REDOX AUXILIARY MEDIATED CATALYSIS OF ORGANIC THERMAL REACTIONS.

STILBENE ISOMERIZATION AND AZA-CLAISEN REARRANGEMENT

by

CHINENYEZE I. NWANKWOALA

SILAS C. BLACKSTOCK, COMMITTEE CHAIR
MICHAEL K. BOWMAN
KEVIN H. SHAUGHNESSY
MICHAEL P. JENNINGS
YUPING BAO

A DISSERTATION

Submitted in partial fulfillment of the requirements
for the degree of Doctor of Philosophy
in the Department of Chemistry and Biochemistry
in the Graduate School of
The University of Alabama

TUSCALOOSA, ALABAMA

2018

Copyright Chinenyeze I. Nwankwoala 2018
ALL RIGHTS RESERVED

ABSTRACT

This work focuses on the development of new general methods of reducing the activation barriers of organic thermal reactions using a diarylamino redox auxiliary (RA) group. Electron removal from the RA weakens bonds and/or changes the conformation of the appended structure to activate its chemical transformation. The electron transfer activation is catalytic, hence the name redox auxiliary catalysis (RAC). This work involves the development of RAC for two thermal organic reactions which normally require high temperatures: stilbene isomerization and the aza-Claisen rearrangement. The outcome is to enable these reactions at room temperature.

Stilbenes may exist as *cis* and *trans* isomers, and photochemical switching between these forms allows for stilbenes use in molecular machines, light-controlled storage devices, and molecular switches including light responsive biological systems. The thermal *cis* to *trans* isomerization of stilbenes requires a large activation barrier of ~46 kcal/mol, which corresponds to a half-life of $\sim 10^{12}$ years at 303 K. As a result, the thermal isomerization of *cis*-stilbene is negligible at room temperature. This barrier to isomerization can be dramatically reduced using RAC, thus yielding a photo electrochromic stilbene which is switched in one direction with photons and in the other direction with electron loss. The oxidized RA unit ($RA^{\cdot+}$) preferentially stabilize twist transition state, thereby reducing the isomerization barrier. Electron transfer between $RA^{\cdot+}$-*trans*-stilbene and RA-*cis*-stilbene completes a catalytic cycle. To date, we have synthesized eight different RA-stilbenes containing electron donating and withdrawing substituents. The RAC *cis* to *trans* stilbene isomerization rate enhancement is found to be $\geq 10^5$.

RA catalysis has also been investigated as a way to promote [3,3]-sigmatropic rearrangement of 1,5-hexadienes (Cope rearrangement) at room temperature. The parent Cope substrate has an activation barrier of ~33.5 kcal/mol and requires temperatures above 200 ºC. Our RA-appended diene undergoes a facile [3,3]-sigmatropic rearrangement at room temperature upon a one electron oxidation of the RA to give predominantly an aza-Claisen product instead of the anticipated Cope product.

LIST OF ABBREVIATIONS AND SYMBOLS

Å angstrom	1 A = 10^{-10} m
anal.	analytical
aq.	Aqueous
AC	aza-Claisen
B3LYP	Becke, 3-parameter, Lee-Yang-Parr
B.p.	boiling point
Bn	benzyl
br.	broad
Bu	butyl
Bz	benzoyl
ca.	circa
cal	calorie 1 cal = 4.184 J
calc.	calculated
CAN	ceric ammonium nitrate
cm	centimeter
conc.	concentrated
CV	cyclic voltammetry
Δ	heat
δ	chemical shift

°C	degrees centigrade, 0 °C = 273.15 K
d	day
d	doublet
dd	doublet of doublets
ddd	doublet of doublet of doublets
ddt	doublet of doublet of triplets
dm	doublet of multiplets
dt	doublet of triplets
DMF	dimethylformamide
DMSO-d_6	deuterated dimethylsulfoxide
dppf	1,1′-bis(diphenylphosphino)ferrocene
ε	molar extinction coefficient
E^o	redox potential or energy or entgegen (trans)
EA	elemental analysis
e.g.	exempli gratia (lat.) - for instance
EI-MS	electron impact mass spectrometry
λmax	energy of the longest-wavelength (lowest-energy)
EPR	electron paramagnetic resonance (spectroscopy)
eq.	equivalents
eqn.	equation
eu	entropy unit
Et	ethyl
ET	electron transfer

EtOH	ethanol
eV	electron volt, 1 eV = 96.485 kJ mol1
exp.	experimental
Fc	ferrocene
*p	fluorescence quantum yield
FT-IR	Fourier transformation infrared spectroscopy
ΔG	change in free energy of activation
g	gram
ΔH	change in enthalpy of activation
h	hour
HOAc	acetic acid
HOMO	highest occupied molecular orbital
HRMS	high resolution mass spectroscopy
Hz	hertz, s^{-1}
i.e.	id est (lat.) - that is to say
ISC	intersystem crossing
J	Joule
J	coupling constant
K	Kelvin
kcal	kilocalorie
kJ	kilojoule
LED	light-emitting device
lit.	literature

LUMO	lowest unoccupied molecular orbital
M	molarity
m	meter
m	multiplet
M.p.	melting point
Me	methyl
melt.	melting
mg	milligram
MHz	megahertz
min	minute
mL	milliliter
mm	millimeter
mmol	millimole
MO	molecular orbital
mol	mole
MS	mass spectrometry
mV	millivolt
μA	microamperes
Mw	weight-average molecular weight
NAr_2	bis(4-methoxyphenyl)amine
N_2	nitrogen
NaOt-Bu	sodium tert-butoxide
nm	nanometer

NMR	nuclear magnetic resonance (spectroscopy)
O	ortho
ORTEP	Oak Ridge thermal ellipsoid plot
p*	perpendicular geometry (phantom state)
p	para
$Pd(dba)_2$	bis-(dibenzylideneacetone)palladium
$Pd_2(dba)_3$	Tris(dibenzylideneacetone)dipalladium (0)
pet	petroleum
Ph	phenyl
pH	pondus hydrogenii
ppm	parts per million
Pr	propyl
p-TsOH	*p*-Toluenesulfonic acid
$P(t\text{-}Bu)_3$	tri-tert-butylphosphine
q	quartet (NMR)
quant	quantitative
$TBABF_4$	n-tetrabutylammoniumtetrafluoroborate
NBu_4PF_6	n-tetrabutylammonium hexafluorophosphate
RA	redox auxiliary
RAC	redox auxiliary catalysis
r.t.	room temperature
ref.	reference
ΔS	change in entropy of activation

s	second
s	singlet
SCE	standard calomel electrode
t	triplet (NMR)
t*	triplet state
TFA	trifluoracetic acid
THF	tetrahydrofuran
TLC	thin-layer chromatography
TMEDA	tetramethylethylenediamine
TMS	trimethylsilyl
TS	transition state
UV/Vis	ultraviolet/visible (spectroscopy)
V	Volt
vs.	versus
W	Watt
Z	zusammen (cis)

ACKNOWLEDGMENTS

Looking over my years of schooling, this quote sums up my, to say the least. “The race is not given to the swift or strong, but the one who endures to the end,” inspired by Ecclesiastes 9:11. From my many challenges, and journey throughout my years in Nigeria and America, I can truly say I have grown as not only a scientist; but an individual. I know the growth during this time, specifically at the University of Alabama, is not only through God, but His use of my advisor, dissertation committee, colleagues, family, and friends. This has been a tough road thus far, however, it has challenged me in ways that I didn’t expect but also brought on unexpected ideas and growth in character.

Dr. Silas C. Blackstock, thank you for your keen intellect, drive, support, and advisement throughout the years. Please know that I mean this with a sincere heart, I was truly blessed to have you as an advisor. Someone who pushed me to go beyond my limits and saw the scientist within myself. Thank you for helping me see it as well and the constant encouragement throughout my time at the University of Alabama. To my dissertation committee (Dr. Michael K. Bowman, Dr. Michael P. Jennings, Dr. Kevin Shaughnessy and Dr. Yuping Bao), thank you for taking the time to review my work and being candid about improvements and further research that could improve my work. Thank you for using this opportunity to push my research beyond what I thought was capable. To my colleagues, thank you for your constant friendship and much-needed laughs on some of the toughest days of my schooling. Your support, and brilliant minds, helped me tremendously and I am grateful to call you not only colleagues; but friends.

To my father (Dennis Umunakwe) and late mother (Irene Umunakwe), thank you for being with me since the beginning. It is your love that has gotten me thus far. To my wife, Chloe Nwankwoala, words can't express how blessed I am to have you by my side. You are a true help-mate in my life and I am grateful for all the prayers, patience and love in my schooling and life. You are my gift from God. To my friends, thank you for the calls and strong friendship that kept me going to this school end. I know you will continue to be with me as my journey continues.

"A nation falls through a lack of guidance, but victory comes through the counsel of many," Proverbs 11:14.

Thank you for helping me have victory in my journey. It is because of you all that I did not fall.

CONTENTS

ABSTRACT.....ii

LIST OF ABBREVIATIONS AND SYMBOLS iv

ACKNOWLEDGMENTS.....x

LIST OF TABLES.....xvi

LIST OF FIGURES xviii

LIST OF SCHEMES xxiii

COMPOUND STRUCTURE LEGEND xxv

CHAPTER ONE INTRODUCTION TO REDOX AUXILIARY CATALYSIS AND SINGLE ELECTRON TRANSFER IN ORGANIC CHEMISTRY 1

1.1 Introduction.....1

1.2 Electron Transfer Catalysis 4

1.3 Photoredox Catalysis 6

1.4 Redox Auxiliary Catalysis.....9

1.5 Our Research Goals.....13

CHAPTER TWO REDOX-AUXILIARY CATALYSIS FOR ISOMERIZATION OF STILBENES 17

2.1 Photochromism and Photoswitches.....17

2.2 Research Goals.....23

2.3 Synthesis of Redox Appended Stilbenes *cis*-7a-e and *trans*-7a-e 25

2.4 Thermal Isomerization of Redox Appended *cis*-Stilbenes 26

2.4.1 *Cis* to *trans* Isomerization of *cis*-dianisylmethoxyaminostilbene (*cis*-OMe-St-NAR$_2$ *cis*-7a) 26

2.4.2 Kinetic Analysis....29

2.4.3 Results of the Thermal Isomerization of *cis*-aminostilbenes (*cis*-St-NAR$_2$) *cis*-7b 35

2.4.4 Results of the Thermal Isomerization of *cis*-dianisylchloroaminostilbene (*cis*-Cl-St-NAR$_2$) *cis*-7c....36

2.4.5 Results of the Thermal Isomerization of *cis*-dianisyltrifluoromethylaminostilbene (*cis*-CF$_3$-St-NAR$_2$) *cis*-7d 37

2.4.6 Results of the thermal isomerization of dianisylmethylaminostilbene (*cis*-Me-StNAr$_2$) *cis*-7e 38

2.4.7. Summary of the Activation parameters of *p*-substituted aminostilbenes *cis*-7a-e.....39

2.5 Photochemistry of Redox-Auxiliary Appended Stilbenes....40

2.5.1 Photochemistry and Optical Spectrum of *trans*-7a 40

2.5.2 Photochemical *trans*-*cis* Isomerization of *trans*-7b-e 47

2.5.3 Summary of the Photochemical Properties of Redox Appended Stilbenes.....50

2.5.4 Photochemical *trans*-*cis* Isomerization of Ortho-substitued stilbenes *trans*-7f-g.....50

2.6 Electrochemical Properties of Redox-Auxiliary Stilbenes....53

2.7 Electron Transfer Catalysis of *cis*-to-*trans* Isomerization of aminostilbenes *cis*-7a-e 60

2.7.1 Results of the Redox Auxiliary Promoted Isomerization of *cis*-7a....61

2.7.2 Results of the Redox Auxiliary Promoted Isomerization of *cis*-7b....72

2.7.3 Results of the Redox Auxiliary Promoted Isomerization of *cis*-7c....74

2.7.4 Results of the Redox Auxiliary Promoted Isomerization of *cis*-7d....75

2.7.5 Results of the Redox Auxiliary Promoted Isomerization of *cis*-7e....76

2.7.6 Summary of the Results of the Neutral and the Radical Processes....80

2.7.7 Thin cell Photo-Electro Device (PED)....82

2.8 Conclusions.....83

2.9 Experimental Details.....84

CHAPTER THREE REDOX AUXILIARY CATALYSIS BIS(DIARYLAMINO) STILBENES.....108

3.1 Introduction.....108

3.2 Synthesis.....109

3.3 Thermal Isomerization of *cis*-NAR$_2$-St-NAR$_2$ *cis*-9.....110

3.4 Kinetic Analysis.....113

3.5 Photochemistry and Optical Spectrum of *trans*-9.....117

3.6 Electrochemical Properties of Bis(diarylamino)stilbene.....122

3.7 Results of the redox auxiliary catalysis of *cis*-NAr$_2$-St-NAr$_2$ *cis*-9.....123

3.8 Thin cell Photo-Electro Device (PED).....132

3.9 Conclusions.....133

3.10 Experimental details.....134

CHAPTER FOUR [3,3]-SIGMATROPIC REARRANGEMENT OF 3-AMINO-1,5-HEXADIENES.....139

4.1 Introduction.....139

4.2 Mechanism of the Cope and Claisen rearrangements.....140

4.3 Catalysis of the Cope and Claisen rearrangements.....142

4.4 Our Research Goals.....143

4.5 Synthesis of Redox Appended 1,5-Hexadienes.....144

4.6 Results of the Redox Auxiliary Mediated Rearrangement of 3-amino-1,5-Hexadienes.....145

4.7 Explanation of Results.....149

4.8 Experimental Results of CRET and Other Oxidants.....152

4.9 Conclusions.....154

4.10 Experimental details.....155

REFERENCES 168

APPENDIX A NMR SPECTRA 183

APPENDIX B X-RAY CRYSTALLOGRAPHIC DATA FOR ***trans*-7a**.....265

APPENDIX C X- RAY CRYSTALLOGRAPHIC DATA FOR ***cis*-7a** 267

APPENDIX D X- RAY CRYSTALLOGRAPHIC DATA FOR ***trans*-7e** 269

APPENDIX E X- RAY CRYSTALLOGRAPHIC DATA FOR ***trans*-7g**.....271

APPENDIX F EMISSION SPECTRUM OF 395-410 nm LED 273

APPENDIX G EMISSION SPECTRUM OF 430 nm LED.....274

APPENDIX H THERMAL ISOMERIZATION DATA FOR ***cis*-7a-e** 275

APPENDIX I RADICAL ISOMERIZATION DATA FOR ***cis*-7a-e**.....283

APPENDIX J UV-VIS OF CRET 294

LIST OF TABLES

2.1 Thermal isomerization of 0.0731 M ***cis*-7a** to ***trans*-7a** in DMSO at 140 °C.....31

2.2 The first order rate constants for the thermal isomerization of ***cis*-7a** to ***trans*-7a**.....33

2.3 Activation parameters of the thermal isomerization of ***cis*-7a** in DMSO 34

2.4 Thermal isomerization of 0.0731 M ***cis*-7b** to ***trans*-7b** in DMSO at 140 °C 35

2.5 Thermal isomerization of 0.0731 M ***cis*-7c** to ***trans*-7c** in DMSO at 140 °C 36

2.6 Thermal isomerization of 0.0731 M ***cis*-7d** to ***trans*-7d** in DMSO at 140 °C 37

2.7 Thermal isomerization of 0.0731 M ***cis*-7e** to ***trans*-7e** in DMSO at 140 °C 38

2.8 The activation parameters of p-substituted stilbenes in DMSO at 140 °C 39

2.9 Summary of the photochemical properties of redox appended stilbenes. 50

2.10 Oxidation potentials of para-substituted aminostilbenes 59

2.11 Redox auxiliary promoted *cis-trans* isomerization of 3.02 x 10^{-5} M ***cis*-7a** in cyclohexane: benzene = 98:2 using 5 mol % CRET in DCM at 30°C 63

2.12 First order rate constants of the RA promoted *cis-trans* isomerization of 3.02 x 10^{-5} M ***cis*-7a** in cyclohexane: benzene = 98:2 using 5 mol % CRET in DCM at 30°C 65

2.13 Summary of the activation parameters for the RA promoted neutral/radical isomerization of ***cis*-7a**.....67

2.14 Redox auxiliary promoted *cis-trans* isomerization of 3.02 x 10^{-5} M ***cis*-7b** in cyclohexane: benzene = 98:2 using 5 mol % CRET in DCM at 30°C 73

2.15 Redox auxiliary promoted *cis-trans* isomerization of 3.39 x 10^{-5} M ***cis*-7c** in cyclohexane: benzene = 98:2 using 5 mol % CRET in DCM at 30°C 74

2.16 Redox auxiliary promoted *cis-trans* isomerization of 3.02 x 10^{-5} M ***cis*-7d** in cyclohexane: benzene = 98:2 using 5 mol % CRET in DCM at 30°C 75

2.17 Redox auxiliary promoted *cis-trans* isomerization of 3.39 x 10^{-5} M ***cis*-7e** in cyclohexane: benzene = 98:2 using 5 mol % CRET in DCM at 30°C 77

2.18 First order rate constants of the RA promoted cis-trans isomerization of 3.39 x 10^{-5} M ***cis*-7e** using 5 mol % CRET in DCM at 30°C 78

2.19 Summary of the activation parameters for the RA promoted neutral/radical isomerization of ***cis*-7e** 79

2.20 Summary of the results of the processes 80

3.1 First order rate constants for the thermal isomerization of ***cis*-9** in DMSO.....115

3.2 Activation parameters of the thermal isomerization of ***cis*-9** in DMSO 116

3.3 Redox auxiliary promoted isomerization of ***cis*-9** at 30 ºC.....129

4.1 Oxidation products of 3-diarylamino-1, 5-hexadienes 148

LIST OF FIGURES

1.1 Molecular orbitals of the neutral molecules, radical anions, and radical cations 4

1.2 (a) Heck-type reaction (b) radical cross-dehydrogenative coupling reactions (c) trifluoromethylation (d) Alkoxycarbonylation 5

1.3 Photocatalysts 7

1.4 Schematic of the redox auxiliary effect 10

1.5 Diarylamino redox auxiliary **(RA)**.....13

2.1 Energy profile of the thermal equilibrium of *trans* and *cis*-stilbene.....19

2.2 A schematic representation of the *trans*-and *cis*-isomerization of stilbene 21

2.3 The electronic absorption spectra of *cis*- and *trans*-stilbene 22

2.4 The model structures of the *cis* and *trans*-stilbene. Modeled by using B3LYP-631G*.....28

2.5 ^{1}H NMR of ***cis*-7a** undergoing a thermal isomerization to ***trans*-7a** 28

2.6 First order plots of ln [***cis*-7a**] vs time t at 150 °C 32

2.7 The eyring plot of the thermal isomerization of ***cis*-7a** in DMSO.....33

2.8 Graph of ln [***cis*-7b**] vs time at 140 ºC.....35

2.9 Graph of ln [***cis*-7c**] vs time at 140 ºC 36

2.10 Graph of ln [***cis*-7d**] vs time at 140 ºC.....37

2.11 Graph of ln [***cis*-7e**] vs time at 140 ºC 38

2.12 Optical spectrum of ***cis*-7a** and ***trans*-7a** (3.01×10^{-5} M).....41

2.13 The optical spectrum of ***trans*-7a** (3.01×10^{-5} M**)** 42

2.14 The optical spectrum of ***trans*-7a** (2.21 x 10^{-4} M in C_6D_6) irradiated with a 430 nm LED at room temperature in a 0.1cm quartz cuvette 43

2.15 An expanded view of the methoxy region of the ^{1}H NMR spectrum of ***trans*-7a** before irradiation and an isomeric mixture (2.43 x 10^{-4} M solution) of 60:40 ***trans*-7a:*cis*-7a** at the PSS 44

2.16 The Full NMR spectrum of synthetically made ***cis*-7a** 45

2.17 An expanded view of the methoxy region of the ^{1}H NMR spectrum of ***cis*-7a** 46

2.18 An expanded view of the aromatic region of the ^{1}H NMR spectrum of ***cis*-7a** 46

2.19 Photoisomerization of 5.49 x 10^{-5} M solution of ***trans*-7b** 48

2.20 Photoisomerization of 3.79 x 10^{-5} M solution of ***trans*-7c** 48

2.21 Photoisomerization of 2.88 x 10^{-5} M solution of ***trans*-7d** 49

2.22 Photoisomerization of 2.71 x 10^{-5} M solution of ***trans*-7e** 49

2.23 Photoisomerization of 1.49 x 10^{-5} M solution of ***trans*-7f** in 2 % benzene in cyclohexane using 395-410 nm (7W) LED at 23 ºC 52

2.24 Photoisomerization of 1.49 x 10^{-5} M solution of ***trans*-7g** in 2 % benzene in cyclohexane using 395-410 nm (7W) LED at 23 ºC 52

2.25 Cyclic voltammogram of ***trans*-7a** (1.00 mM in DCM with 0.1 M nBu_4PF_6) at a scan rate of 50 mV/s 54

2.26 Cyclic voltammogram of ***trans*-7b** (1.00 mM in DCM with 0.1 M nBu_4PF_6) at a scan rate of 50 mV/s 55

2.27 Cyclic voltammogram of ***trans*-7c** (1.00 mM in DCM with 0.1 M nBu_4PF_6) at a scan rate of 50 mV/s 55

2.28 Cyclic voltammogram of ***trans*-7d** (1.00 mM in DCM with 0.1 M nBu_4PF_6) at a scan rate of 50 mV/s 56

2.29 Cyclic voltammogram of ***trans*-7e** (1.00 mM in DCM with 0.1 M nBu_4PF_6) at a scan rate of 50 mV/s 56

2.30 Cyclic voltammogram of ***trans*-7f** (1.00 mM in DCM with 0.1 M nBu_4PF_6) at a scan rate of 50 mV/s 57

2.31 Cyclic voltammogram of ***trans*-7g** (1.00 mM in DCM with 0.1 M nBu_4PF_6) at a scan rate of 50 mV/s 57

2.32 Optical spectrum of addition of CRET (5 mol % in DCM) to 4.04 X 10^{-5} M solution of ***cis*-7a** in 2 % benzene in cyclohexane.....63

2.33 First order plot of the ln[***cis*-7a**] vs time at 30 ºC for the redox auxiliary promoted *cis-trans* isomerization of using 10 mol % CRET.....64

2.34 Eyring plot of the radical isomerization of ***cis*-7a** 65

2.35 Graph of k vs mol % of CRET for the radical isomerization of ***cis*-7a**.....66

2.36 The optical spectrum of the addition of 5 mol % of CRET to 4.04 x 10^{-5} M solution of ***cis*-7a** at PSS.....68

2.37 The addition of CRET (5 mol%) to ***cis*-7a** (2.86 X 10^{-3} M) at 30 ºC 69

2.38 Cap and stick diagram of the crystal structure of ***trans*-7a** 71

2.39 Cap and stick diagram of the crystal structure of ***cis*-7a** 71

2.40 Optical spectrum of the addition of CRET (5 mol% in DCM) to 3.02 X 10^{-5} M solution of ***cis*-7b** in 2 % benzene in cyclohexane.....72

2.41 First order plot of the ln[***cis*-7b**] vs time at 30 ºC for the redox auxiliary promoted *cis-trans* isomerization of using 5 mol % CRET.....73

2.42 Optical spectrum of the addition of CRET (5 mol% in DCM) to 3.39 X 10^{-5} M solution of ***cis*-7c** in 2 % benzene in cyclohexane.....74

2.43 First order plot of the ln[***cis*-7c**] vs time at 30 ºC for the redox auxiliary promoted *cis-trans* isomerization of using 5 mol % CRET.....75

2.44 First order plot of the ln[***cis*-7c**] vs time at 30 ºC for the redox auxiliary promoted *cis-trans* isomerization of using 5 mol % CRET.....76

2.45 Optical spectrum of the addition of CRET (5 mol% in DCM) to 3.08 X 10^{-5} M solution of ***cis*-7e** in 2 % benzene in cyclohexane.....76

2.46 First order plot of the ln[***cis*-7e**] vs time at 30 ºC for the redox auxiliary promoted *cis-trans* isomerization of using 5 mol % CRET.....77

2.47 Eyring plot of the RA radical isomerization of ***cis*-7e**.....78

2.48 Photo-electro cell device designed to test the effect of electricity on the *cis* isomers of *para*-redoxstilbenes 82

2.49 Photo-electro cell device 83

3.1 Bis(diarylamino)stilbene photo-electro switch 108

3.2 ^{1}H NMR of ***cis*-9** undergoing a thermal isomerization to ***trans*-9** form in DMSO at 150 ºC 112

3.3 First order plots of ln [***cis*-9**] vs time t at different temperatures 114

3.4 Eyring and Arrhenius plots of the thermal isomerization of ***cis*-9** in DMSO 116

3.5 Optical spectrum of ***cis*-9** and ***trans*-9** (3.02×10^{-5} M) in cyclohexane:benzene = 2:98 at room temperature in 1cm quartz cuvette 118

3.6 Optical spectrum of ***trans*-9** (2.47×10^{-5} M in 2 % benzene in cyclohexane) irradiated with a 430 nm LED at room temperature in a 1cm quartz cuvette 119

3.7 ^{1}H NMR of ***cis*-9** (1.58×10^{-2} M in C_6D_6) (a) Spectrum before irradiation in black (b) Spectrum after irradiation with 430 nm LED light (7W) in blue. PSS is established at a 60:40 ***cis*-9:*trans*-9** ratio at room temperature 120

3.8 An expanded view of the alkyl region of the ^{1}H NMR spectrum of ***cis*-9** 121

3.9 Cyclic voltammogram of ***trans*-7f** (1.00 mM in DCM with 0.1 M nBu_4PF_6) at a scan rate of 50 mV/s 123

3.10 Optical spectrum of addition of CRET (3.5 mol% in DCM) to 3.03×10^{-5} M solution of ***cis*-9** in 2 % benzene in cyclohexane 124

3.11 Optical spectrum of addition of CRET (3.0 mol% in DCM) to 3.03×10^{-5} M solution of ***cis*-9** in 2 % benzene in cyclohexane 125

3.12 Optical spectrum of addition of CRET (2.5 mol% in DCM) to 3.03×10^{-5} M solution of ***cis*-9** in 2 % benzene in cyclohexane 125

3.13 Photoisomerization of 2.47×10^{-5} M solution of ***trans-9*** in 2 % benzene in cyclohexane using 430nm LED (7W) at 23 ºC 126

3.14 The optical spectrum of the addition of 2.5 mol % to 2.47×10^{-5} M solution of ***cis-9*** in 2 % benzene in cyclohexane at PSS 127

3.15 The ^{1}HNMR of (a) ***trans*-9** (b) isomeric mixture of ***cis*-9** and ***trans*-9** (91% *cis*: 9% *trans*) (c) isomeric mixture at PSS (40 % *cis*: 60 % *trans*) (d) after addition of 3 mol % CRET 128

3.16 First order plot of the ln[***cis*-9**] vs time at 30 ºC for the redox auxiliary promoted *cis-trans* isomerization of using 3.5 mol % CRET 129

3.17 First order plot of the ln[***cis*-9**] vs time at 30 ºC for the redox auxiliary promoted *cis-trans* isomerization of using 3.0 mol % CRET 130

3.18 First order plot of the ln[***cis*-9**] vs time at 30 ºC for the redox auxiliary promoted *cis-trans* isomerization of using 2.5 mol % CRET 130

3.19 Graph of k vs mol % of CRET for the radical isomerization of ***cis*-9**…….....131

3.20 Photo-electro cell device of **NAr_2-St-NAr_2** 132

4.1 The depiction of possible TSs for the Cope rearrangement.....142

4.2 3-amino-1,5-hexadiene and the rearrangement products.....152

4.3 The cyclic voltammogram of **10** 154

LIST OF SCHEMES

1.1 The mechanism of single electron oxidation 2

1.2 SET in organic chemistry 3

1.3 The mechanism of base promoted homolytic aromatic substitution (BHAS) 5

1.4 Simplified Molecular Orbital Depiction of $Ru(bpy)_3^2$ photochemistry 9

1.5 The redox auxiliary catalyzed [2 + 2] cycloadditions 11

1.6 (a) Simple alkene: resistant to one electron oxidation, poor substrates
(b) Redox auxiliary strategy for radical cation reactions 11

1.7 The postulated mechanism of the photo-electro catalysis of azobenene 12

1.8 The 4a-4b system and the postulated RA-substituted photoelectrochromic system 13

1.9 The catalytic cycle of the isomerization of Z-E stilbenes 15

1.10 Schematic of the redox-auxiliary promoted [3,3]-sigmatropic rearrangement of 1, 5-hexadienes 16

2.1 Examples of photochromic devices switches 18

2.2 Isomerization of stilbene 20

2.3 Mechanism of photoisomerization of stilbene 21

2.4 Isomerization and oxidative cyclization of stilbene 23

2.5 Proposed redox auxiliary promoted *cis-trans* isomerization of stilbene 24

2.6 Synthesis of *para*-substituted bromostilbene 25

2.7 Synthesis of RA stilbenes 26

2.8 Thermal isomerization ***cis*-7a** at 140 ºC 27

2.9 Photocyclization of *cis*-stilbene 51

2.10 The isomerization/dimerization reactions of the *cis*-stilbene radical cation.....61

2.11 The catalytic cycle of the *cis-trans* isomerization of stilbene.....70

2.12 Mechanism of the cation radical isomerization of *cis*-RA stilbene 82

3.1 Synthesis of 4,4′-dibromostilbene.....110

3.2 Synthesis of bis(diarylamino)stilbenes 110

3.3 Thermal isomerization ***cis*-9** in DMSO at 150 ºC 111

3.4 The catalytic cycle of the isomerization of bis(diarylamino)stilbene 133

4.1 A [3,3]- sigmatropic rearrangement of 1,5-Hexadiene 139

4.2 Cope rearrangement of 1,5-hexadienes showing a chair-like six-membered pericyclic transition state and a biradical intermediate when radical stabilizing groups are attached to C_2 and C_5 positions 140

4.3 Cope and aza-Claisen rearrangements of a redox appended 1,5-hexadiene 144

4.4 The synthesis of 3-amino-1,5-Hexadienes.....145

4.5 The redox auxiliary mediated rearrangement of 3-diarylamino-1,5-Hexadienes.....146

4.6 Cope rearrangement of 3-amino-1,5-hexadiene 149

4.7 Aza-Claisen rearrangement of 3-amino-1,5-hexadiene 150

4.8 The transition state of the Cope and aza-Claisen rearrangement of 3-diarylamino-1,5-hexadiene 151

COMPOUND STRUCTURE LEGEND

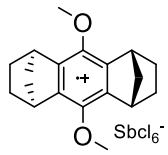

CRET

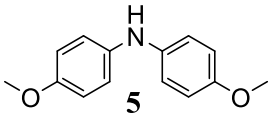

5

RA

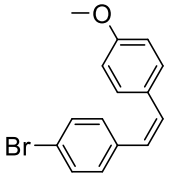

***cis*-6a**

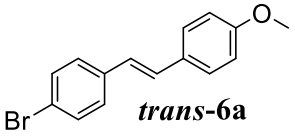

***trans*-6a**

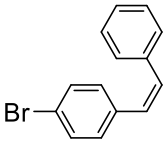

***cis*-6b**

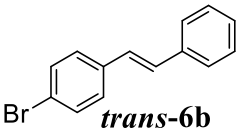

***trans*-6b**

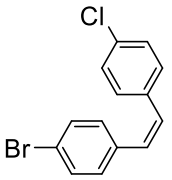

***cis*-6c**

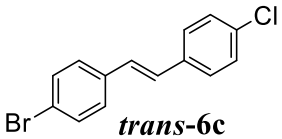

***trans*-6c**

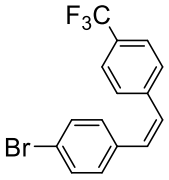

***cis*-6d**

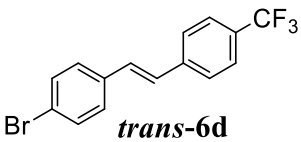

***trans*-6d**

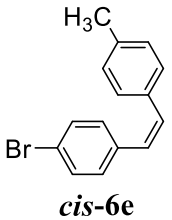

***cis*-6e**

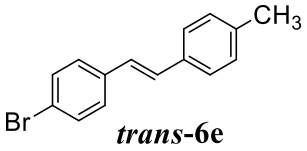

***trans*-6e**

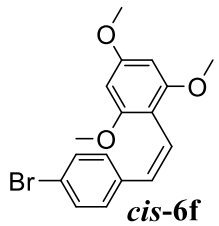

***cis*-6f**

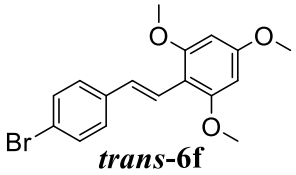

***trans*-6f**

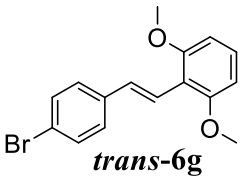

***trans*-6g**

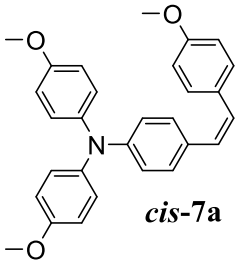

***cis*-7a**

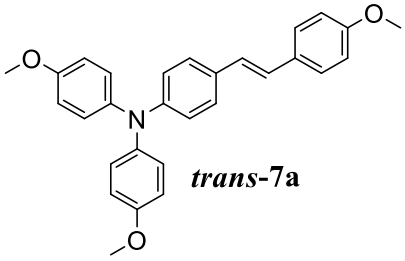

***trans*-7a**

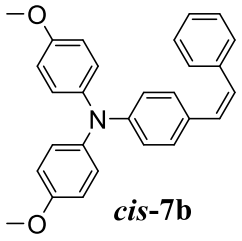

***cis*-7b**

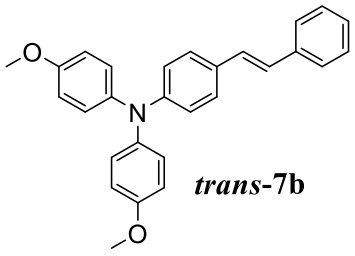

***trans*-7b**

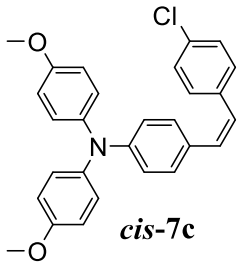

***cis*-7c**

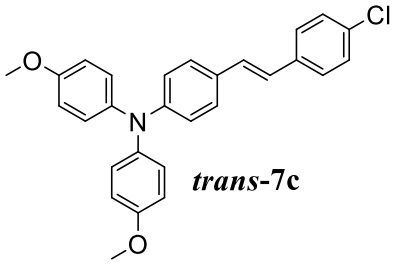

***trans*-7c**

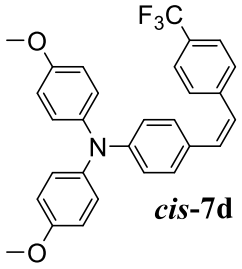

***cis*-7d**

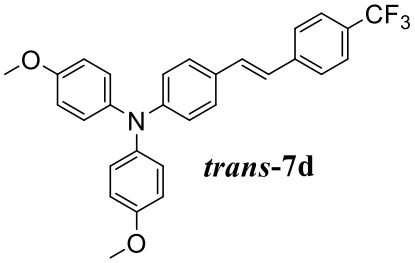

***trans*-7d**

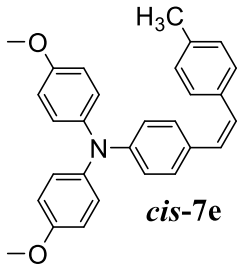

***cis*-7e**

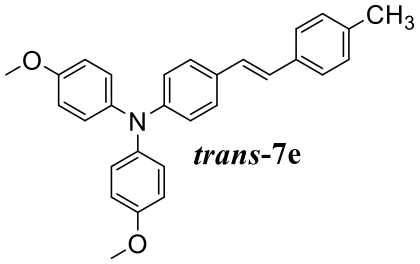

***trans*-7e**

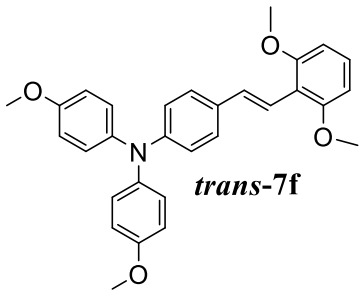

***trans*-7f**

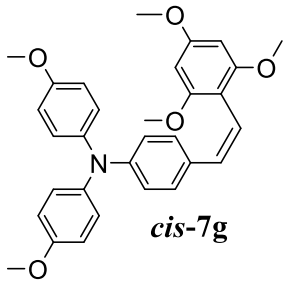

***cis*-7g**

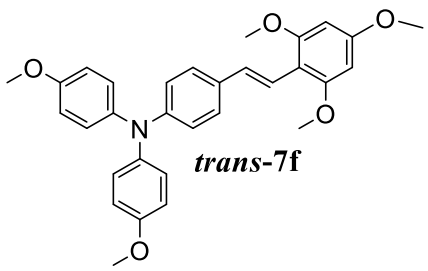

***trans*-7f**

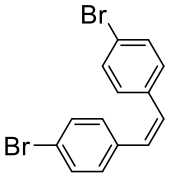

***cis*-8**

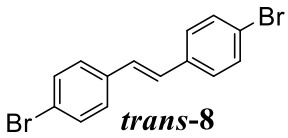

***trans*-8**

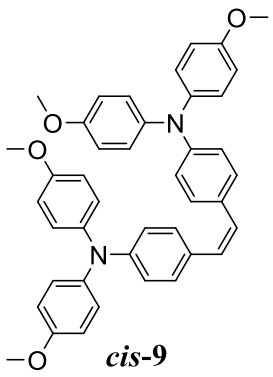

***cis*-9**

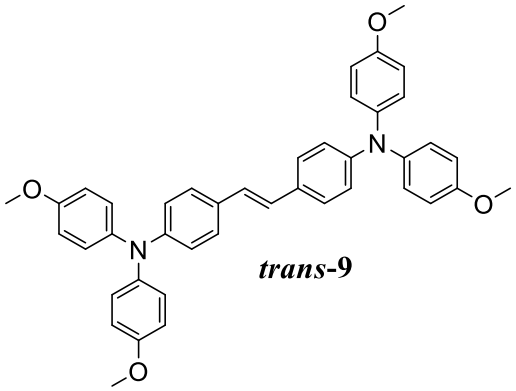

***trans*-9**

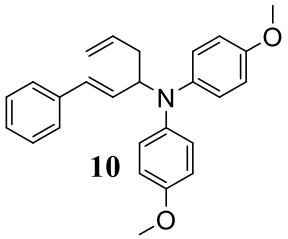

10

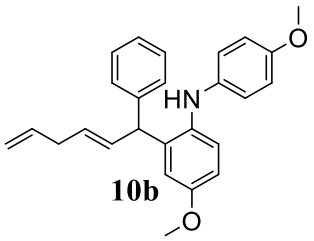

10b

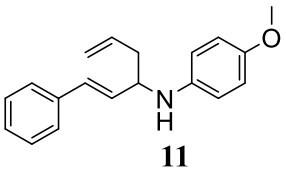

11

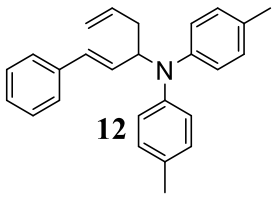

12

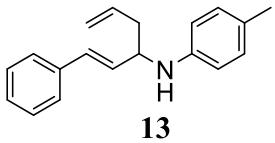

13

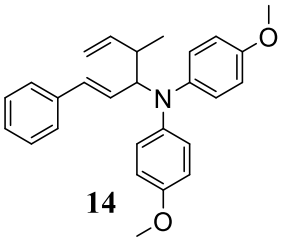

14

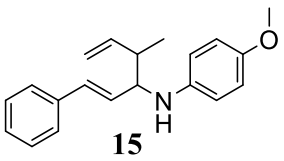

15

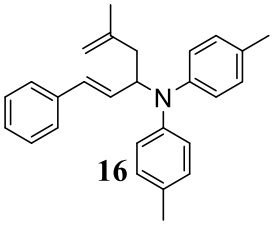

16

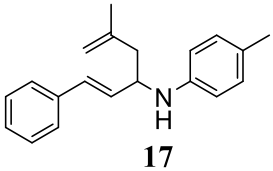

17

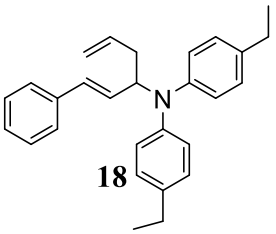

18

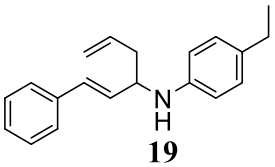

19

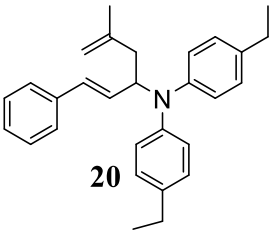

20

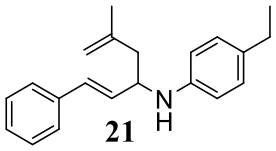

21

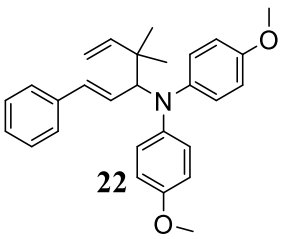

22

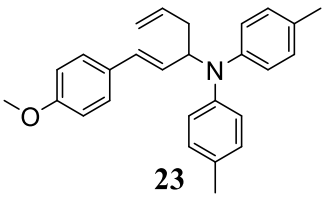

23

CHAPTER ONE

INTRODUCTION TO REDOX AUXILIARY CATALYSIS AND SINGLE ELECTRON OXIDATION IN ORGANIC CHEMISTRY

1.1 Introduction

An oxidation-reduction (redox) reaction is a chemical reaction that involves a transfer of electrons between two species, resulting in a change in the oxidation state of the molecule, atom, or ion.[1] Redox processes are found in nature, as well as in virtually every area of chemistry, including inorganic, organic, biochemistry, macromolecules, electroplating, electrochemistry, metallurgy, etc.[2] A redox process can be induced thermally or photoinduced. Several reviews on chemical and electrochemical electron transfer have been published.[3-8]

The single electron transfer (SET) process also known as electron transfer is important in organic chemistry because it generates reactive intermediates. These intermediates can undergo several pathways to produce important synthetic compounds.[8] SET is defined by the commission of physical organic chemistry division of the IUPAC as a "reaction mechanism characterized by the transfer of single electron between the species occurring on the reaction coordinate of one of the elementary steps".[9] These reactions constitute a type of redox process and include both chemical and electrochemical systems. One of the earliest examples of single electron oxidation was performed by Michael Faraday in 1834 when he electrolyzed an aqueous potassium acetate salt and observed the formation of organic gas at the anode.[10] Two decades later, this process became known as Kolbe reaction[11] because he showed that the gases formed during the

electrolysis were due to the decarboxylation of the acetate to produce CO_2 gas and ethane.[12] The reaction mechanism involves single electron oxidation of the acetate to produce carboxyl radicals, which then release CO_2 and form methyl radicals. These radicals can either homocouple to produce ethane or undergo a second single-electron oxidation to produce a cation as shown in Scheme 1.1.[13] These discoveries by Faraday and Kolbe brought attention to the single electron transfer processes and led to both experimental and theoretical developments of this field in chemistry and biology. The applications of single electron transfer in organic synthesis have been well documented,[14-16] and these reactions continue to receive attention.

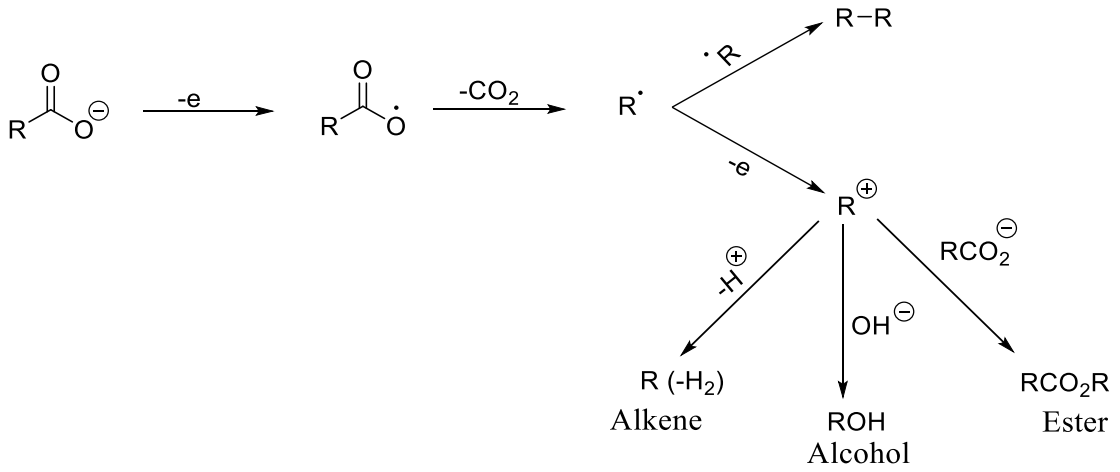

Scheme 1.1. The mechanism of single electron oxidation.[13]

Inorganic electron transfer reactions differ from the organic electron transfer reaction in that the electron transfer occurs between two metal complexes instead of occurring between two organic molecules. The transfer of electrons between one or more bridging ligands requires less energy, leading to the formation of a kinetically stable specie. Organic electron transfer processes (Scheme 1.2)[16] involve the formation or cleavage of strong bonds; thus, the bond energies are greater than 50 kcal mol $^{-1}$. In contrast, the ligand to metal bond energies of

complexes in inorganic electron transfers is usually less than or equal to 10 kcal mol.[1] Cation radicals and anions are generated after SET for species with an even number of electrons, while cations and anions are generated from odd electron species. In inorganic SET, the interaction between the donor and the acceptor depends primarily on the ligand, the nature of the donor and acceptor, and the solvent used for the reaction. There is no formation or breakage of chemical bonds. However, the change in bond geometry (distances and sometimes angles) in each reactant and rearrangements of the likely configurations of the environment (solvent molecules) around the reactants play an important role in this process.[17]

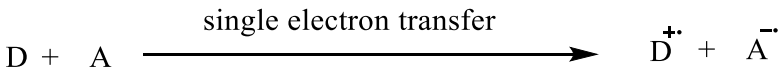

Even Electron species

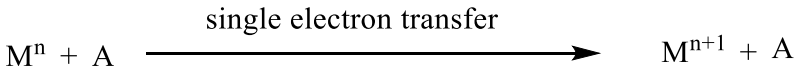

M= metal; n, n+1 = oxidation state of the metal

Odd Electron species

Scheme 1.2. SET in organic chemistry.[16]

The reactivity of radical cations formed through single electron transfer is well known[18-19]. The molecular orbitals of the neutral, radical anions and cations are shown in Figure 1.1[18] The neutral molecules have higher bond breaking energies than their corresponding radical anions and cations, hence they have a higher activation energy.

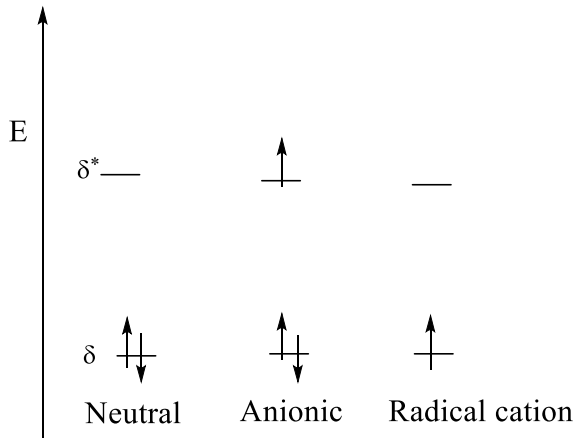

Figure 1.1. Molecular orbitals of the neutral molecules, anions, and radical cations.[18]

1.2 Electron Transfer Catalysis

Electron transfer catalysis is a reaction where the initial and final states are at the same oxidation level and the intervening steps take place at an oxidation level one step above (hole catalysis) or below (electron catalysis) that of the substrate.[1] Redox catalysis is a type of electron transfer catalysis. It takes place in multi-step reactions where an intermediate has either one oxidation-state level above or below that of the substrates and products. Numerous chemical reactions, previously believed to occur by the movement of electron pairs, are now understood as processes in which there is an initial electron transfer from a nucleophile (reductant) to an electrophile (oxidant). This initial single electron transfer produces a radical ion pair, which leads to the final products through additional steps involving the cleavage and formation of chemical bonds.[20-22] The subsequent steps are very fast, making the initial single electron transfer the rate determining step in an overall irreversible transformation. The rate determining electron transfer step is usually endergonic ($\Delta G^{o}_{et} > 0$) and thereby thermodynamically unfavorable.

Base-promoted homolytic aromatic substitution (BHAS) is another type of electron-catalyzed reaction that has generated new interest and opportunities in electron transfer catalysis

and radical chemistry.[22] In the last few years, BHAS has led to new transformations such as the Heck-type reaction,[23] radical cross-dehydrogenative coupling reactions,[24] arene trifluoromethylation[25] and alkoxycarbonylation[26] as shown in Figure 1.2

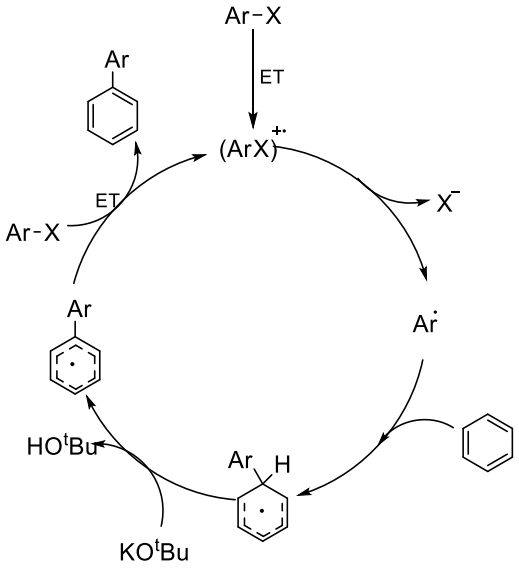

Scheme 1.3 The mechanism of base promoted homolytic aromatic substitution (BHAS).[22]

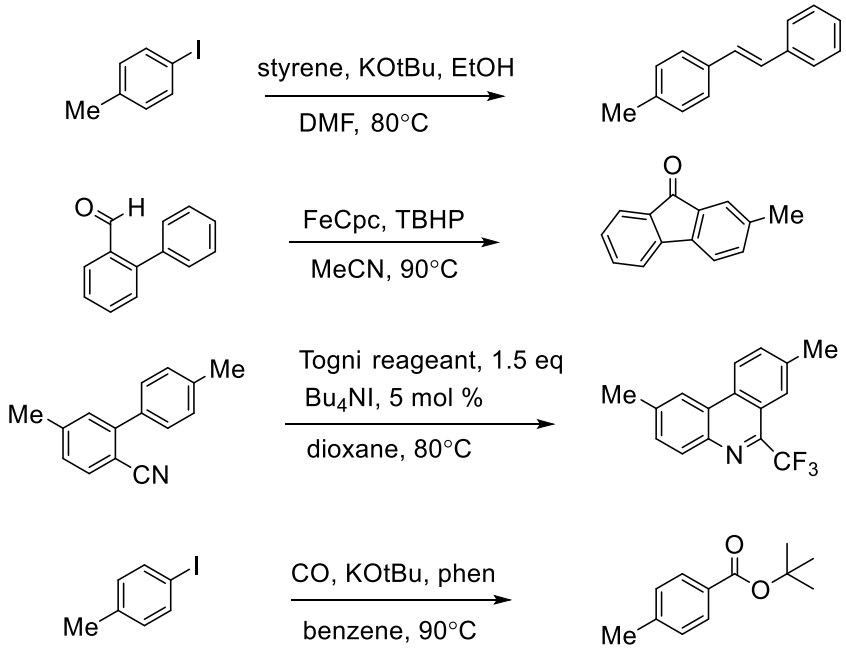

Figure 1.2. (a) Heck-type reaction (b) radical cross-dehydrogenative coupling reactions (c) trifluoromethylation (d) alkoxycarbonylation.[22]

SET is an effective means of promoting symmetry-forbidden or slow pericyclic reactions by the addition or removal of an electron.[27] Radical cations are reactive intermediates that can be formed from neutral species by oxidative SET. This approach has been used to accelerate the rates of [3,3]-sigmatropic rearrangements and the other pericyclic reactions by lowering the barrier for the reaction.[28] The idiosyncrasy of the transition state of a pericyclic reaction is the cyclic conjugated system, and the acceleration of these reactions is usually explained in terms of the delocalization stabilization of these cyclic systems.[28] Woodward proposed the application of electron transfer catalysis to pericyclic reactions via the formation of the final product by back electron transfer from the product radical ion in 1942.[29] Since then, much progress has been made towards the theoretical understanding[28, 30] of the radical cation pericyclic reactions. This has led to the application of these reactions in the synthesis of natural products.[31] Examples of cation- radical pericyclic reactions are cation- radical Diels Alder, cation-radical olefin cyclodimerization, Cope reaction, and electrocyclic reactions.[28, 32]

1.3 Photoredox Catalysis

An important aim in the field of catalysis is the development of new modes of small molecule activation. One approach toward the catalytic activation of organic molecules which has received much attention lately is visible light photoredox catalysis and it is one of the most expanding areas of radical chemistry.[33] Photoredox catalysis is now considered as a mild means of achieving unique chemical reactivity. This type of catalysis harnesses the energy of light to increase the rate of a chemical reaction through SET events.[34-35] The reaction relies on the ability of metal complexes and organic dyes to engage in single-electron-transfer (SET) processes with organic substrates upon photoexcitation with visible light.[36] It employs small quantities of a photo-sensitive compound that when excited by light, can facilitate the transfer of

electrons between chemical compounds that would have either reacted slowly or not reacted at all. The resultant stable, long-lived photoexcited species can act as both a strong oxidant and a strong reductant concurrently, thereby engineering an overall redox neutral reaction by allowing oxidation and reduction to occur at separate steps in the reaction mechanism.[36] In contrast to traditional redox reactions (e.g. electrochemistry), the reaction medium can be either oxidative or reductive (but not both) and, in turn, provides access to previously inaccessible redox-neutral reaction platforms.[34]

The most commonly used visible light photocatalysts are polypyridyl complexes of ruthenium (tris(2,2′-bipyridine) ruthenium(II)) $Ru(bpy)_3^{2+}$ and iridium (tris[2-phenylpyridinato-C^2,N]iridium(III) $Ir(ppy)_3$ (Figure 1.3).[37-38] The oxidation and reduction potentials of the photocatalysts are dependent on the ligands and groups present on the ligands. Each photocatalyst possesses different oxidation and reduction potentials, and can therefore be used to create new synthetic transformations or explain unknown mechanistic pathways.

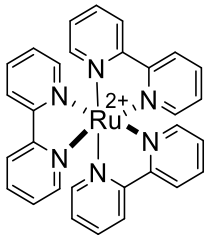

1a

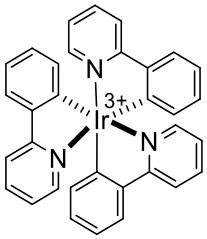

1b

Figure 1.3. Photocatalysts (a) (tris(2,2′-bipyridine) ruthenium(II)) $Ru(bpy)_3^{2+}$ (b) iridium (tris[2-phenylpyridinato-C^2,N]iridium(III) $Ir(ppy)_3$.[37-38]

The activity of a photoredox catalyst can be described in three steps. First, a molecule of the catalyst in its ground state interacts with light and moves into a long-lived excited state, where the electrons are not distributed among the lowest-energy combination of available states.[39] The photoexcitation involves the movement of an electron in one of the photocatalyst's

metal-centered t_{2g} orbitals (HOMO) to the ligand-centered π^* orbital (LUMO) upon absorption of a photon in the visible region (Scheme 1.4).[36] This transition is known as a metal to ligand charge transfer (MLCT) and results in species in which the metal has effectively been oxidized to a higher oxidation state and the ligand framework has undergone a single-electron reduction. Second, the initially occupied singlet MLCT state undergoes rapid intersystem crossing (ISC) to give the lowest-energy triplet MLCT state.[40] Photoexcitation of $Ru(bpy)_3^{2+}$ generates a higher-energy electron, which may be expelled from the π^* orbital when the photocatalyst acts as a reductant. Simultaneously, photoexcitation reveals a lower-energy hole in the t_{2g} orbital, which may accept an electron when the photocatalyst acts as an oxidant (Scheme 1.4).[36] Finally, a second single electron transfer occurs to return the catalyst to its original oxidation state and electron arrangement. As a result of this distinct property of the $Ru(bpy)3^{2+}$ photoexcited state, redox reactions of $*Ru(bpy)3^{2+}$ may proceed either by oxidative or by reductive quenching.

Modern photoredox catalysis have been applied to the development of a wide array of novel synthetic methodologies,[35, 41] water splitting,[42] carbon dioxide reduction,[43] and novel solar cell materials.[44]

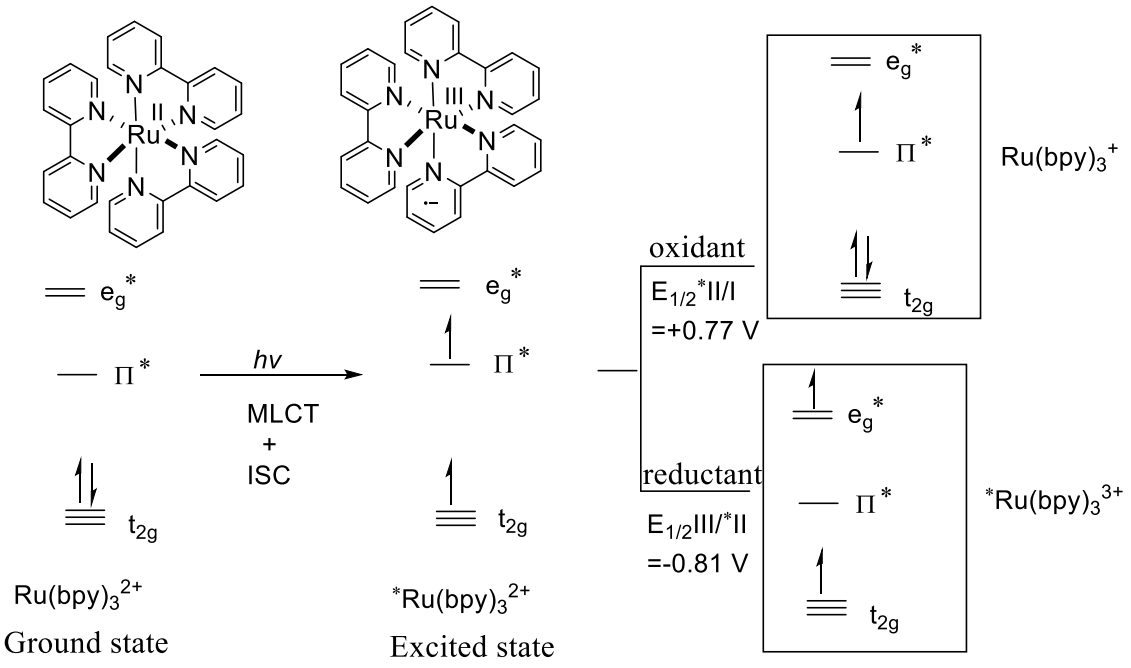

Scheme 1.4. Simplified Molecular Orbital Depiction of $Ru(bpy)_3^2$ Photochemistry.[36]

1.4 Redox Auxiliary Catalysis

Redox auxiliary catalysis is the appending of a stable redox-switchable group (redox auxiliary, RA) to a reactive site which then enhances the reactivity of the redox appended molecule.[45] This reaction involves the changing of the oxidation state of the RA to enhance a chemical transformation. A redox auxiliary is a group that changes its oxidation state reversibly and can act as a chemical switch when attached to a molecular substrate as illustrated in Figure 1.4. The intermediates in the cycle are either one oxidation state above or below the substrates and products. In other words, redox auxiliary catalysis is an electron transfer reaction that involves the temporary addition or removal of an electron. This new method of electron transfer catalysis can be applied to very slow chemical transformations that require high temperatures and serve to increase the rate of such reactions. The term “hole transfer” is an electron transfer reaction that involves radical cations, and the position left by the hole is of primary interest.

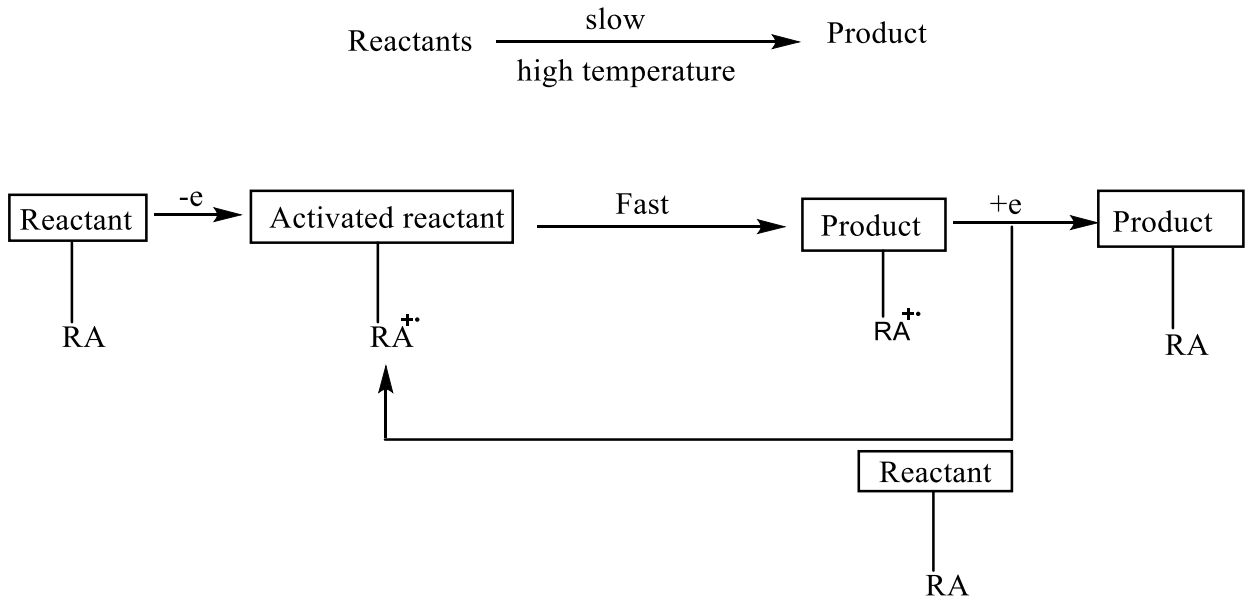

Figure 1.4. Schematic of the redox auxiliary effect.

The redox auxiliary unit is attached to a reaction site and upon removal of an electron by a one electron oxidant, reduces the activation barrier for the reaction thereby increasing the rate of the formation of the product. Redox catalysis is a developing field and has had useful applications in materials science and organic synthesis.[45-47] Okada et. al.[48] used the word "redox tag" to describe the alkoxyphenyl group attached to unactivated olefins to enhance the electron-transfer-induced intramolecular (electrocatalytic formal) [2 + 2] cycloadditions (Scheme 1.5). The radical cation of the aliphatic cyclic enol ether generated by anodic oxidation underwent successful [2 + 2] cycloadditions with several unactivated alkenes possessing the aromatic "redox tag". The alkoxyphenyl group enhances the complete formation of the cyclobutane ring **2** through intramolecular electron transfer between alkoxphenyl group possessing the redox tag and the cyclobutene radical cation.

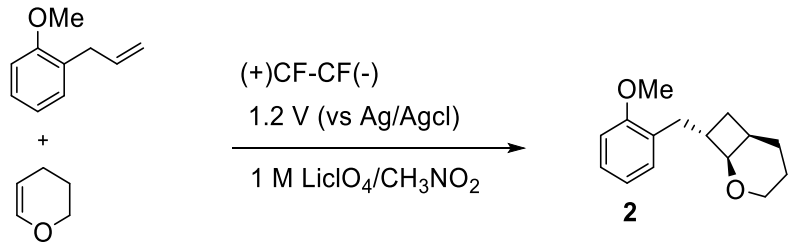

Scheme 1.5. The redox auxiliary catalyzed [2 + 2] cycloadditions.[48]

T. P. Yoon[49-50] appended an easily removable electron rich redox auxiliary group onto an unactivated alkene to enhance the Diels-Alder and [2 + 2] cycloadditions upon oxidation by a one electron transfer oxidant. The attachment of this easily oxidized redox auxiliary moiety promoted the photocatalytic conversion of the alkene to the radical cation, which then reduced the activation barrier of the reaction. The radical cations resulting from the one electron oxidation underwent many Diels-Alder and [2 + 2] cycloadditions. These were then followed by the removal of the sulfide group to afford cycloadducts that could not be directly synthesized by reactions of simple unfunctionalized alkenes as shown in Scheme 1.6. They concluded that the use of a redox auxiliary group provides a method to overcome a fundamental constraint on the feasibility of photoreactions.

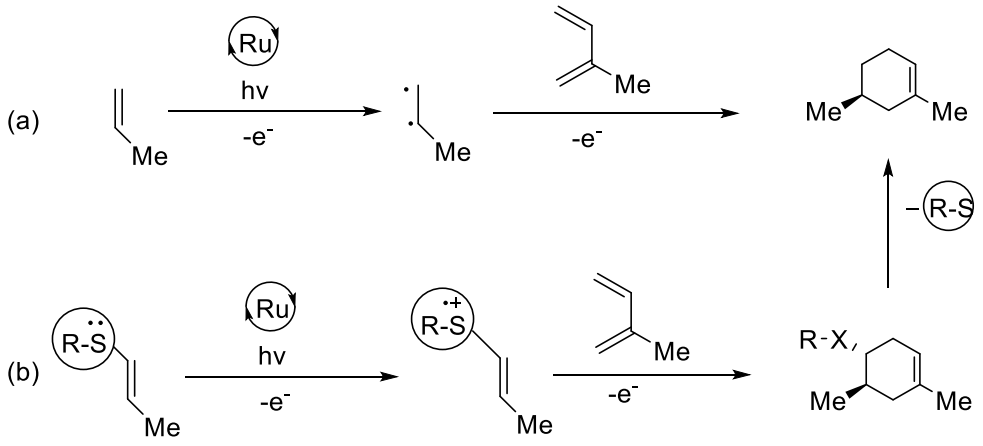

Scheme 1.6. (a) Simple alkene: resistant to one electron oxidation, poor substrates (b) Redox auxiliary strategy for radical cation reactions.

Redox auxiliary chemistry is limited in general applicability, as well as in scope because the product of a propagation step must be a stronger oxidant than the oxidized starting material for a chain reaction to take place. Blackstock and coworkers[45] have developed a strategy to overcome this limitation. They used the term redox auxiliary catalysis to describe this novel method of carrying out redox auxiliary chemistry and stated that the active catalyst in this reaction is the oxidized species of the diaryl amino auxiliary group attached at the reactive function. Upon a one electron oxidation of this redox auxiliary to the radical cation, an electronic perturbation is transferred to the reactive function from the redox auxiliary which reduces the activation barrier of the chemical process, thereby enhancing the rate of the reaction. This novel redox auxiliary catalysis has been applied in the design of photochromic devices and molecular switches.[45] Scheme 1.7 shows the postulated mechanism of a redox appended azobenzene, which is capable of undergoing a reversible conformation change between the *trans* and *cis* forms upon absorbing light, and the redox auxiliary mediated isomerization from the *cis* to the *trans*.[51]

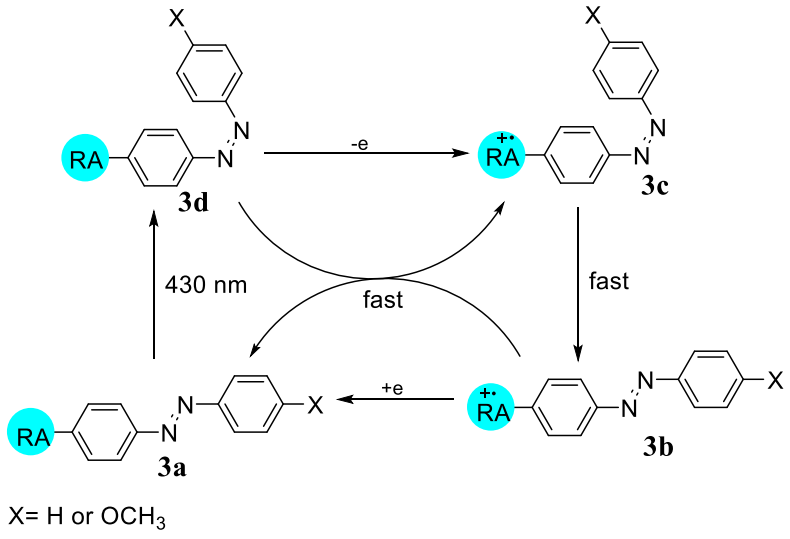

Scheme 1.7. The postulated mechanism of the photo-electro catalysis of azobenene.[51]

In another project, the Blackstock's group appended a diaryl amine redox active group on the skeleton of norbornadiene to enhance its electrochemical conversion to quadricyclane upon changing the oxidation state of the redox auxiliary.[52] This yielded a material that is isomerized in one direction photochemically (**4a** to **4b**), and in another direction (**4b** to **4a**) by a one electron oxidation of the redox auxiliary group (Scheme 1.8).

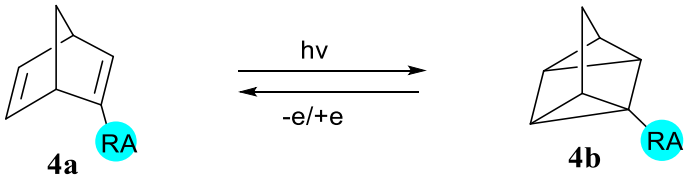

Scheme 1.8. The **4a-4b** system and the postulated RA-substituted photoelectrochromic system.[52]

1.5 Our Research Goals

Our goal is to develop a new general method for ET-catalysis of organic thermal reactions. This can be achieved by attaching a diaryl amino redox auxiliary group **5** to the skeleton of the substrates to reduce the activation barriers of these highly thermal organic reactions. The oxidation of the attached RA by a one electron oxidant CRET **6**, is expected to trigger an increase in the rate of these transformations.

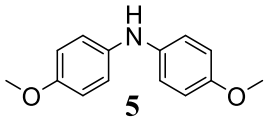

5

Figure 1.5. Diarylamino redox auxiliary **(RA)**.

In the first project, we attached the diaryl amino redox auxiliary to the skeleton of stilbenes to enhance the rate of the *cis* to *trans* isomerization upon oxidation of the RA. Stilbenes can be switched reversibly between two states and this conformational change from *cis* to *trans*

allows for the incorporation of the molecule in molecular machines, light controlled storage devices, molecular switches and biological systems.[53-54] The thermal *cis* to *trans* isomerization of stilbenes requires a large activation barrier of about 46 kcal/mol[54-56] (corresponding to a half-life of $\sim 10^{12}$ years at 303 K) unlike azobenzene that has a barrier of about 25 kcal/mol,[57-58] and is negligible at room temperature due to this large barrier. The *trans*-stilbene is more thermally stable and only a small energy difference of about 5 kcal/mol[59] between the two isomers. As a result of these characteristics, isomerization from *cis* to *trans* stilbene requires very high temperatures (> 210 ºC)[60] and long reaction times. Iodine[61] and diaryl disulfide[62] catalyzed *cis* to *trans* isomerization of are the most frequently used methods for obtaining pure *trans*-isomer. Unfortunately, these methods also do not go to completion, require very high temperatures, as well as purification by column chromatography.

Our goal is to reduce the activation barrier of the *cis* to *trans* stilbene isomerization by oxidizing an appended diaryl amino RA with a one electron oxidant, as illustrated in the catalytic cycle (Scheme 1.9). This method of *cis* to *trans* isomerization of stilbene will convert the neutral *cis*-stilbene to the cation radical. The cation radical is envisioned to undergo a chain process in which it will isomerize to the more stable *trans*-stilbene radical cation. The electron hole transfer between the *trans*-stilbene radical cation and the neutral *cis*-stilbene completes catalytic cycle. This one electron oxidation of the RA is expected to be catalytic, occur at lower temperatures and produce pure *trans*-stilbenes.

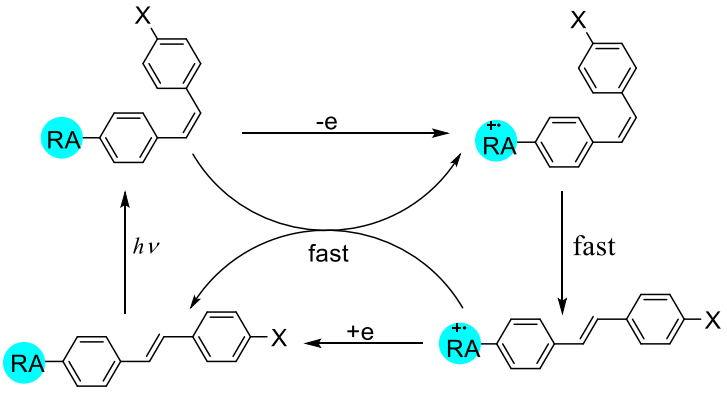

Scheme 1.9. The catalytic cycle of the *cis-trans* isomerization of stilbene.

In the second project, we appended the RA on the skeleton of 1,5-hexadienes to enhance the rate of the [3,3]-sigmatropic rearrangement. Previous studies have established that the energy barrier for the Cope rearrangement of 1,5-hexadienes is 33.5 kcal/mol[63-66] for the chair pathway and requires a temperature above 200 ºC. We postulated that the aryl amino redox group (Figure 1.5) appended on the skeleton of the 1,5-hexadiene could lower the barrier of the [3,3]-sigmatropic rearrangement upon oxidation of this redox group by changing the oxidation state from the neutral to the cationic form. The cationic state is envisioned to reduce the bond strength of the migrating C-C bond, thereby reducing the barrier for the rearrangement of redox appended 1,5-hexadiene to give the Cope product or, alternatively, the aza-Claisen product if the redox auxiliary takes part in the reaction.

We reasoned that a one-electron oxidant such as CRET **6** will generate a redox appended 1,5-hexadiene radical cation from the redox appended hexadiene. This is postulated to undergo a fast [3,3]-Cope rearrangement or possibly a [3,3]-aza-Claisen rearrangement (Scheme 1.10). The

expectation is that the oxidation of the amine will turn on the Cope or aza-Claisen reactivity of the redox appended 1,5-hexadiene at room temperature or maybe even at lower temperatures.

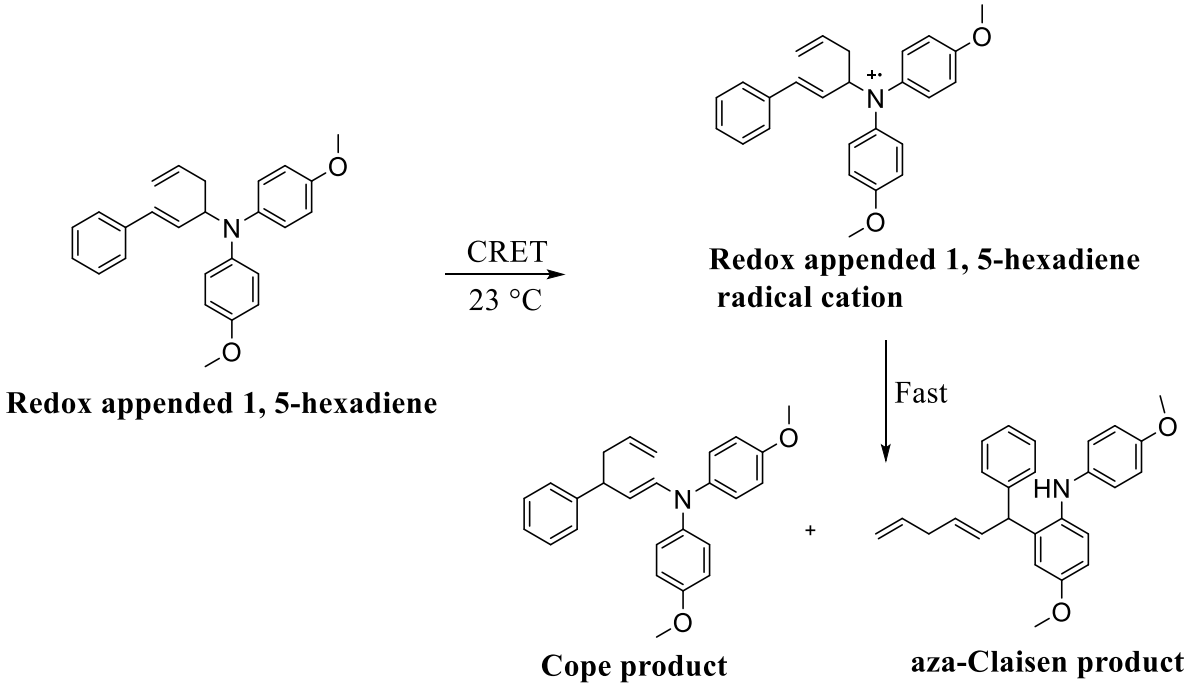

Scheme 1.10. Schematic of the redox-auxiliary promoted [3,3]-sigmatropic rearrangement of 1, 5-hexadienes.

CHAPTER TWO

REDOX AUXILIARY ISOMERIZATION OF STILBENES

2.1 Photochromism and Photoswitches

Stilbene is a photochromic molecule and one of the most studied aromatic compounds from both theoretical and experimental viewpoints.[67-68] Stilbenes are attractive molecular switches because of their easy synthesis, chemical and thermal stability, and tunable switching rates. Photochromism is the light-induced reversible transformation of chemical species between two isomers having different absorption spectra.[69] These chemical changes can be reversed thermally or by irradiation with light of a different wavelength. The various types of photochromic molecules and their corresponding isomers are shown in Scheme 2.1

Chemists have developed different types of synthetic photoswitches that can undergo a reversible change in structure upon irradiation with light (Scheme 2.1).[70] These photoswitches are usually characterized by the absorption of their isomeric forms, as well as by the photostationary state (PSS). The PSS is a steady state reached by a reacting chemical system when the light has been absorbed by at least one of the components. The versatility of these photoswitchable molecules provides tremendous potential for utilization in several fields, ranging from chemistry, physics, and materials science to biology and medicine.[67]

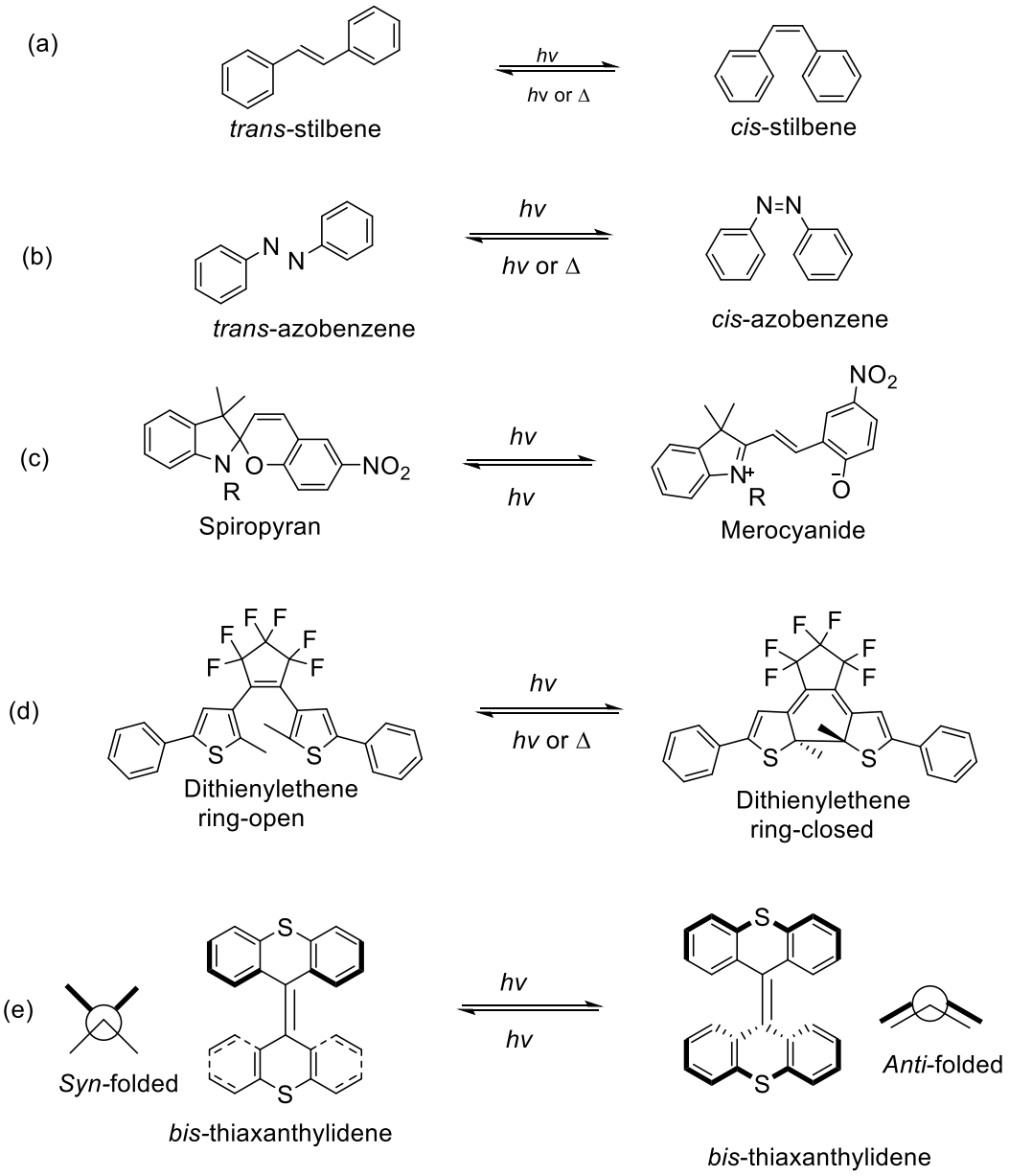

Scheme 2.1. Examples of photochromic switches.[70]

The electronic and energy levels of *trans*- and *cis*-stilbene and stilbenoid compounds have been modeled using several methods.[71-77] The ground state of *cis*-stilbene is propeller shaped with out of plane twisting of the phenyl rings by 30-50º, whereas the *trans*-stilbene shows only a small deviation from planarity.[56, 78] *Cis*-stilbene has a larger dihedral angle than the *trans*-

stilbene and as a result, *cis-stilbene* has a higher ground state energy. A small energy difference ΔH of about 5 kcal/mol exists between the two isomers of stilbene (Figure 2.1).[79-81] Unlike the *cis*-azobenzene, which has about 25.8 kcal/mol[82-84] thermal isomerization barrier, the activation barrier of the thermal back reaction of *cis*-stilbene is about 46 kcal/mol.[56, 85-87] This makes the *cis*-stilbene thermally stable and not easily isomerized to the *trans*- isomer by heating. Experimental results show that a reasonable rate of isomerization from *cis* to *trans* can only be obtained at temperatures above 210 ºC.[88-89] However, modifications of the parent stilbene could influence the activation barrier and promote the *cis* to *trans* isomerization.

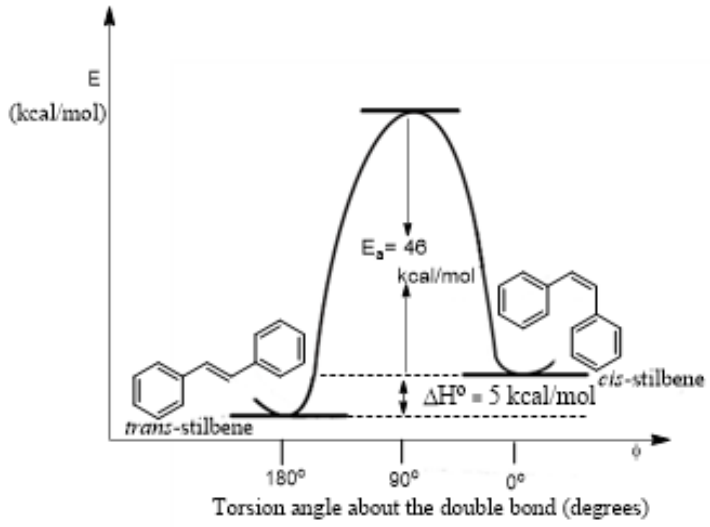

Figure 2.1. Energy profile of the thermal equilibrium of *trans* and *cis*-stilbene. E = energy (kcal/mol), ϕ = torsion angle about the double bond (degrees), ΔH^o = free reaction enthalpy (kcal/mol).

Stilbene exhibits reversible *trans-cis* isomerization upon irradiation. The light induced isomerization of stilbene and its simple derivatives has been studied for more than half a century[90] and leads to a photostationary state (PSS). The percentages of *trans* and *cis* isomers at the PSS, $(\%\ trans)_{pss}$ and $(\%\ cis)_{pss}$ are directly related to $\Phi_{tran\text{-}cis}$ and $\Phi_{cis\text{-}trans}$ and the molar absorptivity ε_{cis}, and ε_{trans}, at the irradiation wavelength (Equation 2.1).[91]

$$\left(\frac{[trans]}{[cis]}\right)_{PSS} = \frac{\varepsilon_{cis}\ \Phi_{cis\text{-}trans}}{\varepsilon_{trans}\ \Phi_{trans\text{-}cis}} \qquad 2.1$$

Lewis and his coworkers[92] and Yamashita.[93] studied the photochemistry of stilbene using mercury lamp in isooctane and hexane respectively. Lewis et al. observed the quantum yield (Φ) of 0.35 and 0.32 for *trans* ⟶ *cis* and *cis* ⟶ *trans* respectively when they irradiated a 2.5 x 10^{-5} M solution of the parent stilbene with 254 μm mercury line. The photochemical isomerization of *cis* and *trans*-stilbene in n-hexane was studied kinetically in the temperature range of 10 −30 ℃ using the mercury lines of 313 and 334 μm by Yamashita.[93] He observed the quantum yields of 0.04 and 0.27 for the *cis* ⟶ *trans* and *trans* ⟶ *cis* isomerization respectively. PSS of 92 % *cis*,[94] 93% *cis*[95], 90%,[96] and 69% *cis*[97] have been reported when the photoisomerization was carried out in pentane, hexane, benzene and cyclohexane respectively.

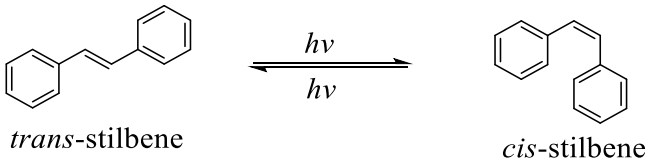

Scheme 2.2. Isomerization of stilbene.

The triplet sensitized isomerization of *cis* or *trans* stilbene leads to a photostationary state (PSS) and depends on the energy of the triplet sensitizer. This PSS composition was about 60 % *cis* and 40 % *trans* for high energy triplet sensitizers.[98] Photolysis of stilbene can be achieved by an excited molecule having a triplet energy of above 60 kcal/mol and both isomers compete for sensitization. This leads to a decrease in quantum yields. Photoisomerization occurs via interconversion to the triplet state or through a common intermediate called the phantom triplets p* which relaxes to the ground state isomers (Scheme 2.3)[98]

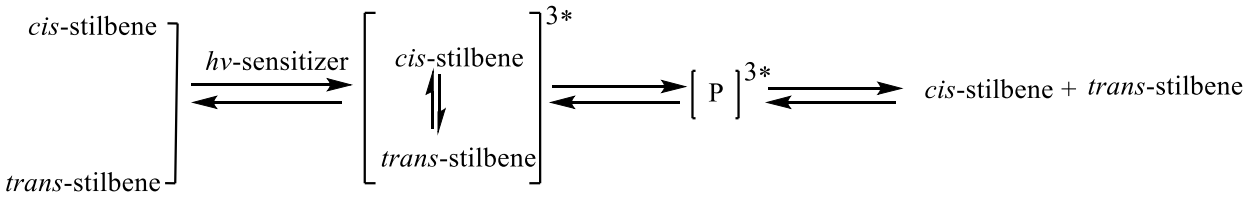

Scheme 2.3. Mechanism of photoisomerization of stilbene.[98]

The one-dimensional potential energy scheme for the isomerization of stilbene was proposed by Saltiel [99] (Figure 2.2). The reaction coordinate corresponds to a large amplitude motion of the phenyl rings and requires a large amount of ethylenic twisting. A large barrier exists between the *trans* and *cis* isomers in the ground electronic state. The *trans* stilbene has a potential minimum in the first excited state and a barrier exists for the twisting motion of the ethylene bond. This barrier to torsional motion is absent in *cis*-stilbene (Figure 2.2) is obtained from a mixing of the first excited (due to $\pi \rightarrow \pi^*$ transition) of stilbenes with one or more higher lying, doubly excited configurations that have a minimum at the 90° twisted form (phantom state). The decay to the ground state *cis*-or *trans*-stilbene is fast once the molecule reaches the twisted form (90°).[90]

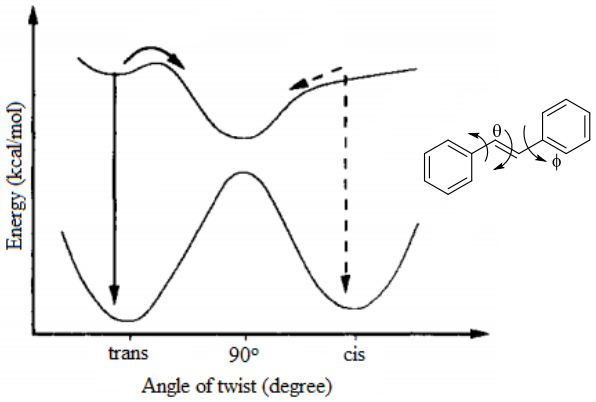

Figure 2.2. A schematic representation of the *trans*-and *cis*-isomerization of stilbene.[90]

F.F. Crim[100] converted the *trans*-stilbene to the *cis*-isomer using tunable ultraviolet probe pulses. The probe pulses come from nonlinear frequency conversion of light from an amplified Ti: sapphire laser. Figure 2.3 shows the electronic absorption spectra of *cis*- and *trans*-stilbene as dashed and solid lines respectively, and the vertical arrows mark the probe wavelengths used by Crim and coworkers. There is a weak vibrational progression in the *trans*-stilbene spectrum that is absent in the *cis*-stilbene spectrum, and the maximum of the long wavelength transition lies at a slightly lower energy in the *trans*-isomer. This is because the steric crowding of the ortho hydrogen causes the phenyl groups to twist slightly out of coplanarity.[101] The twisting out of coplanarity leads to a decreased conjuagtion, as a result, the *cis*-stilbene has a lower molar absorptibity than the *trans*. It is easy to choose an appropriate irradiation wavelength to arrive at a photostationary state which is either *cis*- or *trans*-rich but the pure isomers of stilbenes can only be obtained by subsequent separation techniques.

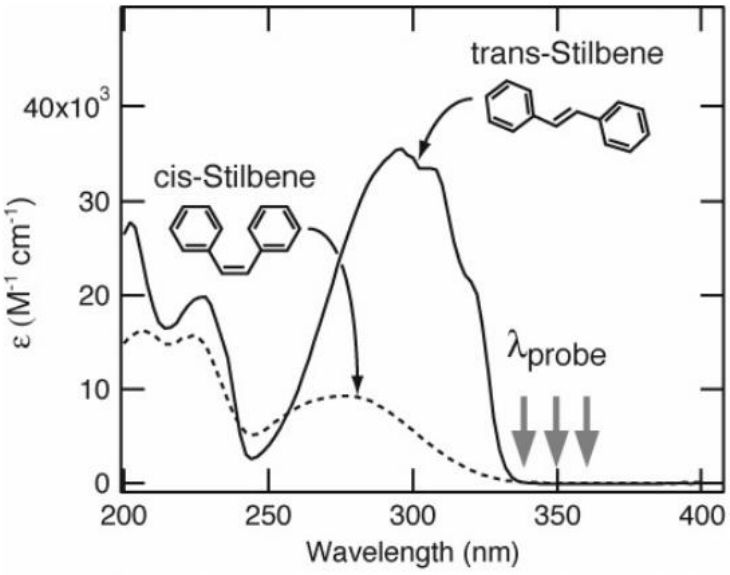

Figure 2.3. The electronic absorption spectra of *cis*- and *trans*-stilbene. The dashed and solid lines represents the *cis*- and *trans*-stilbene respectively.[100-101]

Chemical bond rearrangement during the phototransformation results in electronic and structural changes of the molecules, such as changes in absorption spectra, fluorescence spectra and electrical conductivity. These changes can be utilized in the design of optical memory media, photoswitching devices, and light-driven actuators. For such applications, photochromic molecules should fulfill the following requirements: (1) facile synthesis, (2) thermal stability of both isomers, (3) fatigue resistant property, (4) high sensitivity, (5) rapid response, and (6) reactivity in the solid state.[102]

Stilbenes are known to undergo some competing reactions once excited.[103-105] One of the side reactions is the photocyclization of *cis*-stilbenes to yield 4a,4b-dihydrophenanthrene intermediate, which is rapidly converted to phenanthrene in the presence of an oxidant (Scheme 2.4).[103, 106-107] The dihydrophenanthrene is thermally unstable and will relax back to the *cis*-stilbene in the absence of an oxidant. The oxidation of 4a,4b-dihydrophenanthrene is irreversible and this must be avoided for stilbenes-derived molecular switches.

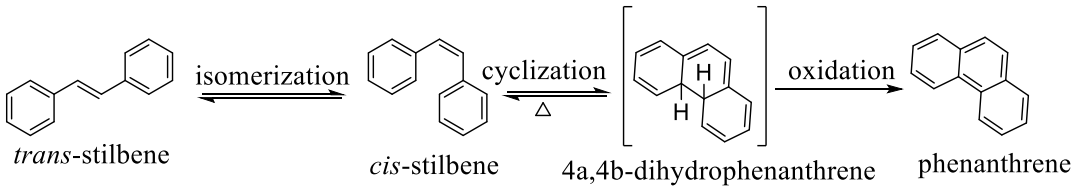

Scheme 2.4. Isomerization and oxidative cyclization of stilbene.[103, 106]

2.2 Research Goals

Stilbenes can be switched reversibly between *cis* and *trans* states and this inducible conformational change allows for the incorporation of the molecule in molecular machines, light controlled storage devices, molecular switches, and biological systems. Unfortunately, the *cis* to *trans* isomerization of stilbenes is very slow, requiring high temperatures and exhibiting low

quantum yields if performed photochemically. We hypothesize that the incorporation of a diaryl amino redox auxiliary (RA) to the skeleton of stilbenes (**St-NAr$_2$**) will enhance the rate of the *cis* to *trans* isomerization upon oxidation of the amine RA (Scheme 2.5). This method of *cis* to *trans* isomerization of stilbene involves one-electron oxidation of the ***cis*-St-NAr$_2$** to ***cis*-St-NAr$_2^{\bullet+}$** which is proposed to undergo a facile isomerization to the ***trans*-St-NAr$_2^{\bullet+}$** and upon reduction yield the ***trans*-St-NAr$_2$**. It is expected that this cycle will be catalytic upon ***trans*-St-NAr$_2^{\bullet+}$** electron transfer thus propagating a chain reaction with the ***cis*-St-NAr$_2$**.

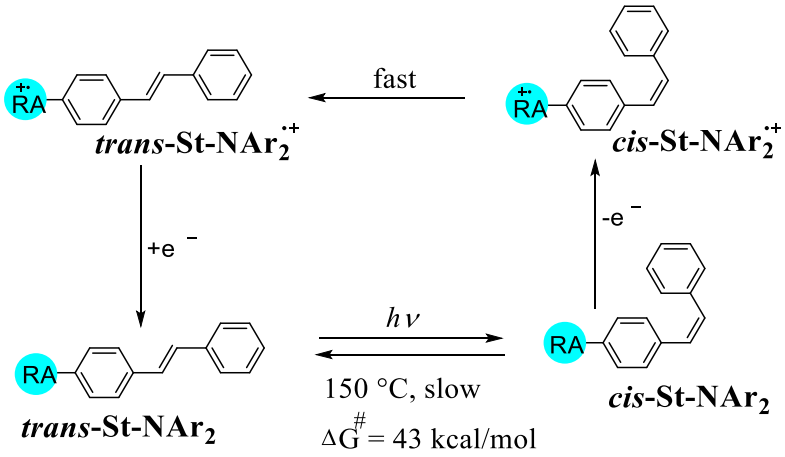

Scheme 2.5. Proposed redox auxiliary promoted *cis-trans* isomerization of stilbene.

The substituent effect on the *cis-trans* isomerization of stilbenes is a relevant factor to be considered in the design of stilbene-derived molecular switches. Substitution on the phenyl or vinylene group could significantly perturb the C=C torsional barrier and/or induce spin-orbit coupling that enhances the intersystem crossing process.[108] We investigated the variation in the rates and the energetics of the thermal isomerization of *para*-substituted stilbenes ***cis*-7a-e** by heating a solution of the stilbene derivatives ***cis*-7a-e** in DMSO. The strong electron donating and electron withdrawing substituents in conjugation with the olefinic bond are expected to accelerate the thermal isomerization of the *cis*-RA stilbenes by resonance stabilization of the

biradical transition state. This rate acceleration occurs because these substituents tend to elongate the olefinic bond and decrease its bond order, thereby reducing the rate-determining barrier of the pi-bond rotation.

2.3 Synthesis of Redox Appended Stilbenes *cis*-7a-e and *trans*-7a-e

Stilbenes derivatives can be prepared by Wittig reaction[109] of an aryl aldehyde with (4-bromobenzyl) triphenylphosphonium salt to give a mixture of the *cis* and *trans* isomers and triphenylphosphine oxide (Scheme 2.6). The Wittig reaction is a versatile method for the preparation of substituted stilbenes because the reaction is not sensitive to atmospheric oxygen unlike the McMurry reaction,[110] thus allowing for simpler experimental procedures. The *trans*-isomer is less soluble in the reaction solvent (usually methanol if sodium/sodium methoxide is used as a base) and precipitates on standing. This makes it easy to separate the *trans* and *cis* isomers. The *trans* isomer can also be recrystallized from hexane as well as purified by column chromatography.

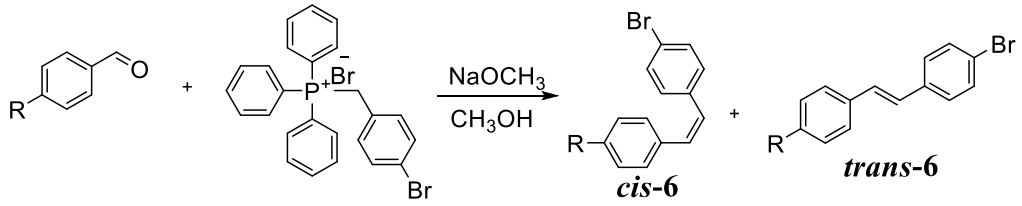

	Yields (%)	
R	*cis*	*trans*
a=OCH_3	47	43
b=H	43	49
c=Cl	50	41
d=CF_3	43	47
e=CH_3	49	43

Scheme 2.6. Synthesis of *para*-substituted bromostilbenes.

The intermediates **6a-e** in the synthesis of redox auxiliary appended stilbenes ***7*a-e** are well-known compounds.[111-112] The key reaction for the An_2N-stilbene (***7*a-e**) construction is the

Buchwald/Hartwig coupling of bromostilbenes **6** and dianisyl amine **5** to give **7a-e** in good yields (Scheme 2.7). The resulting *cis* or *trans* aminostilbenes were purified by column chromatography on silica gel to afford the desired RA-stilbene substrates.

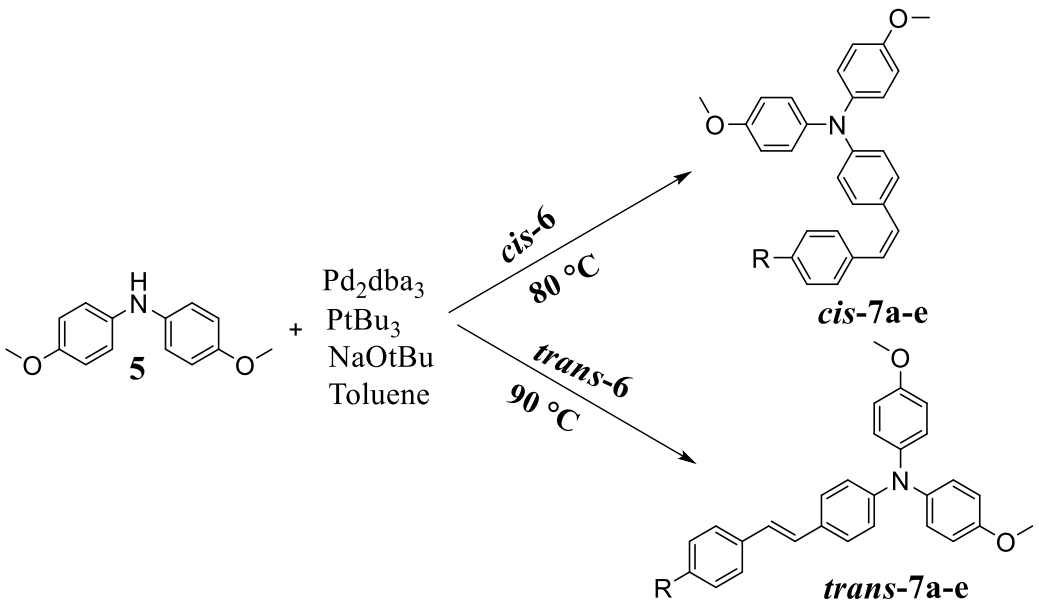

	Yields (%)	
R	*cis*	*trans*
a=OCH_3	84	92
b=H	93	95
c=Cl	86	90
d=CF_3	89	91
e=CH_3	90	93

Scheme 2.7. Synthesis of RA stilbenes.

2.4 Thermal Isomerization of Redox Appended *cis*-Aminostilbenes.

2.4.1 *Cis* to t*rans* isomerization of *cis*-dianisylmethoxyaminostilbene (*cis*-Ome-St-NAR_2) *cis*-7a

The work presented in this thesis involved the investigation of the kinetics of the thermal isomerization of *cis* stilbenes, in addition to obtaining the activation parameters from the temperature dependence of the thermal *cis* decay. The investigation of the thermal *cis*-to-*trans* isomerization was conducted experimentally by using NMR spectroscopy.

In order to determine the extent of rate acceleration for the conversion of ***cis*-Ome-St-NAR2** to ***trans*-Ome-St-NAR2** by RA catalysis, it was necessary to measure the rate of thermal conversion of ***cis*-Ome-St-NAR2** as a basis for comparison. The evaluation of the thermal rates (Scheme 2.8) requires information about the isomeric composition at different temperatures. This was performed by dissolving ***cis*-Ome-St-NAR2** in DMSO-D_6 in NMR tube and heating the sample at different temperatures. The ^{1}H NMR spectra were taken at various time intervals and the changes in the integrations of the peaks corresponding to the two isomers were recorded. Since most signals in the ^{1}H NMR spectra of the *trans* and *cis* isomers (Scheme 2.8) are well separated, changes in the *trans* and *cis* ratio were easily determined. The measurement of these signals belonging to the same proton in both the *cis* and *trans* isomers allows the concentration of the *cis* and *trans* isomers to be calculated. An accurate determination of this value is very useful in the study of the kinetics of the isomerization.

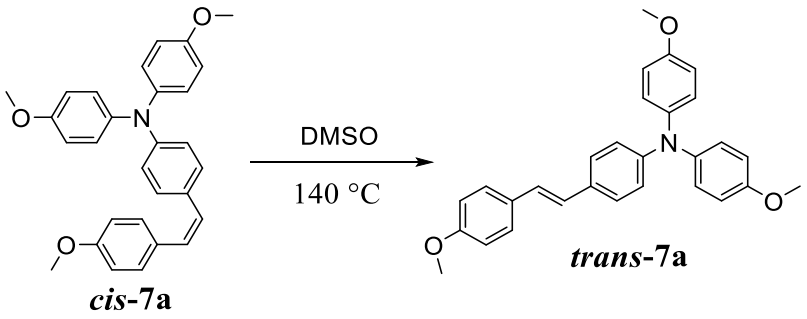

Scheme 2.8. Thermal isomerization ***cis*-7a** at 140 ºC.

The ^{1}H NMR spectrum of the olefinic and aromatic protons of the *cis* and *trans* stilbene indicates that the two rings in the *trans* isomer are coplanar with the double bond and hence deshielded. In the *cis* isomer, the aromatic rings are tilted (Figure 2.4) and the olefinic protons are shielded. As a result, the olefinic protons in ***trans*-7a** appear at a higher chemical shift than those of ***cis*-7a**. The ^{1}H NMR spectra of ***cis*-7a** and ***trans*-7a** show five distinct protons in the

olefinic and aromatic regions labeled a-e for the *cis* form and a´- e´ for the *trans* form, as illustrated in Figure 2.5.

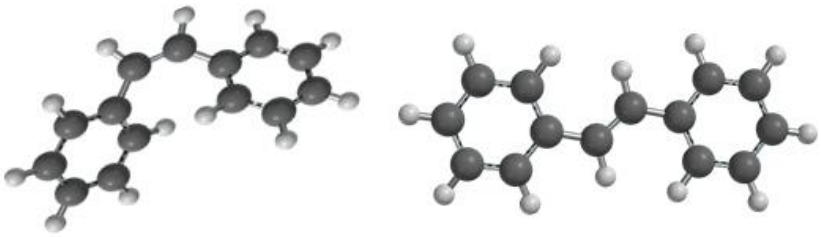

cis-stilbene *trans*-stilbene

Figure 2.4. The model structures of the *cis* and *trans*-stilbene. Modeled by using B3LYP-631G*.

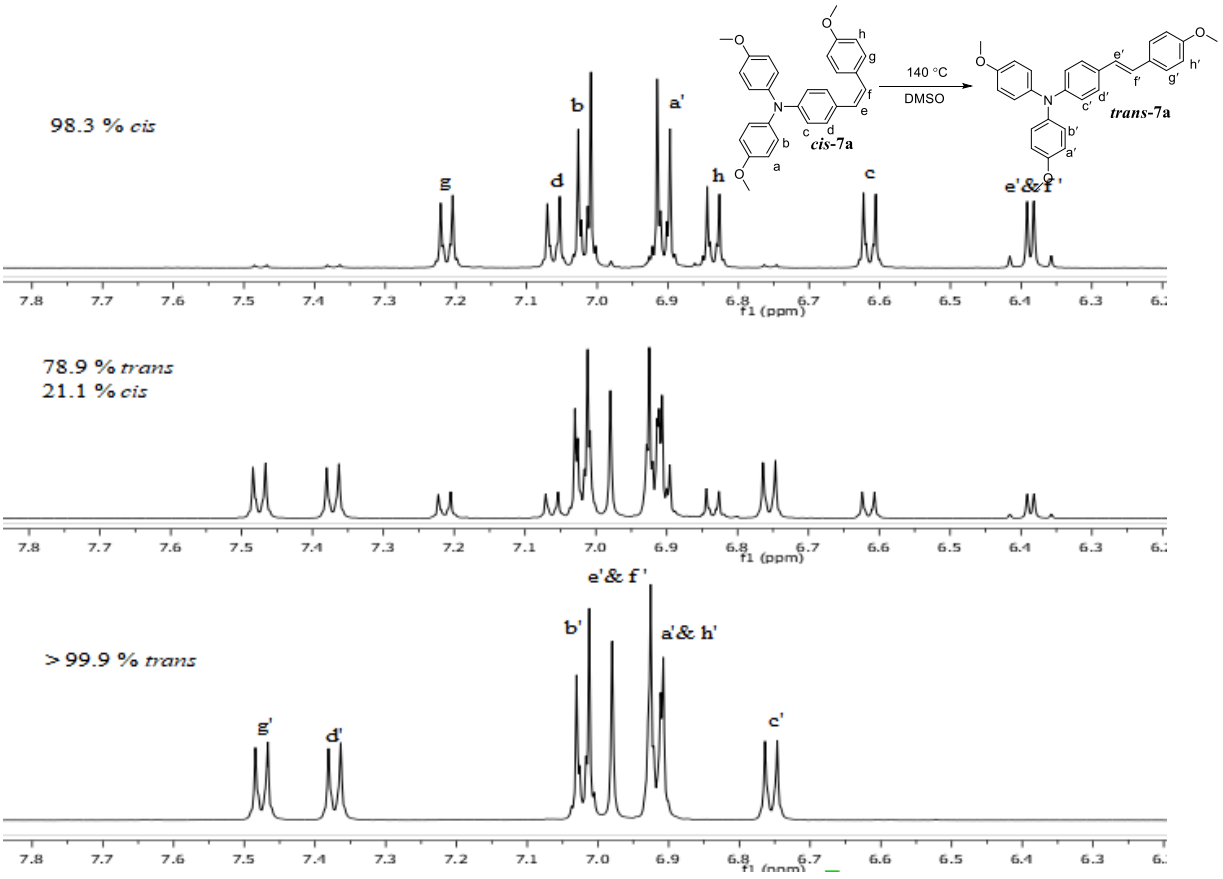

Figure 2.5. ^{1}H NMR of ***cis*-7a** undergoing a thermal isomerization to ***trans*-7a** in DMSO at 150 ^{o}C

2.4.2 Kinetic Analysis

The rate constant of a chemical reaction always depends on the temperature of the reaction and is described by the Arrhenius equation:

$$\frac{d\ln K}{dT} = \frac{E_a}{RT} \qquad 2.2$$

where E_a is the activation energy and the equation can be integrated to give

$$\ln k = \ln A - \frac{E_a}{RT} \qquad 2.3$$

This equation can also be written as

$$k = Ae^{-\frac{E_a}{RT}} \qquad 2.4$$

The constant A is called the pre-exponential factor and defines the rate due to the frequency of collisions in the correct orientation, R is the gas constant, T is the absolute temperature and k is the rate constant. A plot of ln k vs 1/T gives a straight line which has $-E_a/R$ as the slope and ln A as the y-intercept. The minimum amount of energy which the reactants must acquire before they transform into products, E_a, can be calculated from the slope of the graph.

Eyring developed an alternative to Arrhenius equation known as the Eyring equation. His equation describes the variance of the rate of a chemical reaction with temperature. He viewed the activated complex as a distinct chemical species that exists at the transition state and the potential energy is highest along the reaction pathway. In this model, the activated complex is considered to be in equilibrium with the reactants. The rate of the reaction is equal to the number of activated complexes decomposing to form products, which is given by concentration of the high-energy complex multiplied by the frequency of surmounting the barrier. An Eyring plot

allows the activation parameters $\Delta S^{\ddagger}$ and $\Delta H^{\ddagger}$ to be obtained from the temperature dependence of the rate constant according to the equation below:

$$\ln(\frac{k}{T}) = -\frac{\Delta H^{\ddagger}}{RT} + \ln(\frac{K_B}{h}) + \frac{\Delta S^{\ddagger}}{R} \qquad 2.5$$

where k is the rate constant, h is the Planck's constant, T is the absolute temperature, K_B is the Boltzmann's constant and R is the gas constant. A plot of ln(k/T) versus 1/T gives a straight line with a slope of $-\Delta H^{\ddagger}/R$ and the intercept as $\ln(\frac{K_B}{h}) + \frac{\Delta S^{\ddagger}}{R}$. The enthalpy of activation ΔH is derived from the slope of the plot, and the entropy of activation ΔS is derived from the intercept. The free energy of activation ΔG^{*} is given by

$$\Delta G^{\ddagger} = \Delta H^{\ddagger} - T\Delta S^{\ddagger} \qquad 2.6$$

The Eyring equation from the transition state theory can also be stated as

$$k = \frac{K_B T}{h} e^{-\frac{\Delta G^{\ddagger}}{RT}} \qquad 2.7$$

$$(\frac{K_B}{h}) = 2.08 \times 10^{10}\ K^{-1}s^{-1} \text{ and } \ln(\frac{K_B}{h}) = 23.8$$

$\Delta H^{\ddagger}$ can also be obtained from E_a and vice versa.

$$\Delta H^{\ddagger} = E_a - RT \quad (\text{where T is the median temperature}) \qquad 2.8$$

The Van 't Hoff equation (eqn 2.9) can also be used to determine the enthalpy of the reaction.

$$\ln(\frac{k_2}{k_1}) = -\frac{\Delta H^{\ddagger}}{R}\ (\frac{1}{T_2} - \frac{1}{T_1}) \qquad 2.9$$

Where k_1 is the rate constant at absolute temperature T_1, and k_2 is the rate constant at absolute temperature T_2.

To perform the kinetic study of the thermal *cis* to *trans* isomerization of ***cis*-7a**, the compound was dissolved in deareated DMSO (0.0731M) and placed in an NMR tube. The NMR

tube was sealed with parafilm, immersed in a constant temperature oil bath, and the spectrum was recorded at 140 ºC and time intervals of 30, 90, 150, 220, 308, 495, 750, 1050 and 1300 minutes as shown in Table 2.1. For each spectrum, the methoxy signals were integrated to evaluate the % *cis*/% *trans* of the sample, giving the corresponding concentration of ***cis*-7a** was a function of time (Table 2.1). The data obtained from the experiment fit the first order kinetic equation

$$\ln [a]_t = -k_1 t + \ln [a]_o \qquad 2.10$$

where a is the concentration of the ***cis*-7a** at time t and k is the rate constant for the first order process. A plot of ln [***cis*-7a**] against time (Figure 2.6) gave a straight line where the slope of the plot is -k and the corresponding thermal half-lives were obtained by using the kinetic equation below where $t_{1/2}$ is the half-life.

$$t_{1/2} = \frac{ln\, 2}{k} \qquad 2.11$$

Time (minutes)	**% *cis***	**[*cis*]**	**ln[*cis*]**
0	95.6	0.0699	-2.66
30	90.3	0.0660	-2.72
90	85.6	0.0626	-2.77
150	77.5	0.0567	-2.87
220	70.4	0.0515	-2.97
308	62.4	0.0456	-3.09
495	51.2	0.0374	-3.29
750	39.7	0.0290	-3.54
1050	29.1	0.0213	-3.85
1300	16.2	0.0118	-4.44

.

Table 2.1. Thermal isomerization of 0.0731 M ***cis*-7a** to ***trans*-7a** in deaerated DMSO at 140 °C.

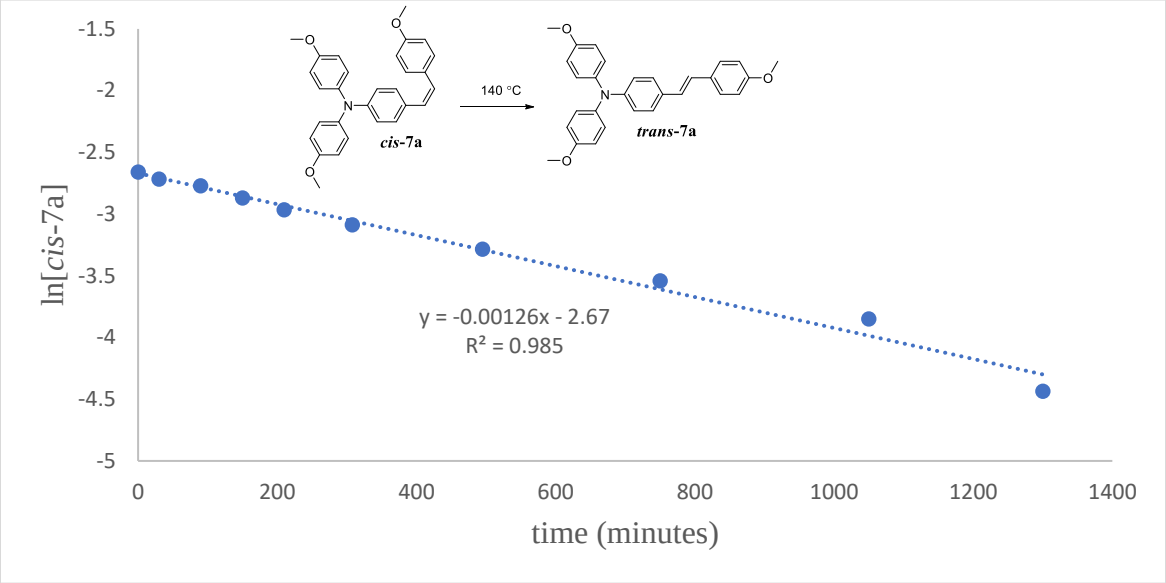

Figure 2.6. First order plot of ln [***cis*-7a**] vs time t at 140 °C.

k_{413K} = 2.10 ± 0.09 x 10^{-5} s^{-1}

$\Delta G^{\ddagger}_{413k}$ = 33.3 ± 0.1 kcal/mol

To evaluate the enthalpy and entropy activation parameters for this isomerization, the rate of the process was measured at several addition temperatures (120 ºC, 130 ºC, and 150 ºC). Results of the experiments are given in Table 2.2 to yield $\Delta H^{\ddagger}$= 21.3 kcal/mol and $\Delta S^{\ddagger}$= -29.8 eu for the thermal *cis*-to *trans* isomerization ***cis*-7a**. The Eyring plot of the graph of ln (k/T) vs I/T gave a straight line (Figure 2.7). The slope and intercept were used to calculate the $\Delta H^{\ddagger}$ and $\Delta S^{\ddagger}$ respectively (Table 2.3). The $\Delta G^{\ddagger}_{413K}$ for the thermal isomerization of ***cis*-7a** to ***trans*-7a** was determined to be ~33.2 kcal/mol at 413 K, which is substantially lower than 42.3 kcal/mol[60] at 496 K for the neutral parent stilbene. The high negative entropy of activation (-31.4 eu) means that the disorder in the molecule has decreased, which is due to the loss of rotational degrees of freedom in the formation of the highly ordered TS. This implies that the transition state has much more charge separation than the *cis* ground state.[113-117] $\Delta S^{\ddagger}$ can become more negative than

expected if a significant amount of order is required in the solvent to make favorably enthalpy interactions.[118]

T (K)	k (s^{-1})	ln (k/T)	1/T
423	4.92×10^{-5}	-16.0	0.00236
413	2.10×10^{-5}	-16.8	0.00242
403	8.88×10^{-6}	-17.6	0.00248
393	6.92×10^{-6}	-17.9	0.00255

Table 2.2. The first order rate constants for the thermal isomerization of ***cis*-7a** to ***trans*-7a** in DMSO.

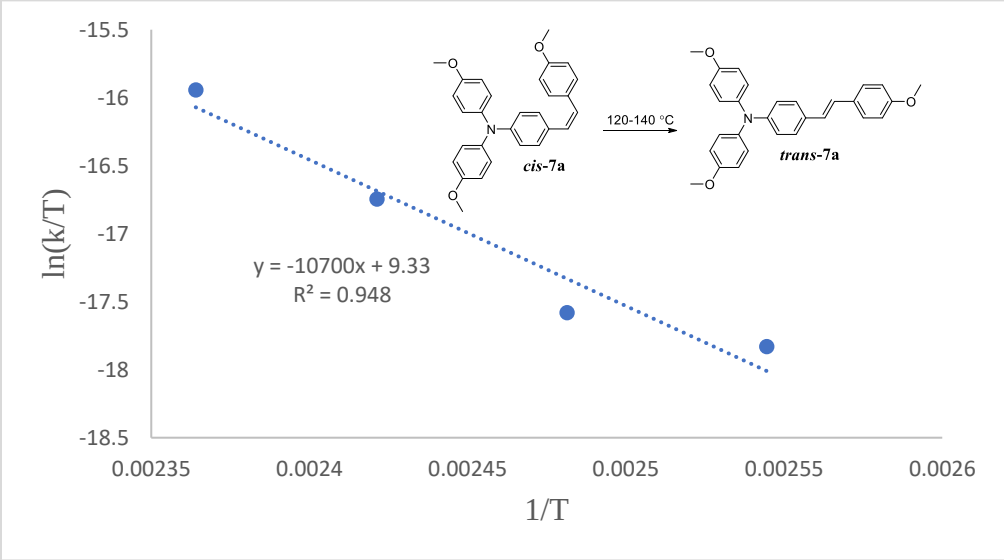

Figure 2.7. The eyring plot of the thermal isomerization of ***cis*-7a** in DMSO.

Activation parameters	Experimental Values
$\Delta H^{\ddagger}$	21.3 ± 0.8 kcal/mol
$\Delta S^{\ddagger}$	-29.8 ± 2 cal mol^{-1} K^{-1}
$\Delta G^{\ddagger}_{413K}$	33.2 ± 1.6 kcal/mol

Table 2.3. Activation parameters of the thermal isomerization of ***cis*-7a** in DMSO.

The rate of the thermal *cis*-trans isomerization of stilbenes is very slow due to a large barrier to rotation. This large barrier to rotation around the carbon-carbon double bond means that the two isomers cannot easily interconvert. Thermal energy is needed to allow the *cis* isomer to overcome this barrier, but the rate can be enhanced by modifying the structure of stilbenes using a redox active substituent. The effect of substitution on the *cis-trans* isomerization plays an important role in the development of stilbene-based molecular switches. This effect was examined in this work because a previous report[119] indicates that substitution increases or decreases the rate of *cis-trans* isomerization of stilbenes. It is expected that enhancing the degree of single bondedness of the double bond will decrease the activation barrier and hence, increase the rate of *cis-trans* isomerization. The examination of the rate of substituted ***cis*-7b-e** was studied at 140 ºC in DMSO and the results are shown in Table 2.4-2.8 and the first order plots of the concentration against time are shown in Figure 2.8-2.11.

2.4.3 Results of thermal isomerization of *cis*-aminostilbene (*cis*-St-NAR$_2$) *cis*-7b

Time (minutes)	% cis	[*cis*]	ln[*cis*]
0	0.972	0.0711	-2.64
110	0.883	0.0645	-2.75
250	0.823	0.0602	-2.80
480	0.753	0.0550	-2.87
710	0.694	0.0507	-3.02
925	0.497	0.0363	-3.50
1325	0.254	0.0186	-4.11
1876	0.108	0.00790	-4.80

Table 2.4. Thermal isomerization of 0.0731 M ***cis*-7b** to ***trans*-7b** in deaerated DMSO at 140 °C.

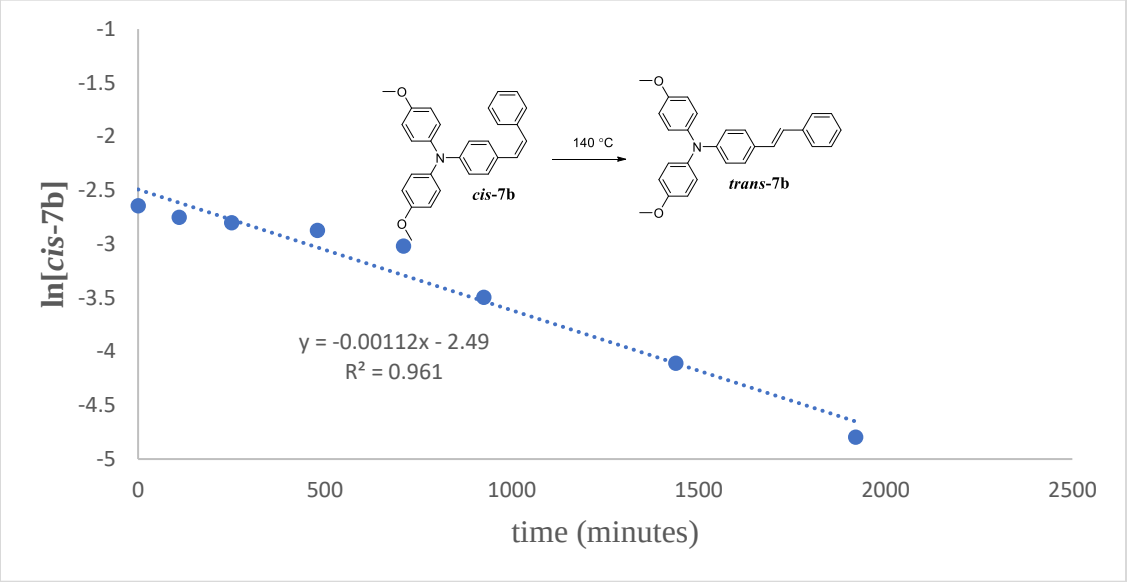

Figure 2.8. Graph of ln [***cis*-7b**] vs time at 140 ºC.

k_{413K} = 1.86 ± 0.10 x 10^{-5} s^{-1}

$\Delta G^{\ddagger}_{413K}$ = 33.4 kcal/mol

2.4.4 Results of the thermal isomerization of *cis*-dianisylchloroaminostilbene (*cis*-Cl-St-NAR$_2$) *cis*-7c

Time(minutes)	% cis	[*cis*]	ln[*cis*]
0	97.2	0.0711	-2.64
90	87.3	0.0638	-2.75
220	83.0	0.0607	-2.80
350	77.2	0.0564	-2.87
510	66.7	0.0343	-3.37
630	41.5	0.0303	-3.50
800	22.5	0.0164	-4.11
1340	9.05	0.00661	-5.02

Table 2.5. Thermal isomerization of 0.0731 M ***cis*-7c** to ***trans*-7c** in deaerated DMSO at 140 °C.

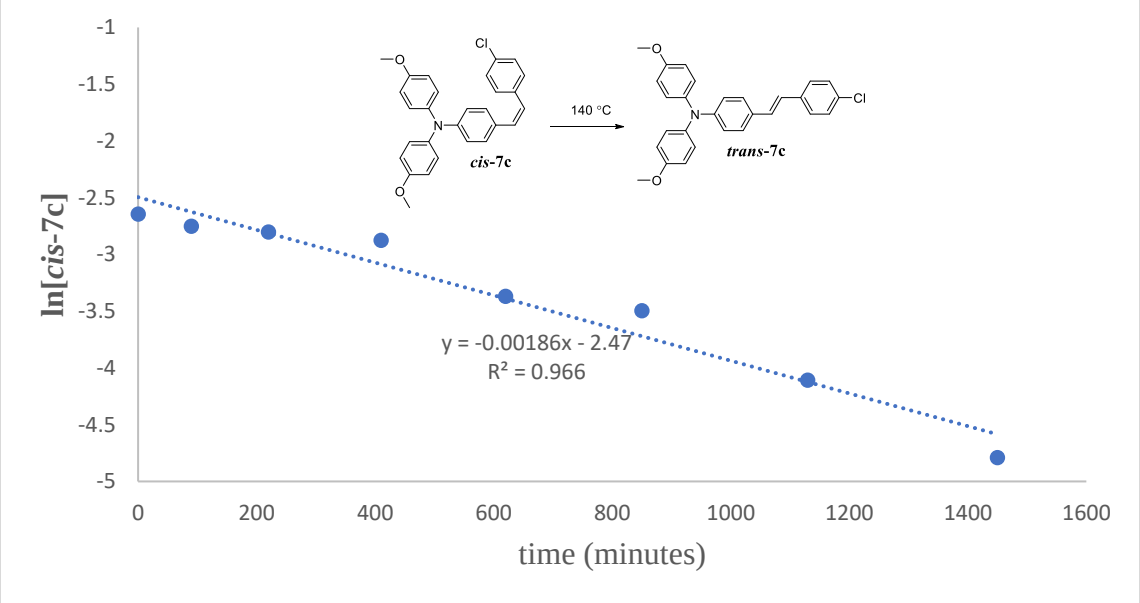

Figure 2.9. Graph of ln [***cis*-7c**] vs time at 140 ºC.

$k_{413K} = 3.10 \pm 0.2 \times 10^{-5}\ s^{-1}$

$\Delta G^{\ddagger}_{413K} = 33.0$ kcal/mol

2.4.5 Results of the thermal isomerization of *cis*-dianisyltrifluoromethylaminostilbene (*cis*-CF_3-St-NAR_2) *cis*-7d

Time (minutes)	% *cis*	[*cis*]	ln[*cis*]
0	0.926	0.0677	-2.69
75	0.845	0.0618	-2.78
200	0.632	0.0462	-3.07
350	0.456	0.0333	-3.40
640	0.381	0.0279	-3.58
900	0.265	0.0194	-3.94
1095	0.159	0.0116	-4.45
1840	0.0178	0.00130	-6.64

Table 2.6. Thermal isomerization of 0.0731 M ***cis*-7d** to ***trans*-7d** in deaerated DMSO at 140 °C.

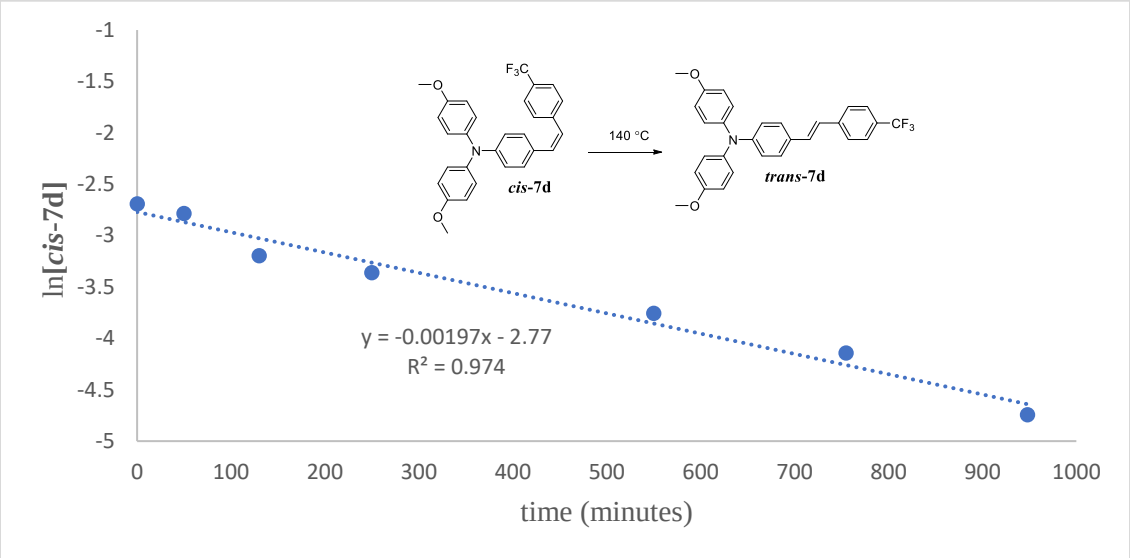

Figure 2.10. Graph of ln[***cis*-7d**] vs time at 140 ºC

k_{413K} = 3.28 ± 0.2 x 10^{-5} s^{-1}

$\Delta G^{\ddagger}_{413K}$ = 32.9 kcal/mol

2.4.6 Results of the thermal isomerization of dianisylmethylaminostilbene (*cis*-Me-St-NAr_2) *cis*-7e

Time (minutes)	% *cis*	ln [*cis*]	ln[*cis*]
0	96.2	0.0703	-2.65
50	90.4	0.0661	-2.72
230	84.4	0.0617	-2.79
358	75.2	0.0550	-2.90
550	52.1	0.0381	-3.27
725	38.4	0.0281	-3.57
832	28.1	0.0205	-3.89
950	24.6	0.0180	-4.02

Table 2.7. Thermal isomerization of 0.0731 M ***cis*-7e** to ***trans*-7e** in deaerated DMSO at 140 °C

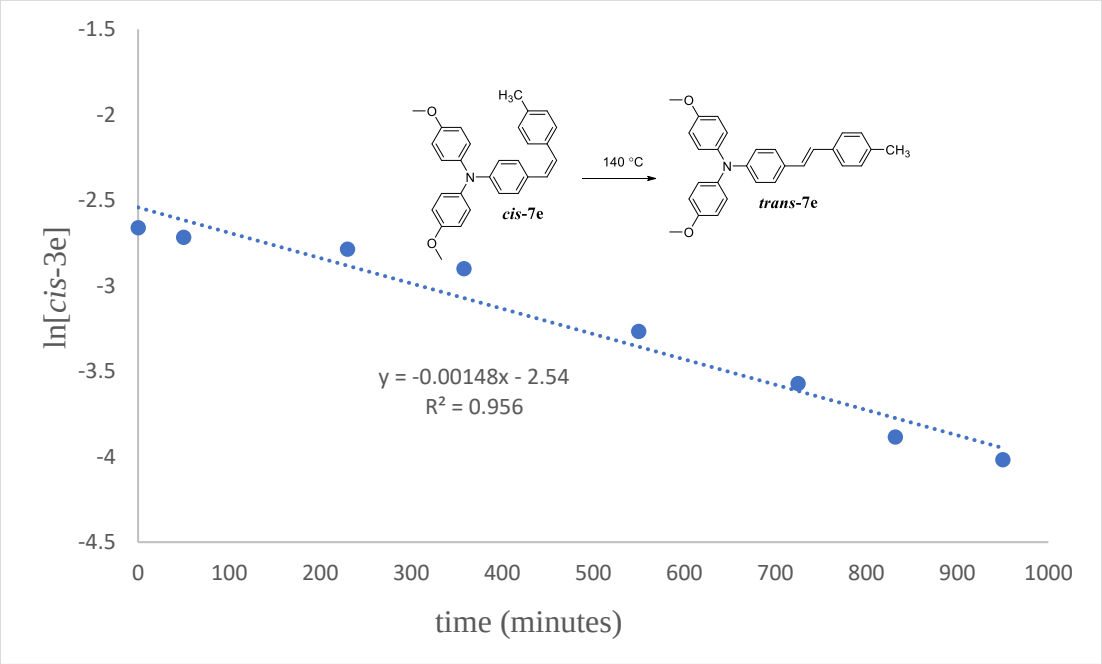

Figure 2.11. Graph of ln [***cis*-7e**] vs time at 140 ºC.

k_{413K} = 2.47 ± 0.3 x 10^{-5} s^{-1}

$\Delta G^{\ddagger}_{413K}$ = 33.2 kcal/mol

2.4.7. Summary of the activation parameters of *p*-substituted aminostilbenes *cis*-7a-e

Substrate	k_{413K} (s^{-1})	$t_{1/2\ 413K}$ (minutes)	$\Delta G^{\ddagger}_{413K}$ (± 1.0 kcal/mol)
***cis*-7a**	2.10×10^{-5}	550	33.3
***cis*-7b**	1.86×10^{-5}	618	33.4
***cis*-7c**	3.10×10^{-5}	372	33.0
***cis*-7d**	3.28×10^{-5}	351	32.9
***cis*-7e**	2.47×10^{-5}	468	33.2

Table 2.8. The activation parameters of *p*-substituted aminostilbenes in DMSO at 413 K (140 ºC).

The results of the investigation of the effect of substituents on the *cis-trans* isomerization of stilbene indicate that electron donating substituents are able to accelerate the thermal isomerization of *para*-substituted stilbenes. Previous studies[91] indicate that the activation and π-bond energies of the central C=C bond are influenced by the interactions between the two π-electrons and the *para* eletron donating substituents. This interaction decreases the energy required for bond-twisting.

Electron donating substituents attached in conjugation with the olefinic bond will tend to elongate the olefinic bond by resonance stabilization of the biradical transition state. This increases the single bond character of the C=C bond, lowers the rate determining barrier and the molecule will quickly relax to a lower energy twisted configuration ($\theta \cong 90^{o}$) leading to an increased isomerization rate. Non-radiative internal conversion of this twisted state leads to a transition state which decays equally to the ground states of the *trans* and *cis* isomers. This configurational isomerization of stilbenes about a single double bond is known as a One-Bond-

Flip (OBF) mechanism.[91] Our result agrees with previously published results[119] that describes the substituent effect on benzylic radical stability, which is consistent with the biradical nature of the transition state.

The thermal barrier of the *cis* to *trans* isomerization of stilbenes can also be significantly reduced by combining the electron donating diaryl amino group on one ring and an electron withdrawing substituent on the para position of the other ring (***cis*-7e**). This is an example of a push-pull stilbene. Push-pull stilbenes also exhibit enhanced rates of thermal *cis* to *trans* isomerization due to the high contribution of the charge-separated resonance form in which the central carbon-carbon bond is single. This leads to a reduced energy barrier for the *cis* to *trans* rotation of the molecule. For example, ***cis*-7e (*cis*-CF_3-St-NAR_2)** has a much lower activation barrier (32.9 ± 1.0 kcal/mol) than the parent stilbene (46 ± 2 kcal/mol)[120]. The isomerization of push-pull stilbenes also involves the 90º twisted configuration, which represents an energy maximum (the activated state of the isomerization process).

2.5 Photochemistry of Redox-Auxiliary appended stilbenes

2.5.1 Photochemistry and optical spectrum of *trans*-7a

The reversible photochemical reactions of stilbenes play important roles in the development of light-gated molecular switches. The intensity of the light source, the molar absorptivity of the substrate at a specific wavelength of light and the quantum yield determine the efficiency of a photochemical reaction. The UV-absorption spectrum of ***trans*-7a** exhibits two main absorptions near 394 nm (A-band) and 302 nm (B-band). The A-band of ***trans*-7a** is attributed $\pi \rightarrow \pi^*$ transition. In contrast to ***trans*-7a**, the A-band of ***cis*-7a** is blue-shifted, much broader, and has a considerably lower molar absorption coefficient than ***trans*-7a** (Figure 2.12). The molar absorptivity of ***cis*-7a** is less than that of ***trans*-7a** because the steric crowding of the

ortho sites causes the phenyl groups to twist slightly out of coplanarity. This leads to a decreased conjugation in ***cis*-7a**. It is easy to choose an appropriate irradiation wavelength to arrive at a photostationary state which is either *cis*- or *trans*-rich because the spectra of *trans*- and *cis*-stilbenes are different due to the decreased conjuagtion in the *cis* form as a result of the twist out of coplanarity.

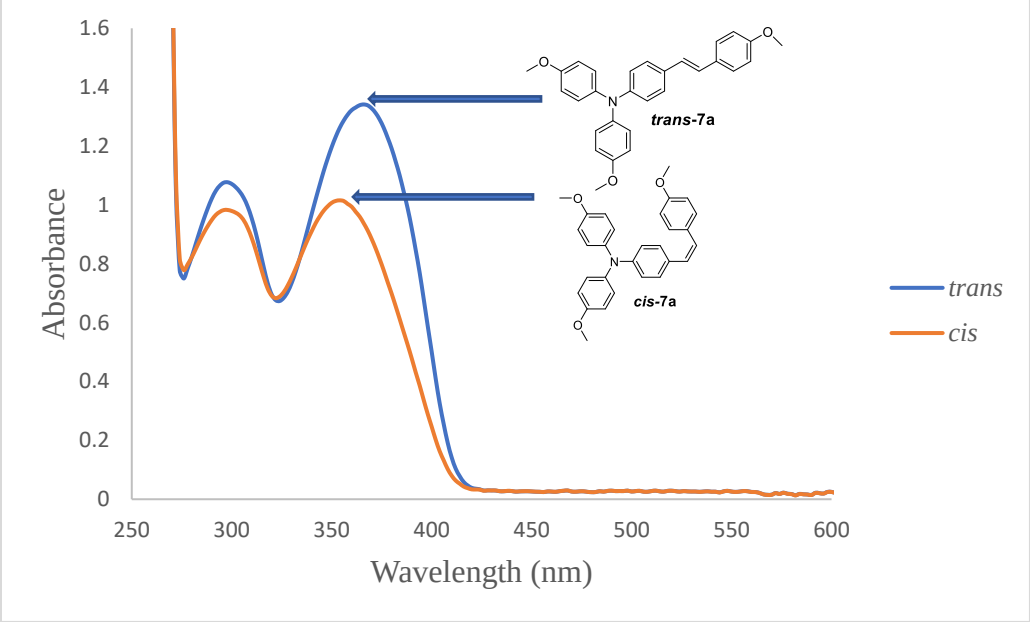

Figure 2.12. Optical spectrum of ***cis*-7a** and ***trans*-7a** (3.01×10^{-5} M) in cyclohexane:benzene = 2:98 at room temperature in 1cm quartz cuvette.

Upon excitation, *trans*-*cis* isomerization of stilbene proceeds through a torsional potential. This potential reaches a surface minimum at the perpendicular geometry in the excited state. There is an equal probability of forming the *cis* and *trans* conformers at this minimal position.[121-122] This change in conformation associated with the *cis* to *trans* isomerization of stilbenes can induce an electronic and/or mechanical response. The photochemical behavior of stilbenes may be changed by the introduction of substituents which may affect the properties of the molecule. Examples of these properties include π-electron cloud, the electron densities at

different positions and the changes in the separation between the energy levels brought about by the twisting around the C-C central bonds.[123]

The photochemical *trans-cis* isomerization of ***trans*-7a** was investigated via irradiation of a dilute cyclohexane solution (approximately 3.01 x10^{-5} M) at 25 ºC with a 395-410 nm LED light source (7W). Irradiation of the sample caused a progressive decrease of the maximum absorption (λ_{max}) at 374 nm with a concomitant increase in the absorption intensity at 302 nm. A well defined isosbestic point at 332 nm was obtained after the irradiation of ***trans*-7a**, providing further evidence for a transformation between two species. The time to reach the photostationary state (PSS) was determined by following the maximum absorption at 374 nm. After about 3 minutes, no changes in the absorbance was observed (Figure 2.13), and there were no decomposition products detected by the UV/Vis spectroscopy due to the absence of a peak at 450 nm.[104]

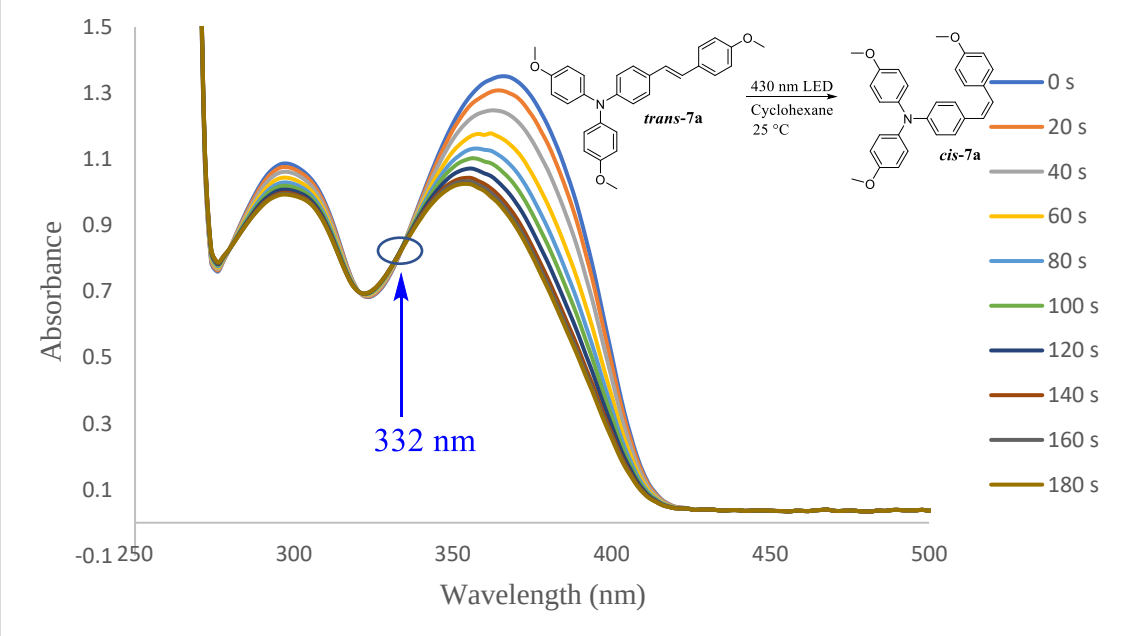

Figure 2.13. The optical spectrum of ***trans*-7a** (3.01 x 10^{-5} M in 2 % benzene in cyclohexane) irradiated with a 430 nm LED at room temperature in a 1cm quartz cuvette.

The same experiment was repaeated for 2.43 x 10^{-4} M solution of ***trans*-7a** in C_6D_6 using a 0.1cm path length cuvette. This was necessary in order to determine the ratio of ***trans*-7a** and ***cis*-7a** at the PSS. The PSS was reached was reached after 18 minutes of irradiation with a 430 nm LED source (Figure 2.14). The ^{1}H NMR spectrum of the PSS solution in C_6D_6 (Figure 2.15) was used to distinguish the substrate from the product formed after irradiation.

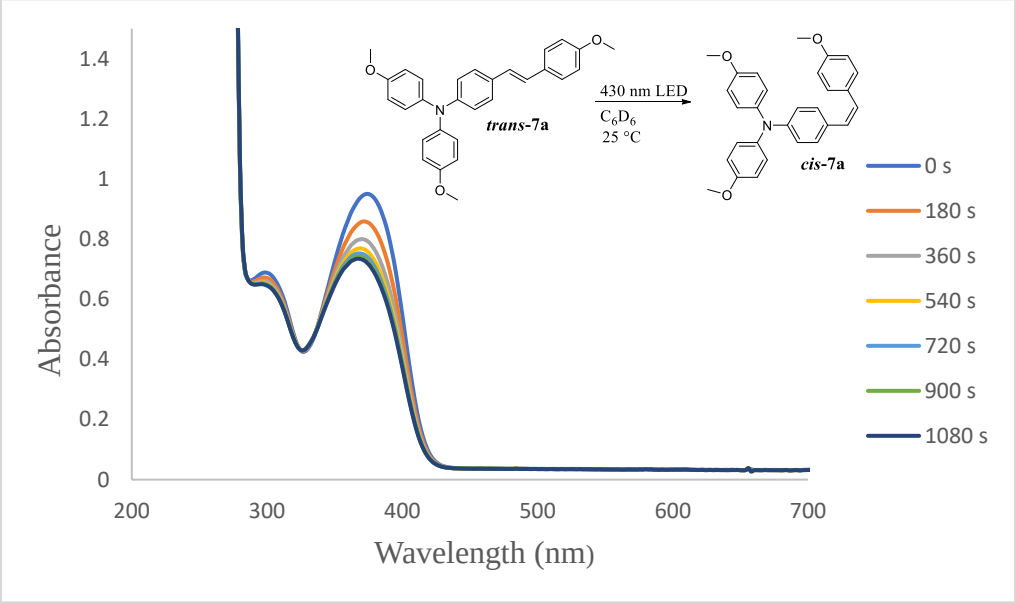

Figure 2.14. The optical spectrum of ***trans*-7a** (2.21 x 10^{-4} M in C_6D_6) irradiated with a 430 nm LED at room temperature in a 0.1cm quartz cuvette.

It was impossible to use the spectrum of 100 % of ***cis*-7a** to measure the molar absorptivity of ***cis*-7a** (ε_{cis}). But the ε_{cis} can be measured by using the isomeric ratio of ***cis*-7a:** ***trans*-7a** at the PSS. This ratio was determined by using NMR spectroscopy at room temperature (Figure 2.15). The UV/Vis spectrum of ***trans*-7a** at PSS and the isomeric ratio ***cis*-7a: *trans*-7a** was then used to measure the molar absorptivity of the compound (ε_{cis}) using the equation below.

$$\varepsilon_{cis} = \frac{A_{pss} - (cxl)\varepsilon_{trans}}{cl(1-x)} \quad \text{.....2.12}$$

Where x is the decimal fraction of ***trans*-7a** at the PSS, A_{pss} is the absorbance at PSS, l is the path length of the cuvette and c is the concentration of ***trans*-7a**.

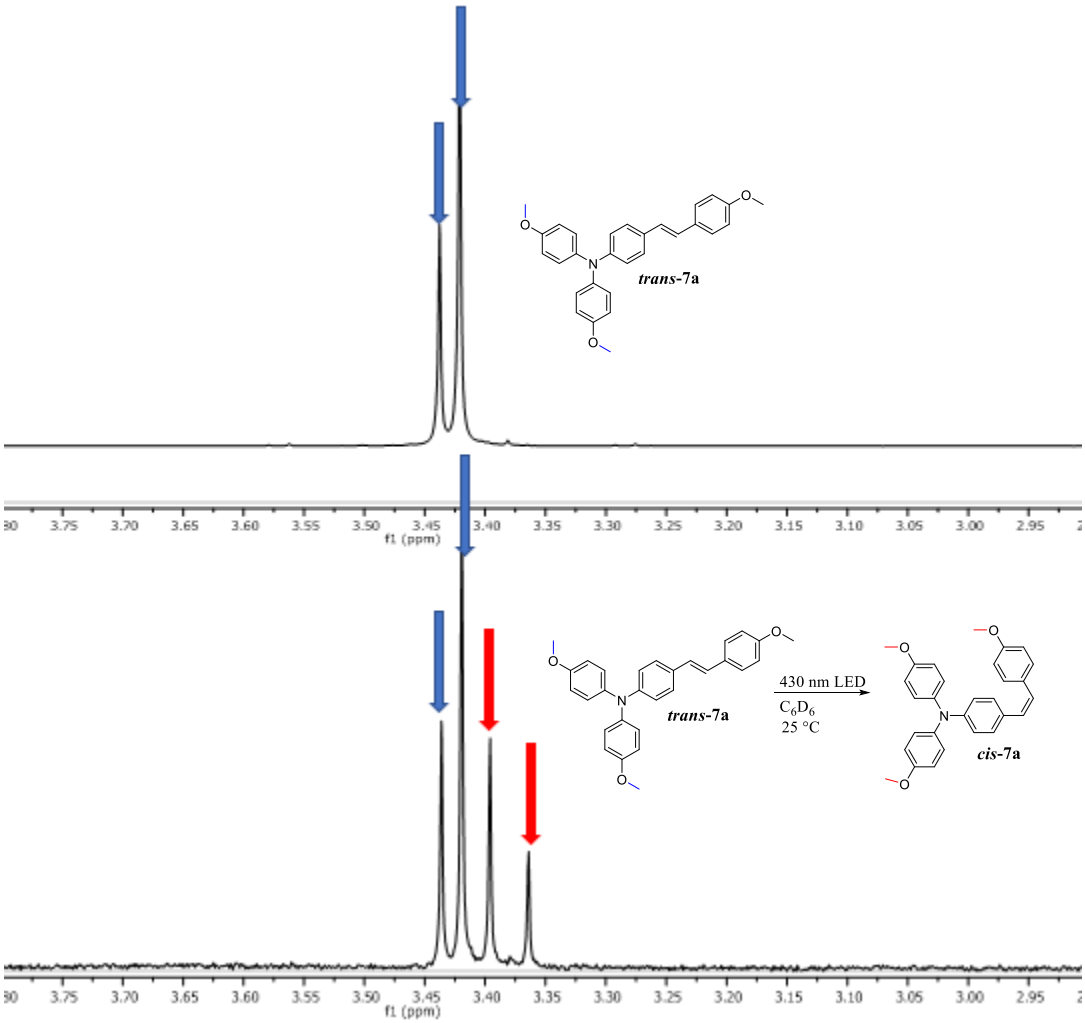

Figure 2.15. An expanded view of the methoxy region of the ^{1}H NMR spectrum of ***trans*-7a** before irradiation and an isomeric mixture (2.43 x 10^{-4} M solution) of 60:40 ***trans*-7a:*cis*-7a** at the PSS after irradiation with a 430 nm LED. Blue arrows indicate the *trans* isomer.

Alternatively, the ε_{cis} can also be measured from chemically made ***cis*-7a**. Unfortunately, 100% pure ***cis*-7a** was difficult to synthesize, however the synthesis yielded a sample that has an

isomeric composition of 98:2 for ***cis*-7a:*trans*-7a** according to the NMR (Figures 2.16-2.18). The UV/Vis spectrum of a known concentration (2.85 x 10^{-2} M) of this synthetically made ***cis*-7a** was obtained and the ε_{cis} was determined using the equation 2.12 above.

It was easy to determined this ratio by ^{1}H NMR because the two isomers have slightly different chemical shifts due to their different structural orientations. In contrast to *trans*-stilbene, the two arene rings in *cis*-stilbene are twisted from the coplanar orientation relative to the central double bond. Upon rotation of the aromatic parts of the molecule, the two protons adjacent to the central double bond may come into the shielding cone of the anisotropic ring current. The protons of the *cis* isomer are shielded as a result of the tilted phenyl rings and therefore appear at higher chemical shifts.

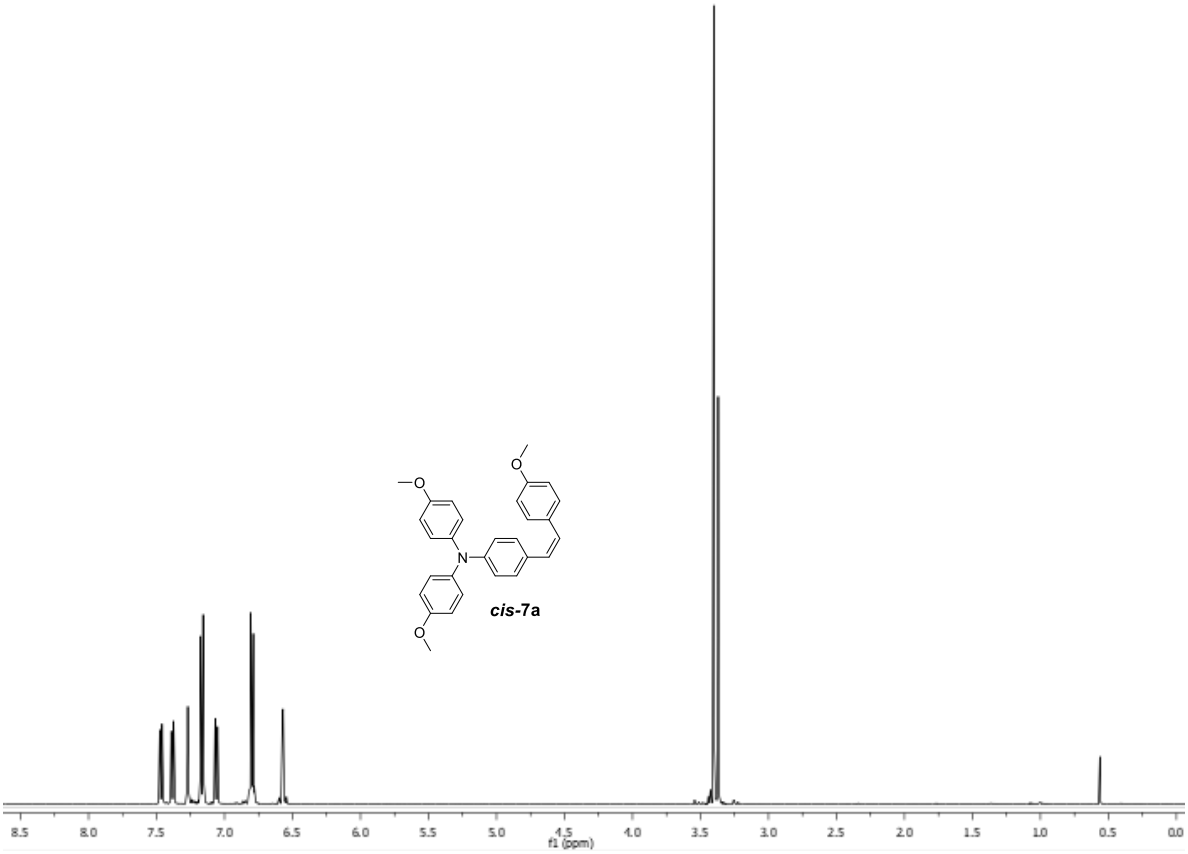

Figure 2.16. The Full NMR spectrum of synthetically made ***cis*-7a** (2.85 x 10^{-2} M) containing an isomeric mixture of 98:2 ***cis*-7a:*trans*-7a** in C_6D_6. Blue arrows indicate the *cis* isomer.

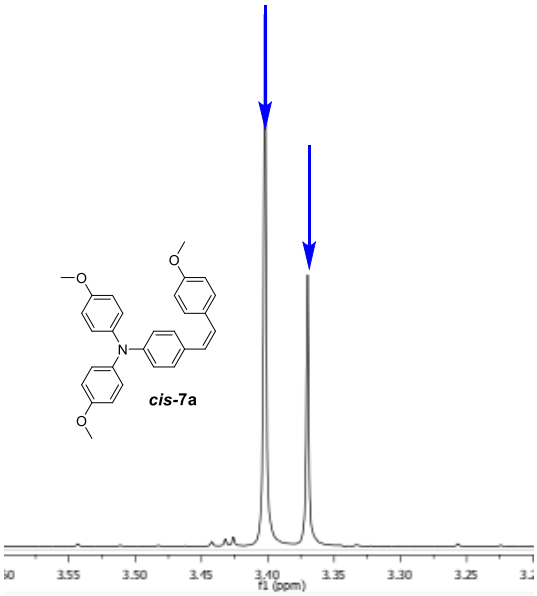

Figure 2.17. An expanded view of the methoxy region of the ^{1}H NMR spectrum of the synthetically made ***cis*-7a** (2.85 x 10^{-2} M in C_6D_6) containing an isomeric mixture of 98:2 ***cis*-7a:*trans*-7a**. Blue arrows indicate the *cis* isomer. Blue arrows indicate the *cis* isomer.

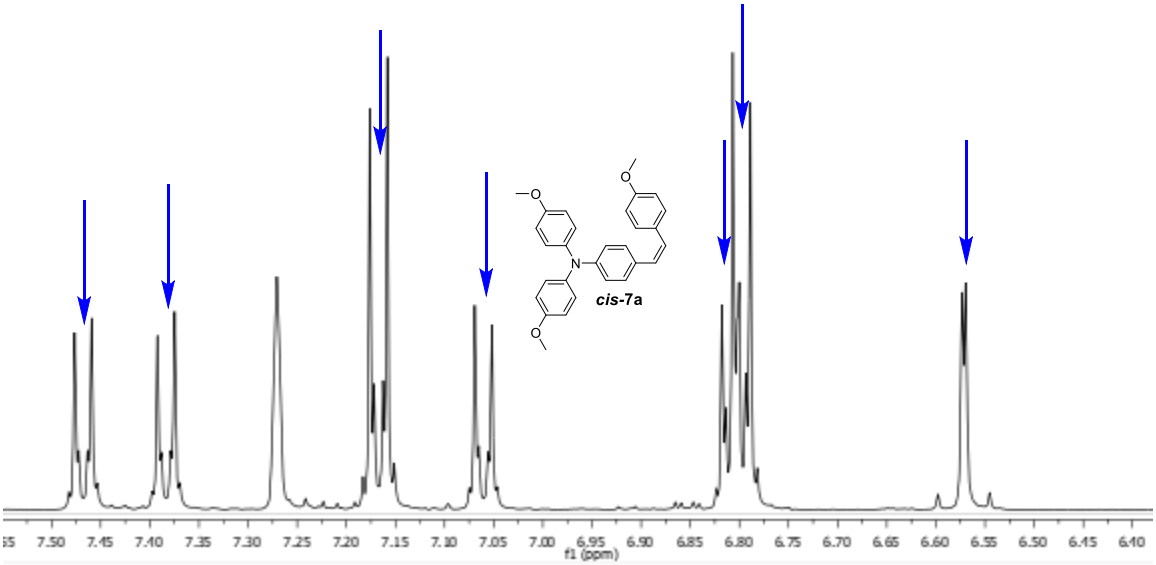

Figure 2.18. An expanded view of the aromatic region of the ^{1}H NMR spectrum of the synthetically made ***cis*-7a** (2.85 x 10^{-2} M in C_6D_6) containing an isomeric mixture of 98:2 ***cis*-7a:*trans*-7a**. Blue arrows indicate the *cis* isomer.

2.5.2 Photochemical *trans-cis* Isomerization of *trans*-7b-e

The photochemistry of para-substituted stilbenes is a unique way of following the different time-scale processes occurring within molecules after irradiation. Photoisomerization of stilbenes is well known and has been studied extensively.[90] The UV-Vis spectroscopy is an efficient method of monitoring the *trans-cis* siomerization of stilbenes since the wavelenghth of the maximum absorption and the extinction coefficient of the *trans*-stilbenes differ substantially from those of the *cis*. As a result, the wavelength of the maximum absorption of the *trans* isomer provided a conveninent means of studying the *trans* to *cis* photoisomerization. The *trans* to *cis* photoisomerization is known to proceed through the lowest excited singlet state or through the twisted singlet intermediate known as the phantom state p*. In this mechanism, a torsional potential reached a surface minimum at the perpendicular geometry p* in the excited state upon excitation.[124-125] Aminostilbenes have a similar isomerization pathway in the electronically excited states. Photochemical *cis-trans* isomerization can also occur by the intersystem crossing pathway (through the biradical twisted triplet state).[126]

The photochemical behavior of stilbenes may be changed by the introduction of substituents which affect the charge distribution of the molecules. This work investigated the electronic effects of the substitution on the photoisomerization reaction of para-(4,4′)-substituted stilbenes. The absorption spectra of *p*-substituted aminostilbenes ***trans*-7b-e** in cyclohexane are shown in Figures 2.19-2.22. Substituted *trans*-4-aminostilbenes have photochemical behavior similar to that of stilbenes. However, para-(4,4′)-substituted *trans*-aminostilbenes have a more planar geometry about the nitrogen atom, extended amino conjugation and an increase in the intramolecular charge transfer character in the excited state. This results in a bathochromic shift

of the $\pi \rightarrow \pi^*$ absorption band in the absorption spectrum. Consequently, the maximum absorbance is shifted to longer wavelength in ***trans*-7b-e** in comparison to ***cis*-7b-e** (Table 2.9).

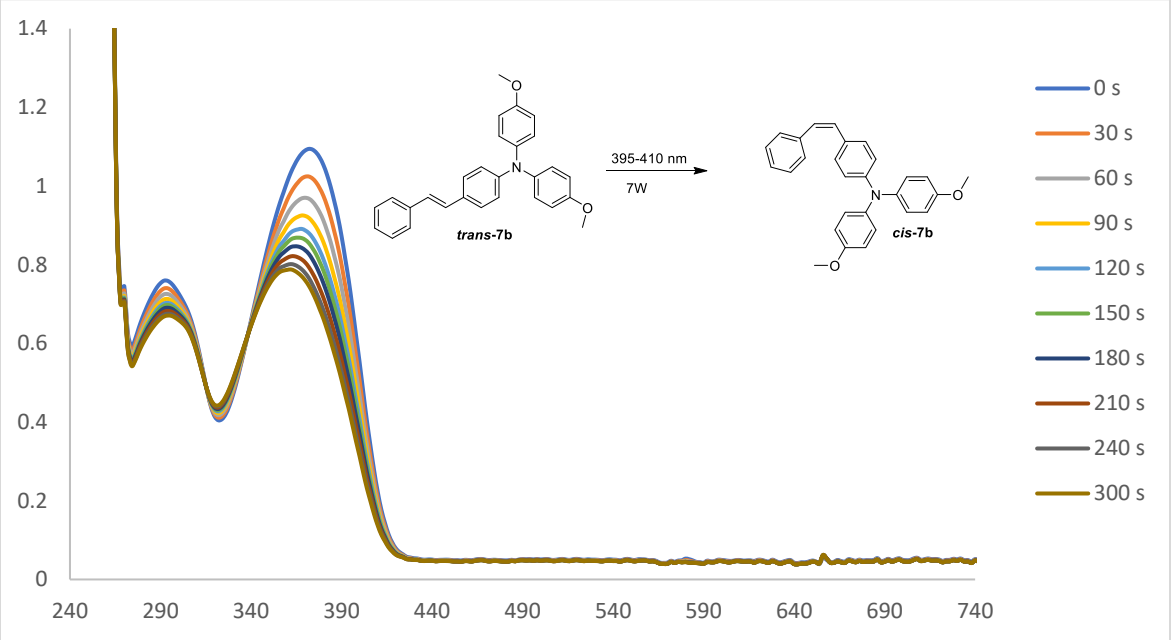

Figure 2.19. Photoisomerization of 5.49 x 10^{-5} M solution of ***trans*-7b** in 2 % benzene in cyclohexane using 395-410 nm (7W) LED at 23 ºC.

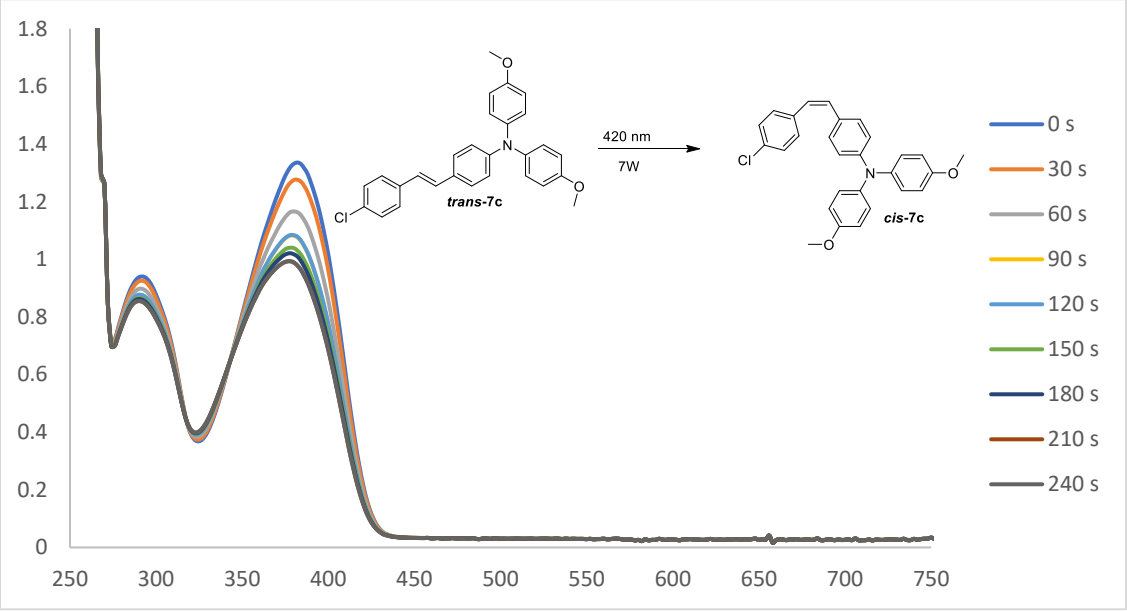

Figure 2.20. Photoisomerization of 3.79 x 10^{-5} M solution of ***trans*-7c** in 2 % benzene in cyclohexane using 395-410 nm (7W) LED at 23 ºC.

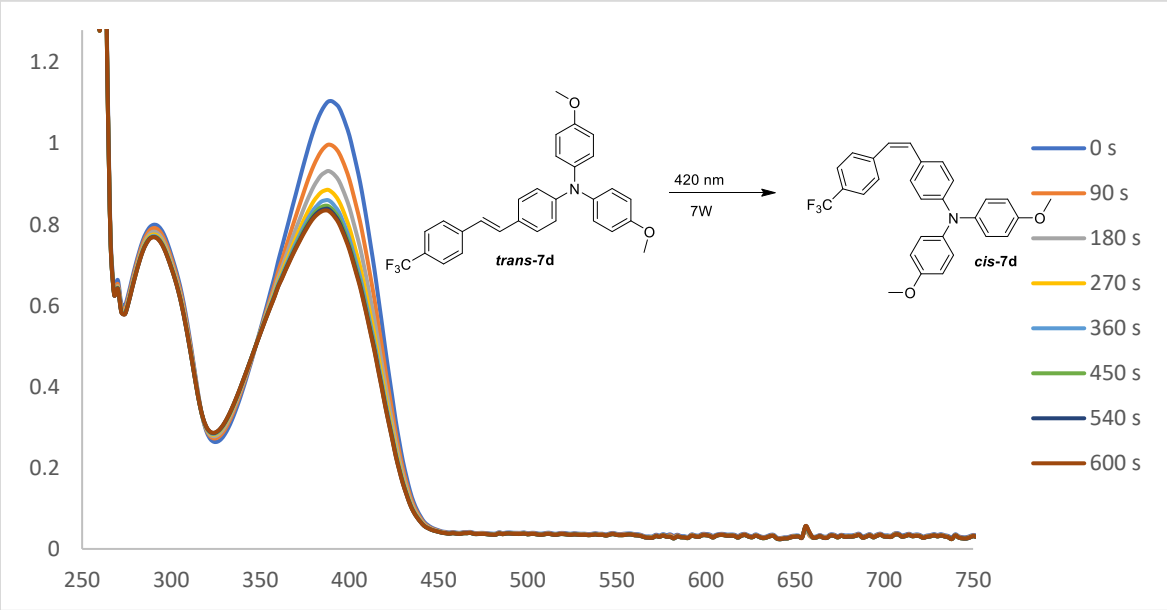

Figure 2.21. Photoisomerization of 2.88 x 10^{-5} M solution of ***trans*-7d** in 2 % benzene in cyclohexane using 395-410 nm (7W) LED at 23 ºC.

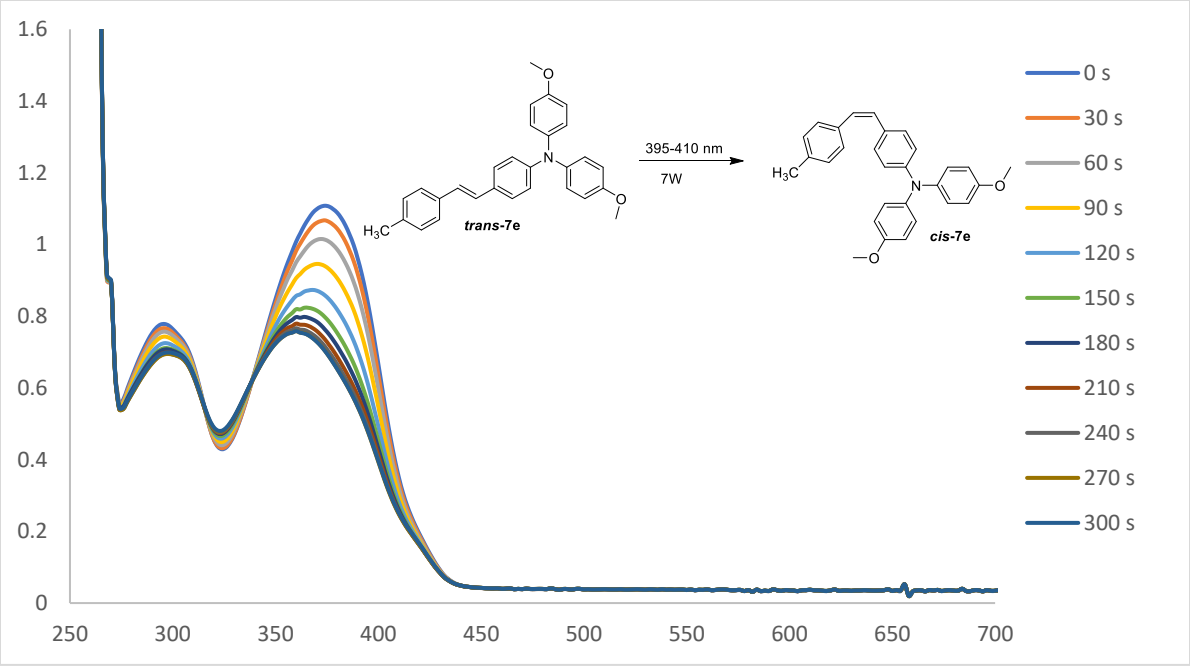

Figure 2.22. Photoisomerization of 2.71 x 10^{-5} M solution of ***trans*-7e** in 2 % benzene in cyclohexane using 395-410 nm (7W) LED at 23 ºC.

2.5.3 Summary of the Photochemical Properties of Redox Appended Stilbenes

Substrate	λmax (nm)	ε_{cis} ($M^{-1}cm^{-1}$)	ε_{trans} ($M^{-1}cm^{-1}$)	PSS (%)	Isosbestic Points (nm)	Excitation wavelength (nm)
***trans*-7a**	374	24800	44300	85.5	332	385-410
***trans*-7b**	372	22,800	39,100	85.9	336	385-410
***trans*-7c**	382	20800	37800	59.8	342	385-410
***trans*-7d**	390	23700	39400	61.3	346	385-410
***trans*-7e**	374	23200	40900	85.6	338	420

Table 2.9. Summary of the photochemical properties of redox appended stilbenes.

2.5.4 Photochemical *trans*-*cis* Isomerization of Ortho-substituted Stilbenes *trans*-7f-g

Photoisomerization of stilbene can begin from either the *cis* or *trans* geometry. When the reaction proceeds from the *cis* isomer, the photo-excited molecule has two competing reaction pathways; one is a torsional *cis–trans* isomerization reaction, and a photocyclization reaction due to electronic rearrangement. The product of the reaction is the *trans*-stilbene for the former and 4a,4b-dihydrophenanthrene (DHP) for the latter (Scheme 2.9).[96, 127] The cyclization reaction of *cis*-stilbene to form DHP proceeds through the electronically excited singlet state of the *cis*-stilbene. The intermediate reaches a perpendicular geometric orientation before the molecule decays to the electronic ground state non-adiabatically. This intermediate then loses hydrogen in presence of oxidative reagent to form the phenanthrene.

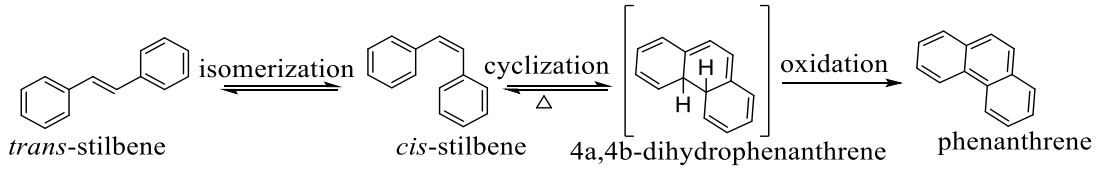

Scheme 2.9. Photocyclization of *cis*-stilbene.[103, 106]

Substitution at the ortho position of the stilbene can be used to inhibit oxidative cyclisation at that position.[128] The introduction of substituents can lead to steric overcrowding around the double bond. If the substituents are large enough, the planarity of the double bond is disrupted. These types of compounds still undergo photoisomerization, but will not cyclize to form DHP. As a result of this, we synthesized two ortho substituted stilbenes (***trans*-7f and *trans*-7g**) and compared their photochemistry to those of structurally of similar compounds ***trans*-7a** and ***trans*-7b**. The absence of a long wavelength absorption near 450 nm indictaes the absence of DHP formation in the previous photochemical experiments of ***trans*-7a-e**.[104]

The photochemical *trans-cis* isomerization of ***trans*-7f and *trans*-7g** were studied via irradiation of a dilute cyclohexane solutions (approximately 1.49 x 10^{-5} M of ***trans*-7f** and 3.01 x 10^{-5} M for ***trans*-7g**) at 25 ºC with a 395-410 nm LED light source (7W). Irradiation of the sample caused a progressive decrease of the maximum absorption (λ_{max}) at 364 nm and 368 nm for ***trans*-7f** and ***trans*-7g** respectively with a concomitant decrease in the absorption intensity at 304 nm and 300 nm for ***trans*-7f** and ***trans*-7g**. A well defined isosbestic point at 338 nm obtained after the irradiation of ***trans*-7f** and ***trans*-7g** (Figures 2.23 and 2.24) and the absence of a long wavelength absorption at about 450 nm provided further evidence for a *trans* to *cis* isomerization without the formation of DHP. Our results also show a little increase in the *cis* ratio at the PSS compared to those of the structurally of similar compounds ***trans*-7a** and ***trans*-7b**.

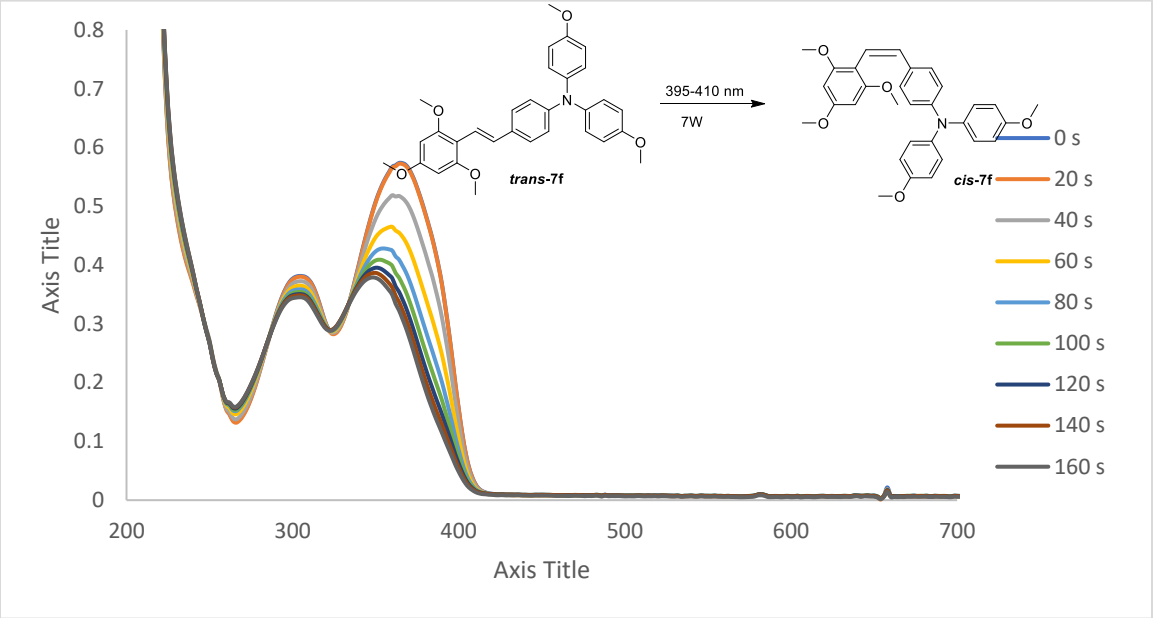

Figure 2.23. Photoisomerization of 1.49 x 10^{-5} M solution of ***trans*-7f** in 2 % benzene in cyclohexane using 395-410 nm (7W) LED at 23 ºC.

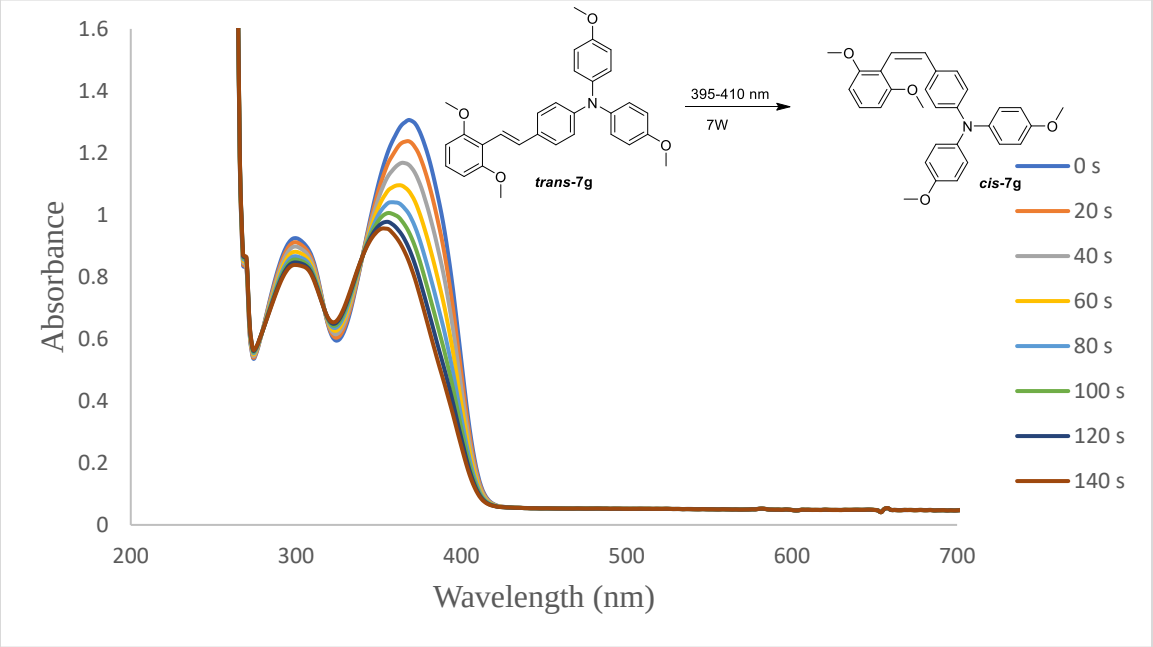

Figure 2.24. Photoisomerization of 1.49 x 10^{-5} M solution of ***trans*-7g** in 2 % benzene in cyclohexane using 395-410 nm (7W) LED at 23 ºC.

2.6 Electrochemical Properties of Redox-Auxiliary stilbenes

Cyclic voltammetry is commonly used for the initial redox characterization of a molecule (i.e., the redox potentials, and the stability of the different oxidations states) and for qualitative investigation of chemical reactions that accompany electron transfer. The redox behavior of ***trans*-7a** was investigated by cyclic voltammetry (CV) experiment at ambient temperature with standard calomel electrode (SCE) as a reference electrode and tetrabutylammonium hexafluorophosphate nBu_4PF_6 as the electrolyte (Figure 2.25). The CV in CH_2Cl_2 showed a reversible oxidation potential of 0.58V. This result means that the cationic radical is stable at room temperature and the radical formation is not accompanied by a subsequent side reaction such as cyclization and dimerization. It also means that the reaction is fast enough to maintain the concentrations of the oxidized and reduced forms in equilibrium with each other at the electrode surface. However, the proper equilibrium ratio at a given potential can be determined by the Nernst Equation:

$$E = E^0 - \frac{RT}{nF} ln\left(\frac{[R]}{[0]}\right)$$

2.13

Where O and R are the oxidized and reduced forms respectively.

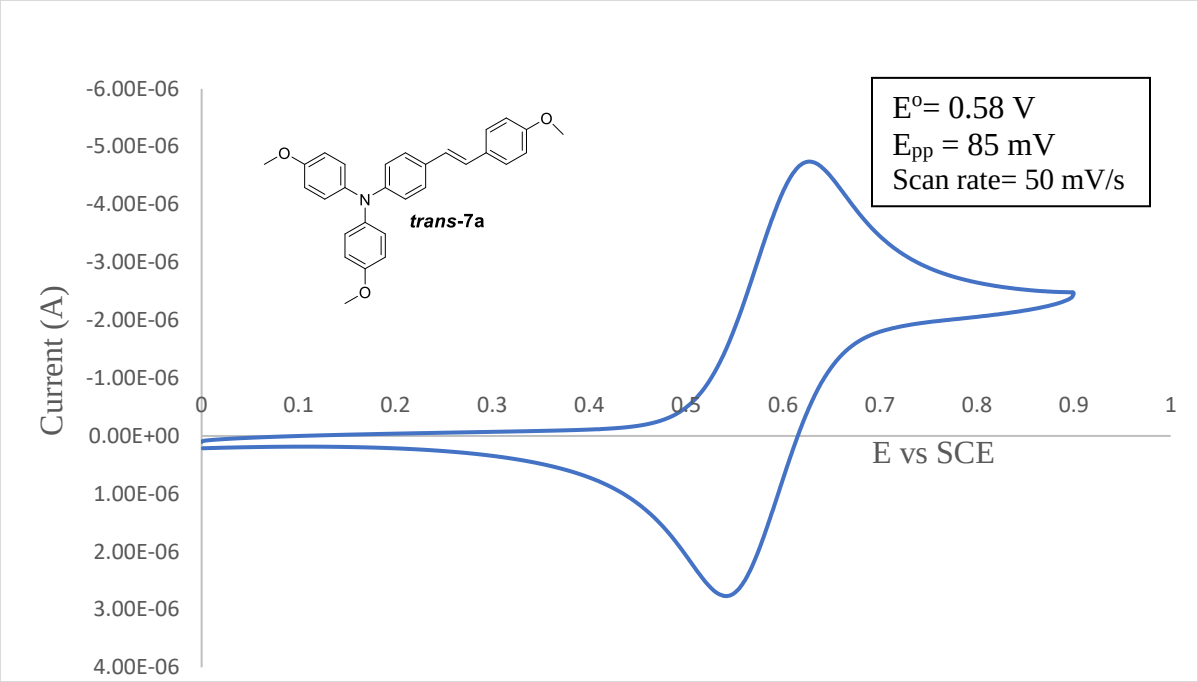

Figure 2.25. Cyclic voltammogram of ***trans*-7a** (1.00 mM in DCM with 0.1 M nBu_4PF_6) at a scan rate of 50 mV/s.

To estimate the effects of varying the substituents on the stilbene electronic structure, the cyclic voltammetry measurements were performed (Figures 2.26-2.31). The voltammogram results (Table 2.10) shows the measured oxidation potentials (versus SCE) of six aminostilbenes ***trans*-7b-g**. The average of the forward and return peak potentials was reported as the formal oxidation potential for the redox couple.

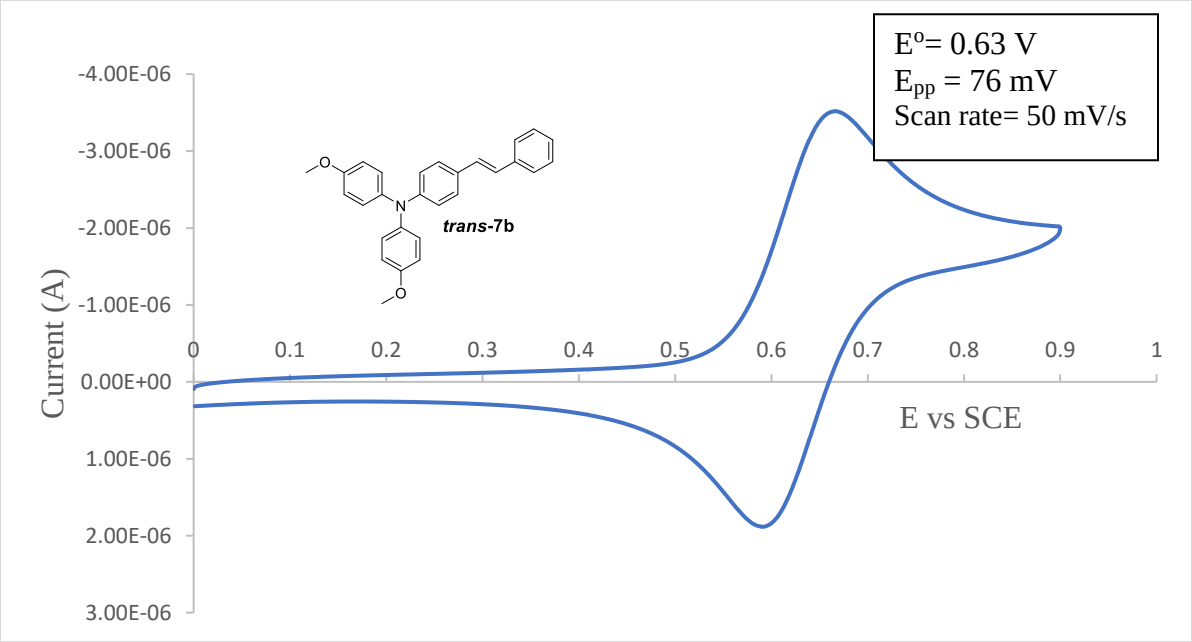

Figure 2.26. Cyclic voltammogram of ***trans*-7b** (1.00 mM in DCM with 0.1 M nBu_4PF_6) at a scan rate of 50 mV/s.

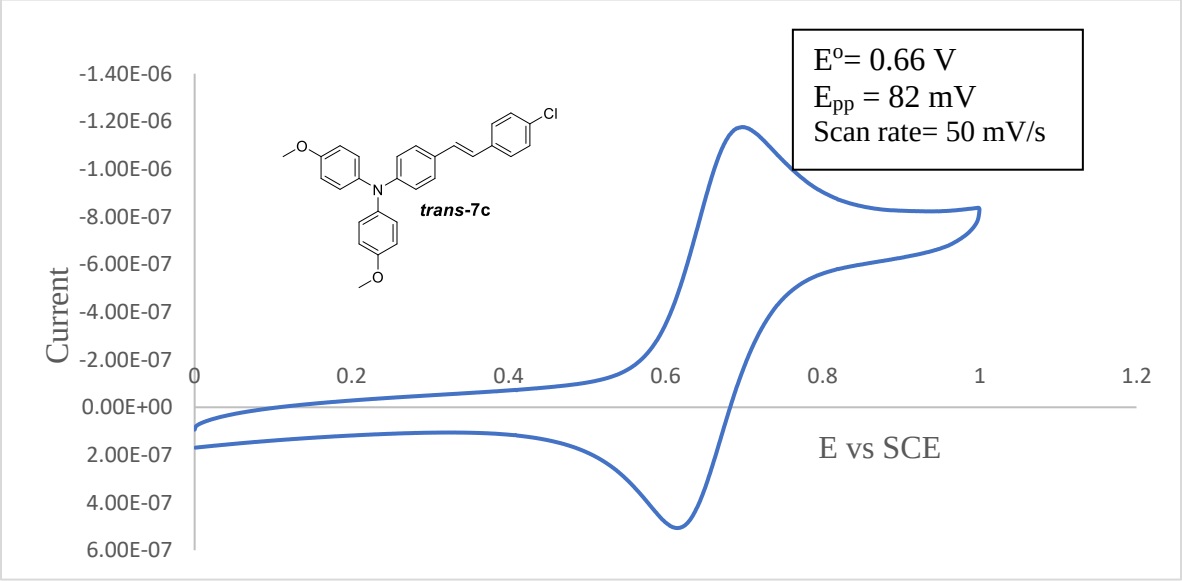

Figure 2.27. Cyclic voltammogram of ***trans*-7c** (1.00 mM in DCM with 0.1 M nBu_4PF_6) at a scan rate of 50 mV/s.

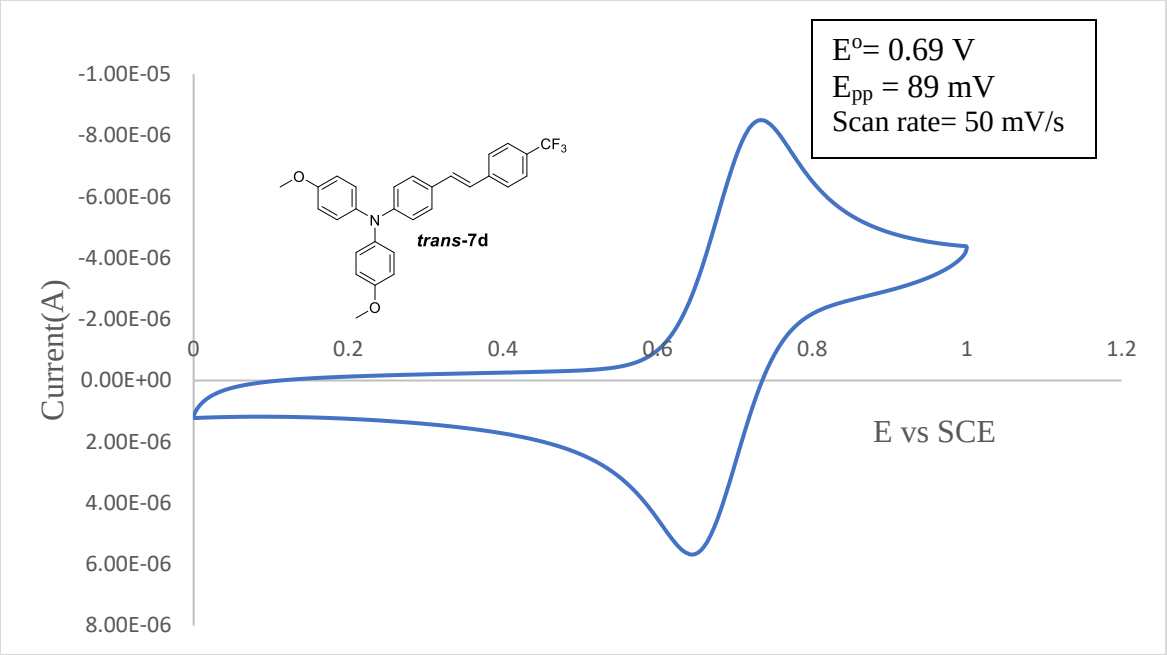

Figure 2.28. Cyclic voltammogram of ***trans*-7d** (1.00 mM in DCM with 0.1 M nBu_4PF_6) at a scan rate of 50 mV/s.

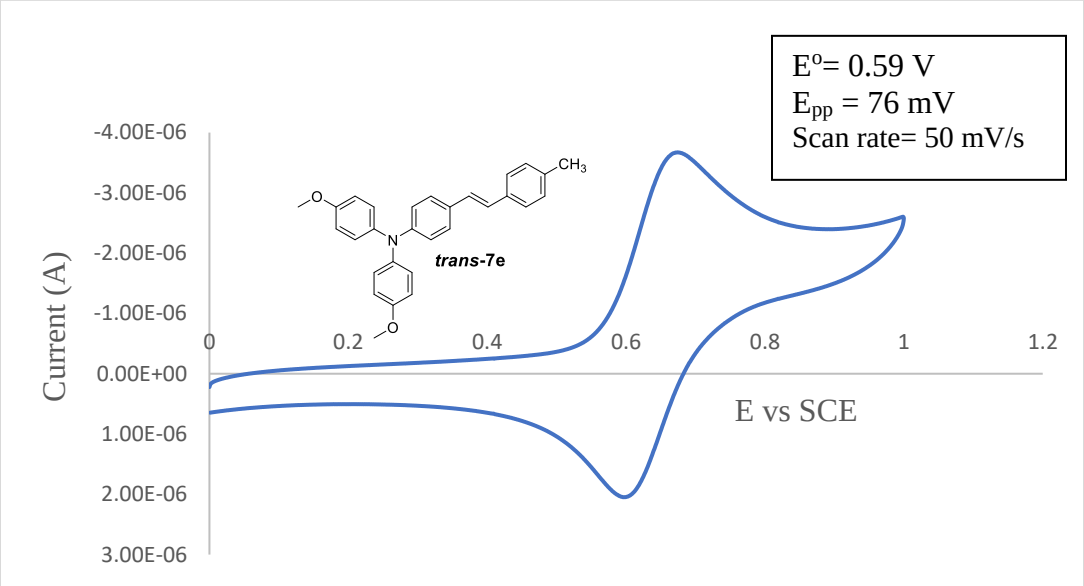

Figure 2.29. Cyclic voltammogram of ***trans*-7e** (1.00 mM in DCM with 0.1 M nBu_4PF_6) at a scan rate of 50 mV/s.

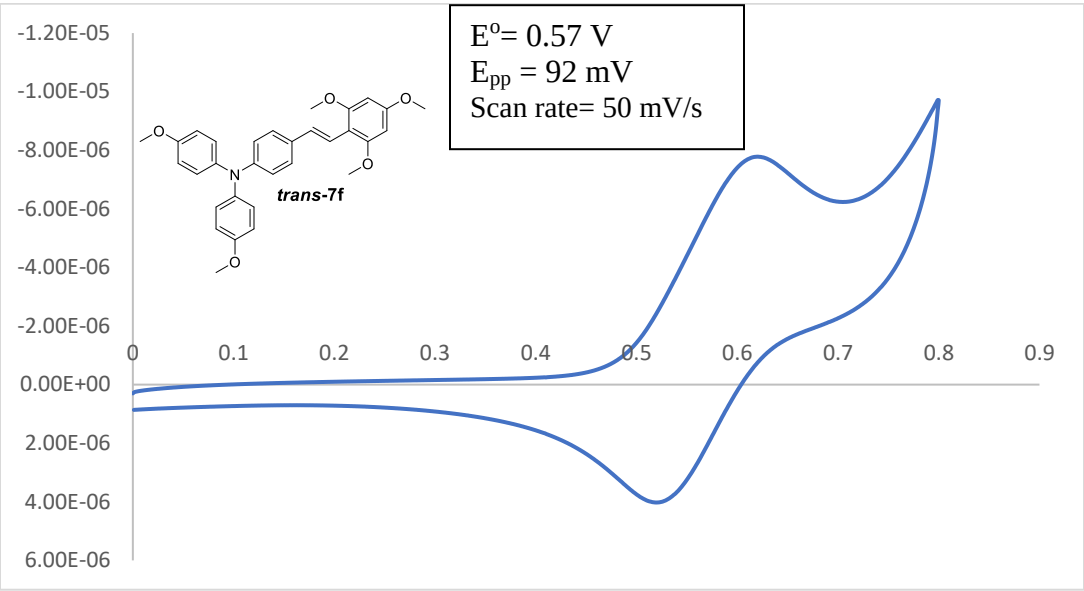

Figure 2.30. Cyclic voltammogram of ***trans*-7f** (1.00 mM in DCM with 0.1 M nBu_4PF_6) at a scan rate of 50 mV/s.

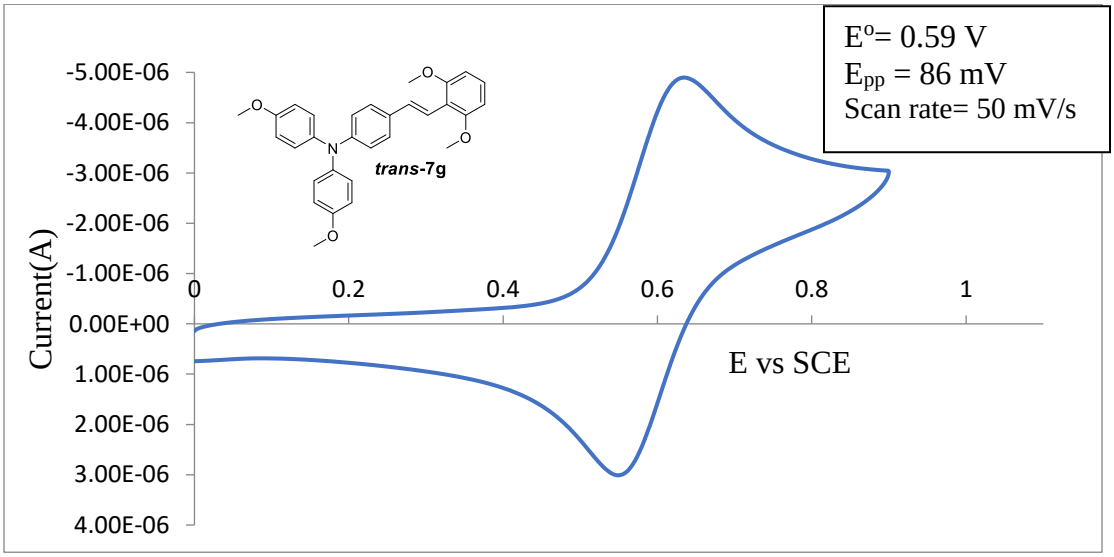

Figure 2.31. Cyclic voltammogram of ***trans*-7g** (1.00 mM in DCM with 0.1 M nBu_4PF_6) at a scan rate of 50 mV/s.

These results show that the oxidation potentials of stilbenes can be varied by changing the substitution pattern and the electron density within the π- electronic system. Stilbenes

substituted with electron withdrawing groups have higher oxidation potentials compared those with electron donating groups. The electron donating groups stabilize the oxidized species through the electron-donating effect while the electron withdrawing groups promote a positive shift in the peak potential due to the destabilization of the radical cation formed, making it more electron deficient. This agrees with the electron withdrawing property of the CF_3 and Cl resulting in the reduction of electron density in the aromatic ring. The oxidation potentials of the various para-substituted aminostilbenes are summarized in Table 2.10. The Cyclic voltammograms were recorded in 0.1 M nBu_4NPF_6 in dichloromethane vs SCE at 0 V. The potential of the Fc/Fc^+ couple versus SCE was 0.45 V.[129]

Substrate	E^o
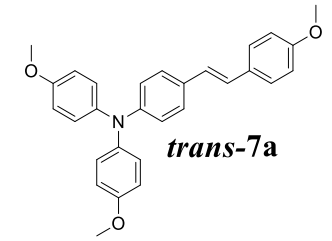 ***trans*-7a**	0.58 V
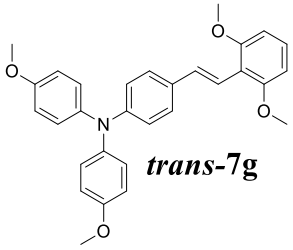 ***trans*-7g**	0.59 V
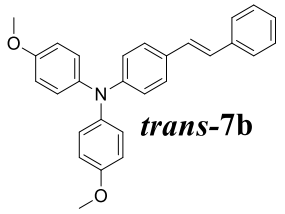 ***trans*-7b**	0.63 V
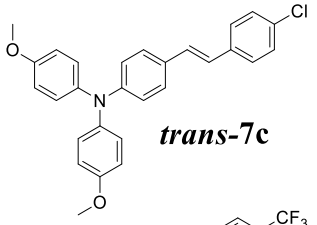 ***trans*-7c**	0.67 V
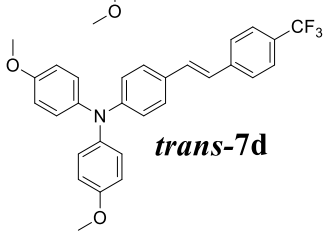 ***trans*-7d**	0.69 V
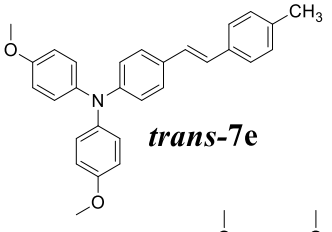 ***trans*-7e**	0.59 V
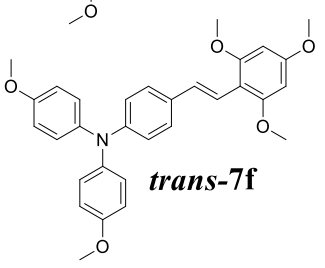 ***trans*-7f**	0.59 V

Table 2.10. Oxidation potentials of para-substituted aminostibenes. Cyclic voltammogram was recorded in 1.00 mM of analyte in DCM with 0.1 M nBu_4PF_6 at a scan rate of 50 mV/s.

2.7 Electron Transfer Catalysis of *cis*-to-*trans* isomerization of aminostilbenes *cis*-7a-e

There are several ways of converting *cis*-stilbenes to the t*rans* isomer. In the previous chapter, we stated that the *cis*-stilbene is thermally stable at room temperature and isomerization can only be observed at temperatures greater than 210 ºC. Photoisomerization of *cis*-stilbenes have been extensively studied but it leads to a photostationary state,[130] and the formation of DHP,[131] which can be trapped oxidatively with hydrogen acceptors. Iodine[61] and diaryl disulfide[62] catalyzed *cis* to *trans* isomerization of stilbenes are the most commonly used methods for obtaining the *trans*-isomer. Unfortunately, these methods also do not go to completion, require very high temperatures, as well as purification by column chromatography.

The *cis*-*trans* isomerization of stilbene radical cations is also a known reaction.[132-133] Although this reaction is fast, it requires about 100 mol % of the oxidant, and the efficiency of the reaction is inhibited by the competition between dimerization and isomerization (Scheme 2.10). The reversible dimerization of the *cis*-stilbene radical cation must be avoided to achieve the one-way *cis*-*trans* isomerization of the *cis*-stilbene radical cation.

We reasoned that the incorporation of radical-stabilizing substituents on the para position of the parent stilbene would significantly increase the rate of isomerization and eliminate the formation of the dimerization product. These substituents are expected to enhance the separation and localization of the positive charge. To achieve this, we attached a diaryl amino redox auxiliary (RA) to the skeleton of stilbenes. The oxidation of the RA by a one electron oxidant (CRET) is expected to enhance the rate of the *cis* to *trans* isomerization. We envisioned this one electron oxidation of the RA to be catalytic, occur at lower temperatures and give pure *trans*-stilbenes without the formation of a dimer or dihydrophenanthrene. The results of this experiment are presented in the next section.

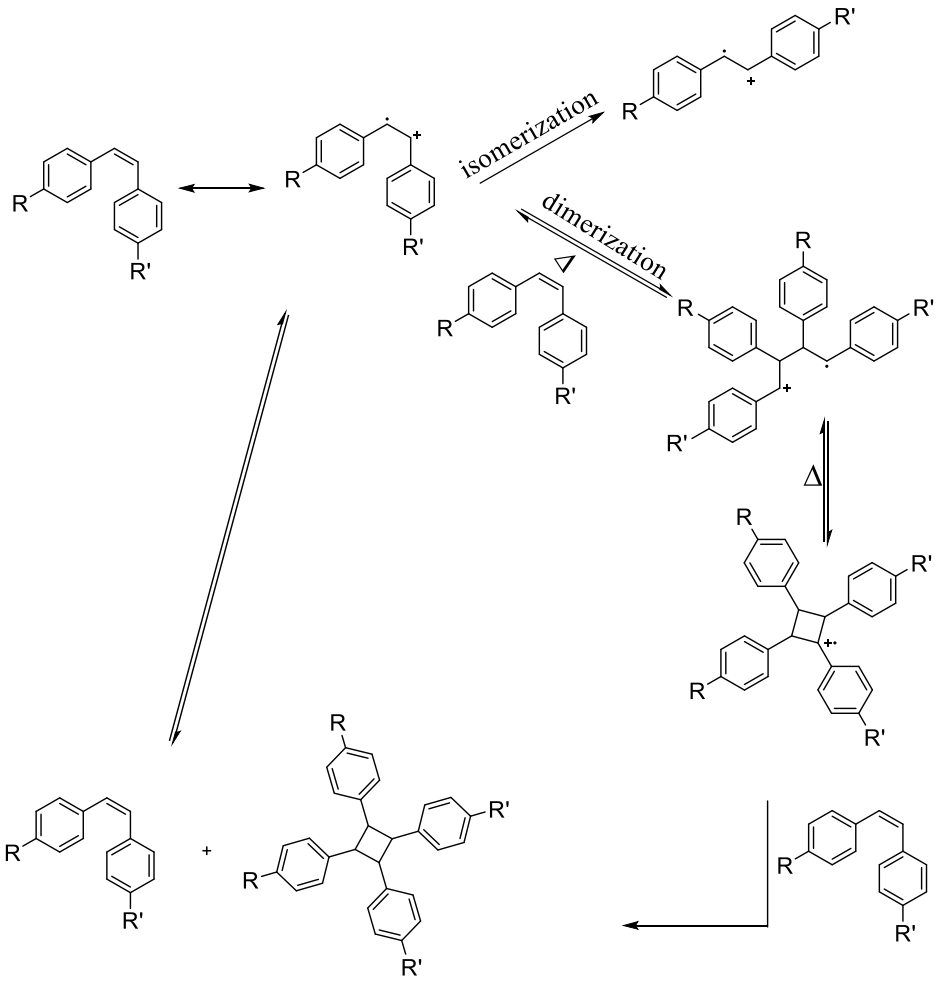

Scheme 2.10. The isomerization/dimerization reactions of the *cis*-stilbene radical cation.[132, 134]

2.7.1 Results of the redox auxiliary promoted isomerization of *cis*-OMe-St-NAr$_2$ *cis*-7a

The kinetic studies of the redox auxiliary mediated *cis* to *trans* isomerization of ***cis*-7a** was monitored by UV-Vis spectroscopy. Since the wavelenghth of the maximum absorption and the extinction coefficient of the *trans*-stilbene differ substantially from that of the *cis*, the wavelength of the maximum absorption of the *trans* isomer provided a means of studying the kinetics of the redox auixiliary promoted *cis-trans* isomerization. A 3.02 x 10^{-5} M solution of ***cis*-7a** was prepared in a mixture of 2% deaerated benzene in cyclohexane and 42.3 μL (5 mol %) of CRET solution (1.07 X 10^{-4} M) in DCM was injected into a 3mL solution of the prepared ***cis*-7a**.

The progress of the isomerization was followed by monitoring the increase of the absorbances at 374 nm (λmax of *trans*) and the decrease of the absorbance at about 302 nm (Figures 2.32). At the end of the isomerization (when the absorbances at 394 nm and 302 nm remained constant), the obtained spectrum looked similar to the spectrum of ***trans*-7a** and both spectra had the same λ_{max} and molar absorptivity, ε. An isosbestic point at about 336 nm indicates that there was no dimerization or dihydrophenanthrene product formed. The experiment was repeated for different amounts of CRET (6 mol %, 7 mol%, 8 mol%, 9 mol%, 10 mol%). See Appendix I for experimental results.

To understand the thermodynamic effect of the addition of the RA on ***cis*-7a**, it was necessary to experimentally measure the $\Delta G^{\ddagger}$ for the *cis* to *trans* RA-promoted isomerization of ***cis*-7a**. The $\Delta G^{\ddagger}_{413K}$ for the thermal isomerization ***cis*-7a** was previously measured to be approximately 33.3 kcal mol^{-1}, which is lower than the thermal isomerization barrier of the parent stilbene (~ 46 kcal/mol).[135] The $\Delta G^{\ddagger}$ for the RA-promoted isomerization can be obtained by plotting of graph of ln [***cis*-7a**] against time at 30 ºC (Figures 2.33). The slope of the graph gives the rate constant -k for the first order process, which is used in calculating the free energy of activation $\Delta G^{\ddagger}$ for reaction.

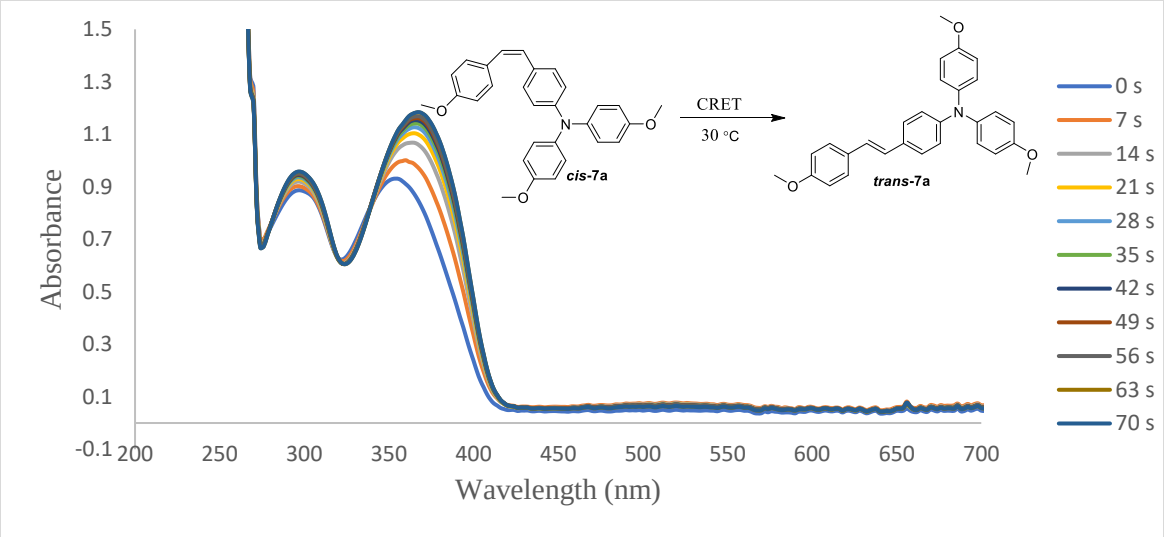

Figure 2.32. Optical spectrum of addition of CRET (5 mol% in DCM) to 3.02 X 10^{-5} M solution of ***cis*-7a** in 2 % benzene in cyclohexane.

Time (seconds)	% cis	[*cis*]	ln[*cis*]
0	91.4	2.76 x 10^{-5}	-10.5
4	60.3	1.82 x 10^{-5}	-10.9
11	34.2	1.03 x 10^{-5}	-11.5
18	22.5	6.78 x 10^{-6}	-11.9
25	15.5	4.67 x 10^{-6}	-12.3
32	11.4	3.44 x 10^{-6}	-12.6
39	8.33	2.52 x 10^{-6}	-12.9
46	5.99	1.81 x 10^{-6}	-13.2
53	4.02	1.22 x 10^{-6}	-13.6
60	2.32	6.99 x 10^{-7}	-14.2
67	0.545	1.65 x 10^{-7}	-15.6

Table 2.11. Redox auxiliary promoted *cis-trans* isomerization of 3.02 X 10^{-5} M ***cis*-7a** in cyclohexane: benzene = 98:2 using 5 mol % CRET in DCM at 30 ºC.

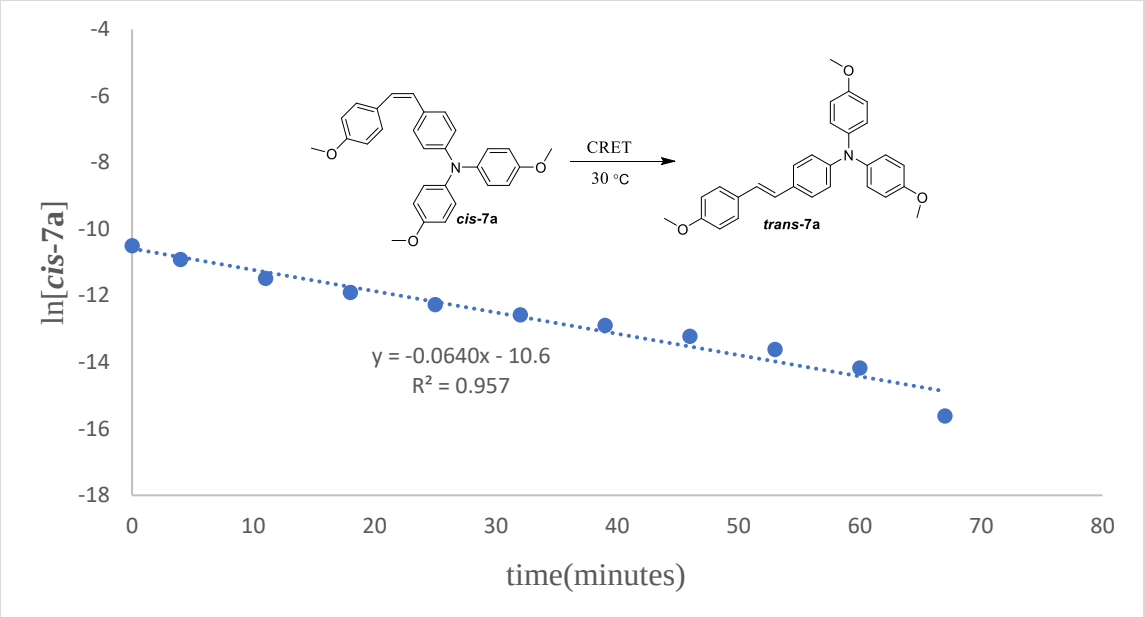

Figure 2.33. First order plot of the ln[***cis*-7a**] vs time at 30 ºC for the redox auxiliary promoted *cis-trans* isomerization of ***cis*-7a** in cyclohexane: benzene = 98:2 using 5 mol % CRET in DCM.

The $\Delta G^{\ddagger}$ of the RA-promoted radical isomerization of stilbene was obtained by evaluating the reaction at different temperatures (25 ºC – 50 ºC) using 5 mol % of CRET (Table 2.12). An Eyring plot of the rate constant ln (k/T) against 1/T gave a linear fit (Figure 2.34), whose slope and intercept were used to calculate the $\Delta H^{\ddagger}$ (9.36 kcal/mol) and $\Delta S^{\ddagger}$ (-32.8 e.u) respectively. The graph of the rate constant against the mol % of CRET (Figure 2.35) was extrapolated to obtain the k for the addition of 100 mol % CRET. The RAC *cis* to *trans* stilbene isomerization rate enhancement at 303 K was obtained by dividing the rate of the radical process for 5 mol % CRET by the rate of the neutral process at the same temperature. This was found to be 10^7 times faster relative to the neutral. A summary of the activation parameters for the RA promoted neutral/radical isomerization of ***cis*-7a** is shown in Table 2.13.

T(K)	k	ln(k/T)	1/T
298	0.0532	-8.63	0.00336
303	0.0640	-8.49	0.00330
308	0.0929	-8.11	0.00325
313	0.1276	-7.81	0.00320
318	0.1599	-7.60	0.00315
323	0.1781	-7.50	0.00310
328	0.211	-7.35	0.00305

Table 2.12. First order rate constants of the RA promoted *cis-trans* isomerization of 3.02 X 10^{-5} M ***cis*-7a** in cyclohexane: benzene = 98:2 using 5 mol % CRET in DCM.

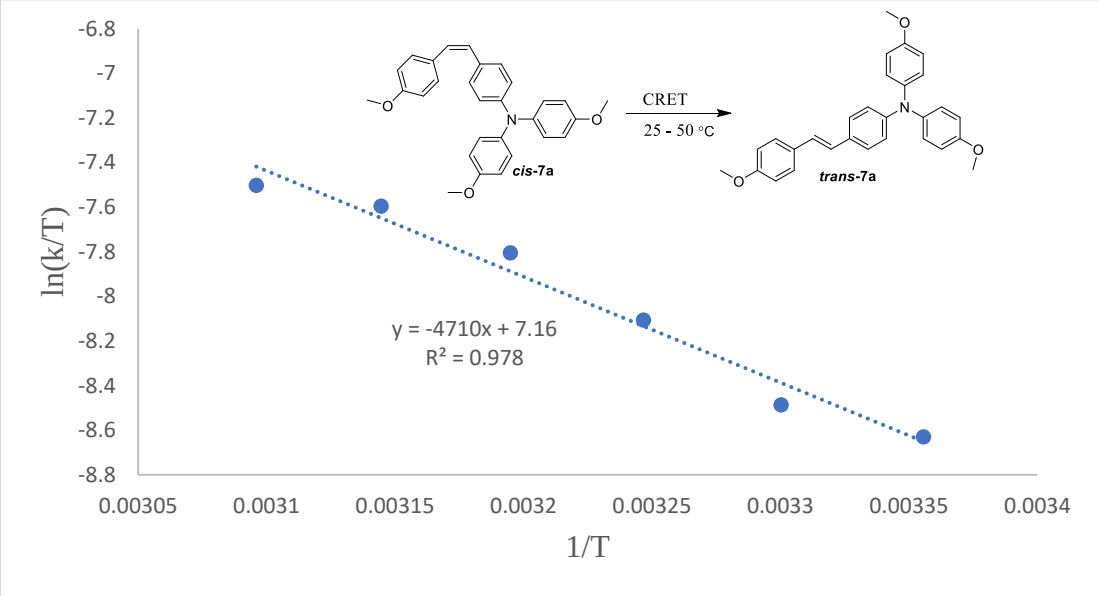

Figure 2.34. Eyring plot of the radical isomerization of ***cis*-7a**.

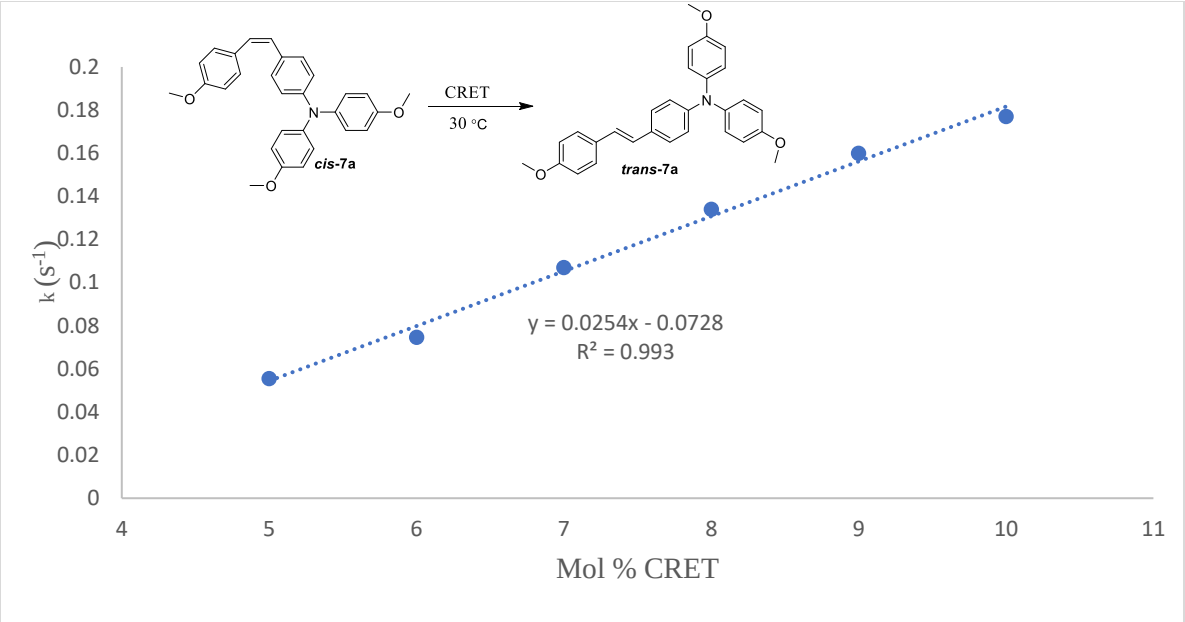

Figure 2.35. Graph of k vs mol % of CRET for the radical isomerization of ***cis*-7a**.

Neutral isomerization	**Activation parameters**
K_{413K} (s^{-1})	2.10 x 10^{-5}
$\Delta G^{\ddagger}_{413K}$ (kcal/mol)	33.2
$\Delta S^{\ddagger}$ (eu)	-28.8
$\Delta H^{\ddagger}$ (kcal/mol)	21.3
$\Delta G^{\ddagger}_{303K}$ (kcal/mol)	29.8
k_{303K} (s^{-1})	1.42 x10^{-9}
Radical isomerization	
k_{303K} (s^{-1}) 5 mol % CRET	0.0625
k_{303K} (s^{-1}) 100 mol % CRET	2.47
$\Delta G^{\ddagger}_{303K}$ (kcal/mol) 100 mol % CRET	17.2
$\Delta H^{\ddagger}$ (kcal/mol)	9.44
$\Delta S^{\ddagger}$ (eu)	-32.8
$\Delta\Delta G$ (kcal/mol)	12.9
Rate acceleration for 5 mol % CRET	4.40 x 10^{7}
Rate acceleration for 100 mol % CRET	1.74 x 10^{9}

Table 2.13. Summary of the activation parameters of the RA promoted neutral/radical isomerization of ***cis*-7a**.

To confirm that the catalytic ability of CRET to induce the *cis-trans* isomerization of stilbenes, a new sample of ***cis*-7a (**4.04 x 10^{-5} M) was irradiated in a 1 cm path length cuvette for 3 minutes to reach the PSS (86 % *cis*:14 % *trans*). This was followed by the addition of a catalytic amount (5 mol %) of CRET in DCM to regenerate the *trans* isomer in about 70 seconds

at 30 ºC, thus exponentially increasing the rate at which the *cis* isomer isomerizes back to the *trans* isomer (Figure 2.36). The incorporation of the RA to the skeleton of stilbene (**OMe-St-NAr$_2$**) enhanced the rate of the *cis* to *trans* isomerization upon oxidation of the amine RA by a one-electron oxidant. The oxidation of ***cis*-OMe-St-NAr$_2$** to ***cis*-OMe-St-NAr$_2$**$^{\bullet+}$ underwent a facile isomerization to the ***trans*-OMe-St-NAr$_2$**$^{\bullet+}$ and upon reduction yield the ***trans*-OMe-St-NAr$_2$**. This cycle was catalytic upon the formation of ***trans*-OMe-St-NAr$_2$**$^{\bullet+}$ electron transfer thus, propagating a chain reaction with the ***cis*-OMe-St-NAr$_2$**.

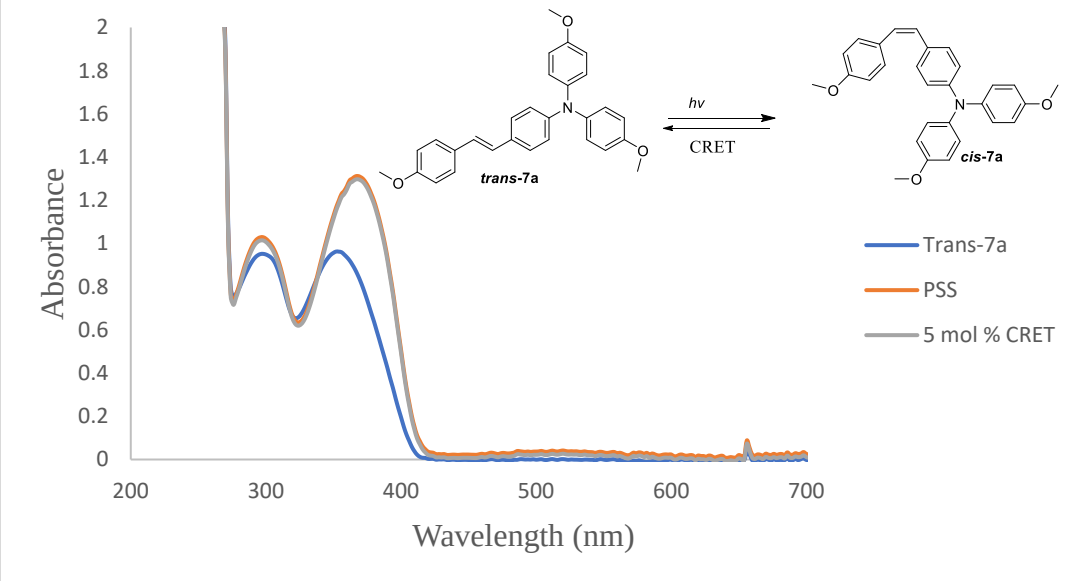

Figure 2.36. The optical spectrum of the addition of 5 mol % of CRET to 4.04 x 10^{-5} M solution of ***cis*-7a** at PSS.

Furthermore, ^{1}H NMR experiment was carried out to confirm the structure and identity of the electro generated product in the *cis-trans* switching of ***cis*-7a** formed after the redox catalysis of ***cis*-7a**. This was done by dissolving a known amount of ***cis*-7a** containing an isomeric mixture of 98 % *cis* and 2 % *trans* in deuterated benzene and followed by the addition of 5.0 mol % of CRET to the solution at 30 ºC. The reaction was quenched after about 70 seconds by the addition of activated zinc powder. The ^{1}H NMR spectrum of the product (Figure 2.37) showed a complete

conversion of the ***cis*-7a** to the ***trans*-7a**. This agrees with results obtained from the previous UV-Vis experiment (Figure 2.36).

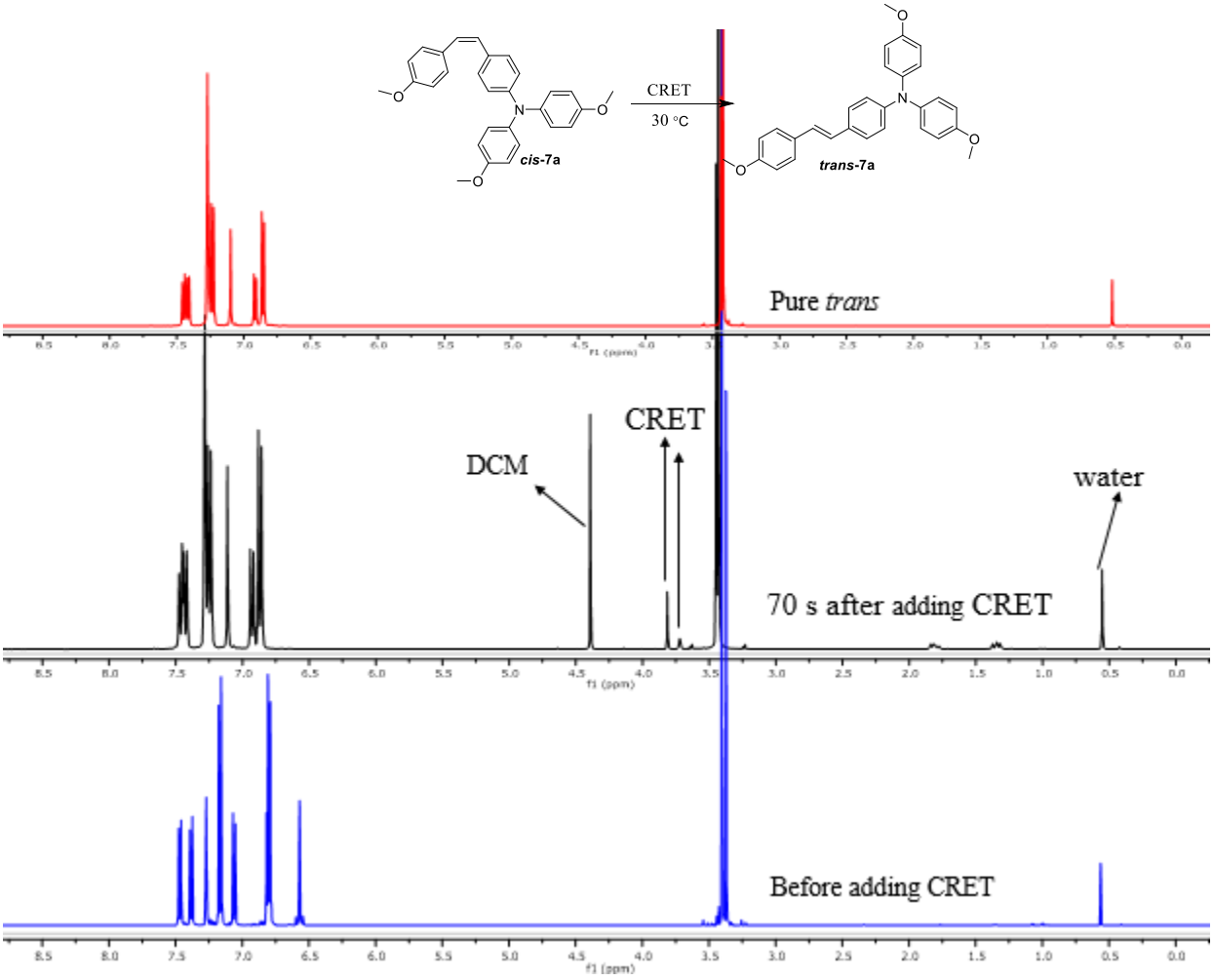

Figure 2.37. The addition of CRET (5 mol %) to ***cis*-7a** (2.86 X 10^{-3} M) at 30 ºC. The spectrum shows ***cis*-7a** before CRET addition **(blue)**, ***cis*-7a** after CRET addition at 30 ºC **(black)** and pure ***trans*-7a (red)**.

These results agree with our hypothesis that the activation barriers of the *cis* to *trans* isomerization of stilbenes can be reduced by oxidizing an appended diaryl amino RA with a one electron oxidant. This converts the neutral *cis*-stilbene to the cation radical. The cation radical will then undergo a chain process in which it will isomerize to the more stable *trans*-stilbene radical cation. The electron hole transfer between the *trans*-stilbene radical cation and the neutral *cis*-stilbene completes the catalytic cycle, as shown in Scheme 2.11. This one electron oxidation

of the attached RA was catalytic and occurred at lower temperatures. We did not observe the formation of any side product because the reduced activation barrier of the radical process is lower than the barrier of the competing side reactions.

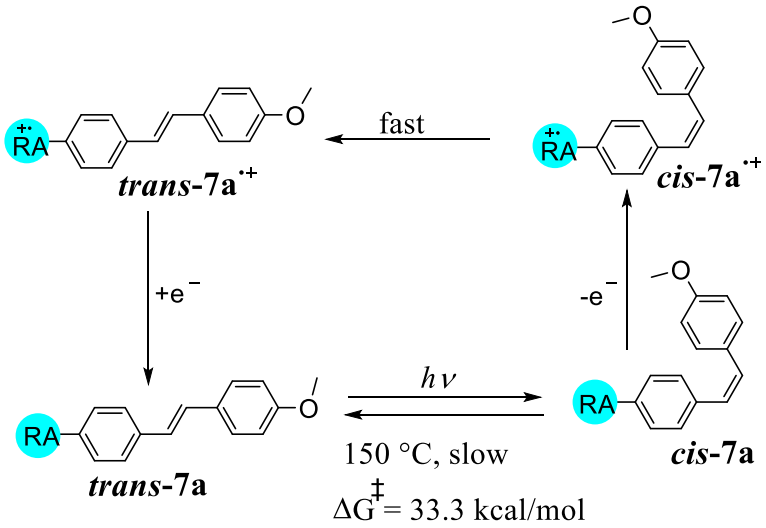

Scheme 2.11. The catalytic cycle of the *cis-trans* isomerization of stilbene.

The crystal structure of ***trans*-7a** (Figure 2.38) shows only a small deviation in the twisting of the phenyl group attached to the RA group. This is necessary because it helps align its pi orbitals with the pi orbitals of the -C=C- group and the lone pair of the nitrogen atom of the RA group and as a result, the stilbene core is nearly planar. The planarity of the stilbene core is important because it helps stabilize ***trans*-7a** by extending the conjugation between the phenyl ring attached to the RA group. The crystal structure of ***cis*-7a** (Figure 2.39) is propeller shaped with out of plane twisting of the phenyl rings by 34.2º unlike that of ***trans*-7a** that shows only a small deviation (2.49 º) from planarity. Both ***trans*-7a** and ***cis*-7a** have 2 structures in their asymmetric units and the alkene C=C bond lengths in ***trans*-7a** and ***cis*-7a** are 1.33Å and 1.34 Å respectively.

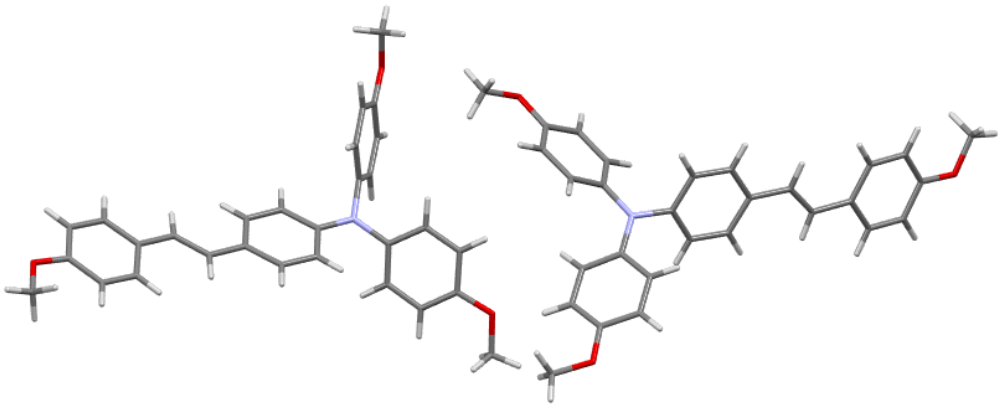

Figure 2.38. Cap and stick diagram of the crystal structure of ***trans*-7a**.

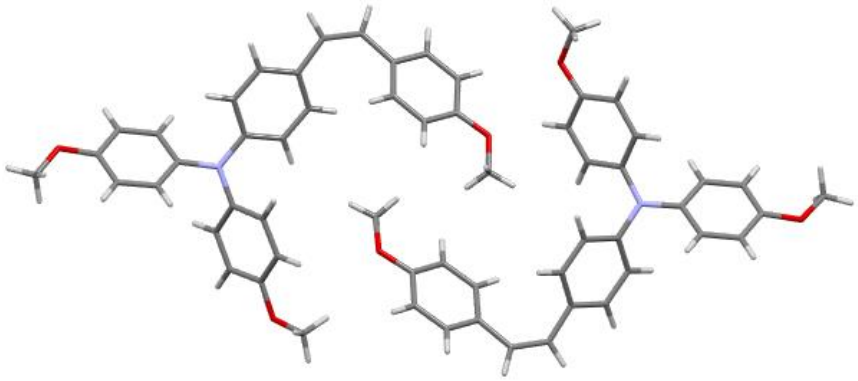

Figure 2.39. Cap and stick diagram of the crystal structure of ***cis*-7a**.

Our studies on the *cis-trans* thermal isomerization of RA stilbenes showed that the rate of isomerization was affected by changing the substituents. This result prompted us to investigate the electronic effects of the substitution on the RA catalysis of para-(4,4')-amino-substituted stilbenes. In this study, we have examined the *cis-trans* isomerization of five 4-X substituted *cis*-stilbenes (where X = OCH_3, CF_3, Cl, H, CH_3) bearing either an electron withdrawing or an electron donating group.

2.7.2 Results of the redox auxiliary promoted isomerization *cis*-7b

The results of the redox catalysis of the *cis-trans* isomerization of ***cis*-7b** are presented in the Figures 2.40-2.41. Following the same procedure as in **2.7.1**, a 3.02 X 10^{-5} M solution of ***cis*-7b** was prepared in a mixture of 2% deaerated benzene in cyclohexane and 5 mol % CRET was injected into a 3 mL of the sample in a 1 cm path length cuvette at 30 ºC. The change in absorbance over time was recorded every 30 seconds with UV-Vis and the graph of the natural logarithm of the change in concentration of ***cis*-7b** was plotted against time. Then k and ΔG‡ of the reaction was obtained. The same experiment was repeated for 3.39 x 10^{-5} M, 3.02 x 10^{-5} M and 3.08 x 10^{-5} M of ***cis*-7c**, ***cis*-7d** and ***cis*-7e** respectively (Figures 2.42, 2.44 and 2.46)

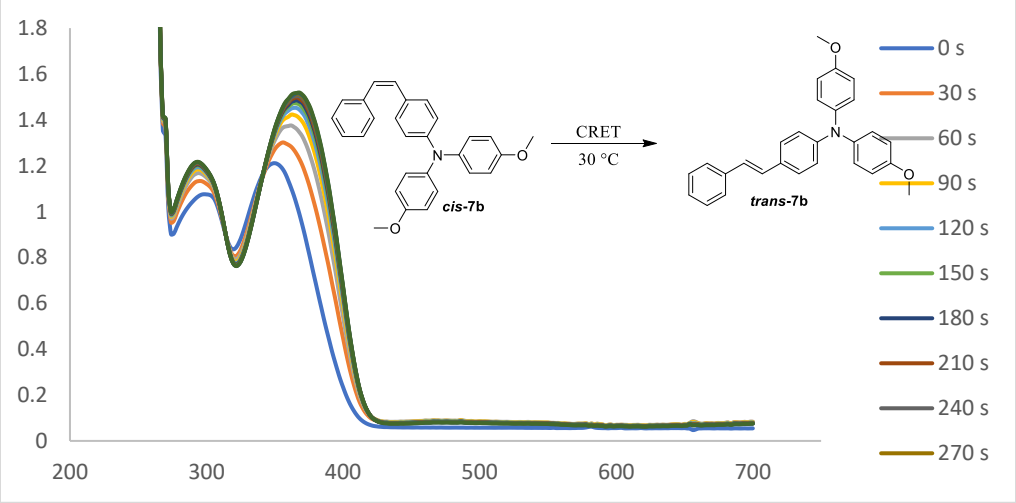

Figure 2.40. Optical spectrum of addition of CRET (5 mol% in DCM) to 3.02 X 10^{-5} M solution of ***cis*-7b** in 5 % deareated benzene in cyclohexane.

Time (seconds)	% *cis*	[*cis*]	ln[*cis*]
0	90.4	3.51×10^{-5}	-10.3
30	66.8	2.60×10^{-5}	-10.6
60	51.2	1.99×10^{-5}	-10.8
90	38.9	1.51×10^{-5}	-11.1
120	29.4	1.14×10^{-5}	-11.4
150	23.9	9.30×10^{-6}	-11.6
180	20.1	7.80×10^{-6}	-11.8
210	17.3	6.73×10^{-6}	-11.9
240	15.2	5.90×10^{-6}	-12.0
270	13.9	5.38×10^{-6}	-12.1
300	12.9	5.02×10^{-6}	-12.2
330	12.1	4.68×10^{-6}	-12.3
360	10.5	4.09×10^{-6}	-12.4

Table 2.14. Redox auxiliary promoted *cis-trans* isomerization of 3.02 X 10^{-5} M ***cis*-7b** in cyclohexane: benzene = 98:2 using 5 mol % CRET in DCM at 30 ºC.

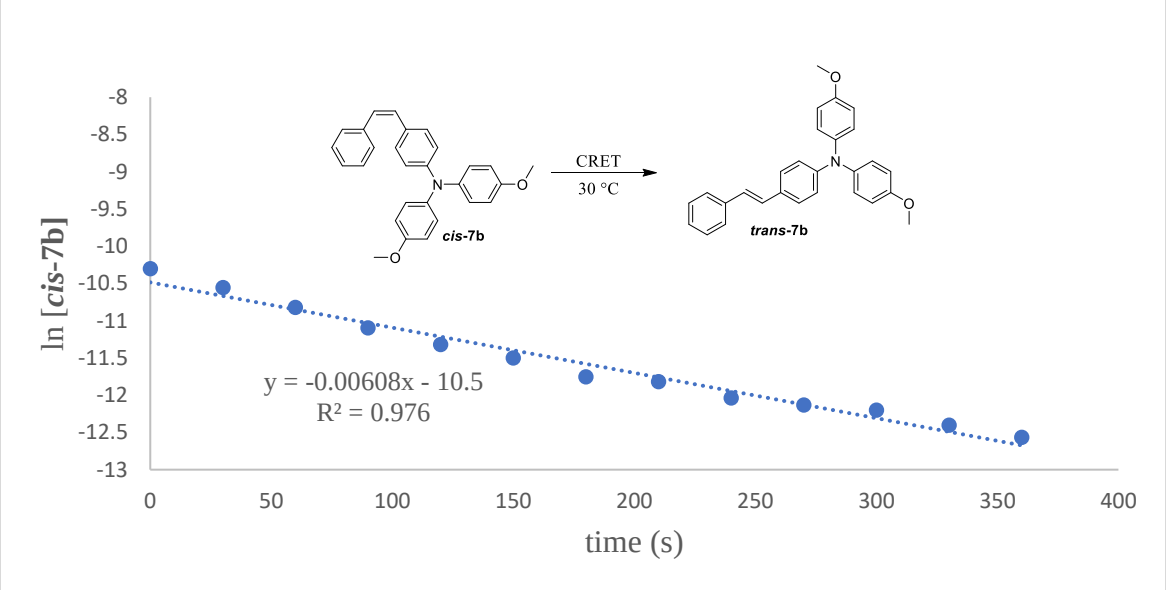

Figure 2.41. First order plot of the ln[***cis*-7b**] vs time at 30 ºC for the redox auxiliary promoted *cis-trans* isomerization of ***cis*-7b** in cyclohexane: benzene =98:2 using 5 mol % CRET in DCM.

2.7.3 Results of the redox auxiliary promoted isomerization of *cis*-7c

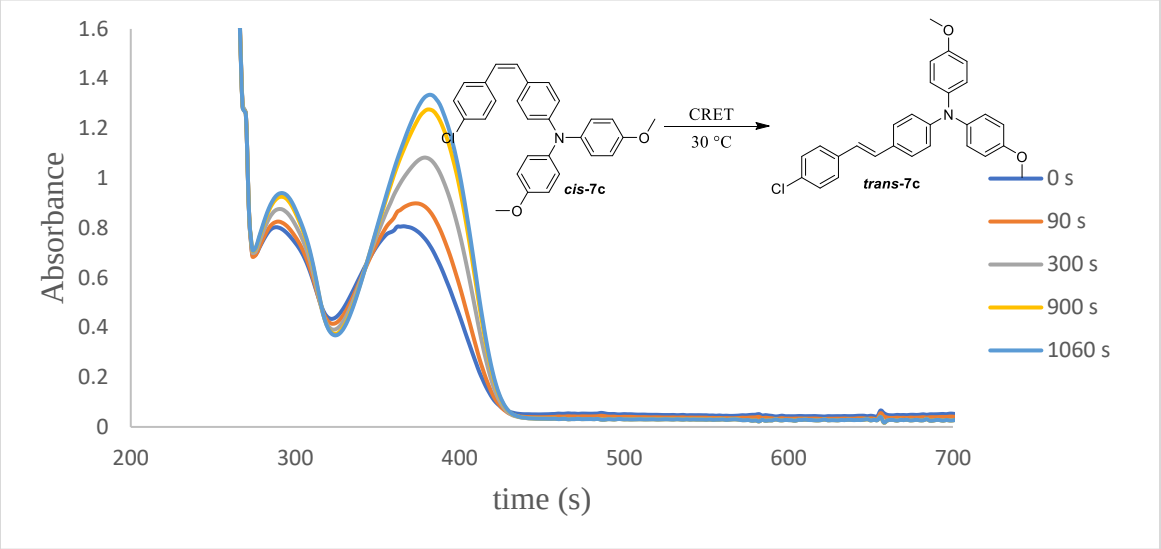

Figure 2.42. Optical spectrum of addition of CRET (5.0 mol% in DCM) to 3.39 X 10^{-5} M solution of ***cis*-7c** in 2 % benzene in cyclohexane.

Time (seconds)	% *cis*	[*cis*]	ln[*cis*]
0	97.0	3.24 x 10^{-5}	-10.3
60	66.0	2.20 x 10^{-5}	-10.7
120	46.2	1.55 x 10^{-5}	-11.1
240	24.5	8.19 x 10^{-6}	-11.7
360	14.8	4.95 x 10^{-6}	-12.2
480	9.49	3.17 x 10^{-6}	-12.7
600	6.10	2.04 x 10^{-6}	-13.1
720	3.77	1.26 x 10^{-6}	-13.6
840	2.39	7.99 x 10^{-6}	-14.0
960	0.683	2.28 x 10^{-7}	-15.3

Table 2.15. Redox auxiliary promoted *cis-trans* isomerization of 3.39 X 10^{-5} M ***cis*-7c** in cyclohexane: benzene = 98:2 using 5 mol % CRET in DCM at 30 ºC.

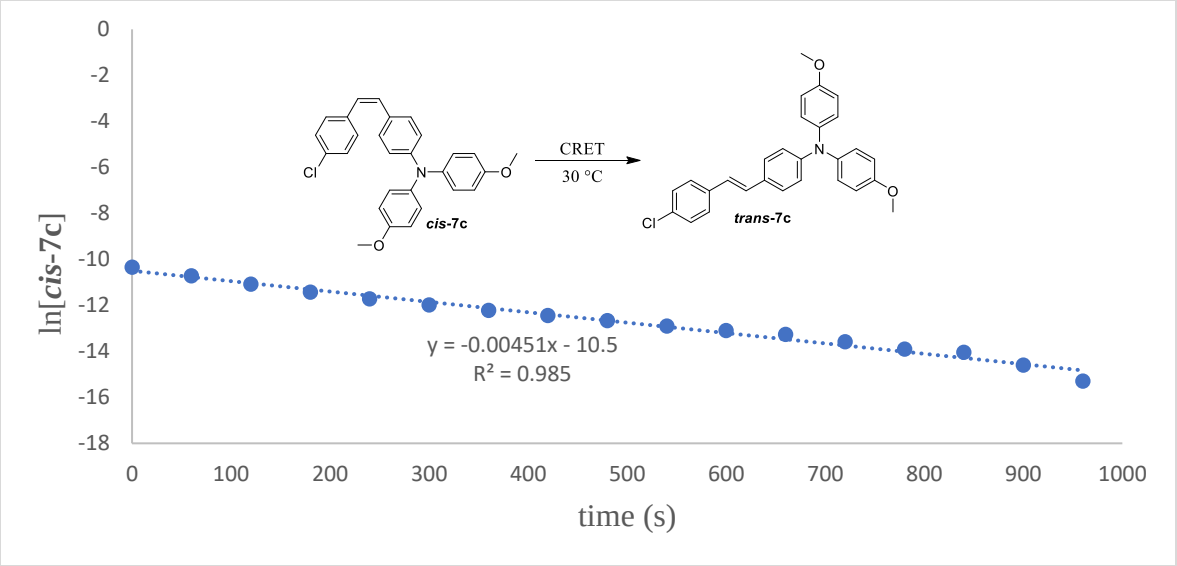

Figure 2.43. First order plot of the ln[***cis*-7c**] vs time at 30 ºC for the redox auxiliary promoted *cis-trans* isomerization of ***cis*-7c** in cyclohexane: benzene =98:2 using 5 mol % CRET in DCM.

2.7.4 Results of the redox auxiliary promoted isomerization of *cis*-7d

Time (seconds)	*% cis*	[*cis*]	ln[*cis*]
0	96.2	3.24E x 10^{-5}	-10.3
180	76.1	2.56 x 10^{-5}	-10.6
360	56.6	1.90 x 10^{-5}	-10.9
540	42.2	1.42 x 10^{-5}	-11.2
720	31.9	1.07 x 10^{-5}	-11.4
900	24.2	8.15 x 10^{-5}	-11.7
1080	18.3	6.17 x 10^{-5}	-12.0
1260	13.7	4.61 x 10^{-5}	-12.3
1440	10.0	3.38 x 10^{-5}	-12.6
1620	7.01	2.36 x 10^{-5}	-13.0
1800	4.83	1.63 x 10^{-5}	-13.3
1980	3.01	1.01 x 10^{-5}	-13.8
2160	1.38	4.64 x 10^{-5}	-14.6

Table 2.16. Redox auxiliary promoted *cis-trans* isomerization of 3.02 X 10^{-5} M ***cis*-7d** in cyclohexane: benzene = 98:2 using 5 mol % CRET in DCM at 30 ºC.

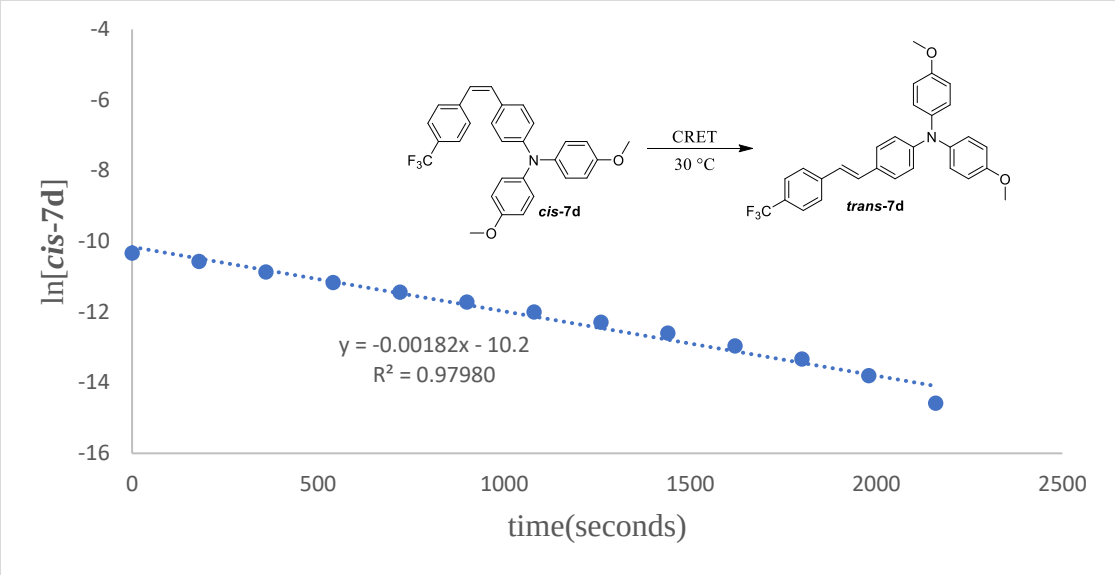

Figure 2.44. First order plot of the ln[***cis*-7d**] vs time at 30 ºC for the redox auxiliary promoted *cis-trans* isomerization of ***cis*-7d** in cyclohexane: benzene =98:2 using 5 mol % CRET in DCM.

2.7.5 Results of the redox auxiliary promoted isomerization of *cis*-7e

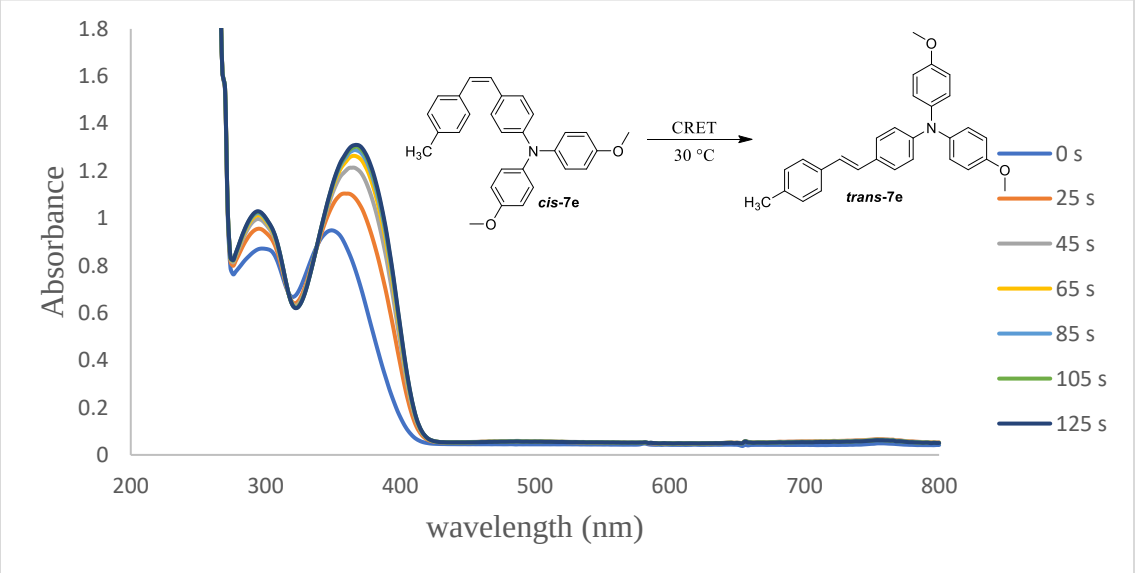

Figure 2.45. Optical spectrum of addition of CRET (5 mol% in DCM) to 3.08 X 10^{-5} M solution of ***cis*-7e** in 5 % benzene in cyclohexane.

Time (seconds)	% *cis*	[*cis*]	ln[*cis*]
0	98.5	3.18×10^{-5}	-10.4
25	42.9	1.38×10^{-5}	-11.2
45	19.6	6.33×10^{-6}	-12.0
65	10.3	3.32×10^{-6}	-12.6
85	5.80	1.87×10^{-6}	-13.2
100	2.86	9.22×10^{-7}	-13.9
125	1.62	5.22×10^{-7}	14.5

Table 2.17. Redox auxiliary promoted *cis-trans* isomerization of 3.02 X 10^{-5} M ***cis*-7e** in cyclohexane: benzene = 98:2 using 5 mol % CRET in DCM at 30 ºC.

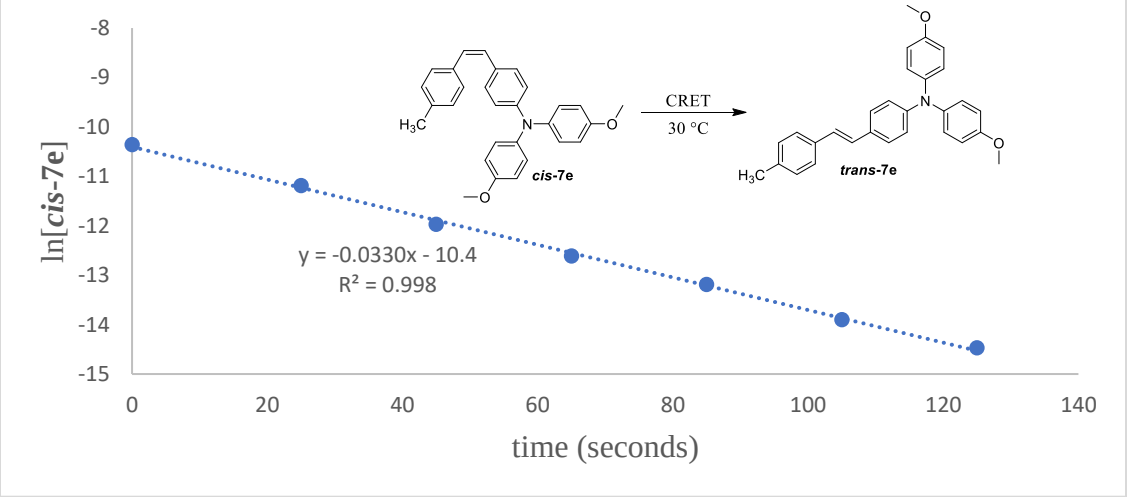

Figure 2.46. First order plot of the ln[***cis*-7e**] vs time at 30 ºC for the redox auxiliary promoted *cis-trans* isomerization of ***cis*-7e** in cyclohexane: benzene =98:2 using 5 mol % CRET in DCM.

The $\Delta G^{\ddagger}$ of the RA-promoted radical isomerization of ***cis*-7e** was obtained by evaluating the reaction at different temperatures (25 ºC – 50 ºC) using 5 mol % of CRET (Table 2.18). An Eyring plot of the rate constant ln (k/T) against 1/T gave a linear fit (Figure 2.47) and the $\Delta H^{\ddagger}$ (10.9 kcal/mol) and $\Delta S^{\ddagger}$ (-29.3 e.u) were obtained from the slope and intercept respectively. The

graph of the rate constant against mol % of CRET was extrapolated to obtain the k for the addition of 100 mol % CRET. The RAC *cis* to *trans* stilbene isomerization rate enhancement at 303 K was obtained by dividing the rate of the radical process for 5 mol % CRET by the rate of the neutral process at the same temperature. This was found to be 10^7 times faster relative to the the neutral (Table 2.19). A summary of the activation parameters for the RA promoted neutral/radical isomerization of ***cis*-7a** is shown in Table 2.20.

T (K)	k	ln(k/T)	1/T	ln(k)
298	0.0226	-9.49	0.00336	-3.79
303	0.0330	-9.12	0.00330	-3.41
308	0.0489	-8.75	0.00325	-3.02
313	0.0657	-8.45	0.00320	-2.72
318	0.0860	-8.22	0.00315	-2.45
323	0.104	-8.04	0.00310	-2.27

Table 2.18. First order rate constants of the RA promoted *cis-trans* isomerization of 3.02 X 10^{-5} M ***cis*-7e** in cyclohexane: benzene = 98:2 using 5 mol % CRET in DCM.

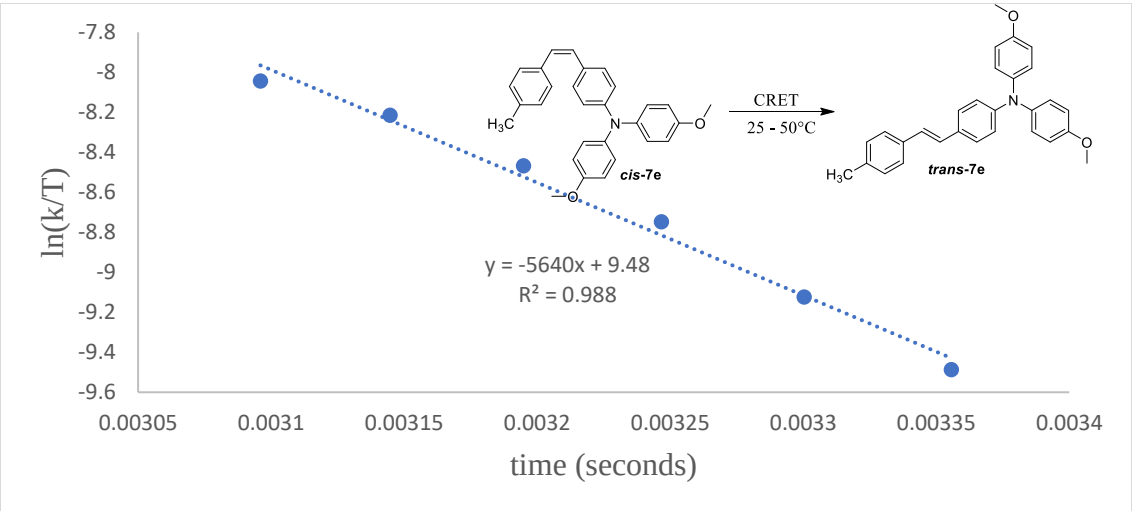

Figure 2.47. Eyring plot of the RA radical isomerization of ***cis*-7e.**

Neutral isomerization	**Activation parameters**
K_{413K} (s^{-1})	2.47 x 10^{-5}
$\Delta G^{\ddagger}_{413K}$ (kcal/mol)	32.3
$\Delta S^{\ddagger}$ (eu)	-24.5
$\Delta H^{\ddagger}$ (kcal/mol)	22.2
$\Delta G^{\ddagger}_{303K}$ (kcal/mol)	30.2
k_{303K} (s^{-1})	1.08 x 10^{-9}
Radical isomerization	
k_{303K} (s^{-1}) 5 mol % CRET	0.0330
k_{303K} (s^{-1}) 100 mol % CRET	1.04
$\Delta G^{\ddagger}_{303K}$ (kcal/mol) 100 mol % CRET	17.7
$\Delta H^{\ddagger}$ (kcal/mol)	10.9
$\Delta S^{\ddagger}$ (eu)	-28.5
$\Delta\Delta G$ (kcal/mol)	12.5
Rate acceleration for 5 mol % CRET	3.31 x 10^{7}
Rate acceleration for 100 mol % CRET	9.63 x 10^{8}

Table 2.19. Summary of the activation parameters for the RA promoted neutral/radical isomerization of ***cis*-7e**.

2.7.6 Summary of the results of the neutral and radical processes

Substrate	k_{413K} (s^{-1})	$\Delta G^{\ddagger}_{413K}$ neutral process	k_{303K} neutral process	k_{303K} (s^{-1}) radical process	$\Delta G^{\ddagger}_{303\,K}$ radical process	Rate acceleration
***cis*-7a OMe-St-NAr_2**	2.10×10^{-5}	33.3	1.42×10^{-9}	0.0625	19.4	4.41×10^{7}
***cis*-7b H-St-NAr_2**	1.86×10^{-5}	34.0	1.19×10^{-9}	0.00608	20.8	5.09×10^{6}
***cis*-7c Cl-St-NAr_2**	3.10×10^{-5}	33.0	5.38×10^{-9}	0.00452	21.0	3.39×10^{5}
***cis*-4d CF_3-St-NAr_2**	3.28×10^{-5}	32.8	1.04×10^{-9}	0.00182	21.8	1.75×10^{5}
***cis*-4e Me-St-NAr_2**	2.47×10^{-5}	33.2	1.08×10^{-9}	0.0357	19.8	3.71×10^{7}

Table 2.20. Summary of the results of the neutral and radical processes.

In summary, the occurrence of the isomerization at lower temperature indicates that the activation energy for the isomerization of the stilbene radical cation is substantially lower than that of the neutral stilbene, as shown the Table 2.13. There was no formation of phenanthrene nor any cyclization product due to the absence of UV-Vis peaks at λ_{max} 450 nm and 480 nm for phenanthrene[104] and the dimeric product[133] respectively. This indicates that neither the cyclization of the stilbene radical cation to the dihydrophenanthrene radical cation nor the dimerization of the stilbene radical cation competes with the isomerization process of this reaction.

The rate of the isomerization of the *p*-substituted *cis*-stilbene radical increased with the introduction of electron-donating substituents on the para positions of the phenyl ring not

containing the RA group. The substituent's ability to delocalize the radical cation in the transition state structure affects the rate of the reaction. Delocalizing the radical cation stabilizes the transition state structure. From the valence bond viewpoint, stabilization is a result of the interaction of the radical center with the nonbonding electron pair of the electron donating groups. The electron donating groups decrease the barrier for the *cis* to *trans* transformation by localizing the positive charge (hole) on the electron donating groups. This would account for the stabilizing ability of the electron donating groups vs the destabilizing influence of the electron withdrawing groups.[136] The substitutions in ***cis*-7a** and ***cis*-7e** enhance the separation and delocalization of the positive charge on the nitrogen atom of the RA group and an unpaired electron on the olefinic carbon (charge-spin separation). This induces a twisted conformation with a large twist angle and more C-C single-bond character for the central C=C double bond (Scheme 2.11). The increase in the single bond character of the C-C bond increases the rate of isomerization of the *cis*-stilbene radical cation. So, the ability of substrates ***cis*-7a** and ***cis*-7e** to stabilize the radical cation leads a stabilized lower energy transition state thereby enhancing their isomerization rate.

The mechanism of the radical *cis-trans* isomerization of RA-stilbenes is shown in Scheme 1.12. The *trans*-stilbene-RA$^{\bullet+}$ is chemically stable and can exchange an electron with the neutral *cis* isomer thereby generating a catalytic cycle for isomerization of *cis*-stilbene-RA.

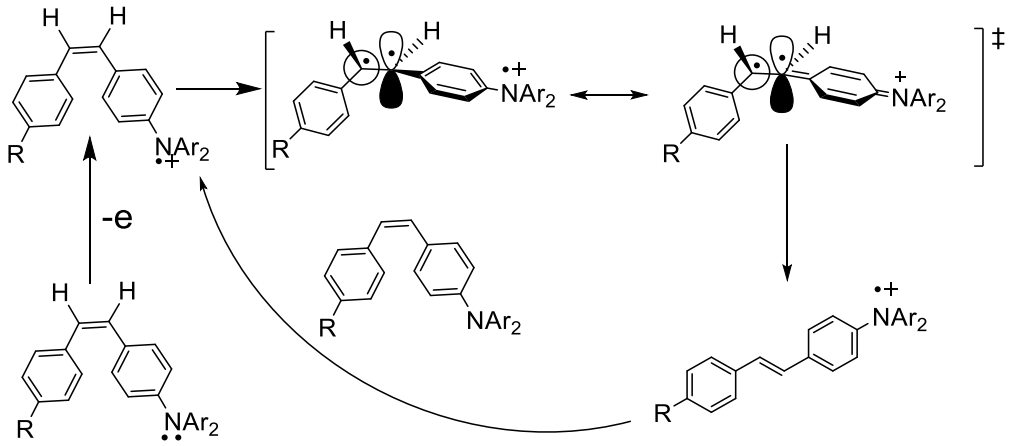

Scheme 2.12. Mechanism of the cation radical isomerization of *cis*-RA stilbenes.

2.7.7 Thin cell Photo-Electro Device (PED)

After showing that we can exponentially increase the rate of *cis*-to *trans* isomerization of para-redox stilbenes through catalytic electron transfer cycle with a one electron oxidant, it was necessary to reproduce the results using a different oxidation method. We anticipated that applying 1.8 V would oxidize the *cis* isomer and cause a facile isomerization to the *trans* isomer (via a catalytic electron transfer cycle) similar to that of Scheme 2.11. Figure 2.48 illustrates the design of the photo-electro cell device used to test the effect of electricity on the *cis* isomers.

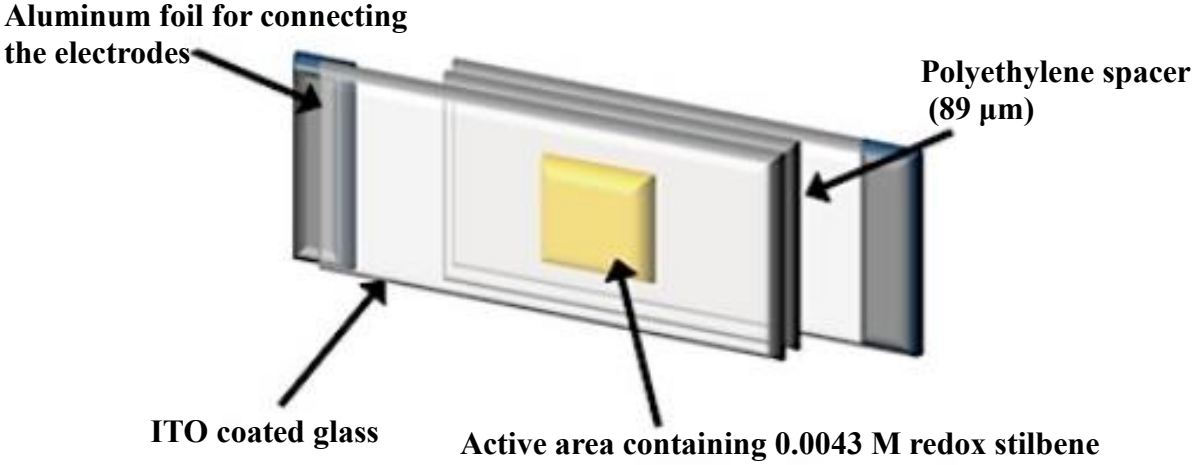

Figure 2.48. Photo-electro cell device designed to test the effect of electricity on the *cis* isomers of *para*-redoxstilbenes. Picture adapted from M.D Kelley's dissertation.[137]

Trans*-7a** was chosen for this experiment because the *cis*-isomer (cis*-7a**) has the fastest radical catalyzed *cis-trans* isomerization rate when compared to ***cis*-7b-e**. Isomerization of ***trans*-7a** to ***cis*-7a** was achieved by irradiating ***trans*-7a** (4.30×10^{-3} M) with 405 nm LED for 120 seconds, and then 1.8V was immediately applied to the sample for 200 seconds to regenerate the ***trans*-7a** isomer as shown in Figure 2.49. This illustrates that isomerization from ***trans*-7a** to ***cis*-7a** was obtained by irradiating with 405 nm light, therefore turning "OFF" the switch. The switch was then turned back "ON" by applying a 1.8 V to the ***cis*-7a**, thus regenerating the ***trans*-7a**.

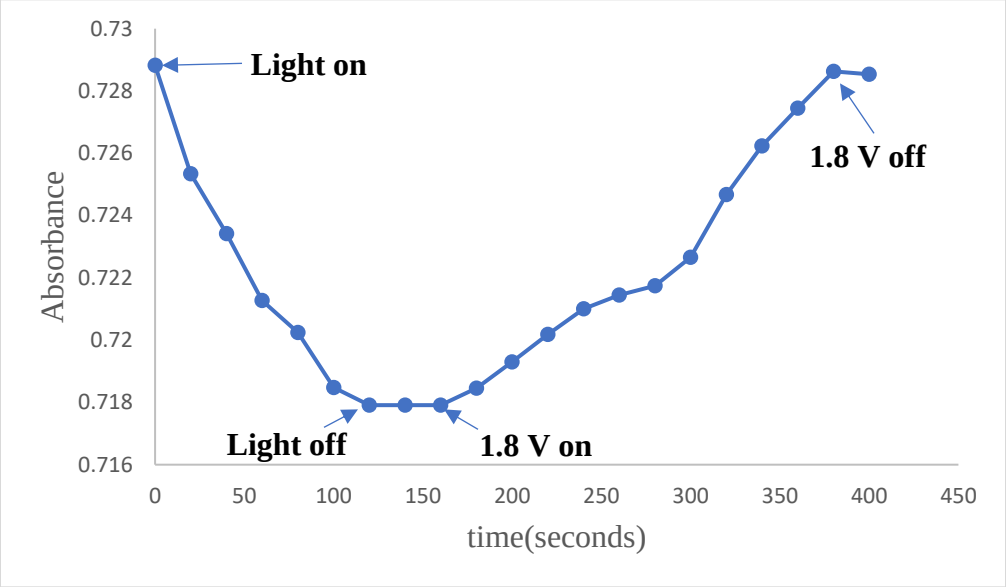

Figure 2.49. Photo-electro cell device. Irradiation for 120 seconds with 405 nm LED corresponds to the decreases in absorbance. Application of 1.5 V for 200 seconds corresponds to the increases in absorbance.

2.8 Conclusions

The results obtained in this chapter support our hypothesis that the activation barriers of the *cis* to *trans* isomerization of stilbenes can be reduced by oxidizing an appended diaryl amino

RA with a one electron oxidant. This method of *cis* to *trans* isomerization of stilbene converts the neutral *cis*-RA-stilbene to the cation radical which will then initiate a chain reaction in which *cis*-RA-stilbene radical cation will isomerize to the more stable *trans*-stilbene radical cation.

Electron donating substituents attached in conjugation with the olefinic bond will tend to elongate the olefinic bond by resonance stabilization. This increases the single bond character of the C=C bond, thereby lowering the rate determining barrier and enhancing the isomerization of the *cis*-stilbene radical cation. The lower energy transition state is as a result of the interaction between the odd electron in the benzylic radical and RA. The benzyl-type radical intermediate has additional resonance stabilization and consequently, the energy of the transition state is reduced.

2.9 Experimental details

Materials and instrumentation. Deuterated solvents were purchased from Cambridge isotopes and used without further purification. All Pd-catalyzed reactions were performed under N_2 atmosphere. $Pd(dba)_2$ and $Pd_2(dba)_3$ were purchased from Ark Pharm Inc while $P(tBu)_3$ and NaOtBu were purchased from Alfa Aesar. $Pd(dba)_2$, $Pd_2(dba)_3$, $P(tBu)_3$ and NaOtBu were all weighed out in a dry box. $TBAPF_6$ was purchased from Oakwood Chemical and purified by 2-3 recrystallizations from ethanol and dried under vacuum at 70 ºC for 10 hours.[138] Activity III alumina was prepared by the addition of 6% H_2O to basic alumina (Aldrich, activated Brockmann I, ~150 mesh). Sodium methoxide (25 % weight in methanol) was purchased from Sigma Aldrich.

Purification of solvents. Methylene chloride, cyclohexane, and benzene were purified according to standard literature procedures by washing with H_2SO_4, water, saturated $NaHCO_3$ and distilled over calcium hydride.[139]

Preparation of Tol_3TBABF_4 gel[140]- In a 50 mL oven dried glass jar equipped with a stir bar, 5.33 g of $TBABF_4$ was dissolved in 15 mL of toluene by gently heating. The stirring was stopped after 5 min or when $TBABF_4$ dissolved to allow the colorless solution phases to settle. The bottom phase was Tol_3TBABF_4 gel (10 mL, 1.62 M) and the top phase was toluene (5 mL) as determined by ^1H NMR spectroscopy.[137] The jar was then capped and stored in a cabinet at room temperature under ambient conditions.

Apparatus- ^1H and ^{13}C NMR spectra were recorded on Bruker AV-360 or AV-500 NMR spectrophotometers using $CDCl_3$, C_6D_6, and DMSO-d_6 as solvents and referenced to the residue H-signals of the deuterated solvents. FT-IR spectra were recorded on a JASCO 4100 equipped with a Pike Technologies MIRacle^{TM} ATR cell for analyzing solid samples. UV-Vis optical spectra were recorded on a HP8452A Diode Array Spectrophotometer. Electrochemistry was performed using a PAR 273 electrochemical potentiostat (EG&G Instruments). Redox potentials were referenced to an SCE standard potential and also measured relative to the Fc/Fc^+ redox couple. Typically, purified CH_2Cl_2 containing $TBAPF_6$ (0.1 M) as a supporting electrolyte was used as the solvent for electrochemical measurements. Automated column chromatography was performed on a Teledyne ISCO CombiFlash® Rf 200i or by manual flash column chromatography using silica gel (Silicycle®, 60 Å, 230-400 mesh) as a stationary phase and with elution solvent mixtures reported as volume ratios. X-ray diffraction data were gathered on a Siemens CCD SMART diffractometer and the software package *SHELXTL/PC*, version 6.14 package[141] was used for structure solution and refinement. Melting points were recorded on a Mel Temp apparatus by Laboratory Devices and are uncorrected. The Buchwald/Hartwig amination reactions were carried out in a dry box (OMNI-LAB System) from Vacuum

Atmosphere company. The sonicator (Solid state/ultrasonic FS-14) and the Isotemp constant temperature circulator (Model 80) were purchased from Fischer Scientific.

Photo-electrochemical cell

ITO glass cleaning procedure[137]- ITO coated glass was purchased from Delta Technologies (part no. CB-50IN-1111). The slide was rinsed and soaked in ACS grade acetone for 5.0 min. It was then sonicated for 10 min in diluted aqueous soap solution. After sonication, the slide was rinsed thoroughly with distilled water, acetone, and methylene chloride respectively. The surface was then dried using a stream of dry N_2 gas. The ITO side of the slide was determined using multi-meter resistance measurement.

Preparation of plastic spacer- Polyethylene Plastic Sheeting (Husky Brand) was purchased from Lowes and used as a spacer in PECD. The thickness of the spacer as indicated on the label was 88.9 μm. This thickness was checked with a caliper and found to be correct. A square area: (~1.5 cm^2) was cut out of the plastic sheet before applying it to a clean ITO glass substrate.

The light sources for irradiation- See Appendix H for the excitation spectra of the LED light souces.

LED light wavelength (nm)	Power	Source	Input volatge
430	7 X 1 W	Zhongshan LED Technology Co., Ltd	90-264 V
395-410	1 X 7 W	ADJ Products on Amazon	100-240 V

Synthesis

CRET

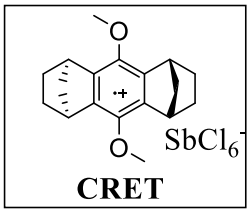

CRET

The synthesis and purification of CRET (cation radical electron transfer) reagent was carried out by following the reported procedure by Rathore R *et al.*[142] The UV-Vis spectrum of CRET in dichloromethane has a λ_{max} = 518 nm, shoulder at 486 nm (see Appendix J.1) and a reported extinction coefficient of 7300 M^{-1} cm^{-1} at 518 nm. The purity can be evaluated by UV-Vis analysis as follows. 1.00 mg of CRET was dissolved in 10 mL of anhyd DCM in a volumetric flask and the absorbance was monitored at 518 nm using a 1 cm quartz cuvette. The solution showed an absorbance of 1.20 at 518 nm (concentration = 1.65×10^{-4} M, ε_{518} = 7270 M^{-1} cm^{-1}, lit[142] ε_{518} = 7300 M^{-1} cm^{-1} , 99.6 % pure). The authors reported that CRET which is > 99% pure can be stored in a glass bottle at ambient temperatures indefinitely but we stored our sample of the pure CRET in a refrigerator (- 2 ºC).

Dianisylamine 5

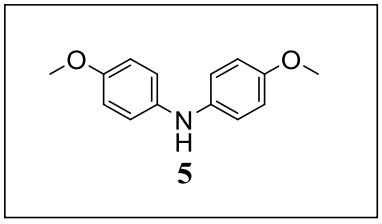

5

5 was prepared as previously reported.[51, 143] p-anisidine (4.93 g, 40.0 mmol) and p-bromoanisole (7.39 g, 39.5 mmol) were added to a 100 mL flamed-dried round bottomed (rb) flask containing a magnetic stir bar in a dry box. Toluene (anhyd 60 mL) was added to the flask and the mixture was stirred. $Pd(dba)_2$ (0.115 g, 0.200 mmol, 0.500 mol %), $P(tBu)_3$ (0.0405 g, 0.200 mmol, 0.500 mol %,) were added into the mixture and the mixture was stirred for about one minute. NaOtBu (5.77 g, 60.0 mmol, 1.50 eq) was then added and the flask was capped with a rubber septum, removed from the dry box and stirred under N_2 for 1 hr at 90 °C. The reaction mixture was monitored via TLC (ethyl acetate: hexane =1:4) until it showed the disappearance of the starting

materials at about 1 hr. The mixture was then cooled to room temperature, filtered through a plug of about 5 g of activated basic alumina (activity III) in a fritted funnel which was then rinsed with 200 mL of ethyl acetate. The product solution was concentrated in vacuo to yield the crude product which was recrystallized in hexane to afford the pure **5** (8.71 g, 95.0 %) as nearly colorless crystals. mp 102 ºC ^{1}H NMR (360 MHz, $CDCl_3$): δ (ppm) 6.94 (d, J = 8.9 Hz, 4H), 6.83 (d, J = 8.9 Hz, 4H), 5.29 (s, 1H), 3.78 (s, 6H). ^{13}C NMR (125 MHz, $CDCl_3$): δ (ppm) 154.2; 138.0; 119.6; 114.7; 55.7

(4-bromobenzyl) triphenylphosphonium bromide, $Ph_3BrBnP^+Br^-$

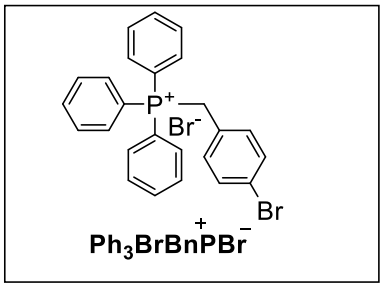

This phosphonium salt was prepared as previously reported.[144] A solution of 10.0 g (40.0 mmol) of 4-Bromobenzyl bromide and 12.6 g (48.1 mmol) of triphenylphosphine in 100 ml of dry toluene was refluxed for 12 h. After cooling to room temperature, a precipitate formed which was filtered off and washed with ~10 mL of toluene. Drying in vacuo afforded (4-bromobenzyl)triphenylphosphonium bromide. White powder, yield (19.7 g, 96.1 %). mp 274-275 ºC ^{1}H NMR (360 MHz, $CDCl_3$): δ 7.81-7.73(m, 9H), 7.64-7.59 (m, 6H), 7.20 (d, 8.40 Hz, 2H), 7.07 (dd, 8.40 Hz, 2.5 Hz, 2H), 5.59 (d, 14.3 Hz, 2H).

General Wittig procedure for the preparation of *cis*-6a-e and *trans*-6a-e.[145]

The ***cis*-6a** and ***trans*-6a** were synthesized by adapting a previously reported procedure.[145] A solution of sodium methoxide (0.720 g, 13.3 mmol (source is 25 % w/v NaOme in methanol, from Sigma Aldrich)) in methanol (15 mL) was added dropwise to a suspension of the (4-bromobenzyl) triphenylphosphonium bromide salt (6.27 g, 12.2 mmol) and *p*-anisaldehyde (1.39 g, 10.2 mmol) in methanol (20 mL) under N_2 with stirring at room temperature. After completion of the addition, the resulting solution was stirred for 1 h at room temperature and then the

mixture was poured into cold water (60 mL), treated with 10 mL of saturated $NaHCO_3$, extracted with EtOAC (3 x 15 mL) and the EtOAC extracts were combined and dried over anhyd $MgSO_4$. The solution was gravity filtered and solvent removed under reduced pressure to give a crude product as a white solid. The resulting solid, which contains a mixture of *cis* & *trans*-stilbenes and triphenylphosphonium oxide, was then taken up in hexane (50 mL) to give a slurry which was then cooled in a freezer (~ -20 ºC) for 6 hours and then cold suction filtered through a frit funnel to recover 1.37 g (47.4 %) of the pure ***trans*-6a** as a colorless solid. The mother liquor containing a mixture of the phosphonium oxide and ***cis*-6a** was evaporated in vacuo to give an oily compound, which was then dissolved in 20 mL ethyl acetate/hexane (1:8) and suction filtered through a plug of silica gel (~0.5 in height x 1.0 in diameter in a 25 mL filter funnel)) with rinsing using ethyl acetate/hexane (1:8) to remove the phosphonium oxide and isolate the pure ***cis*-6a** as a yellow oil (1.27 g, 44.0 %) after solvent removal in vacuo. Total yield = 2.64 g, 91.4 %

[An alternative procedure for isolating ***cis*-6a** is also described here. The above oily residue containing the *cis* isomer and Ph_3PO was dissolved in ~20 mL chloroform/hexane (1:1), cooled to -20 ˚C for 6 h to precipitate Ph_3PO, which was removed by suction filtration through a frit funnel, followed by solvent removal in vacuo to give pure ***cis*-6a** as a colorless oil.]

cis-4-bromo-4′-methoxystilbene _cis_-6a

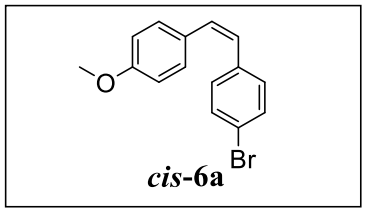

***cis*-6a**

***cis*-6a** has previously been reported.[146-147] The compound was obtained as a colorless oil (1.27 g, 44.0 %). ^{1}H NMR (500 MHz, $CDCl_3$) δ (ppm) 7.45 (d, J = 8.4 Hz, 2H), 7.26 (d, J = 8.8 Hz, 2H), 7.23 (d, J = 8.4 Hz, 2H), 6.86 (d, J = 8.8 Hz, 2H), 6.66 (d, J = 12.1 Hz, 1H), 6.51 (d, J = 12.1 Hz, 1H), 3.87 (s, 3H).

***trans*-4-bromo-4′-methoxystilbene *trans*-6a**

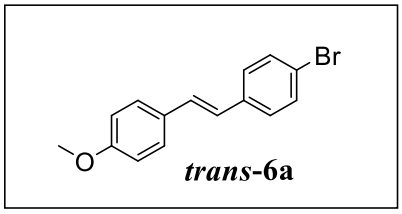

***trans*-6a**

***trans*-6a** has previously been reported.[148] The compound was obtained as a colorless solid (1.37 g, 47.4 %). mp 199-200 °C, lit 200-201 °C[148] ^{1}H-NMR (500 MHz, $CDCl_3$): δ (ppm) 7.48 (d, J = 8.2 Hz, 2H), 7.47 (d, J = 8.2 Hz, 2H), 7.37 (d, J = 8.2 Hz, 2H), 7.07 (d, J =16.2 Hz, 1H), 6.94-6.91 (m, 3H), 3.88 (s, 3H).

***cis*-4-bromostilbene *cis*-6b**

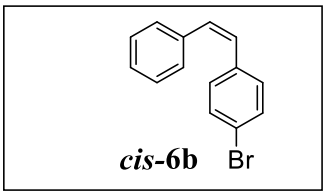

***cis*-6b**

***cis*-6b** has been previously reported.[148-149] It was synthesized by using the above Wittig procedure from benzaldehyde (509 mg, 4.80 mmol), (4-bromobenzyl) triphenylphosphonium bromide (2.95 g, 5.76 mmol) and sodium methoxide (0.342 g, 6.34 mmol) in 20 mL of methanol. The crude product containing a mixture of ***cis*-6b**, ***trans*-6b** and phosphonium oxide was purified by column chromatography on silica gel using hexane to give pure ***cis*-6b** as a colorless oil (0.537 g, 43.2%) and the pure ***trans*-6b** as a colorless solid (0.607 g, 48.8 %.) (elutes second). ^{1}H NMR of ***cis*-6b** (360 MHz, $CDCl_3$) δ (ppm) 7.37 (d, 2H), 7.29-7.20 (m, 5H), 7.13 (d, 2H), 6.66 (d, J = 12.2 Hz, 1H), 6.53 (d, J = 12.2 Hz, 1H)

***trans*-4-bromostilbene *trans*-6b**

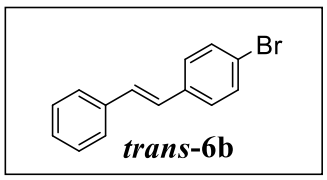

***trans*-6b**

***trans*-6b** has been previously reported.[148] It was obtained as colorless solid (0.607 g, 48.8 %.) as indicated above. mp 139-140 °C, lit 115-117 °C,[149] ^{1}H NMR (360 MHz, $CDCl_3$): δ (ppm) 7.48 - 7.41 (m, 4H), 7.36 - 7.30 (m, 4H), 7.26 - 7.21 (m, 1H), 7.06 (d, J = 16.3 Hz, 1H), 6.99 (d, J = 16.3 Hz, 1H)

***cis*-4-bromo-4′-chlorostilbene *cis*-6c**

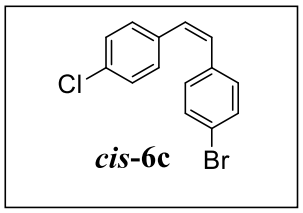

***cis*-6c**

***cis*-6c** has been previously reported.[150] The compound was prepared by using the above Wittig procedure from 4-chlorobenzaldehyde (703 mg, 5.00 mmol), (4-bromobenzyl) triphenylphosphonium bromide (3.07 g, 6.00 mmol) and sodium methoxide (0.357 g, 6.60 mmol) in 25 mL of methanol. The resultant work up included the extraction of the basic aqueous/methanol solution with ethyl acetate (3 x 15 mL), drying over anhyd $MgSO_4$ and evaporation in vacuo to give the crude product as a colorless solid. The crude product was taken up in cyclohexane, filtered through a frit funnel and washed with acetone (15 mL) to recover the ***trans*-6c** which is insoluble in both solvents. The mother liquor was evaporated in vacuo and purified by column chromatography on silica gel using hexane to give 730 mg of ***cis*-6c** as a colorless oil (49.7 %). ^{1}H NMR (360 MHz, $CDCl_3$): δ (ppm) 7.42 (d, 2H, J = 8.5 Hz), 7.27 (d, 2H, J = 8.5 Hz), 7.20 (d, 2H, J = 8.5 Hz), 7.14 (d, 2H, J = 8.5 Hz), 6.63 (d, 1H, J = 12.1 Hz), 6.58 (d, 1H, J = 12.1 Hz)

***trans*-4-bromo-4′-chlorostilbene *trans*-6c**

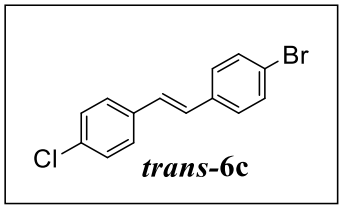

***trans*-6c**

***trans*-6c** has been previously reported.[151] The crude product ***trans*-6c** product was recovered from the filtration of the cyclohexane solution mentioned above and washed with 15 mL of acetone to give the 593 mg of ***trans*-6c** as a colorless solid (40.4 % yield). mp 225-227°C, lit 226-228 °C[151] ^{1}H NMR (500 MHz, $CDCl_3$): δ (ppm) 7.54 (d, 2H, J = 8.5 Hz), 7.49 (d, 2H, J = 8.5 Hz), 7.42 (d, 2H, J = 8.5 Hz), 7.38 (d, 2H, J = 8.5 Hz), 7.32 (s, 2H), 7.10 (d, 1H, J = 16.5 Hz), 7.05 (d, 1H, J = 16.5 Hz)

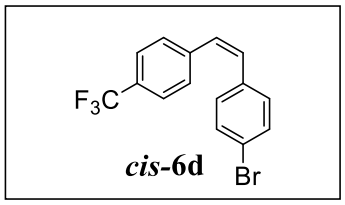

***cis*-6d**

***cis*-4-bromo-4′- trifluoromethylstilbene *cis*-6d**

***cis*-6d** was prepared by using the general Wittig procedure described above from 4-(trifluoromethyl)benzaldehyde (871g, 5.00

mmol), (4-bromobenzyl)triphenylphosphonium bromide (3.07 g, 6.00 mmol) and sodium methoxide (0.428 g, 7.92 mmol) in 25.0 mL of methanol. The resultant work up included the extraction of the basic/aqueous methanol slurry with ethyl acetate (3 x 15 mL), drying over anhyd $MgSO_4$ and evaporation in vacuo to give the crude product which is shown by NMR analysis to contain both ***cis*** and ***trans*-6d**. The stilbene isomers were separated and obtained in pure form by column chromatography on silica gel using hexane to give ***cis*-6d** as a colorless oil (852 mg, 52.1 % yield) and ***trans*-6d** as a colorless solid. ^{1}H NMR of ***cis*-6d** (360 MHz, $CDCl_3$): δ (ppm) 7.50 (d, 2H, J = 8.5 Hz), 7.33 (d, 4H, 8.5 Hz), 7.09 (d, 2H, J = 8.5), 6.65 (s, 2H). ^{13}C NMR (125 MHz, DMSO-D_6): 141.2, 135.8, 131.9, 131.4, 131.1, 129.8, 129.7, 128.0(q), 125.7(q), 123.5, 121.3.

^{19}F NMR (360 MHz, DMSO-D_6): -61.1. ESI-HRMS calcd for $C_{15}H_{10}BrF_3$: 325.9918, found 325.9932

***trans*-4-bromo-4′- trifluoromethylstilbene *trans*-6d**

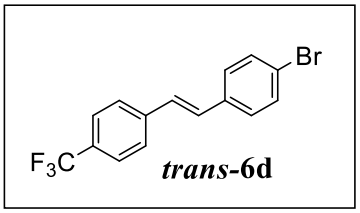

trans-6d has been previously reported.[147] It was obtained as a white solid (705 mg, 43.1 % yield). m.p 146-147 °C, lit 147-148 °C;[147] ^{1}HNMR ($CDCl_3$, 500 MHz) δ (ppm): 7.49 (d, J = 8.4 Hz, 2H), 7.44 (d, J = 8.4 Hz, 2H), 7.37 (d, J = 8.4 Hz, 2H), 7.34 (d, J = 8.4 Hz, 2H), 7.05 (d, J = 16.5 Hz, 1H), 7.00 (d, J = 16.5 Hz, 1H)

***cis*-4-bromo-4′-methylstilbene *cis*-6e**

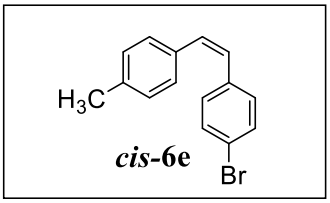

cis-6e has been previously reported.[152] It was synthesized by using the general Wittig procedure from *p*-tolualdehyde (721 mg, 6.00 mmol), (4-bromobenzyl) triphenylphosphonium bromide (3.69 g, 7.20 mmol) and sodium methoxide (0.357 g, 6.60 mmol). The resultant work up included the

extraction of the basic/aqueous methanol slurry with ethyl acetate (3 x 15 mL), drying over anhydrous $MgSO_4$ and evaporation in vacuo to give the crude product as a colorless solid. The crude product was taken up in a mixture of 30 mL of toluene/methanol (1:3), filtered through a frit funnel and washed with 20 mL of acetone to give ***trans-6e***. The mother liquor was evaporated in vacuo, redissolved in ethyl acetate/hexane = 1:8 and filtered through a plug of silica gel to afford the ***cis-6e*** as a colorless oil (803 mg, 49.2 % yield) after evaporation of the solvent. ^{1}H NMR (360 MHz, $CDCl_3$): δ (ppm) 7.36 (d, 2H, J = 8.2 Hz), 7.15-7.12 (m, 4H), 7.06(d, 2H, 8.5 Hz), 6.60 (d, 1H, 12.1 Hz), 6.47 (d, 1H, J = 12.1 Hz), 2.34 (s, 3H)

trans-4-bromo-4′-methylstilbene _trans_-6e

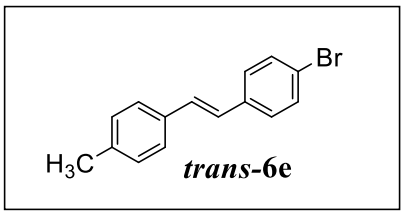

trans-6e

trans-6e has been previously reported.[111] It was obtained as a white solid (702 mg, 43.0 % yield) mp 212-214 °C, lit 213-214 °C[111] ^{1}H NMR (360 MHz, $CDCl_3$): δ (ppm) 7.48 (d, 2H, 8.2 Hz), 7.43-7.36 (m, 4H), 7.18 (d, 2H, J = 8.5), 7.08 (d, 1H, 16.2 Hz), 6.99 (d, 1H, J = 16.2 Hz), 2.37 (s, 3H)

Synthesis of ortho-substituted 4-bromostilbenes 6f and 6g

***cis*-4-bromo- 2′,4′,6′-trimethoxystilbene, *cis*-6f**

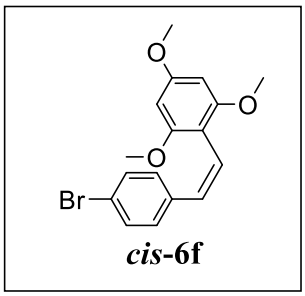

cis-6f

cis-6f was synthesized by using a modified Wittig procedure.[112] Potassium t-butoxide (288 mg, 3.00 mmol) was added in small portions to a solution of (4-bromobenzyl)triphenylphosphonium bromide (1.43 g, 2.80 mmol) in anhyd THF (10 ml) in a rb flask at 0-5 °C under N_2 atmosphere. The resulting mixture stirred at 80 °C for 30 min. Formation of orange color was observed in the reaction. The reaction was cooled to room temperature and 2,4,6-trimethoxybenzaldehyde (0.500 g, 2.50 mmol) was added in one portion. The resulting reaction

mixture was again refluxed at 80 °C for 30 min and then cooled to room temperature. Ethyl acetate (10 ml) was added to the reaction mixture and the solvent was evaporated under vacuo, taken up in water (20 mL), and extracted with ethyl acetate (2 x 50 ml). The organic layer was collected, dried over anhydrous sodium sulfate, filtered and evaporated to dryness to give the crude product. The crude product containing a mixture of ***cis*-6f** and ***trans*-6f** (13.8 % *cis*: 86.2 % *trans*) was purified by silica gel column chromatography using EtOAc/hexane (1:12) to give the ***cis*-6f** as a colorless oil (100 mg, 11.5 %) and ***trans*-6f** as a colorless solid (736 mg, 84.3%). ^{1}H NMR of ***cis*-6f** ($CDCl_3$, 360 MHz): δ 7.28 (d, 2H, 9.03 Hz), 7.03 (d, 2H, 9.03 Hz), 6.57 (d, 2H, 11.8 Hz), 6.44 (d, 2H, 11.8 Hz), 6.11 (s, 2H), 3.84 (s, 3H), 3.61 (s, 6H). ^{13}C NMR (125 MHz, $CDCl_3$): 161.1, 158.3, 138.1, 130.7, 129.7, 129.5, 121.8, 120.1, 107.7, 90.7, 55.4, 55.3

***cis*- *and trans*-4-bromo- 2′,4′,6′-trimethoxystilbene, *cis*-6f and *trans*-6f**

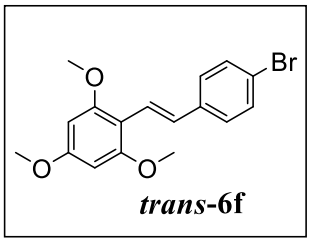

***trans*-6f**

Colorless solid (736 mg, 84.3%). m.p. 99-100 °C, lit = 95-96 °C[112]; ^{1}H NMR ($CDCl_3$, 360 MHz): δ 7.45-7.36 (m, 6H), 6.18 (s, 2H), 3.89 (s, 6H), 3.85 (s, 3H)

***trans*-4-bromo- 2′,6′-trimethoxystilbene *trans*-6g**

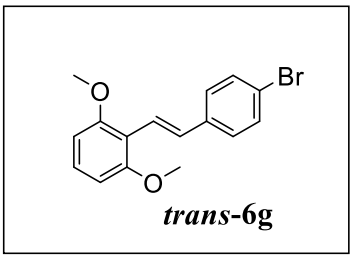

***trans*-6g**

***trans*-6g** has been previously reported.[153-154] 2,6-dimethoxybenzoic acid (0.314 g, 1.72 mmol), 4-bromostyrene (0.278 g, 2.68 mmol), palladium (II) trifluoroacetate (0.106 g, 0.320 mmol), and silver (I) carbonate (1.51 g, 5.50 mmol) were suspended in DMF (20 mL) and DMSO (1.0 mL) under air atmosphere. The reaction mixture was heated at 120 ^{o}C for 3 h, cooled and poured into ethyl acetate (100 mL). The mixture was filtered and the filtrate was washed sequentially with aqueous HCl (1 M, 2 × 80 mL) and brine (40 mL). Then the organic

layer was collected, dried with $MgSO_4$, filtered and concentrated in vacuo. Column chromatography of the residue on silica gel using ethyl acetate/hexane (1:8) yielded ***trans*-6g** as a greenish yellow oil (512 mg, 93.1 %). ^1H NMR (360 MHz, $CDCl_3$) δ 7.53-7.43(m, 3H), 7.42 (d, J = 8.4 Hz, 2H), 7.18 (t, J = 8.4 Hz, 1H), 6.59 (d, J = 8.4 Hz, 2H), 3.90 (s, 6H)

Buchwald/Hartwig amination for the synthesis of dianisylaminostilbenes *trans*-7a -f and *cis*-7a-e.

Original reports by Buchwald *et al.* and Hartwig *et al.* of this kind of N-arylation general prodecure were previously published and our procedure is adapted therefrom.[155-156]

Di-p-anisylamine **5** (0.229 g, 2.00 mmol) and 4-bromo-4-substituted stilbene (2.00 mmol) were added into a 100 mL flamed-dried rb flask in a dry box. Toluene (anhyd 6 mL) was added to the flamed-dried flask and stirred. $Pd(dba)_2$ (11.5 mg, 0.02 mmol, 1.00 mol %), $P(tBu)_3$ (4.05 mg, 0.02 mmol, 1.00 mol %,) were added into the mixture and the mixture was stirred for about one minute. NaOtBu (0.288 g, 3.00 mmol, 1.50 eq) was then added and the flask was capped with a rubber septum, removed from the dry box and stirred under N_2 for 4 h at 90 °C. The reaction mixture was monitored via TLC (ethyl acetate: hexane =1:8) until it showed the disappearance of the starting materials in about 4 h. The mixture was then cooled to room temperature, filtered through a plug of about 5 g of activated basic alumina in a fritted funnel and washed with 15 mL of ethyl acetate. The product was concentrated in vacuo to yield the crude product which was purified by column chromatography to yield desired *p*-dianisylaminostilbene.

***cis*-4-(dianisylamino)-4'-methoxystilbene, *cis*-7a**.

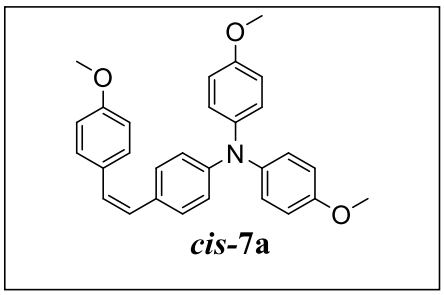

***cis*-7a**

The synthesis of ***cis*-7a** was prepared by using the Buchwald/Hartwig amination for the synthesis of dianisylaminostilbene from **5** (0.229 g, 2.00 mmol) and ***cis*-6a (**0.584 g, 2.02 mmol). The resultant work up included the

filtration of the reaction mixture through a plug of about 5 g of activated basic alumina in a fritted funnel and washed with 15 mL of ethyl acetate and evaporated in vacuo to give the crude product. The crude product was purified by column chromatography on silica gel using diethyl ether/hexane (1:4) to afford a yellow solid containing mainly the *cis* isomer (98.5% ***cis-6a***: 1.50 % ***trans-6a***). Recrystallization in a mixture of diethyl ether/hexane mixture (5:1) afforded ***cis*-7a** as yellow crystals (838 mg, 95.8 %). mp 75-76 °C. ^{1}H NMR (500 MHz, C_6D_6) δ (ppm): 7.47 (d, J = 8.9 Hz, 2H), 7.38 (d, J = 8.9 Hz, 4H), 7.17 (d, J = 8.9 Hz, 4H), 7.06 (d, 2H), 6.78-6.82 (m, 6H), 6.59 (d, J = 12.2 Hz, 1H), 6.56 (d, J = 12.2 Hz, 1H), 3.40 (s, 6H), 3.37 (s, 3H). ^{13}C NMR (125 MHz, DMSO-D_6): 158.6, 156.2, 147.6, 140.2, 130.1, 129.9, 129.7, 128.9, 128.5, 128.0, 127.2, 119.9, 115.4, 114.5, 55.7, 55.5 ESI-HRMS calcd for $C_{28}H_{25}NO_2$: 437.1991, found 437.1993. UV-Vis (1.5 % benzene in cyclohexane) λ_{max} = 354 nm, ε = 24800 cm^{-1} M^{-1}

***trans*-4-dianisylamino-4'-methoxystilbene, *trans*-7a**

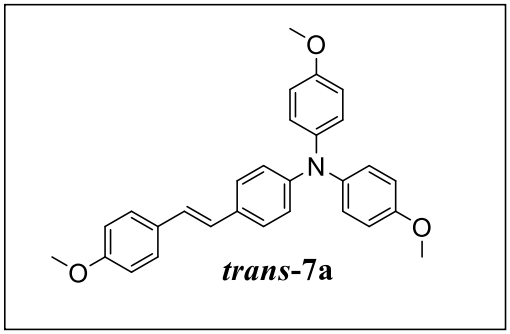

***trans*-7a** has been previously reported.[157] It was prepared by using the Buchwald/Hartwig amination for the synthesis of dianisylaminostilbene from **5** (0.229 g, 2.00 mmol) and ***trans*-6a (**0.584 g, 2.02 mmol). The resultant work up included the filtration of the reaction mixture through a plug of about 5 g of activated basic alumina in a fritted funnel and washed with 15 mL of ethyl acetate and evaporated in vacuo to give the crude product. The crude product was purified by column chromatography on silica gel using diethyl ether/hexane (1:4) to give a nearly colorless Buchwald/Hartwig amination described above and purified by column chromatography on silica gel using diethyl ether/hexane=1:4 to give a yellow solid (841 mg, 96.1 % yield); mp 120-121 °C, lit 117-118 °C[157]. ^{1}H NMR (500 MHz, DMSO-D_6) δ (ppm) : 7.48 (d,

8.9 Hz, 2H) 7.37 (d, 8.9 Hz, 2H), 7.02 (d, 8.9 Hz, 4H), 6.98 (s, 2H), 6.92 (m, 6H), 6.75(d, 8.9 Hz, 2H), 3.77 (s, 3H), 3.75 (s, 6H) ^{13}C NMR (125 MHz, DMSO-D_6): 159.0, 156.2, 148.0, 140.4, 130.6, 129.9, 127.8, 127.5, 127.0, 126.3, 125.8, 119.9, 115.4, 114.6, 55.7, 55.5 ESI-HRMS calcd for $C_{28}H_{25}NO_2$:437.1991, found 437.1991. UV-Vis (1.5 % benzene in cyclohexane) λ_{max} = 374 nm, ε = 44300 cm^{-1} M^{-1}

***cis*-4-(dianisylamino)stilbene, *cis*-7b**

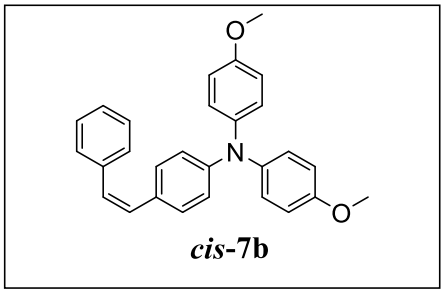

***cis*-7b**

***cis*-7b** was prepared by using the Buchwald/Hartwig amination for dianisylaminostilbene described above from **5** (0.229 g, 2.00 mmol) and ***cis*-6b (**0.523 g, 2.02 mmol). The crude product was purified by column chromatography on silica gel using diethyl ether/hexane (1:4) to give a nearly colorless oil containing mainly the *cis* isomer (93.1 % *cis*: 6.90 % *trans*). 752 mg, 92.3 % yield; ^{1}H NMR (500 MHz, DMSO-D_6) δ (ppm): 7.27-717 (m, 5H). 7.00-7.04 (m, 6H), 6.89 (d, 8.81 Hz, 5H), 6.59 (d, 8.81 Hz, 2H), 6.47 (s, 2H), 373 (s, 6H). ^{13}C NMR (125 MHz, DMSO-D_6): 156.3, 147.9, 140.2, 137.8, 130.1, 129.8, 128.8, 128.5, 128.2, 127.4, 127.3, 127.2, 118.7, 115.4, 55.7 ESI-HRMS calcd for $C_{28}H_{25}NO_2$: 407.1885, found 407.1894. UV-Vis (1.5 % benzene in cyclohexane) λ_{max} = 350 nm, ε = 22800 cm^{-1} M^{-1}

***trans*-4-(dianisylamino)stilbene, *trans*-7b**

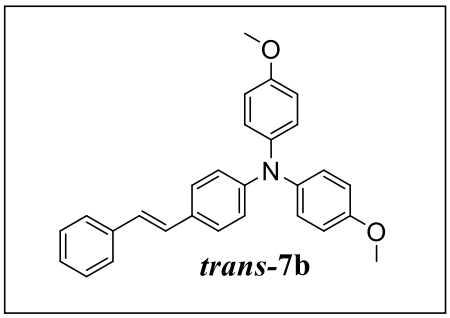

***trans*-7b**

***trans*-7b** has been previously reported.[158] It was synthesized by using the Buchwald/Hartwig amination for the synthesis of dianisylaminostilbene described above from **5** (0.229 g, 2.00 mmol) and ***trans*-6b (**0.523 g, 2.02 mmol). The crude product was purified by column

chromatography on silica gel using diethyl ether/hexane =1:4 to give ***trans*-7b** as a yellow solid (773 mg, 94.9 % yield); mp 117-119 °C, lit 117-118 °C;[158] ^{1}H NMR (360 MHz, $CDCl_3$): , δ (ppm) 7.49 (d, J = 7.3 Hz, 2H), 7.35-7.32 (m, 4H), 7.22 (t, J = 7.3 Hz, 1H), 7.08-7.03 (m, 5H), 6.97-6.91 (m, 3H), 6.84 (d, 8.5 Hz, 4H), 3.81 (s, 6H), ^{13}C NMR (125 MHz, $CDCl_3$): 156.0, 148.3, 140.8, 137.9, 129.6, 128.6, 128.4, 127.2, 127.0, 126.6, 126.2, 126.1, 120.5, 114.7, 55.5; ESI-HRMS calcd for $C_{28}H_{25}NO_2$: 407.1885, found 407.1891. UV-Vis (1.5 % benzene in cyclohexane) λ_{max} = 372 nm, ε = 39100 cm^{-1} M^{-1}

***cis*-4-dianisylamino-4'-chlorostilbene, *cis*-7c**

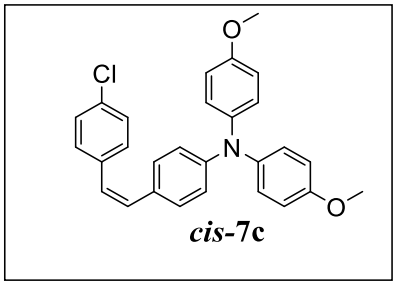

***cis*-7c**

***cis*-7c** was prepared by using the Buchwald/Hartwig amination for the synthesis of dianisylaminostilbene described above from **5** (0.229 g, 2.00 mmol) and ***cis*-6c (**0.593 g, 2.02 mmol), Pd_2dba_3 (18.3 mg, 1.00 mol %), DPPF (22.1 mg, 2.00 mol %) and NaOtBu (0.288 g, 1.50 eq). The crude product was purified by column chromatography on silica gel using diethyl ether/hexane (1:4) to give a nearly colorless oil containing mainly the *cis* isomer (98.5 % *cis*:1.50 % *trans*). 833 mg, 94.2 % yield; ^{1}H NMR (500 MHz, C_6D_6) δ (ppm): 7.24 (d, J = 8.9 Hz, 2H), 7.22 (d, J = 8.9 Hz, 2H), 7.17 (d, J = 8.9 Hz, 4H), 7.14 (d, J = 8.9 Hz, 2H), 7.02 (d, J = 8.9 Hz, 2H), 6.82 (d, J = 8.9 Hz, 4H), 6.53 (d, J = 12.1 Hz, 1H), 6.34 (d, J = 12.1 Hz, 1H), 3.41 (s, 6H) ^{13}C NMR (125 MHz, DMSO-D_6): 156.3, 148.6, 140.3, 136.9, 131.6, 129.5, 129.1, 129.0, 128.1, 127.9, 127.3, 124.6, 119.5, 115.5, 55.7 ESI-HRMS calcd for $C_{28}H_{24}ClNO_2$: 441.1496, found 441.1498. UV-Vis (1.5 % benzene in cyclohexane) λ_{max} = 360 nm, ε = 20800 cm^{-1} M^{-1}

***trans*-4-dianisylamino-4'-chlorostilbene, *trans*-7c**

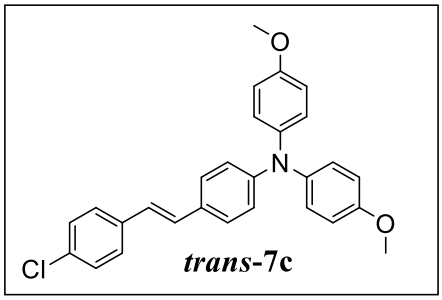

***trans*-7c**

***trans*-7c** was prepared by using the Buchwald/Hartwig amination for the synthesis of dianisylaminostilbene described above from **5** (0.229 g, 2.00 mmol), ***trans*-6c** **(**0.593 g, 2.02 mmol), Pd_2dba_3 (18.3 mg, 1.00 mol %), DPPF (22.1 mg, 2.00 mol %) and NaOtBu (0.288 g, 1.50 eq). The crude product was purified by column chromatography on silica gel using diethyl ether/hexane = 1:4 to afford a greenish-yellow powder (825 mg, 90.3 %) ^{1}H NMR (500 MHz, C_6D_6) δ (ppm): 7.38 (d, J = 8.9 Hz, 2H), 7.21-7.24 (m, 8H), 7.12 (d, J = 8.9 Hz, 2H), 6.99 (d, J = 16.1 Hz, 1H), 6.85-6.88 (m, 5H), 3.43 (s, 6H) ^{13}C NMR (125 MHz, DMSO-D_6): 156.6, 148.6,140.2, 137.0, 131.6, 129.5, 129.1, 129.0, 128.1, 127.9, 127.2, 124.6, 119.5,115.4, 55.7 ESI-HRMS calcd for $C_{28}H_{24}ClNO_2$: 441.1496, found 441.1499. UV-Vis (1.5 % benzene in cyclohexane) λ_{max} = 382 nm, ε = 37800 cm^{-1} M^{-1}

***cis*-4-dianisylamino-4'-trifluoromethylstilbene, *cis*-7d**

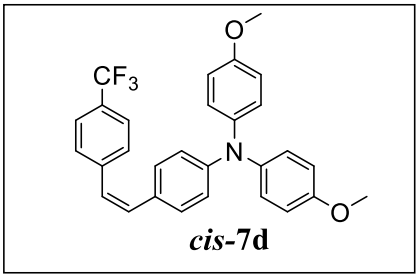

***cis*-7d**

***cis*-7d** was prepared by using the Buchwald/Hartwig amination for the synthesis of dianisylaminostilbene from **5** (0.229 g, 2.00 mmol) and ***cis*-6d** (0.658 g, 2.02 mmol). The crude product was purified by column chromatography on silica gel using diethyl ether/hexane (1:4) to give a nearly colorless oil containing mainly the *cis* isomer (98.1 % *cis*:1.90 % *trans*). 847 mg, 89.1 % yield; ^{1}H NMR (360 MHz, DMSO-D_6) δ (ppm): 7.64 (d, J = 8.9 Hz, 2H) , 7.49 (d, 8.9 Hz, 2H), 7.05 (d, J = 8.9 Hz, 6H), 6.92 (d, J = 8.9 Hz, 4H), 6.61-6.65 (m, 3H), 6.52 (d, J = 12.1 Hz, 1H), 3.75 (s, 6H) ^{19}F NMR (360 MHz, DMSO-D_6): -62.0 (s) ^{13}C NMR (125 MHz, DMSO-D_6): 156.3,148.2, 142.0, 139.9, 132.1,129.9, 129.5, 127.6, 127.5, 125.7(q), 125.4,125.2, 125.0 (q), 118.3, 115.2, 55.7 ESI-HRMS calcd for $C_2H_{24}F_3NO_2$:

475.1759, found 475.1762. UV-Vis (1.5 % benzene in cyclohexane) λ_{max} = 370 nm, ε = 23700 cm^{-1} M^{-1}

trans-4-dianisylamino-4'-trifluoromethylstilbene, _trans_-7d

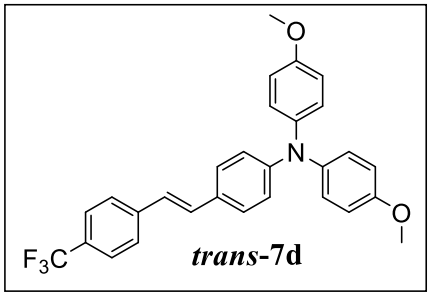

***trans*-7d**

***trans*-7d** was prepared by using the Buchwald/Hartwig amination for the synthesis of dianisylaminostilbene from **5** (0.229 g, 2.00 mmol) and ***trans*-6d (**0.593 g, 2.02 mmol). The crude product was purified by column chromatography on silica gel using diethyl ether/hexane (1:4) to give ***trans*-7d** as greenish-yellow crystals (866 mg, 91.1 % yield); mp 103-104 °C ^{1}H NMR (500 MHz, DMSO-D_6) δ (ppm): 7.75 (d, J = 8.3 Hz, 2H), 7.68 (d, 8.3 Hz, 2H), 7.45 (d, J = 8.3 Hz, 2H), 7.32 (d, J = 16.2 Hz, 2H), 7.11 (d, 16.2 Hz, 1H), 7.05 (d, J = 8.3 Hz, 4H), 6.93 (d, J = 8.3 Hz, 4H), 6.76 (d, J = 8.3 Hz, 2H), 3.75 (s, 6H) ^{19}F NMR (360 MHz, DMSO-D_6): -61.8 (s)

^{13}C NMR (125 MHz, DMSO-D_6): 156.2, 148.0, 142.3, 140.2, 131.8, 130.2, 129.5, 127.6, 127.5, 125.7 (q), 125.8 (q), 125.4, 125.2, 117.9, 115.3, 55.7 ESI-HRMS calcd for $C_2H_{24}F_3NO_2$: 475.1759, found 475.1760. UV-Vis (1.5 % benzene in cyclohexane) λ_{max} = 390 nm, ε = 39400 cm^{-1} M^{-1}

cis-4-dianisylamino-4'-methylstilbene, _cis_-7e

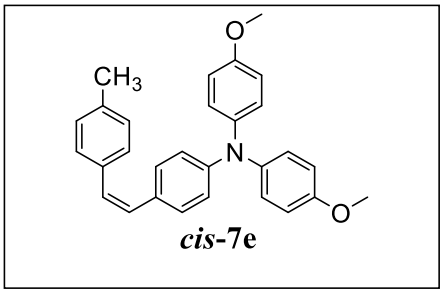

***cis*-7e**

***cis*-7e** was prepared by using the Buchwald/Hartwig amination for the synthesis of dianisylaminostilbene from **5** (0.229 g, 2.00 mmol) and ***cis*-6e** (0**.**552 g, 2.02 mmol). The crude product was purified by column chromatography on silica gel using ethyl acetate/hexane (1:6) to give the desired product as a light yellow solid (754 mg, 89.5 % yield). Recrystallization of the product in hexane afforded light yellow crystals. mp

92-94 °C ^{1}H NMR (500 MHz, DMSO-D_6) δ (ppm): 7.17 (d, J = 8.7 Hz, 2H), 7.08 (d, J = 8.7 Hz, 2H), 7.05 (d, J = 8.7 Hz, 2H), 7.02 (d, J = 8.7 Hz, 2H), 6.90 (d, 8.7 Hz, 4H), 6.59 (d, J = 8.7 Hz, 4H), 6.59 (d, J =8.9 Hz, 2H), 6.42 (s, 2H), 3.73 (s, 6H) 2.26 (s, 3H)

^{13}C NMR (125 MHz, DMSO-D_6): 156.3, 147.9, 141.2, 140.3, 136.7, 134.8, 133.0, 129.8, 129.4, 128.7, 128.2, 127.3, 118.8,115.4, 55.7, 21.2 ESI-HRMS calcd for $C_{29}H_{27}NO_2$: 421.2042, found 421.2043. UV-Vis (1.5 % benzene in cyclohexane) λ_{max} = 350 nm, ε = 23200 cm^{-1} M^{-1}

***trans*-4-dianisylamino-4'-methylstilbene, *trans*-7e**

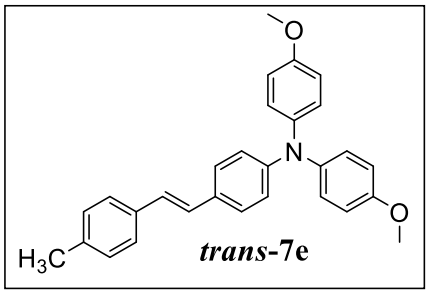

***trans*-7e**

***trans*-7e** has been previously reported.[157] It was prepared by using the Buchwald/Hartwig amination for the synthesis of dianisylaminostilbene from **5** (0.229 g, 2.00 mmol) and ***trans*-6e (**0.552 g, 2.02 mmol). The crude product was purified by column chromatography on silica gel using ethyl acetate/hexane (1:6) to give the desired product as a light yellow solid (780 mg, 92.5 % yield). Recrystallization of the product in hexane afforded light yellow crystals. mp 99-100 °C ^{1}H NMR (500 MHz, DMSO-D_6) δ (ppm): 7.44 (d, J = 8.7 Hz, 2H), 7.40 (d, 8.7 Hz, 2H), 7.16 (d, J = 8.7 Hz, 2H), 7.09 (d, 16.3 Hz, 1H), 7.05-6.92 (m, 9H), 6.76 (d, J = 8.7 Hz, 2H), 3.75 (s, 6H), 2.30 (s, 3H) ^{13}C NMR (125 MHz, DMSO-D_6): 156.2, 148.2, 140.5, 135.7, 135.1, 129.7, 129.6, 127.7, 127.1, 127.0, 126.4, 126.0, 119.6, 115.1, 55.7, 21.5 ESI-HRMS calcd for $C_{29}H_{27}NO_2$: 421.2045, found 421.2044. UV-Vis (1.5 % benzene in cyclohexane) λ_{max} = 374 nm, ε = 40900 cm^{-1} M^{-1}

***trans*-4-dianisylamino-2′,4′,6′-trimethoxystilbene, *trans*-7f**

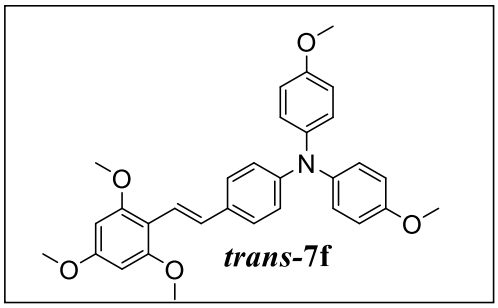

***trans*-7f**

***trans*-7f** was synthesized by using the Buchwald/Hartwig amination for the synthesis of dianisylaminostilbene from **5** (0.229 g, 2.00 mmol) and ***trans*-6f (**0.705 g, 2.02 mmol). The crude product was purified by column chromatography on silica gel using ethyl acetate/hexane (1:4) to give ***trans*-7f** as a yellow solid. Recrystallization of the product in hexane yielded yellow crystals (849 mg, 85.4 % yield). mp 147-149 °C; ^{1}H NMR (360 MHz, C_6D_6) δ (ppm): 8.06 (d, J = 16.6 Hz, 1H), 7.97 (d, 16.6 Hz, 1H), 7.68 (d, J = 8.6 Hz, 2H), 7.25-7.20 (m, 6H), 6.84 (d, J = 8.6 Hz, 4H), 6.25 (s, 2H), 3.51 (s, 6H), 3.48 (s, 6H), 3.43 (s, 3H) ^{13}C NMR (125 MHz, DMSO-D_6): 160.2 159.8, 155.9, 147.7, 141.5, 133.4, 130.2, 127.2,126.4, 121.8, 118.5, 114.8, 109.3, 99.2,55.1, 54.8, 54.6 ESI-HRMS calcd for $C_{31}H_{31}NO_5$: 497.2202, found 497.2204. UV-Vis (1.5 % benzene in cyclohexane) λ_{max} = 364 nm, ε = 38500 cm^{-1} M^{-1}

***trans*-4-dianisylamino-2′,6′-dimethoxystilbene*trans*-7g**

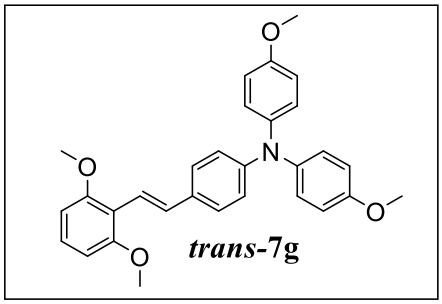

***trans*-7g**

***trans*-7g** was synthesized by using the Buchwald/Hartwig amination for the synthesis of dianisylaminostilbene from **5** (0.229 g, 2.00 mmol) and ***trans*-6g (**0.645 g, 2.02 mmol). The crude product was purified by column chromatography on silica gel using ethyl acetate/hexane (1:4) to give ***trans*-7g** as a greenish yellow solid. Recrystallization of the product in ethyl acetate/hexane (1:8) yielded greenish yellow crystals (861 mg, 91.2 %). mp 175-177 °C; ^{1}H NMR (500 MHz, DMSO-D_6) δ (ppm): 7.39 (d, J = 15.9 Hz, 1H), 7.30 (d, J = 8.5 Hz, 2H), 7.19-7.15 (m, 2H), 7.02 (d, J = 8.5 Hz, 4H), 6.91 (d, 8.5 Hz, 4H), 6.77 (d, J = 8.5 Hz, 4H), 6.68 (d, J = 8.5 Hz, 2H), 3.83 (s, 6H), 3.74 (s, 6H) ^{13}C NMR (125

MHz, DMSO-D_6): 158.4, 156.1, 147.9, 140.6, 131.8, 131.2, 128.4, 127.4, 126.9, 120.2, 117.6, 115.4, 114.4, 104.6, 56.2, 55.7, ESI-HRMS calcd for $C_{30}H_{29}NO_4$: 467.2097, found 467.2104. UV-Vis (1.5 % benzene in cyclohexane) λ_{max} = 374 nm, ε = 33700 cm^{-1} M^{-1}

Procedure used for measurements

Photochemical Experiments

Solutions of ***trans*-7a-e** in 2 % benzene in cyclohexane used for the optical spectra (Figures 2.12, 2.18-2.21) were prepared by successive dilution. 1 mg of the substrate was dissolved in about 1.00 mL of benzene and a 500 μL gas-tight syringe was used to transfer a volume of this solution to an empty volumetric flask. This flask was filled to the 30.0 mL mark with cyclohexane to give the required concentration. About 3.00 mL of the solution was placed in a 10 mm quartz cuvette and the optical spectrum was measured. *T**rans*-7a** (1.0 mg, 2.29 x 10^{-3} mmol) was dissolved in 1.0 mL benzene in a volumetric flask to give a 2.29 x 10^{-3} M solution. A 500 μL gas-tight syringe was used to transfer 328 μL of the ***trans*-7a** solution to an empty volumetric flask. This flask was filled to the 30 mL mark with cyclohexane to give a 2.50 x 10^{-5} M solution. 3.0 mL of the solution was placed in a quartz cuvette and the optical spectrum was measured. The same procedure was used for preparing the solutions of ***trans*-7b-e** that were used for the photoisomerization experiments.

Photoisomerization of *trans*-7a-c and *trans*-7e using a 385-410nm LED in deaerated 2 % benzene in cyclohexane

The solution of ***trans*-7a-c** and ***trans*-7e** prepared by using the above procedure was placed in a quartz cuvette and the optical spectrum was measured. The sample was then irradiated with a 385-410 nm LED (7 W) and the subsequent optical spectra were measured at different time intervals. The spectrum was taken every 20 s for ***trans*-7a** and 30 s for ***trans*-7b, *trans*-7c** and ***trans*-7e**.

Photoisomerization of *trans*-7d using a 420 nm LED in deaerated 2 % benzene in cyclohexane

The solution of ***trans*-7d** prepared by using the above procedure was placed in a 1cm quartz cuvette and the optical spectrum was measured. The sample was then irradiated with a 430 nm LED (7 W) and the subsequent optical spectra were measured at different time intervals. The spectrum was taken every 90 s.

Kinetic studies of the thermal isomerization of 0.0731 M *cis*-7a-e in DMSO-d_6

The thermal isomerization kinetics of ***cis*-7a** was studied by ^{1}H NMR spectroscopy at different temperatures (120 ºC, 130 ºC, 140 ºC and 150 ºC). A solution of 25.6 mg of ***cis*-7a** in 0.80 mL of deaerated DMSO-d_6 (7.31×10^{-2} M) was put in an NMR tube. The NMR tube was sealed with parafilm, immersed in a constant temperature oil bath, and the spectrum was recorded at 140 ºC after 30, 90, 150, 220, 308, 495, 750, 1050 and 1300 minutes. For each spectrum, the methoxy signals were integrated to evaluate the % *cis*: % *trans* of the sample, giving the corresponding concentration of ***cis*-7a** as a function of time. The thermal isomerization rates (k) were obtained from the slope of the first order plots of the natural logarithm of the concentration of the *cis* against time. The resulting k values at different temperatures were used to plot Eyring and Arrhenius plots from which the activation and thermodynamic parameters were obtained. The experiment was repeated at 120 ºC, 130 ºC, and 150 ºC and their respective time intervals and concentrations are shown in Appendix H. The experiment was repeated at 150 ºC and 140 ºC for ***cis*-7b**, ***cis*-7c** and ***cis*-7d** and their thermodynamic parameters (Appendix H) were obtained by applying the Van't Hoff's and Eyring equations.

Electrochemical Experiments

The cyclic voltammograms of *trans*-7a-e -1.00 mM in dichloromethane (0.100 M nBu_4PF_6) at 50.0 mV/s scan rate.

For each cyclic voltammogram, nBu_4PF_6 (0.968 g, 2.50 mmol) was dissolved in freshly distilled methylene chloride (25.0 mL) in a volumetric flask to give a 0.100 M solution. About (8.0 mL) of this solution was placed in a four-neck electrochemical cell equipped with a magnetic stir bar. A blank CV scan (0.0 to 1.2 V vs SCE, 50 mV/s) was measured to ensure there were no impurities in the prepared solution. An amount of ***trans*-7a-e** which would give a 1.00 mM solution was added to the blank solution and stirred to dissolve the solid. The potential was scanned from 0.00 to 1.00 V vs SCE at a rate of 50.0 mV/s. The following amounts were used; 4.00 mg of ***trans*-7a**, ***trans*-7c**, ***trans*-7e**, ***trans*-7f** and ***trans*-7g**, 3.30 mg of ***trans*-7b** and ***trans*-7d**, 3.30 mg of ***trans*-7b** and ***trans*-7d**.

Kinetic analysis of the redox auxiliary catalysis of the isomerization of *cis*-7a-e with CRET 5 mol % of CRET at 30 ºC in the absence of oxygen

30.0 mL of 3.02 x 10^{-5} M of ***cis*-7a** in 2 % benzene in cyclohexane was prepared by serial dilution in a volumetric flask. 1.50 mg of the substrate was dissolved in 1.0 mL of benzene and a 500 μL gas-tight syringe was used to transfer 264 μL of this solution to an empty volumetric flask. This flask was filled to the 30.0 mL mark with cyclohexane to give the required concentration (3.02 x 10^{-5} M) and degassed. The solution (3.00 mL) was placed in a 1cm path length quartz cuvette by using a 10 mL syringe and the optical spectrum was measured. A 1.07 x 10^{-4} M stock solution of orange CRET was prepared by dissolving CRET (1.30 mg, 2.15 mmol) in 20.0 mL of dry CH_2Cl_2 in a 25 mL volumetric flask. Using a 100 μL glass syringe (42.3 μL, 5.00 mmol %) of the CRET solution was injected into the ***cis*-7a** solution and the cuvette was shaken for 4 seconds to ensure thorough mixing. Subsequent optical spectra were recorded every 7 seconds until the completion of the reaction. Full conversion to ***cis*-7a** to ***trans*-7a** was achieved in about 70 s, and no further change was observed at longer times. The experiment was repeated using a greater amount of CRET. The radical isomerization rates (*k*) were obtained from

the slope of the first order plots of the natural logarithm of the concentration of the *cis* against time. The resulting *k* values were used to the activation barrier of the radical process. The same procedure was used for the radical isomerization of ***cis*-7b-e**. The following amounts were used; ***cis*-7b (**1.40 mg), ***cis*-7c** (1.52 mg), ***cis*-7d** (1.63 mg) and ***cis*-7e** (1.45 mg) and their respective times in between spectra were 30 s, 90 s, 120 s and 10 s.

Kinetic analysis of the redox auxiliary catalysis of the isomerization of *cis*-7a-e with CRET 5 mol % of CRET at 30 ºC in the absence of oxygen

30.0 mL of 3.02 x 10^{-5} M of ***cis*-7a** in 2 % benzene in cyclohexane was prepared by serial dilution in a volumetric flask. 1.50 mg of the substrate was dissolved in 1.00 mL of benzene and a 500 μL gas-tight syringe was used to transfer 264 μL of this solution to an empty volumetric flask. This flask was filled to the 30 mL mark with cyclohexane to give the required concentration (3.02 x 10^{-5} M) without degassing. The solution (3.00 mL) was placed in a 1cm path length quartz cuvette by using a 10 mL syringe and the optical spectrum was measured. A 1.07 x 10^{-4} M stock solution of orange CRET was prepared by dissolving CRET (1.30 mg, 2.15 mmol) in 20 mL of dry CH_2Cl_2 in a 25.0 mL volumetric flask. Using a 100 μL glass syringe (42.3 μL, 5.00 mmol) of the CRET solution was injected into the ***cis*-7a** solution and the cuvette was shaken for 4 seconds to ensure thorough mixing. Subsequent optical spectra were recorded every 5 seconds until the completion of the reaction. The radical isomerization rates (*k*) was obtained from the slope of the first order plots of the natural logarithm of the concentration of the *cis* against time. The resulting k value did not differ significantly from the previous experiment carried out in the absence of air.

Preparation of photo electrochromic device (PECD)

***Trans*-7a -** (1.90 mg, 0.00435 mmol) was dissolved in 1.00 mL Tol_3TBABF_4 gel. The gel solution was applied to ITO glass anode (equipped with spacer); the ITO glass cathode was then

added to complete sandwich-type device. The ITO sandwich was held together with two closed jaw compressor clamps for the duration of the experiment. For a picture of PECD, see Figure 2.42. Cycling conditions were: 120 s irradiation with 405 nm LED and 0.00 V, then 1.80 V for 120 s with no irradiation applied in cyclic voltammetry module using a scan rate of 100 V/s, V_1 potential = 1.50 V and a hold time of 120 s. UV-Vis spectra of the cell solution were recorded every 20.0 s.

CHAPTER THREE

REDOX AUXILIARY CATALYSIS OF BIS(DIARYLAMINO)STILBENE

3.1 Introduction

We showed in Chapter 2 that incorporating a RA group at the 4-position of stilbene causes an increase in the rate of the thermal isomerization from *cis*-to-*trans* compared to the parent stilbene. These *para*-RA-appended stilbenes can undergo a facile *cis* to *trans* isomerization upon removal of an electron. To better understand these systems, it is important to understand the effects of introducing an additional RA group at the 4′-position of ***cis*-7b** (Figure 3.1). The *trans* isomer (***trans*-9**) isomerizes to the *cis* isomer (***cis*-9**) by photo-absorption, and the *cis* isomer (***cis*-9**) then rapidly isomerizes to the *trans* isomer (***trans*-9**) upon one electron oxidation.

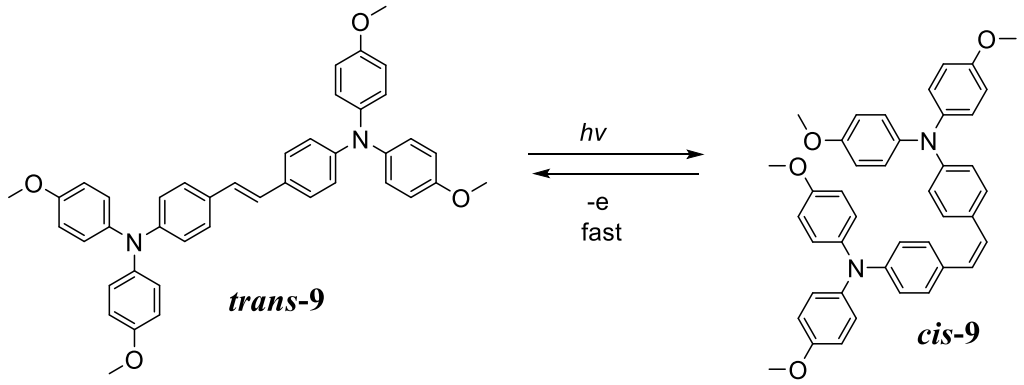

Figure 3.1 Bis(diarylamino)stilbene photo-electro switch. The *trans* isomer (***trans*-9**) isomerizes to the *cis* isomer (***trans*-9**) by photo-absorption, and the *cis* isomer (***cis*-9**) then undergoes a facile isomerization to the *trans* isomer (***trans*-9**) upon a one electron oxidation.

We hypothesized that having two RA groups at the 4- and 4′- positions of the stilbene will cause the bis(para-diarylamino) stilbene, ***trans*-9**, to behave similarly to ***trans*-7a**. The addition of the extra RA at the 4′-position is expected to increase the rate of the thermal *cis*-to-*trans* isomerization and decrease the activation barrier $\Delta G^{\ddagger}$ for the thermal isomerization of ***cis*-9**. In this chapter, we will investigate the effects of the additional RA group on the thermal *cis*-to-*trans* isomerization rate of ***cis*-9** and redox catalysis of the *cis*-to-*trans* isomerization.

The diarylamine **5** was used as the RA group because of it is chemically stable in both neutral and radical cation forms. The incorporation of the RA to the 4, 4′- positions of stilbene (**NAr_2-St-NAr_2**) will enhance the rate of the *cis* to *trans* isomerization upon oxidation of the amine RA by a one-electron oxidant. The basic premise of our work is that the radical cation, **NAr_2-St-$NAr_2^{\bullet+}$**, will be much more reactive toward *cis*-to-*trans* isomerization than its neutral *cis* form. The oxidation of the ***cis*-NAr_2-St-NAr_2** to ***cis*-NAr_2-St-$NAr_2^{\bullet+}$** will undergo a facile isomerization to the ***trans*-NAr_2-St-$NAr_2^{\bullet+}$** and upon reduction yield the ***trans*- NAr_2-St-NAr_2**.

3.2 Synthesis

The Wittig reaction[109] was employed in the synthesis of the intermediates ***cis*-8** and ***trans*-8** because it is a versatile method for the preparation of substituted stilbenes (Scheme 3.1). The reaction is not sensitive to atmospheric oxygen, thus allowing for simpler experimental procedures. The *trans*-isomer (***trans*-8**) is less soluble in hexane and this makes it easy to separate the ***trans*-8** from ***cis*-8**. The key reaction is the Buchwald/Hartwig coupling of the 4,4′-dibromostilbene and diaryl amino RA **5** to give ***trans*-9** and ***cis*-9** in good yields (Scheme 3.2). The resulting *cis* or *trans* aminostilbene was purified by column chromatography on silica gel to afford the desired compound**.**

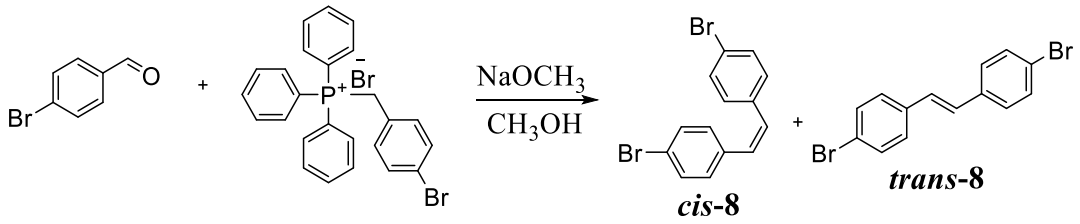

Scheme 3.1. Synthesis of 4,4′-dibromostilbene.

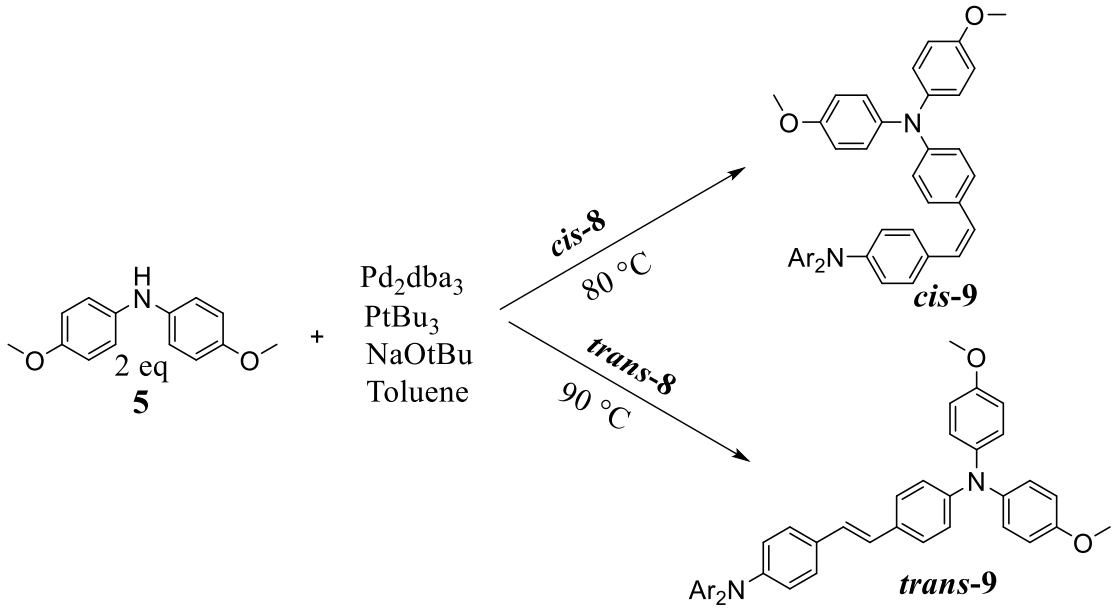

Yields (%)	*cis*	*trans*
	47	43

Scheme 3.2. Synthesis of bis(diarylamino)stilbenes.

3.3 Thermal Isomerization of *Cis*-bis(diarylamino)stilbenes (*cis*-NAr$_2$-St-NAr$_2$) *cis*-9

The work presented in this chapter involves the investigation of the kinetics of the thermal isomerization of *cis*-bis(diarylamino)stilbene ***cis*-9**, in addition to obtaining the activation parameters from the temperature dependence of the thermal *cis* decay. The investigation of the thermal *cis*-to-*trans* isomerization was conducted experimentally by using NMR spectroscopy.

In order to determine the extent of rate acceleration for the conversion of ***cis*-NAr$_2$-St-NAr$_2$** to ***trans*-NAr$_2$-St-NAr$_2$** by RA catalysis, it was necessary to measure the rate of thermal conversion of ***cis*-NAr$_2$-St-NAr$_2$** as a basis for comparison. The evaluation of the thermal rates (Scheme 3.3) requires information about the isomeric composition at different temperatures. This was performed by dissolving ***cis*-NAr$_2$-St-NAr$_2$** in DMSO-D_6 in NMR tube and heating the sample at different temperatures. The ^{1}H NMR spectra were taken at various time intervals and the changes in the integrations of the peaks corresponding to the two isomers were recorded. Since most signals in the ^{1}H NMR spectra of the *trans* and *cis* isomers are well separated, changes in the ***trans*-NAr$_2$-St-NAr$_2$** and ***cis*-NAr$_2$-St-NAr$_2$** ratios were easily determined. The measurement of these signals belonging to the same proton in both the *cis* and *trans* isomers allows the concentration of the *cis* and *trans* isomers to be calculated. An accurate determination of this value is very useful in the study of the kinetics of the isomerization.

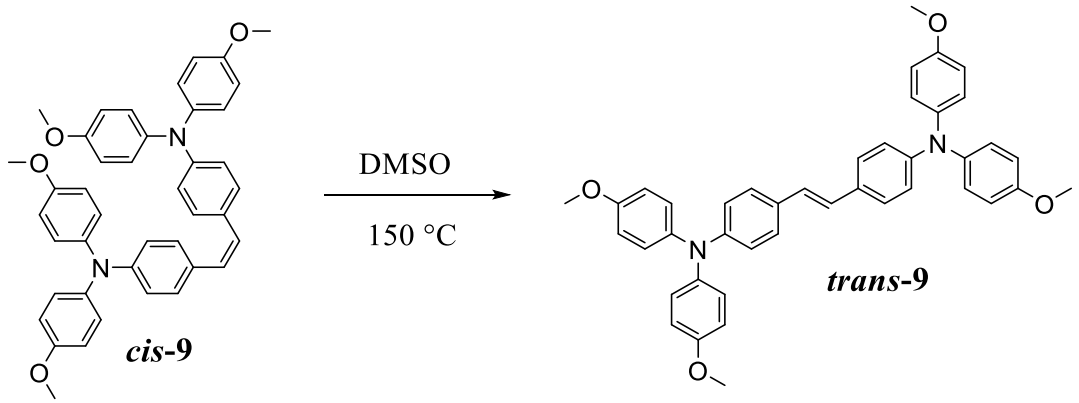

Yields (%)	*cis*	*trans*
	84	95

Scheme 3.3. Thermal isomerization ***cis*-9** in DMSO at 150 ºC.

The ^{1}H NMR spectrum of the olefinic and aromatic protons of the ***cis*-NAr$_2$-St-NAr$_2$** and ***trans*-NAr$_2$-St-NAr$_2$** indicates that the two rings in the *trans* isomer are coplanar with the double

bond and hence deshielded. In the *cis* isomer, the aromatic rings are tilted and the olefinic protons are shielded. As a result, the olefinic protons in ***trans*-9** appear at a higher chemical shift than those of ***cis*-9**. The ^{1}H NMR spectra of ***cis*-9** and ***trans*-9** show five distinct protons in the olefinic and aromatic regions labeled a-e for the *cis* form and a´- e´ for the trans form, as illustrated in Figure 3.2.

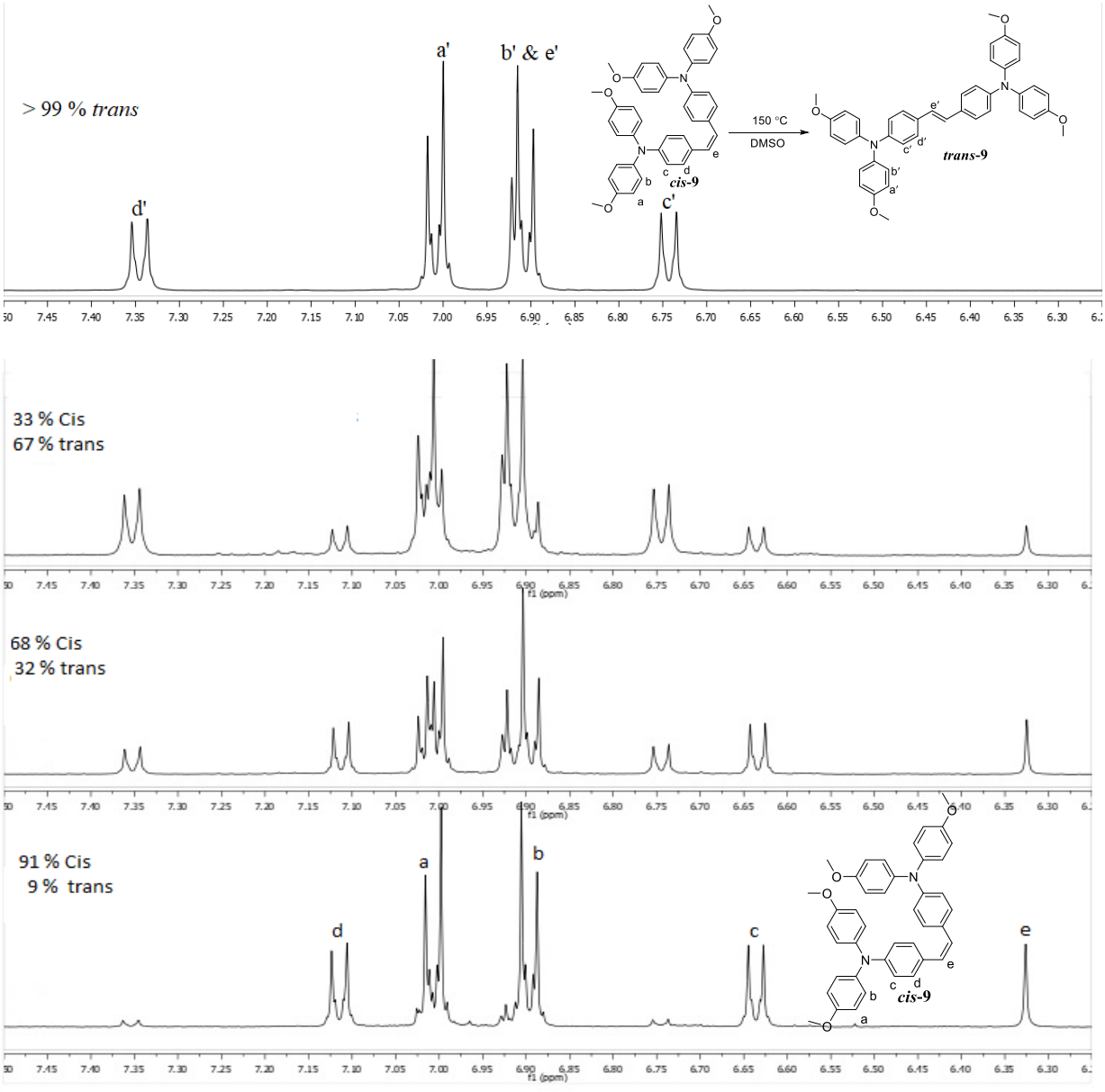

Figure 3.2. ^{1}H NMR of ***cis*-9** undergoing a thermal isomerization to ***trans*-9** form in DMSO at 150 ºC.

3.4 Kinetic Studies

To perform the kinetic studies of the thermal *cis* to *trans* isomerization of ***cis*-9**, the compound was dissolved in DMSO and placed in an NMR tube. The NMR tube was immersed in a constant temperature oil bath and the spectrum was recorded at six different temperatures (100 ºC,110 ºC, 120 ºC, 130 ºC, 140 ºC, 150 ºC) and time intervals. For each spectrum, the changes in the number of protons under corresponding peaks in ^{1}H NMR spectra were recorded and the corresponding concentration of ***cis*-9** was obtained at the various times (t). The data obtained from the experiment fit the kinetic equation

$$\ln [a] = k_1 t$$

where a is the concentration of the ***cis*-9**, remaining concentration at time t and k is the rate constant for the first order process. A plot of ln [***cis*-9**] against time (Figure 3.3) gave a straight line in all experiments. The slope of the plot is the rate constant k (Table 3.1), and the corresponding thermal half-lives were obtained by using the kinetic equation below where $t_{1/2}$ is the half-life.

$$t_{1/2} = \frac{ln\, 2}{k}$$

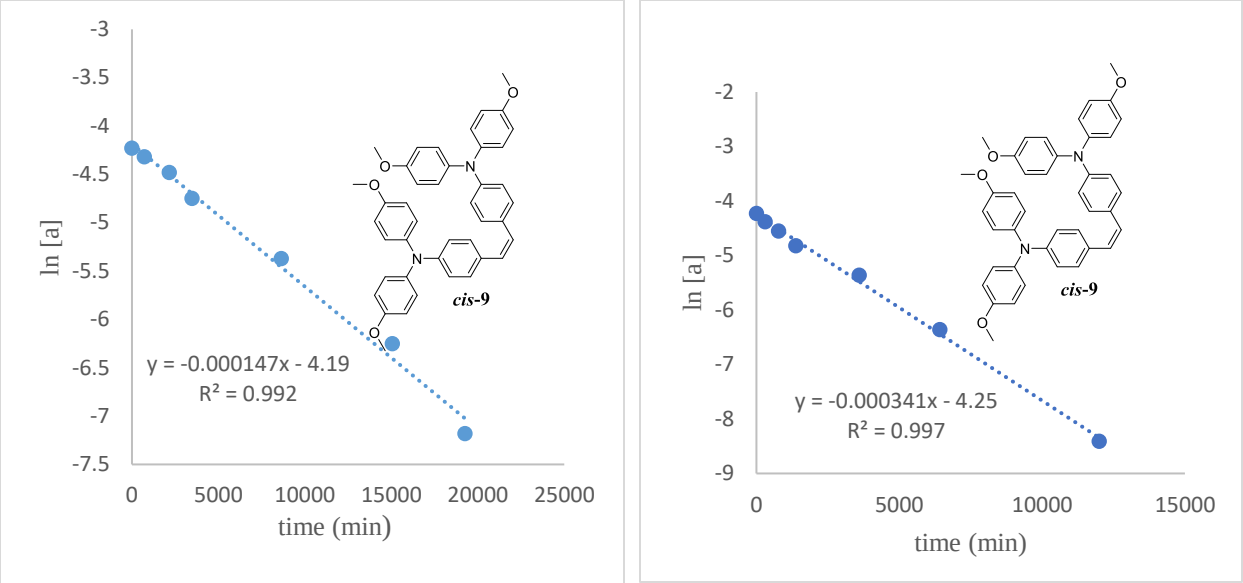

Figure 3.3. First order plots of ln [***cis*-9**] vs time t at different temperatures.

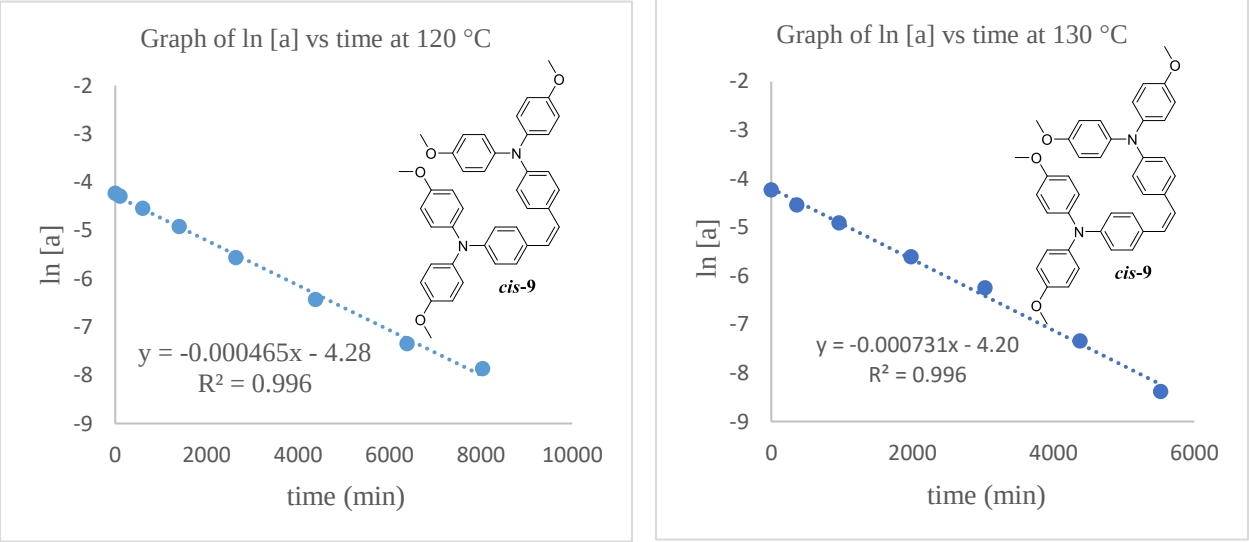

Figure 3.3. First order plots of ln [***cis*-9**] vs time t at different temperatures.

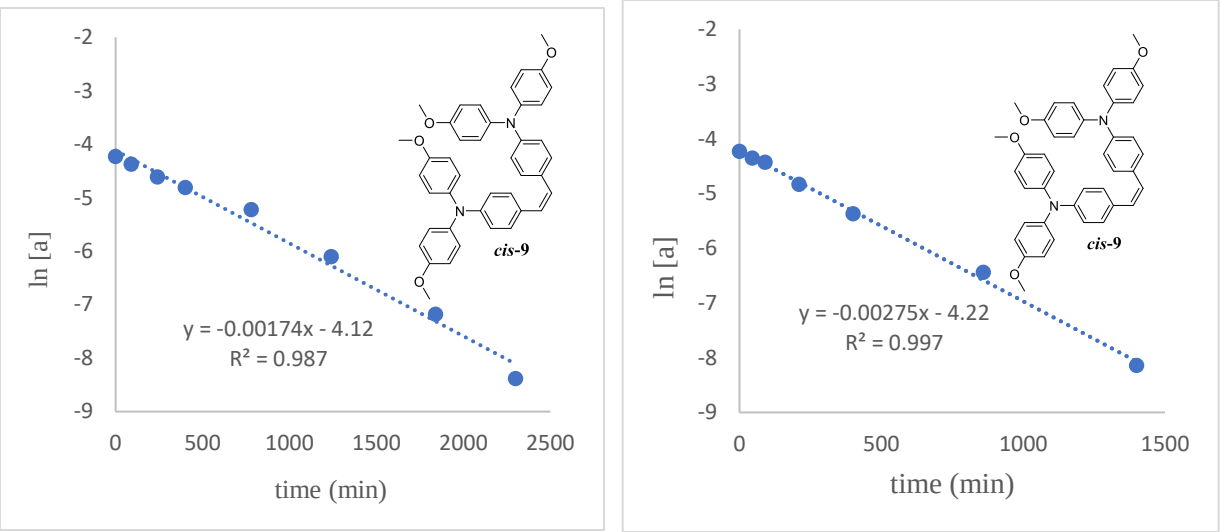

Figure 3.3. Continued. First order plots of ln [***cis*-9**] vs time t at different temperatures.

T(K)	I/T	k (s^{-1})	ln k	ln(k/T)
373	0.00268	2.45E-06	-12.9	-18.8
383	0.00261	5.68E-06	-12.1	-18.0
393	0.00254	7.73E-06	-11.8	-17.7
403	0.00248	5.50 E-05	-11.3	-17.3
413	0.00242	2.90E-05	-10.4	-16.5
423	0.00236	4.58E-05	-9.99	-16.0

Table 3.1. The first order rate constants for the thermal isomerization of ***cis*-9** in DMSO.

The activation parameters for the thermal *cis* to *trans* isomerization were estimated by applying the temperature dependent Eyring equation in order to understand the thermodynamic effect of the RA. The graph of ln (k/T) vs I/T gave a straight line (Figure 3.4). The slope and

intercept were used to calculate the $\Delta H^{\ddagger}$ and $\Delta S^{\ddagger}$ respectively (Table 3.2). The $\Delta G^{\ddagger}_{413K}$ for the thermal isomerization of ***cis*-9** to ***trans*-9** was determined to be approximately 32.6 kcal/mol, which is substantially lower than 46 kcal/mol[60] for the neutral parent stilbene.

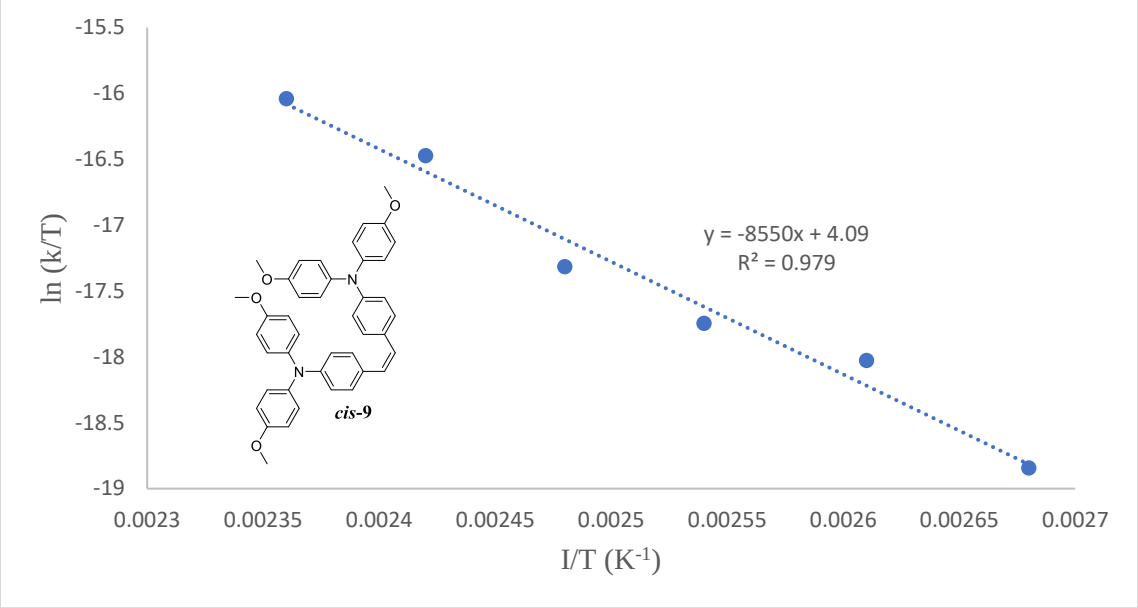

Figure 3.4. Eyring and Arrhenius plots of the thermal isomerization of ***cis*-9** in DMSO.

Activation parameters	Experimental Values
$\Delta H^{\ddagger}$	17.0 ± 0.1 kcal
$\Delta S^{\ddagger}$	-39.2 ± 0.1 cal mol^{-1} K^{-1}
E_a	17.8 ± 0.1 kcal/mol
$\Delta G_{413K}^{\ddagger}$	33.2 ± 0.1 kcal/mol

Table 3.2. Activation parameters of the thermal isomerization of ***cis*-9** in DMSO.

The rate of the thermal *cis*-trans isomerization of stilbenes is very slow due to a large barrier to rotation. This large barrier to rotation around the carbon-carbon double bond means

that the two isomers cannot easily interconvert. Thermal energy is needed to allow the *cis* isomer to overcome this barrier, but the rate can be enhanced by modifying the structure of stilbenes using two RA groups. It is expected that two RA groups will enhance the degree of single bondedness of the double bond by resonance, and hence will decrease the activation barrier. This leads to an increased the rate of *cis*-*trans* isomerization of ***cis*-9**.

3.5 Photochemistry and optical spectrum of *trans*-9

The reversible photochemical reactions of stilbenes play important roles in the development of light-gated molecular switches. The intensity of the light source, the molar absorptivity of the substrate at a specific wavelength of light and the quantum yield determine the efficiency of a photochemical reaction. The UV-absorption spectrum of ***trans*-9** exhibits two main absorption near 394 nm (A-band) and 302nm (B-band). The A-band of ***trans*-9** is attributed $\pi \rightarrow \pi^*$transition. In contrast to ***trans*-9**, the A-band of ***cis*-9** is blue-shifted, much broader, and has a considerably lower molar absorption coefficient than ***trans*-9** (Figure 3.5).The molar absorptivity of ***cis*-9** is less than that of ***trans*-9** because the steric crowding of the ortho sites causes the phenyl groups to twist slightly out of coplanarity. This leads to a decreased conjugation in ***cis*-9**. It is easy to choose an appropriate irradiation wavelength to arrive at a PSS which is either *cis*- or *trans*-rich because the spectra of *trans*- and *cis*-stilbenes are different due to the decreased conjuagtion in the *cis* form as a result of the twist out of coplanarity.

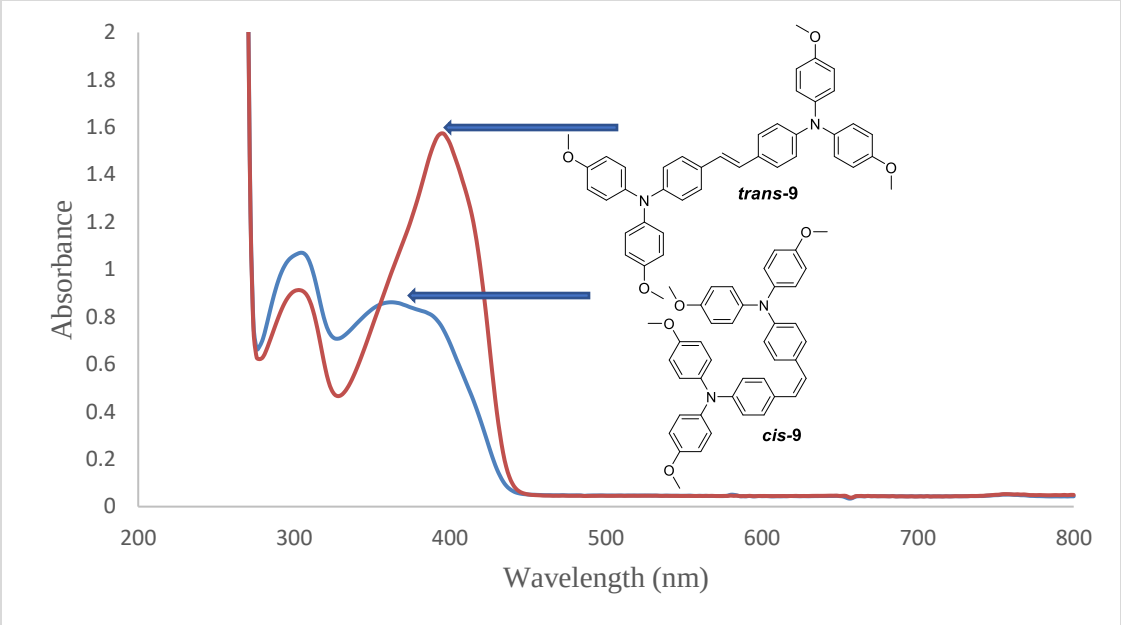

Figure 3.5. Optical spectrum of ***cis*-9** and ***trans*-9** (3.02×10^{-5} M) in cyclohexane:benzene = 2:98 at room temperature in 1cm quartz cuvette.

Upon excitation, *trans-cis* isomerization of stilbene proceeds through a torsional potential. This potential reaches a surface minimum at the perpendicular geometry in the excited state. There is an equal probability of forming the *cis* and *trans* conformers at this minimal position.[121-122] This change in conformation associated with the *cis* to *trans* isomerization of stilbenes can induce an electronic and/or mechanical response. The photochemical behavior of stilbenes may be changed by the introduction of substituents which may affect the properties of the molecule. Examples of these properties include π-electron cloud, the electron densities at different positions and the changes in the separation between the energy levels brought about by the twisting around the C-C central bonds.[123]

The photochemical *trans-cis* isomerization of ***trans*-9** was investigated via monochromatic irradiation of a dilute cyclohexane solution (approximately 2.47×10^{-5} M) at 25 ºC with a 430 nm LED light source (7W). Irradiation of the sample caused a progressive

decrease of the maximum absorption (λ_{max}) at 394 nm with a concomitant increase in the absorption intensity at 302 nm. A well defined isosbestic point at 352 nm (Figure 3.6) obtained after the irradiation of ***trans*-9**, providing further evidence for a transformation between two species. The time to reach the PSS was determined by following the maximum absorption at 394 nm. After about 3 minutes, no changes in the absorbance was observed (Figure 3.6), and there were no decomposition products detected by the UV/Vis spectroscopy. This was confirmed by the ^{1}H NMR spectrum of the PSS solution in C_6D_6, which was used to distinguish the substrate from the product formed after irradiation.

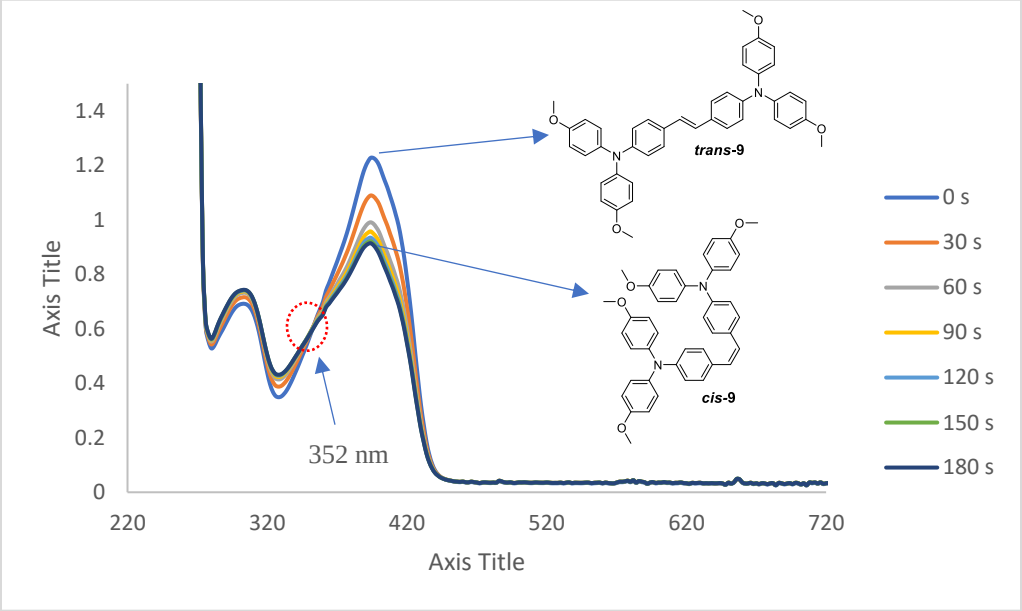

Figure 3.6. Optical spectrum of ***trans*-9** (2.47 x 10^{-5} M in 2 % benzene in cyclohexane) irradiated with a 430 nm LED at room temperature in a 1cm quartz cuvette.

It was impossible to use the spectrum of 100 % of ***cis*-7a** to measure the molar absorptivity of ***cis*-9** (ε_{cis}). But the ε_{cis} can be measured by using the isomeric ratio of ***cis*-9:** ***trans*-9** at the PSS. This ratio was determined by using NMR spectroscopy (Figures 3.7 and 3.8) at room temperature. The UV/Vis spectrum of ***trans*-9** at the PSS and the isomeric ratio ***cis*-9:**

***trans*-9** was then used to measure the molar absorptivity of the compound (ε_{cis}) using the equation below.

$$\varepsilon_{cis} = \frac{A_{pss} - (cxl)\varepsilon_{trans}}{cl(1-x)}$$

Where x and A_{pss} are the decimal fraction of the *trans* isomer at the PSS and the absorbance at the PSS respectively.

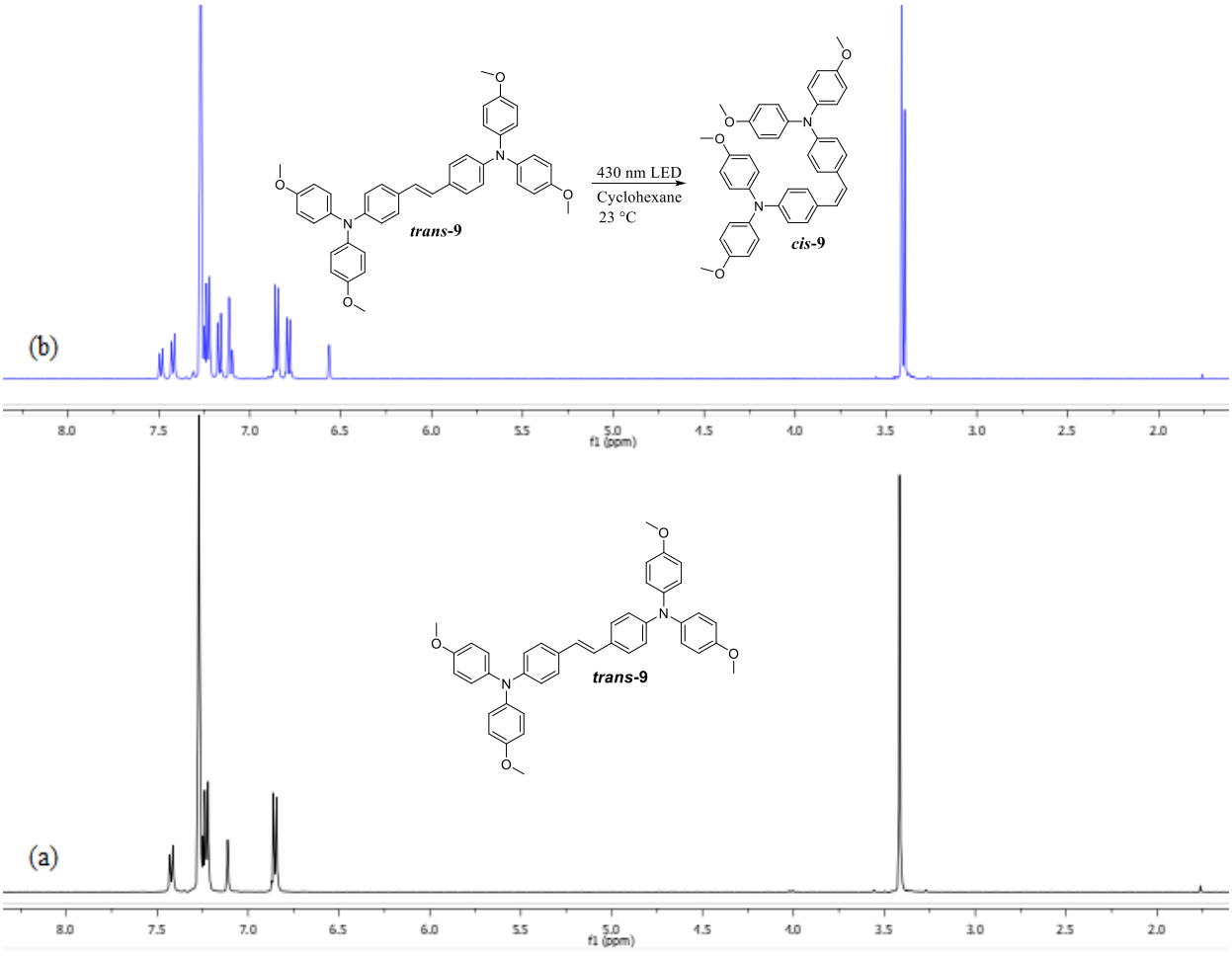

Figure 3.7. ^{1}H NMR of ***cis*-9** (1.58 X 10 $^{-2}$ M in C_6D_6) (a) Spectrum before irradiation in black (b) Spectrum after irradiation with 430 nm LED light (7W) in blue. PSS is established at a 60:40 ***cis*-9:*trans*-9** ratio at room temperature.

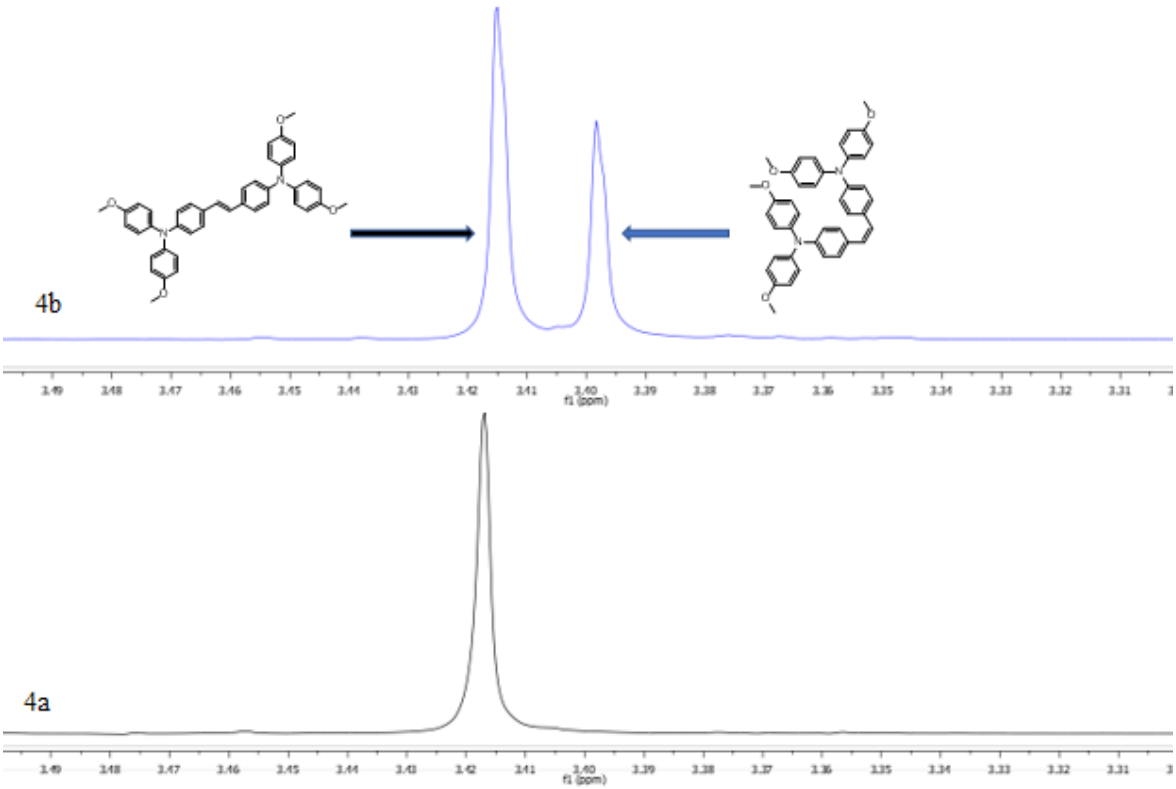

Figure 3.8. An expanded view of the alkyl region of the ^{1}H NMR spectrum of ***cis*-9** (1.58 x 10-2M in C_6D_6) (a) Spectrum before irradiation in black (b) Spectrum after irradiation with 430 nm LED light (7W) in blue. PSS is established at a 60:40 ***cis*-9:*trans*-9** ratio at room temperature.

It was easy to determine this ratio by ^{1}H NMR (Figure 3.7) since the two isomers have slightly different chemical shifts due to their different structural orientations. In contrast to *trans*-stilbene, the two arene rings of the *cis*-stilbene are twisted from the coplanar orientation relative to the central double bond. Upon rotation of the aromatic parts of the molecule, the two protons adjacent to the central double bond may come into the shielding cone of the anisotropic ring current. The protons of the *cis* isomer are shielded as a result of the tilted phenyl rings and therefore appear at higher chemical shifts.

The *trans* to *cis* photoisomerization of stilbenes proceed through the lowest excited singlet state or through the twisted singlet intermediate known as the phantom state p*. In this

mechanism, a torsional potential reaches a surface minimum at the perpendicular geometry p* in the excited state upon excitation.[124-125] Aminostilbenes have a similar isomerization pathway in the electronically excited states and their photochemical behavior is similar to that of the parent stilbene. However, para-(4,4′)-substituted aminostilbenes (***trans*-9**) have a more planar geometry about the nitrogen atom, extended amino conjugation, an increase in the twisted intramolecular charge transfer (TICT) character in the excited state and a very large dipole moment (32 D[159]). Since the polarization field of the solvent is large and apparently sluggish compared to the reactive time scale, the solute can become trapped in the solvent cage. This polarization caging of the reactant increases the activation energy of reaction, causing a significant reduction in the rate of the *trans* to *cis* isomerization.[90]

The extended amino conjugation in para-(4,4′)-substituted aminostilbenes results in a bathochromic shift of the $\pi \rightarrow \pi^*$ absorption band in the absorption spectrum. The strong donor (RA) tends to participate in the charge delocalisation at the triplet state. This electronic resonance interaction destablizes the activated transition state, thereby increasing the activation barrier of the *trans-cis* isomerization and also hinders the photoisomerization rate.[160]

3.6 Electrochemical Properties of Bis(diarylamino)stilbene

The redox behavior of ***trans*-9** was investigated by cyclic voltammetry (CV) experiment at ambient temperature with standard calomel electrode (SCE) as a reference electrode and tetrabutylammonium hexafluorophosphate nBu_4PF_6 as the electrolyte (Figure 3.9). The CV in CH_2Cl_2 showed paired oxidation potentials with reversible redox couples at +0.51V and +0.64V owing to sequential oxidations of the two diarylamine appendages. This result means that the cationic radical is stable at room temperature and the radical formation is not accompanied by a subsequent side reaction such as cyclization and dimerization. It also means that the reaction is

fast enough to maintain the concentrations of the oxidized and reduced forms in equilibrium with each other at the electrode surface.

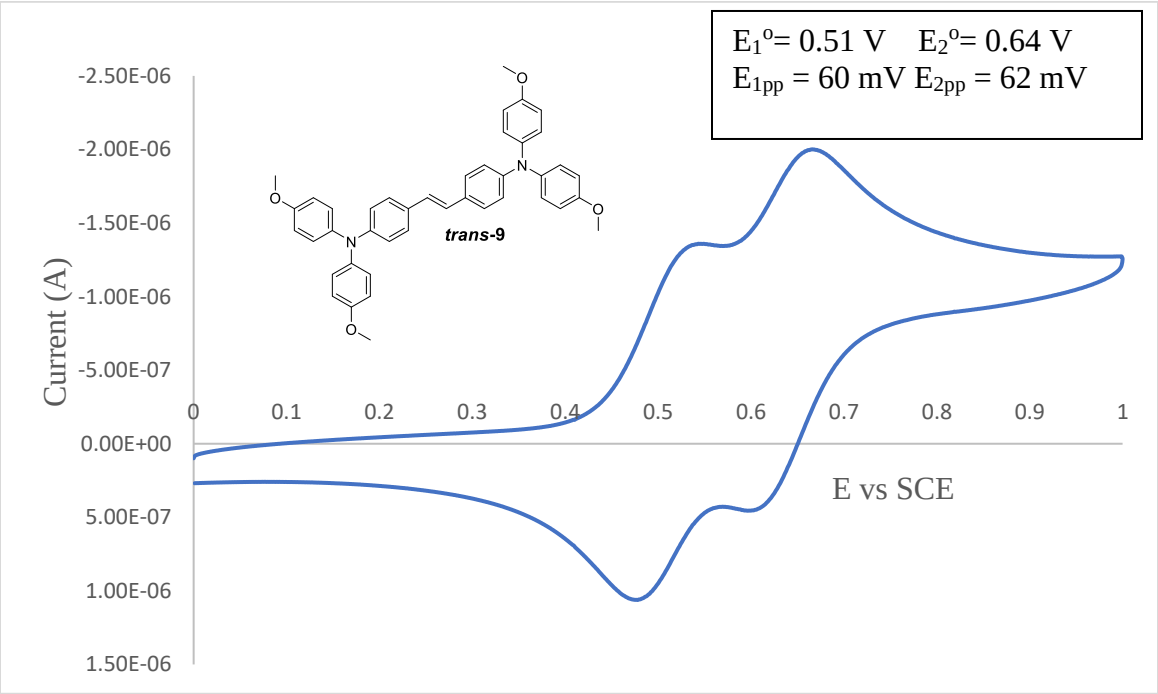

Figure 3.9. Cyclic voltammogram of ***trans*-9** (1.00 mM in DCM with 0.100 M nBu_4PF_6 at a scan rate of 50.0 mV/s.

3.7 Results of the redox auxiliary catalysis of *cis*-NAr_2-St-NAr_2 *cis*-9

The kinetic studies of the redox auxiliary mediated *cis* to *trans* isomerization of ***cis*-9** was monitored by UV-Vis spectroscopy. Since the wavelenghth of the maximum absorption and the extinction coefficient of the *trans*-stilbene differ substantially from that of the *cis*, the wavelength of the maximum absorption of the *trans* isomer provided a means of studying the kinetics of the redox auixiliary promoted *cis*-*trans* isomerization. A known amount of the compound was dissolved in a mixture of 2% deaerated benzene in cyclohexane and various amounts of CRET (5 mol%, 6 mol %, 7 mol%, 8 mol%, 9 mol%) were injected into the solution

at 30 ºC. The progress of the isomerization was followed by monitoring the increase of the absorbances at 394 nm (λmax of *trans*) and the decrease of the absorbance at about 302 nm (Figures 3.9-3.11) At the end of the isomerization (when the absorbances at 394 nm and 302 nm remained constant), the obtained spectrum looked similar to the spectrum of ***trans*-9** and both spectra had the same λ_{max} and molar absorptivity, ε. A clean isosbestic point at about 352 nm indicates that there was no dimerization or dihydrophenanthrene product formed.

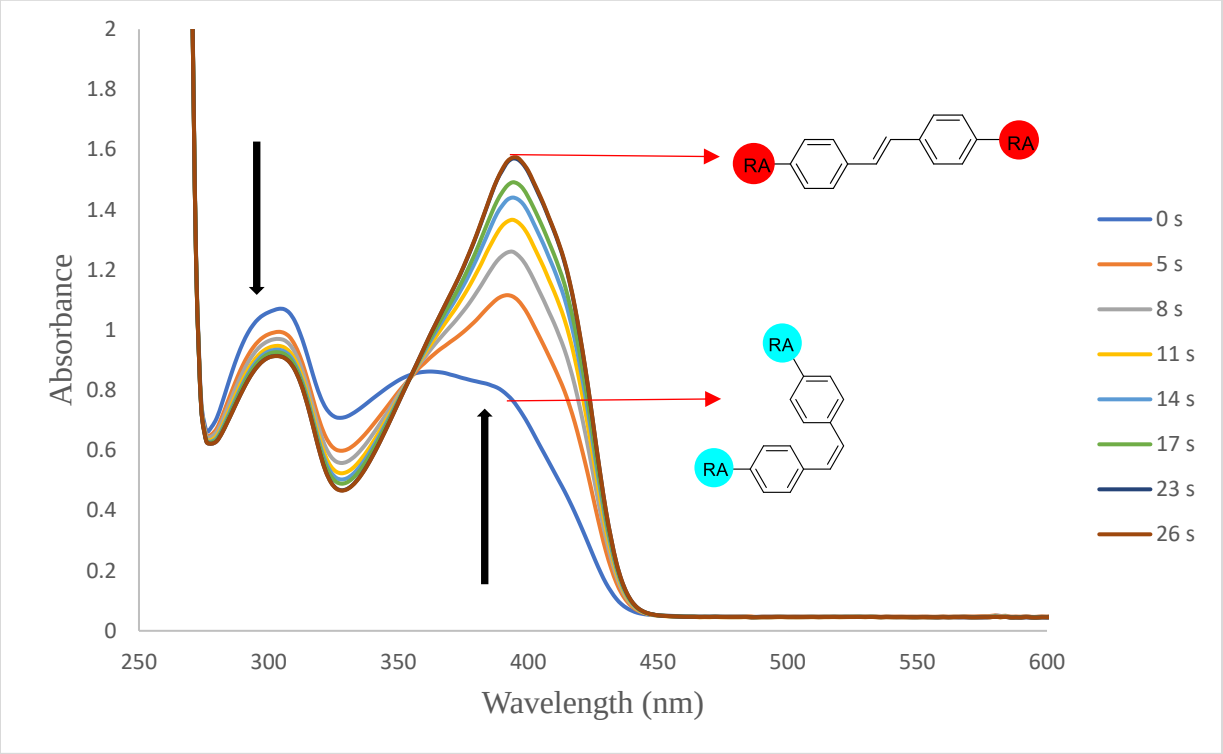

Figure 3.10. Optical spectrum of addition of CRET (3.50 mol % in DCM) to 3.03 X 10^{-5} M solution of ***cis*-9** in 2 % benzene in cyclohexane.

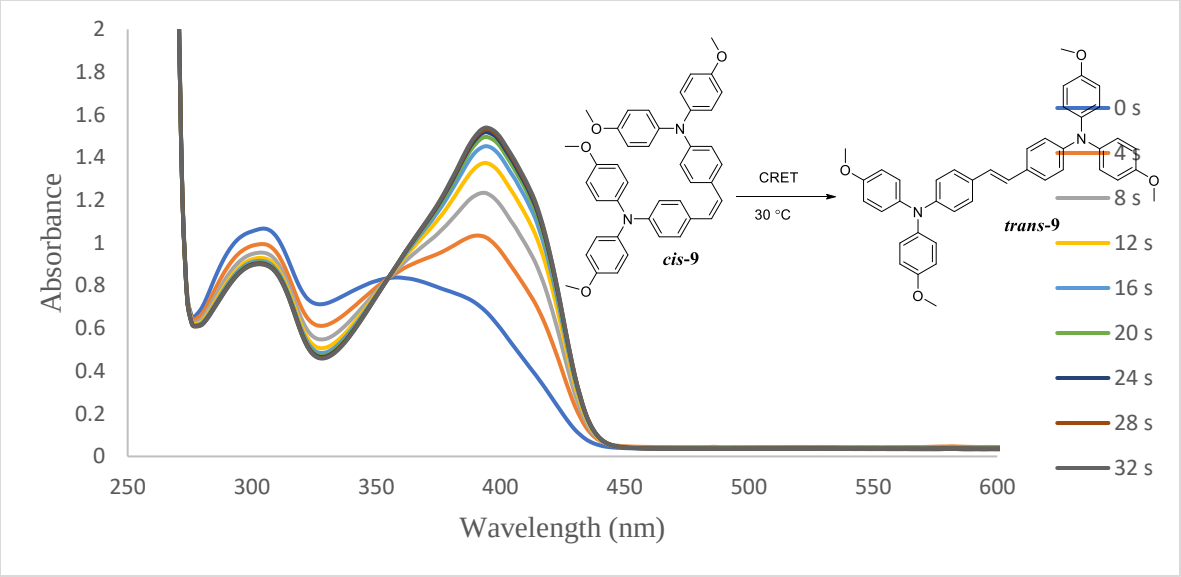

Figure 3.11. Optical spectrum of addition of CRET (3.00 mol % in DCM) to 3.03 X 10^{-5} M solution of ***cis*-9** in 2 % benzene in cyclohexane.

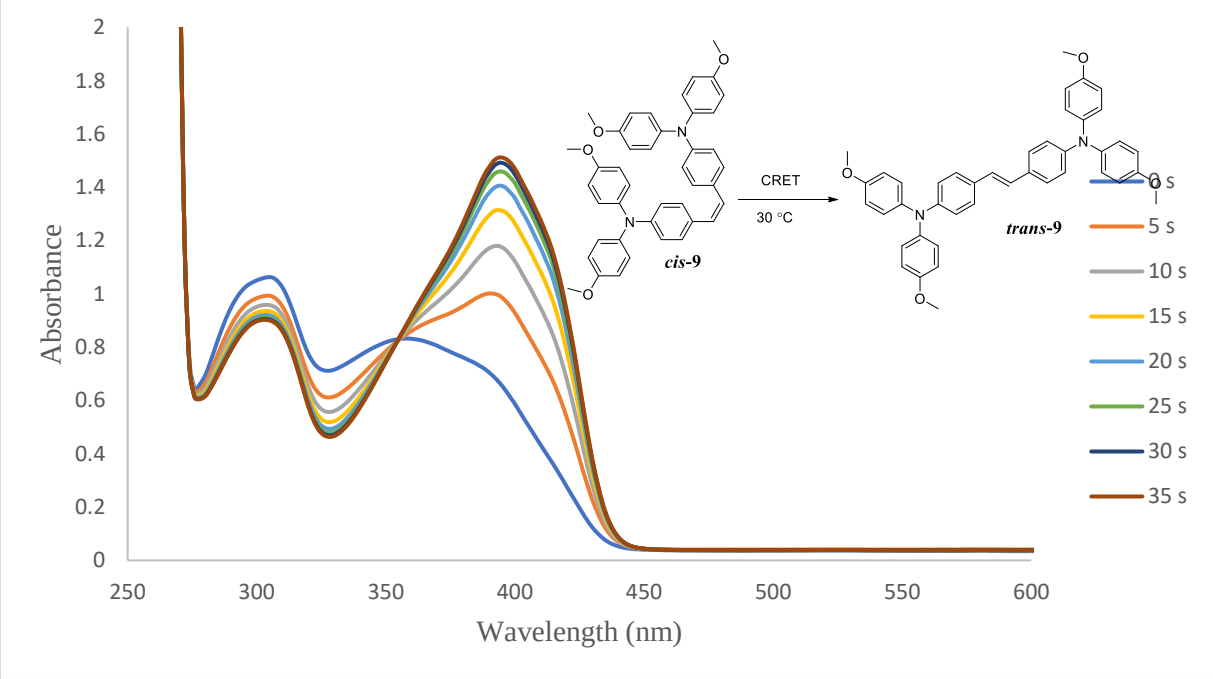

Figure 3.12. Optical spectrum of addition of CRET (2.50 mol % in DCM) to 3.03 X 10^{-5} M solution of ***cis*-9** in 2 % benzene in cyclohexane.

To confirm that the catalytic ability of CRET to induce the *cis-trans* isomerization of stilbenes, a new sample of ***cis*-9** was irradiated for 6 minutes to reach the PSS (40% *cis*: 60% *trans*). This was followed by the addition of a catalytic amount (3.0 mol %) of CRET to regenerate the *trans* isomer in about 12 seconds, thus exponentially increasing the rate at which the *cis* isomer isomerizes back to the *trans* isomer (Figures 3.12 and 3.13). The incorporation of the RA to the skeleton of stilbene (**NAr_2-St-NAr_2**) enhanced the rate of the *cis* to *trans* isomerization upon oxidation of the amine RA by a one-electron oxidant. The oxidation of the ***cis*-NAr_2-St-NAr_2** to ***cis*-NAr_2-St-NAr_2**$^{\bullet+}$ led to a facile isomerization to the ***trans*-NAr_2-St-NAr_2**$^{\bullet+}$, which upon reduction yielded the ***trans*-NAr_2-St-NAr_2**. This cycle was catalytic upon *the* formation of ***trans*- NAr_2-St-NAr_2**$^{\bullet+}$ electron transfer, thus propagating a chain reaction with the ***cis*-NAr_2-St-NAr_2**. The occurrence of this isomerization at low temperatures indicates that the activation energy for the isomerization of the *cis*-stilbene radical cation is substantially lower than that of the neutral ***cis*-NAr_2-St-NAr_2**.

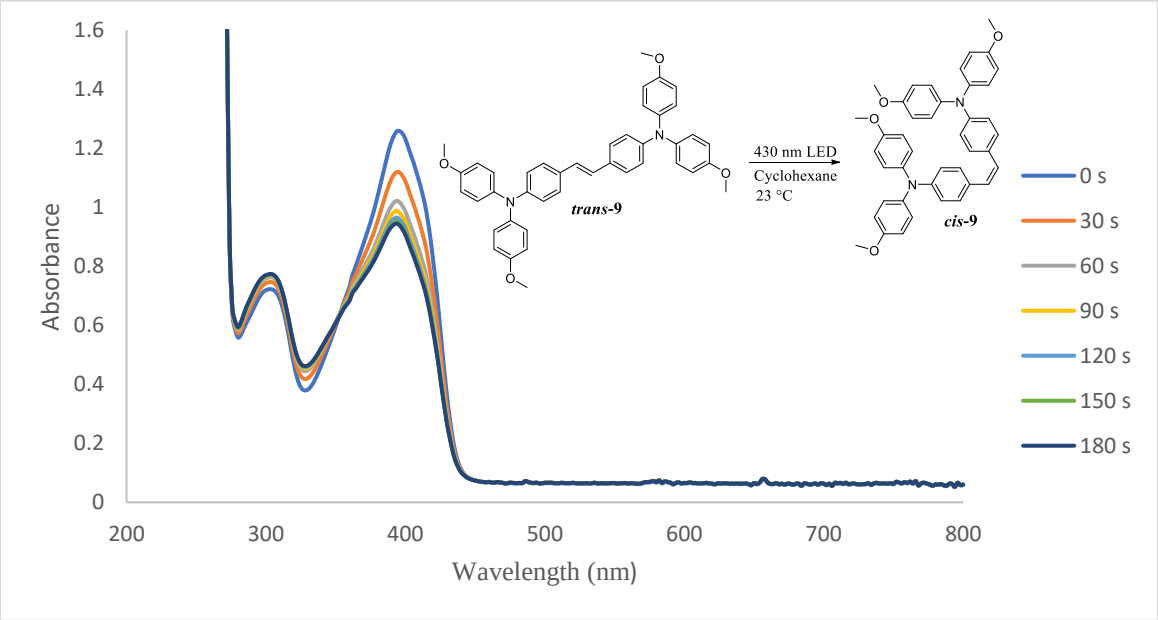

Figure 3.13. Photoisomerization of 2.47 x 10^{-5} M solution of ***trans*-9** in 2 % benzene in cyclohexane using 430nm LED (7W) at 23 ºC.

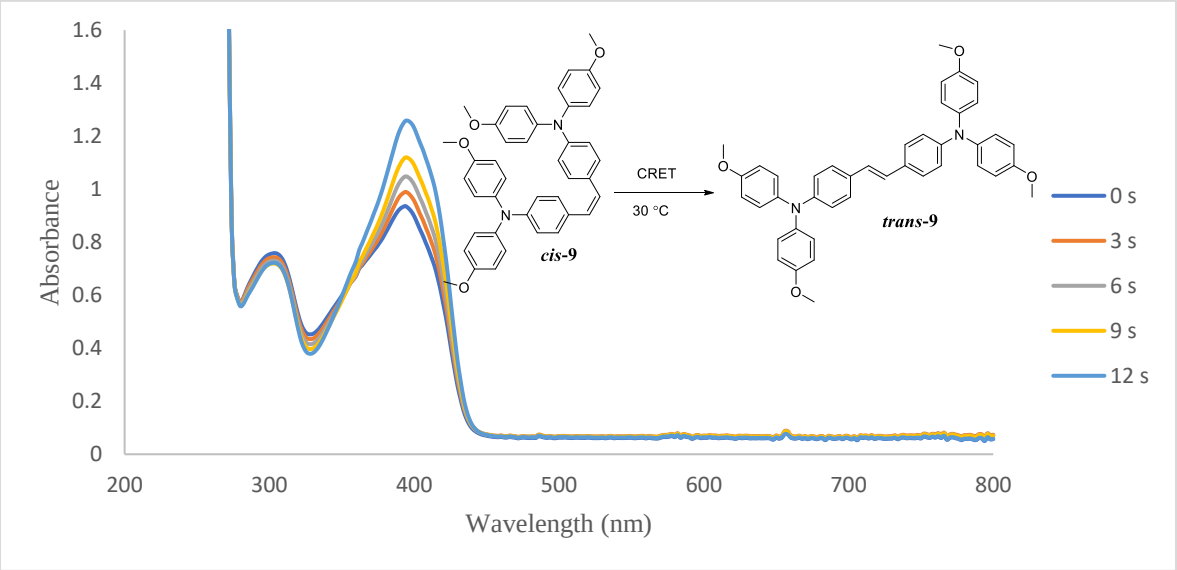

Figure 3.14. The optical spectrum of the addition of 2.50 mol % to 2.47 x 10^{-5} M solution of ***cis*-9** in 2 % benzene in cyclohexane at PSS.

Furthermore, ^{1}H NMR experiment was carried out to confirm the structure and identity of the product formed after the redox catalysis of ***cis*-9**. This was done by dissolving a known amount of ***cis*-9** in deuterated benzene and irradiating with 430 nm LED light (7W) until the PSS was reached. This was followed by the addition of 3.0 mol % of CRET to the solution and the reaction was stopped after about 12 seconds by the addition of activated zinc powder. The ^{1}H NMR spectrum of the product did not show any presence of the *cis* isomer, and it matched the ^{1}H NMR of ***trans*-9** as shown in Figure 3.14. To confirm this result, 3.0 mol % of CRET was added to a deuterated solution of benzene containing an isomeric mixture of 93 % *cis* and 7 % *trans*. The reaction was quenched with activated zinc after about 40 seconds and ^{1}H NMR of the product showed a complete conversion of the ***cis*-9** isomer to the ***trans*-9**

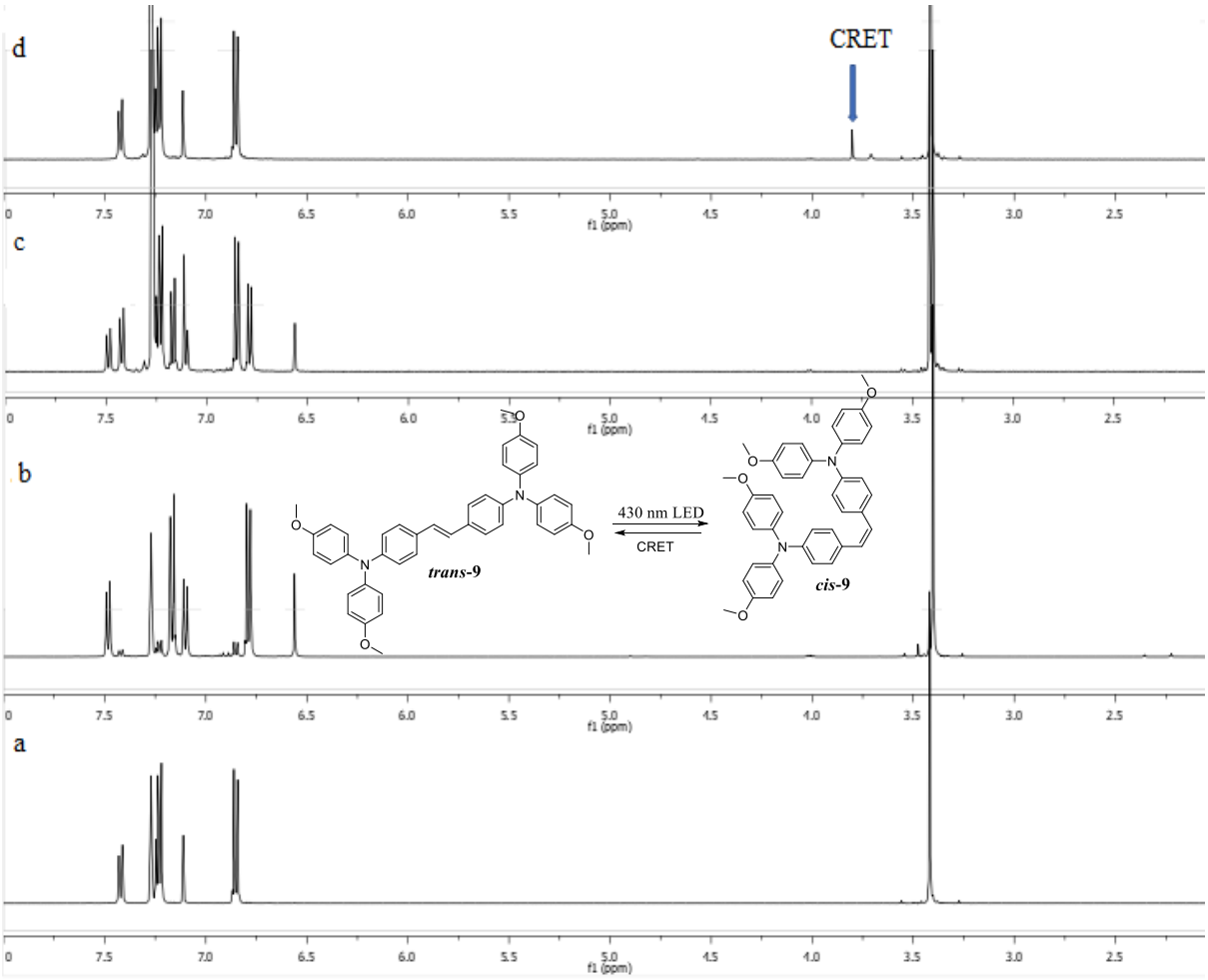

Figure 3.15. The ^{1}HNMR of (a) 2.21 x 10^{-4} M ***trans*-9** (b) isomeric mixture of ***cis*-9** and ***trans*-9** (91% *cis*: 9% *trans*) (c) isomeric mixture at PSS (40 % *cis*: 60 % *trans*) (d) after addition of 3 mol % CRET.

To understand the thermodynamic effect of the addition of the RA on ***cis*-9**, it was necessary to experimentally measure the ΔG‡ for the *cis* to *trans* RA-promoted isomerization of ***cis*-9**. The ΔG‡ for the thermal isomerization ***cis*-9** was measured to be approximately 29.3 kcal mol^{-1}, which is lower than the ΔG‡ for thermal isomerization of the parent stilbene (46 kcal/mol[56]). The ΔG‡ for the RA-promoted isomerization can be obtained by plotting of graph of ln [***cis*-9**] against time at 30 ºC (Figure 3.15-3.18). The slope of the graph gives the rate constant

k for the first order process and k can be used in calculating the free energy of activation ΔG‡ for reaction.

Time (seconds)	% *cis*: % *trans*	[*cis*]	In [*cis*]
0	92.7: 7.3	2.74E-05	-10.5
5	50.4: 49.6	1.49E-5	-11.1
8	31.1: 68.9	9.20E-6	-11.6
11	17.8: 88.2	5.27E-6	-12.2
14	8.6: 91.4	2.54E-6	-12.9
17	4.95: 95.5	1.24E-6	-13.4
23	0: 100	0	-14.4

Table 3.3. The changes in concentration over time for the redox auxiliary promoted isomerization of 2.96 x 10^{-5} M ***cis*-9** at 30 ºC in cyclohexane: benzene = 98:2 using 3.5 mol % CRET in DCM.

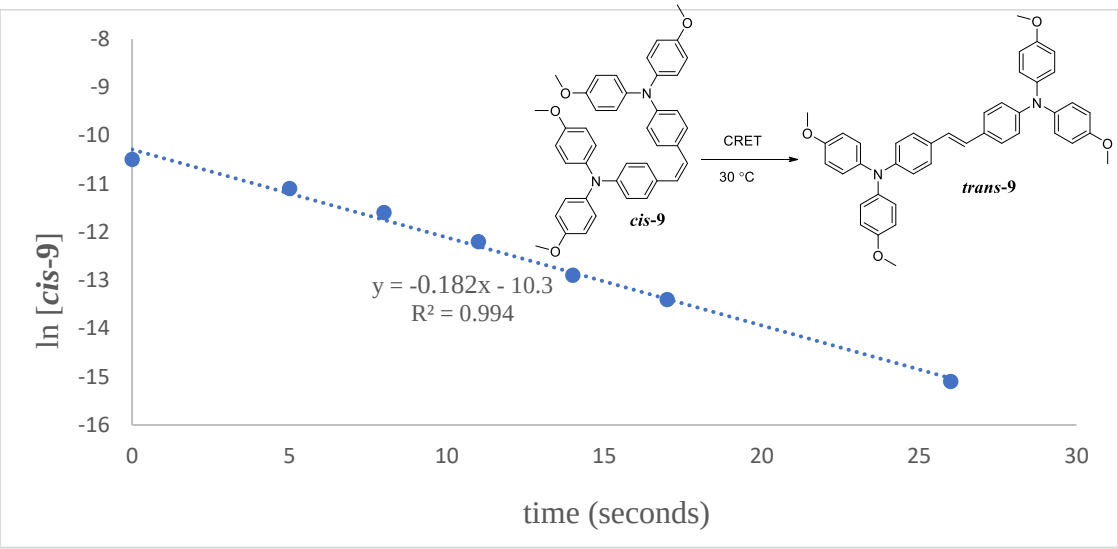

Figure 3.16. First order plot of the ln[***cis*-9**] vs time at 30 ºC for the redox auxiliary promoted *cis-trans* isomerization of 2.47 x 10^{-5} M ***cis*-9** in cyclohexane: benzene = 98:2 using 3.5 mol % CRET in DCM.

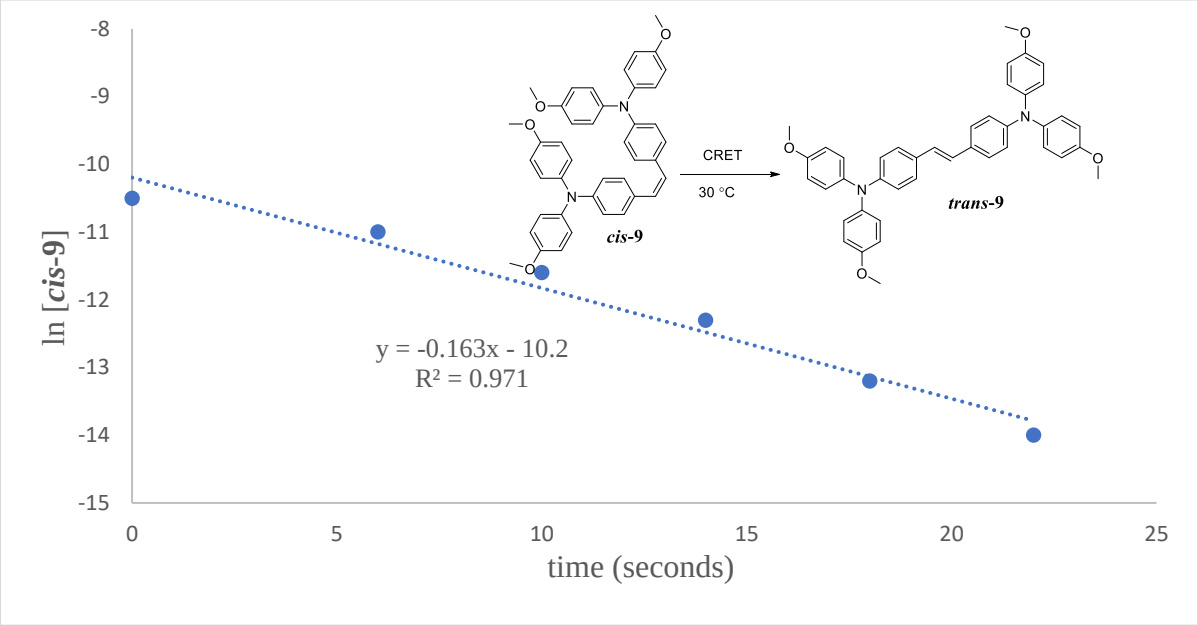

Figure 3.17. First order plot of the ln[***cis*-9**] vs time at 30 ºC for the redox auxiliary promoted *cis-trans* isomerization of 2.47 x 10^{-5} M ***cis*-9** in cyclohexane: benzene = 98:2 using 3.0 mol % CRET in DCM.

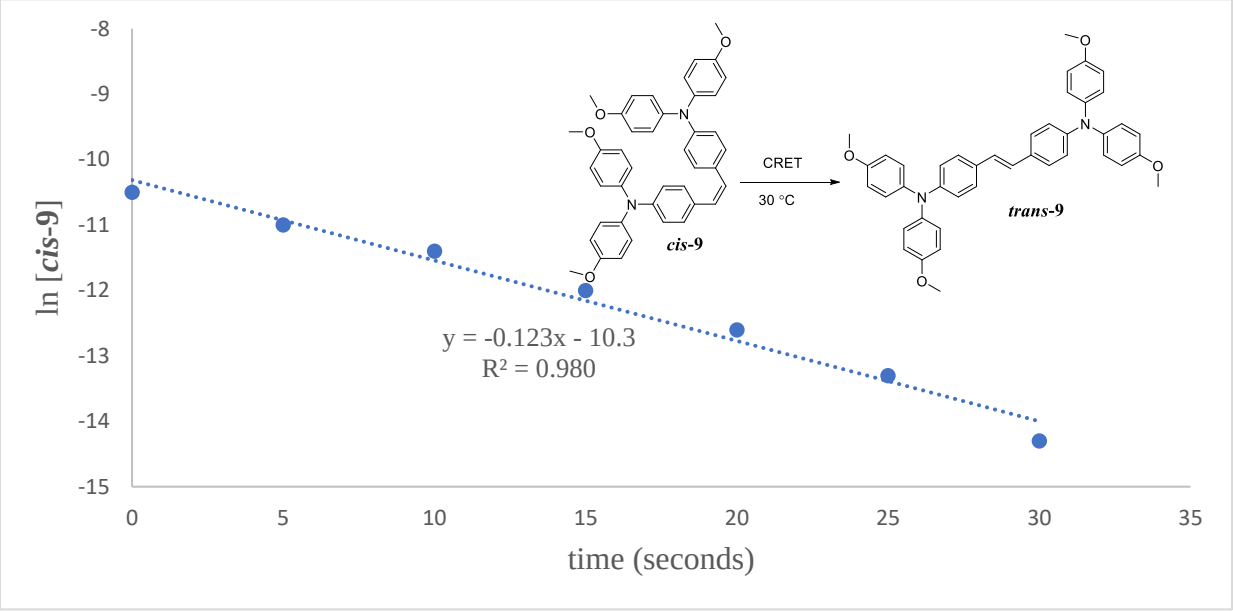

Figure 3.18. First order plot of the ln[***cis*-9**] vs time at 30 ºC for the redox auxiliary promoted *cis*-trans isomerization of 2.47 x 10^{-5} M ***cis*-9** in cyclohexane: benzene = 95:5 using 2.5 mol % CRET in DCM.

A graph of the rate constant was plotted against the mol % of CRET (Figure 3.19) and extrapolated to obtain the k for the addition of 100 mol % CRET. The rate acceleration of the *cis-trans* isomerization of ***cis*-9** for 100 mol % of CRET addition (10^{11}) was obtained by dividing the rate of the radical process for 100 mol % of CRET by the rate of the neutral process. The RA-promoted radical isomerization increased the rate of the *cis-trans* isomerization of ***cis*-9** by 10^{11} and the $\Delta G^{\ddagger}$ was experimentally found to be 14.1 kcal/mol.

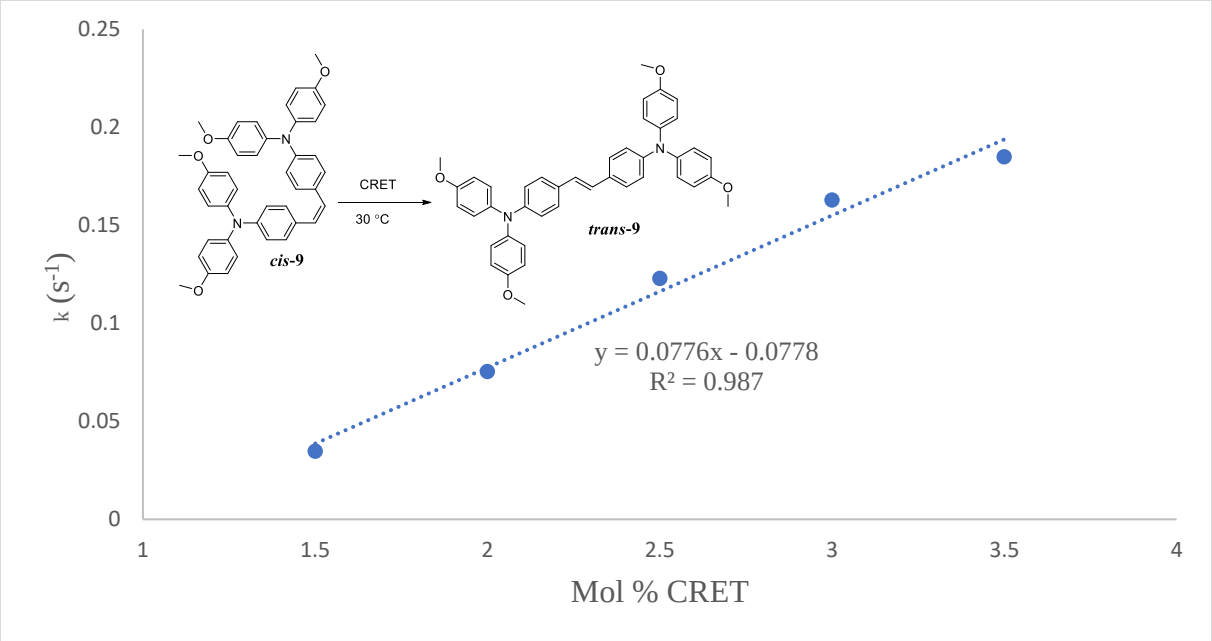

Figure 3.19. Graph of k vs mol % of CRET for the radical isomerization of 2.47 x 10^{-5} M ***cis*-9**.

But for 5 mol % CRET, k = 0.310 s^{-1}

Rate acceleration for *cis-trans* isomerization of ***cis*-9** for 5 mol % of CRET =

$$\frac{rate\ of\ the\ radical\ catalyzed\ process}{rate\ of\ the\ neutral\ process}$$

$$= \frac{0.310}{1.02\ x\ 10^{-8}} = 3.03\ X\ 10^{7}$$

$\Delta G^{\ddagger}$ of the radical catalyzed process for 5 mol % of CRET = 18.5 ± 0.1 kcal/mol

3.8 Thin cell Photo-Electro Device (PED)

After showing that we can exponentially increase the rate of *cis*-to *trans* isomerization of bis(diarylamino)stilbene through catalytic electron transfer cycle with a one electron oxidant, it was necessary to reproduce the results using a different oxidation method. We anticipated that applying 1.8 V would oxidize the *cis* isomer and cause a facile isomerization to the *trans* isomer (via a catalytic electron transfer cycle).

Isomerization of ***trans*-9f** to ***cis*-9f** was achieved by irradiating the ***trans*-9f** sample with 430 nm LED for 90 seconds, and then 1.8V was immediately applied to the sample for 120 seconds to regenerate the ***trans*-9f** isomer as shown in Figure 3.20. This illustrates that isomerization from ***trans*-9f** to ***cis*-9f** was obtained by irradiating with 430 nm light, therefore turning "OFF" the switch. The switch was then turned back "ON" by applying a 1.8 V to the ***cis*-9f**, thus regenerating the ***trans*-9f**.

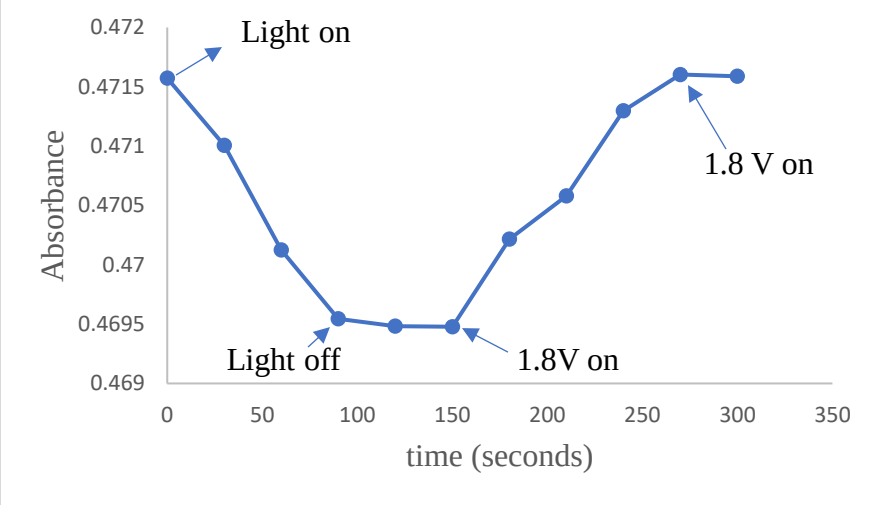

Figure 3.20. Photo-electro cell device. Irradiation of 1.05 x 10^{-4} M ***cis*-9** for 90 seconds with 430 nm LED corresponds to the decreases in absorbance. Application of 1.5 V for 120 seconds corresponds to the increases in absorbance.

3.9 Conclusions

These results agree with our hypothesis that the activation barriers of the *cis* to *trans* isomerization of stilbenes can be reduced by oxidizing an appended diaryl amino RA with a one electron oxidant. This method of isomerization of stilbene converts the neutral *cis*-stilbene to the cation radical. The cation radical will then undergo a chain process in which it will isomerize to the more stable *trans*-stilbene radical cation. The electron hole transfer between the *trans*-stilbene radical cation and the neutral *cis*-stilbene completes catalytic cycle, as shown in Scheme 3.4. This one electron oxidation of the attached RA was catalytic, occurred at lower temperatures, produced pure *trans*-stilbenes and did not produce any side products. The rate acceleration was due to the reduced activation barrier of the radical process being lower than the barrier of the competing side reactions.

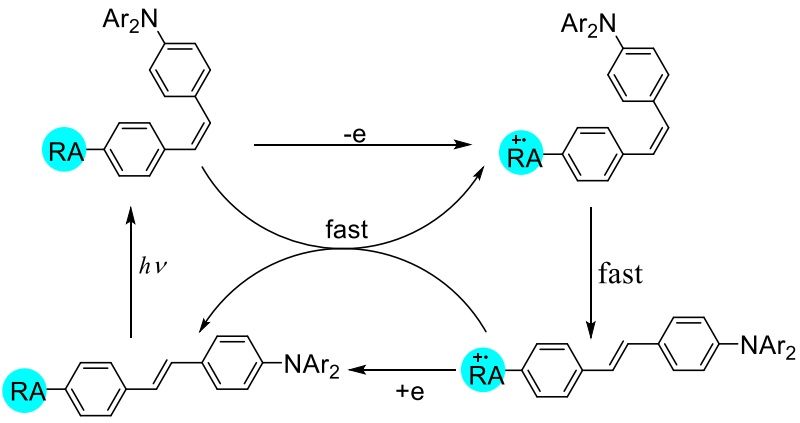

Scheme 3.4. The catalytic cycle of the isomerization of bis(diarylamino)stilbene.

3.10 Experimental details

Synthesis of (4-bromobenzyl) triphenylphosphonium bromide

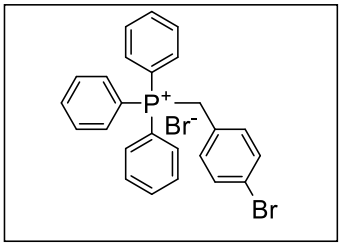

A solution of 10.0 g (48.0 mmol) of 4-(bromomethyl) bromobenzene and 12.6 g (48 mmol) of triphenylphosphine in 100 ml of dry toluene was refluxed for 12 h. After cooling to room temperature, a precipitate formed which was filtered off and washed with toluene. Drying in vacuo afforded (4-bromobenzyl) triphenylphosphonium bromide. White powder, yield (19.7 g, 96.1%).[144]

General Witting procedure for the preparation of *cis*-8 and *trans*-8.[145]

A solution of sodium methoxide (0.797 g, 14.8 mmol) in methanol (15.0 mL) was added dropwise to a suspension of the (4-bromobenzyl) triphenylphosphonium bromide salt (9.10 g, 14.8 mmol) and p-bromobenzaldehyde (2.28 g, 12.3mmol) in methanol (20 mL) under N_2 at room temperature. After completion of the addition, the resulting solution was stirred for 1 h at room temperature. At the end of the reaction, the mixture was poured into cold water (60 mL), treated with saturated $NaHCO_3$, extracted with 3 x 10 mL of CH_2Cl_2 and dried over $MgSO_4$. The solvent was removed under reduced pressure and the crude product was recrystallized in hexane, filtered through a frit funnel and washed with acetone to give the pure ***trans*-8** as a colorless solid (1.96 g, 47.1 %). The mother liquor containing a mixture of the phosphonium oxide and ***cis*-8** was filtered through a short pad of silica gel using ethyl acetate/hexane = 1:8 to afford the pure ***cis*-8** as a yellow oil (1.80 g, 44.0 %). Total yield= 3.76 g, 91.1%

***cis*-4,4′-dibromostilbene *cis*-8**

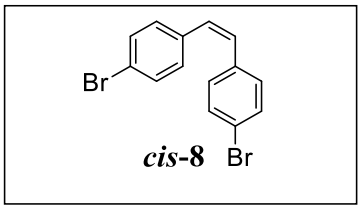

***cis*-8**

Yellow oil, 1.80 g, 44.0 % δ (ppm) ^{1}H NMR (360 MHz, $CDCl_3$): 7.36 (d, J = 8.5 Hz, 4H), 7.08 (d, J = 8.5 Hz, 4H), 6.54 (s, 2H)[144]

***trans*-4,4′-dibromostilbene 6a**

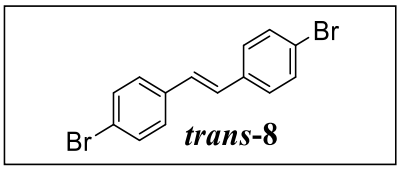

***trans*-8**

White solid, 1.96 g, 47.1 % yield. δ (ppm) ^{1}H NMR (360 MHz, $CDCl_3$): δ (ppm) 7.50 (d, J = 8.6 Hz, 4H), 7.38 (d, J = 8.6 Hz, 4H), 7.03 (s, 2H). mp 211-212 (Lit. 210-212 ºC)[145]

Synthesis of Tetraanisyldiaminostilbene (TADAS) *cis*-9 and *trans*-9 [161]

***cis*-9**

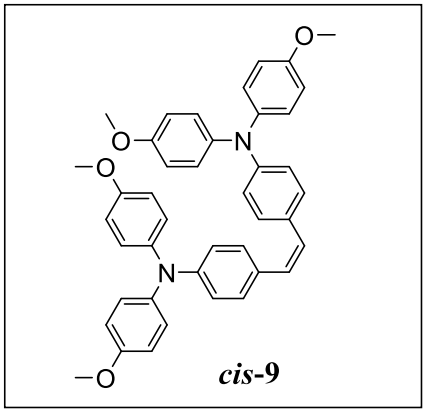

***cis*-9**

5 (0.459 g, 2.00 mmol) and and 4,4′-dibromo-substituted stilbene ***cis*-8** (0.334g, 1.00 mmol) were added into a 100 mL flamed-dried rb flask in a dry box. Toluene (anhyd. 4 mL) was added to the flamed-dried flask and stirred. $Pd(dba)_2$ (11.5 mg, 2 mol %), $P(tBu)_3$ (4.05 mg, 2.00 mol %,) were added into the mixture and the mixture was stirred for about one minute. NaOtBu (0.288 g, 3.00 mmol, 1.50 eq) was then added and the flask was capped with a rubber septum, removed from the dry box and stirred under N_2 for 4 h at 90 °C. The reaction mixture was monitored via TLC (ethyl acetate: hexane =1:8) until it showed the disappearance of the starting materials in about 4 hr. The mixture was then cooled to room temperature, filtered through a plug of about 5 g of activated basic alumina in a fritted funnel and washed with 50 mL of ethyl acetate. The product was concentrated in vacuo to yield the crude product which was purified by column chromatography on silica gel using ethyl acetate/hexane

=1:4 to give *bis*-dianisylaminostilbene ***cis*-9** as a yellow oil containing mainly the *cis* isomer (91.9 % *cis*: 8.10 % *trans*). 1.15 g, 90.3 % yield

mp 72-74 °C; ^{1}H NMR (500 MHz, C_6D_6) δ (ppm): 7.48 (d, J = 8.9 Hz, 4H), 7.17 (d, J = 8.9 Hz, 8H), 7.10 (d, J = 8.9 Hz, 4H), 6.79 (d, 8H), 6.56 (s, 2H), 3.40 (s, 12H); ^{13}C NMR (125 MHz, C_6D_6): 55.7 115.4, 119.1, 127.2, 128.1, 129.2, 129.7, 147.7, 156.2; ESI-HRMS calcd for $C_{42}H_{38}N_2O_4$: 634.2832, found 634.2845

***trans*-9**

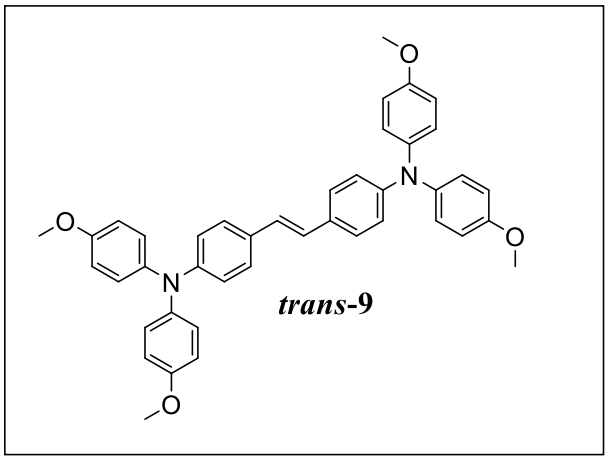

***trans*-9**

The synthesis of ***trans*-9** was carried out by using the above Buchwald/Hartwig amination procedure. The reaction mixture was cooled to room temperature, filtered through a plug of about 5.00 g of activated basic alumina in a fritted funnel and washed with 50.0 mL of ethyl acetate. The product was concentrated in vacuo to yield the crude product which was purified by column chromatography silica gel using ethyl acetate/hexane =1:4 to give *bis*-dianisylaminostilbene ***trans*-9** as a greenish yellow solid (1.17 g 92.1 % yield). mp 164-166 °C; ^{1}H NMR (500 MHz, C_6D_6) δ (ppm): 7.42 (d, J = 8.7 Hz, 4H), 7.25-7.22 (m, 12H), 7.11 (s, 2H), 3.42 (s, 12H), 6.85 (d, J = 8.7 Hz, 8H)

^{13}C NMR (125 MHz, DMSO-D_6): 55.7, 115.4, 120.0, 125.8, 126.9, 127.4, 130.0, 140.4, 147.9, 156.2; ESI-HRMS calcd for $C_{42}H_{38}N_2O_4$: 634.2832, found 634.2841

Preparation of the stock solution of *trans*-9 (3.04 x 10^{-5} M) in deaerated 2 % benzene in cyclohexane

The stock solution of ***trans*-9** (3.04 x 10^{-5} M) in 2 % benzene in cyclohexane (Figures 3.6) was prepared by successive dilution. 1.00 mg (1.58 x 10^{-3} mmol) of the substrate was dissolved in about 1.00 mL of benzene and a 1000 μL gas-tight syringe was used to transfer 500 μL of this solution to an empty volumetric flask. The solution was filled to the 26.0 mL mark with cyclohexane to give the required concentration (3.04 x 10^{-5} M). 3.0 mL of this solution was placed in a 10 mm quartz cuvette and the optical spectrum was measured every 30 s.

Photoisomerization of *trans*-9 using a 420 nm LED in deaerated 2 % benzene in cyclohexane

3.00 mL of the solution of ***trans*-9** (3.04 x 10^{-5} M) prepared by using the above procedure was placed in a quartz cuvette. The sample was then irradiated with a 420 nm LED (7 W) and the subsequent optical spectrum was taken every 30 s.

Kinetic studies of the thermal isomerization of 0.0790 M *cis*-9 in DMSO-d_6

The thermal isomerization kinetics of ***cis*-9** was studied by ^{1}H NMR spectroscopy at different temperatures (100 ºC, 110 ºC, 120 ºC, 130 ºC, 140 ºC and 150 ºC). A solution of 25.1 mg of ***cis*-9a** in 0.5 mL of deaerated DMSO-d_6 (7.90 x 10^{-2} M) was put in an NMR tube. The NMR tube was sealed with parafilm, immersed in a constant temperature oil bath, and the spectrum was recorded. For each spectrum, the methoxy signals were integrated to evaluate the % *cis*: % *trans* of the sample, giving the corresponding concentration of ***cis*-9a** as a function of time. The thermal isomerization rates (*k*) were obtained from the slope of the first order plots of the natural logarithm of the concentration of the *cis* against time. The resulting *k* values at different temperatures were used to plot Eyring and Arrhenius plots from which the activation and thermodynamic parameters were obtained.

Preparation of photo electrochromic device (PECD)

***Trans*-9f** (2.81 mg, 0.00440 mmol) was dissolved in 1.0 mL Tol_3TBABF_4 gel. The gel solution was applied to ITO glass anode (equipped with spacer); the ITO glass cathode was then added to complete sandwich-type device. The ITO sandwich was held together with two closed jaw compressor clamps for the duration of the experiment. Cycling conditions were: 90 sec irradiation with 430 nm LED and 0.00 V, then 1.50 V for 120 s with no irradiation (Cyclic Voltammetry Scan Rate: 100 V/s). Spectrophotometer Reading- 30 s intervals.

CHAPTER FOUR

[3,3]-SIGMATROPIC REARRANGEMENT OF 3-AMINO-1,5-HEXADIENES

4.1 Introduction

The Cope and Claisen rearrangements are among the most important reactions in organic chemistry. The Claisen rearrangement was discovered by Raney Claisen in 1912[162] while rearrangement was discovered by Arthur Cope in 1948.[163] The reactions have a very high negative entropy of activation[64, 164] and generally, require very high temperatures, sometimes exceeding 200 ºC.[118] Both reactions belong to the same class of organic reactions known as [3,3]-sigmatropic rearrangements. The [3,3]- sigmatropic rearrangements are intramolecular processes that involve the migration of a sigma bond adjacent to one or more pi systems to a new position within the molecule. For example, the migration of C-X sigma bond from position 3 to position 1 in Scheme 4.1.[165]

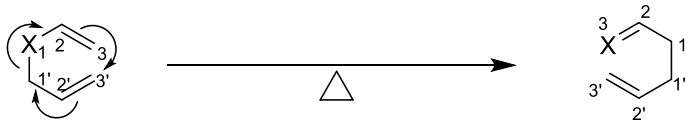

Scheme 4.1. A [3,3]- sigmatropic rearrangement of 1,5-Hexadiene.

The rearrangement is called the Cope when X is carbon and the Claisen when X is oxygen, nitrogen or sulfur. These reactions have been subjects of intensive researches for almost a century, both as subjects of intensive theoretical investigations,[166] and as a powerful tool for

organic synthesis.[31] Hence, synthetic chemists have widely employed them as a guiding concept in the design of a wide range of complex structures. These transformations are advantageous for the construction of congested stereocenters, such as in the synthesis of natural products, fragrances, flavor compounds as well as in biological processes.[167]

4.2 Mechanism of the Cope and Claisen Rearrangements

The Cope and the Claisen rearrangements involve the [3,3] migration of a σ bond in a thermally activated molecule and have the same mechanism. Interestingly, the mechanism of these reactions has remained controversial even though these reactions have been studied extensively.[66, 168-169] Early speculation on the mechanism of the rearrangement of 1,5-hexadiene focused on a concerted process whose transition state involved a new bond formation assisting the bond cleavage. Two major reaction pathways have been proposed for the rearrangement of 1,5-hexadienes. Doering and Roth[170] believe that 1,5-hexadienes and other related compounds undergo [3,3]-sigmatropic rearrangements in a concerted mechanism that involves a chair-like six-membered pericyclic transition state while Dewar[168] and Houk[64] believe that the reactions proceed by a biradical intermediate when radical stabilizing groups are attached to C_2 and C_5 positions (Scheme 4.2).

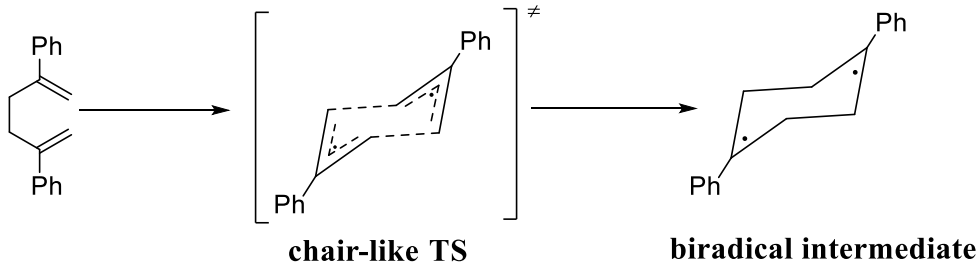

Scheme 4.2. Cope rearrangement of 1,5-hexadienes showing a chair-like six-membered pericyclic transition state and a biradical intermediate when radical stabilizing groups are attached to C_2 and C_5 positions.

In order to determine the actual mechanism of the Cope rearrangement of 1,5-hexadienes, Doering and coworkers[171] studied the substituent effects on the transition state of the reaction. They used the term "Chameleonic" to describe the ability of the bond lengths to change in response to radical stabilizing substituents. Theoretical calculations[63, 172] show that substituents do not only stabilize the Cope rearrangement TS, but also alter the geometry to maximize this stabilization. These computed bond lengths in the transition structures are all consistent with a chameleonic nature of the TS. Secondary kinetic isotope effects measured by Gajewski and Conrad[173] provided a direct experimental evidence that the reaction has a variable TS, in which the bond lengths change with the presence and placement of radical-stabilizing substituents. They defined these bond length changes as the bond breaking and the bond making kinetic isotope effects and the ratio of these two indicates the extent to which bond making/breaking has occurred at the transition state. They showed that this ratio was large for hexadienes having phenyl substituents at C_2 and C_5, indicating that more bond making than bond breaking occurred at the cyclohexanediyl-like transition state of the reaction. This is because the phenyls at this position stabilize such an intermediate, indicating that cyclohexanediyl is a possible intermediate thereby opposing the involvement of two allylic radicals. However, other studies indicate that the TS could be an intermediate between the two extreme structures, either two allyl radicals or a 1,4-cyclohexane diyl (Figure 4.1).[174-176]

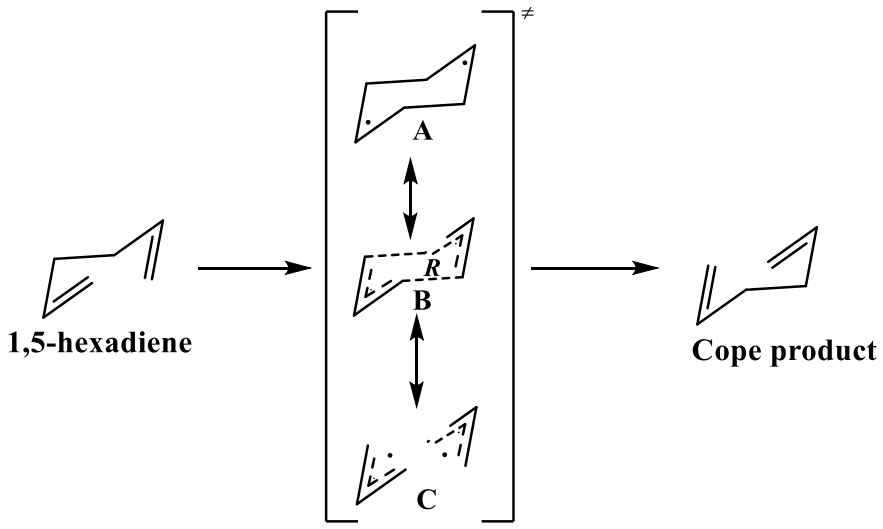

Figure 4.1. The depiction of possible TSs for the Cope rearrangement. In the two diradical extremes, bond making either precedes (**A**) or lags (**C**) bond breaking, while in TS **B** bond making and bond breaking occur synchronously. The interallylic distance (***R***) is expected to increase in going from TS **A** to TS **C**.[177]

4.3 Catalysis of the Cope and Claisen rearrangements

Thermal amino-Claisen rearrangements have been less attractive due to the high reaction temperatures (220-350 °C). Catalysis of the Cope and Claisen rearrangements has been of interest for a very long time; beginning with a 1912 report by Claisen when he showed that ammonium chloride could catalyze a Claisen rearrangement.[178] Since then, numerous other compounds, mainly Bronsted and Lewis acids such as BF_3, BCl_3, CF_3COOH, $ZnCl_2$, HCl, H_2SO4, H_3PO_4 and $AlCl_3$, bases such as KOH, NaH, and KH, and transition metal complexes such as Na_2PtCl_4 and $Pd(OAc)_2/PPh_3$ have been used to catalyze the reactions. These compounds have shown catalytic activities ranging from little to dramatic at lower reaction temperatures. In some cases, these catalysts have been used in stoichiometric or greater amounts if necessary to promote aromatic amino-Claisen rearrangements. The synthetic utility of these rearrangements is limited due to by-product formation, long reaction times, high reaction temperatures, large amounts of catalyst as well as unsatisfactory yields.[162, 179-181]

4.4 Our Research Goals

Our goal is to develop redox-auxiliary (RA) promoted [3,3]-sigmatropic rearrangement of 1,5-hexadienes at room temperature by using a one electron transfer oxidant to lower the energy barrier of the reaction. Previous studies have established that the energy barrier for the Cope rearrangement of 1,5-hexadienes is 33.5 kcal/mol for the chair pathway.[65-66, 172] As a result of this barrier, the aza-Claisen and Cope rearrangements require very high temperatures. For example, uncatalyzed simple allyl vinyl amines undergo [3,3]-sigmatropic transformation at about 250 °C, while the activated aromatic analogs require 200–210 °C.[179] We postulated that an aryl amino redox group appended on the skeleton of the 1,5-hexadiene could lower the barrier of a [3,3]-sigmatropic rearrangement upon oxidation of the redox group by changing this group from the neutral to the cationic state. The cationic state is envisioned to reduce the bond strength of the migrating C-C bond thereby reducing the barrier for the rearrangement of **10** to give the Cope product **10a** or, alternatively, the aza-Claisen (AC) product **10b** if the redox auxiliary takes part in the reaction.

A one-electron oxidant such as **CRET** will be capable making $\mathbf{10}^{+\cdot}$ which is postulated to undergo a [3,3]-Cope rearrangement or [3,3]-aza-Claisen rearrangement. The expectation is that the oxidation of the amine will turn on the Cope reactivity of **10** at room temperature or maybe even at lower temperatures. It is possible for this process to be catalytic because oxidizing the neutral amine could trigger an electron transfer catalysis cycle in which the amine cation radical undergoes a Cope reaction and then electron transfer with another unreacted Cope substrate to create a chain reaction. This process might as well be stoichiometric if the product structure is not able to oxidize the reactant structure, as in the AC transformation. In this case, the RA will take part in the reaction as shown in Scheme 4.3 and will not function as a RA as designed. Such

a dramatic change in reaction rates which accompany this reaction may find interesting applications in the design of sensors and triggering devices in materials science.

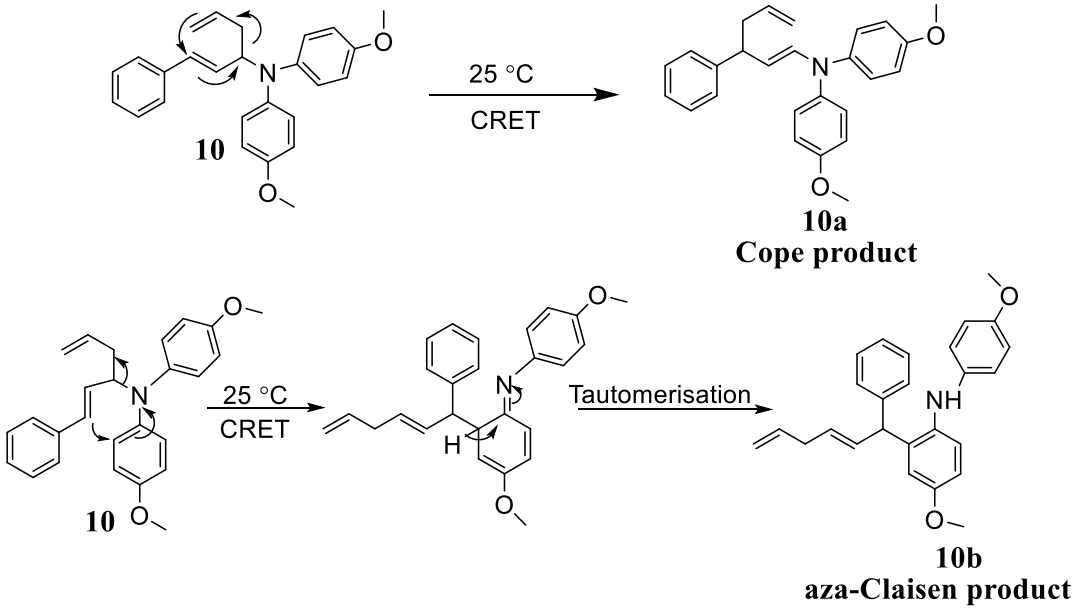

Scheme 4.3. Cope and aza-Claisen rearrangements of redox appended 1,5-hexadiene.

4.5 Synthesis of redox appended 1,5-hexadienes

The first step in the synthesis of redox appended 1,5-hexadienes is the condensation of commercially available substituted primary anilines and aromatic aldehydes to make the α, β-unsaturated imines (Schiff base). This was followed by the addition of 1.2 equivalents of the Grignard reagent to the Schiff under an inert atmosphere to afford the secondary amine **11**. All the corresponding homoallylic secondary amines were obtained in yields ranging from 85% to 99 %. The key reaction in Scheme 4.4 is the Buchwald/Hartwig coupling of the para-substituted bromoanisole and homoallylic secondary amine. The resulting 3-diarylamino,1,5-hexadiene **10** was purified by column chromatography to afford the desired compound in excellent yields.

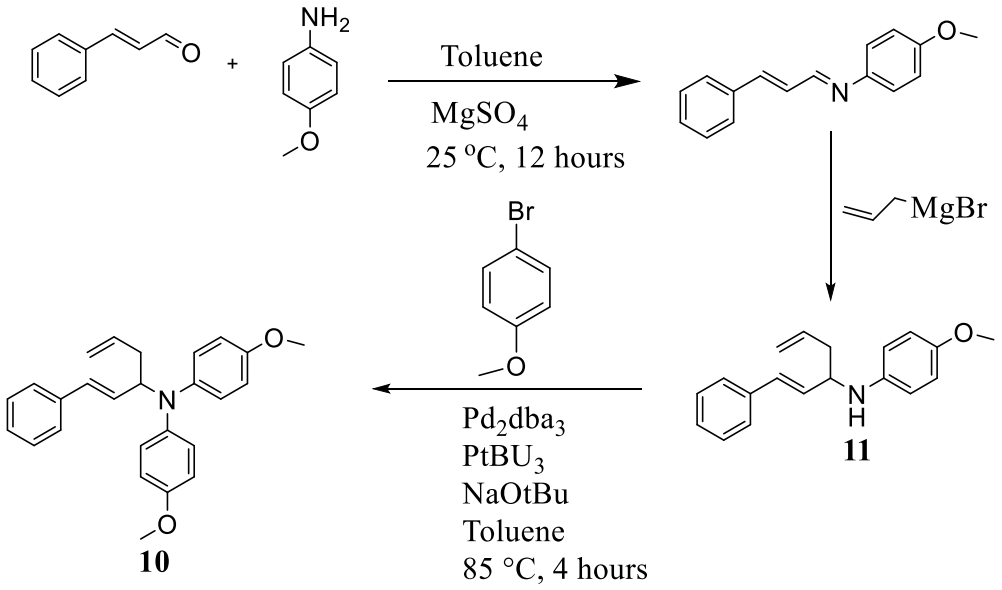

Scheme 4.4. The synthesis of 3-amino-1,5-Hexadienes.

4.6 Results of the Redox Auxiliary Mediated Rearrangement of 3-amino-1,5-Hexadienes

As stated earlier, the Cope rearrangement of 1,5-hexadienes is a slow reaction that occurs at very high temperatures with high activation energy.[64, 182] The main goal of this redox auxiliary promoted [3,3]-sigmatropic rearrangements is to reduce the high temperature required for the Cope or aza-Claisen rearrangement. To achieve this, it is very important to have a reference temperature at which the thermal reaction takes place. Therefore, we evaluated the uncatalyzed rearrangement of **10** and this evaluation showed that the reaction proceeds thermally at about 175 °C. After about 2 hours at 175 °C, a mixture of the AC product **10b** and three other minor products were formed. There were about 80 % unreacted starting material at the end of the reaction. However, the reaction did not produce any Cope product **10a**.

Based on this result, we proceeded to study the redox auxiliary promoted [3,3]-sigmatropic rearrangement of **10** at room temperature using 20.0 mol % of a one-electron transfer oxidant, CRET. The purpose of attaching the diarylamino RA on the skeleton of the 1,5-

hexadiene was to lower the barrier of the cope rearrangement upon oxidation of this RA group by changing it from the neutral to the cationic state. The cationic state was expected to reduce the bond strength of the C-C bond thereby reducing the barrier for the rearrangement of **10** to give the Cope product **10a**. But to our greatest surprise, in the process of trying to redox activate the Cope reaction of the 1,5-diene, the RA group at C3 also created an allyl phenyl amine, which upon oxidation of the amine, underwent a facile [3,3] AC rearrangement as the primary reaction pathway to give **10b**. So, the design to activate one [3,3] bond shift resulted in the activation of another [3,3] bond shift in the substrate (Scheme 4.5). The oxidation products of this reaction were successfully purified by column chromatography using benzene: hexane = 1:1 after several unsuccessful attempts to yield the products **10b- e** as shown in Scheme 4.5. The structures and the double bond configurations of these oxidation products were fully characterized by using mass spectrometry and NMR. The above result indicates that the Cope and AC rearrangements of substituted 3-amino-1,5-hexadiene differ from the parent reaction due to the lower enthalpy of activation. This impact was particularly pronounced in the case of **10** because of the resonance stabilization provided by the introduction of the RA, which could change its oxidation state reversibly.

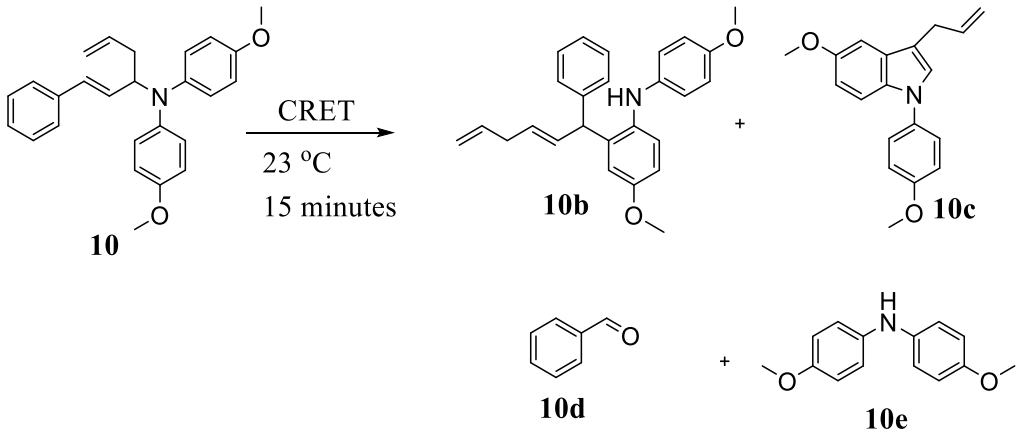

Scheme 4.5. The RA mediated rearrangement of 3-diarylamino-1,5-Hexadienes.

Encouraged by the success recorded in this reaction and the purification of the oxidation products of **10**, the RA promoted AC rearrangement of structurally similar compounds **12**,**14**,**16**,**18 and 20** were also studied. This is necessary to determine the scope of this rearrangement with regard to the diversity of the amine substrates (Table 3.1). The substrates smoothly underwent the desired transformation to give the AC product as the major product. The best result was obtained in **14** which produced AC product as the major product in 75 % yield in contrast to **10** which produced about 65 % AC product. This increase in the rate of formation of the AC product of **14** is known as the Thorpe-Ingold effect[183] and is due to steric interaction caused by the methyl substitution, which makes the bond angle between the two reacting groups narrower than those of **10**,**12**,**16**,**18 and 20**. The narrow bond angle enhances the interaction between the p orbitals thereby promoting the rearrangement of **14** due to the formation of small rings. Furthermore, the introduction of the methyl group in **14** reduced the conformational freedom in the molecule. The steric repulsion caused by this substituent increased the probability of the molecule taking the conformation that favors the formation of the AC product. As a result, the conformation of the nitrogen atom changed from the planar to the twisted form making it possible for the p orbitals to align properly. This maximizes the resonance stabilization in the molecule thereby increasing the rate of the reaction. The substantial decrease in the yields of the side products in **14** might also be due to the absence of one of the acidic hydrogens H_a and H_b in **10** (Table 4.1). Based on this result, we reasoned that **22** might give exclusively the aza-Claisen product due to an increased Thorpe-Ingold effect.[183] Unfortunately, several attempts to synthesize **22** were unsuccessful. The synthesis of this substrate in future might solve the problems associated with the formation of side products[162, 184] in [3,3]-rearrangement of amino-1,5-hexadienes.

	Substrates	Oxidation products		
		b	c	d
10	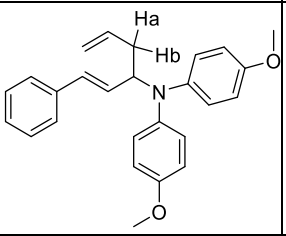	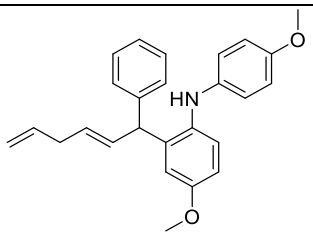	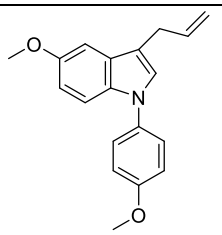	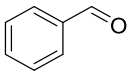
12	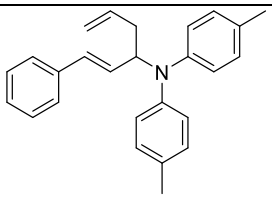	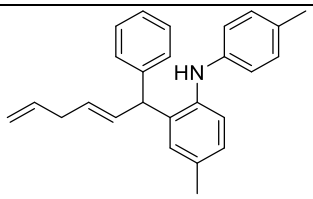	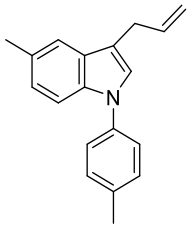	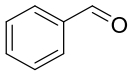
14	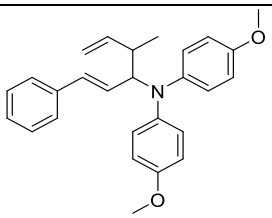	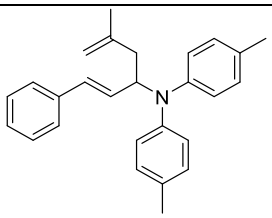	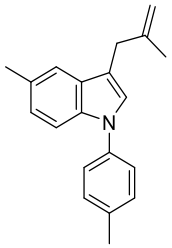	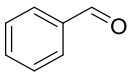
16	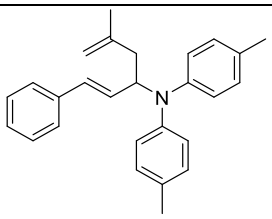	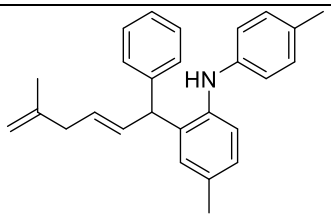	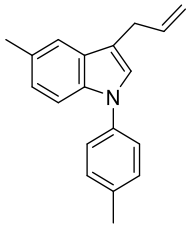	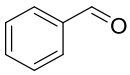
18	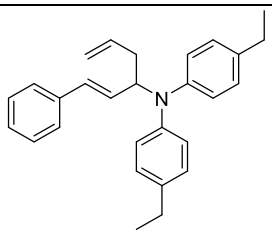	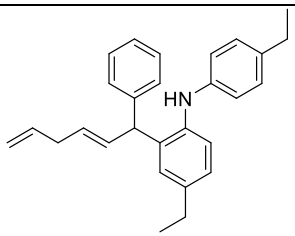	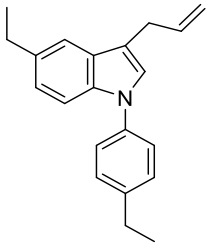	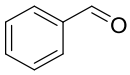
20	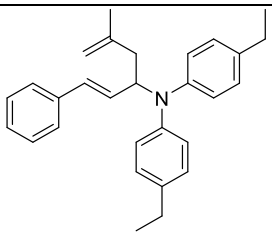	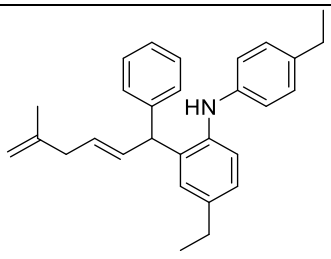	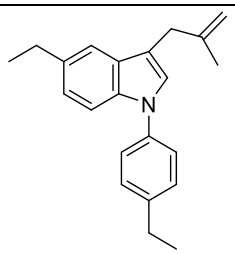	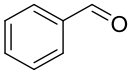

Table 4.1. Oxidation products of 3-diarylamino-1, 5-hexadienes.

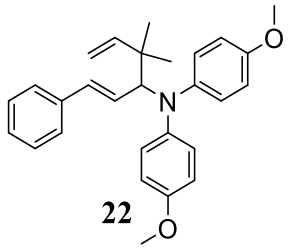

22

4.7 Explanation of Results

In sigmatropic rearrangements where one σ bond is broken and a new σ bond is made, the secondary kinetic deuterium isotope effects on each bond change is independent and would be expected to relate to the extent of bond breaking and bond making respectively.[173] If bond making preceeds bond breaking significantly in the Cope rearrangement, then Cope TS will have a 1,4-diyl character. The amino group at the C3 position may have little effect on the reaction as shown in Scheme 4.6. Theoretical calculations by Bauld and coworkers[28] suggest that the parent 1,5-hexadiene cation radical **10**$^{+\cdot}$ would cyclize either to a chair or boat cyclohexane-1,4-diyl cation radical intermediate with a low energy barrier. But the second cleavage step would require a relatively high activation, suggesting that the cation radical cleavage is the key step in a cation radical cyclization cleavage mechanism. The boat transition state is often disfavoured due to non-bonding interactions. Since the cleavage of the intermediate is the key step in this reaction and requires a high activation barrier, then the Cope product **10b**$^{+\cdot}$ will not be the predominant product of the reaction.

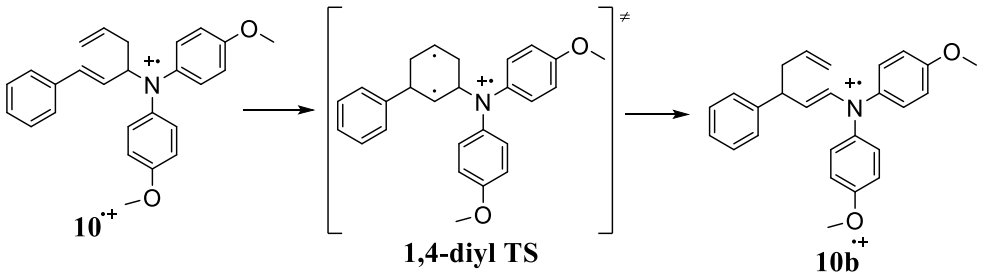

Scheme 4.6. Cope rearrangement of 3-amino-1,5-hexadiene.

If bond making preceeds bond breaking significantly as in the aza-Claisen rearrangement, then the AC TS will be strongly stabilized by amino radical cation at C3 position (Scheme 4.7). This stronger diarylamino stabilization of the TS for the AC path compared to the Cope path could lead to the formation of predominantly the AC product. The formation of a resonance-stabilized iminium cation at the TS is the thermodynamic driving force of this reaction. In addition, the structure/conformation of the substrates play a big role in the determination of the reaction route. B3LYP DFT calculations indicates that the "pre-Cope" conformation is about 1-2 kcal/mol higher in energy (so less populated) than two of the "pre-aza-Claisen" conformations. The stronger RA stabilization of the TS for the AC path compared to the Cope path and the structure/conformation of the substrates could account for the predominant formation of the AC product **10b**.

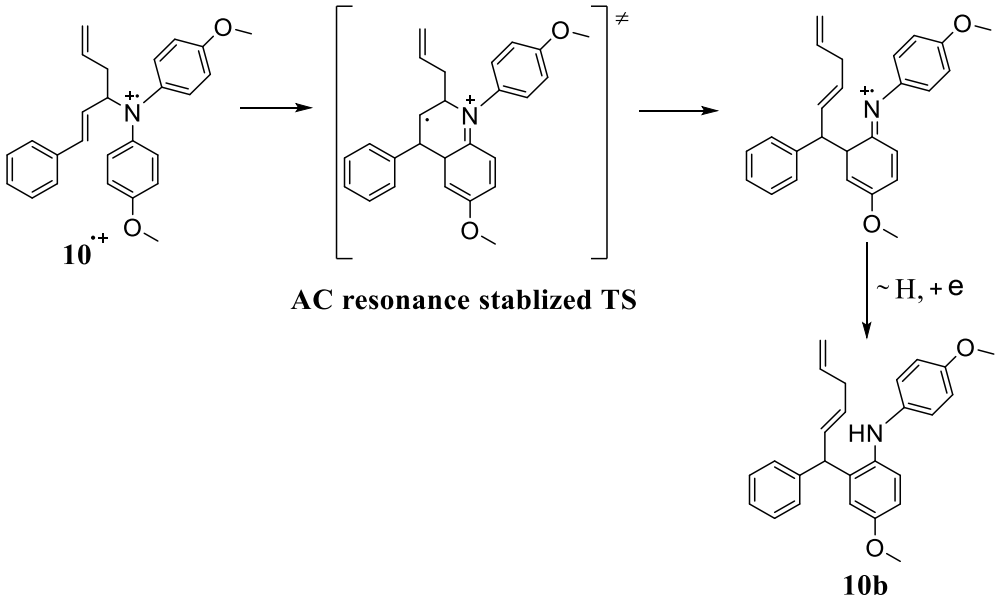

Scheme 4.7. AC rearrangement of 3-amino-1,5-hexadiene.

The unique characteristic of the transition state of a pericyclic reaction such as the AC rearrangement of 3-amino-1,5-hexadiene is the cyclic conjugated system (Scheme 4.8). The rate

enhancement of these reactions is often discussed in terms of the delocalization stabilization (aromaticity or antiaromaticity) of the cyclic systems. The effects of aromaticity or antiaromaticity play a big role in the dramatic acceleration of [3,3]-sigmatropic rearrangement or even a complete disappearance of the reaction barrier. Our results indicate that a one electron oxidation of our substrates to form the cation radicals is found to lower the activation energy drastically, and this agrees with experimental observations relative to cation-radical pericyclic reactions.[28]

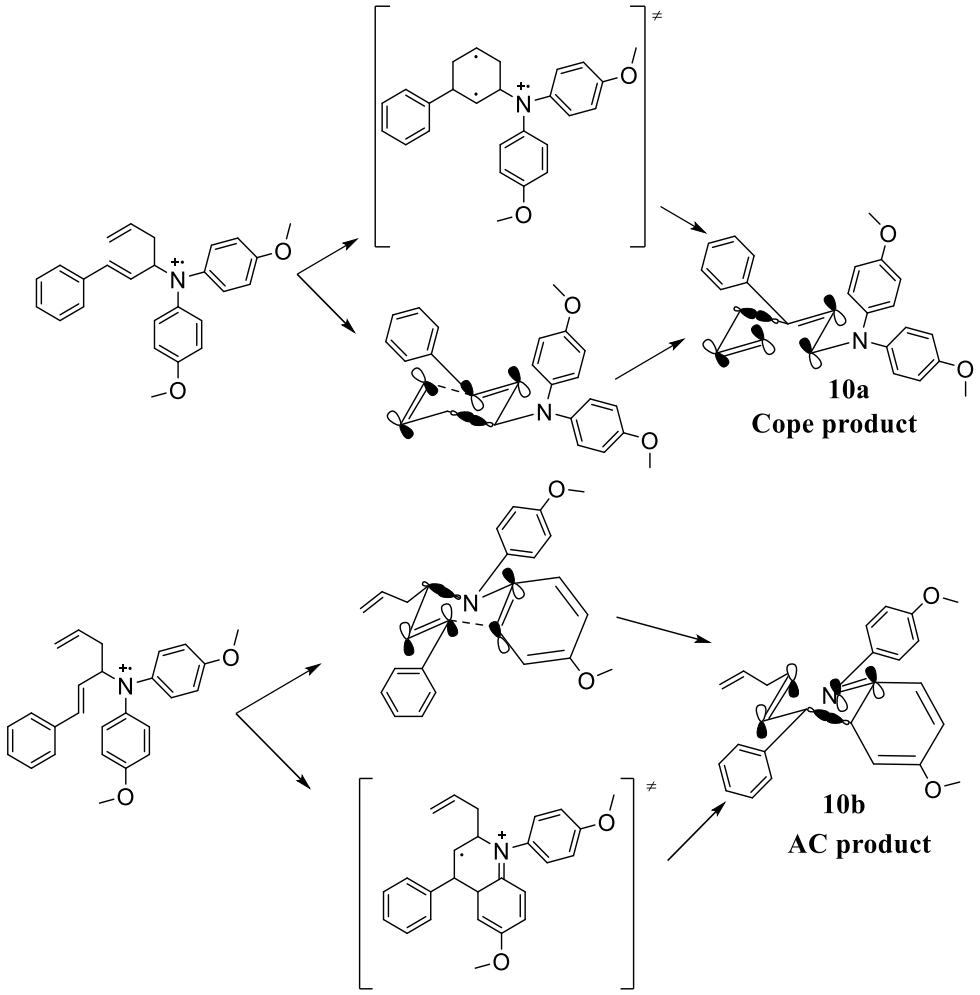

Scheme 4.8. The TS of the Cope and AC rearrangement of 3-diarylamino-1,5-hexadiene.

4.8 Experimental Results of CRET and Other Oxidants

To develop this method into a useful synthetic carbon-carbon bond reaction, it is necessary to determine if other oxidants could promote the rearrangement of **10** to **10b** efficiently. Three other oxidants namely trifluoracetic acid (TFA), Ceric ammonium nitrate (CAN) and *p*-Toluenesulfonic acid (*p*-TsOH) were investigated to see if they could enhance the sigmatropic rearrangement of **10**. Different mole ratios of these oxidants were added to a known amount of the substrate to determine the amount of an oxidant needed for a complete conversion of the starting material to the AC product. Nitromethane was used an internal standard in these reactions. The conversion **12** to the oxidation products was monitored by the disappearance of the doublet of triplets at 4.75 ppm and the appearance of the doublet of doublets at 2.67ppm in **12b** (Figure 4.2). About 20 mol % of each of the oxidants was used for the reaction since we have previously established that about 20 mol % CRET was needed for a complete rearrangement of our substrates to form predominantly the AC product (Table 4.3). Our results indicate that although these three oxidants can enhance the rearrangement of 3-diarylamino-1,5-hexadienes, however their reactions required longer reaction times than CRET.

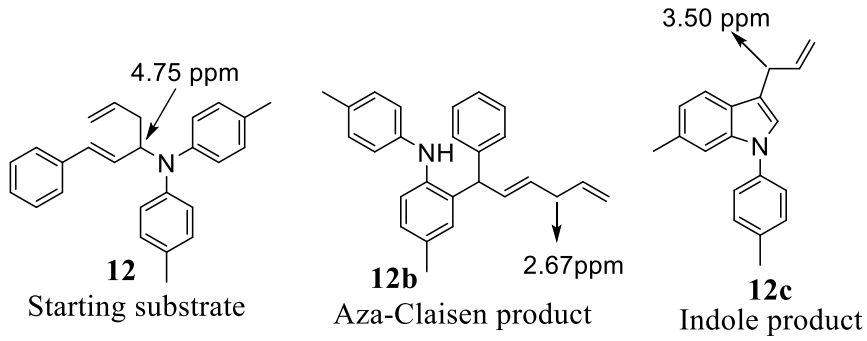

Figure 4.2. 3-diarylamino-1,5-Hexadiene and the rearrangement products.

Having established that 3-diarylamino-1,5-hexadienes **10**,**12**,**14**,**16**,**18**,**20** and any other structurally similar compound will undergo the aza-Claisen rearrangement upon the addition of

0.20 equivalent of the one-electron transfer oxidant CRET, we proceeded to investigate **23** and **24**. To our greatest surprise, the addition of up to one equivalent of the oxidant to the $CDCl_3$ solution of both **23** and **24** did not yield any result even after heating the reaction mixture at 40 ºC for 12 hours. This result indicates that the allyl group attached at the α-position to the nitrogen in 3-diarylamino-1,5-hexadienes plays a role in the AC rearrangement of the substrates. The allyl group changes the conformation of the nitrogen atom from planar to twisted form making it possible for the p orbitals to align properly thereby promoting the reaction. This effect was missing in both **23** and **24** and as a result, no AC product was observed after oxidation of the substrates.

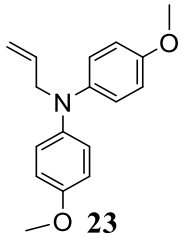

23

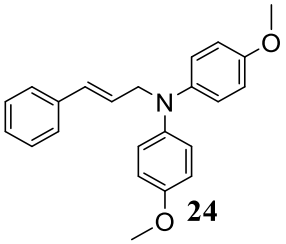

24

The electrochemistry of our substrates was investigated by cyclic voltammetry. Solutions of the compounds (1.0 mM) were prepared in anhydrous CH_2Cl_2 with 0.1 M tetrabutylammonium hexafluorophosphate as the supporting electrolyte. Platinum electrode, platinum wire, and SCE were used as the working, counter and reference electrodes, respectively. The cyclic voltammogram of **10** (Figure 4.3) shows an irreversible single electron oxidation wave seen at 0.89 V vs. SCE. This indicates that the oxidation of the 3-amino-1,5-hexadines to form the aza-Claisen product is not a reversible reaction and agrees with the observed experimental results.

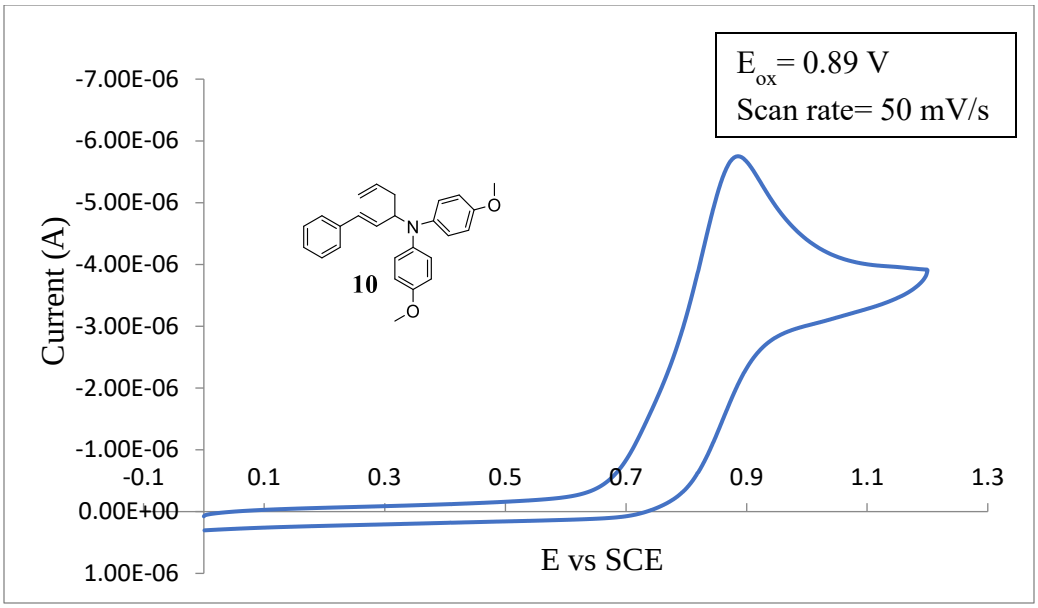

Figure 4.3. The cyclic voltammogram of **10** (1.00 mM in DCM with 0.1 M nBu4PF_6) at a scan rate of 50 mV/s.

4.9 Conclusions

In summary, we have developed a new method of promoting the [3,3]-sigmatropic rearrangement of 3-diarylamino-1,5-hexadienes by using a redox auxiliary. The rearrangement was accomplished at room temperature and even lower temperatures, which represents a drastic decrease in the reaction temperature of greater than 175 ºC for thermal rearrangement. The addition of 20 mol % CRET to these 1,5-hexadienes caused the substrates to undergo an AC rearrangement instead of the anticipated Cope reaction. The stronger RA stabilization of the transition state for the AC pathway compared to the Cope pathway, and conformation of the structure could account for the predominant formation of the AC product. These stabilizing interactions in the transition state involve the delocalization of electrons and are due to the involvement of the RA in the reaction. The RA, in this case, did not function as an RA as designed but rather took part in the reaction. This led to a decrease in the activation energy of the

reaction. We believe this new method of enhancing the rates of [3,3] transformation of 3-amino-1,5-hexadienes could be applied to the development of new synthetically complex molecules, sensors and triggering devices in materials science.

4.10 Experimental Details

Materials and instrumentation. Starting materials and solvents were purchased from Aldrich Chemical Co., Alfa Aesar, EMD Millipore, Oakwood Chemical, Ark Pharm Inc., Chem-Impex International, Inc., TCI America, Cambridge isotopes and used without further purification. All Pd-catalyzed reactions were performed under N_2 atmosphere. $Pd(dba)_2$, $Pd_2(dba)_3$, $P(tBu)_3$ and NaOtBu were all weighed out in a dry box. Activity III alumina was prepared by the addition of 6% H_2O to basic alumina (Aldrich, activated Brockmann I, ~150 mesh).

Apparatus- ^1H and ^{13}C NMR spectra were recorded on Bruker AM-360 or AM-500 Bruker spectrophotometers using $CDCl_3$, C_6D_6, and DMSO-d_6 as solvents and tetramethylsilane as the reference. Chemical shifts were reported by using the following abbreviations: s, singlet; d, doublet; dd, doublet of doublets; ddd, doublet of doublet of doublets; ddt, doublet of doublet of triplets; dm, doublet of multiplets; dt, doublet of triplets; t, triplet; q, quartet; m, multiplet; br, broad; J, coupling constants (Hz). FT-IR spectra were recorded on a Bruker Alpha FTIR instrument (Bruker Optics Inc., Billerica, MA) with the use of KBR pellets. UV-Vis Optical spectra were recorded on a HP8452A Diode Array Spectrophotometer. Electrochemistry was performed on a PAR 273 electrochemical potentiostat (EG&G Instruments). Redox potentials ($E^{ox}_{1/2}$ and $E^{red}_{1/2}$) were measured by Cyclic Voltammetry was on a PAR 273 electrochemical potentiostat (Pt electrode, scan rate 50 mV/s) in CH_2Cl_2 containing $TBAPF_6$ (0.1 M) as a supporting electrolyte. Because the substrates gave irreversible waves, their $E^{ox}_{1/2}$ values

were obtained as Eapp (anodic peak potential), assuming a one-electron oxidation process. Column Chromatography was performed on a Teledyne ISCO CombiFlash® Rf 200i or by flash column chromatography using silica gel (Silicycle®, 60 Å, 230-400 mesh) as a stationary phase and the solvent mixtures were reported as volume ratios.

Purification of solvents. Methylene chloride, cyclohexane, and benzene were purified according to standard literature procedures by washing with H_2SO_4, water, saturated $NaHCO_3$ and distilled over calcium hydride.

Tetrabutylammonium hexafluorophosphate ($TBAPF_6$). This compound was purified by recrystallizing in ethanol and dried under vacuum at 70 ºC for 10 hours.[138]

CRET. The synthesis and purification of CRET was carried out by following the reported procedure by Rathore R et.al.[142]

Synthesis:

General Method for the synthesis of 3-diarylamino-1,5-Hexadienes.

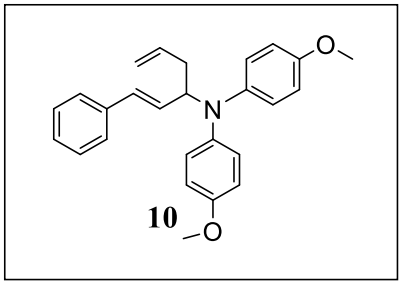

Appropriate secondary amine **10** (838 mg, 3.00 mmol) and p-bromoanisole (573 mg, 3.06 mmol) were added into a 100 mL flamed-dried round-bottomed flask in a dry box. Toluene (anhyd. 4 mL) was added to the flamed-dried flask and stirred. $Pd_2(dba)_3$ (27.5 mg, 0.03 mmol), $P(tBu)_3$ (12.1 mg, 0.06 mmol) were added into the mixture and stirred for about one minute. NaOtBu (0.432 g, 4.5 mmol, 1.5 eq) was then added to the mixture, capped with a rubber septum, removed from the dry box and stirred under N_2 for 4 hr at 90 °C. The reaction mixture was monitored via TLC (hexane: benzene =1:4) until it showed the disappearance of the starting materials. The mixture was filtered through activated basic alumina and washed with 200 mL of ethyl acetate. The product was concentrated in vacuo to yield the

crude product which was purified by column chromatography on silica gel using benzene: hexane = 1:4 to afford the desired compound as a yellow oil (1.10 g, 95.1 % yield)

^{1}H NMR (500 MHz, $CDCl_3$) δ (ppm) 2.25-2.32 (ddd,14 Hz, 7Hz, IH), 2.25-2.61 (ddd, 14.1 Hz, 7 Hz, 1H), 3.62 (s, 3H), 4.53-4.59 (dt, 13.9 Hz, 6.9 Hz, 1H), 4.98-5.04 (m, 2H), 5.74-5.86 (m, 1H), 6.09-6.15 (dd, 7.1 Hz, 16.4 Hz, 1H), 6.45-6.50 (d, 16.4 Hz, 1H), 6.72-6.75 (d, 8.9 Hz, 4H), 6.81-6.84 (d, 8.9 Hz, 4H), 7.09-7.13(t, 8 Hz, 2H), 7.38 (t, 8.1 Hz, 2H), 7.46 (d, 8.1 Hz, IH)

^{13}C NMR (125 MHz, $CDCl_3$) δ (ppm) 154.8, 140.9, 137.2, 135.9, 131.5, 130.1 128.6, 127.6, 126.5, 124.2, 116.9, 114.6, 60.9, 55.6, 37.7. ESI-HRMS calcd for $C_{26}H_{27}NO_2$: 385.2042, found 385.2037

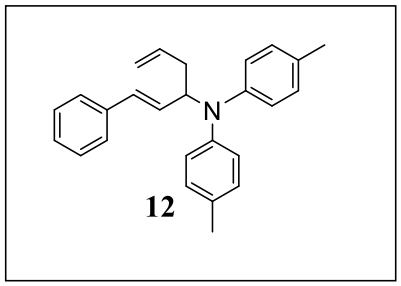

12

12 was prepared by using the general method for the synthesis of 3-diarylamino-1,5-hexadienes from **13** (3 mmol, 790 mg) and 4-bromotoluene (523 mg, 3.06 mmol) in 4.00 mL of toluene. The crude product was purified by column chromatography using benzene: hexane= 1:5 to afford the pure **12** as a yellow oil (1.00 g, 94.5 % yield). ^{1}H NMR (360 MHz, $CDCl_3$) δ (ppm) 2.36 (s, 6H), 2.38-2.46 (ddd, 14.1 Hz, 7.1Hz, 1H), 2.66-2.74 (m, 1H), 4.73-4.77 (dt, 14.1Hz, 7.1 Hz, 1H), 5.11-5.18 (m, 2H), 5.86-5.98 (m, 1H), 6.21-6.28 (dd, 16.2 Hz, 7.1 Hz, 1H), 6.60-6.64 (d, 16.2 Hz, 1H), 6.91-6.94 (d, 8.4 Hz, 4H), 7.12-7.14 (d, 8.4 Hz, 4H), 7.25-7.30 (t, 14.9 Hz, 8.2 Hz, 2H), 7.31-7.33 (t, 7.1 Hz, 2H), 7.35-7.40 (d, 8.2 Hz, 1H)

^{13}C NMR (125 MHz, $CDCl_3$) δ (ppm) 144.5, 1337.2, 135.7, 131.3, 131.1, 129.9, 129.7, 128.5, 127.4, 126.4, 122.9, 116.9, 60.4, 37.4, 20.6. ESI-HRMS calcd for $C_{26}H_{27}N$: 353.2144, found 353.2141

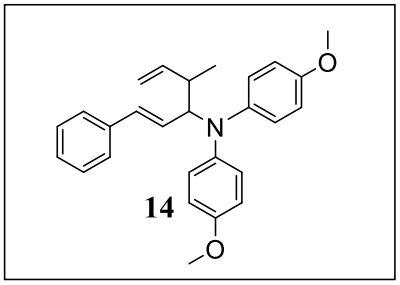

14 was prepared by using the general method for the synthesis of 3-diarylamino-1,5-hexadienes from **15** (3 mmol, 901 mg) and p-bromoanisole (573 mg, 3.06 mmol) in 4.00 mL of toluene. The crude product was purified by column chromatography using benzene: hexane= 1:1 to afford the pure **14** as a yellow oil (1.16 g, 90.6 % yield). ^{1}H NMR (360 MHz, $CDCl_3$) δ (ppm) 1.24-1.27 (d, 3H), 2.69-2.80 (m, 1H), 3.83 (s, 6H), 4.-4.32-4.38 (dd, 1H), 5.02-5.12 (m, 1H), 6.15-6.21 (ddd, 1H), 6.51-6.60 (d, 1H), 6.84-6.89 (d, 4H), 6.95-6.99 (d, 4H), 7.22-7.36 (m, 5H) ESI-HRMS calcd for $C_{27}H_{29}NO_2$: 399.2198, found 399.2196

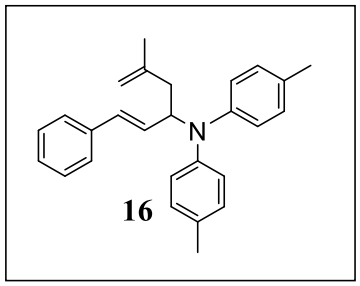

16 was prepared by using the general method for the synthesis of 3-diarylamino-1,5-hexadienes from **17** (3 mmol, 832 mg) and 4-bromotoluene (523 mg, 3.06 mmol) in 4.00 mL of toluene. The crude reaction product was purified by column chromatography on silica gel using benzene: hexane= 1:4 to afford the pure **16** as a yellow oil (1.06 g, 95.8 % yield). ^{1}H NMR 360 MHz ($CDCl_3$) δ 1.77 (s, 3H), 2.27-2.34 (dd, 14.1 Hz, 6.4 Hz, 1H), 2.31 (s, 6H), 2.52-2.57 (dd, 14.1 Hz, 6.4 Hz, 1H), 4.73 (s, 1H), 4.81 (s, 1H), 4.81-4.88 (dt, 14.1 Hz, 6.4 Hz, 1H), 6.14-6.21 (dd, 16.2 Hz, 6.4 Hz, 1H), 6.56-6.60 (d, 16 Hz, 1H), 6.84-6.87(d, 8.3 Hz, 4H), 7.06-7.08 (d, 8.3 Hz, 4H), 7.20-7.23 (m, 1H), 7.29-7.34(m, 3H)

^{13}C NMR 125 MHz, ($CDCl_3$) δ:144.4, 142.4, 137.2, 131.1, 130.9, 130.0, 129.7, 128.5, 127.3, 126.4, 122.8, 112.8, 58.5, 41.2, 22.9, 20.6. ESI-HRMS calcd for $C_{27}H_{29}N$: 367.2300, found 399.2306

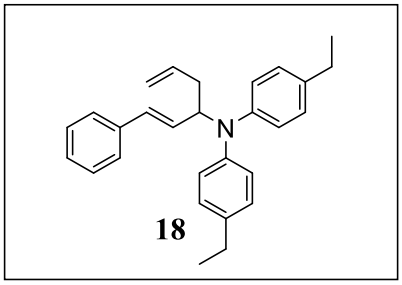

18 was prepared by using the general method for the synthesis of 3-diarylamino-1,5-hexadienes from **13** (3 mmol, 790 mg) and 4-bromoethylbenzene (566 mg, 3.06 mmol) in 4.00 mL of toluene at 80 ºC. The crude product was purified by column chromatography on silica gel using benzene: hexane= 1:2 to afford the pure product as a yellow oil (1.17 g, 87 % yield). ^{1}H NMR 360 MHz ($CDCl_3$) δ 1.41-1.21 (t, 7 Hz, 6H), 2.27-2.35 (ddd,15.3 Hz, 8.4 Hz, 1H), 2.53-2.62 (ddd, 15.3 Hz, 8.4 Hz, 1H), 2.53-2.59 ((q, 7.1 Hz, 4H), 4.63-4.68 (dt, 16 Hz, 7.1 Hz,1H), 4.99- 5.07 (m, 2H), 5.76-5.87 (m, 1H), 6.11-6.18 (dd, 16.4 Hz, 7.1 Hz, 1H), 6.50-6.54 (d, 16.4 Hz, 1H), 6.82-6.85 (d, 8.9 Hz, 4H),7.03-7.05 (d, 8.9 Hz, 4H), 7.15-7.29 (m, 5H) ^{13}C NMR 125 MHz, ($CDCl_3$) 144.6, 137.5, 137.2, 135.8, 131.3, 129.9, 128.5, 128.4, 127.4, 126.4, 122.8, 116.8, 60.4, 37.5, 28.1, 15.6 m/z = 381.2 ESI-HRMS calcd for $C_{28}H_{31}N$: 381.2457, found 381.2461

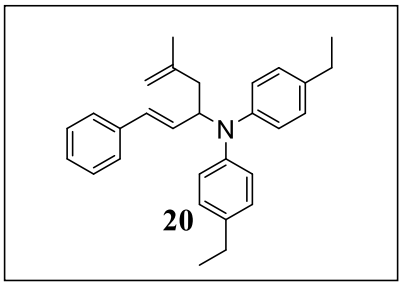

20 was prepared by using the general method for the synthesis of 3-diarylamino-1,5-hexadienes from **17** (3 mmol, 832 mg) and 4-bromoethylbenzene (566 mg, 3.06 mmol) in 4.00 mL of toluene at 80 ºC. The crude product was purified by column chromatography on silica gel using benzene: hexane= 1:2 to give pure **20** as a yellow oil (1.19 g, 82.0 % yield). ^{1}H NMR 360 MHz ($CDCl_3$) δ 1.27-1.31 (t, 8.4 Hz, 6H), 1.82 (s, 3H), 2.23-2.39 (dd, 15.2 Hz, 8.4 Hz, 1H), 2.56-2.63 (dd, 15.2 Hz, 8.4 Hz, 1H), 2.63-2.70 (q, 8.4 Hz, 4H), 4.78 (b, IH), 4.86 (b, IH), 4.86-4.93 (q, 15.2 Hz, 7.1 Hz, 1H), 6.19-6.26 (dd, 16.2 Hz, 7.1 Hz, 1H), 6.60-6.65 (d, 16.2 Hz, 1H), 6.91-6.95 (d, 9.2 Hz, 4H), 7.13-7.15 (d, 9.2 Hz, 4H), 7.24-7.39 (m, 5H) ^{13}C NMR 125 MHz, ($CDCl_3$) 144.6, 142.5, 137.4, 137.3, 131.1, 130.1, 128.5, 128.4, 127.3,

126.4, 122.7, 112.8, 58.5, 41.2, 28.1, 22.9, 15.6 m/z = 395.3 ESI-HRMS calcd for $C_{29}H_{33}N$: 395.2613, found 395.2606

General Method for the synthesis of 3-monoarylamino-1,5-hexadienes (Allylation of imines). Method A.

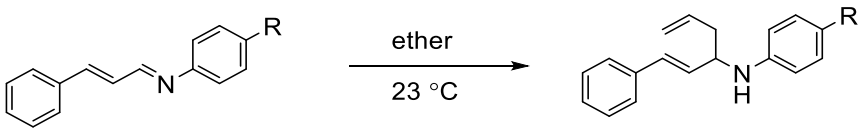

Appropriate imine (5.00 mmol) was dissolved in about 20 ml of Et_2O in a flame dried and N_2 purged round-bottomed flask and cooled to about -10 °C. 1 M allyl magnesium bromide solution (6.0 mL, 6 mmol) as slowly added via syringe to the ice-cold solution over a period of 10 minutes. This solution was allowed to warm up to room temperature and stirred for another 60 minutes. The reaction was cooled in an ice bath and quenched with about 15ml of 10% $NaHCO_3$. The organic layer was extracted with ethyl acetate, dried over $MgSO_4$ and evaporated in vacuo to give the crude product which was purified by column chromatography to afford the pure product.

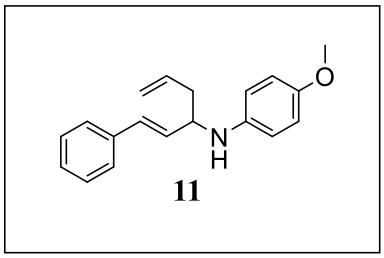

11

11 has been previously reported.[185] It was synthesized by using the general method A for the allylation of imines from 4-methoxy- N-(4-methoxyphenyl)-3-phenylprop-2-en-1-imine (949 mg, 4.00 mmol) and allyl magnesium bromide (697 mg, 4.8 mmol) in 20 ml of diethyl ether at room temperature. The crude reaction product was purified by column chromatography on silica gel using EtOAC/hexane = 1:8 to give a light-yellow oil (886 mg, 79.1 %). ^{1}H NMR 360 MHz ($CDCl_3$) δ 7.38 (d, 2H), 7.32 (t, 2H), 7.23 (t, 1H), 6.78 (d, J = 8.9 Hz, 2 H), 6.66-6.60 (m, 3H), 6.21 (dd, J = 16.0 Hz, 6.1 Hz, 1H), 5.94-5.82 (m, 1H), 5.23-5.16 (m, 2H), 4.00 (ddd, 1H), 3.75 (s, 3H), 3.62 (br s, 1H), 2.55-2.41 (m, 2H),

^{13}C NMR, 125 MHz, ($CDCl_3$) δ 40.6, 55.8, 55.9. 114.9, 115.10, 118.3, 126.5, 127.5, 128.6, 130.1, 130.4, 132.1, 132.7, 134.5, 136.0, 137.2, 141.9, 152.3

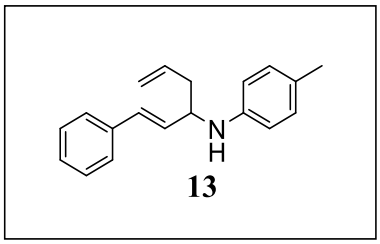

13

13 has been previously reported.[186] It was synthesized by using the general method A for the allylation of imines from N-(4-methylphenyl)-3-phenylprop-2-en-1-imine (885 mg, 4.00 mmol) and allyl magnesium bromide (697 mg, 4.8 mmol) in 20 ml of diethyl ether at 23 ºC. The crude reaction product was purified by column chromatography on silica gel using EtOAC/hexane = 1:8 to give a light-yellow oil (867 mg, 82.3 %). ^{1}H NMR 360 MHz ($CDCl_3$) δ 7.36 (d, 2H), 7.29 (t, 2H), 7.21 (t, 1H), 6.96 (d, J = 8.9 Hz, 2 H), 6.62-6.57 (m, 3H), 6.20 (dd, J = 16.0 Hz, 6.1 Hz, 1H), 5.85 (m, 1H), 5.21-5.14 (m, 2H), 4.02 (ddd, 1H), 3.72 (br s, 1H), 2.52-2.40 (m, 2H), 2.22 (s, 3H)

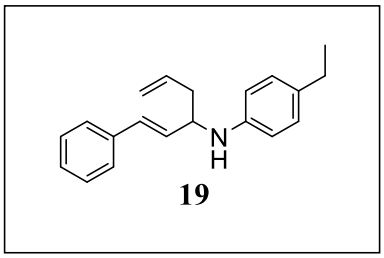

19

19 was synthesized by using the general method A for the allylation of imines from N-(4-ethylphenyl)-3-phenylprop-2-en-1-imine (942 mg, 4.00 mmol) and allyl magnesium bromide (697 mg, 4.8 mmol) in 20 ml of diethyl ether at 23 ºC. The crude reaction product was purified by column chromatography on silica gel using EtOAC/hexane = 1:8 to give a light-yellow oil (814 mg, 73.4 %). ^{1}H NMR 360 MHz ($CDCl_3$) δ 7.38 (d, 2H), 7.31 (t, 2H), 7.23 (t, 1H), 7.01 (d, J = 8.9 Hz, 2 H), 6.64-6.61 (m, 3H), 6.22 (dd, J = 16.0 Hz, 6.1 Hz, 1H), 5.87 (m, 1H), 5.22-5.16 (m, 2H), 4.04 (b, 1H), 3.75 (br s, 1H), 2.57-2.42 (m, 4H), 1.20 (t, 3H)

General Method for the synthesis of 3-monoarylamino-1,5-Hexadienes (Allylation of imines). Method B.

Magnesium turnings (388 mg, 16.00 mmol) were added to 10 mL of Et_2O and 2-methylallyl chloride (1.88 mL, 19.2 mmol) in 5 mL of Et_2O was slowly added under nitrogen over a period

of 15 minutes at 0 ºC. The reaction mixture was stirred at room temperature for 1 h and cooled to about 0 ºC. Then a solution of the appropriate imine (8.00 mmol) was dissolved in about 10 mL of Et_2O and added via syringe to the ice-cold solution over a period of 10 minutes. This solution was then allowed to warm up to 25 ºC and stirred at this temperature for another 60 minutes. The reaction was cooled in an ice bath, quenched with about 30 mL of 10% $NaHCO_3$, extracted with EtOAc (3 x 20 mL) and the combined organic layers dried over $MgSO_4$. Evaporation of the organic layer in vacuo afforded the crude product which was used in the next step without purification.

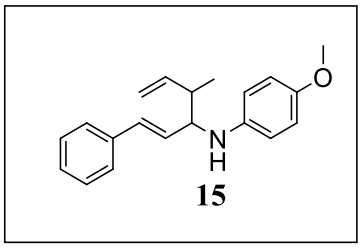

15

The synthesis of **15** was carried out according Method B for the allylation of imines from magnesium turnings (194 mg, 8.00 mmol), crotyl chloride (0.94 mL, 9.86 mmol) and N-(4-methoxyphenyl)-3-phenylprop-2-en-1-imine (949 g, 4.00 mmol) in 20 ml of diethyl ether at 25 ºC. The reaction was quenched with about 30 mL of 10% $NaHCO_3$, extracted with EtOAc (3 x 20 mL) and the combined organic layers dried over $MgSO_4$. Evaporation of the organic layer in vacuo afforded the crude product as a yellow oil which was used in the next step without purification. 0.952 mg, 81.1 % yield. ^{1}H NMR 360 MHz ($CDCl_3$) δ 7.35 (d, 2H), 7.29 (t, 2H), 7.21 (t, 1H), 6.75 (d, 2 H), 6.61-6.54 (m, 3H), 6.13 (dd, 1H), 5.80 (ddq, 1H), 5.13- 5.18 (m, 2H), 3.88 (dd, 1H), 3.72 (s, 3H), 3.64 (br s, 1H), 2.58 (m, 1H), 1.14 (t, 8.2 Hz 3H)

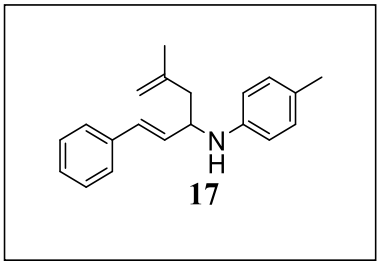

17

17 was synthesized by using the general method B for the allylation of imines from magnesium turnings (388 mg, 16.00 mmol), 2-methylallyl chloride (1.88 mL, 19.2 mmol) and N-(4-methylphenyl)-3-phenylprop-2-en-1-imine (1.77 g, 8.00 mmol)

in 25 ml of diethyl ether at 25 ºC. **17** was obtained as a yellow oil. 2.13 g, 96.2 % yield. ^{1}H NMR 360 MHz ($CDCl_3$) δ 7.36 (d, 7.5 Hz, 1H), 7.29 (t, 7.5 Hz, 2H), 7.21 (t, 7.5 Hz, 1H), 6.96 (d, 14.3 Hz, 8.7 Hz), 6.65-6.58 (m, 3H), 6.21 (dd, 16.1 Hz, 6.2 Hz, 1H), 4.90 (s, 1H), 4.85 (s, 1H), 3.98-4.06 (m, 1H), 3.72 (b, 1H), 2.31-2.44 (m, 2H), 2.22 (s, 3H), 1.75 (s, 3H)

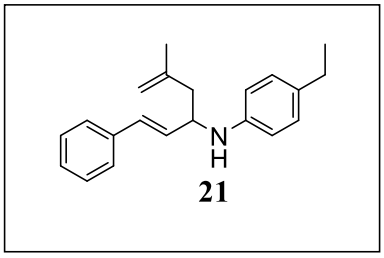

21

21 was synthesized by using the general method B for the allylation of imines from magnesium turnings (194 mg, 8.00 mmol), 2-methylallyl chloride (0.94 mL, 9.86 mmol) and N-(4-ethylphenyl)-3-phenylprop-2-en-1-imine (941 g, 4.00 mmol) in 20 ml of diethyl ether at 25 ºC. **21** was obtained as a yellow oil. 1.11 g, 95.0 % yield. ^{1}H NMR 360 MHz ($CDCl_3$) δ 7.37 (d, 2H), 7.30 (t, 2H), 7.21 (t, 1H), 7.36 (m, 3 H), 7.00 (d, J = 8.9 Hz, 2 H), 6.66-6.61 (m, 3H), 6.21 (dd, J = 16.0 Hz, 6.1 Hz, 1H), 4.88 (d, J= 16.0 Hz, 2H), 4.04 (m, 1H), 3.75 (br s, 1H), 2.53 (q, J= 7.0 Hz, 16.0 Hz, 3H), 2.40 (m, 2H), 1.76 (s, 3H), 1.19 (t, J= 8.0 Hz, 3H)

General method for the synthesis of imines

The appropriate p-substituted aniline (10.0 mmol) was placed in a porcelain mortar along with freshly distilled *trans*-cinnamaldehyde (1.26 mL, 1.0 equiv, 10.0 mmol). This mixture was ground using a pestle for about 15 min until a bright yellow solid was obtained. Recrystallization of the crude product in 25 mL of ether afforded the desired product.

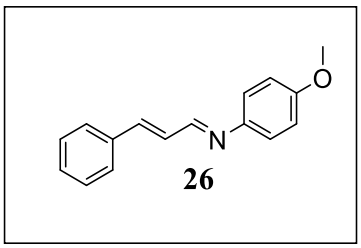

26

26 has been previously reported.[187] It was synthesized by using the general method for the synthesis of imines from *trans*-cinnamaldehyde (1.32 g, 10.0 mmol) and *p*-anisidine (1.23 g, 10 mmol). Recrystallization of the crude product in ether afforded the pure **26** as a yellow solid (2.35 g, 99.1 %). mp: 119 - 120 °C Lit 119 - 121 °C ^{1}H NMR (360

MHz, $CDCl_3$) δ 8.29 (m, 1H), 7.53 (m, 2H), 7.42 - 7.34 (m, 3H), 7.22 (m, 2H), 7.12 (m, 2H), 6.92 (m, 2H), 3.82 (s, 3H)

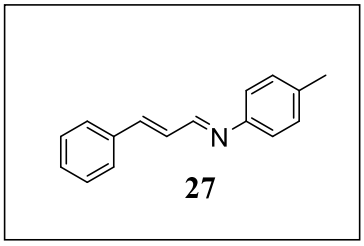

27

27 has been previously reported.[188-189] It was synthesized by using the general method for the synthesis of imines from *trans*-cinnamaldehyde (1.32 g, 10.0 mmol) and *p*-toluidine (1.07 g, 10.0 mmol). Recrystallization of the crude product in ether afforded the pure **27** as a yellow solid (2.09 g, 94.4 %). ^{1}H NMR (360 MHz, $CDCl_3$) δ 8.28 (dd, 5.4, 2.6 Hz, 1H), 7.53 (d, 7.8 Hz, 2H), 7.42 – 7.31 (m, 3H), 7.18 (d, 2H), 7.14 – 7.09 (m, 4H), 2.36 (s, 3H). mp: 76-77 ºC Lit 77 ºC

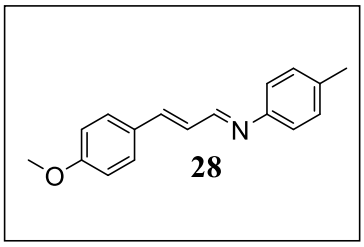

28

28 has been previously reported.[189] It was synthesized by using the general method for the synthesis of imines from *p*-methoxycinnamaldehyde (1.62 g, 10.0 mmol) and *p*-toluidine (1.07 g, 10.0 mmol). Recrystallization of the crude product in ether afforded the pure **27** as a yellow solid (2.31 g, 92.1 %). mp: 76-77 ºC Lit 77 ºC ^{1}H-NMR (360 MHz, $CDCl_3$) δ 8.23 (d, 8.5 Hz, 1H), 7.45 (d, 8.5 Hz, 2H), 7.16 (d, 8.4 Hz, 2H), 7.09-7.04 (m, 3H), 6.97 (dd, 8.4 Hz, 15.8 Hz, 1H), 6.89 (d, 8.7 Hz, 2H), 3.81 (s, 3H), 2.34 (s, 3H)

CAN, TFA or p-TsOH-Catalyzed Rearrangement of 7a under N_2

A two-necked flask containing a solution of **10** (193 mg, 0.50 mmol) in dry $CDCl_3$ (10.0 mL) was purged several times with N_2. The oxidant (CAN, TFA or p-TsOH) (0.100 mmol, 20.0 mol %) was added in one portion, and the mixture was stirred for 60 min under N_2. The reaction was quenched by the addition of zinc dust and the ^{1}H NMR of the crude reaction mixture was taken.

The crude reaction mixture was evaporated to dryness and purified by column chromatography on silica gel using benzene/hexane (1:1) to obtain the oxidation products.

CRET Catalyzed Rearrangement of 3,3-diarylamino-1,5-hexadiene under N_2

A two-necked flask containing a solution of **10** (193 mg, 0.500 mmol) in dry $CDCl_3$ (10 mL) was purged several times with N_2. **CRET** (60.5 mg, 0.100 mmol, 20.0 mol %) was added in one portion, and the mixture was stirred for 20 min under N_2. The reaction was quenched by the addition of zinc dust and the ^1H NMR of the crude reaction mixture was taken. The crude reaction mixture was evaporated to dryness and purified by column chromatography on silica gel using benzene/hexane (1:1) to obtain the oxidation products.

10b

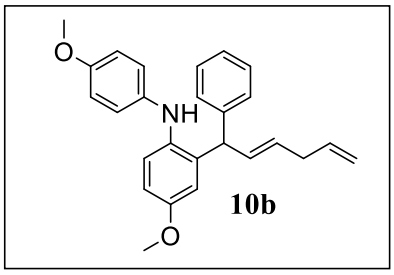

10b

Yellow oil, 126 mg, Yield 65.2 %. H-NMR (360 MHz, $CDCl_3$) δ 7.45 (d, J = 8.9 Hz, 2H), 7.26-7.13 (m, 3H), 7.02 (d, 8.9 Hz, 2H), 6.71-6.58 (m, 6H), 5.84 (ddt, 15.2 Hz, 6.9 Hz, 1.4 Hz, 1H), 5.80-5.70 (m, 1H), 5.29 (ddd, 15.2 Hz, 6.9 Hz, 1.4 Hz, 1H), 4.98-4.90 (m, 2H), 4.80 (b, 1H), 4.78 (d, J = 6.9 Hz, 1H), 3.69 (s, 3H), 3.68 (s, 3H), 2.73 (dd, J = 6.9 Hz, 2H).

^{13}C NMR 125 MHz, ($CDCl_3$) 155.2, 153.5, 142.4, 139.1, 137.2, 136.7, 135.3, 132.6, 130.3, 128.7, 126.6, 122.6, 118.1, 115.6, 115.7, 115.3, 114.8, 111.8, 55.7, 55.4, 49.1, 36.6. ESI-HRMS calcd for $C_{26}H_{27}NO_2$: 385.2042, found 385.2032

13b

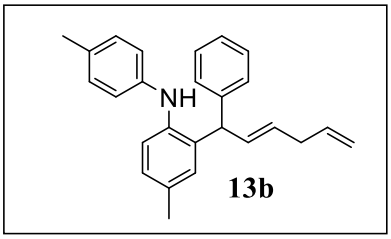

13b was synthesized by using the CRET oxidation method from 177 mg (0.500 mol) of **13** and CRET (60.5 mg, 20.0 mol %) in 10 mL of $CDCl_3$.The crude reaction mixture was purified by column chromatography on silica using DCM/hexane (1:1) to give **13b** as a yellow oil (121 mg, 68.3 %). ^{1}H-NMR (360 MHz, $CDCl_3$) δ 7.34-7.13 (m, 6H) 7.00 (d, 8.9 Hz, 2H), 6.98 (d, 8.9 Hz, 2H), 6.69 (d, 8.9 Hz, 2H), 5.94 (ddt, 15.2 Hz, 6.9 Hz, 1.4 Hz, 1H), 5.90-5.76 (m, 1H), 5.39 (ddd, 15.2 Hz, 6.9 Hz, 1.4 Hz, 1H), 5.13 (b, 1H), 5.06-4.98 (m, 2H), 4.83 (d, 6.9 Hz, 1H), 2.84 (dd, 6.9 Hz, 2H) 2.29 (s, 3H), 2.27 (s, 3H). ^{13}C NMR 125 MHz, ($CDCl_3$) 143.6, 142.2, 138.9, 136.8, 134.6, 132.8, 131.6, 130.2, 130.0, 129.7, 129.1, 128.7, 128.6, 127.8, 126.5, 120.6, 116.9, 115.3, 49.3, 36.8, 20.9, 20.5. ESI-HRMS calcd for $C_{26}H_{27}N$: 353.2144, found 353.2143

16b

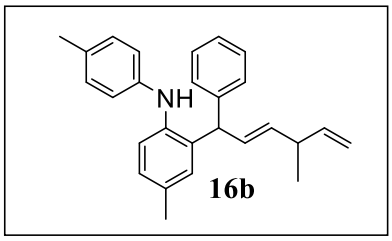

16b was synthesized by using the CRET oxidation method from 184 mg (0.500 mol) of **16** and CRET (60.5 mg, 20.0 mol %) in 10 mL of $CDCl_3$.The crude reaction mixture was purified by column chromatography on silica using DCM/hexane (1:1) to give **16b** as a yellow oil (121 mg, 66.1 %). ^{1}H-NMR (500 MHz, $CDCl_3$) δ 7.35 (d, 8.6 Hz, 2H), 7.26 (d, 8.6 Hz, 1H), 7.21 (d, 8.6 Hz, 2H), 7.16 (d, 8.6 Hz, 1H), 7.03-6.99 (m, 4H), 6.71 (d, 8.6 Hz, 2H), 5.97 (dd, 15.2 Hz, 7.3 Hz, 1H), 5.90-5.76 (m, 1H), 5.39(dt, 15.2 Hz, 7.3 Hz, 1H), 5.15 (b, 1H), 4.87 (d, 7.3 Hz, 1H), 4.76 (b, 1H), 4.71 (b, 1H), 2.81 (d, 7.3 Hz, 2H) 2.31 (s, 3H), 2.29 (s, 3H), 1.74 (s, 3H).

^{13}C NMR 125 MHz, ($CDCl_3$) 144.6, 142.6, 142.2, 138.7, 134.6, 133.4, 131.5, 130.1, 130.0, 129.7, 129.1, 128.7, 128.6, 127.8, 126.5, 120.6, 116.9, 110.8, 49.3, 41.1, 22.5, 20.9, 20.5. ESI-HRMS calcd for $C_{27}H_{29}N$: 367.2230, found 367.2298

20b

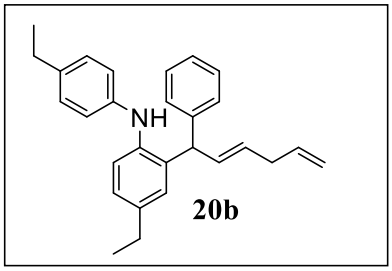

20b

20b was synthesized by using the CRET oxidation method from 191 mg (0.500 mol) of **20** and CRET (60.5 mg, 20.0 mol %) in 10 mL of $CDCl_3$.The crude reaction mixture was purified by column chromatography on silica using DCM/hexane (1:1) to give **20b** as a yellow oil (119 mg, 62.3 %). ^{1}H-NMR (500 MHz, $CDCl_3$) δ 7.25 (d, J = 8.4 Hz, 2H), 7.17 (d, J = 8.4 Hz, 1H), 7.12 (d, J = 8.9 Hz, 2H), 7.12 (d, J = 8.9 Hz, 1H), 6.96-6.92 (m, 4H), 6.64 (d, J = 8.9 Hz, 2H), 5.98 (ddt, J = 15.1 Hz, 7.2 Hz, 1.4 Hz, 1H), 5.81-5.73 (m, 1H), 5.32 (ddd, J = 15.1 Hz, 7.2 Hz, 1H), 5.09 (b, 1H), 4.99-4.92 (m, 2H), 4.78 (d, J = 7.2 Hz, 1H), 2.78 (dd, J = 7.2 Hz, 2H) 2.54-2.48 (m, 4H), 1.14 (t, J = 8.2 Hz, 3H), 1.13 (t, J = 8.4 Hz, 3H), ^{13}C NMR 125 MHz, ($CDCl_3$) 142.2, 142.0, 138.9, 137.9, 136.8, 135.8, 134.4, 132.9, 130.1, 128.9, 128.7, 128.6, 128.5, 126.5, 126.4, 120.4, 117.1, 115.3, 49.4, 36.6, 28.3, 28.1, 15.8, 15.7. ESI-HRMS calcd for $C_{28}H_{31}N$: 381.2457, found 381.245

REFERENCES

1. Eberson, L. E. *Electron transfer reactions in organic chemistry*. Springer: Verlag, 1987.

2. Julliard, M.; Chanon, M. Photoelectron-transfer catalysis: its connections with thermal and electrochemical analogs. *Chem. Rev.*, **1983**, *83*, 425-506.

3. Zhang, J.; Kuznetsov, A. M.; Medvedev, I. G.; Chi, Q.; Albrecht, T.; Jensen, P. S.; Ulstrup, J. Single-molecule electron transfer in electrochemical environments. *Chem. Rev.*, **2008**, *108*, 2737-2791.

4. Ghosh, S.; Soudackov, A. V.; Hammes-Schiffer, S. Electrochemical electron transfer and proton-coupled electron transfer: Effects of double layer and ionic environment on solvent reorganization energies. *J. Chem. Theory Comput.*, **2016**, *12*, 2917-2925.

5. Weinberg, D. R.; Gagliardi, C. J.; Hull, J. F.; Murphy, C. F.; Kent, C. A.; Westlake, B. C.; Paul, A.; Ess, D. H.; McCafferty, D. G.; Meyer, T. J. Proton-Coupled Electron Transfer. *Chem. Rev.*, **2012**, *112*, 4016-4093.

6. Marcus, R. A. Chemical and electrochemical electron-transfer theory. *Annu. Rev. Phys. Chem.*, **1964**, *15*, 155-196.

7. Huynh, M. H. V.; Meyer, T. J. Proton-coupled electron transfer. *Chem. Rev.*, **2007**, *107*, 5004-5064.

8. Ashby, E. C. Single-electron transfer, a major reaction pathway in organic chemistry. An answer to recent criticisms. *Acc. Chem. Res.*, **1988**, *21*, 414-421.

9. Muller, P. Glossary of terms used in physical organic chemistry: (IUPAC Recommendations 1994). *Pure Appl. Chem.*, **1994**, *66*, 1077-1184.

10. Faraday, M. Seventh series of experimental investigations on electricity. *Ann. Phys.*, **1834**, *109*, 433-451.

11. Kolbe, H. Studies on the electrolysis of organic compounds. *Eur. J. Org. Chem.*, **1849**, *69*, 257-294.

12. Vijh, A. K.; Conway, B. E. Electrode kinetic aspects of the Kolbe reaction. *Chem. Rev.*, **1967**, *67*, 623-664.

13. Naber, M. R. *Analysis of experimental variables for the Kolbe electrolysis of organic acids to hydrocarbons.* B.S. Thesis, Massachusetts Institute of Technology, 1980.

14. Wurtz, A. On a new class of organic radicals. *Ann. Chim. Phys.*, **1855**, *44*, 275.

15. Sandmeyer, T. On the replacement of the amide group by chlorine, bromine and cyan in the aromatic substances. *Ber. Dtsch. Chem. Ges.*, **1884**, *17*, 2650.

16. Zhang, N.; Samanta, S. R.; Rosen, B. M.; Percec, V. Single electron transfer in radical ion and radical-mediated organic, materials and polymer synthesis. *Chem. Rev.*, **2014**, *114*, 5848-5958.

17. Marcus, R. A. Electron transfer reactions in chemistry. Theory and experiment. *Rev. Mod. Phy.*, **1993**, *65*, 599.

18. Schmittel, M.; Burghart, A. Understanding reactivity patterns of radical cations. *Angew. Chem. Int. Ed. Engl.*, **1997**, *36*, 2550-2589.

19. Kirchgessner, M.; Sreenath, K.; Gopidas, K. R. Understanding reactivity patterns of the dialkylaniline radical cation. *J. Org. Chem.*, **2006**, *71*, 9849-9852.

20. Rathore, R.; Kochi, J. K. Donor/acceptor organizations and the electron-transfer paradigm for organic reactivity. *Adv. Phys. Org. Chem.*, **2000**, *35*, 193-318.

21. Kochi, J. K. Inner-sphere electron transfer in organic chemistry. Relevance to electrophilic aromatic nitration. *Acc. Chem. Res.*, **1992**, *25*, 39-47.

22. Studer, A.; Curran, D. P. Catalysis of radical reactions: A radical chemistry perspective. *Angew. Chem. Int. Ed.*, **2016**, *55*, 58-102.

23. Shirakawa, E.; Zhang, X.; Hayashi, T. Mizoroki–Heck-type reaction mediated by potassium tert-butoxide. *Angew. Chem.*, **2011**, *123*, 4767-4770.

24. Wertz, S.; Leifert, D.; Studer, A. Cross Dehydrogenative Coupling via Base-Promoted Homolytic Aromatic Substitution (BHAS): Synthesis of fluorenones and xanthones. *Org. Lett.*, **2013**, *15*, 928-931.

25. Zhang, B.; Mück-Lichtenfeld, C.; Daniliuc, C. G.; Studer, A. 6-trifluoromethyl-phenanthridines through radical trifluoromethylation of isonitriles. *Angew. Chem. Int. Ed.*, **2013**, *52*, 10792-10795.

26. Zhang, H.; Shi, R.; Ding, A.; Lu, L.; Chen, B.; Lei, A. Transition-metal-free alkoxycarbonylation of aryl halides. *Angew. Chem. Int. Ed.*, **2012**, *51*, 12542-12545.

27. Tantillo, D. J. Speeding Up Sigmatropic Shifts - To halve or to hold. *Acc. Chem. Res.*, **2016**, *49*, 741-749.

28. Bauld, N. L.; Bellville, D. J.; Pabon, R.; Chelsky, R.; Green, G. Theory of cation-radical pericyclic reactions. *J. Am. Chem. Soc.*, **1983**, *105*, 2378-2382.

29. Woodward, R. The mechanism of the Diels-Alder reaction. *J. Am. Chem. Soc.*, **1942**, *64*, 3058-3059.

30. Saettel, N. J.; Oxgaard, J.; Wiest, O. Pericyclic reactions of radical cations. *Eur. J. Org. Chem.*, **2001**, *2001*, 1429-1439.

31. Ilardi, E. A.; Stivala, C. E.; Zakarian, A. [3, 3]-Sigmatropic rearrangements: recent applications in the total synthesis of natural products. *Chem. Soc. Rev.*, **2009**, *38*, 3133-3148.

32. Bauld, N. L.; Bellville, D. J.; Harirchian, B.; Lorenz, K. T.; Pabon Jr, R. A.; Reynolds, D. W.; Wirth, D. D.; Chiou, H. S.; Marsh, B. K. Cation radical pericyclic reactions. *Acc. Chem. Res.*, **1987**, *20*, 371-378.

33. Romero, N. A.; Nicewicz, D. A. Organic photoredox catalysis. *Chem. Rev.*, **2016**, *116*, 10075-10166.

34. Shaw, M. H.; Twilton, J.; MacMillan, D. W. Photoredox catalysis in organic chemistry. *J. Org. Chem.*, **2016**, *81*, 6898.

35. Tucker, J. W.; Stephenson, C. R. Shining light on photoredox catalysis: theory and synthetic applications. *J. Org. Chem.*, **2012**, *77*, 1617-1622.

36. Prier, C. K.; Rankic, D. A.; MacMillan, D. W. Visible light photoredox catalysis with transition metal complexes: applications in organic synthesis. *Chem. Rev.*, **2013**, *113*, 5322.

37. Campagna, S.; Puntoriero, F.; Nastasi, F.; Bergamini, G.; Balzani, V. Photochemistry and photophysics of coordination compounds: ruthenium. In *Photochemistry and Photophysics of Coordination Compounds I*, Springer: Berlin, 2007; Vol. 281; pp 117-214.

38. Flamigni, L.; Barbieri, A.; Sabatini, C.; Ventura, B.; Barigelletti, F. Photochemistry and photophysics of coordination compounds: iridium. In *Photochemistry and Photophysics of Coordination Compounds II.* Springer: Berlin, 2007; Vol. 281; pp 143-203.

39. Marchini, M.; Bergamini, G.; Cozzi, P. G.; Ceroni, P.; Balzani, V. Photoredox catalysis: The need to elucidate the photochemical mechanism. *Angew. Chem.*, **2017**, 56,12820-12821.

40. Akita, M.; Koike, T. Principles and applications of photoredox catalysis: trifluoromethylation and beyond. *J. Synth. Org. Chem Jpn.* **2016**, *74*, 1036-1046.

41. Narayanam, J. M.; Stephenson, C. R. Visible light photoredox catalysis: applications in organic synthesis. *Chem. Soc. Rev.*, **2011**, *40*, 102-113.

42. Duan, L.; Xu, Y.; Zhang, P.; Wang, M.; Sun, L. Visible light-driven water oxidation by a molecular ruthenium catalyst in homogeneous system. *Inorg. Chem.*, **2009**, *49*, 209-215.

43. Sahara, G.; Ishitani, O. Efficient photocatalysts for CO_2 reduction. *Inorg. Chem.*, **2015**, *54*, 5096-5104.

44. Albery, W. J. Development of photogalvanic cells for solar energy conservation. *Acc. Chem. Res.*, **1982**, *15*, 142-148.

45. Blackstock, S.; Gray, L.; Kelley, M.; Saint-Louis, C. Redox-auxiliary catalysis. U.S 9,469,602 B2, October 18, 2016.

46. Scialdone, O.; Galia, A.; Silvestri, G.; Amatore, C.; Thouin, L.; Verpeaux, J.-N. Electrocarboxylation of benzyl halides through redox catalysis on the preparative Scale. *Chem. Eur. J.*, **2006**, *12*, 7433-7447.

47. Hernández-Muñoz, L. S.; Fragoso-Soriano, R. J.; Vázquez-López, C.; Klimova, E.; Ortiz-Frade, L. A.; Astudillo, P. D.; González, F. J. Modification of carbon surfaces with methyl groups by using ferrocene derivatives as redox catalysts of the oxidation of acetate ions. *J. Electroanal. Chem.*, **2010**, *650*, 62-67.

48. Okada, Y.; Akaba, R.; Chiba, K. Electrocatalytic formal [2+2] cycloaddition reactions between anodically activated aliphatic enol ethers and unactivated olefins possessing an alkoxyphenyl Group. *Org. Lett.*, **2009**, *11*, 1033-1035.

49. Lin, S.; Lies, S. D.; Gravatt, C. S.; Yoon, T. P. Radical cation cycloadditions using cleavable redox auxiliaries. *Org. Lett.*, **2017**, *19*, 368-371.

50. Tyson, E. L.; Farney, E. P.; Yoon, T. P. Photocatalytic [2 + 2] Cycloadditions of enones with cleavable redox auxiliaries. *Org. Lett.*, **2012**, *14*, 1110-1113.

51. Saint-Louis, C. J. *Control of molecular geometries using new photo-electro-switchable azobenzenes*. Ph.D. Dissertation, The University of Alabama, 2015.

52. Gray, L. T. *The Application of Arylamines as Redox Auxiliaries, Polar Crystals, and Organic Semiconductors*. Ph.D. Dissertation, The University of Alabama Libraries, 2012.

53. Browne, W. R.; Feringa, B. L. Making molecular machines work. *Nat. Nanotechnol.*, **2006**, *1*, 25-35.

54. Feringa, B. L. The art of building small: from molecular switches to molecular motors. *J. Org. Chem.*, **2007**, *72*, 6635-6652.

55. Meier, H. The photochemistry of stilbenoid compounds and their role in materials technology. *Angew. Chem. Int. Ed.*, **1992**, *31*, 1399-1420.

56. Han, W. G.; Lovell, T.; Liu, T.; Noodleman, L. Density functional studies of the ground- and excited-state potential-energy curves of stilbene *cis–trans* isomerization. *ChemPhysChem.*, **2002**, *3*, 167-178.

57. Gertz, L. Stilbenes: applications in chemistry, life sciences and materials science. Wiley-VCH Verlag GmbH & Co. KGaA., Weinheim, Germany: 2010.

58. Irie, M.; Fukaminato, T.; Matsuda, K.; Kobatake, S. Photochromism of diarylethene molecules and crystals: Memories, switches, and actuators. *Chem. Rev.*, **2014**, *114*, 12174-12277.

59. Fischer, G.; Muszkat, K.; Fischer, E. The thermodynamic equilibrium between *cis*-and *trans*-isomers in stilbene and some derivatives. *J. Chem. Soc., B,* **1968**, 1156-1158.

60. Taylor, T.; Murray, A. 395. Isomeric change in certain stilbenes. *J. Chem. Soc.,(Resumed),* **1938**, 2078-2086.

61. Muizebelt, W. J.; Nivard, R. J. F. Iodine atom-catalysed isomerisation of symmetrically substituted *cis*-stilbenes. *J. Chem. Soc. B,* **1968**, 913-920.

62. Ali, M. A.; Tsuda, Y. New Method for Isomerization of (Z)-Stilbenes into the (E)-Isomers Catalyzed by diaryl disulfide. *Chem. Pharm. Bull.*, **1992**, *40*, 2842-2844.

63. Hrovat, D. A.; Beno, B. R.; Lange, H.; Yoo, H.-Y.; Houk, K.; Borden, W. T. A Becke3LYP/6-31G* study of the Cope rearrangements of substituted 1, 5-hexadienes provides computational evidence for a chameleonic transition state. *J. Am. Chem. Soc.*, **1999**, *121*, 10529-10537.

64. Black, K. A.; Wilsey, S.; Houk, K. Dissociative and associative mechanisms of Cope rearrangements of fluorinated 1, 5-hexadienes and 2, 2'-bis-methylenecyclopentanes. *J. Am. Chem. Soc.*, **2003**, *125*, 6715-6724.

65. Black, K. A.; Wilsey, S.; Houk, K. Alkynes, allenes, and alkenes in [3, 3]-sigmatropy: functional diversity and kinetic monotony. A theoretical analysis. *J. Am. Chem. Soc.*, **1998**, *120*, 5622-5627.

66. Doering, W. v. E.; Toscano, V.; Beasley, G. Kinetics of the Cope rearrangement of 1, 1-dideuteriohexa-1, 5-diene. *Tetrahedron*, **1971**, *27*, 5299-5306.

67. Meier, H., The photochemistry of stilbenoid compounds and their role in materials technology. *Angew. Chem. Int. Ed. Engl.*, **1992**, *31*, 1399-1420.

68. Likhtenshtein, G. I. *Stilbenes: applications in chemistry, life sciences and materials science*. Wiley Online Library: 2010.

69. Bouas-Laurent, H.; Dürr, H. Organic photochromism (IUPAC technical report). *Pure Appl. Chem.*, **2001**, *73*, 639-665.

70. Szymański, W.; Beierle, J. M.; Kistemaker, H. A.; Velema, W. A.; Feringa, B. L. Reversible photocontrol of biological systems by the incorporation of molecular photoswitches. *Chem. Rev.*, **2013**, *113*, 6114-6178.

71. Gregory, A. R.; Williams, D. F. Stilbene. A critical commentary and some new calculations on its structure and isomerization. *J. Phys. Chem.*, **1979**, *83*, 2652-2662.

72. Chaudhuri, R. K.; Freed, K. F.; Chattopadhyay, S.; Mahapatra, U. S. Theoretical studies of the ground and excited state structures of stilbene. *J. Phys. Chem. A*, **2013**, *117*, 9424-9434.

73. De Wergifosse, M.; Houk, A. L.; Krylov, A. I.; Elles, C. G. Two-photon absorption spectroscopy of *trans*-stilbene, *cis*-stilbene, and phenanthrene: Theory and experiment. *J. Chem. Phys.*, **2017**, *146*, 144305.

74. Molina, V.; Merchán, M.; Roos, B. O. Theoretical study of the electronic spectrum of *trans*-stilbene. *J. Phys. Chem. A*, **1997**, *101*, 3478-3487.

75. Lhost, O.; Brédas, J. Theoretical study of torsion potentials in *trans*-stilbene and substituted *trans*-stilbenes: Modeling torsions in poly (paraphenylene vinylene) and derivatives. *J. Chem. Phys.*, **1992**, *96*, 5279-5288.

76. Galvao, D.; Soos, Z.; Ramasesha, S.; Etemad, S. A parametric method 3 (PM3) study of *trans*-stilbene. *J. Chem. Phys.*, **1993**, *98*, 3016-3021.

77. Choi, C. H.; Kertesz, M. Conformational information from vibrational spectra of Styrene, *trans*-Stilbene, and *cis*-Stilbene. *J. Phys. Chem. A*, **1997**, *101*, 3823-3831.

78. Bromberg, A.; Muszkat, K. The geometry of hindered stilbenes in their ground and excited states. *Tetrahedron*, **1972**, *28*, 1265-1274.

79. Troe, J.; Weitzel, K. M. MNDO calculations of stilbene potential energy properties relevant for the photoisomerization dynamics. *J. Chem. Phys.*, **1988**, *88*, 7030-7039.

80. Saltiel, J.; Ganapathy, S.; Werking, C. The DELTA H for thermal *trans/cis*-stilbene isomerization: do S0 and T1 potential energy curves cross? *J. Phys. Chem.*, **1987**, *91*, 2755-2758.

81. Williams, R. B. Heats of catalytic hydrogenation in solution. I. Apparatus, technique, and the heats of hydrogenation of certain pairs of stereoisomers. *J. Am. Chem. Soc.*, **1942**, *64*, 1395-1404.

82. Tamai, N.; Miyasaka, H. Ultrafast dynamics of photochromic systems. *Chem. Rev.*, **2000**, *100*, 1875-1890.

83. Blevins, A. A.; Blanchard, G. Effect of positional substitution on the optical response of symmetrically disubstituted azobenzene derivatives. *J. Phys. Chem. B*, **2004**, *108*, 4962-4968.

84. Crecca, C. R.; Roitberg, A. E. Theoretical study of the isomerization mechanism of azobenzene and disubstituted azobenzene derivatives. *J. Phys. Chem. A*, **2006**, *110*, 8188-8203.

85. Donald, B. *Advances in Physical Organic Chemistry*. Academic Press: 1989; Vol. 25.

86. Allen, M. T.; Whitten, D. G. The photophysics and photochemistry of. alpha., omega.-diphenylpolyene singlet states. *Chem. Rev.*, **1989**, *89*, 1691-1702.

87. Hammond, G. S.; Turro, N. J. Organic photochemistry. *Science*, **1963**, *142*, 1541-1553.

88. Davies, M.; Evans, F. P. The kinetics of some *cis-trans* isomerization reactions in solutions. *Trans. Faraday Soc.*, **1955**, *51*, 1506-1517.

89. Calvin, M.; Alter, H. W. Substituted Stilbenes. II. Thermal Isomerization. *J. Chem. Phys.*, **1951**, *19*, 768-770.

90. Waldeck, D. H. Photoisomerization dynamics of stilbenes. *Chem. Rev.*, **1991**, *91*, 415-436.

91. Görner, H.; Kuhn, H. J. *Cis-trans* photoisomerization of stilbenes and stilbene-like molecules. In *Advances in Photochemistry*; John Wiley & Sons: 2007; Vol. 19, pp 1-117.

92. Lewis, G. N.; Magel, T. T.; Lipkin, D. The absorption and re-emission of light by *cis*-and *trans*-Stilbenes and the efficiency of their photochemical isomerization. *J. Am. Chem. Soc.*, **1940**, *62*, 2973-2980.

93. Yamashita, S. Photochemical *cis-trans* isomerization of Stilbene. *Bull. Chem. Soc. Jpn.*, **1961**, *34*, 490-493.

94. Saltiel, J.; Chang, D. W.; Megarity, E. D. Positional dependence of the heavy atom effect in the *cis-trans* photoisomerization of bromostilbenes. *J. Am. Chem. Soc.*, **1974**, *96*, 6521-6522.

95. Stegemeyer, H. On the mechanism of photochemical *cis*↔ *trans* isomerization. *J. Phys. Chem.*, **1962**, *66*, 2555-2560.

96. Hammond, G. S.; Saltiel, J.; Lamola, A. A.; Turro, N. J.; Bradshaw, J. S.; Cowan, D. O.; Counsell, R. C.; Vogt, V.; Dalton, C. Mechanisms of photochemical reactions in solution. XXII. 1 Photochemical *cis-trans* isomerization. *J. Am. Chem. Soc.,* **1964**, *86*, 3197-3217.

97. Güsten, H.; Klasinc, L. Quantum yields of the photochemical *cis-trans* isomerization of monosubstituted stilbenes. *Tetrahedron Lett.,* **1968**, *9*, 3097-3101.

98. Bansal, R. K. *Organic reaction mechanisms*. New Academic Science: 2012.

99. Saltiel, J. Perdeuteriostilbene. The role of phantom states in the *cis-trans* photoisomerization of stilbenes. *J. Am. Chem. Soc.,* **1967**, *89*, 1036-1037.

100. Cox, M. J.; Crim, F. F. Vibrational energy flow rates for *cis*-and *trans*-stilbene isomers in solution. *J. Phys. Chem. A,* **2005**, *109*, 11673-11678.

101. Beveridge, D. L.; Jaffe, H. The Electronic Structure and Spectra of cis-and trans-Stibene1. *J. Am. Chem. Soc.,* **1965**, *87*, 5340-5346.

102. Nalwa, H. S. *Nanostructured materials and nanotechnology: concise edition*. Academic Press: 2001.

103. Jørgensen, K. B. Photochemical oxidative cyclisation of stilbenes and stilbenoids—the Mallory-reaction. *Molecules,* **2010**, *15*, 4334-4358.

104. Moore, W. M.; Morgan, D. D.; Stermitz, F. R., The photochemical conversion of stilbene to phenanthrene. The nature of the intermediate. *J. Am. Chem. Soc.,* **1963**, *85*, 829-830.

105. Buckles, R. E. Illumination of *cis*-and *trans*-stilbenes in dilute solutions. *J. Am. Chem. Soc.,* **1955**, *77*, 1040-1041.

106. Dou, Y.; Allen, R. E. Dynamics of the photocyclization of *cis*-stilbene to dihydrophenanthrene. *J. Mod. Opt.,* **2004**, *51*, 2485-2491.

107. Lewis, F. D.; Kurth, T. L.; Kalgutkar, R. S. A push–pull 4a, 4b-dihydrophenanthrene. *Chem. Commun.,* **2001**, 1372-1373.

108. Lin, C.-K.; Prabhakar, C.; Yang, J.-S. o-Amino conjugation effect on the Photochemistry of *trans*-aminostilbenes. *J. Phys. Chem. A,* **2011**, *115*, 3233-3242.

109. Wittig, G.; Haag, W. "Via triphenylphosphine-methylenes as olefin-forming reagents I". *Chem. Ber.,* **1955**, *88*, 1654-1666.

110. McMurry, J. E.; Fleming, M. P. New method for the reductive coupling of carbonyls to olefins. Synthesis of. beta.-carotene. *J. Am. Chem. Soc.*, **1974**, *96*, 4708-4709.

111. Babudri, F.; Farinola, G. M.; Naso, F.; Panessa, D. A novel regio-and stereoselective formal cross-coupling reaction of unsaturated silanes with arenediazonium tetrafluoroborates. *J. Org. Chem.*, **2000**, *65*, 1554-1557.

112. Mudududdla, R.; Sharma, R.; Abbat, S.; Bharatam, P. V.; Vishwakarma, R. A.; Bharate, S. B. Synthesis of 2-phenylnaphthalenes from styryl-2-methoxybenzenes. *Chem. Commun.*, **2014**, *50*, 12076-12079.

113. Abdel-Halim, S. T.; Abdel-Kader, M. H.; Steiner, U. E. Thermal *cis-trans* isomerization of solvatochromic merocyanines: linear correlations between solvent polarity and adiabatic and diabatic transition energies. *J. Phys. Chem.*, **1988**, *92*, 4324-4328.

114. Hicks, J.; Vandersall, M.; Sitzmann, E.; Eisenthal, K. Polarity-dependent barriers and the photoisomerization dynamics of molecules in solution. *Chem. Phys. Lett.*, **1987**, *135*, 413-420.

115. Todd, D. C.; Fleming, G. R. *Cis*-stilbene isomerization: Temperature dependence and the role of mechanical friction. *J. Chem. Phys.*, **1993**, *98*, 269-279.

116. Dokic, J.; Gothe, M.; Wirth, J.; Peters, M. V.; Schwarz, J.; Hecht, S.; Saalfrank, P. Quantum chemical investigation of thermal *cis*-to-*trans* isomerization of azobenzene derivatives: substituent effects, solvent effects, and comparison to experimental data. *J. Phys. Chem. A*, **2009**, *113*, 6763-6773.

117. Carey, F. A.; Sundberg, R. J. *Advanced organic chemistry: part A: structure and mechanisms*. Springer Science & Business Media: US, 2007.

118. Anslyn, E. V.; Dougherty, D. A. *Modern physical organic chemistry*. University Science Books: US, 2006.

119. Calvin, M.; Alter, H. W. Substituted Stilbenes. II. Thermal Isomerization. *J. Chem. Phys.*, **1951**, *19*, 768-770.

120. Taylor, T.; Murray, A. 395. Isomeric change in certain stilbenes. *J. Chem. Soc.*, **1938**, 2078-2086.

121. Yao, H.-H.; Cheng, H.-H.; Cheng, C.-H.; Lin, C.-K.; Yang, J.-S.; Chen, I. C. Charge-transfer and isomerization reactions of *trans*-4-(N-arylamino)stilbenes. *Phys. Chem. Chem. Phys.*, **2016**, *18*, 28164-28174.

122. Dainton, F.; Robinson, E.; Salmon, G. Pulse radiolysis of solutions of stilbene. I. Evidence for triplet and singlet excited state formation. *J. Phys. Chem.*, **1972**, *76*, 3897-3904.

123. Gegiou, D.; Muszkat, K. A.; Fischer, E. Temperature dependence of photoisomerization. V. Effect of substituents on the photoisomerization of stilbenes and azobenzenes. *J. Am. Chem. Soc.,* **1968**, *90*, 3907-3918.

124. Herkstroeter, W. G.; McClure, D. S. Lowest triplet state of stilbene. *J. Am. Chem. Soc.,* **1968**, *90*, 4522-4527.

125. Saltiel, J.; Marinari, A.; Chang, D. W. L.; Mitchener, J. C.; Megarity, E. D. *Trans-cis* photoisomerization of the stilbenes and a reexamination of the positional dependence of the heavy-atom effect. *J. Am. Chem. Soc.*, **1979**, *101*, 2982-2996.

126. Papper, V.; Pines, D.; Likhtenshtein, G.; Pines, E. Photophysical characterization of *trans*-4, 4′-disubstituted stilbenes. *J. Photochem. Photobiol. A,* **1997**, *111*, 87-96.

127. Dou, Y.; Allen, R. E. Dynamics of the photocyclization of *cis*-stilbene to dihydrophenanthrene. *J. Mod. Opt.,* **2004**, *51*, 2485-2491.

128. Hashidzume, A.; Yamaguchi, H.; Harada, A. Molecular Machines and Motors: Recent Advances and Perspectives. In *Topics in Current Chemistry.* Credi, A; Silvi, S; Venturi, M. (Eds.*)* Springer: Bologna, Germany, 2014; pp 71-110

129. Connelly, N. G.; Geiger, W. E. Chemical redox agents for organometallic chemistry. *Chem. Rev.,* **1996**, *96*, 877-910.

130. Lewis, F. D.; Petisce, J. R.; Oxman, J. D.; Nepras, M. J., One-way photoisomerization of *cis*-stilbene via a cation radical chain mechanism. *J. Am. Chem. Soc.*, **1985**, *107*, 203-207.

131. Mallory, F. B.; Mallory, C. W. Photocyclization of stilbenes and related molecules. *Organic reactions,* **2005**, *30*, 1-456.

132. Lewis, F. D.; Bedell, A. M.; Dykstra, R. E.; Elbert, J. E.; Gould, I. R.; Farid, S. Photochemical generation, isomerization, and oxygenation of stilbene cation radicals. *J. Am. Chem. Soc.,* **1990**, *112*, 8055-8064.

133. Kuriyama, Y.; Sakuragi, H.; Tokumaru, K.; Yoshida, Y.; Tagawa, S. Mechanism for isomerization of *cis*-stilbene via its radical cation as investigated by pulse radiolysis. A possible role of a dimeric radical cation as an intermediate. *Bull. Chem. Soc. Jpn.*, **1993**, *66*, 1852-1855.

134. Lewis, F. D.; Kojima, M. Electron-transfer-induced photoisomerization, dimerization, and oxygenation of *trans*- and *cis*-anethole. The role of monomer and dimer cation radicals. *J. Am. Chem. Soc.,* **1988**, *110*, 8664-8670.

135. Santoro, A. V.; Barrett, E. J.; Hoyer, H. W. Kinetics of *cis-trans* isomerization by differential thermal analysis. *J. Am. Chem. Soc.*, **1967**, *89*, 4545-4546.

136. Viehe, H. G.; Janousek, Z.; Merényi, R. *Substituent effects in radical chemistry*. Springer: 1986.

137. Kelley, M. D., *Electrochromic and photoelectrochromic switching devices based on aryl amine redox chemistry*. Ph.D. Dissertation, The University of Alabama, 2014.

138. Zoski, C. G., *Handbook of electrochemistry*. Elsevier: 2006.

139. Perrin, D. D.; Armarego, W. L. F. *Purification of Laboratory Chemicals*. Pergamon Press: Oxford, 1988.

140. Pickett, C. A simple hydrocarbon electrolyte: completing the electron-transfer series [Fe 4 S 4 (SPh) 4] $^{1-/2-/3-/4-\cdot}$ *J. Chem. Soc. Chem. Commun.*, **1985**, 323-326.

141. Sheldrick, G. M. SHELXTL/PC, Version 6.14; Bruker Analytical X-ray Systems: Madison, WI, 2000-2003.

142. Rathore, R.; Burns, C. L.; Deselnicu, M. I. Preparation of 1, 4: 5, 8-Dimethano-1, 2, 3, 4, 5, 6, 7, 8-Octahydro-9, 10-Dimethoxyanthracenium Hexachloroantimonate ($4^{+\cdot}$ $SbCl_6^-$): A Highly Robust Radical-Cation Salt. *Org. Synth.*, **2005**, *82*, 1-9.

143. Surry, D. S.; Buchwald, S. L. Dialkylbiaryl phosphines in Pd-catalyzed amination: a user's guide. *Chem. Sci.*, **2011**, *2*, 27-50.

144. Linseis, M.; Zalis, S.; Zabel, M.; Winter, R. F. Ruthenium stilbenyl and diruthenium distyrylethene complexes: aspects of electron delocalization and electrocatalyzed isomerization of the Z-isomer. *J. Am. Chem. Soc.*, **2012**, *134*, 16671-16692.

145. Talele, H. R.; Chaudhary, A. R.; Patel, P. R.; Bedekar, A. V. Expeditious synthesis of helicenes using an improved protocol of photocyclodehydrogenation of stilbenes. *ARKIVOC*, **2011**, *201*, 15-37.

146. Guo, L.; Yang, C.; Zheng, L.; Xia, W. Visible light-mediated oxidative quenching reaction to electron-rich epoxides: highly regioselective synthesis of α-bromo (di) ketones and mechanism study. *Org. Biomol. Chem.*, **2013**, *11*, 5787-5792.

147. Yang, J.-S.; Hwang, C.-Y.; Hsieh, C.-C.; Chiou, S.-Y. Spectroscopic correlations between supermolecules and molecules. Anatomy of the ion-modulated electronic properties of the nitrogen donor in monoazacrown-derived intrinsic fluoroionophores. *J. Org. Chem.*, **2004**, *69*, 719-726.

148. Heynekamp, J. J.; Weber, W. M.; Hunsaker, L. A.; Gonzales, A. M.; Orlando, R. A.; Deck, L. M.; Vander Jagt, D. L. Substituted *trans*-stilbenes, including analogues of the natural product resveratrol, inhibit the human tumor necrosis factor alpha-induced activation of transcription factor nuclear factor kappaB. *J. Med. Chem.*, **2006**, *49*, 7182-7189.

149. Das, M.; O'Shea, D. F. Z-Stereoselective Aza-Peterson olefinations with bis (trimethylsilane) reagents and sulfinyl Imines. *Org. Lett.,* **2016**, *18*, 336-339.

150. Chau, A.; Cote, B.; Ducharme, Y.; Frenette, R.; Friesen, R.; Gagnon, M.; Giroux, A.; Martins, E.; Yu, H.; Wu, T. Preparation of 1H-phenanthro [9, 10-d] imidazoles as mPGES-1 inhibitors. US20090286772 A1. November 19, 2009.

151. Tewari, R. S.; Kumari, N.; Kendurkar, P. S. Generation and reactions of some dimethyl benzylphosphonate carbanions: synthesis of *trans*-diaryl-substituted ethylenes. *J. Chem. Eng. Data*, **1976**, *21*, 125-131.

152. Eltaief, S.; Aloui, F.; Moussa, S.; Retailleau, P.; Ben Hassine, B. Synthesis and characterisation of new nonracemic quaternary ammonium salts. *Lett. Org. Chem.*, **2012**, *9*, 427-434.

153. Hossian, A.; Bhunia, S. K.; Jana, R. Substrate-dependent mechanistic divergence in decarboxylative Heck reaction at room temperature. *J. Org. Chem.,* **2016**, *81*, 2521-2533.

154. Myers, A. G.; Tanaka, D.; Mannion, M. R. Development of a Decarboxylative Palladation Reaction and Its Use in a Heck-type Olefination of Arene Carboxylates. *J. Am. Chem. Soc.*, **2002**, *124*, 11250-11251.

155. Guram, A. S.; Buchwald, S. L. Palladium-Catalyzed Aromatic Aminations with in situ Generated Aminostannanes. *J. Am. Chem. Soc.*, **1994**, *116*, 7901-7902.

156. Paul, F.; Patt, J.; Hartwig, J. F. Palladium-catalyzed formation of carbon-nitrogen bonds. Reaction intermediates and catalyst improvements in the hetero cross-coupling of aryl halides and tin amides. *J. Am. Chem. Soc.*, **1994**, *116*, 5969-5970.

157. Nandakumar, M. V.; Verkade, J. G. One-Pot Sequential N and C Arylations: An Efficient Methodology for the Synthesis of *trans* 4-N, N-Diaryl Aminostilbenes. *Angew. Chem. Int. Ed.,* **2005**, *44*, 3115-3118.

158. Lin, C.-K.; Yang, J.-S. Fluorescence response of TICT-active aminostilbenes to copper (II) ions: redox reaction vs ion recognition. *Res. Chem. Intermed.,* **2013**, *39*, 19-32.

159. Liptay, W. Dipole moments and polarizabilities of molecules in excited electronic states. In *Excited states*. Lim, E.C. Ed; Elsevier: 1974; Vol. 1, pp 129-229.

160. Papper, V.; Likhtenshtein, G. I. Substituted stilbenes: a new view on well-known systems: New applications in chemistry and biophysics. *J. Photochem. Photobiol. A,* **2001**, *140*, 39-52.

161. Barlow, S.; Risko, C.; Coropceanu, V.; Tucker, N. M.; Jones, S. C.; Levi, Z.; Khrustalev, V. N.; Antipin, M. Y.; Kinnibrugh, T. L.; Timofeeva, T. A mixed-valence bis (diarylamino) stilbene: crystal structure and comparison of electronic coupling with biphenyl and tolane analogues. *Chem. Commun.,* **2005**, 764-766.

162. Lutz, R. P. Catalysis of the Cope and Claisen rearrangements. *Chem. Rev.,* **1984**, *84*, 205-247.

163. Cope, A. C.; Hardy, E. M. The Introduction of substituted vinyl groups. V. A rearrangement Involving the migration of an allyl group in a three-carbon system 1. *J. Am. Chem. Soc.,* **1940**, *62*, 441-444.

164. Negishi, E. Overview of the Negishi protocol with Zn, Al, Zr, and related metals. In *Handbook of organopalladium chemistry for organic synthesis.* John Wiley & Sons, Inc: New York, 2002; pp 229-247.

165. Martín Castro, A. M. Claisen rearrangement over the past nine decades. *Chem. Rev.,* **2004**, *104*, 2939-3002.

166. Sakai, S. Theoretical analysis of the Cope rearrangement of 1, 5-hexadiene. *Int. J. Quantum Chem.,* **2000**, *80*, 1099-1106.

167. Nowicki, J. Claisen, Cope and related rearrangements in the synthesis of flavour and fragrance compounds. *Molecules,* **2000**, *5*, 1033-1050.

168. Dewar, M. J.; Wade Jr, L. E. A study of the mechanism of the Cope rearrangement. *J. Am. Chem. Soc.,* **1977**, *99*, 4417-4424.

169. Hammond, G. S.; DeBoer, C. D. Multiplicity of mechanisms in the cope rearrangement. *J. Am. Chem. Soc.,* **1964**, *86*, 899-902.

170. Doering, W. V. E.; Roth, W. The overlap of two allyl radicals or a four-centered transition state in the cope rearrangement. *Tetrahedron,* **1962**, *18*, 67-74.

171. Doering, W. v. E.; Wang, Y. Perturbation of Cope's Rearrangement: 1, 3, 5-Triphenylhexa-l, 5-diene. Chameleonic or Centauric Transition Region? *J. Am. Chem. Soc.,* **1999**, *121*, 10112-10118.

172. Hrovat, D. A.; Chen, J.; Houk, K.; Borden, W. T. Cooperative and competitive substituent effects on the Cope rearrangements of phenyl-substituted 1, 5-hexadienes elucidated by Becke3LYP/6-31G* calculations. *J. Am. Chem. Soc.,* **2000**, *122*, 7456-7460.

173. Gajewski, J. J.; Conrad, N. D. Variable transition state structure in 3, 3-sigmatropic shifts from. alpha.-secondary deuterium isotope effects. *J. Am. Chem. Soc.,* **1979**, *101*, 6693-6704.

174. Dewar, M. J.; Wade, L. E. Possible role of 1, 4-cyclohexylene intermediates in Cope rearrangements. *J. Am. Chem. Soc.*, **1973**, *95*, 290-291.
175. Gajewski, J. J.; Conrad, N. D., The mechanism of the Cope rearrangement. *J. Am. Chem. Soc.*, **1978**, *100*, 6268-6269.

176. Borden, W. T. *Modern molecular orbital theory for organic chemists*. Prentice Hall: New Jersey, 1975.

177. Hrovat, D. A.; Borden, W. T. A simple mathematical model for the cooperative and competitive substituent effects found in the Cope rearrangements of phenyl-substituted 1, 5-hexadienes. *J. Chem. Theory Comput.*, **2005**, *1*, 87-94.

178. Ralls, J. W.; Lundin, R. E.; Bailey, G. F. Preparation and thermal rearrangement of alkenyl 3-alkenyloxy-2-butenoates. Catalysis of the aliphatic Claisen rearrangement by ammonium chloride. *J. Org. Chem.*, **1963**, *28*, 3521-3526.

179. Hill, R. K.; Gilman, N. W. A nitrogen analog of the Claisen rearrangement. *Tetrahedron Lett.*, **1967**, *8*, 1421-1423.

180. Yoon, T. P.; Dong, V. M.; MacMillan, D. W. Development of a new Lewis acid-catalyzed Claisen rearrangement. *J. Am. Chem. Soc.*, **1999**, *121*, 9726-9727.

181. Heimgartner, H.; Hansen, H.; Schmid, H. *Iminium salts in organic chemistry*. Böhme, H; Viehe, H.G., Ed.; Wiley: New York, 1979; pp 655-732.

182. Nakamura, H; Yamamoto, Y. Palladium-catalyzed carbon skeletal rearrangements: Cope, Claisen, and other [3,3] rearrangements. In *Handbook of organopalladium chemistry for organic Synthesis*. Negishi, E-i., Ed.; John Wiley & Sons, Inc: New York, 2002; pp 2919-2934.

183. Beesley, R. M.; Ingold, C. K.; Thorpe, J. F. CXIX.—The formation and stability of spiro-compounds. Part I. spiro-Compounds from cyclohexane. *J. Chem. Soc. Trans.*, **1915**, *107*, 1080-1106.

184. Nubbemeyer, U. Recent advances in charge-accelerated Aza-Claisen rearrangements. In *Natural products synthesis II*, Springer: Berlin, Heidelberg, 2005; pp 149-213.

185. Shimizu, M.; Kimura, M.; Watanabe, T.; Tamaru, Y. Palladium-catalyzed allylation of imines with allyl alcohols. *Org. Lett.*, **2005**, *7*, 637-640.

186. Yadav, J.; Ather, H.; Rao, P. P.; Rao, R. S.; Nagaiah, K.; Prasad, A. Sulphamic acid: An efficient, cost-effective and recyclable solid acid catalyst for three-component synthesis of homoallylic amines. *Catal. Commun.*, **2006**, *7*, 797-801.

187. Oberg, K. M.; Rovis, T. Enantioselective rhodium-catalyzed [4+ 2] cycloaddition of α, β-unsaturated imines and isocyanates. *J. Am. Chem. Soc.*, **2011**, *133*, 4785-4787.

188. Esteves-Souza, A.; Rodrigues-Santos, C. E.; Del Cistia, C. d. N.; Silva, D. R. d.; Sant'Anna, C. M. R.; Echevarria, A. Solvent-free synthesis, DNA-topoisomerase II activity and molecular docking study of new asymmetrically N, N'-substituted ureas. *Molecules*, **2012**, *17*, 12882-12894.

189. Cho, B. T.; Kang, S. K. Direct and indirect reductive amination of aldehydes and ketones with solid acid-activated sodium borohydride under solvent-free conditions. *Tetrahedron*, **2005**, *61*, 5725-5734.

APPENDIX A

LIST OF NMR SPECTRA

A.1 ^{1}H NMR spectrum (360 MHz) of **5** in $CDCl_3$

A.2 ^{13}C NMR spectrum (125 MHz) of **5** in $CDCl_3$

A.3 ^{1}H NMR spectrum (360 MHz) of (4-bromobenzyl)triphenylphosphonium bromide in $CDCl_3$

A.4 ^{1}H NMR spectrum (500 MHz) of ***cis*-6a** in $CDCl_3$

A.5 ^{1}H NMR spectrum (500 MHz) of ***trans*-6a** in $CDCl_3$

A.6 ^{1}H NMR spectrum (360 MHz) of ***cis*-6b** in $CDCl_3$

A.7 ^{1}H NMR spectrum (360 MHz) of ***trans*-6b** in $CDCl_3$

A.8 ^{1}H NMR spectrum (360 MHz) of ***cis*-6c** in $CDCl_3$

A.9 ^{1}H NMR spectrum (500 MHz) of ***trans*-6c** in $CDCl_3$

A.10 ^{1}H NMR spectrum (360 MHz) of ***cis*-6d** in $CDCl_3$

A.11 ^{13}C NMR spectrum (125 MHz) of ***cis*-6d** in DMSO

A.12 ^{19}F NMR spectrum (360 MHz) of ***cis*-6d** in DMSO

A.13 ^{1}H NMR spectrum (500 MHz) of ***trans*-6d** in $CDCl_3$

A.14 ^{1}H NMR spectrum (360 MHz) of ***cis*-6e** in $CDCl_3$

A.15 ^{1}H NMR spectrum (360 MHz) of ***trans*-6e** in $CDCl_3$

A.16 ^{1}H NMR spectrum (360 MHz) of ***trans*-6f** in $CDCl_3$

A.17 ^{1}H NMR spectrum (360 MHz) of ***cis*-6f** in $CDCl_3$

A.18 ^{13}C NMR spectrum (125 MHz) of ***cis*-6f** in $CDCl_3$

A.19 ^{1}H NMR spectrum (360 MHz) of ***trans*-6g** in $CDCl_3$

A.20 ^{1}H NMR spectrum (500 MHz) of ***cis*-7a** in C_6D_6

A.21 ^{13}C NMR spectrum (125 MHz) of ***cis*-7a** in DMSO-d_6

A.22 ^{1}H NMR spectrum (500 MHz) of ***trans*-7a** in DMSO-d_6

A.23 ^{13}C NMR spectrum (125 MHz) of ***trans*-7a** in DMSO-d_6

A.24 ^{1}H NMR spectrum (500 MHz) of ***cis*-7b** in DMSO-d_6

A.25 ^{13}C NMR spectrum (125 MHz) of ***cis*-7b** in DMSO-d_6

A.26 ^{1}H NMR spectrum (360 MHz) of ***trans*-7b** in $CDCl_3$

A.27 ^{13}C NMR spectrum (125 MHz) of ***trans*-7b** in $CDCl_3$

A.28 ^{1}H NMR spectrum (500 MHz) of ***cis*-7c** in C_6D_6

A.29 ^{13}C NMR spectrum (125 MHz) of ***cis*-7c** in DMSO-d_6

A.30 ^{1}H NMR spectrum (500 MHz) of ***trans*-7c** in C_6D_6

A.31 ^{13}C NMR spectrum (125 MHz) of ***trans*-7c** in DMSO-d_6

A.32 ^{1}H NMR spectrum (360 MHz) of ***cis*-7d** in DMSO-d_6

A.33 ^{13}C NMR spectrum (125 MHz) of ***cis*-7d** in DMSO-d_6

A.34 ^{19}F NMR spectrum (360 MHz) of ***cis*-7d** in DMSO-d_6

A.35 ^{1}H NMR spectrum (500 MHz) of ***trans*-7d** DMSO-d_6

A.36 ^{13}C NMR spectrum (125 MHz) of ***trans*-7d** in DMSO-d_6

A.37 ^{19}F NMR spectrum (360 MHz) of ***trans*-7d** in DMSO-d_6

A.38 ^{1}H NMR spectrum (500 MHz) of ***cis*-7e** in DMSO-d_6

A.39 ^{13}C NMR spectrum (125 MHz) of ***cis*-7e** in DMSO-d_6

A.40 ^{1}H NMR spectrum (500 MHz) of ***trans*-7e** in DMSO-d_6

A.41 ^{13}C NMR spectrum (125 MHz) of ***trans*-7e** in DMSO-d_6

A.42 ^{1}H NMR spectrum (360 MHz) of ***trans*-7f** in C_6D_6

A.43 ^{13}C NMR spectrum (125 MHz) of ***trans*-7f** in DMSO-d_6

A.44 ^{1}H NMR spectrum (500 MHz) of ***trans*-7g** in DMSO-d_6

A.45 ^{13}C NMR spectrum (125 MHz) of ***trans*-7g** in DMSO-d_6

A.46 ^{1}H NMR spectrum (360 MHz) of ***cis*-8** in $CDCl_3$

A.47 ^{1}H NMR spectrum (360 MHz) of ***trans*-8** in $CDCl_3$

A.48 ^{1}H NMR spectrum (500 MHz) of ***cis*-9** in C_6D_6

A.49 ^{13}C NMR spectrum (125 MHz) of ***cis*-9** in in C_6D_6

A.50 ^{1}H NMR spectrum (500 MHz) of ***trans*-9** in C_6D_6

A.51 ^{13}C NMR spectrum (125 MHz) of ***trans*-9** in DMSO-d_6

A.52 ^{1}H NMR spectrum (500 MHz) of **10** in $CDCl_3$

A.53 ^{13}C NMR spectrum (125 MHz) of **10** in $CDCl_3$

A.54 ^{1}H NMR spectrum (360 MHz) of **10b** in $CDCl_3$

A.55 ^{13}C NMR spectrum (125 MHz) of **10b** in $CDCl_3$

A.56 ^{1}H NMR spectrum (360 MHz) of **10c** in $CDCl_3$

A.57 ^{13}C NMR spectrum (125 MHz) of **10c** in $CDCl_3$

A.58 ^{1}H NMR spectrum (360 MHz) of **11** in $CDCl_3$

A.59 ^{1}H NMR spectrum (360 MHz) of **12** in $CDCl_3$

A.60 ^{13}C NMR spectrum (125 MHz) of **12** in $CDCl_3$

A.61 ^{1}H NMR spectrum (360 MHz) of **12b** in $CDCl_3$

A.62 ^{13}C NMR spectrum (125 MHz) of **12b** in $CDCl_3$

A.63 ^{1}H NMR spectrum (360 MHz) of **12c** in $CDCl_3$

A.64 ^{1}H NMR spectrum (360 MHz) of **13** in $CDCl_3$

A.65 ^{13}C NMR spectrum (125 MHz) of **14** in $CDCl_3$

A.66 ^{1}H NMR spectrum (360 MHz) of **15** in $CDCl_3$

A.67 ^{1}H NMR spectrum (360 MHz) of **16** in $CDCl_3$

A.68 ^{13}C NMR spectrum (125 MHz) of **16** in $CDCl_3$

A.69 ^{1}H NMR spectrum (360 MHz) of **16b** in $CDCl_3$

A.70 ^{1}H NMR spectrum (360 MHz) of **17** in $CDCl_3$

A.71 ^{1}H NMR spectrum (360 MHz) of **18** in $CDCl_3$

A.72 ^{13}C NMR spectrum (125 MHz) of **18** in $CDCl_3$

A.73 ^{1}H NMR spectrum (360 MHz) of **18b** in $CDCl_3$

A.74 ^{13}C NMR spectrum (125 MHz) of **18b** in $CDCl_3$

A.75 ^{1}H NMR spectrum (360 MHz) of **19** in $CDCl_3$

A.76 ^{1}H NMR spectrum (360 MHz) of **20** in $CDCl_3$

A.77 ^{13}C NMR spectrum (125 MHz) of **20** in $CDCl_3$

A.78 ^{1}H NMR spectrum (360 MHz) of **21** in $CDCl_3$

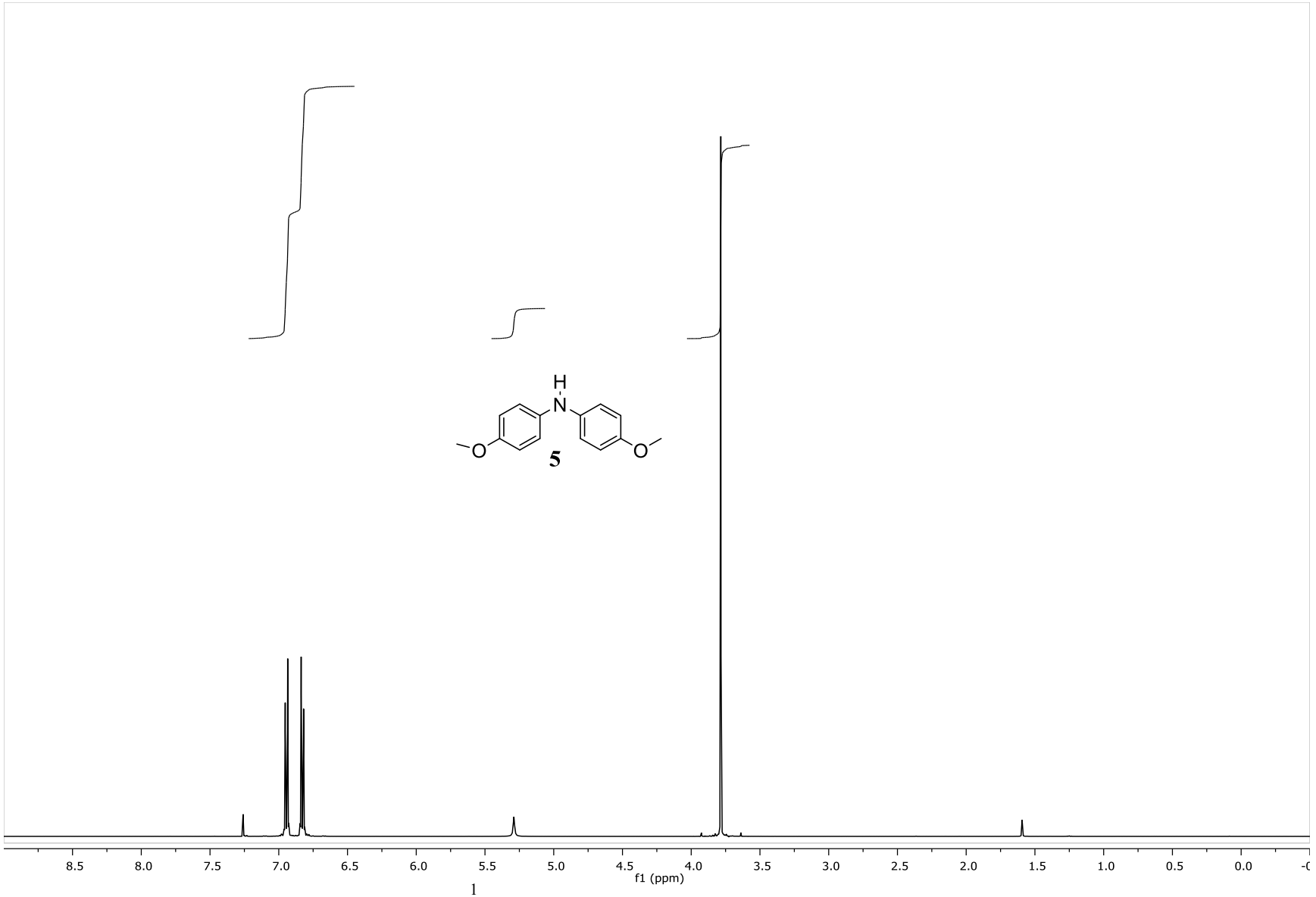

A.1. ^{1}H NMR spectrum (36 MHz) of **5** in $CDCl_3$

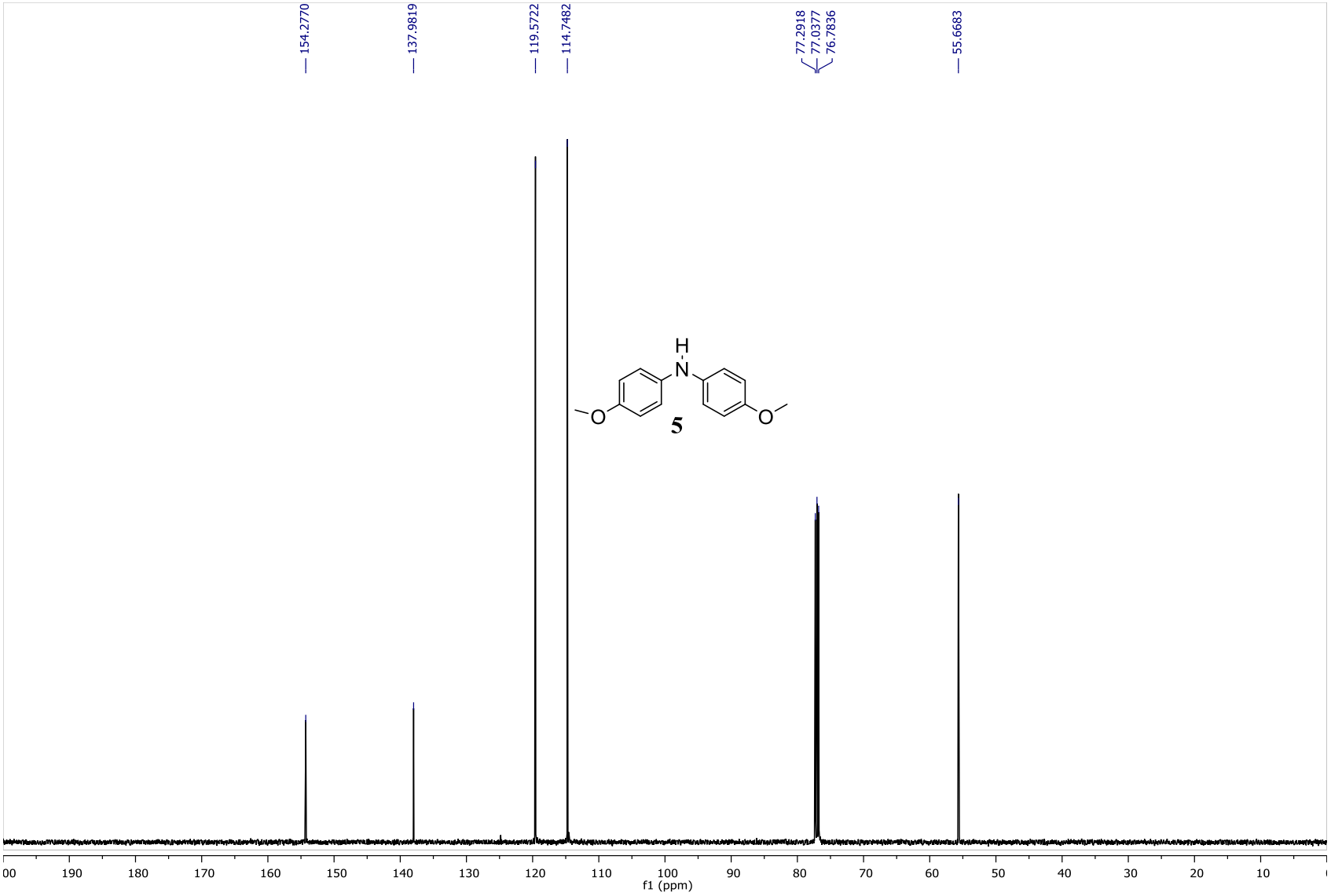

A.2. ^{13}C NMR spectrum (125 MHz) of **5** in $CDCl_3$

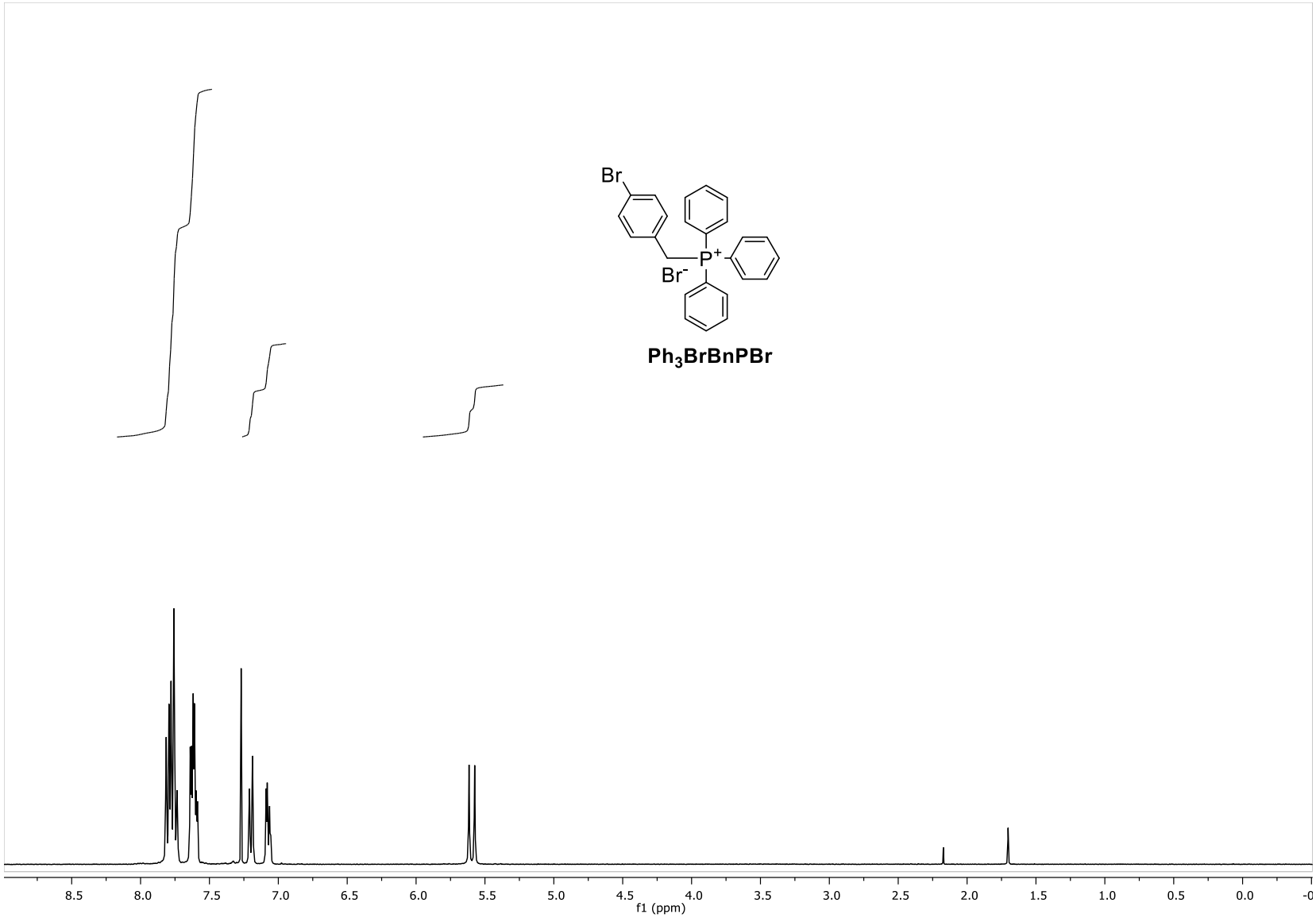

A.3 ^{1}H NMR spectrum (360 MHz) of (4-bromobenzyl)triphenylphosphonium bromide in $CDCl_3$

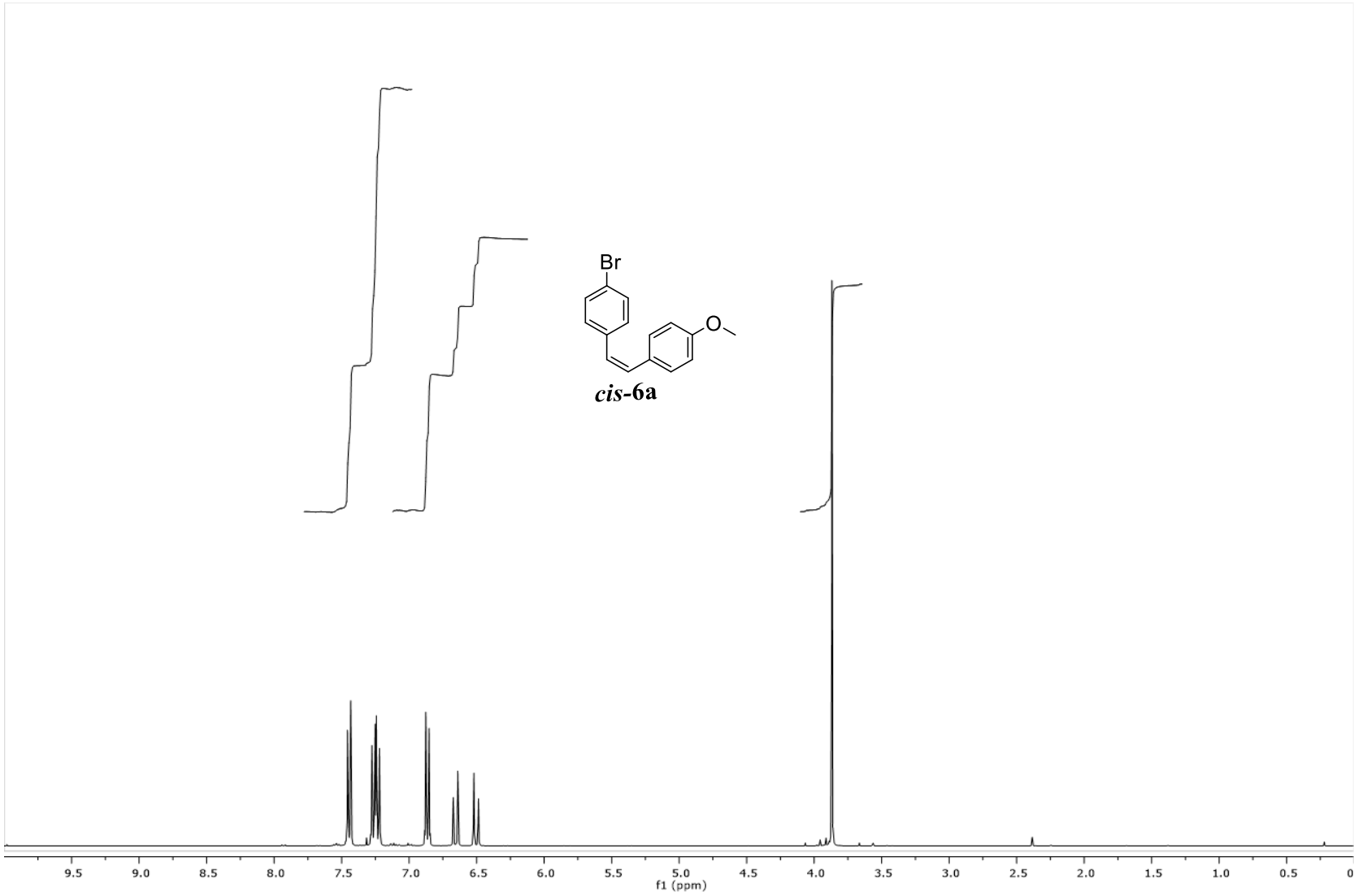

A.4. ^{1}H NMR spectrum (500 MHz) of ***cis*-6a** in $CDCl_3$

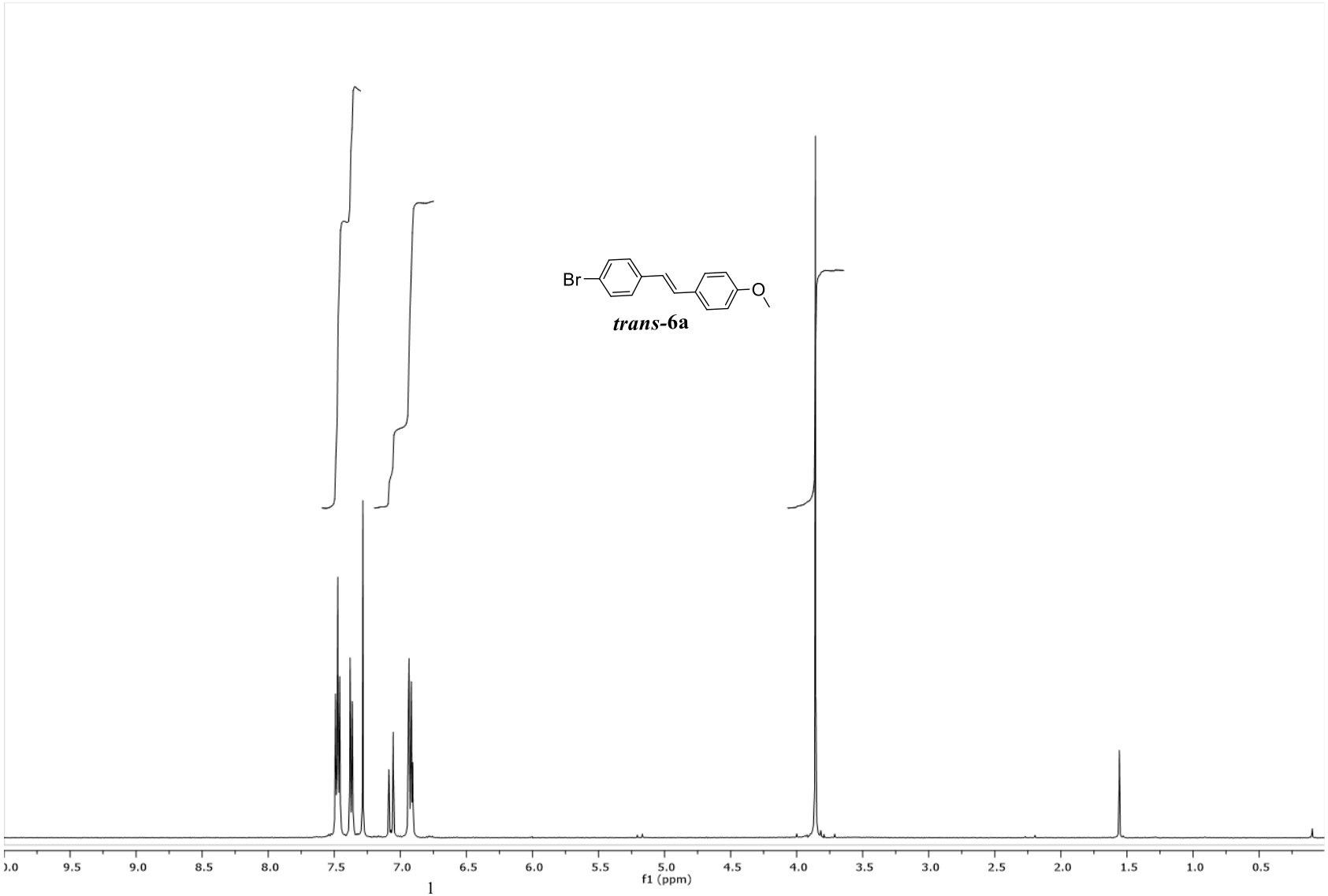

A.5. ^{1}H NMR spectrum (500 MHz) of ***trans*-6a** in $CDCl_3$

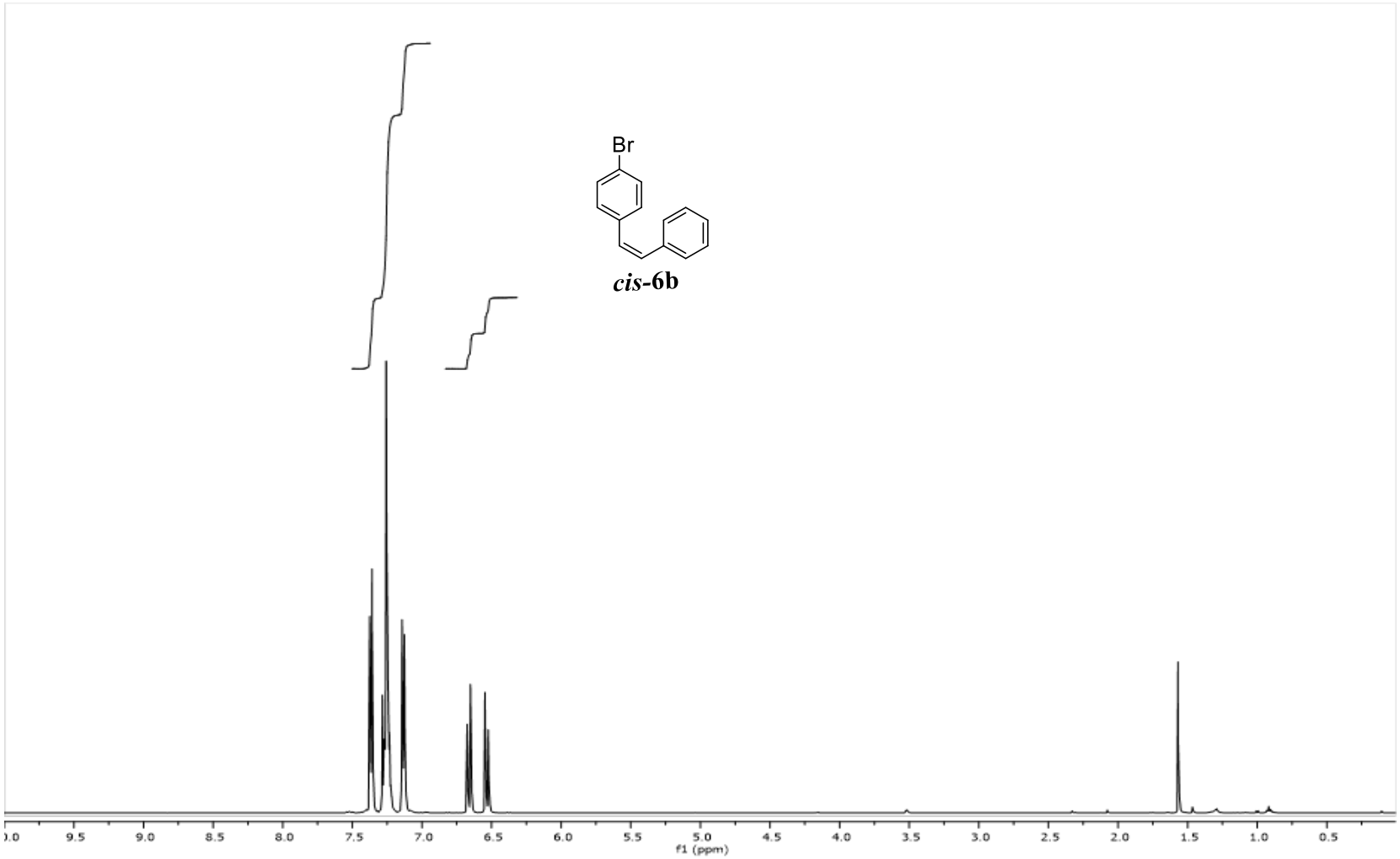

A.6. ^{1}H NMR spectrum (360 MHz) of ***cis*-6b** in $CDCl_3$

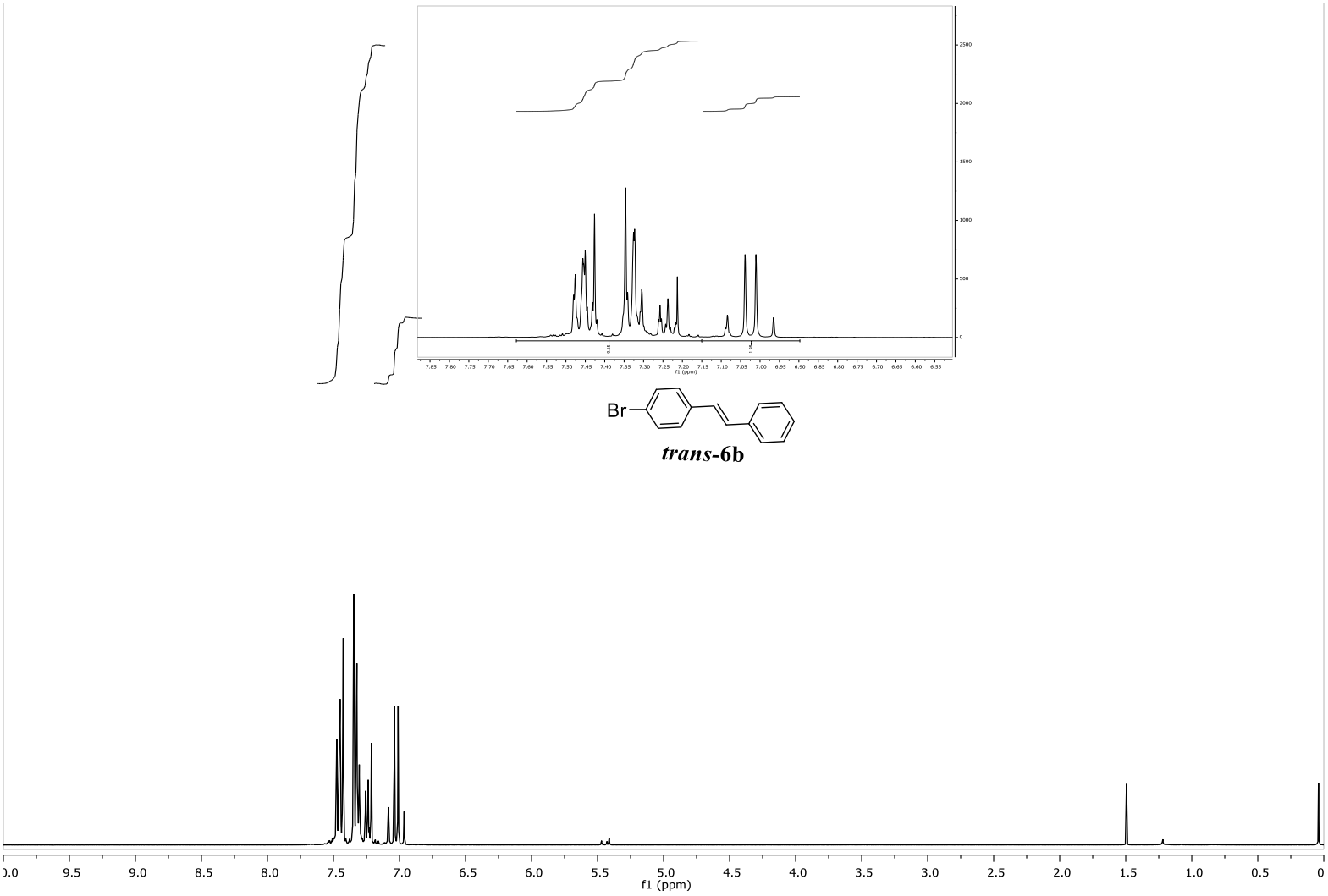

A.7. ^{1}H NMR spectrum (360 MHz) of ***trans*-6b** in $CDCl_3$

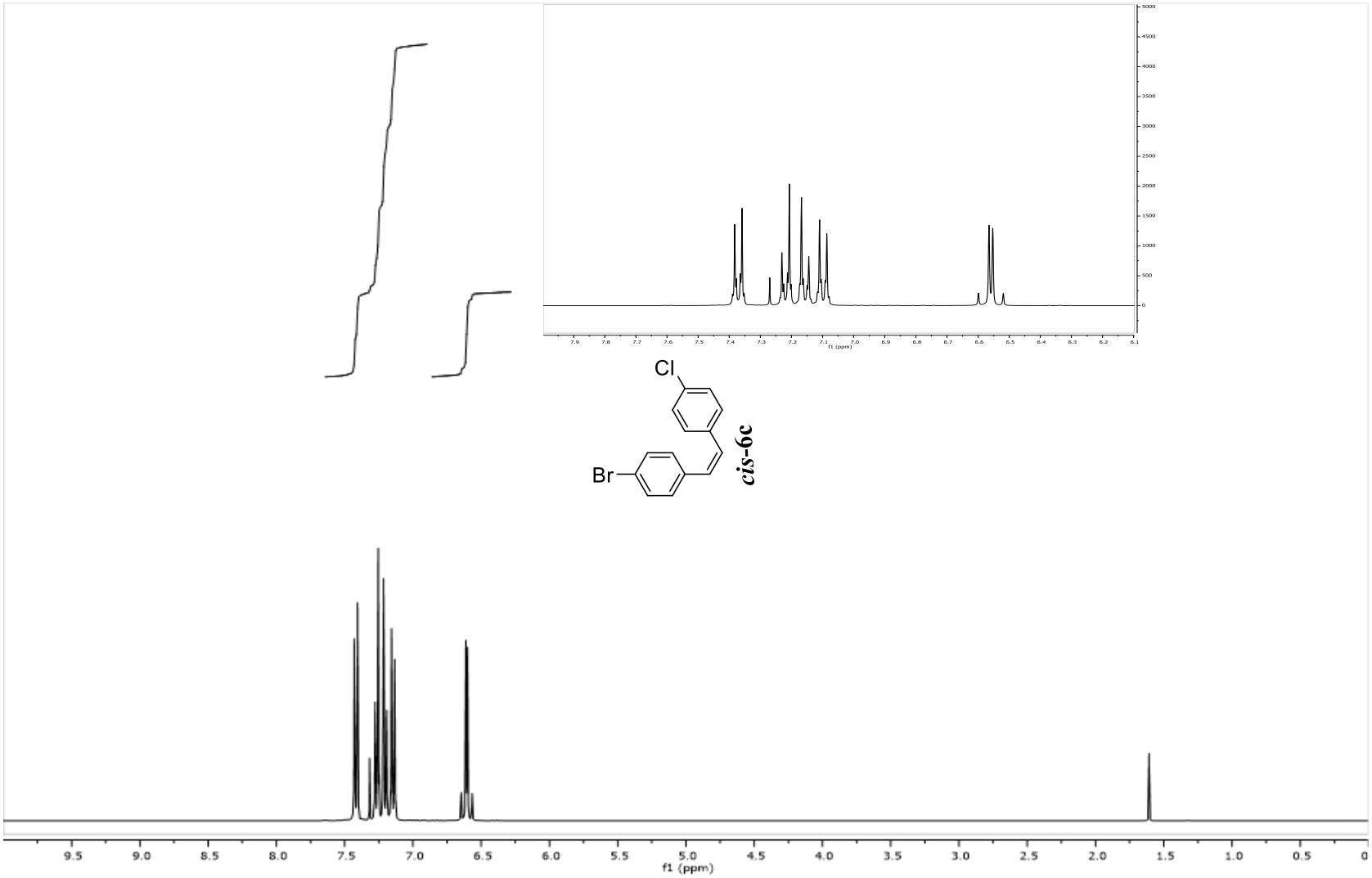

A.8. ^{1}H NMR spectrum (360 MHz) of ***cis*-6c** in $CDCl_3$

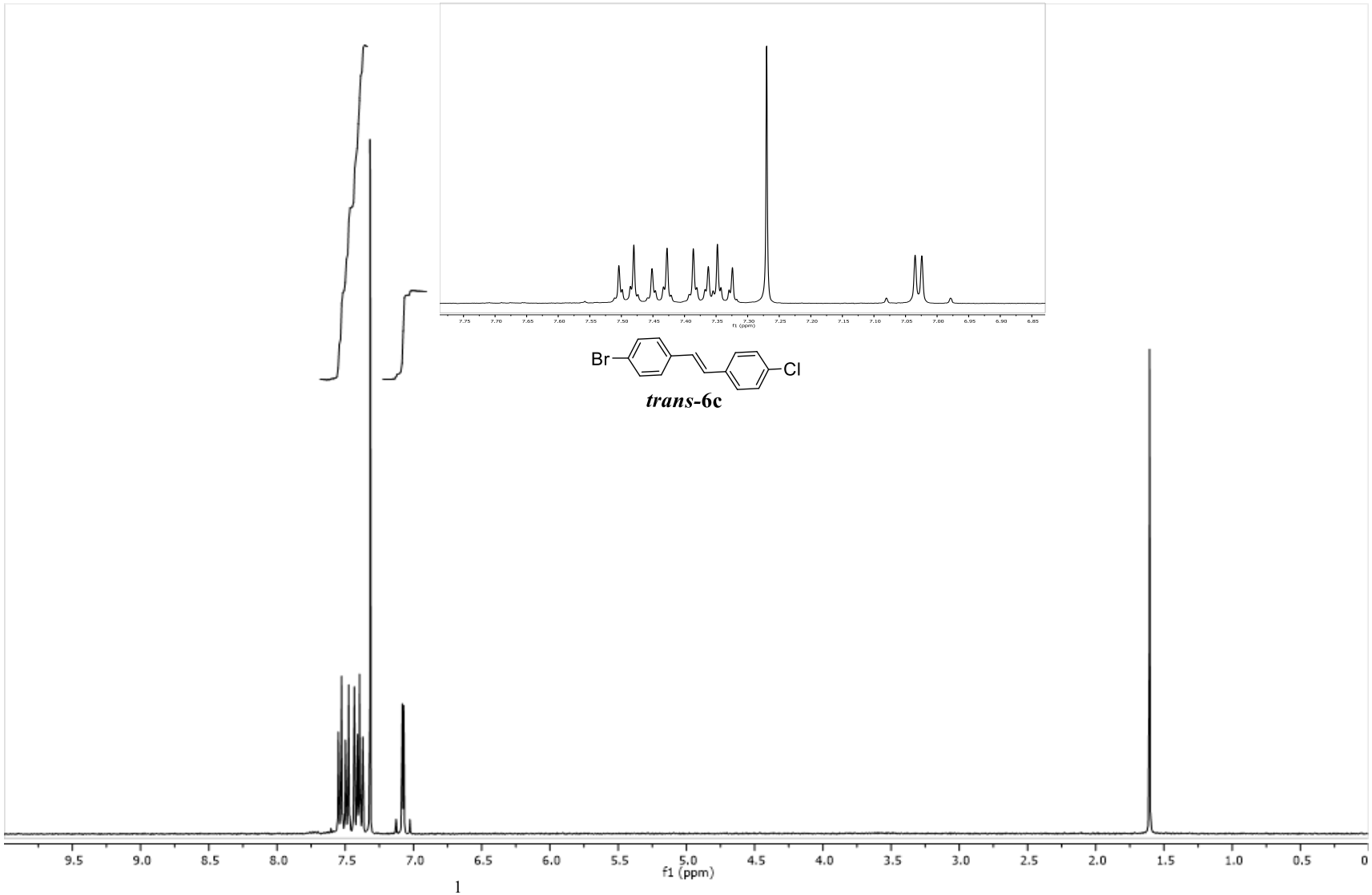

A.9. ^{1}H NMR spectrum (500 MHz) of ***trans*-6c** in $CDCl_3$

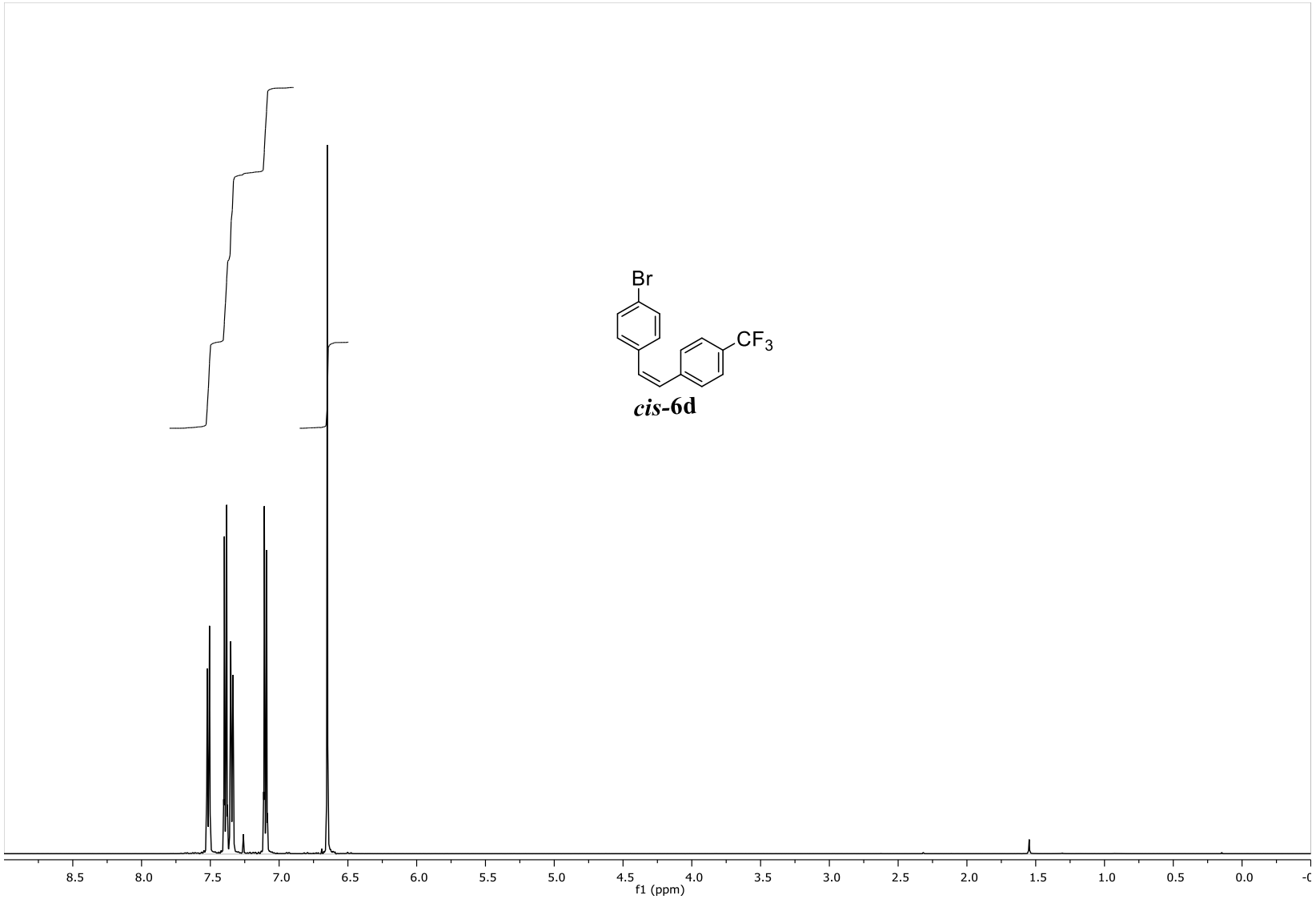

A.10. ^{1}H NMR spectrum (360 MHz) of ***cis*-6d** in $CDCl_3$

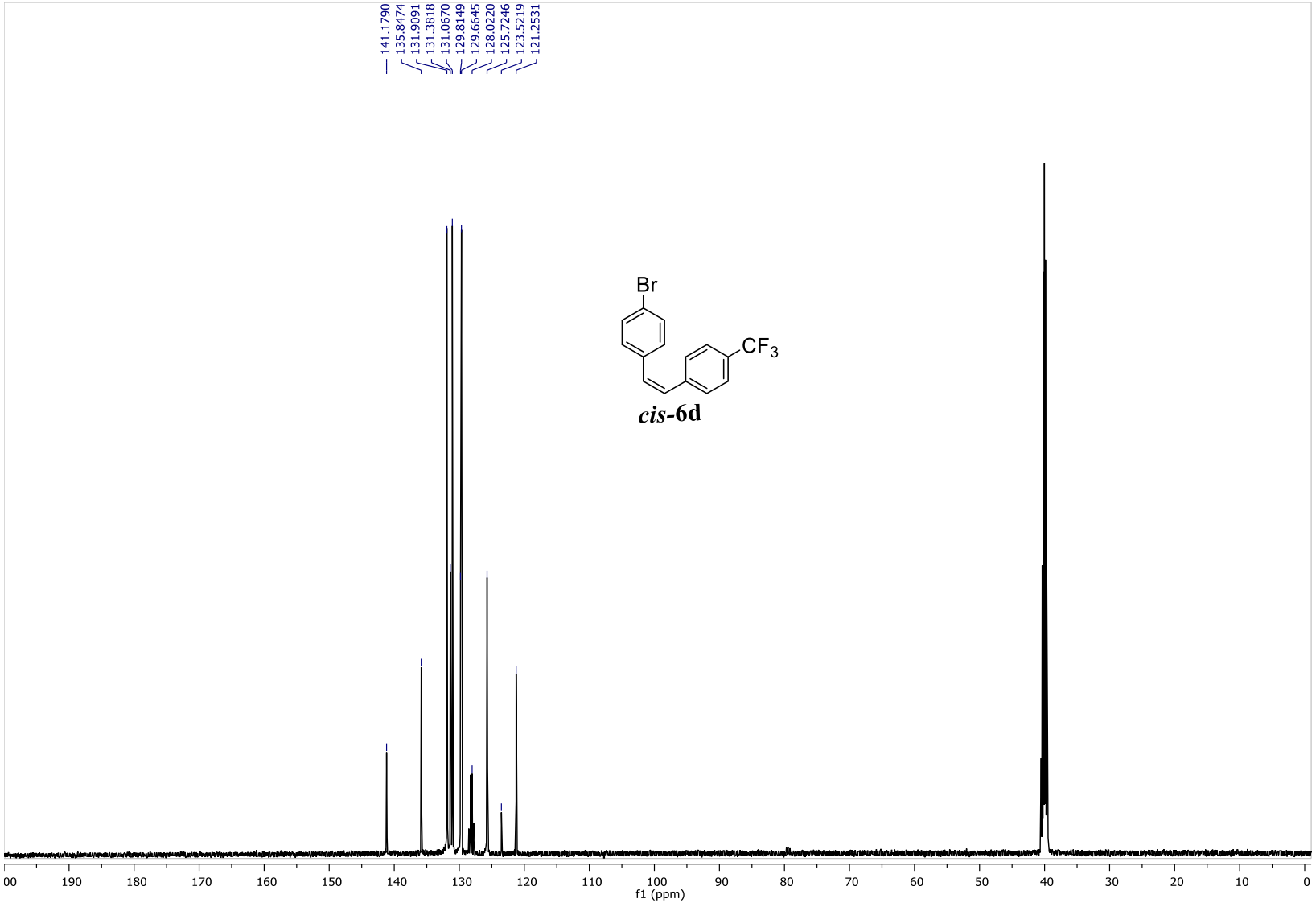

A.11. ^{13}C NMR spectrum (125 MHz) of ***cis*-6d** in DMSO-d_6

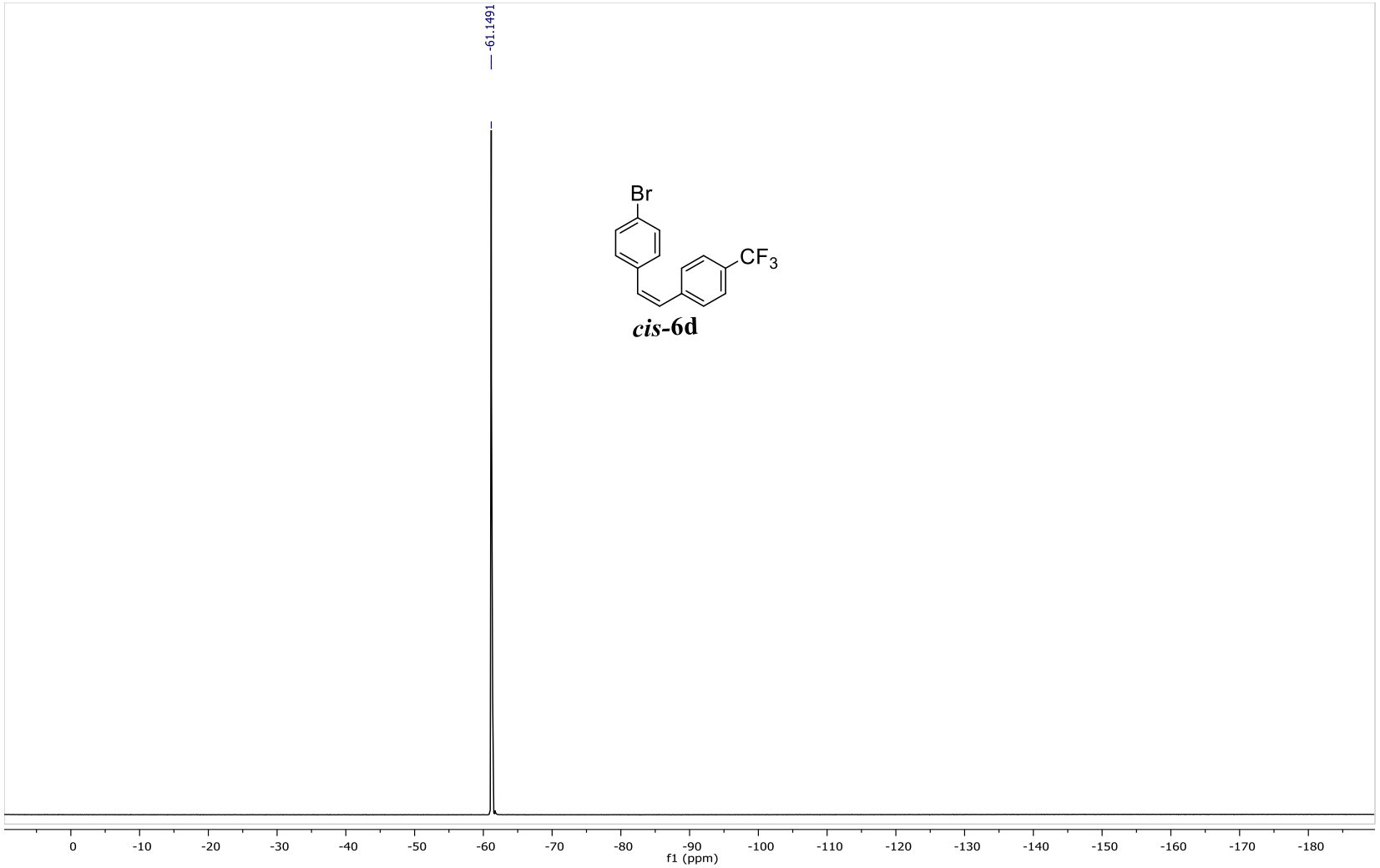

A.12. ^{19}F NMR spectrum (360 MHz) of ***cis*-6d** in DMSO-d_6

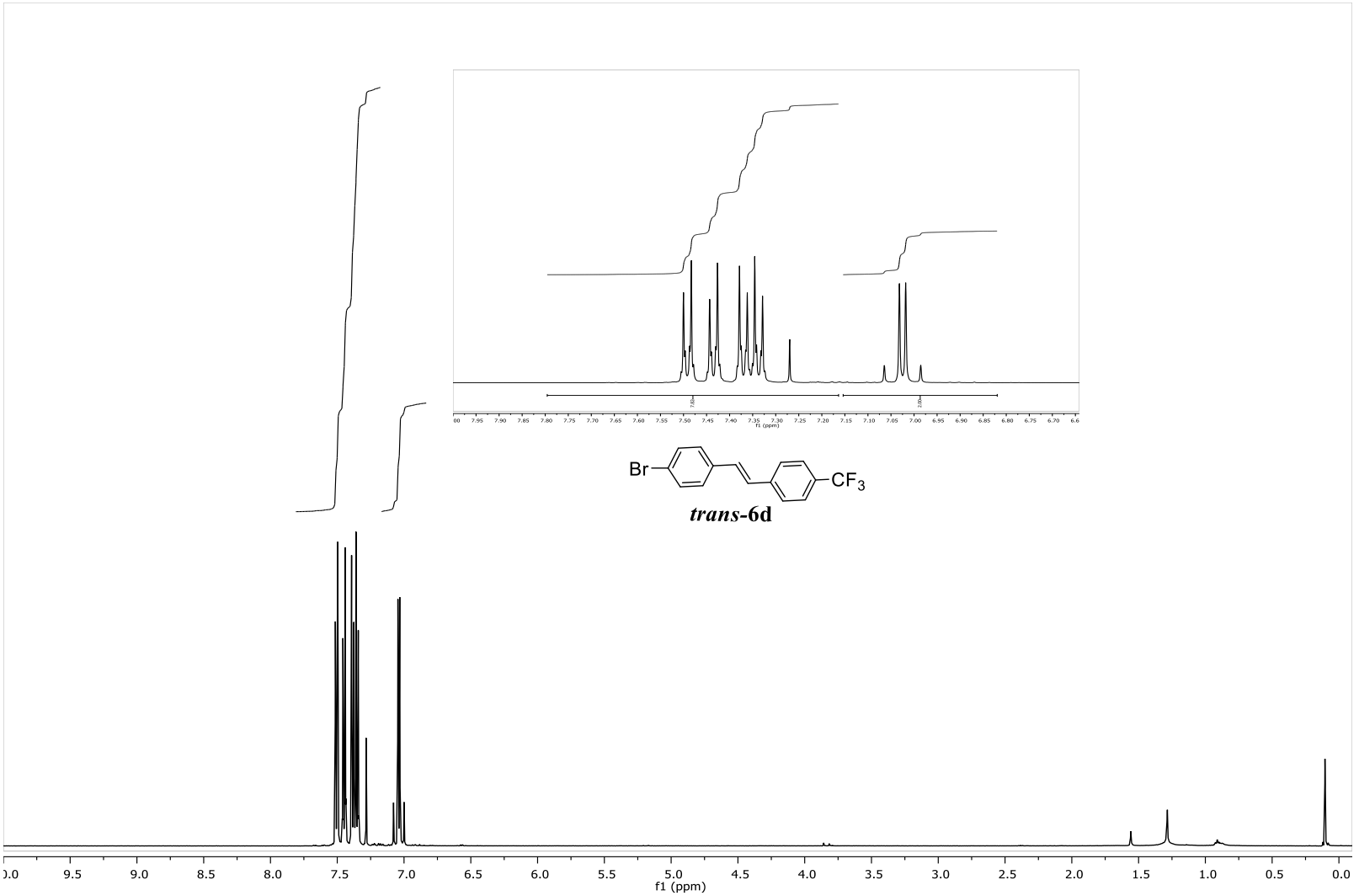

A.13. ^{1}H NMR spectrum (500 MHz) of ***trans*-6d** in $CDCl_3$

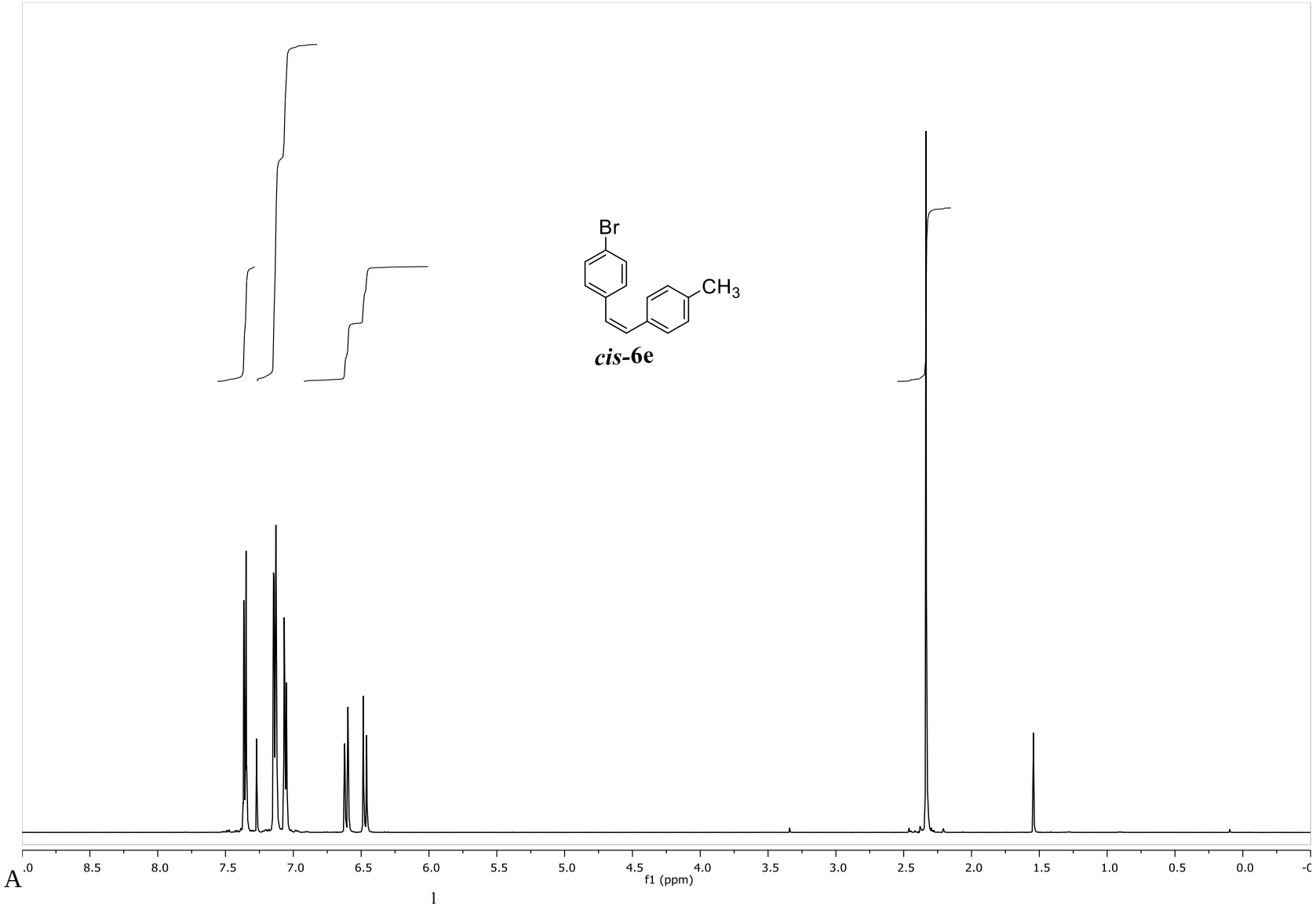

A.14. ^{1}H NMR spectrum (360 MHz) of ***cis*-6e** in $CDCl_3$

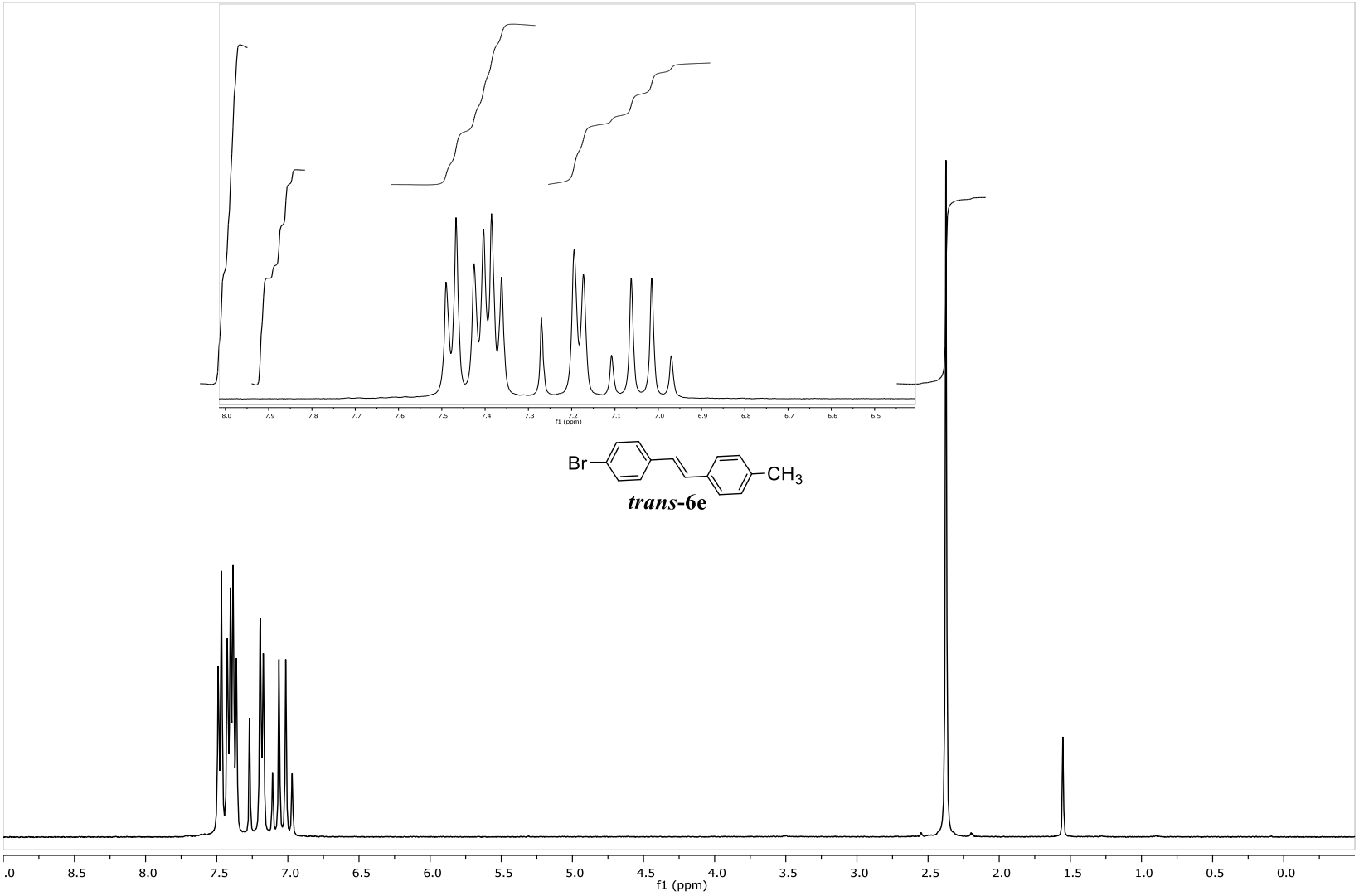

A.15. ^{1}H NMR spectrum (360 MHz) of ***trans*-6e** in $CDCl_3$

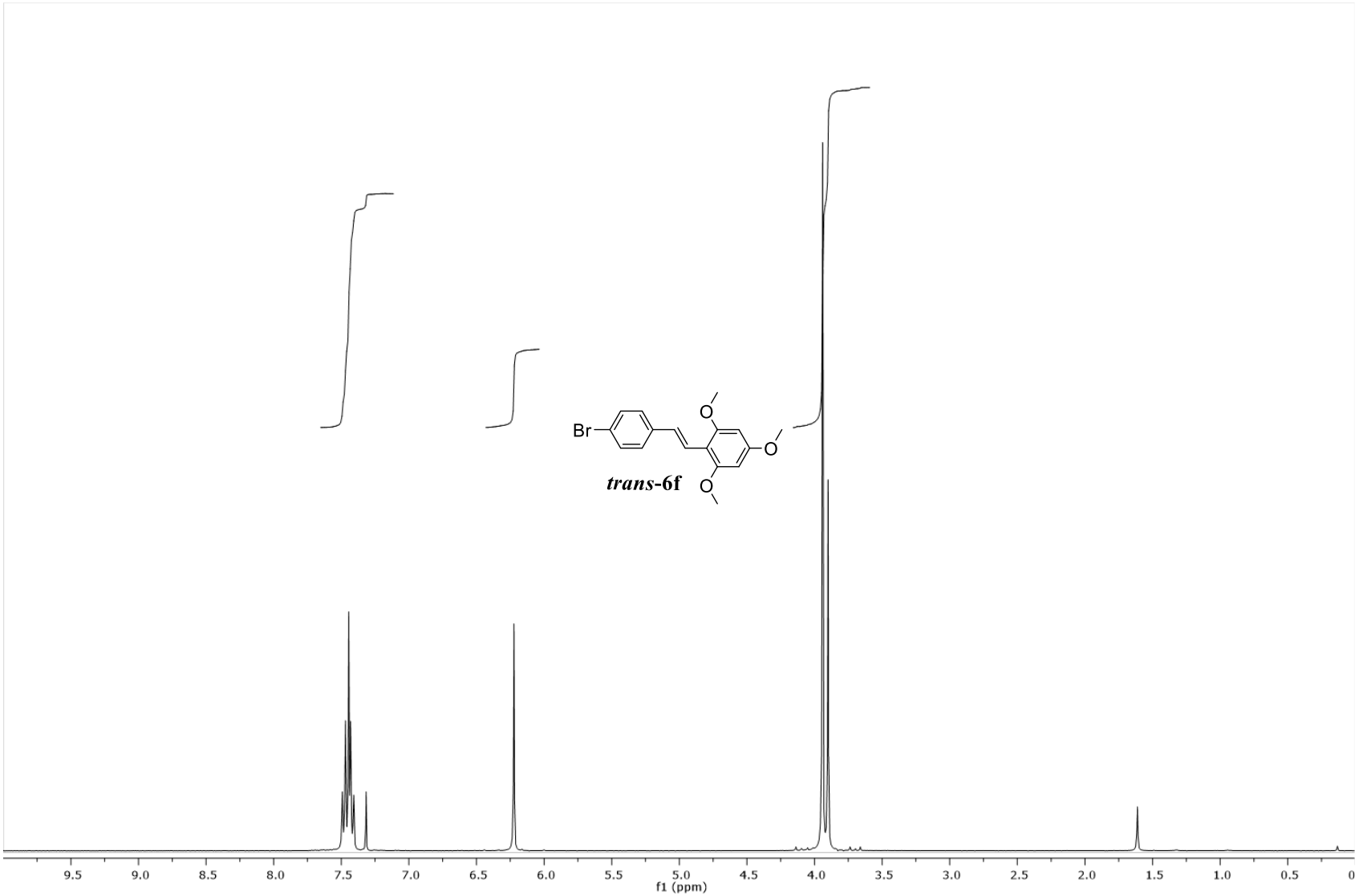

A.16. ^{1}H NMR spectrum (360 MHz) of ***trans*-6f** in $CDCl_3$

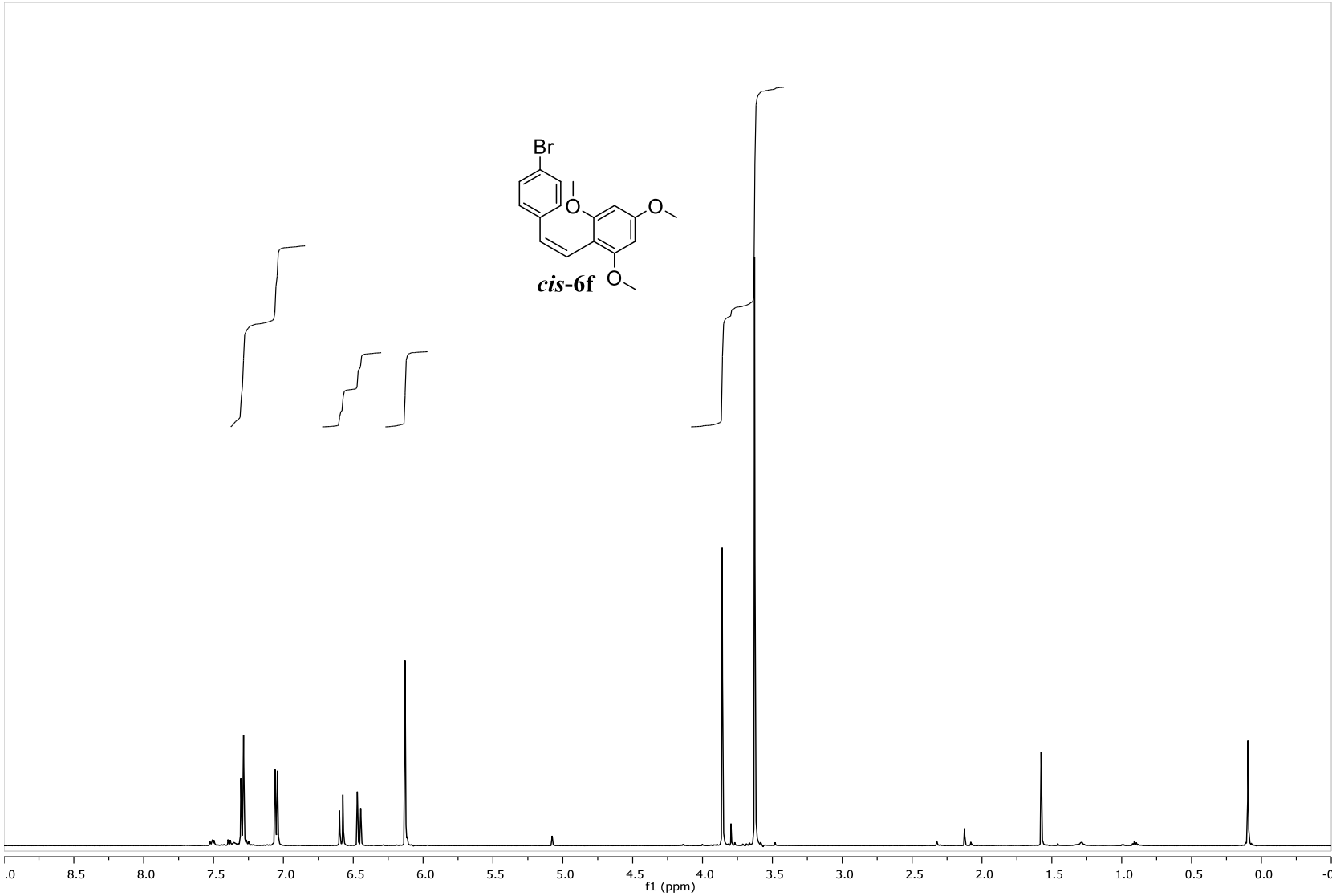

A.17. ^{1}H NMR spectrum (360 MHz) of ***cis*-6f** in $CDCl_3$

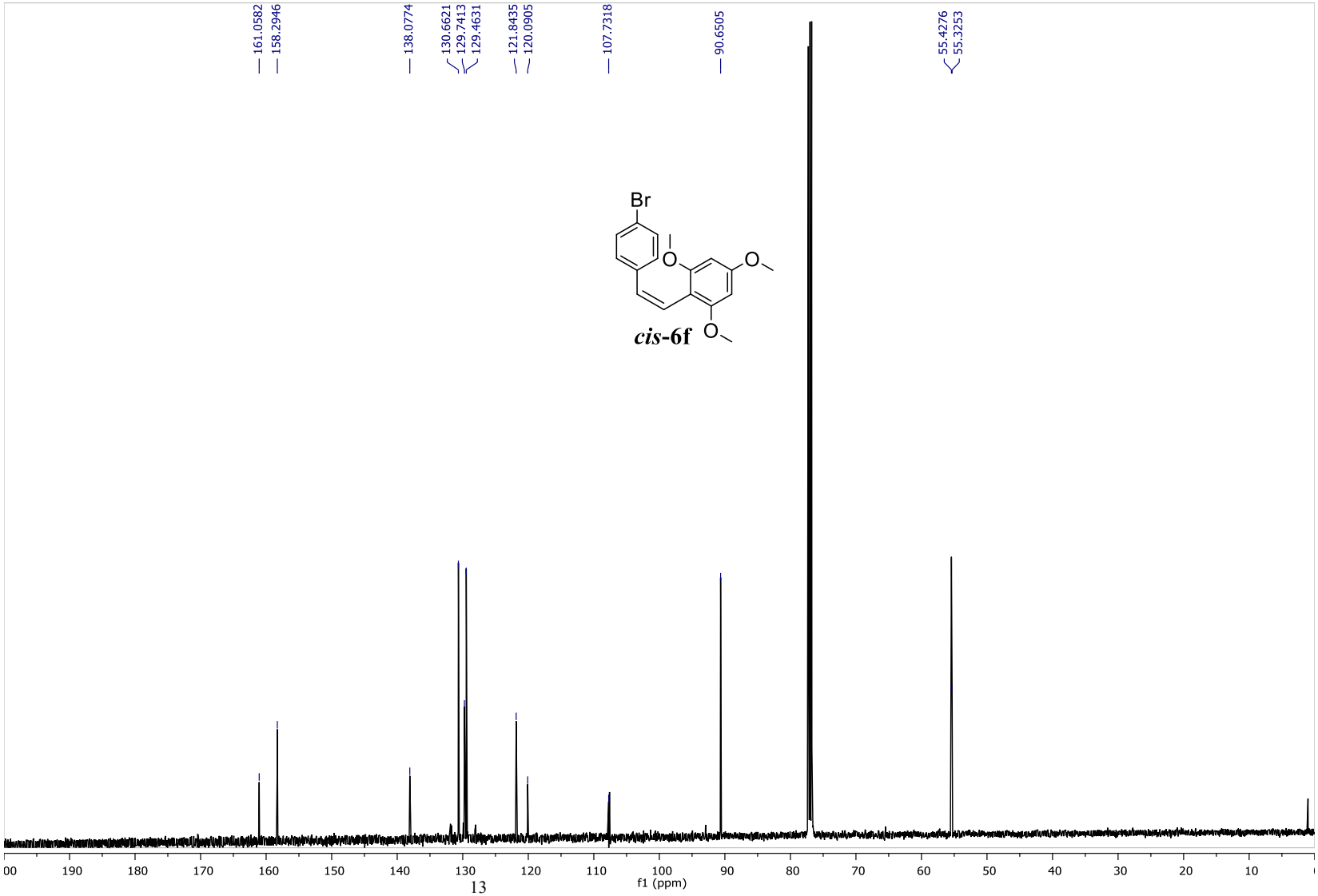

A.18. ^{13}C NMR spectrum (125 MHz) of ***cis*-6f** in $CDCl_3$

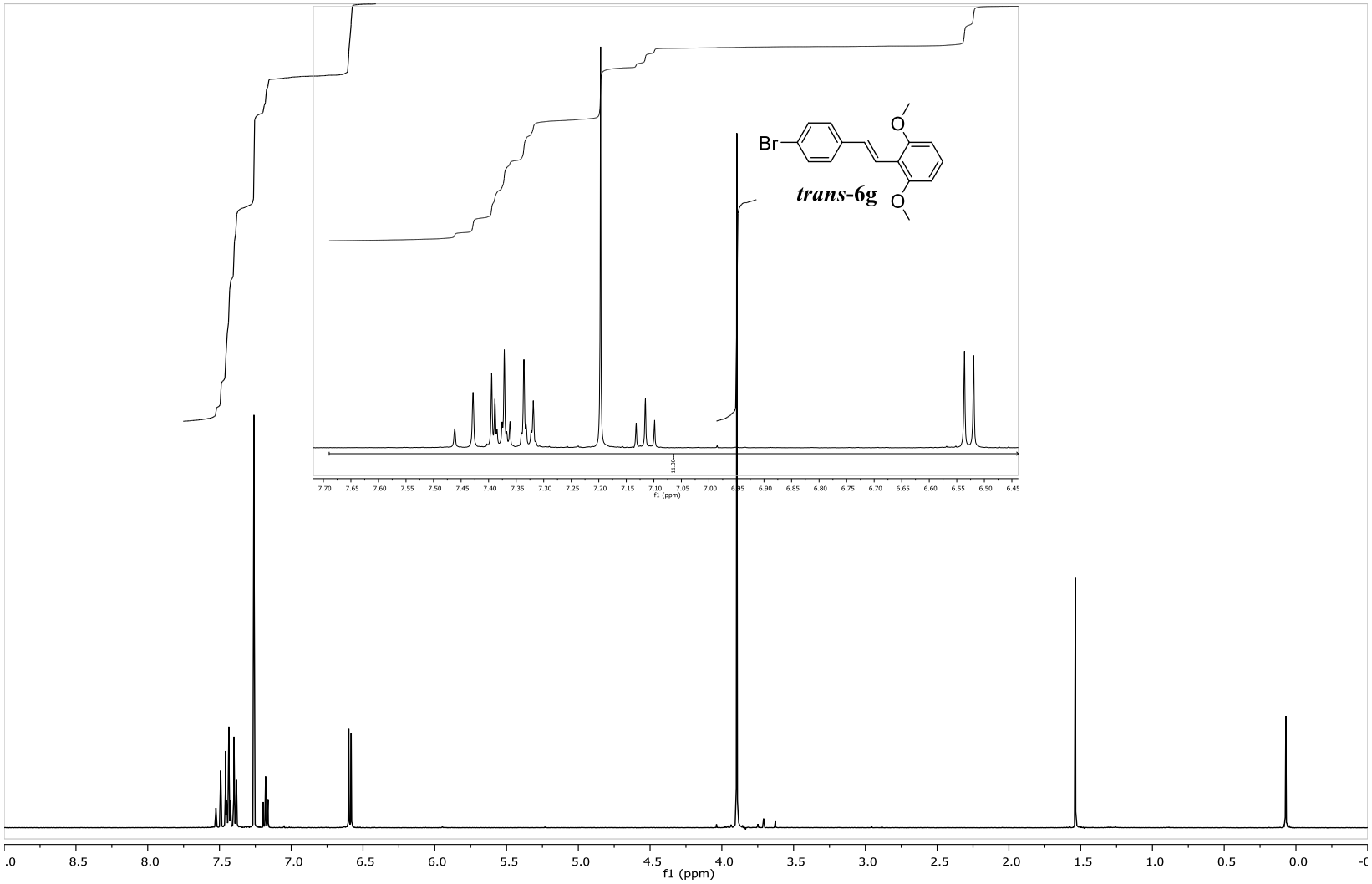

A.19. ^{1}H NMR spectrum (360 MHz) of ***trans*-6g** in $CDCl_3$

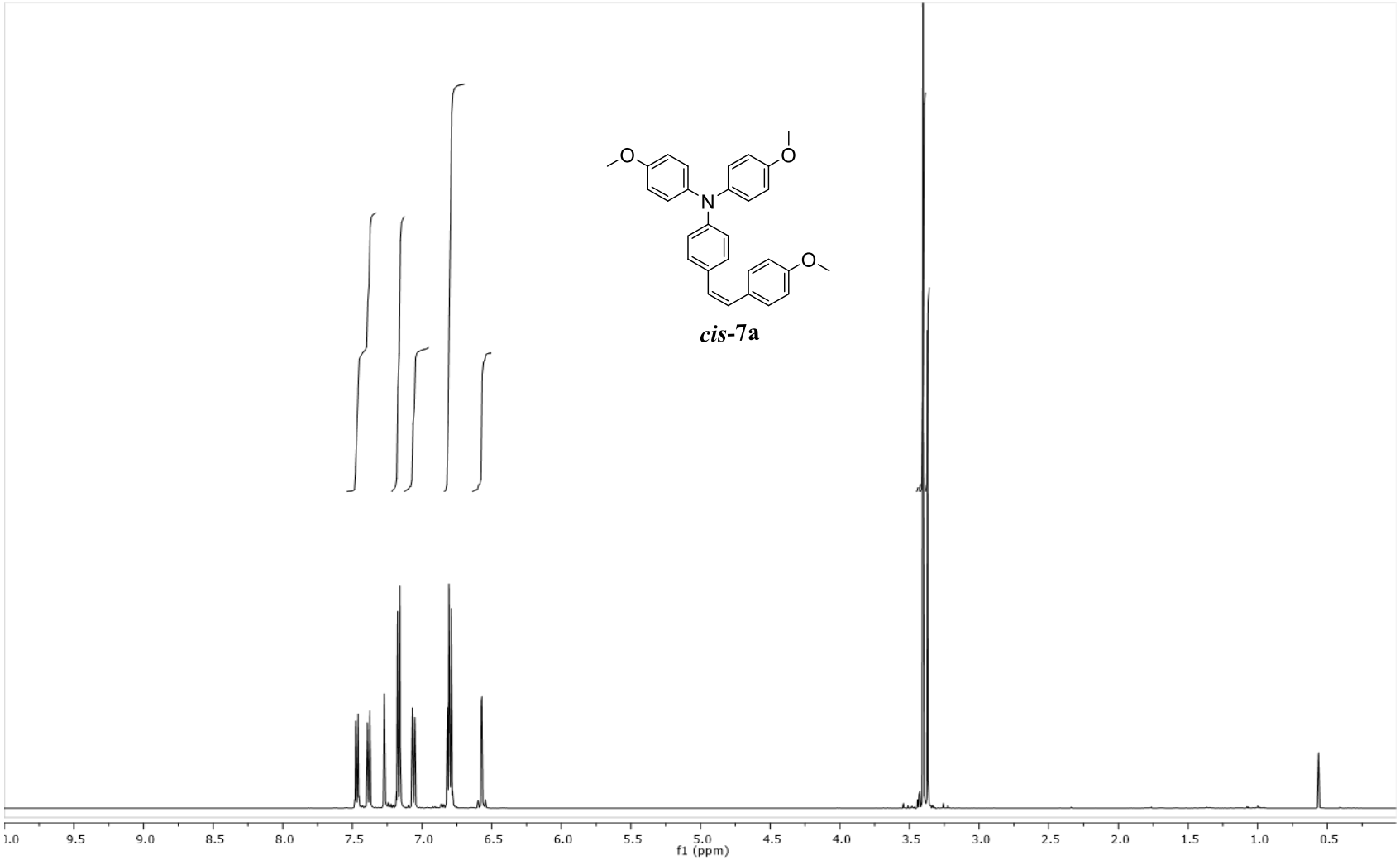

A.20. ^{1}H NMR spectrum (500 MHz) of ***cis*-7a** in C_6D_6

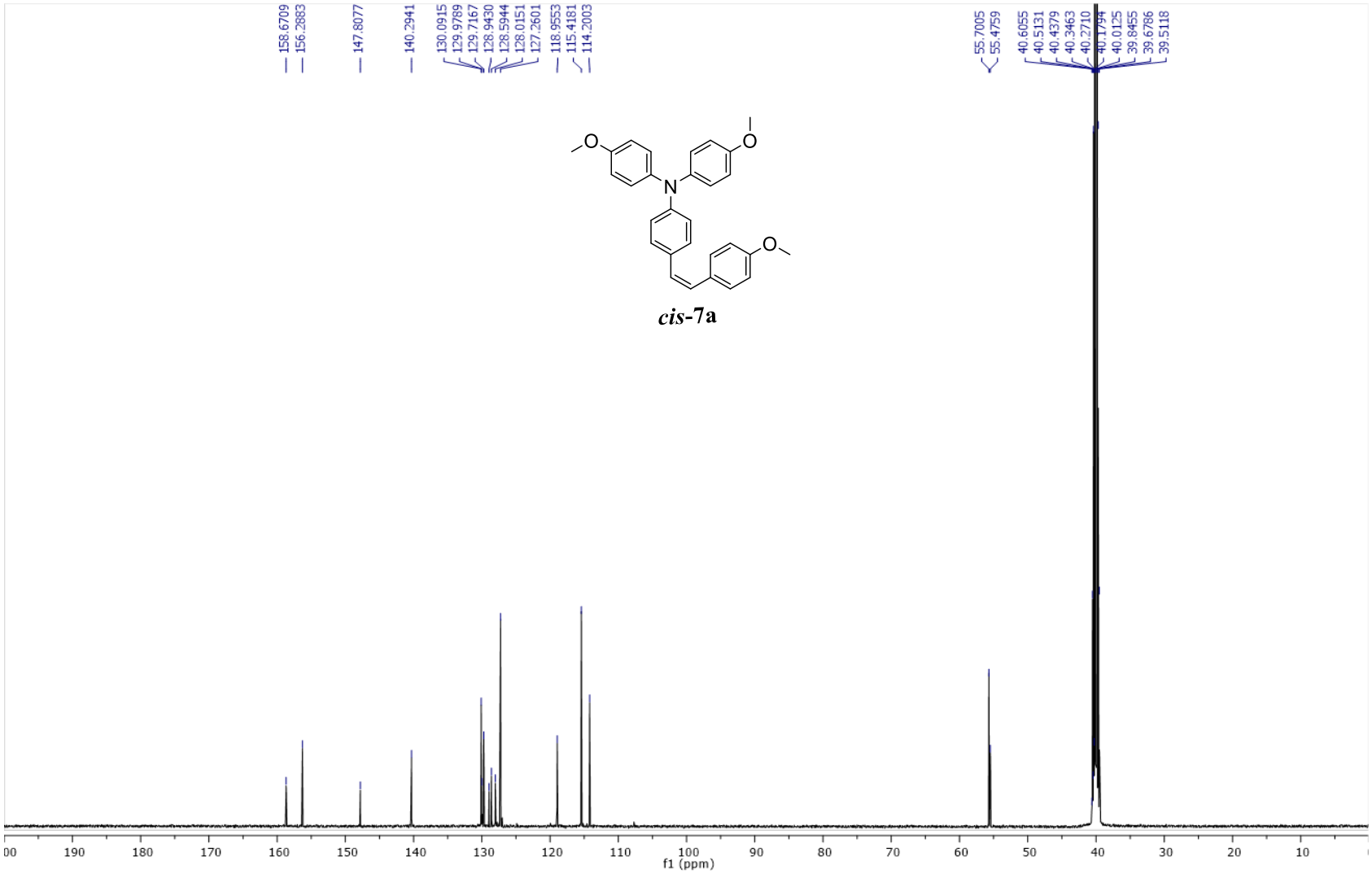

A.21. ^{13}C NMR spectrum (125 MHz) of ***cis*-7a in** DMSO-d_6

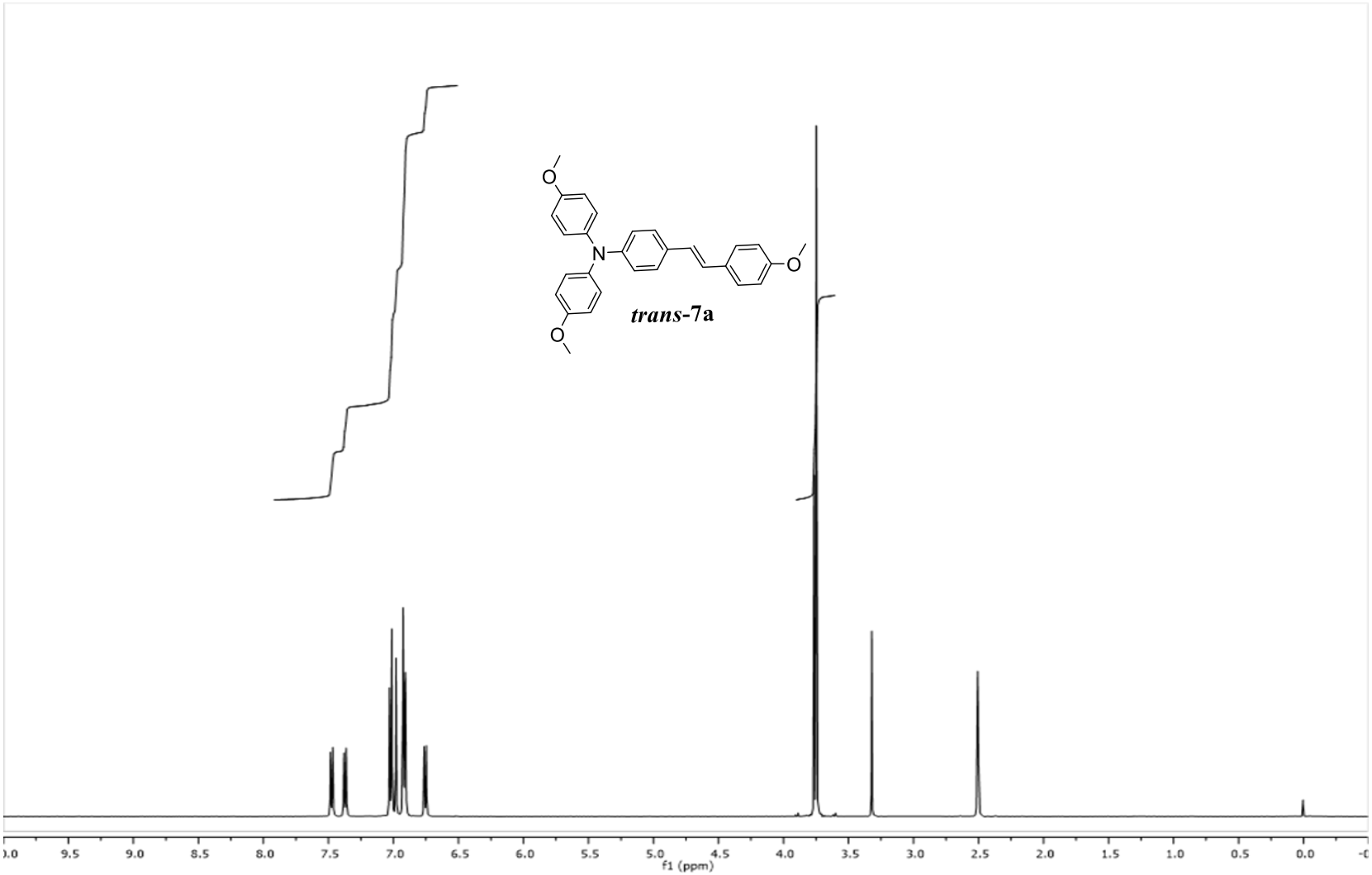

A.22. ^{1}H NMR spectrum (500 MHz) of ***trans*-7a** in DMSO-d_6

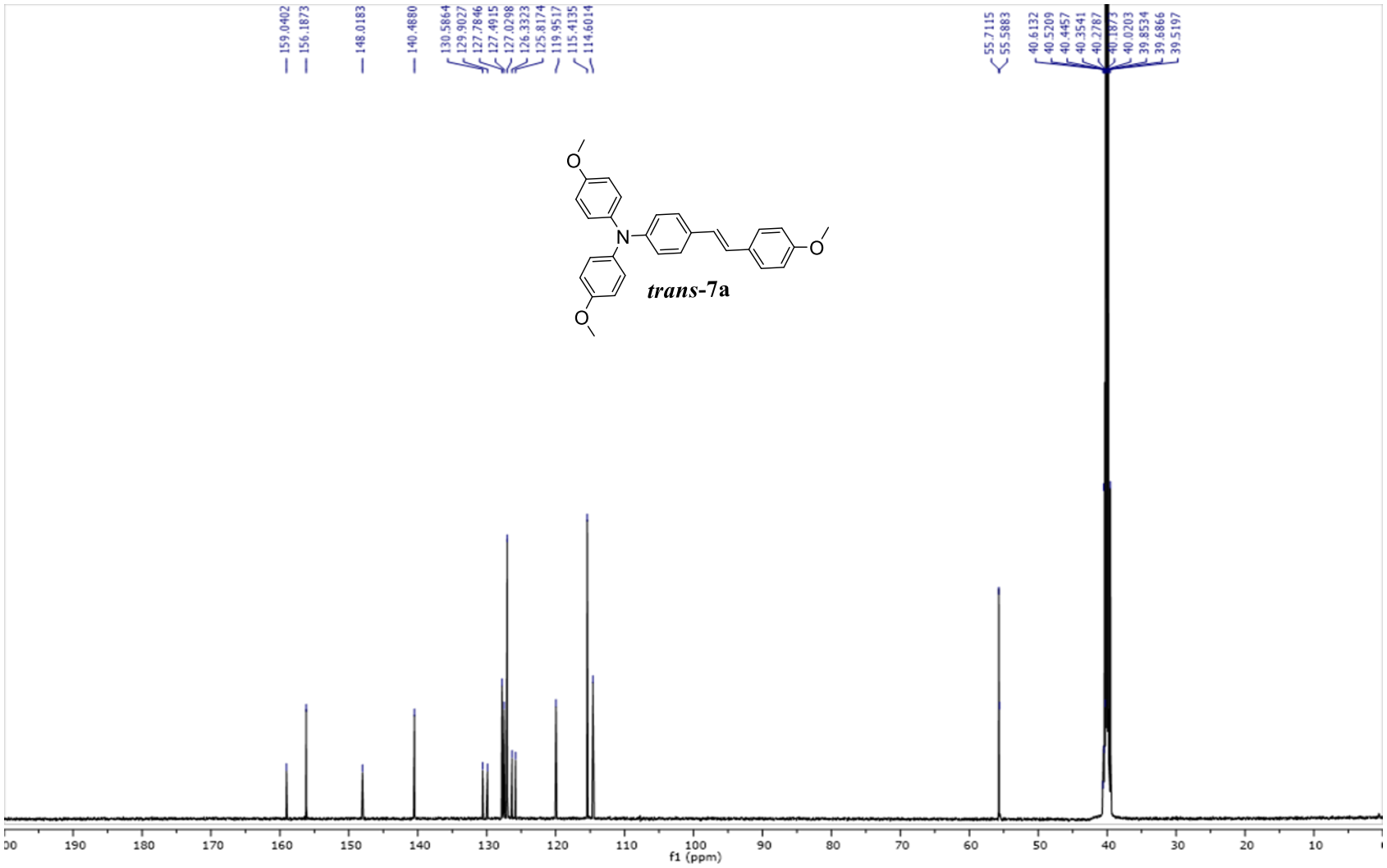

A.23. ^{13}C NMR spectrum (125 MHz) of ***trans*-7a** in DMSO-d_6

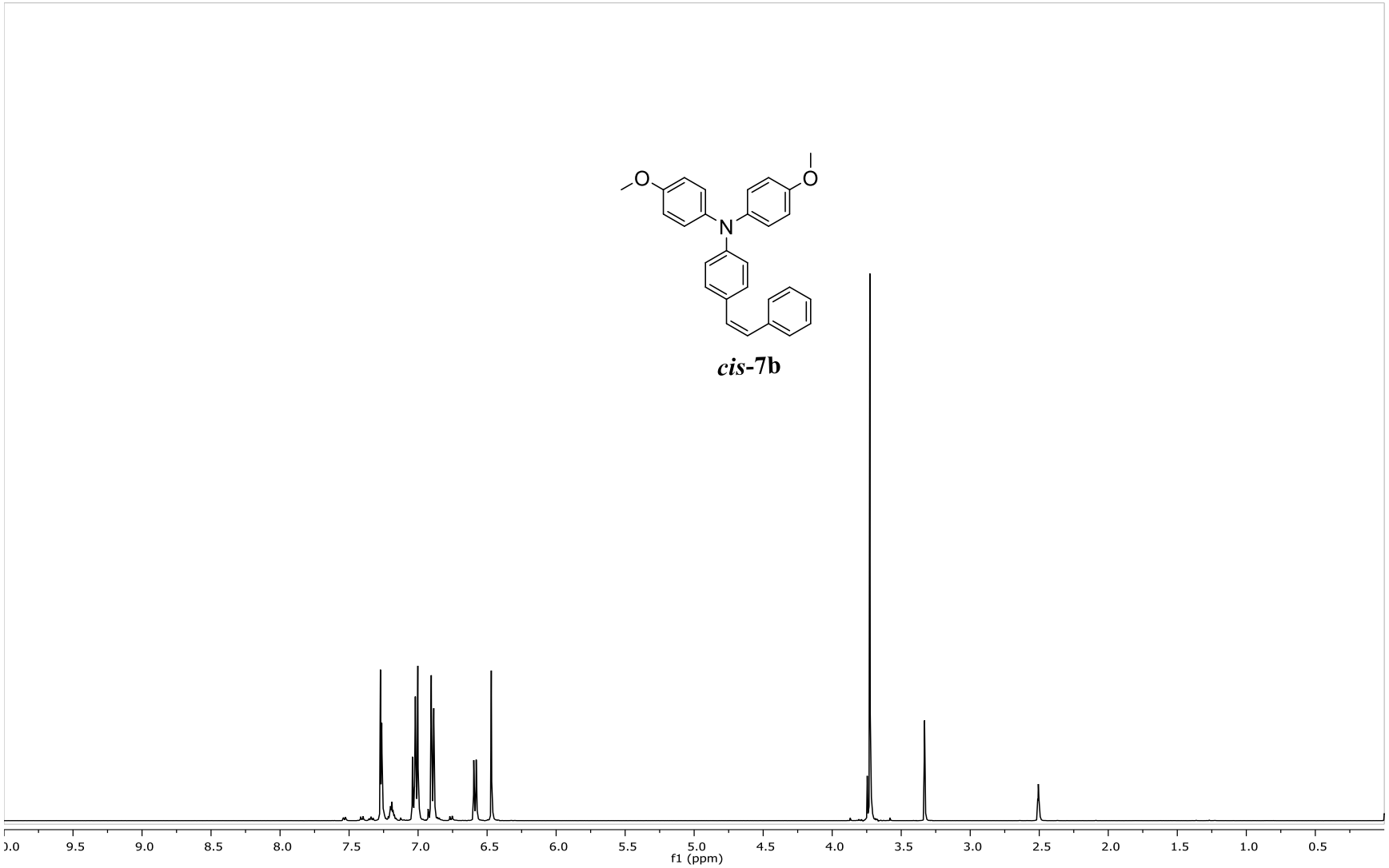

A.24. ^{1}H NMR spectrum (500 MHz) of ***cis*-7b** in DMSO-d_6

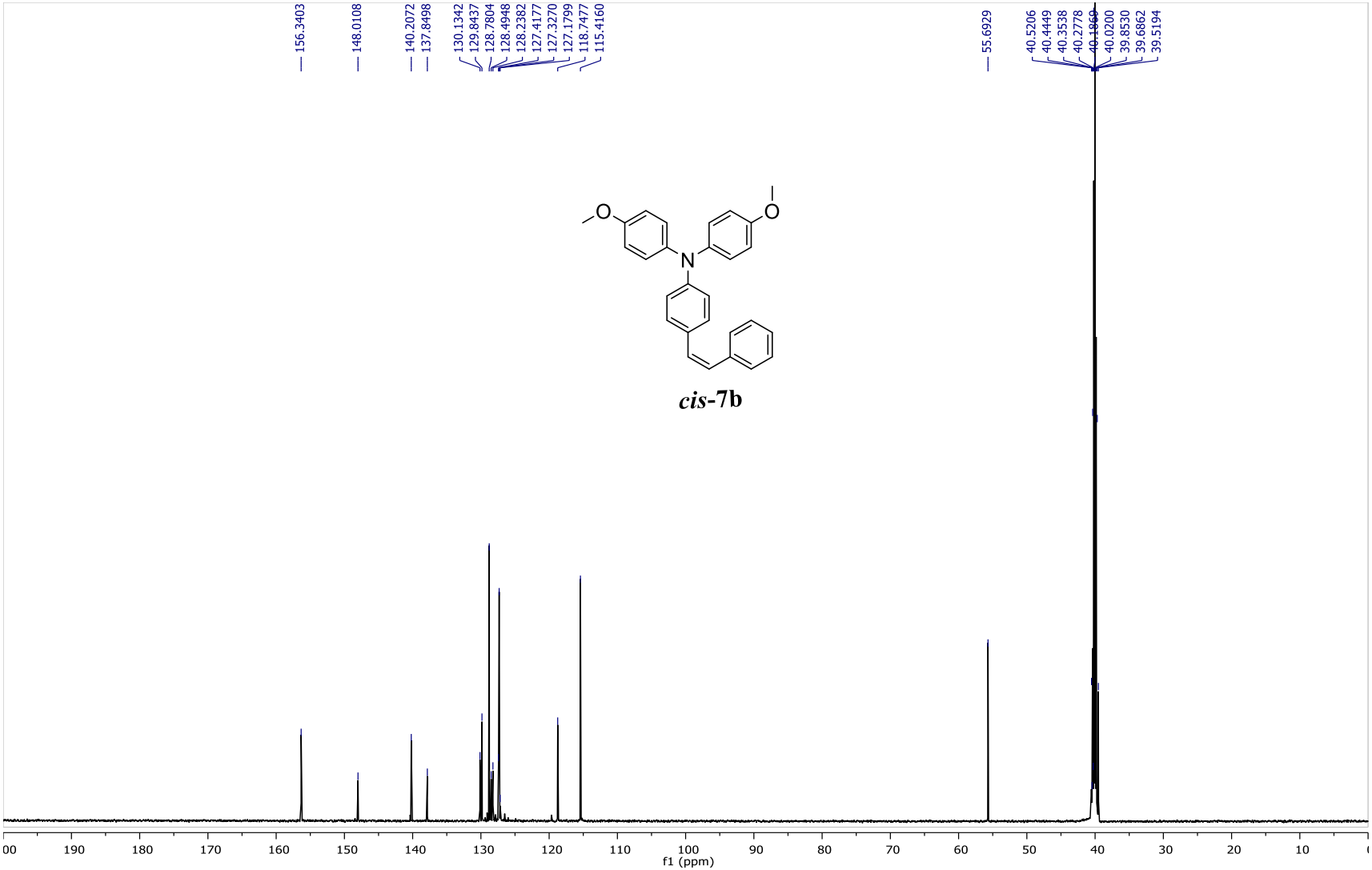

A.25. ^{13}C NMR spectrum (125 MHz) of ***cis*-7b** in DMSO-d_6

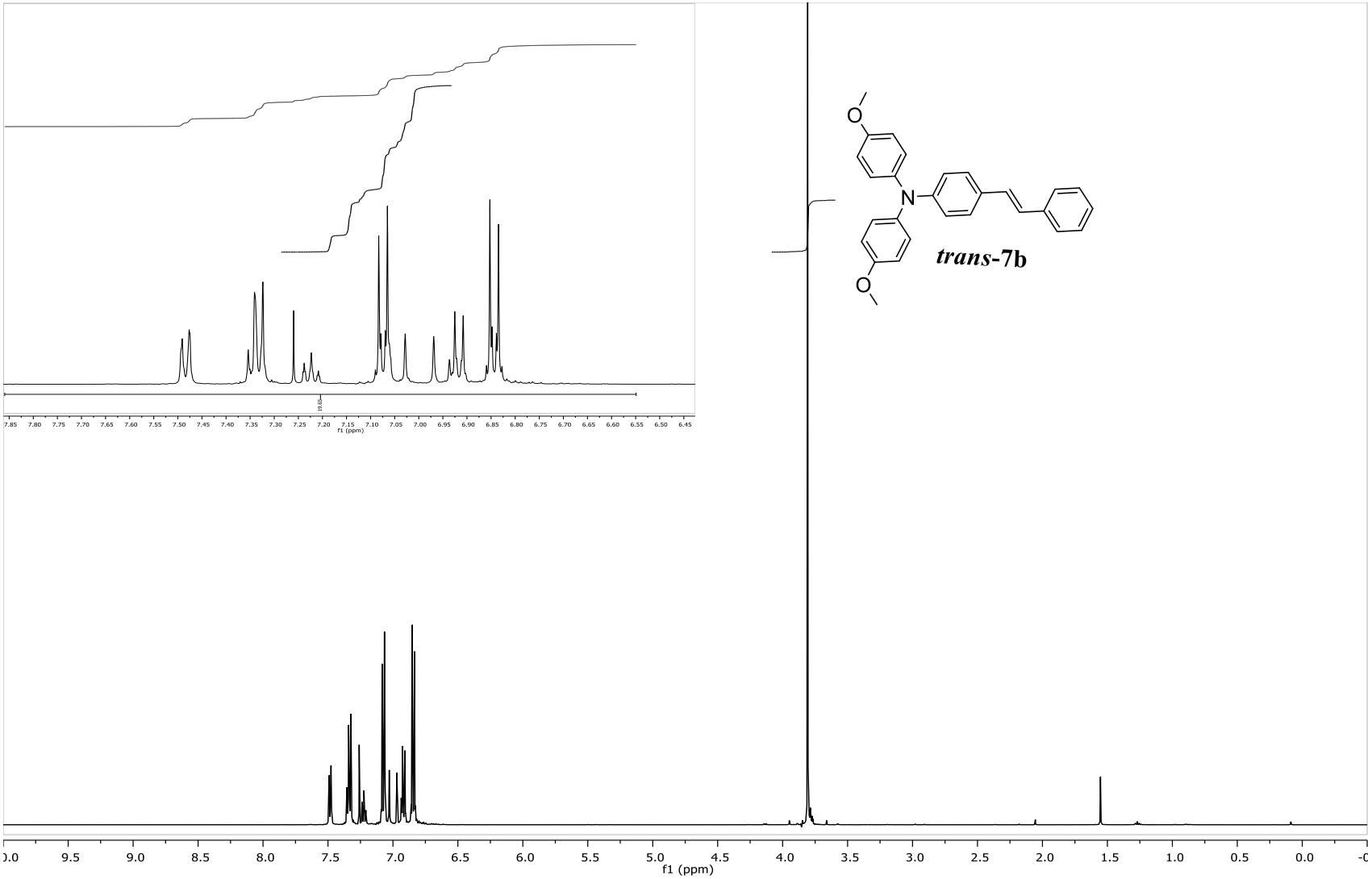

A.26. ^{1}H NMR spectrum (360 MHz) of ***trans*-7b** in $CDCl_3$

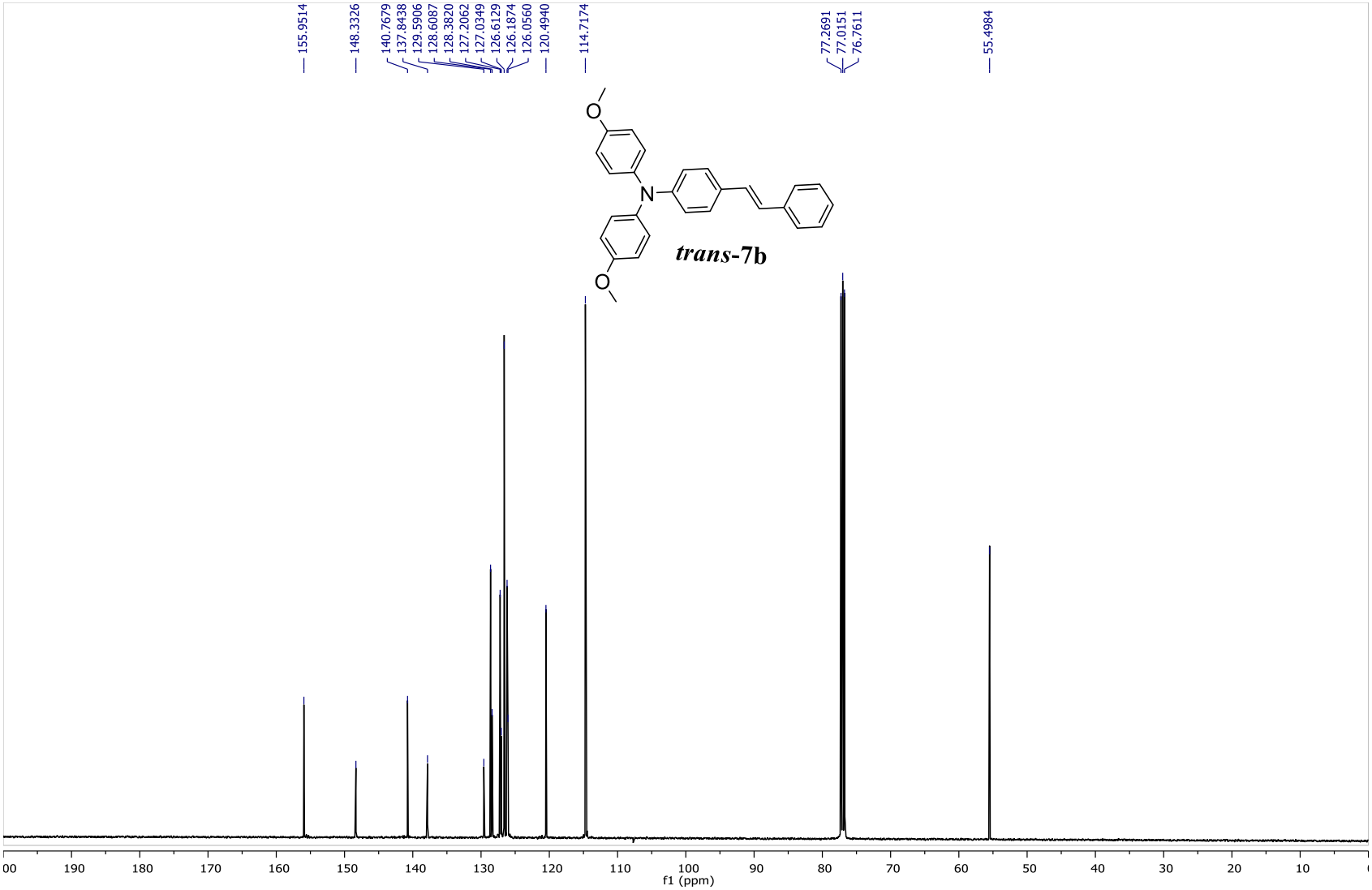

A.27. ^{13}C NMR spectrum (125 MHz) of ***trans*-7b** in $CDCl_3$

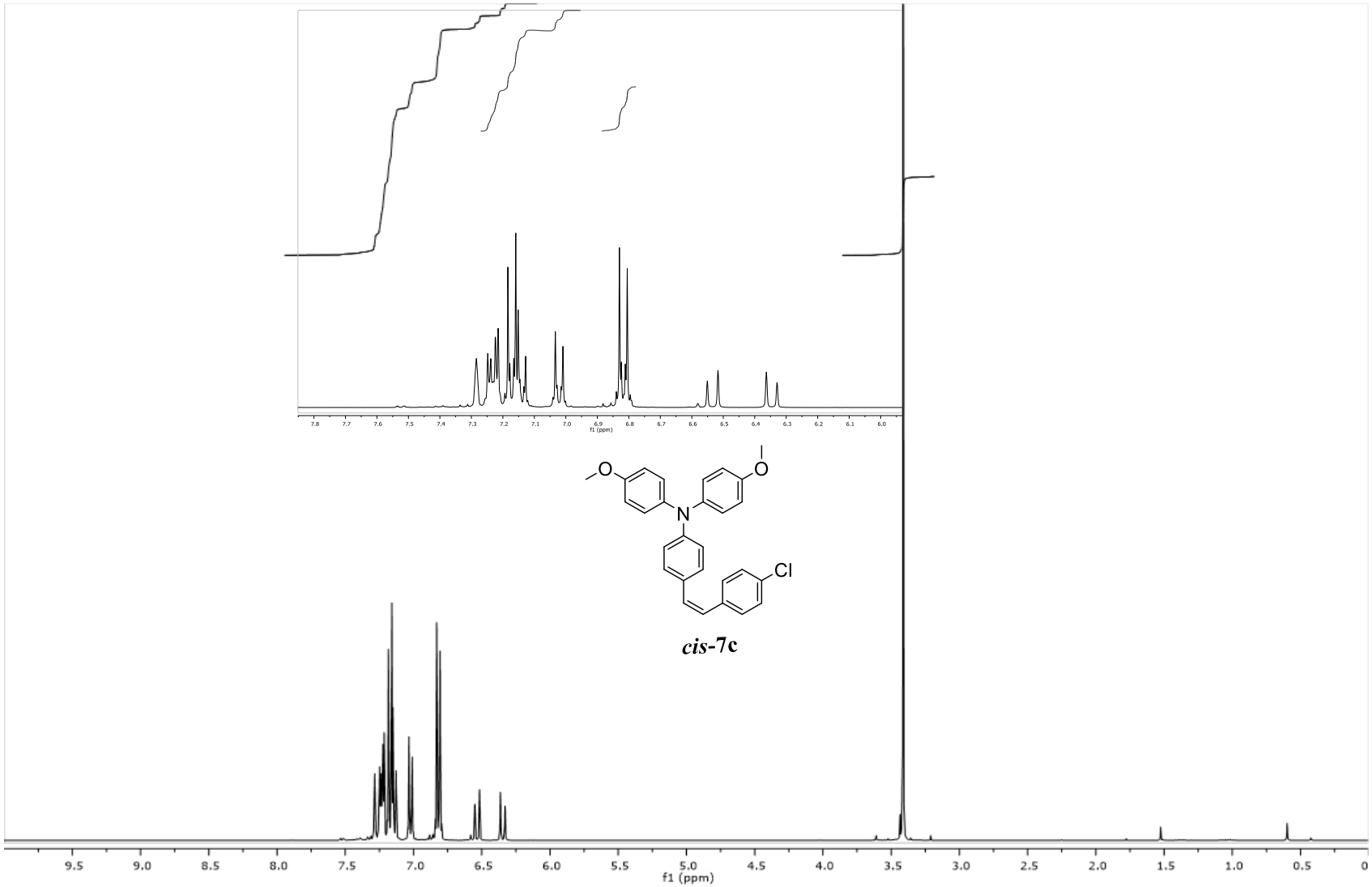

A.28. ^{1}H NMR spectrum (500 MHz) of ***cis*-7c** in C_6D_6

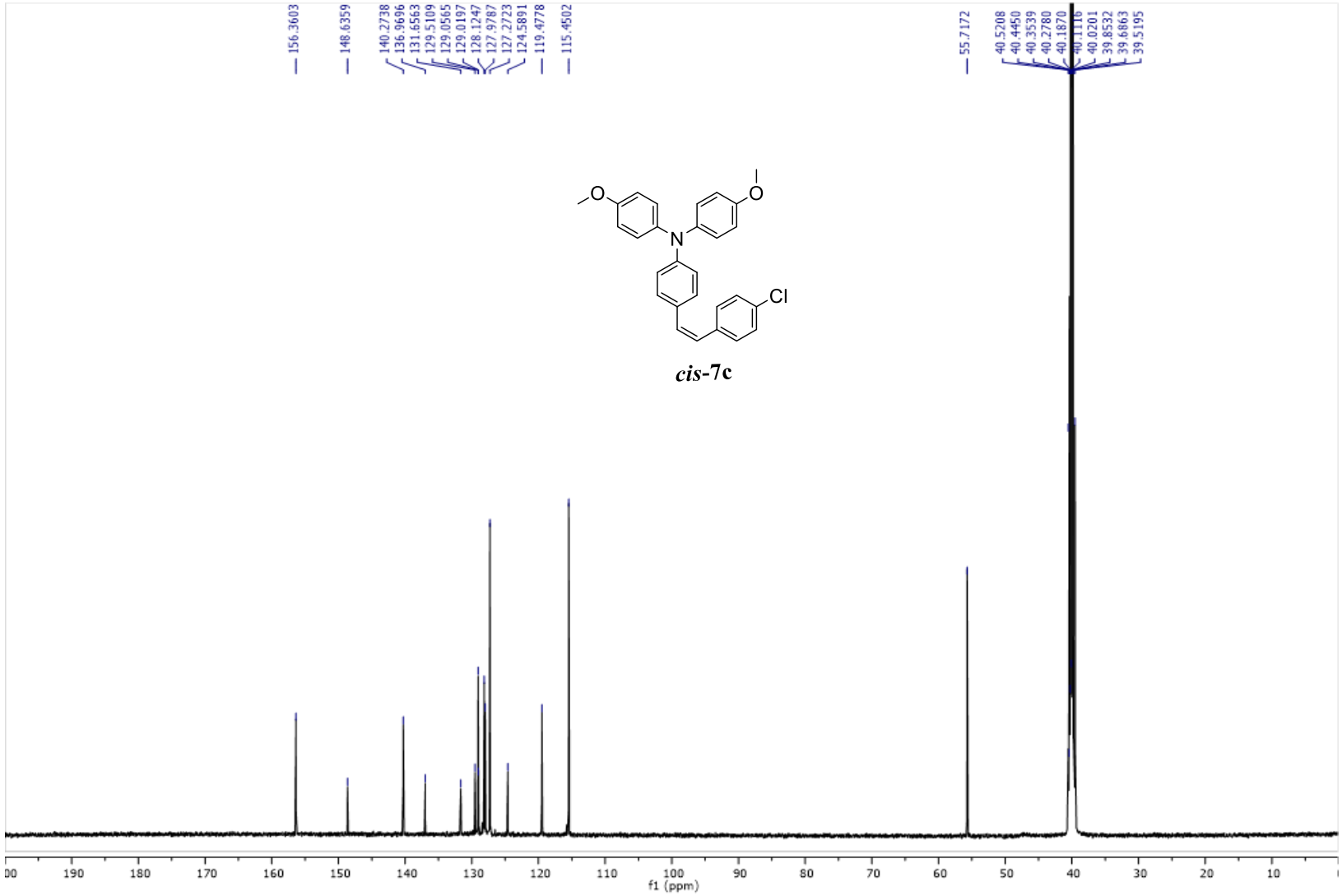

***cis*-7c**

A.29. ^{13}C NMR spectrum (125 MHz) of ***cis*-7c** in DMSO-d_6

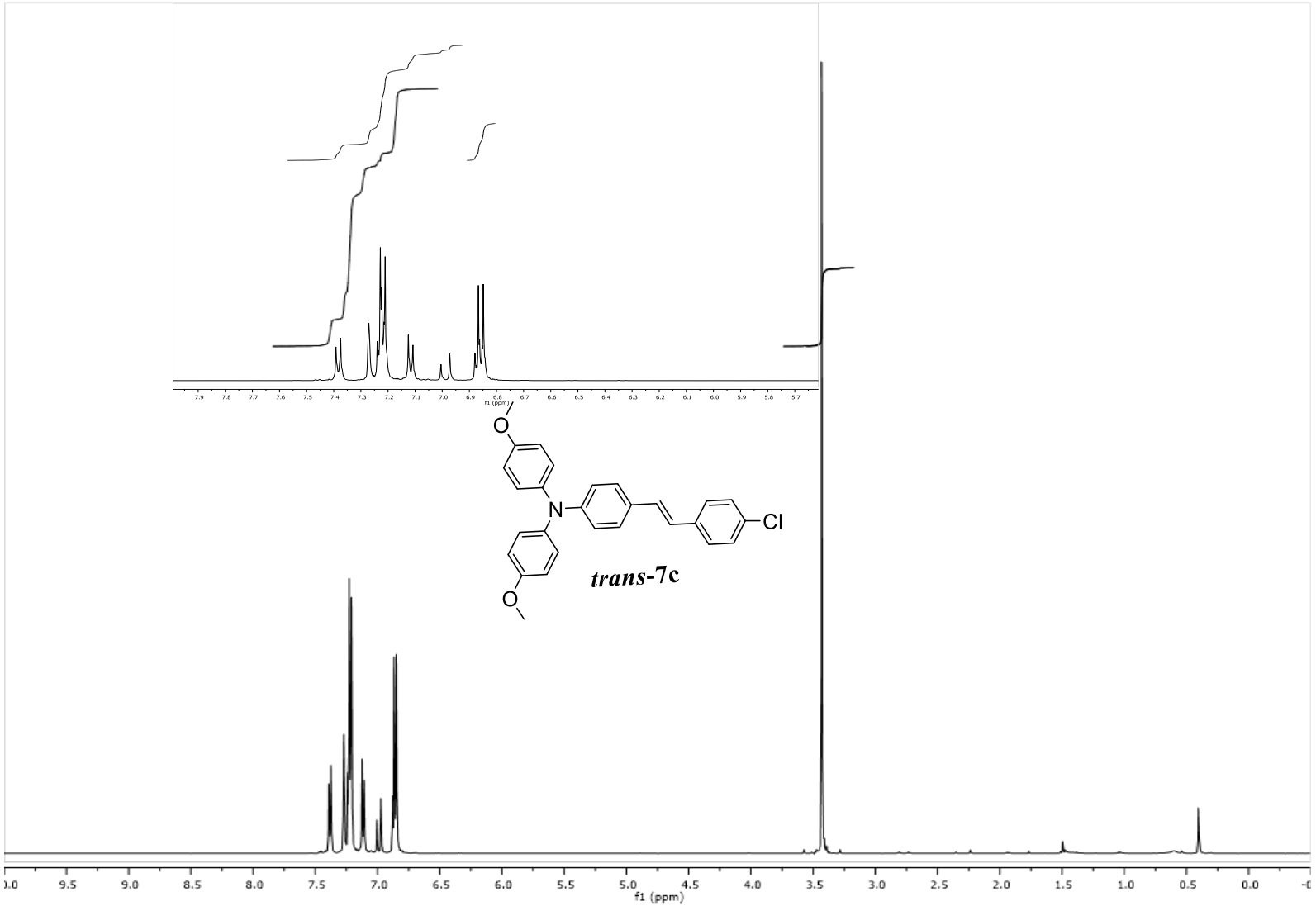

A.30. ^{1}H NMR spectrum (500 MHz) of ***trans*-7c** in C_6D_6

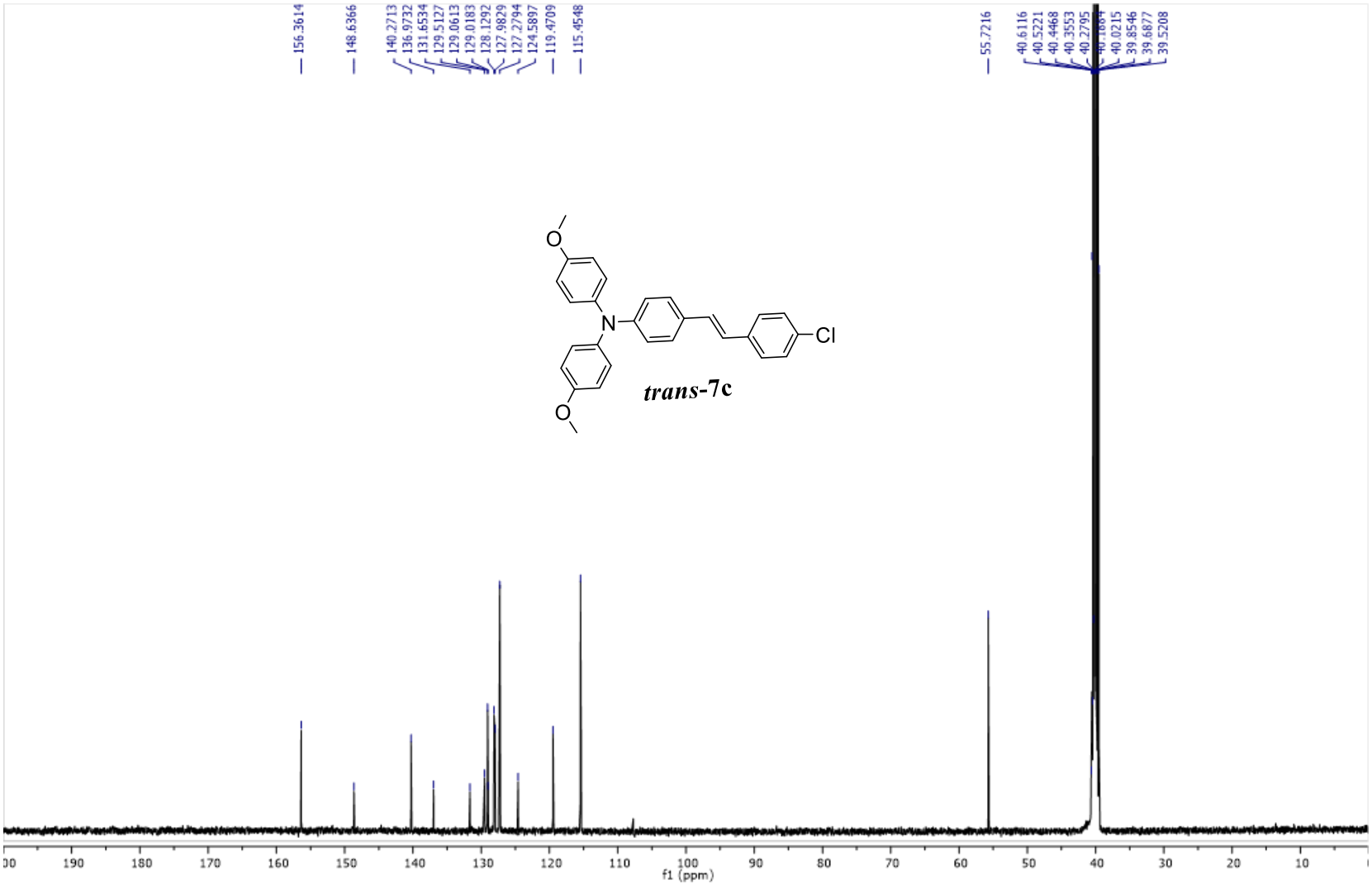

A.31. ^{13}C NMR spectrum (125 MHz) of ***trans*-7c** in DMSO-d_6

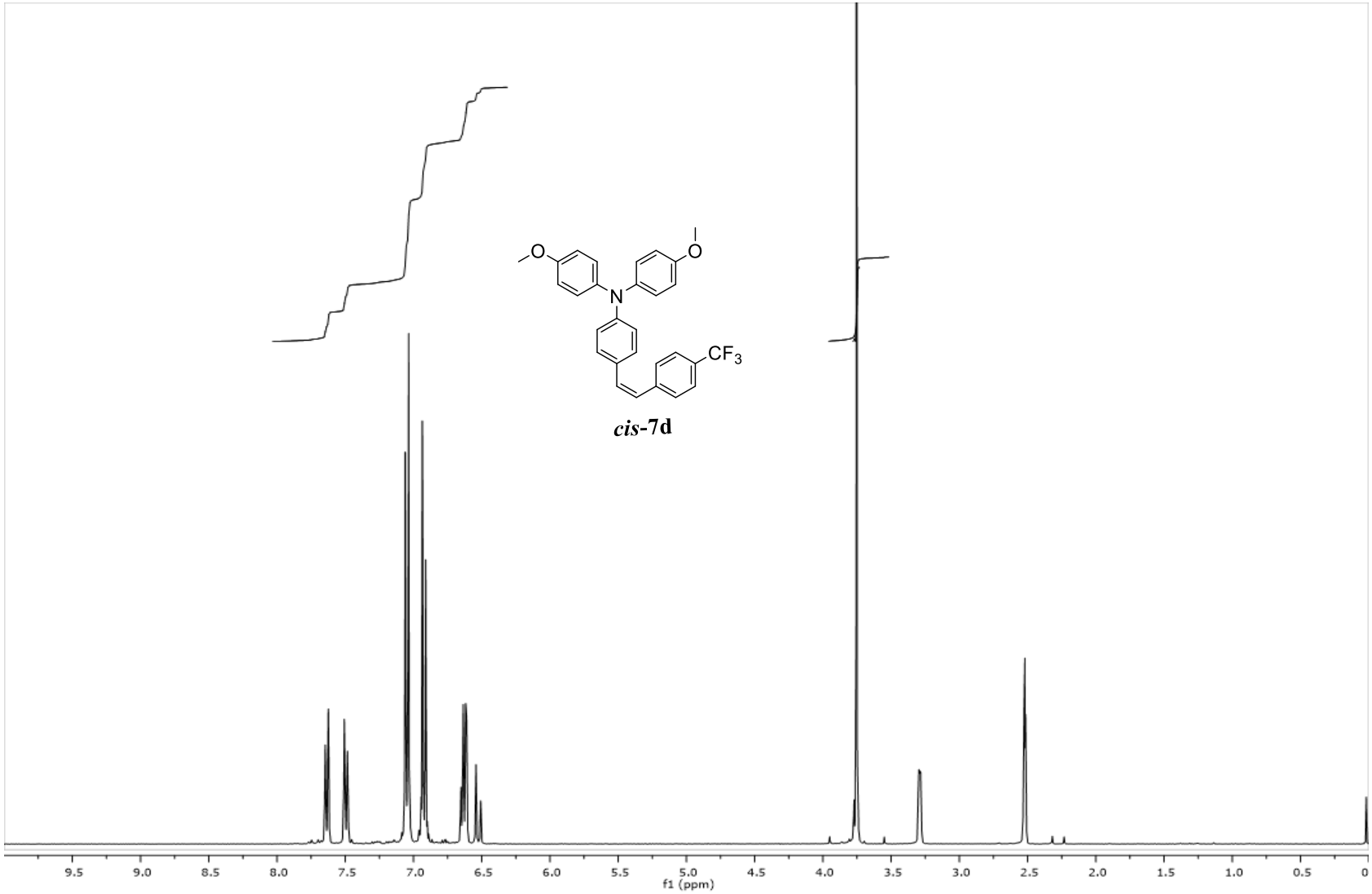

A.32. ^{1}H NMR spectrum (360 MHz) of ***cis*-7d** in DMSO-d_6

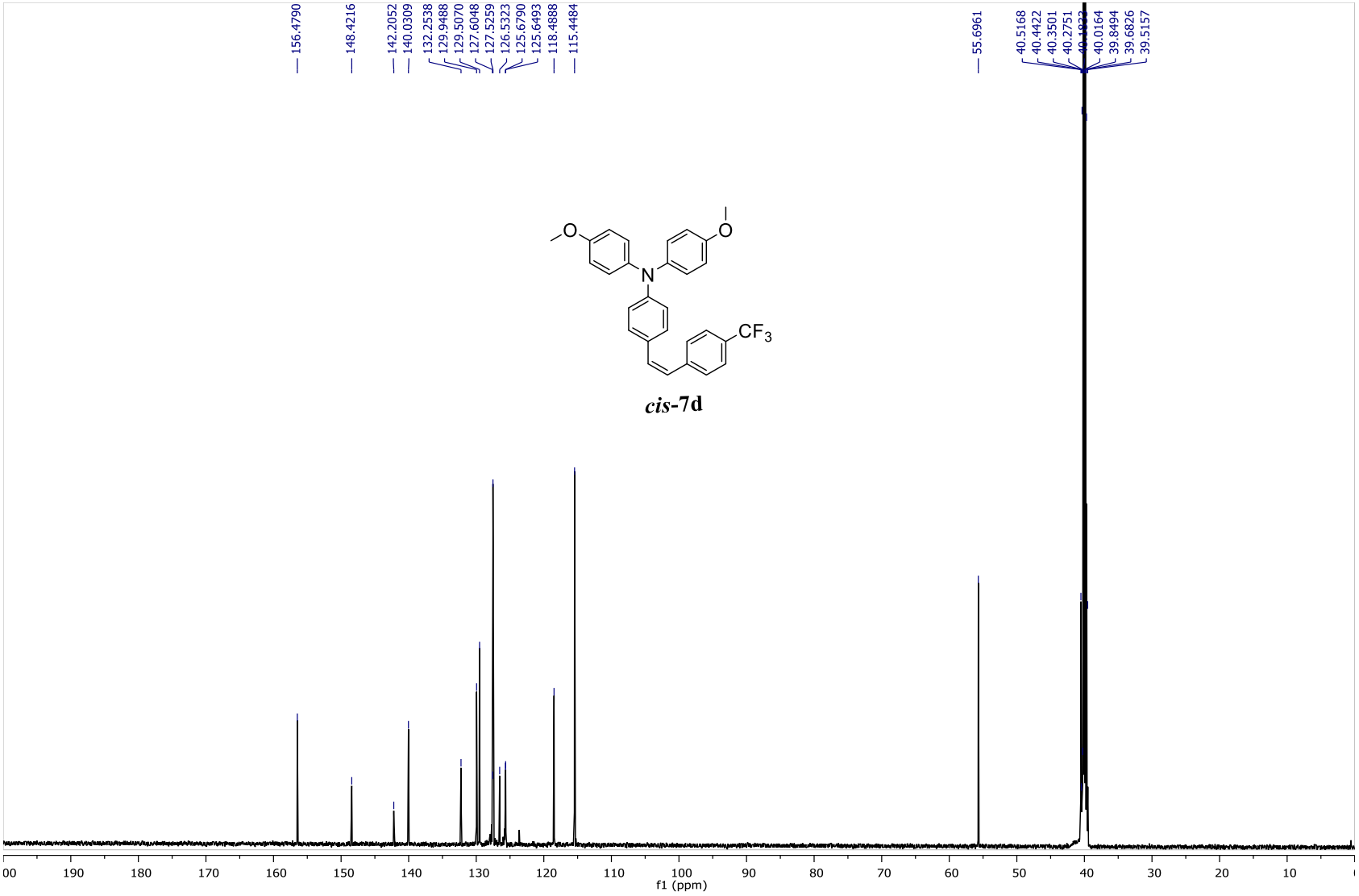

A.33. ^{13}C NMR spectrum (125 MHz) of ***cis*-7d** in DMSO-d_6

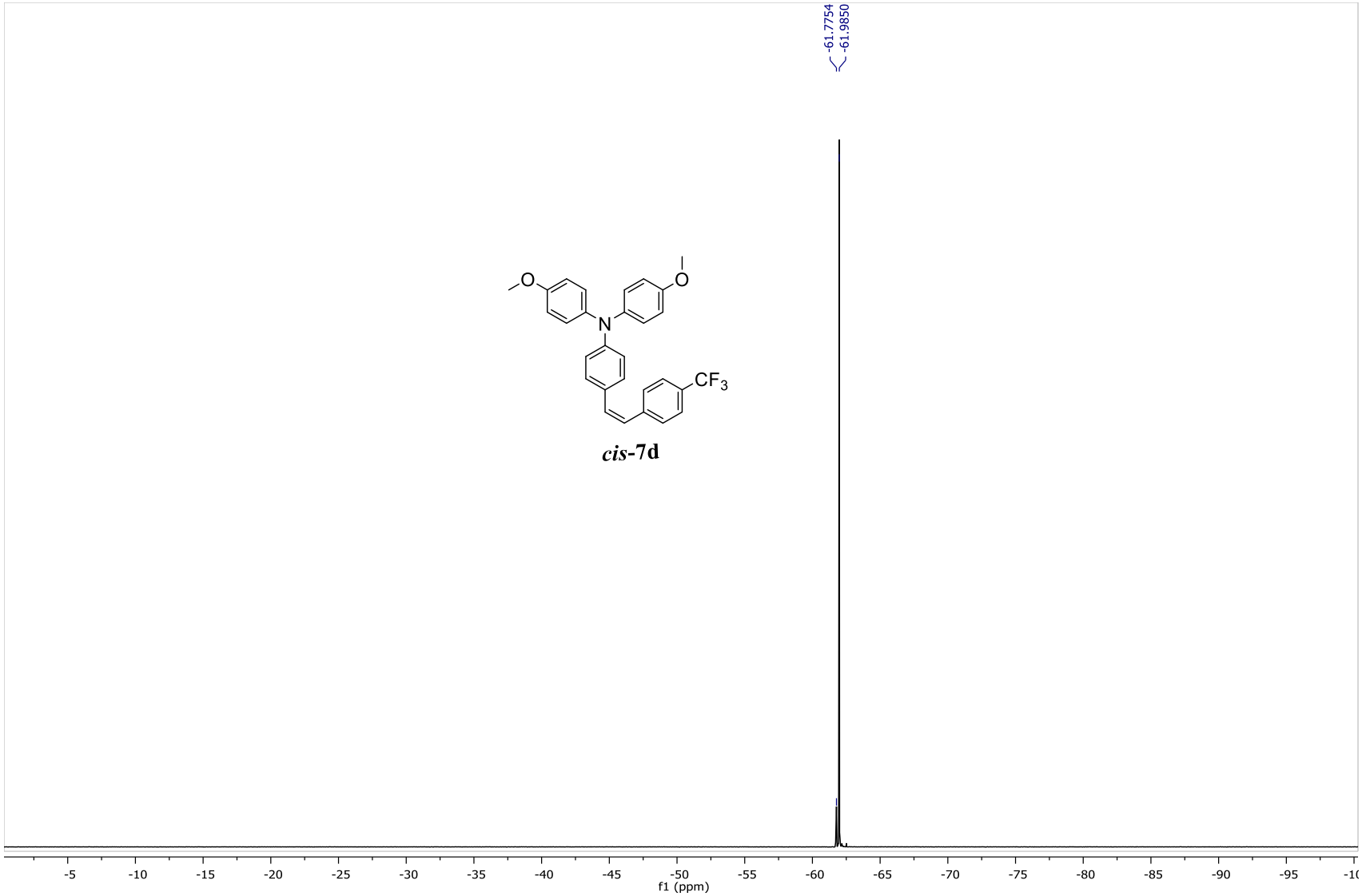

A.34. ^{19}F NMR spectrum (360 MHz) of ***cis*-7d** in DMSO-d_6

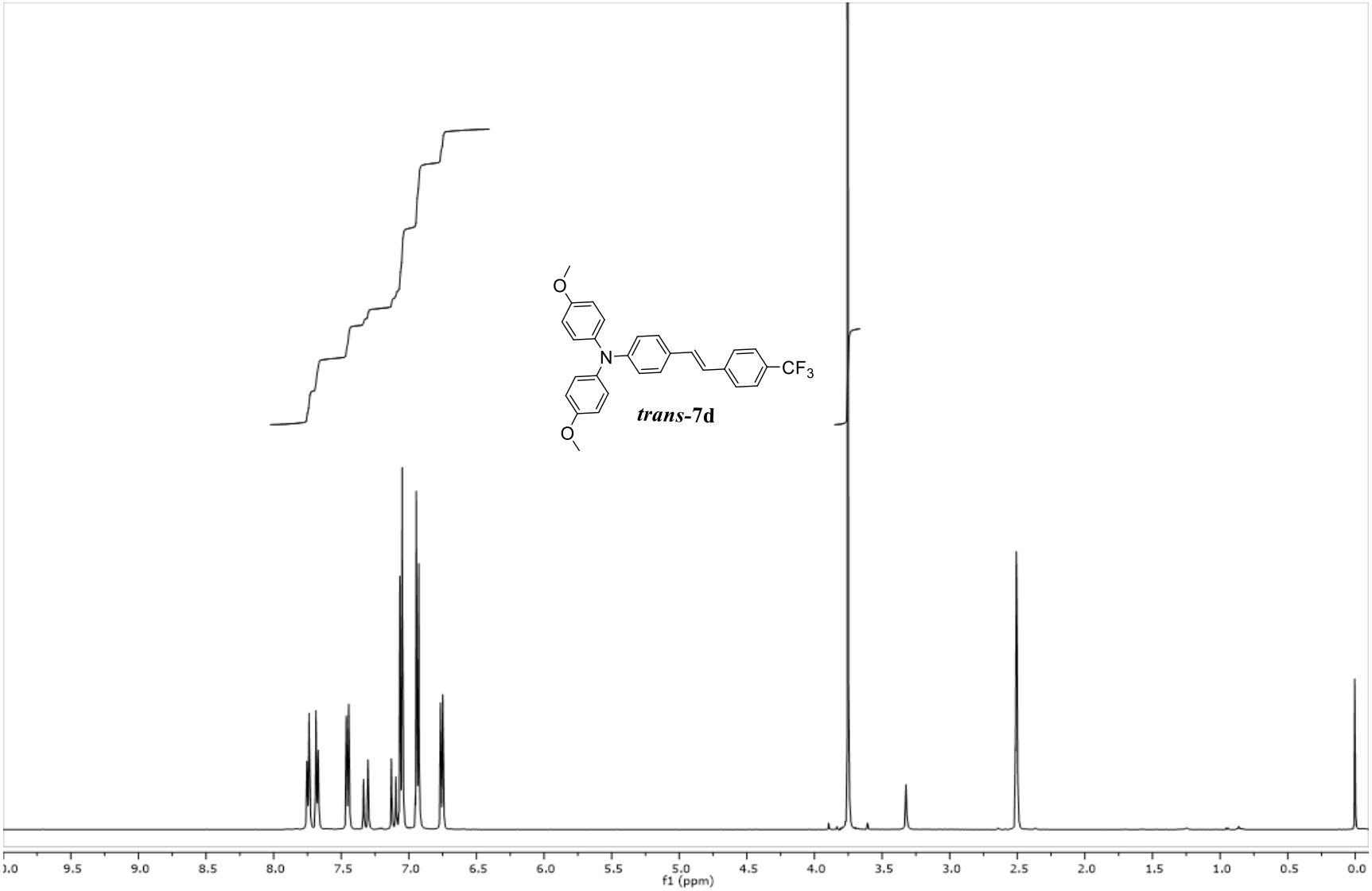

A.35. ^{1}H NMR spectrum (500 MHz) of ***trans*-7d** in DMSO-d_6

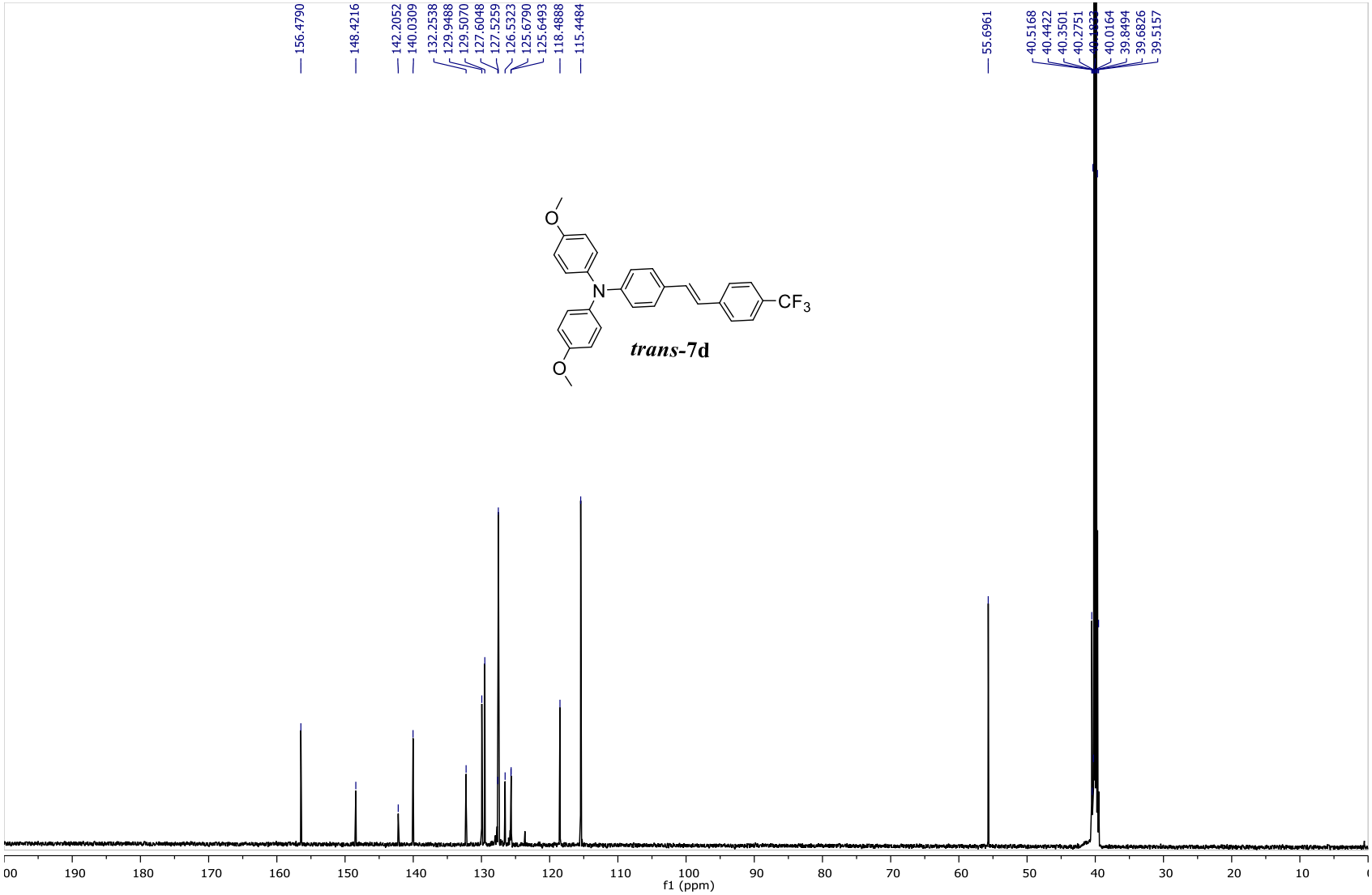

A.36. ^{13}C NMR spectrum (125 MHz) of ***trans*-7d** in DMSO-d_6

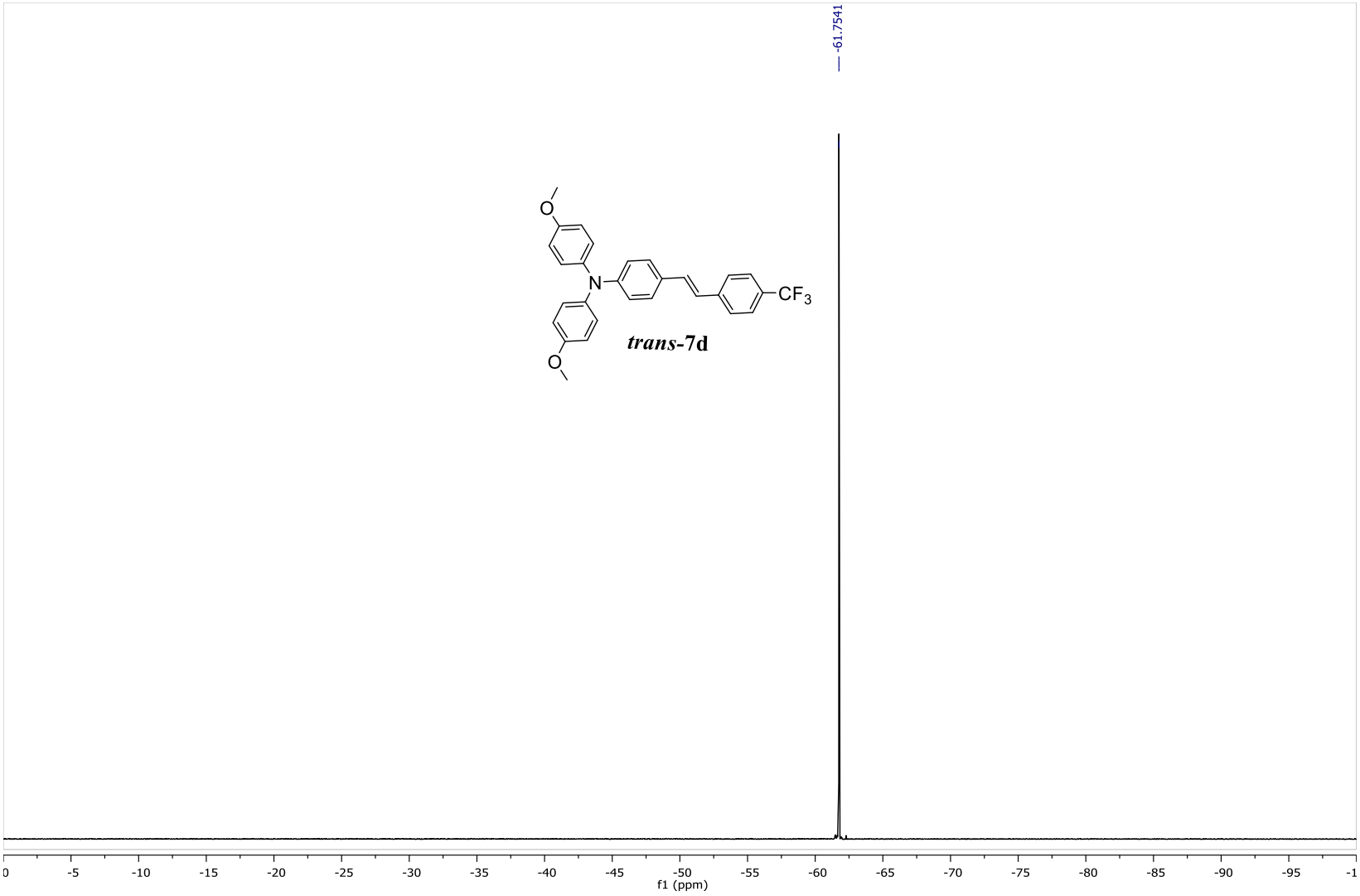

A.37. ^{19}F NMR spectrum (360 MHz) of ***trans*-7d** in DMSO-d_6

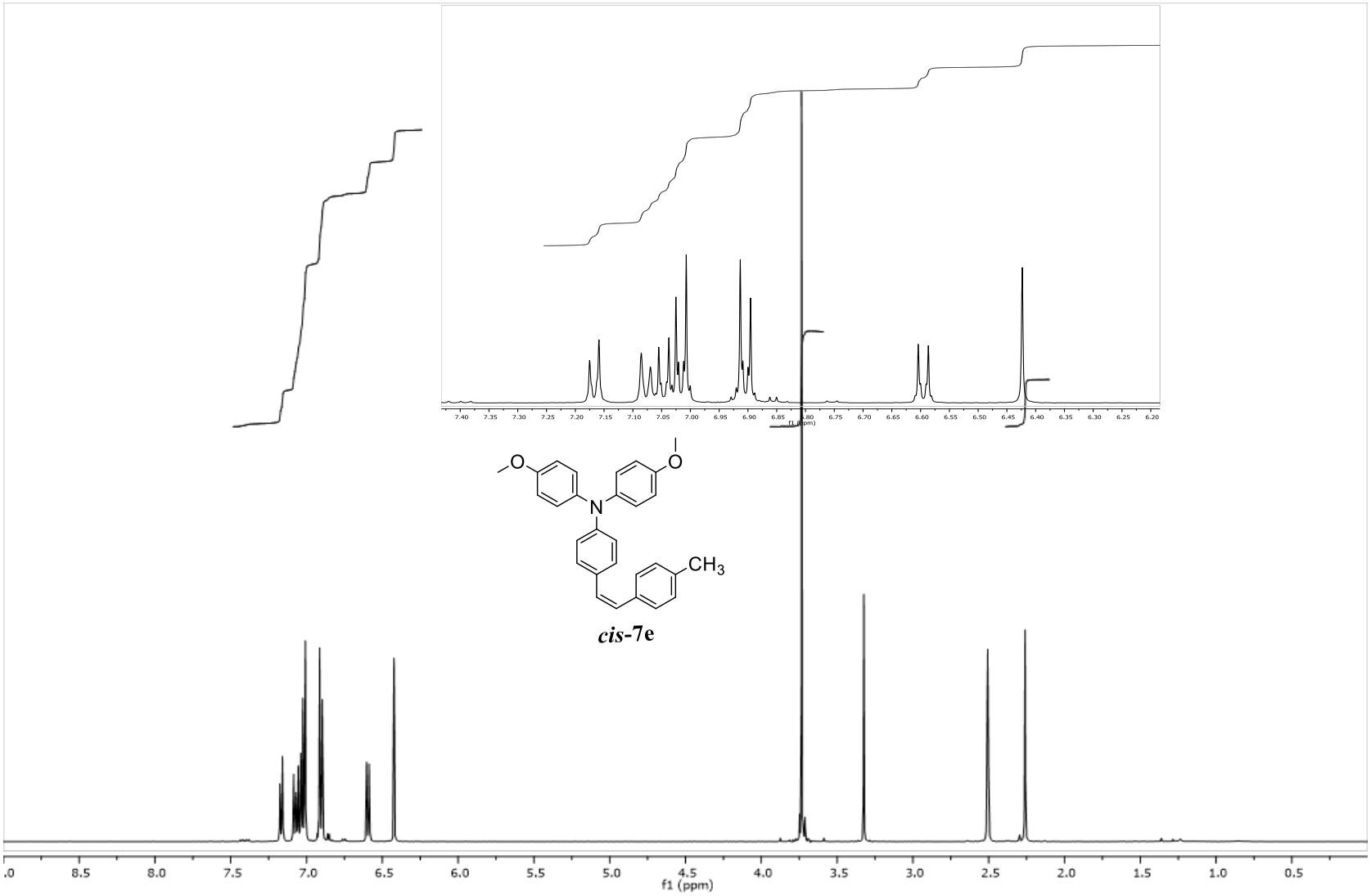

A.38. ^{1}H NMR spectrum (500 MHz) of ***cis*-7e** in DMSO-d_6

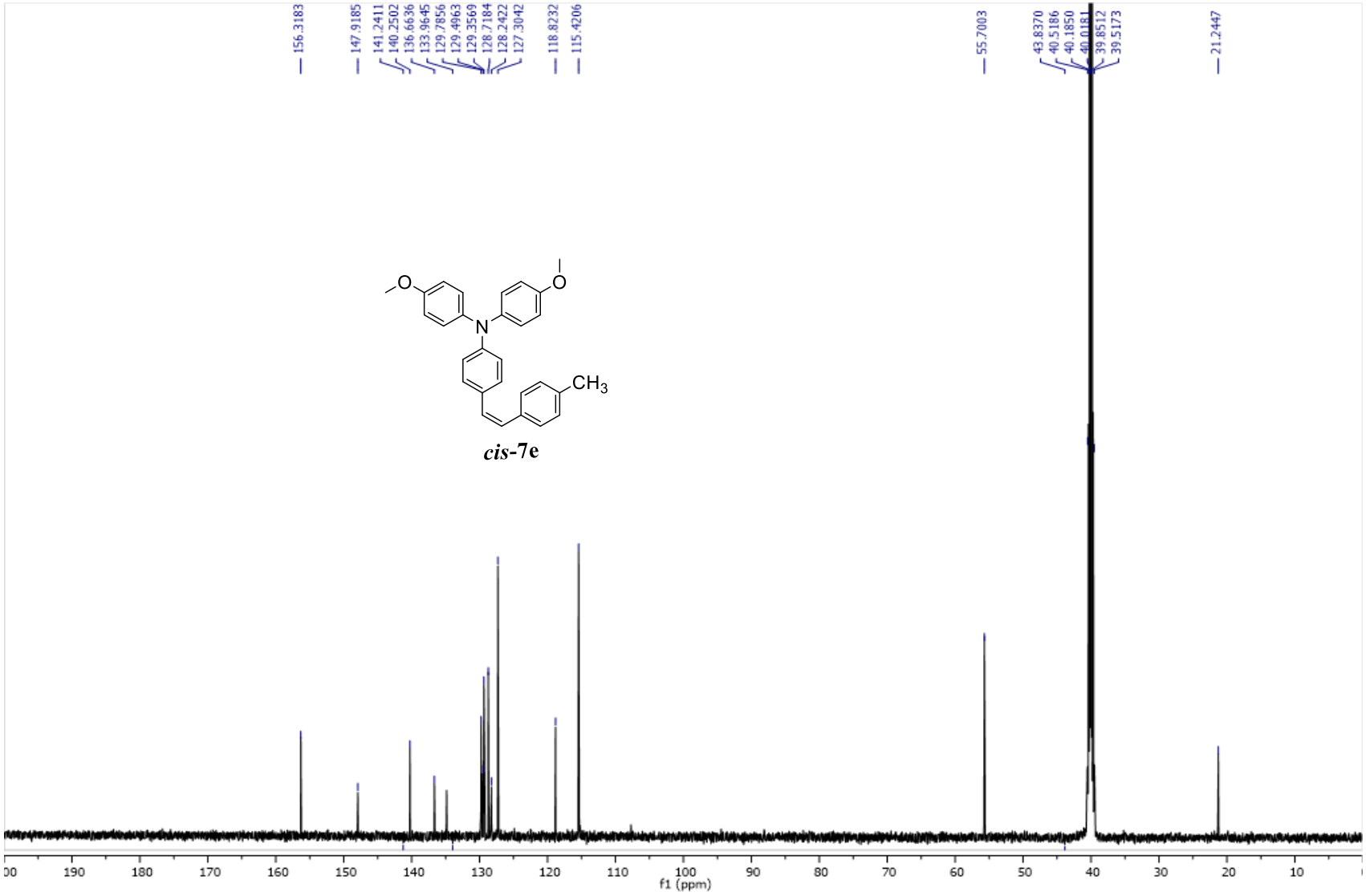

A.39. ^{13}C NMR spectrum (125 MHz) of ***cis*-7e** in DMSO-d_6

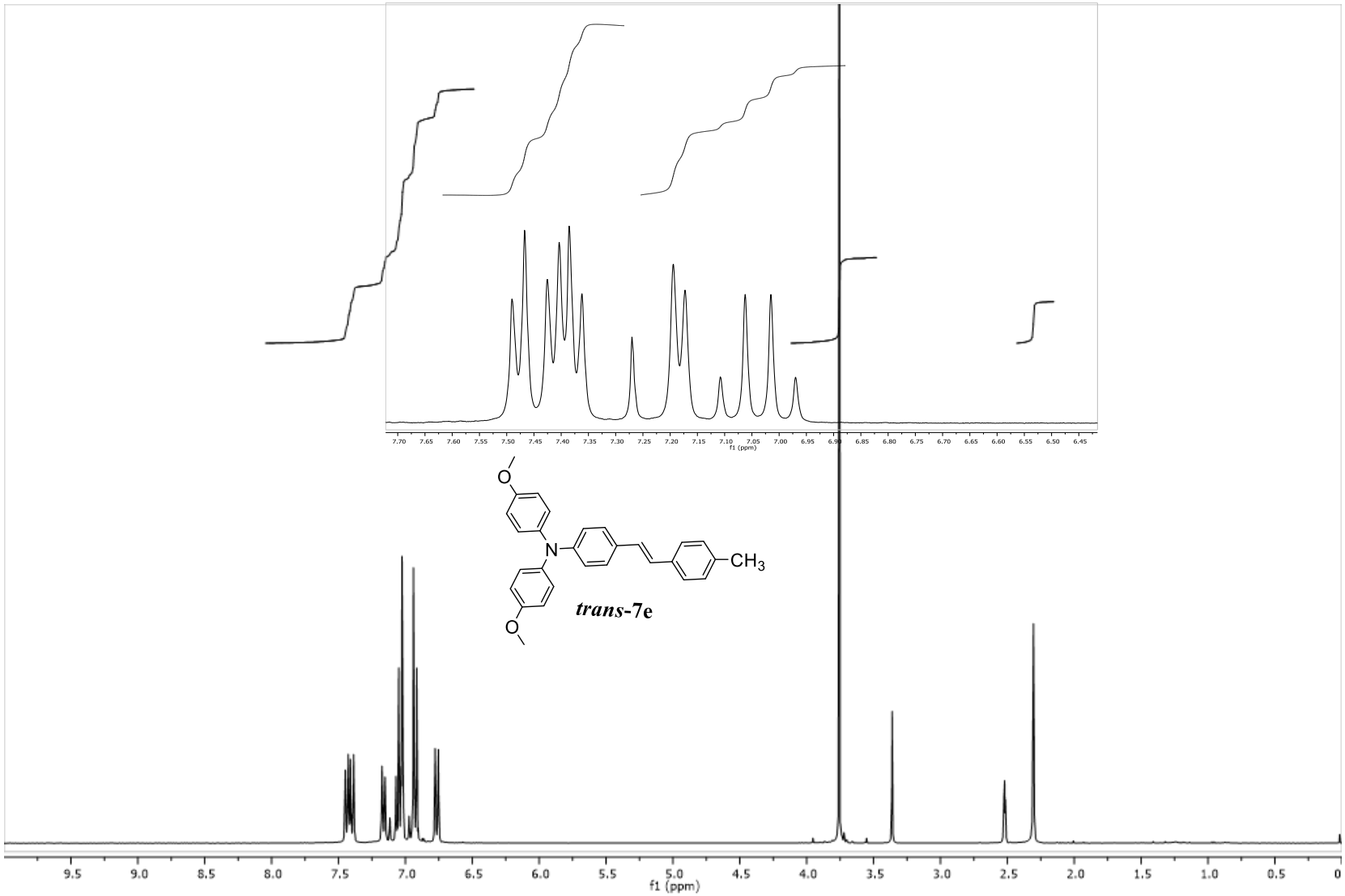

A.40. ^{1}H NMR spectrum (500 MHz) of ***trans*-7e** in DMSO-d_6

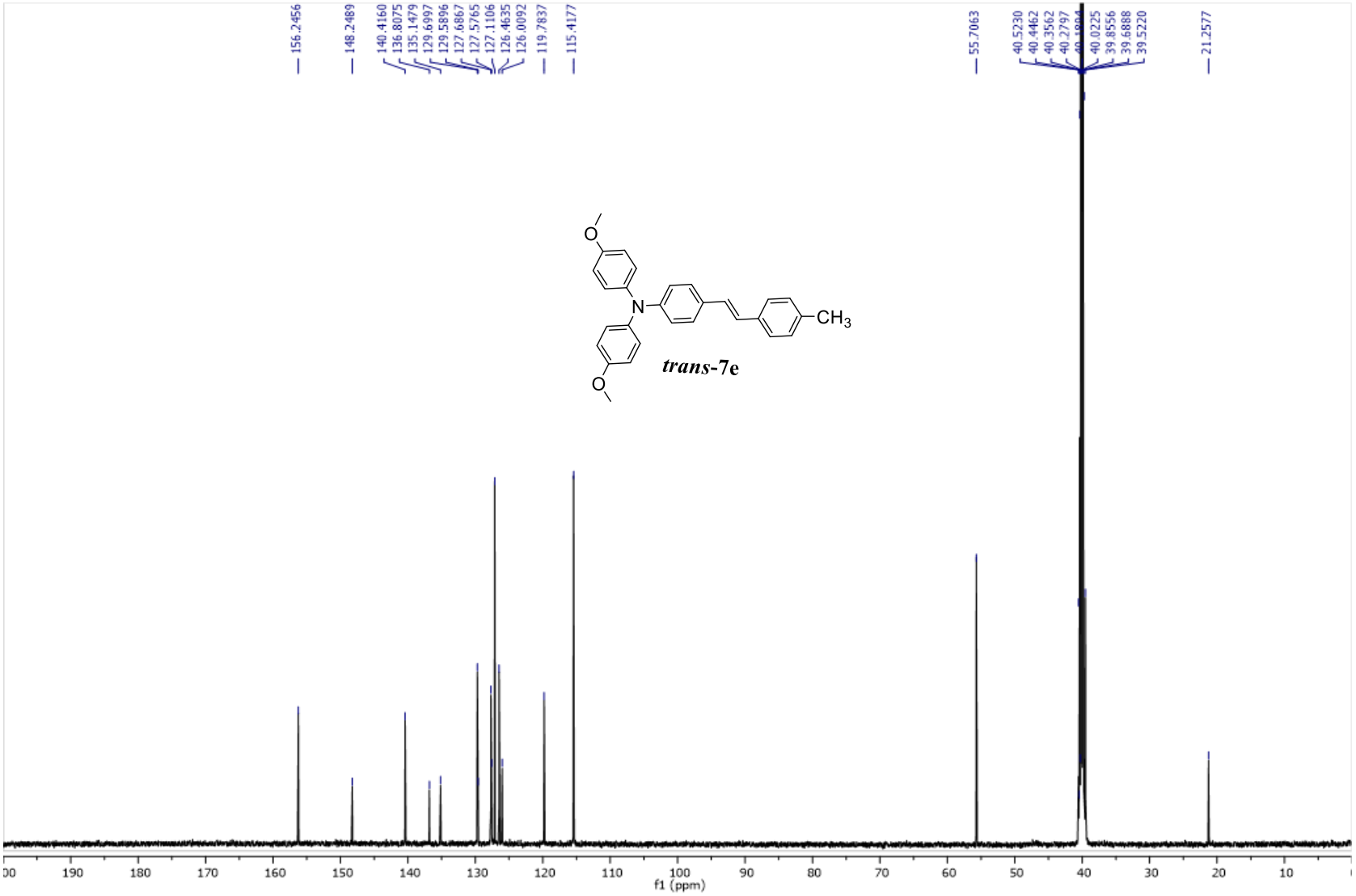

A.41. ^{13}C NMR spectrum (125 MHz) of ***trans*-7e** in DMSO-d_6

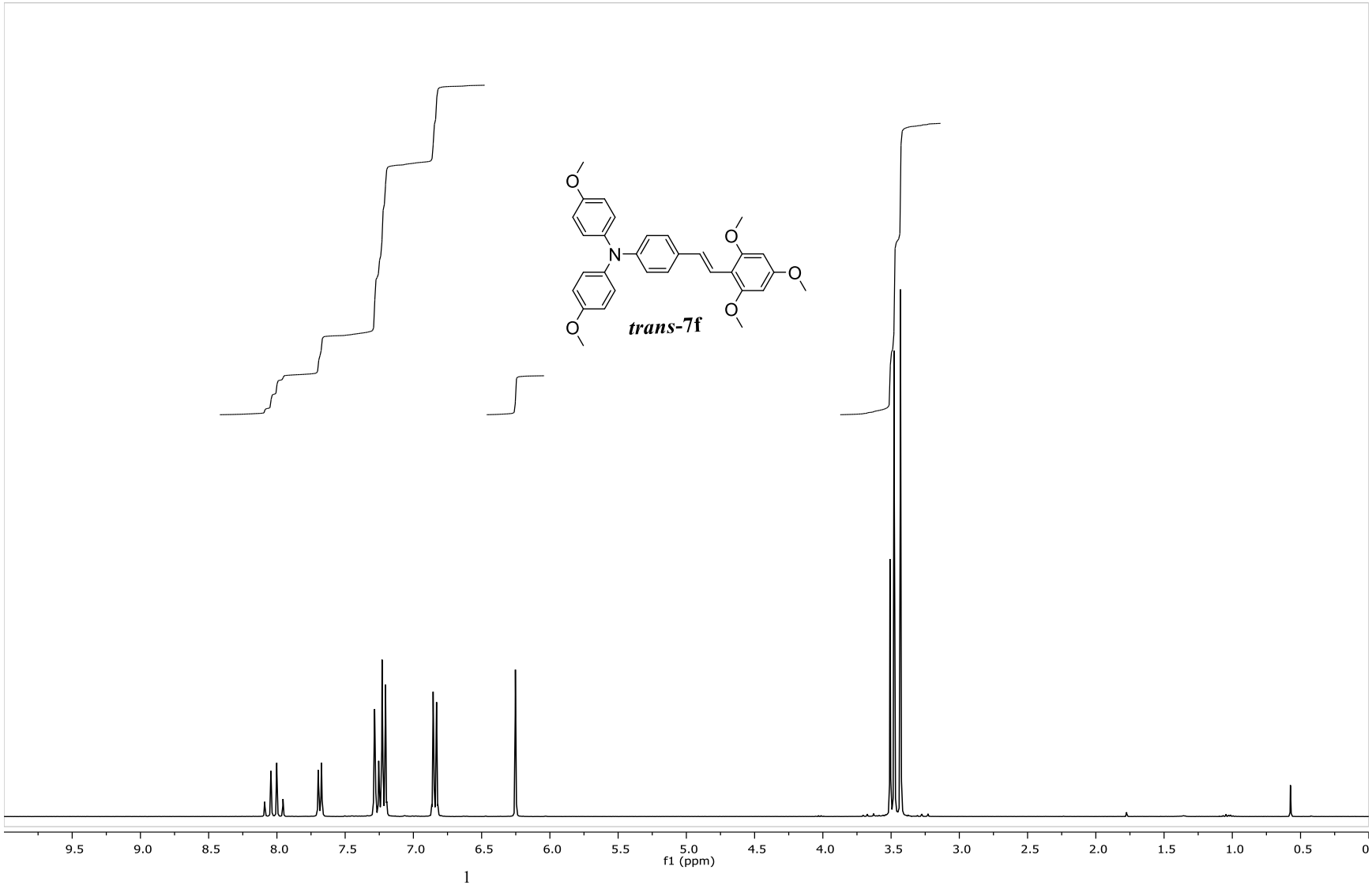

A.42. ^{1}H NMR spectrum (360 MHz) of ***trans*-7f** in C_6D_6

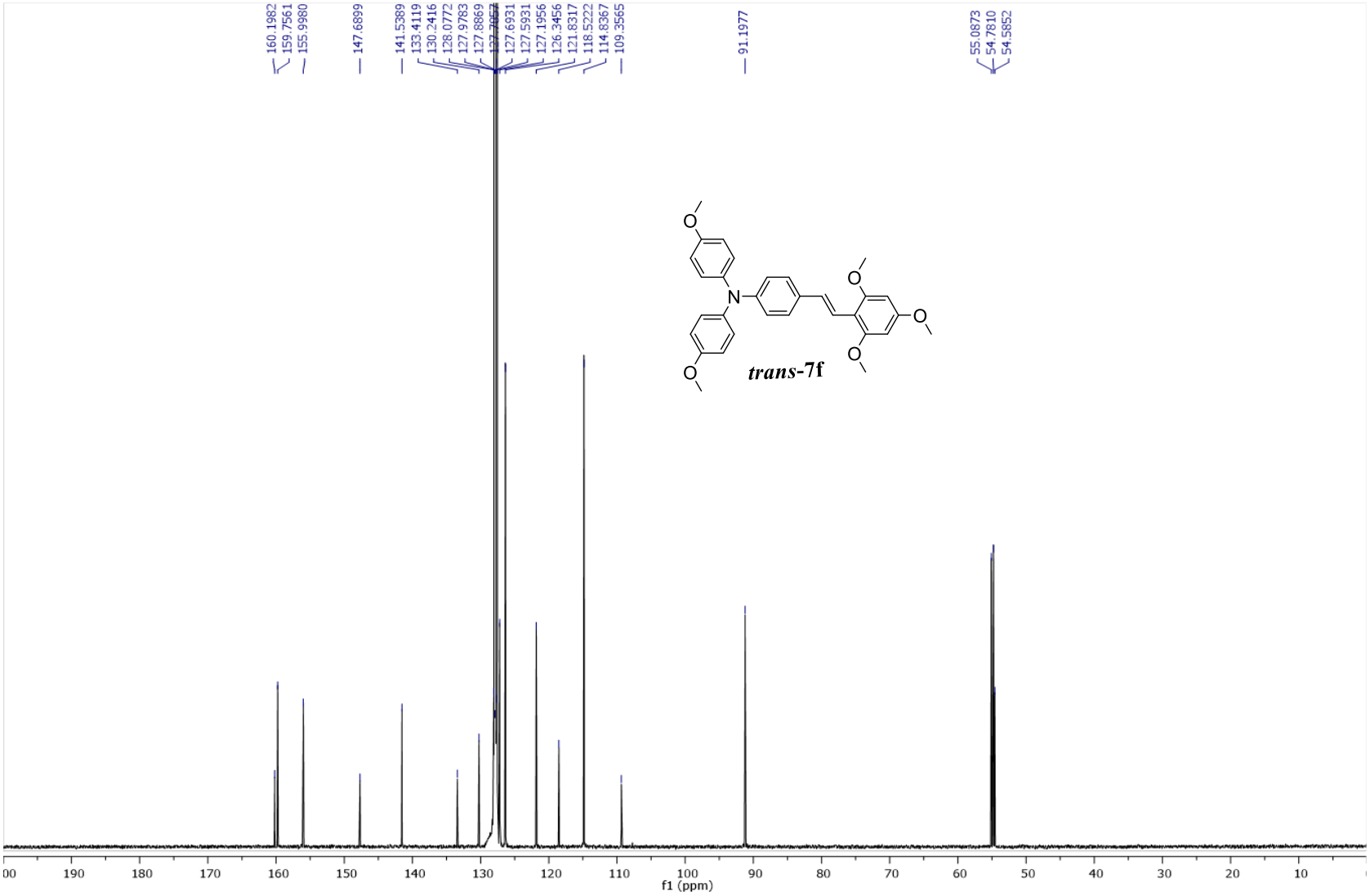

A.43. ^{13}C NMR spectrum (125 MHz) of ***trans*-7f** in DMSO-d_6

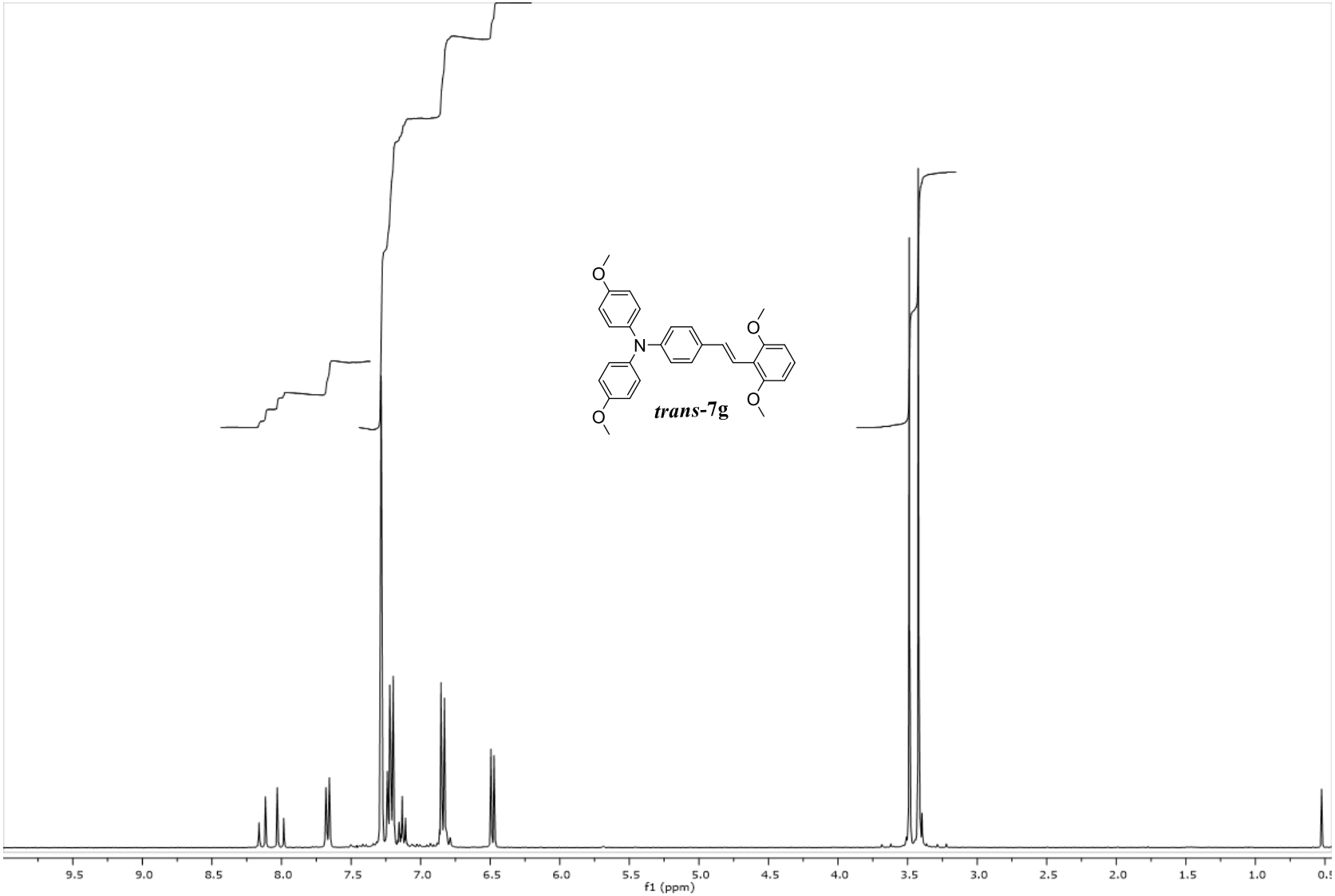

A.44. ^{1}H NMR spectrum (500 MHz) of ***trans*-7g** in DMSO-d_6

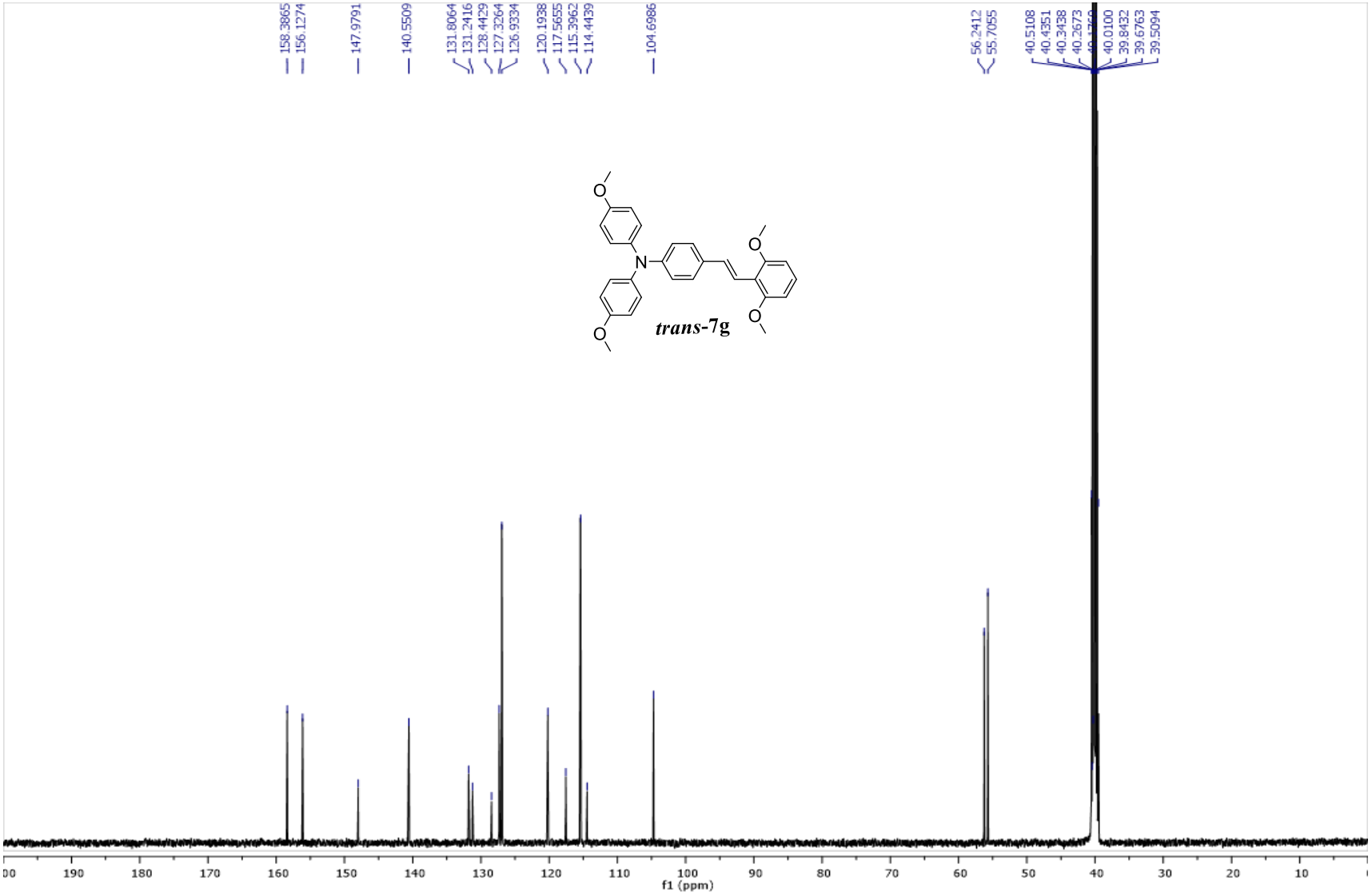

A.45. ^{13}C NMR spectrum (125 MHz) of ***trans*-7g** in DMSO-d_6

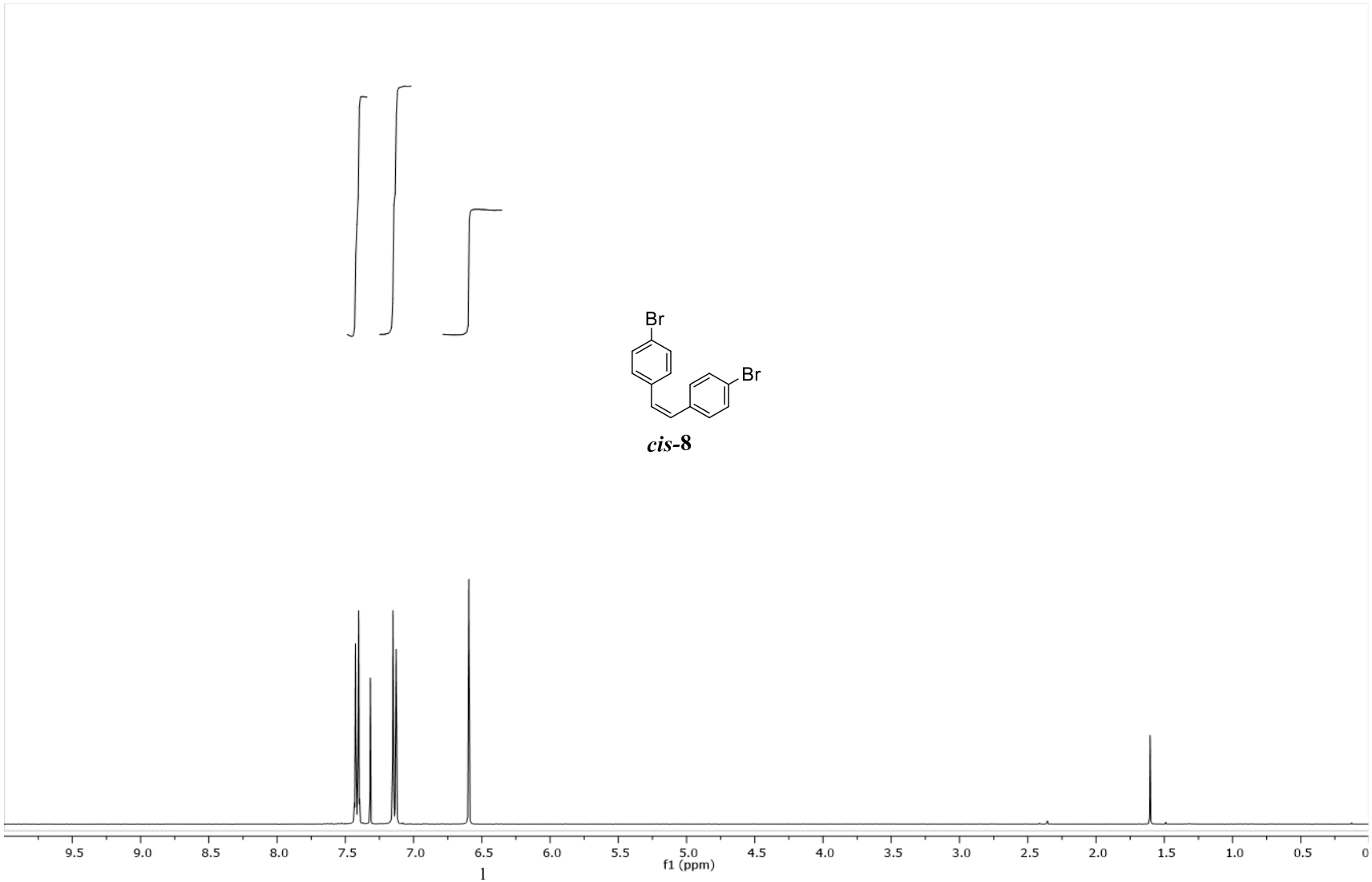

***cis*-8**

A.46. ^{1}H NMR spectrum (360 MHz) of ***cis*-8** in $CDCl_3$

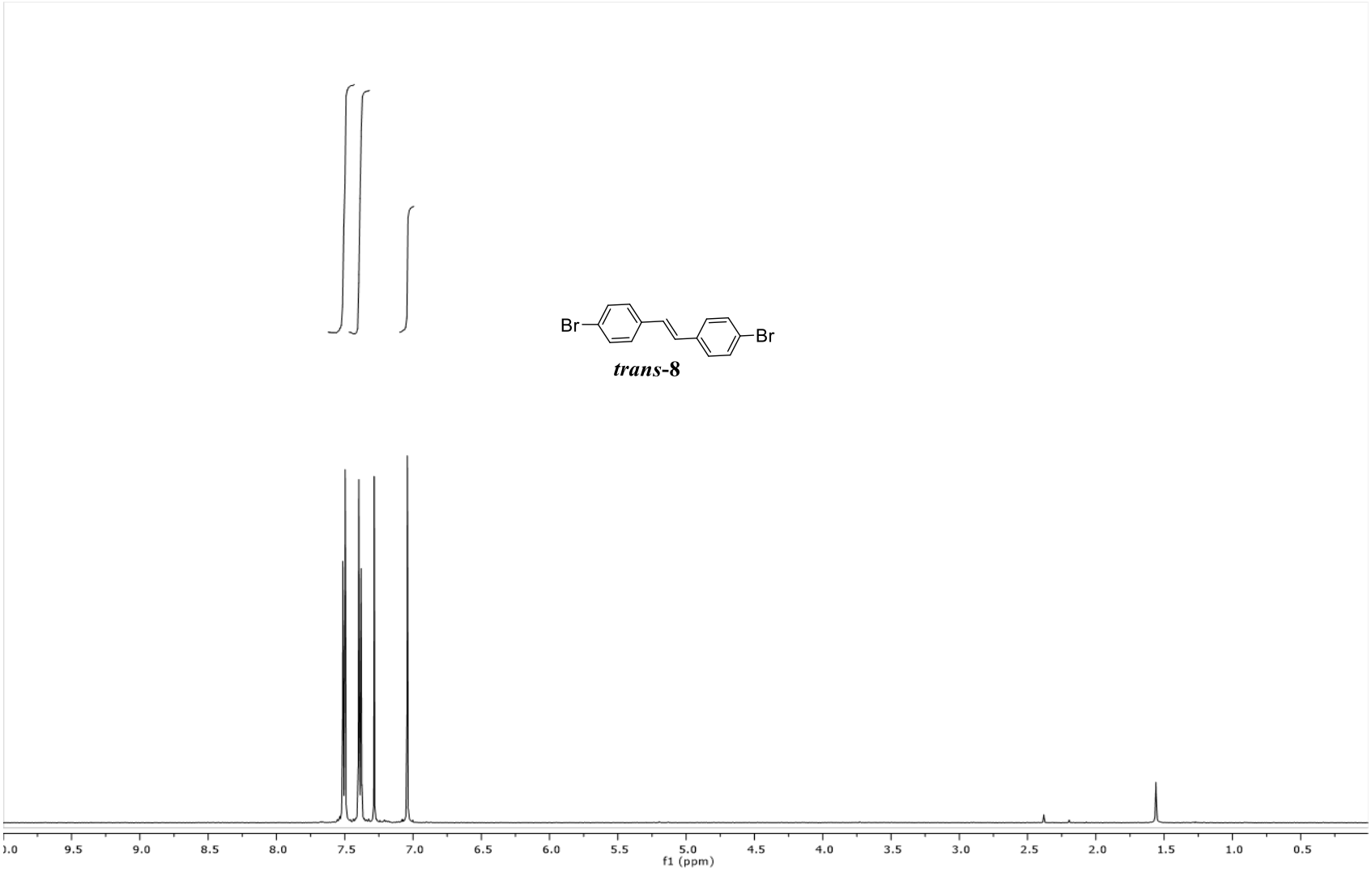

A.47. ^{1}H NMR spectrum (360 MHz) of ***trans*-8** in $CDCl_3$

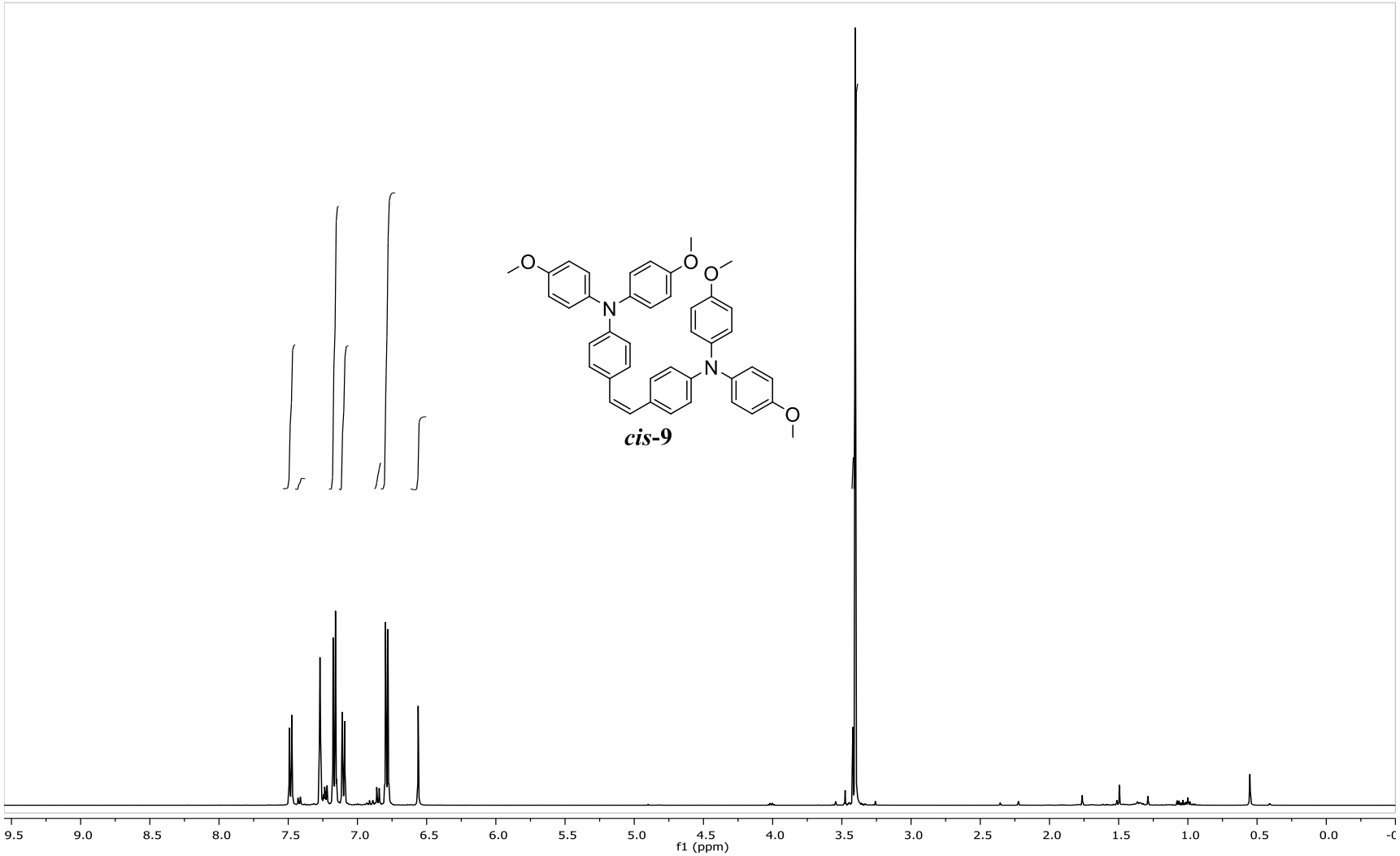

A.48. ^{1}H NMR spectrum (500 MHz) of ***cis*-9** in C_6D_6

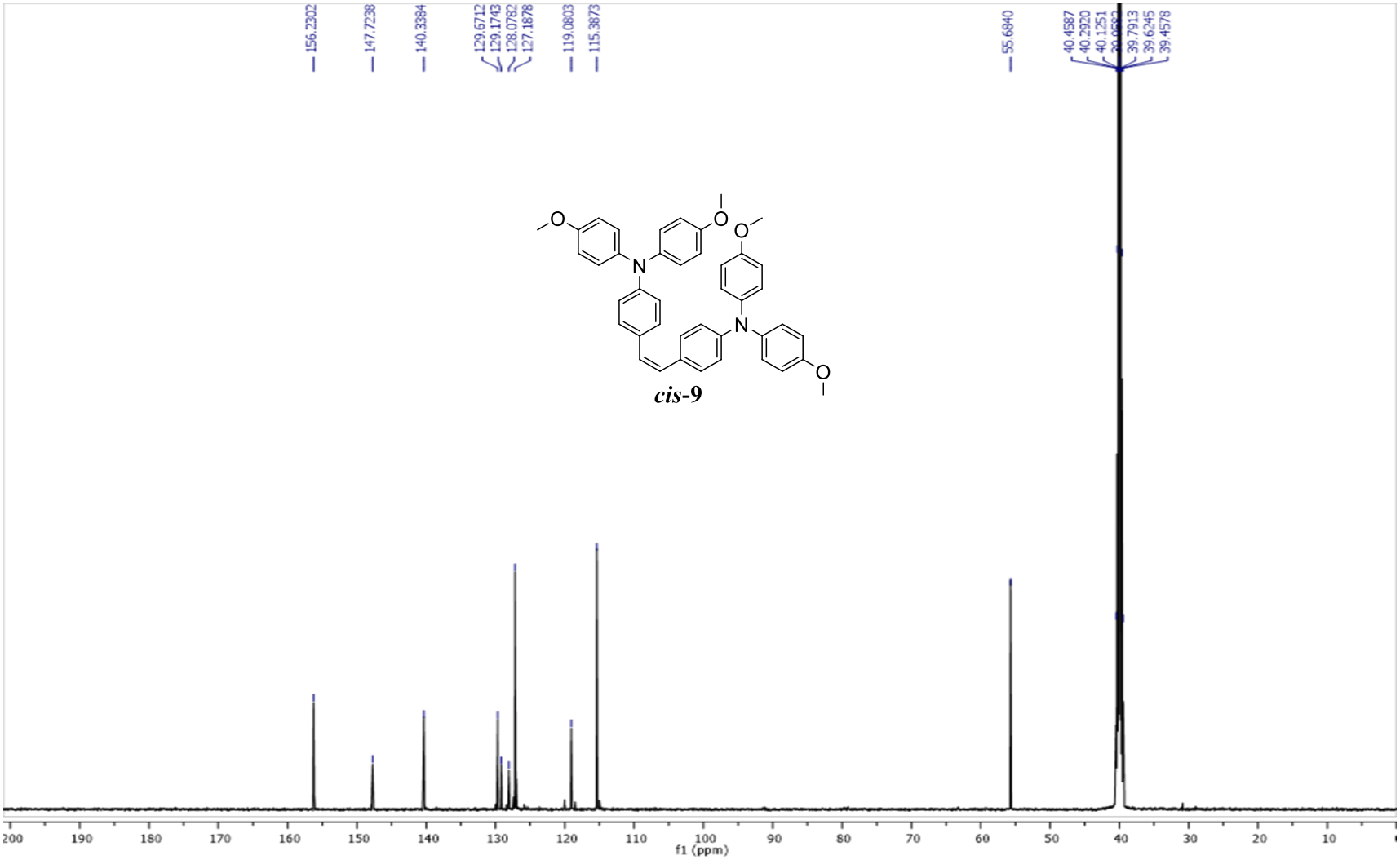

A.49. ^{13}C NMR spectrum (125 MHz) of ***cis*-9** in C_6D_6

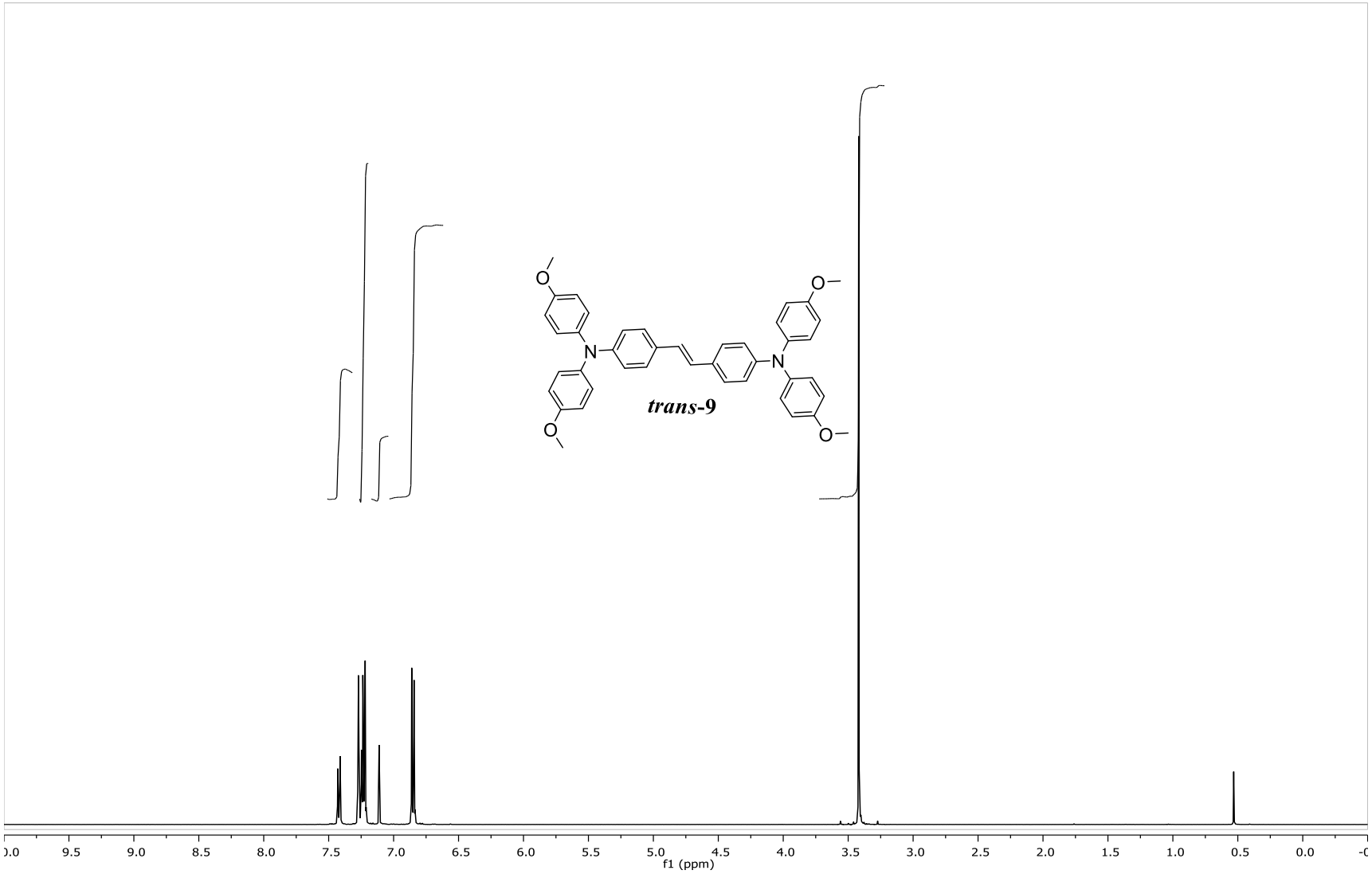

A.50. ^{1}H NMR spectrum (500 MHz) of ***trans*-9** in C_6D_6

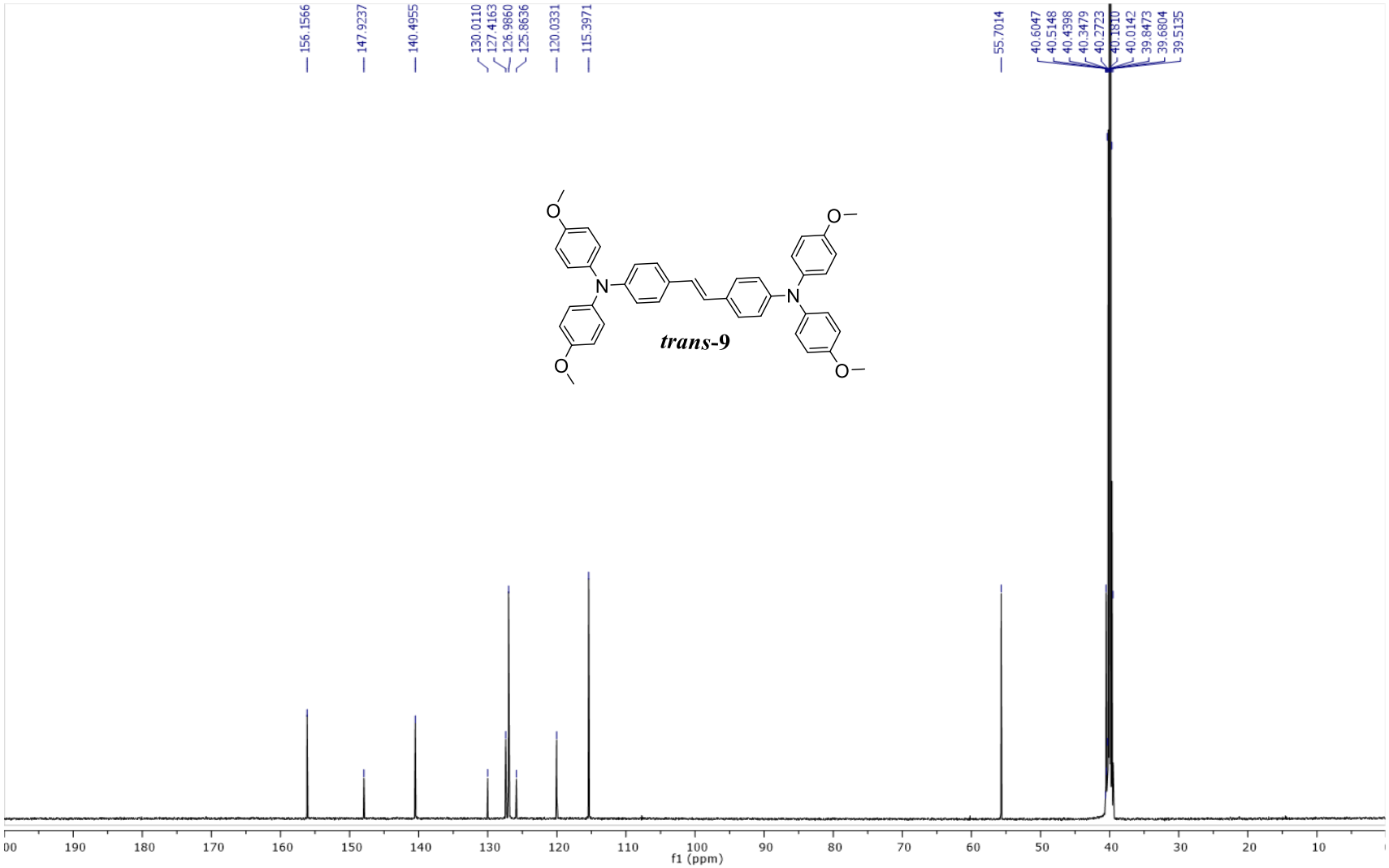

A.51. ^{13}C NMR spectrum (125 MHz) of ***trans*-9** in DMSO-d_6

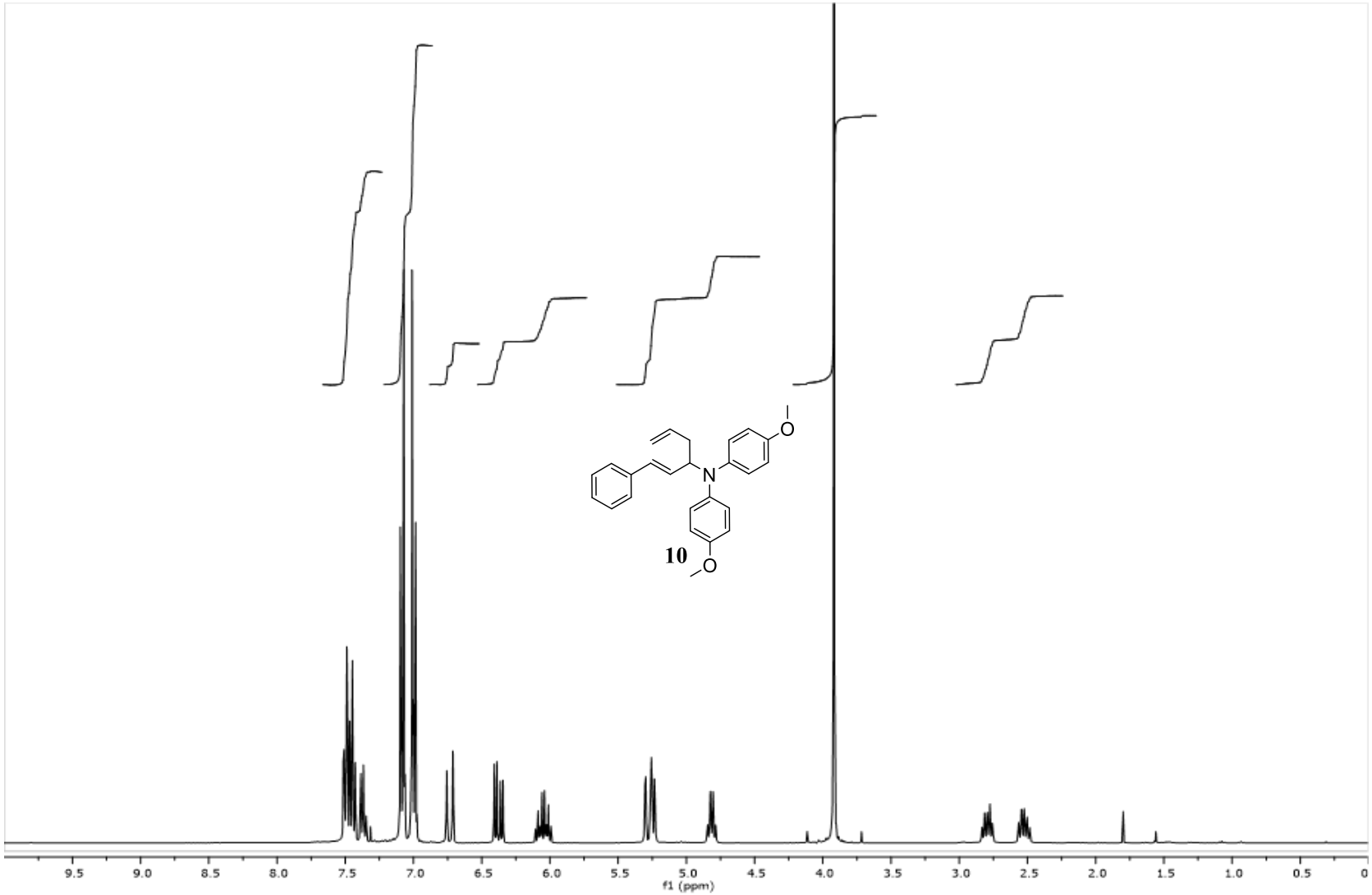

A.52. ^{1}H NMR spectrum (500 MHz) of **10** in $CDCl_3$

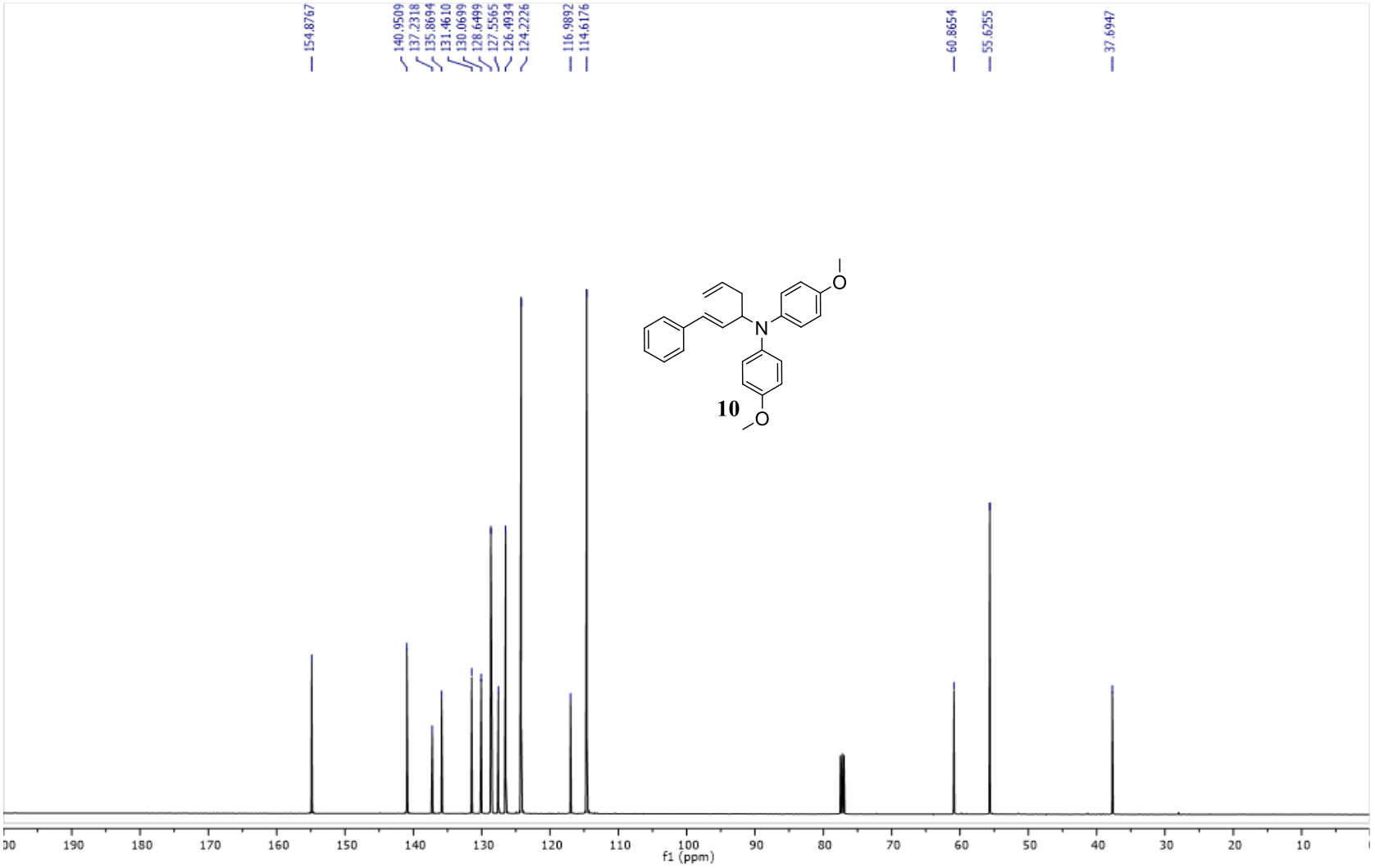

A.53. ^{13}C NMR spectrum (125 MHz) of **10** in $CDCl_3$

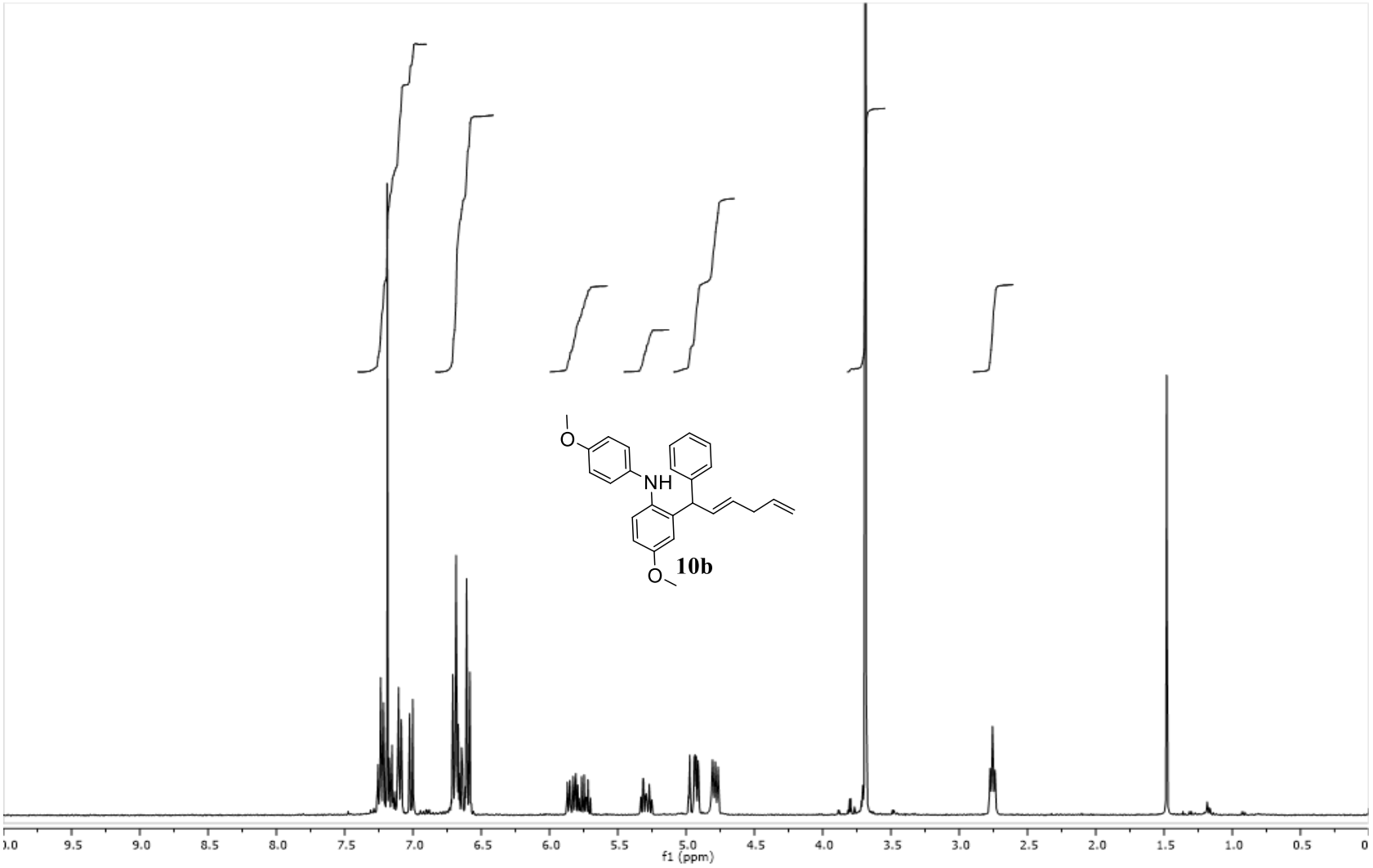

A.54. ^{1}H NMR spectrum (360 MHz) of **10b** in $CDCl_3$

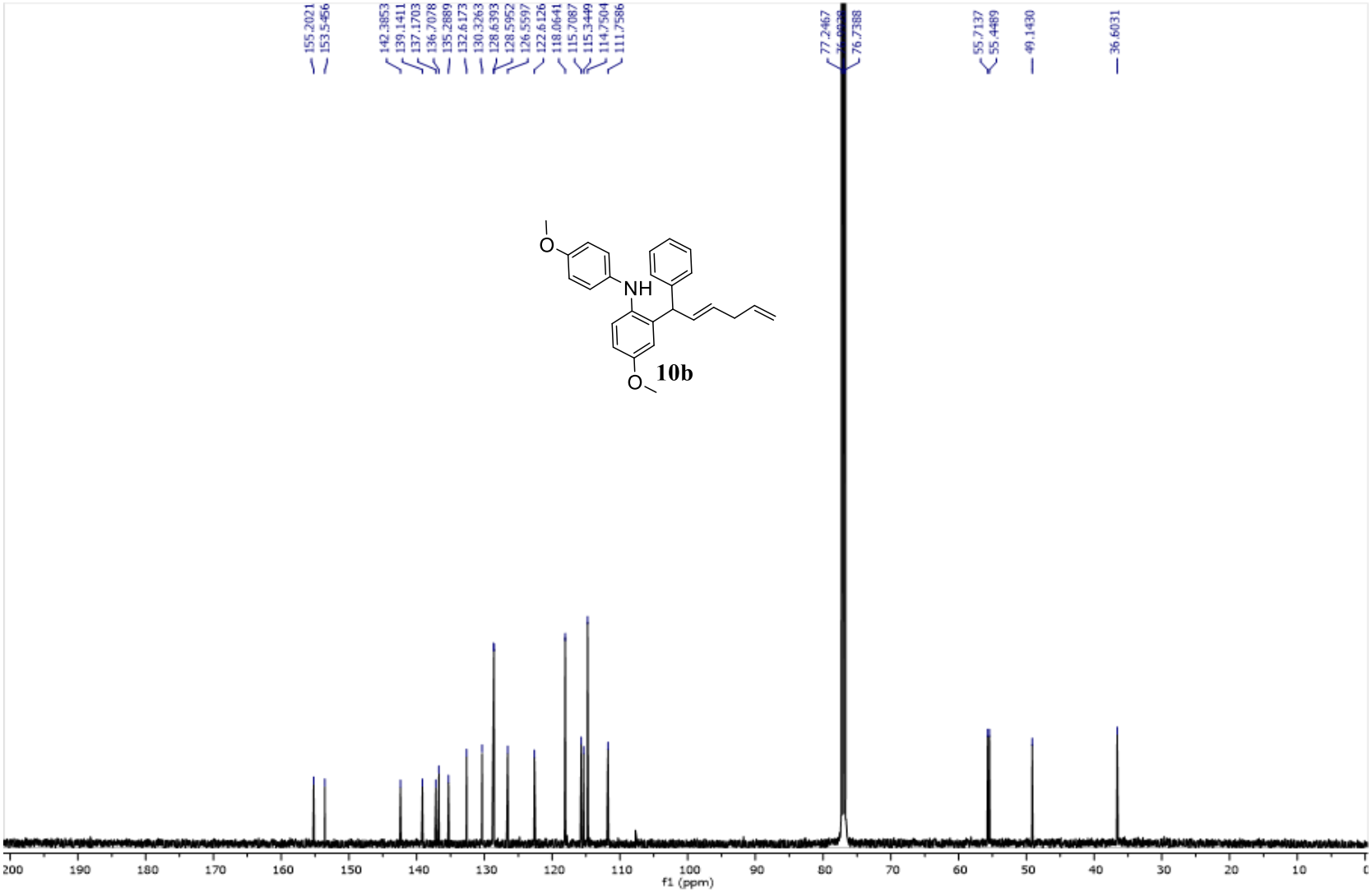

A.55. ^{13}C NMR spectrum (125 MHz) of **10b** in $CDCl_3$

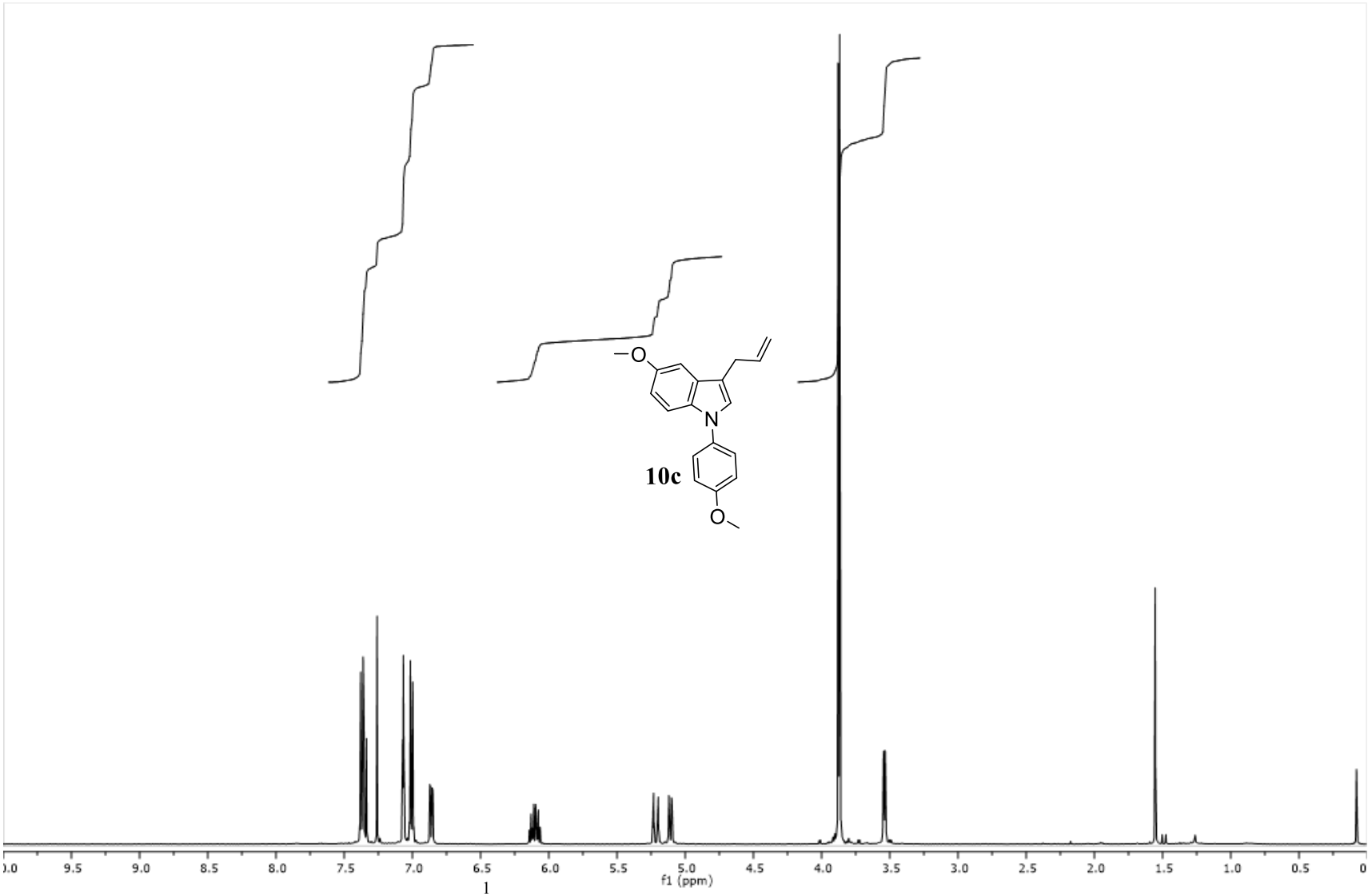

A.56. ^{1}H NMR spectrum (360 MHz) of **10c** in $CDCl_3$

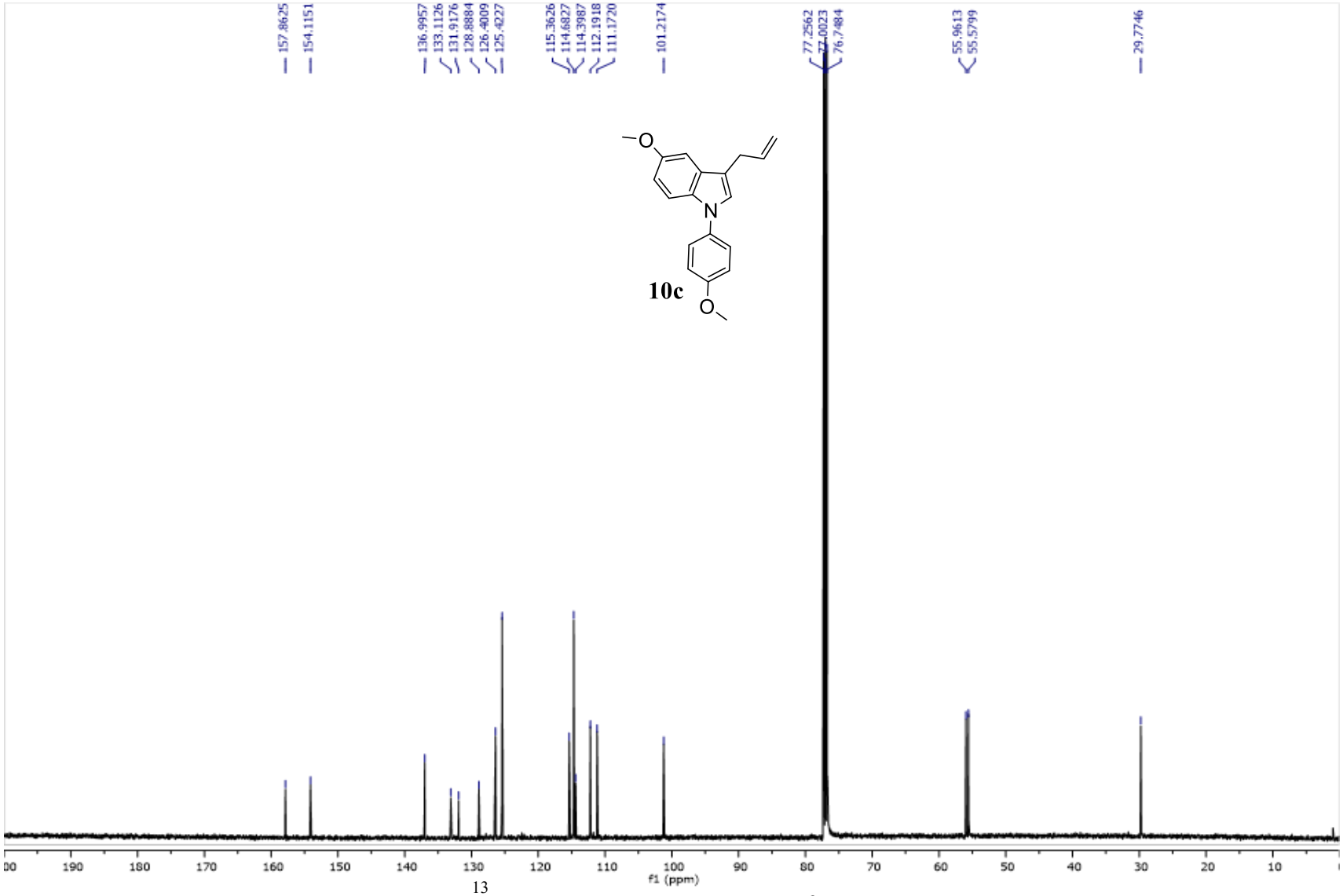

A.57. ^{13}C NMR spectrum (125 MHz) of **10c** in $CDCl_3$

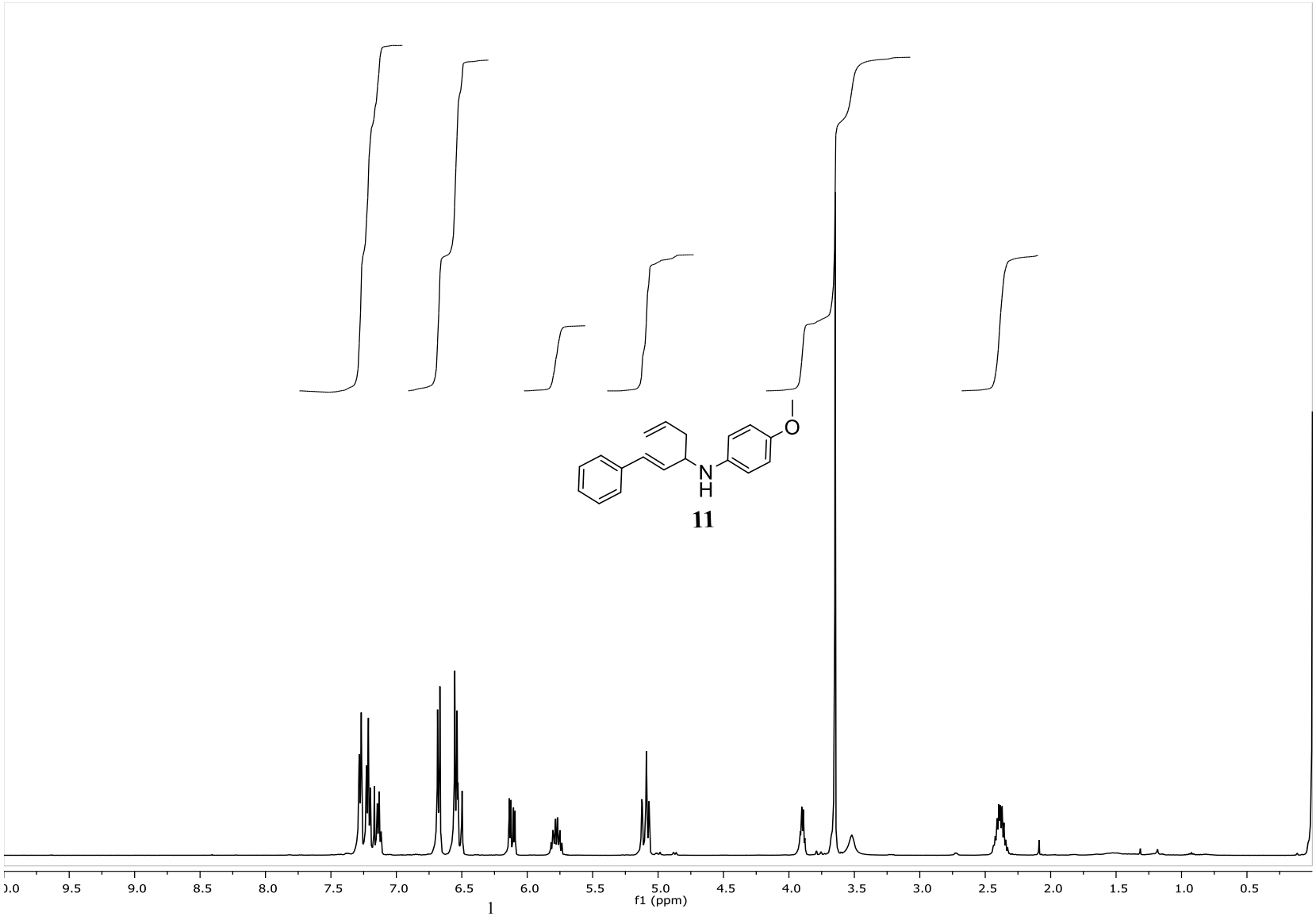

A.58. ^{1}H NMR spectrum (360 MHz) of **11** in $CDCl_3$

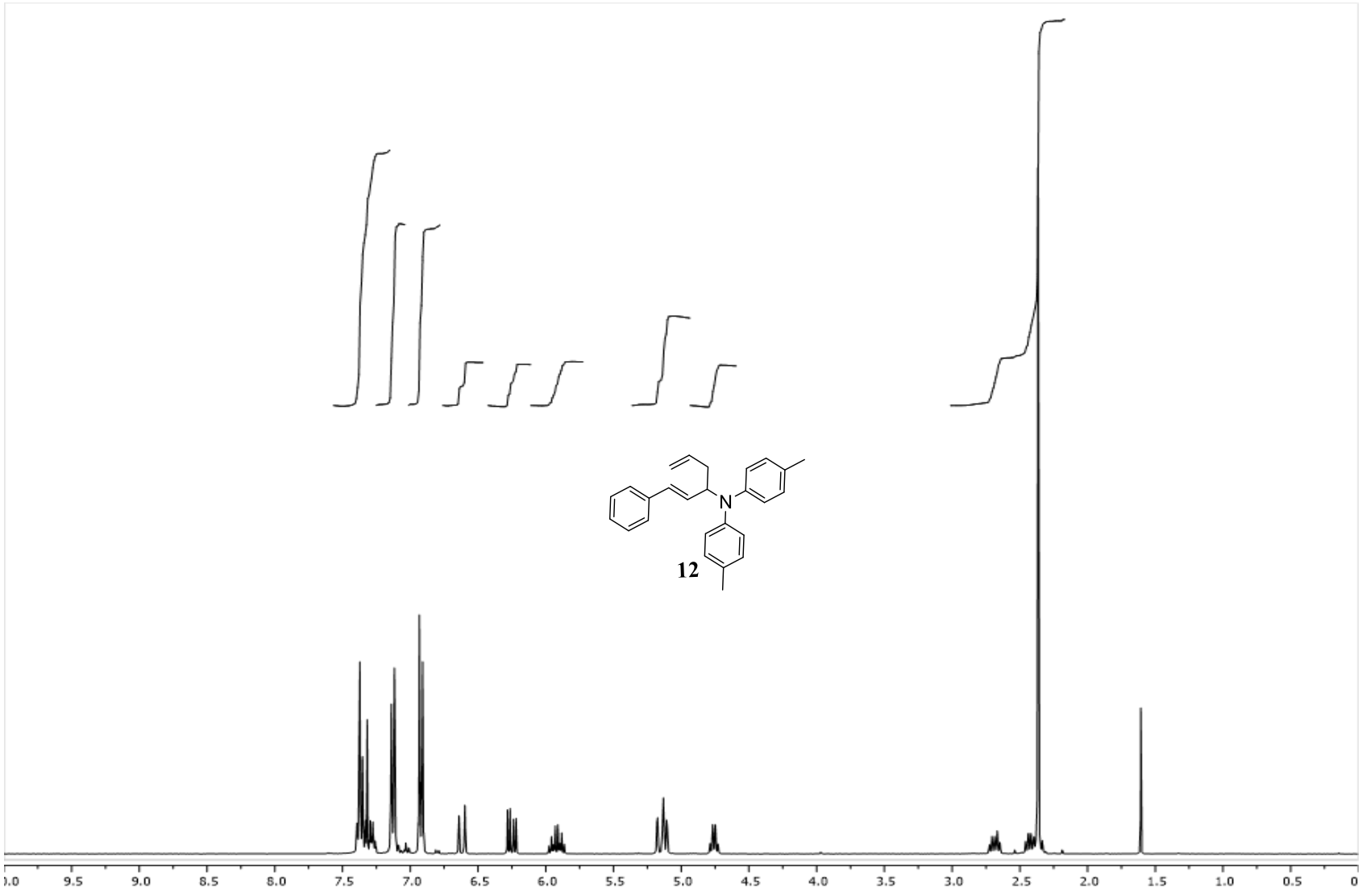

A.59. ^{1}H NMR spectrum (360 MHz) of **12** in $CDCl_3$

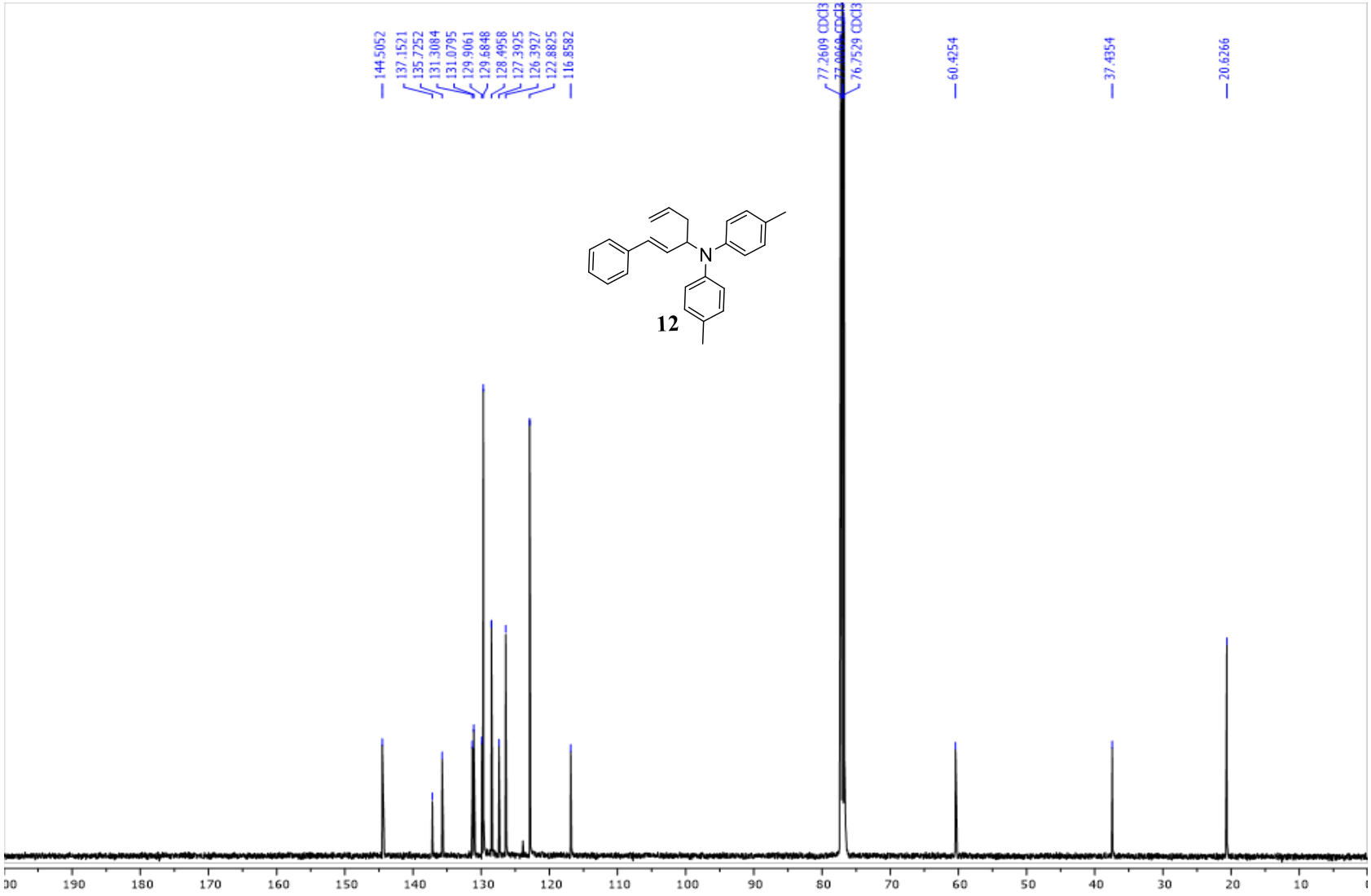

A.60. ^{13}C NMR spectrum (125 MHz) of **12** in $CDCl_3$

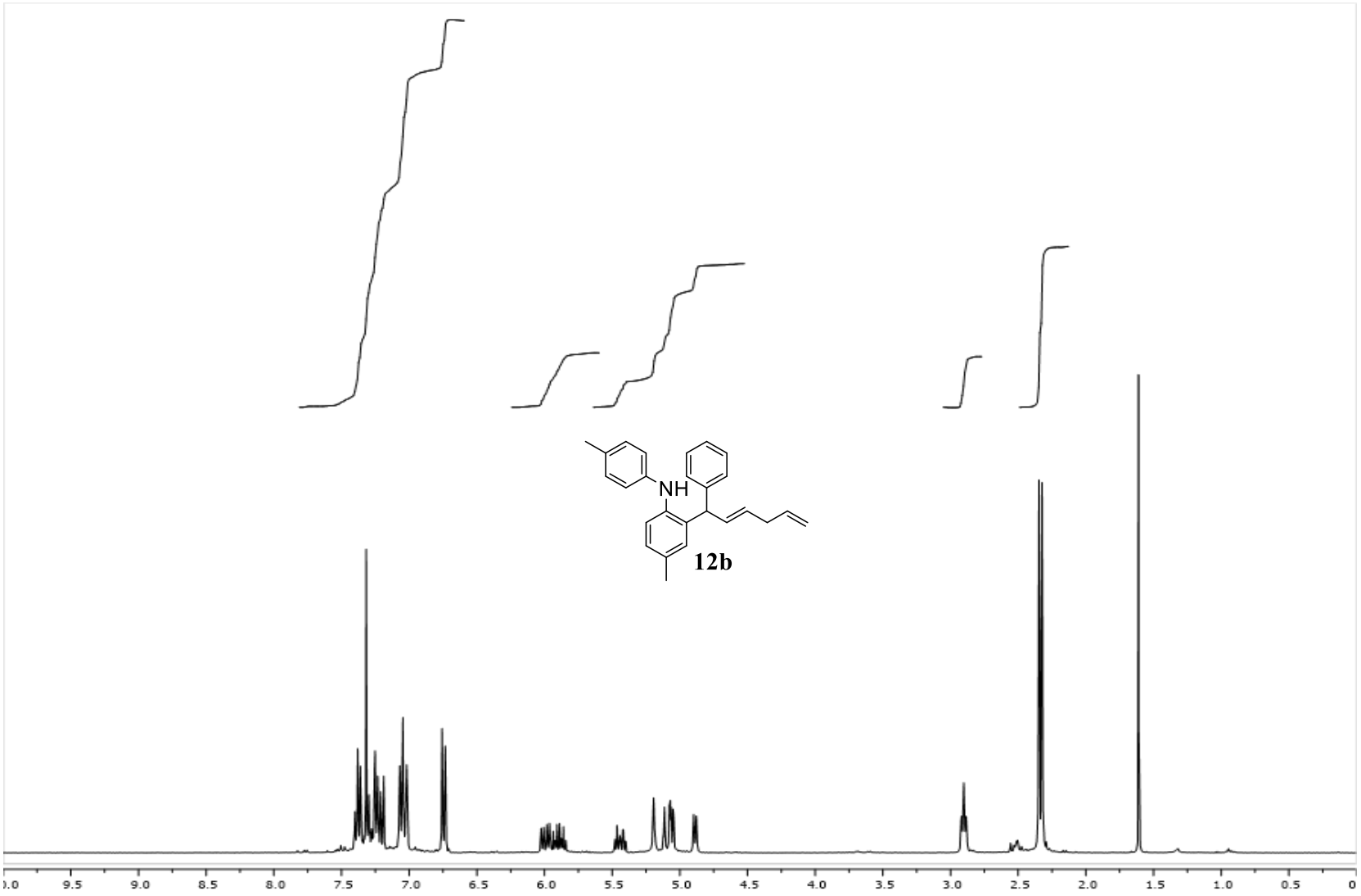

A.61. ^{1}H NMR spectrum (360 MHz) of **12b** in $CDCl_3$

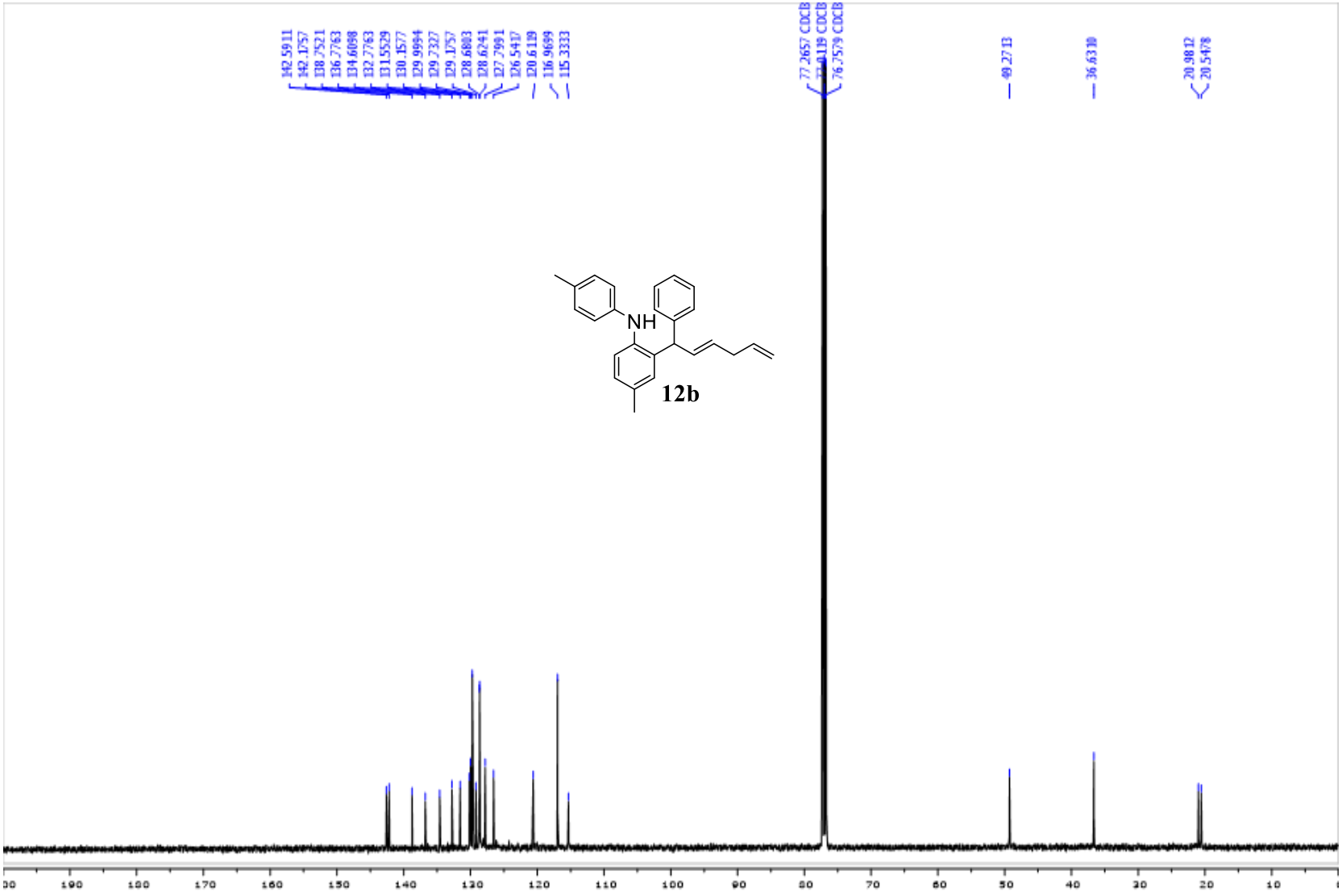

A.62. ^{13}C NMR spectrum (125 MHz) of **12b** in $CDCl_3$

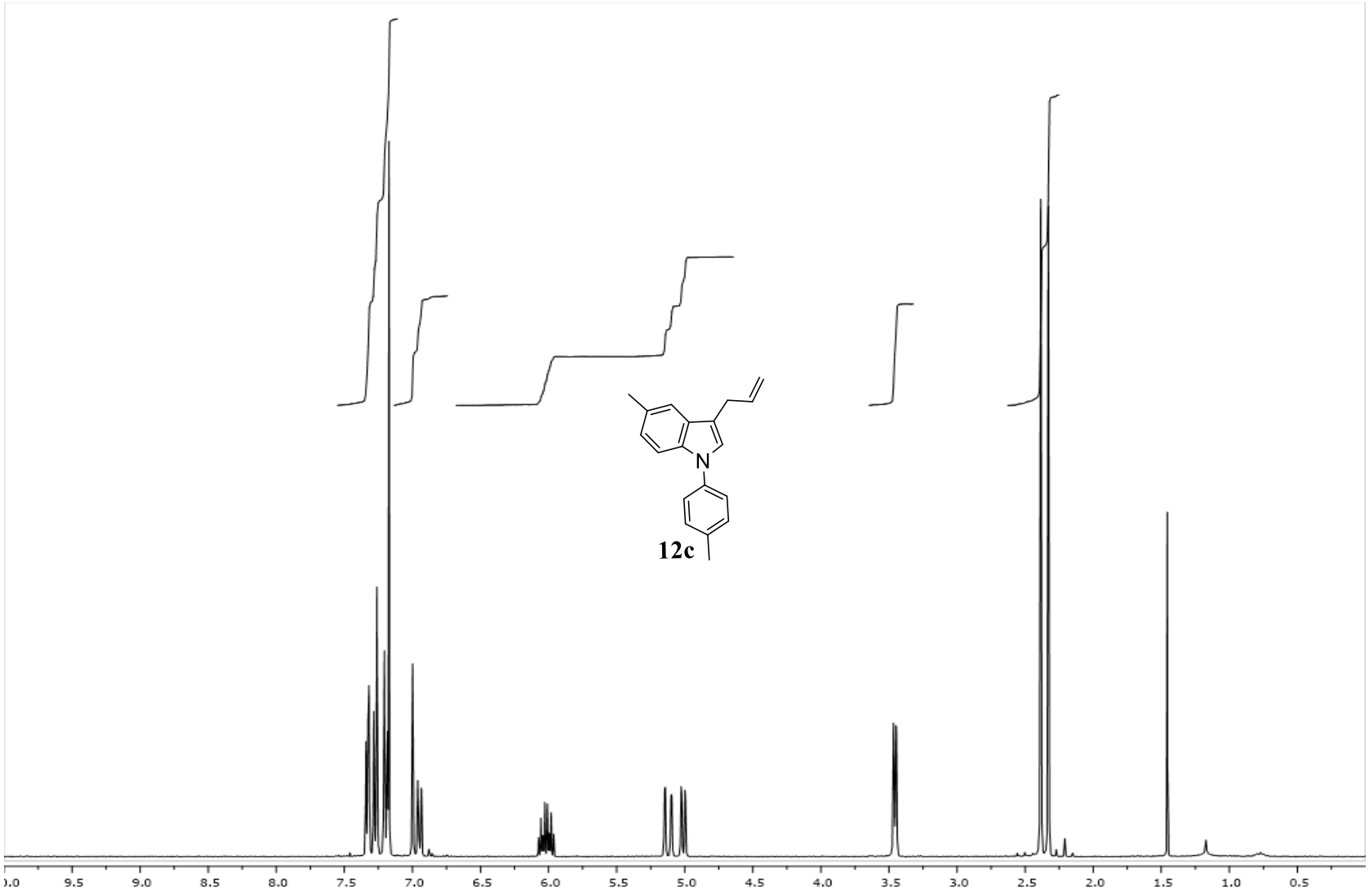

A.63. ^{1}H NMR spectrum (360 MHz) of **12c** in $CDCl_3$

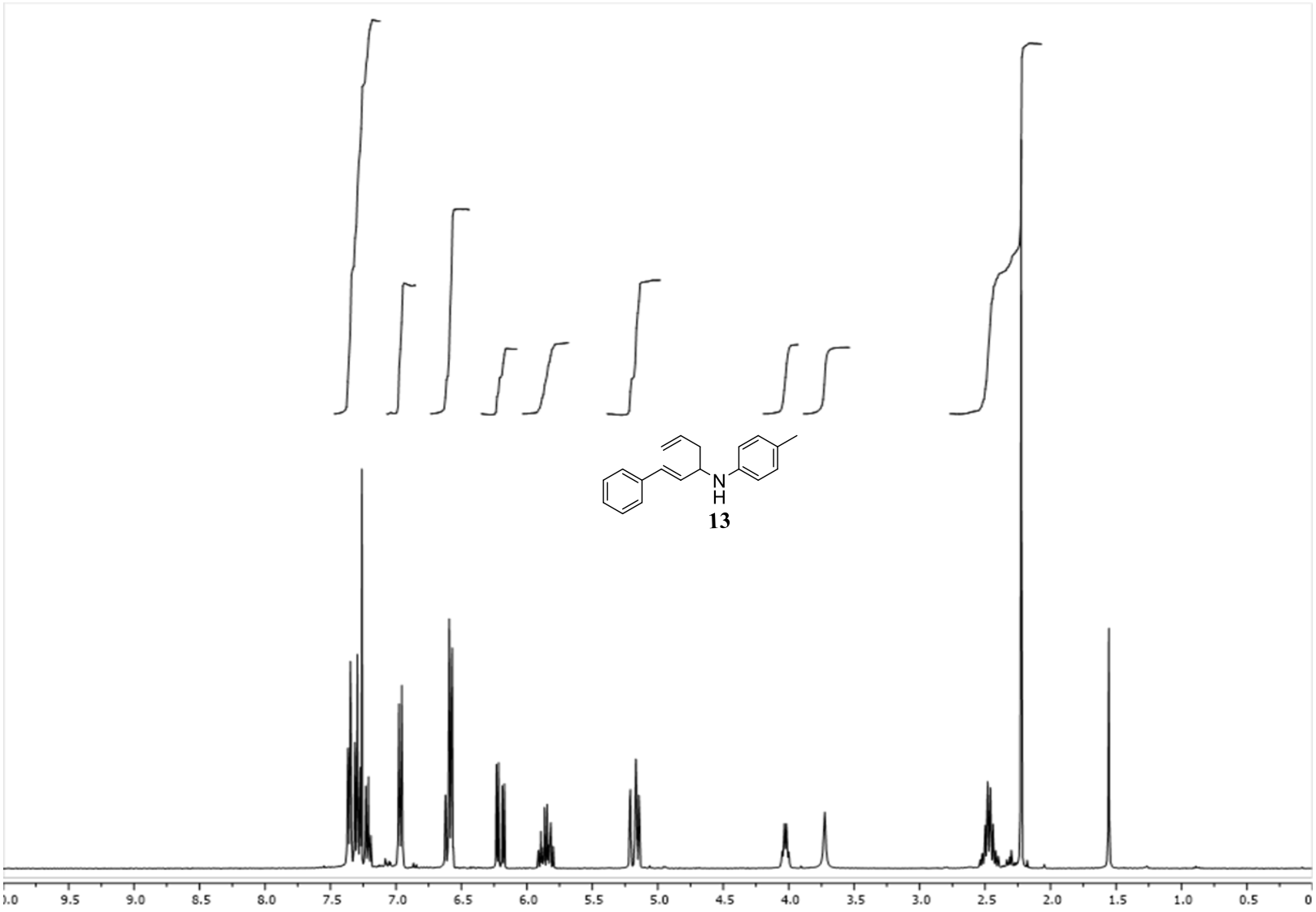

A.64. ^{1}H NMR spectrum (360 MHz) of **13** in $CDCl_3$

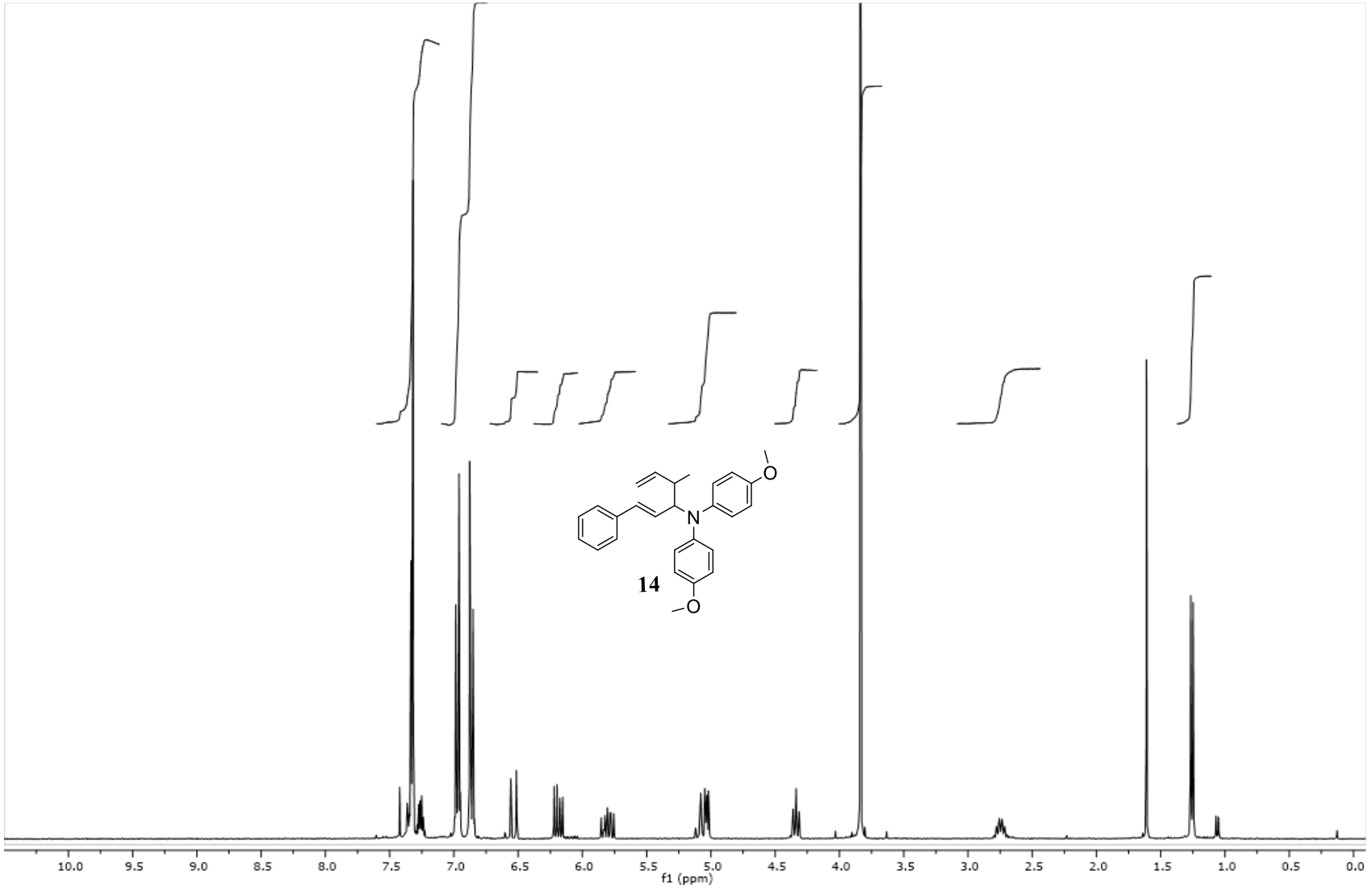

A.65. ^{1}H NMR spectrum (360 MHz) of **14** in $CDCl_3$

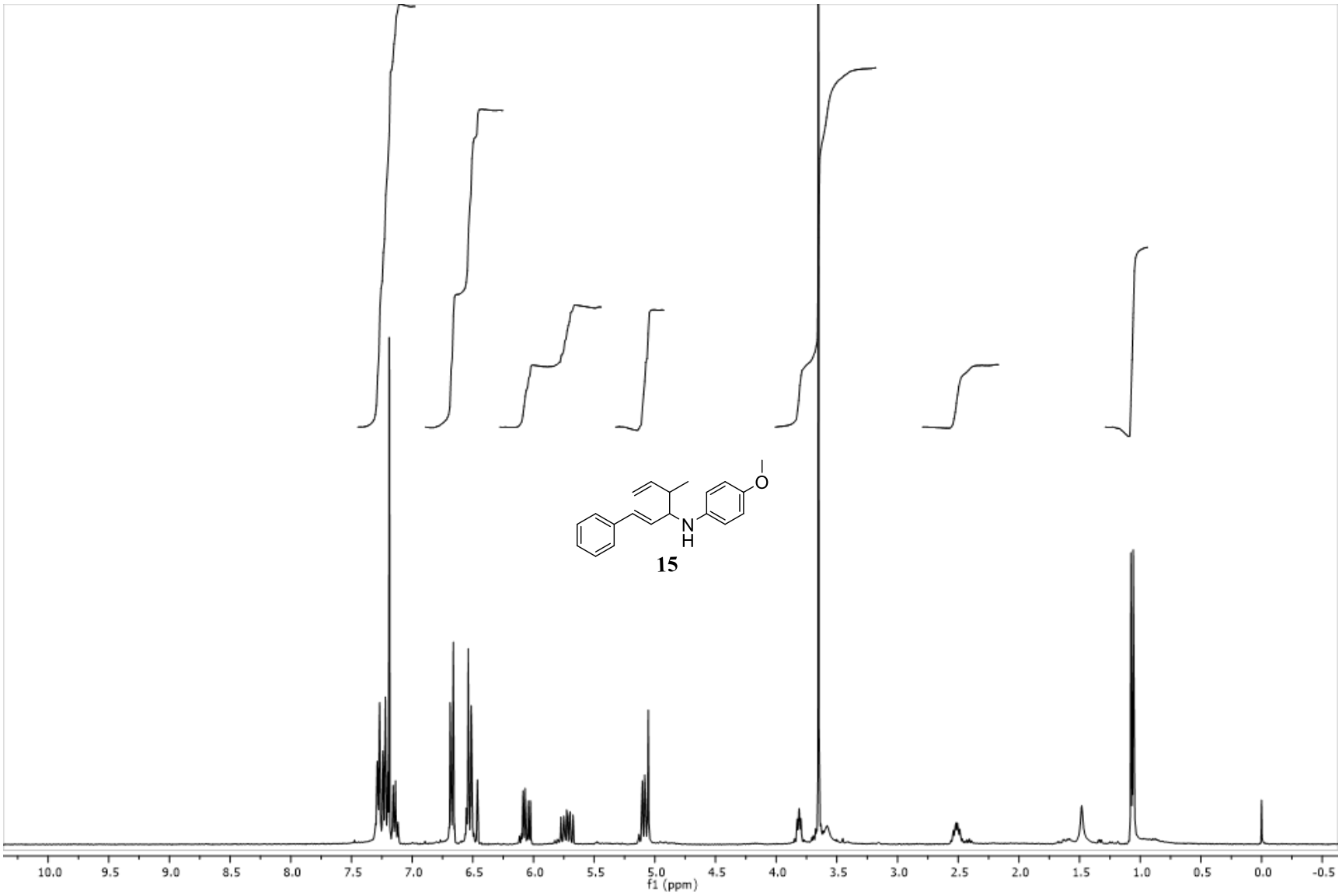

A.66. ^{1}H NMR spectrum (360 MHz) of **15** in $CDCl_3$

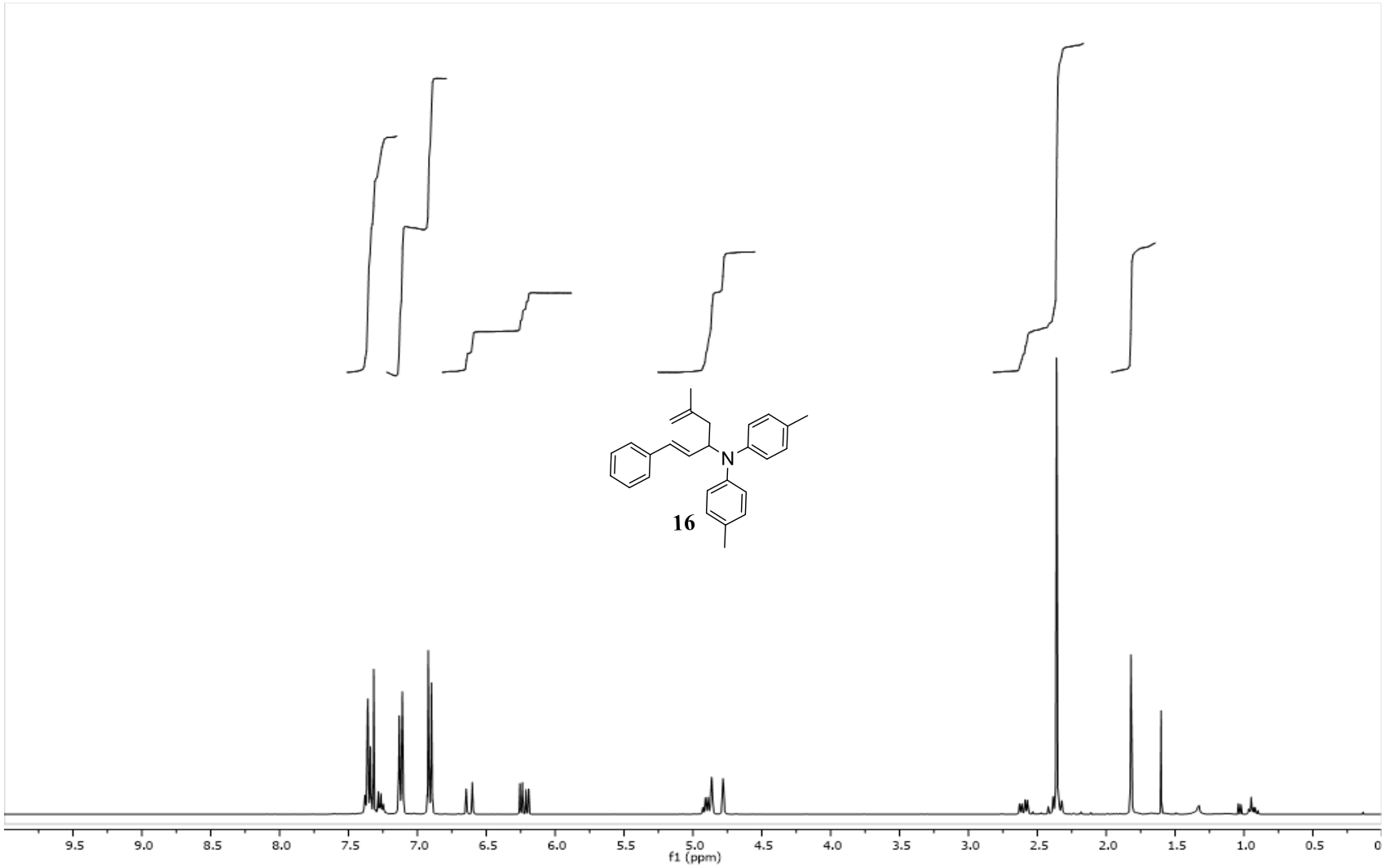

A.67. ^{1}H NMR spectrum (360 MHz) of **16** in $CDCl_3$

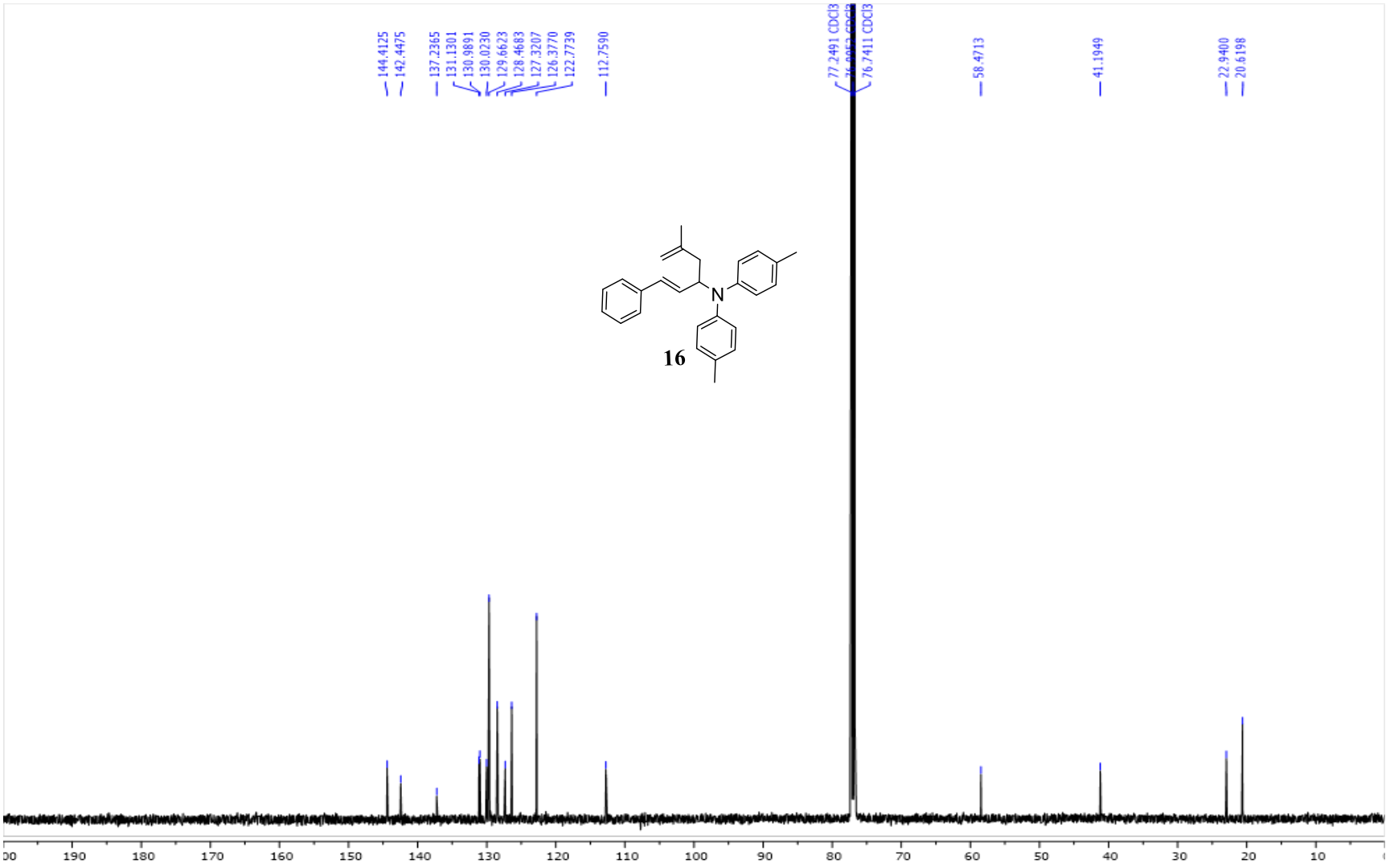

A.68. ^{13}C NMR spectrum (125 MHz) of **16** in

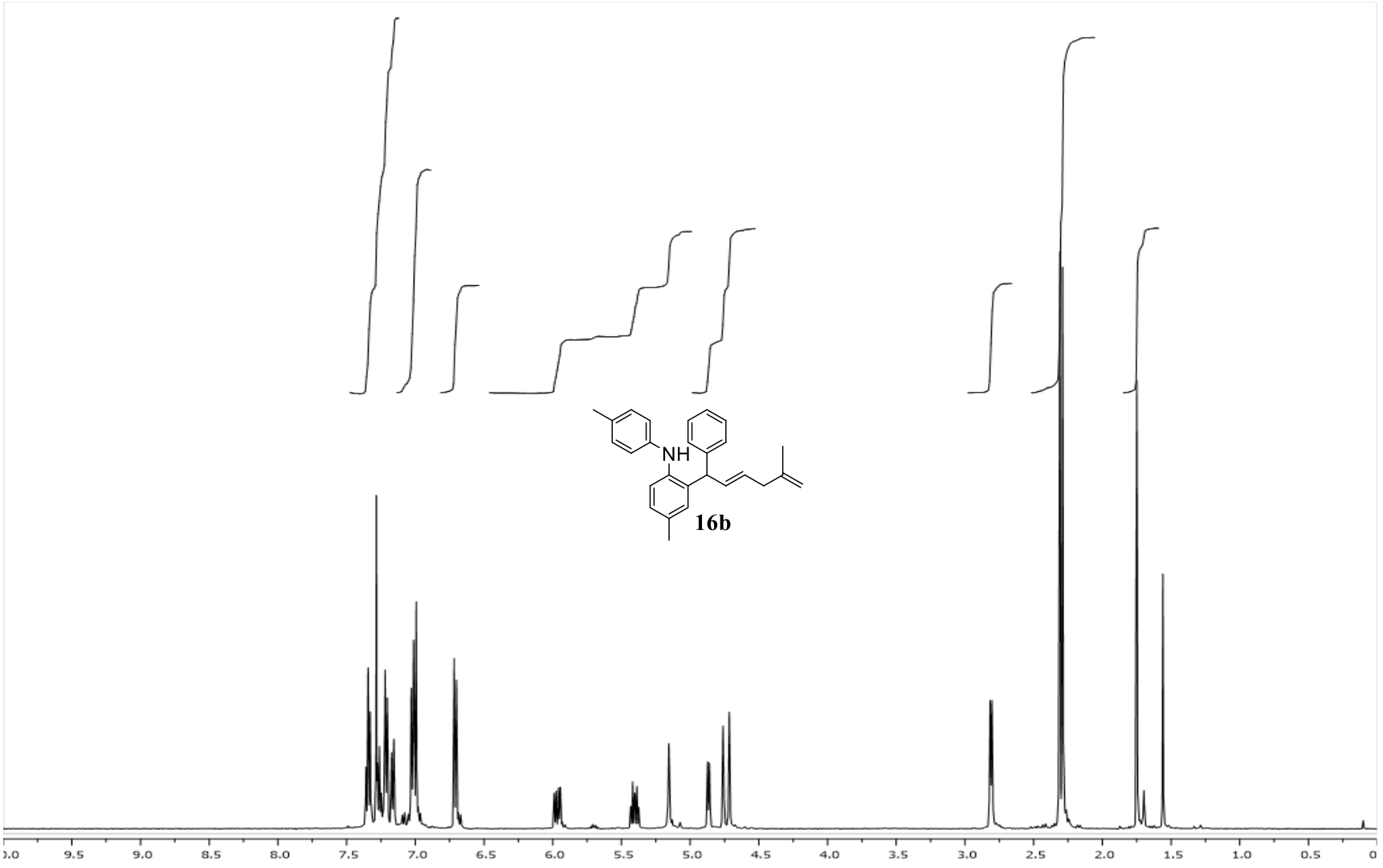

A.69. ^{1}H NMR spectrum (360 MHz) of **16b** in $CDCl_3$

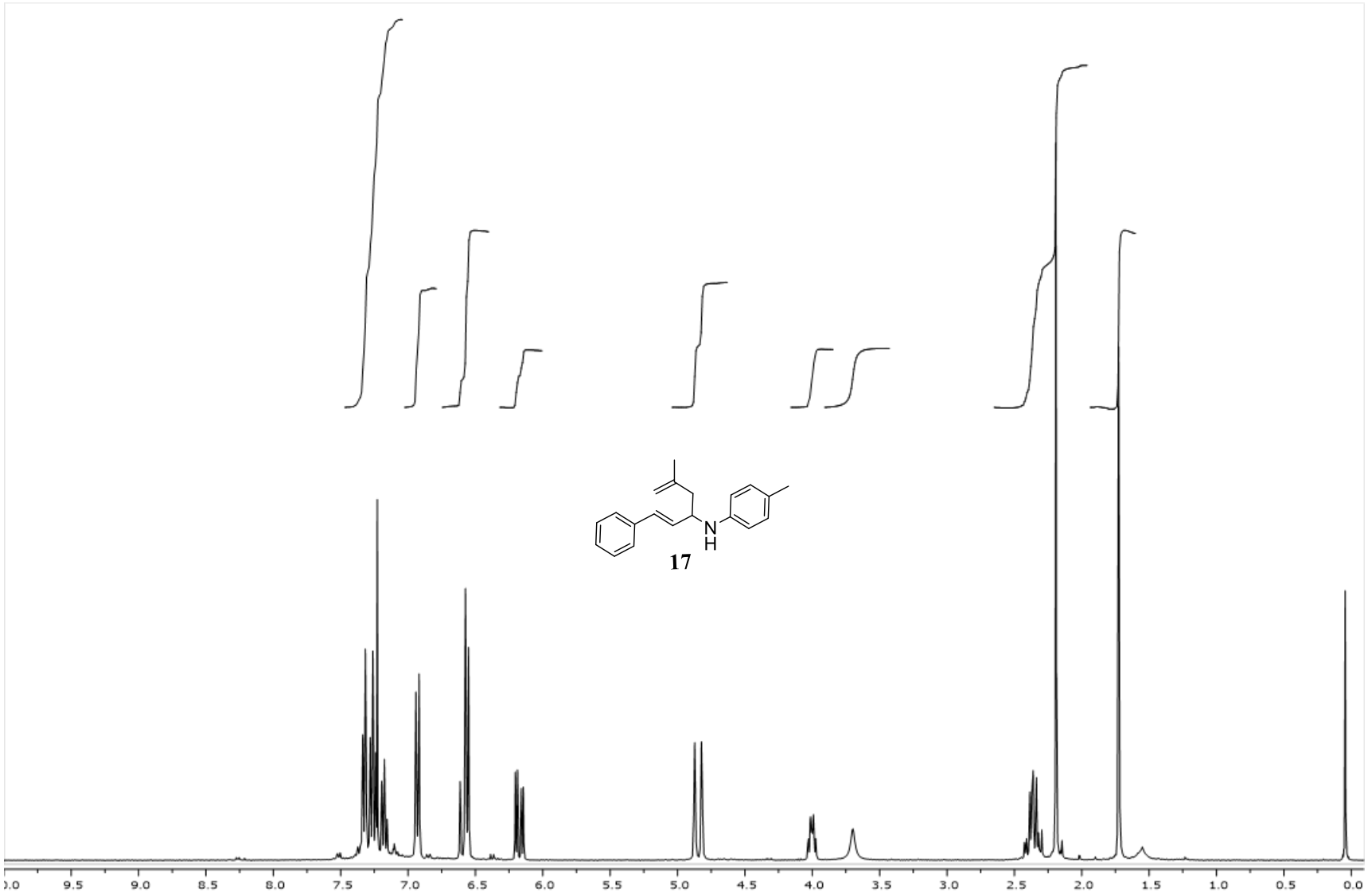

A.70. ^{1}H NMR spectrum (360 MHz) of **17** in $CDCl_3$

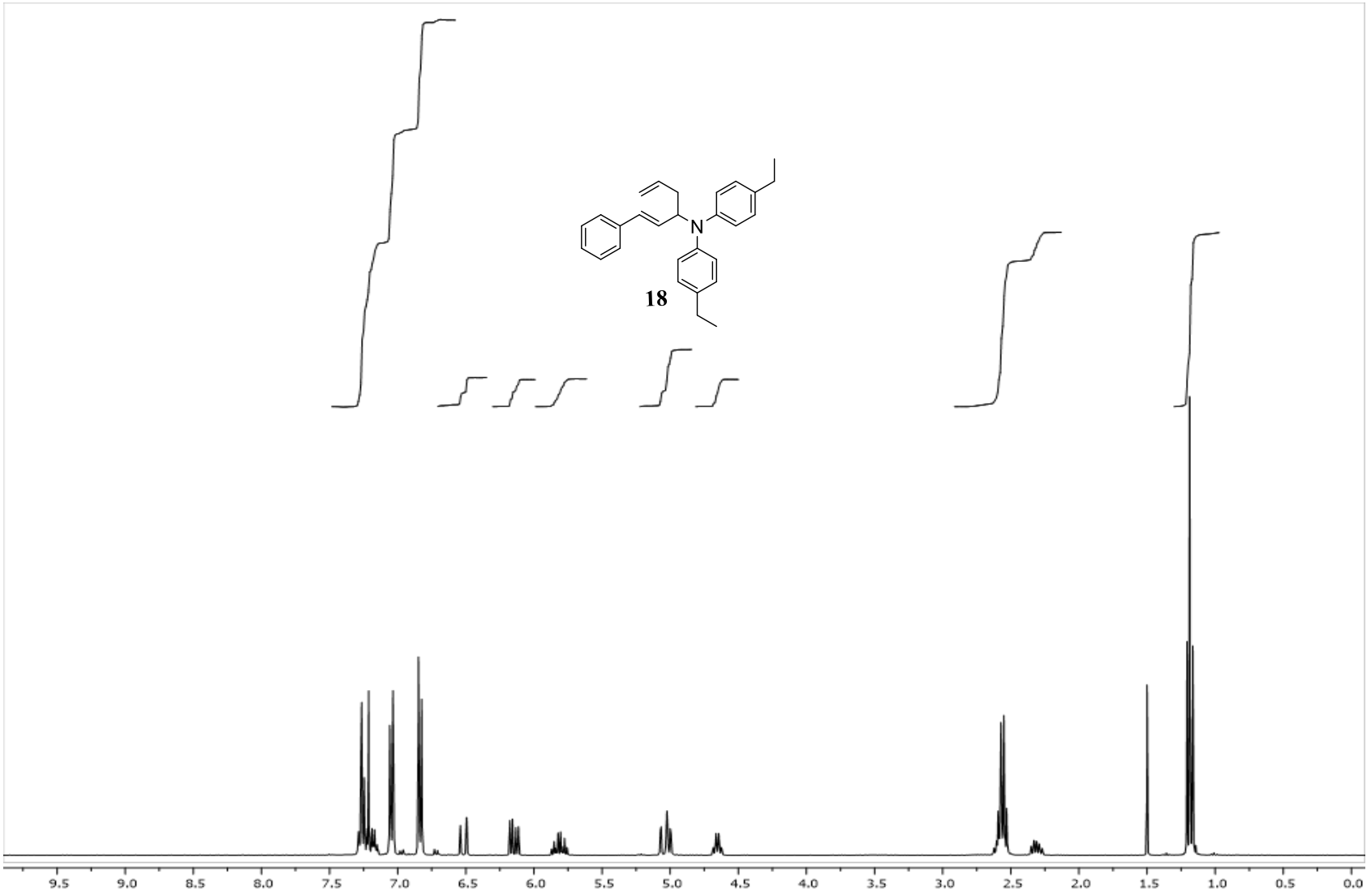

A.71. ^{1}H NMR spectrum (360 MHz) of **18** in $CDCl_3$

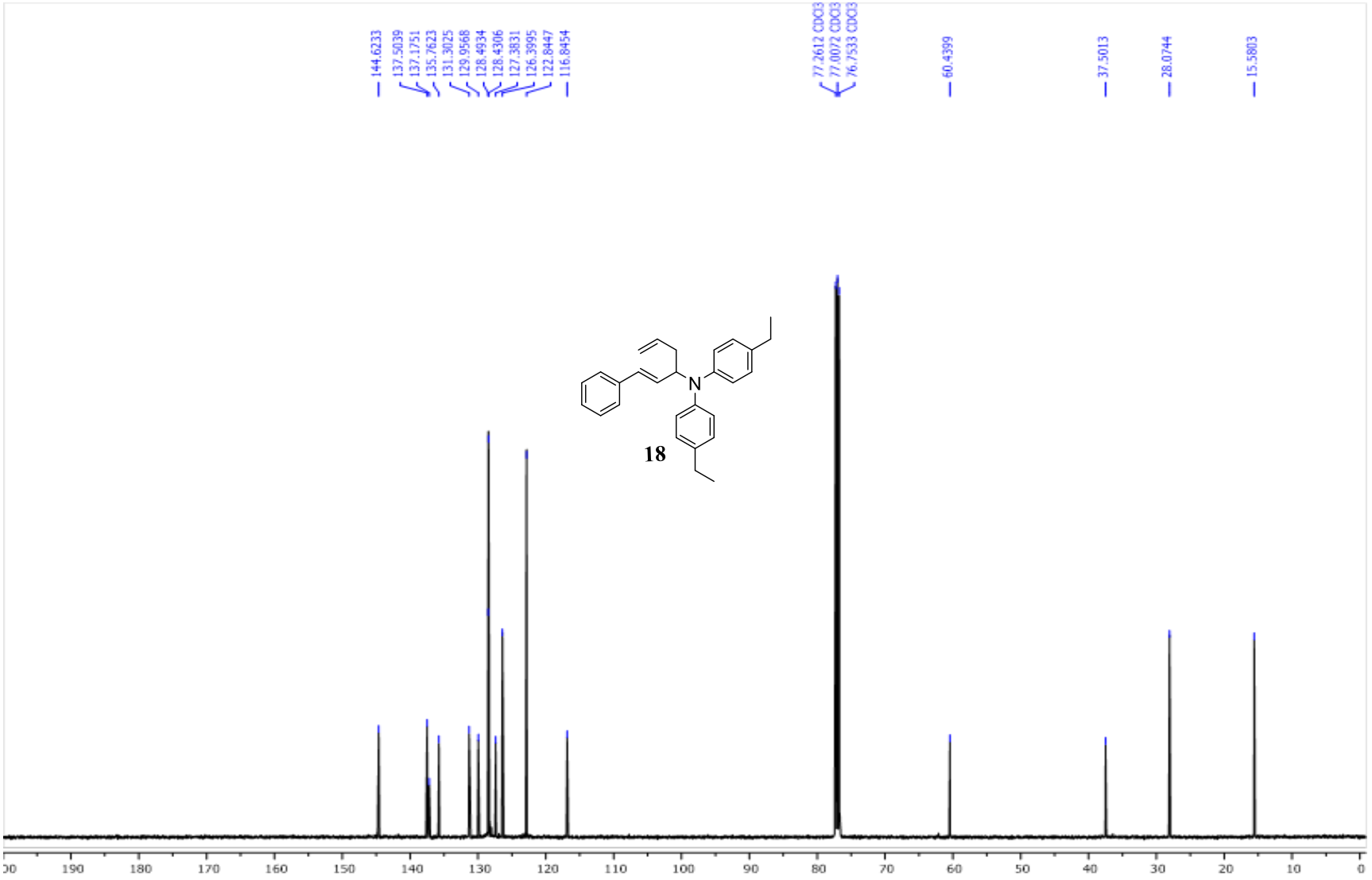

A.72. ^{13}C NMR spectrum (125 MHz) of **18** in $CDCl_3$

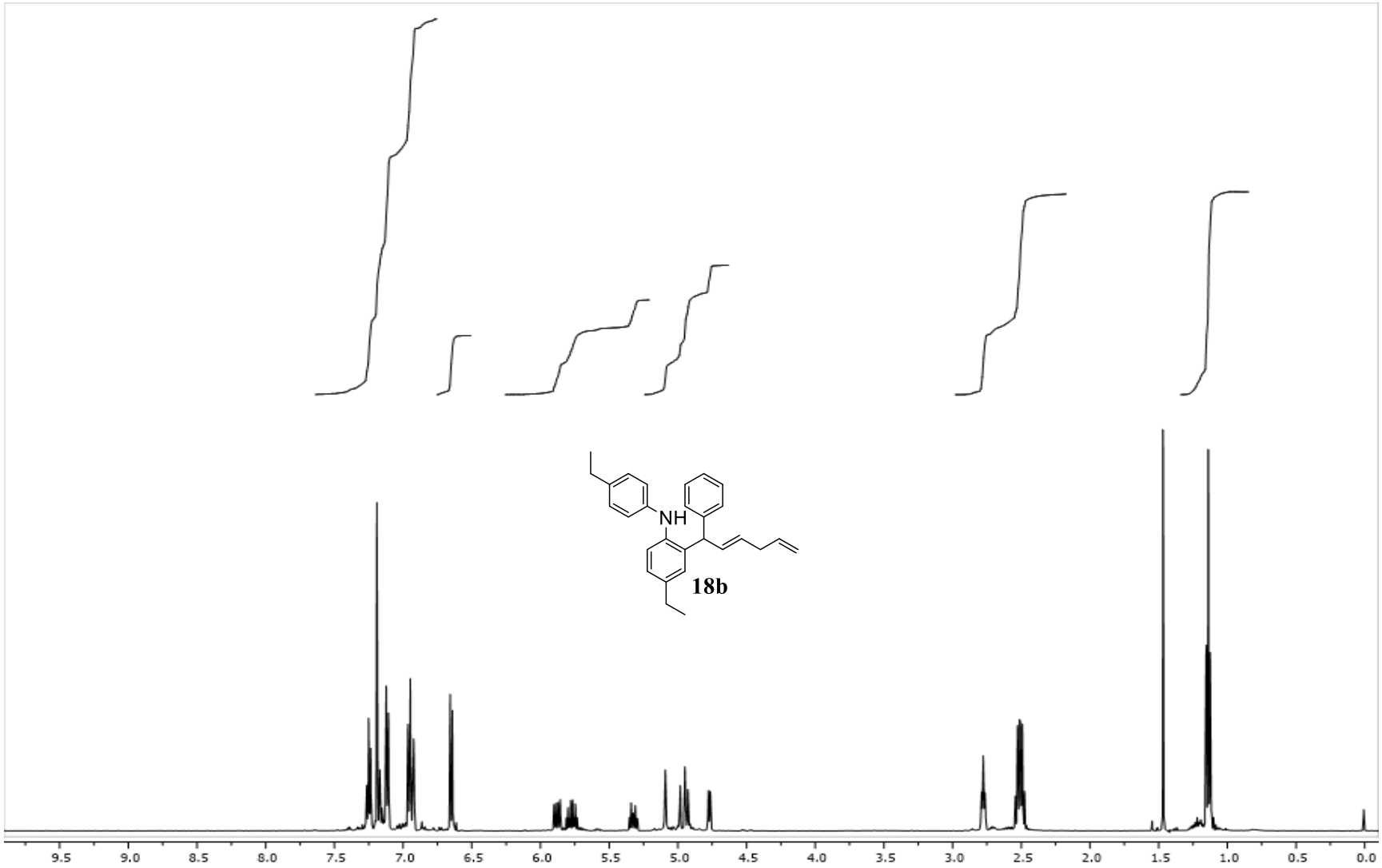

A.73. ^{1}H NMR spectrum (360 MHz) of **18b** in $CDCl_3$

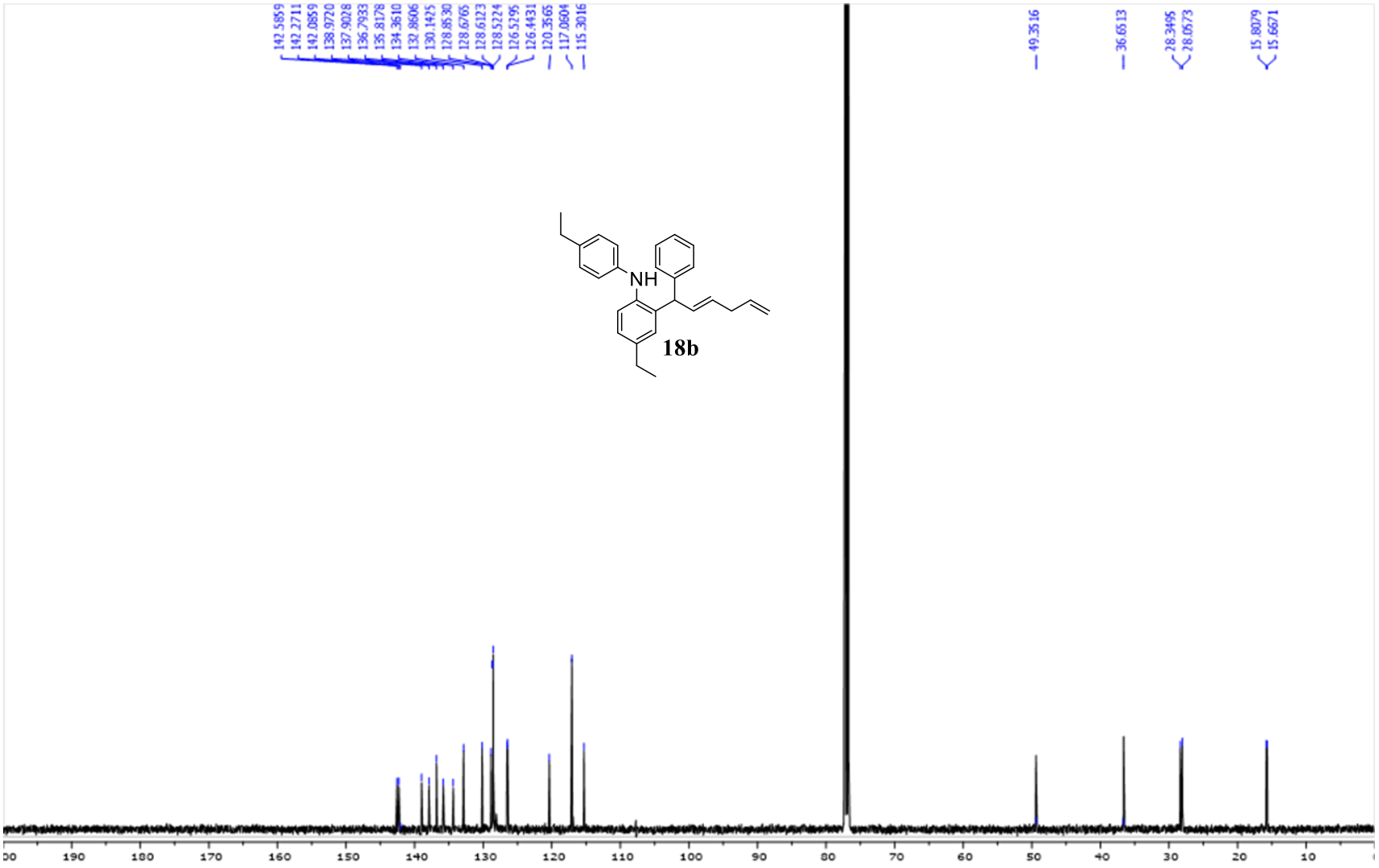

A.74. ^{13}C NMR spectrum (125 MHz) of **18b** in $CDCl_3$

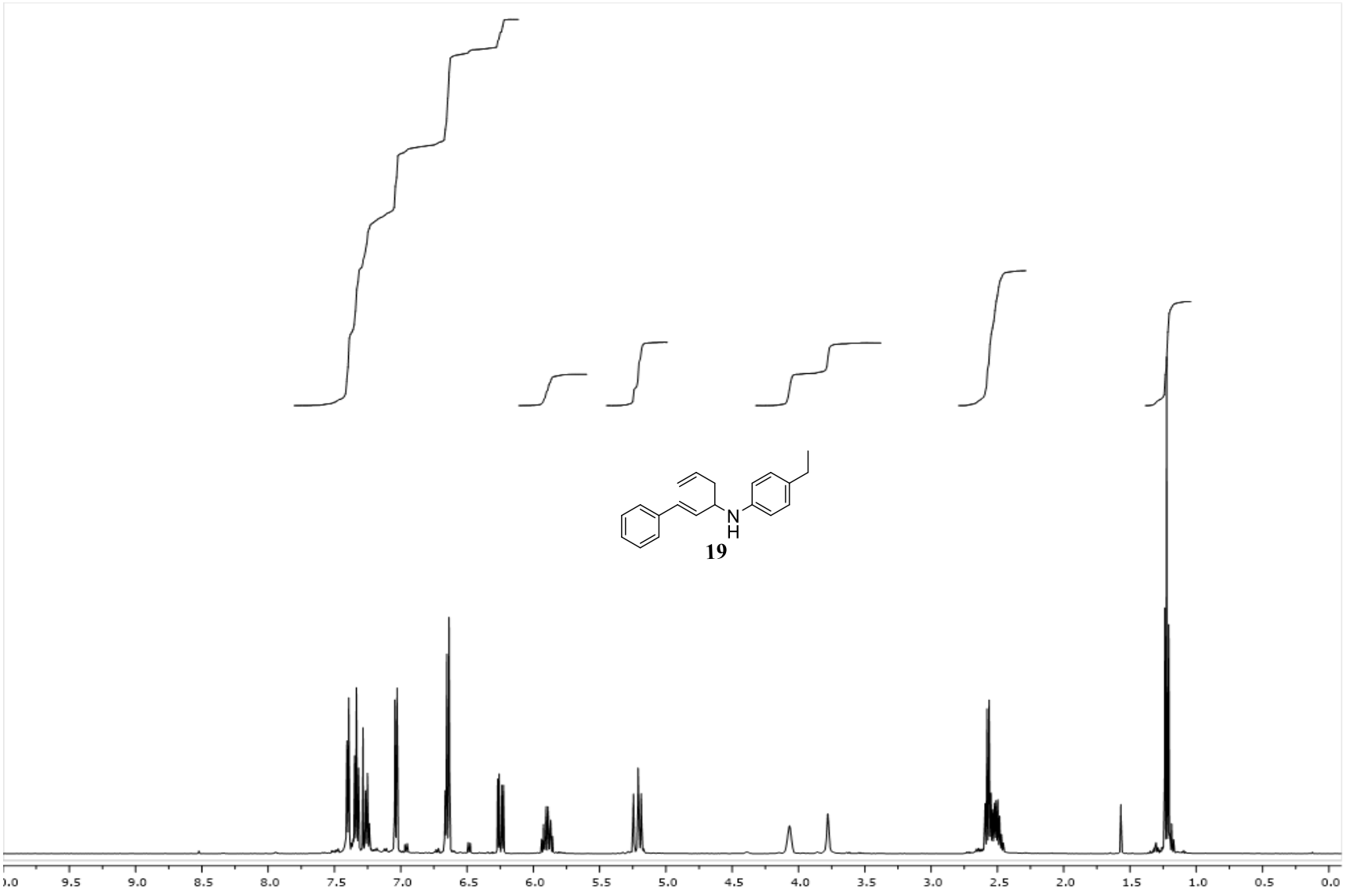

A.75. ^{1}H NMR spectrum (360 MHz) of **19** in $CDCl_3$

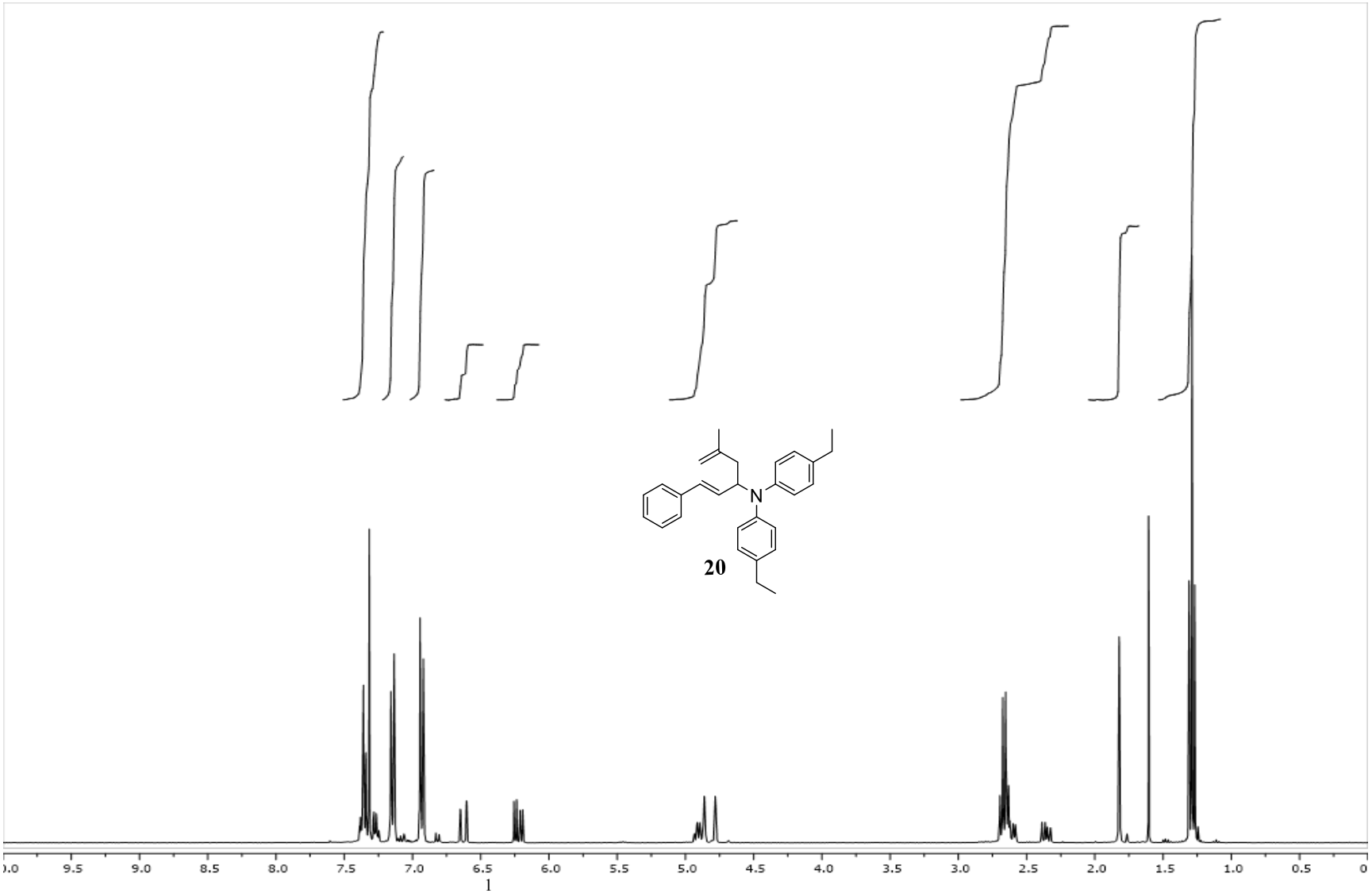

A.76. ^{1}H NMR spectrum (360 MHz) of **20** in $CDCl_3$

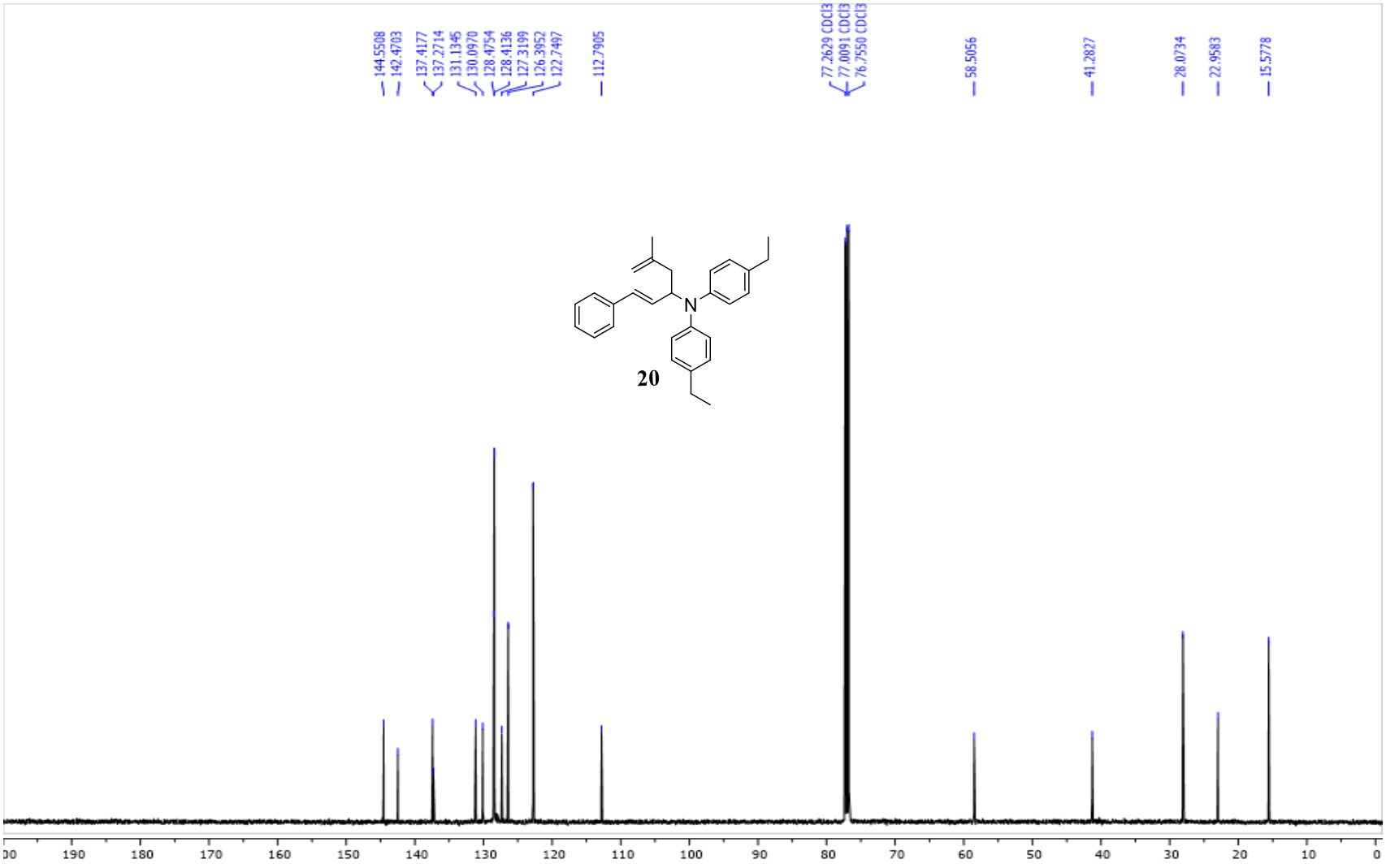

A.77. ^{13}C NMR spectrum (125 MHz) of **20** in $CDCl_3$

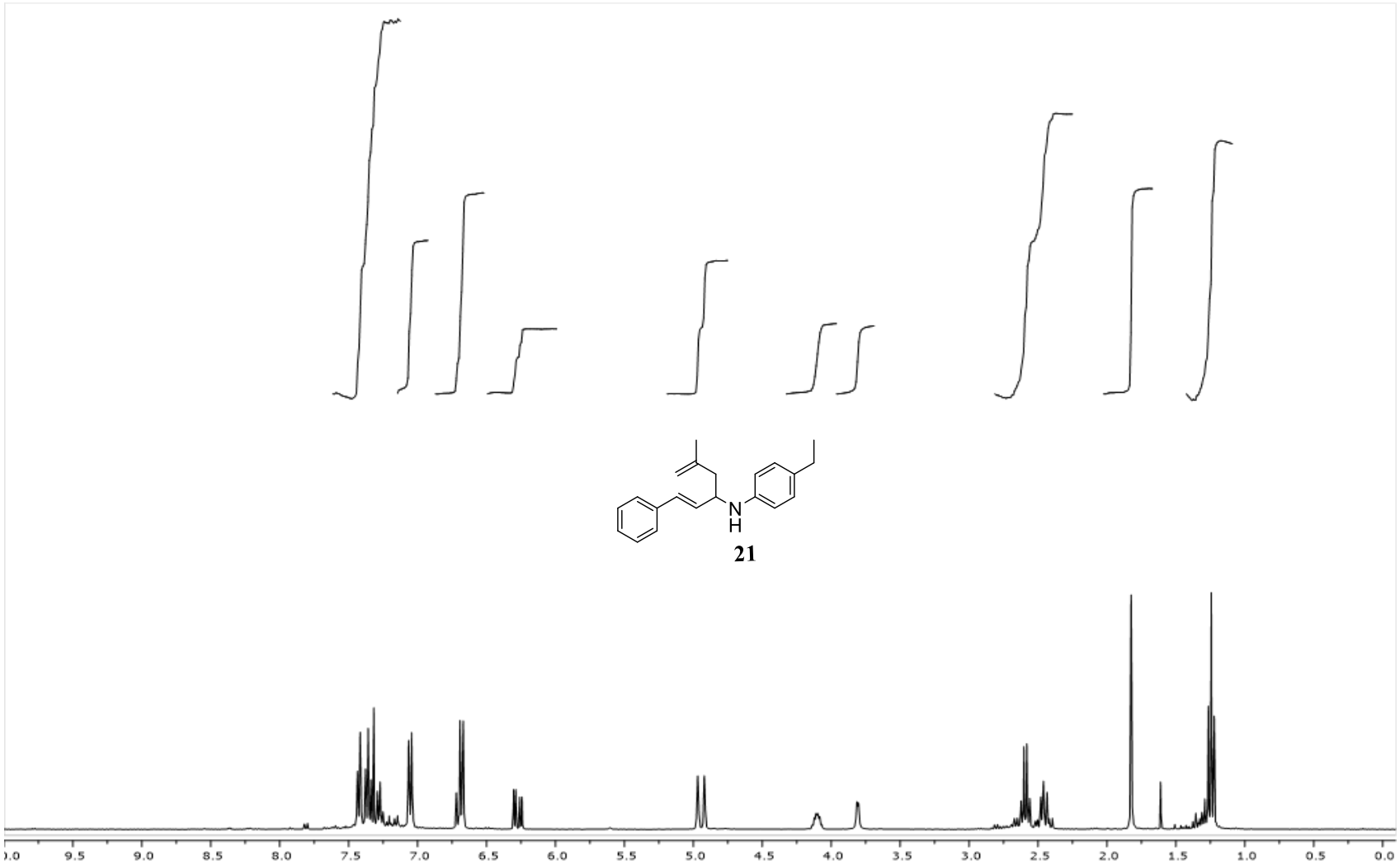

A.78. ^{1}H NMR spectrum (360 MHz) of **21** in $CDCl_3$

APPENDIX B

X-RAY CRYSTALLOGRAPHIC DATA FOR ***trans*-7a**

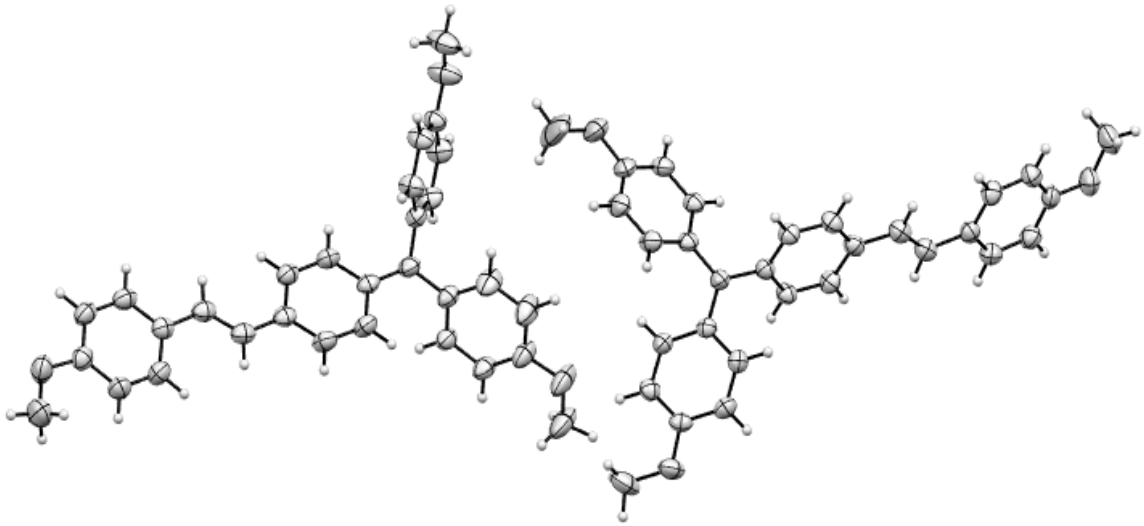

Empirical formula	$C_{29}H_{27}NO_3$
Formula weight	437.53
Temperature	223(2) K
Crystal dimensions (mm)	0.030 x 0.100 x 0.260
Wavelength	0.71073 Å
Crystal system, space group	Triclinic, P-1
Unit cell dimensions	a = 9.9487(14) Å α = 98.8822(18)° b = 11.4364(16) Å β = 89.9943(19)° c = 22.991(3) Å γ = 114.2116(17)°
Volume	2351.4(10) $Å^3$
Z, Calculated density	4, 1.236 mg/m^3

Absorption coefficient	0.080 mm^{-1}
F(000)	928
Theta max	26.105º
Limiting indices	-12<=h<=12, -14<=k<=14, -28<=l<=28
Reflections collected / unique	7099 / 9328 [R(int) = 0.0425]
Completeness to theta = 26.105	99.8 %
Refinement method	Full-matrix least-squares on F^2
Data / restraints / parameters	6351 / 0 / 595
Goodness-of-fit on F^2	1.032
Final R indices [I>2sigma(I)]	R1 = 0.0448, wR2 = 0.1254
R indices (all data)	R1 = 0.0736, wR2 = 0.1254

APPENDIX C

X-RAY CRYSTALLOGRAPHIC DATA FOR ***cis*-7a**

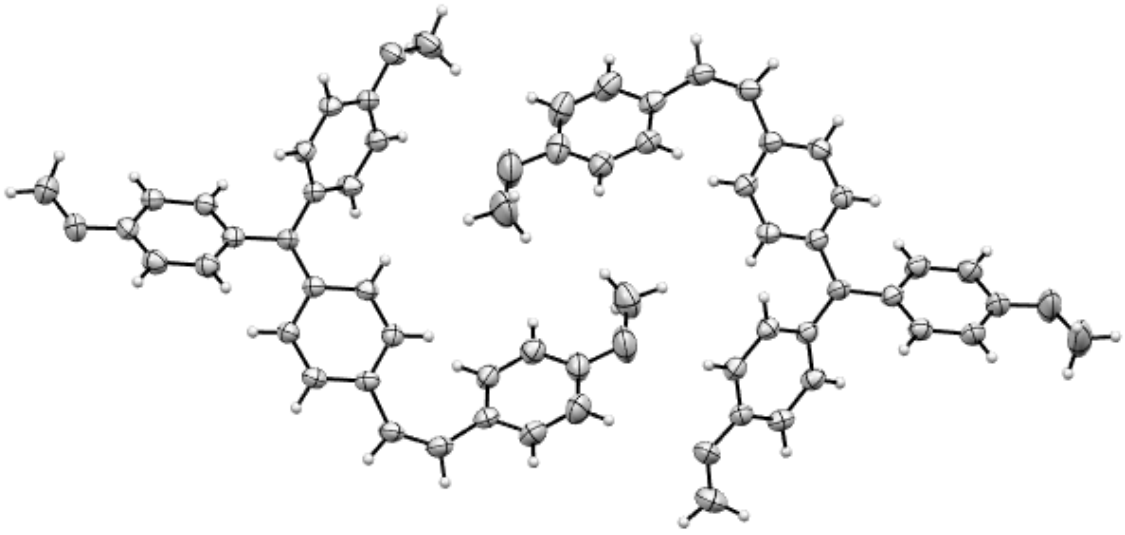

Empirical formula	$C_{29}H_{27}NO_3$
Formula weight	437.53
Temperature	223 K
Crystal dimensions (mm)	0.050 x 0.150 x 0.270
Wavelength	0.71073 Å
Crystal system, space group	Orthorhombic, P n a 21
Unit cell dimensions	a = 8.2483(3) Å α = 90° b = 20.0383(8) Å β = 90° c = 28.6934(11) Å γ = 90°
Volume	4750.1(5) $Å^3$
Z, Calculated density	8, 1.224 mg/m^3

Absorption coefficient	0.079 mm^{-1}
F(000)	1856
Theta max	28.273º
Limiting indices	-26<=h<=26, -38<=k<=38, -11<=l<=11
Reflections collected / unique	8347 / 11053 [R(int) = 0.0419]
Completeness to theta = 28.273	53.4 %
Refinement method	Full-matrix least-squares on F^2
Data / restraints / parameters	6351 / 0 / 595
Goodness-of-fit on F^2	1.02
Final R indices [I>2sigma(I)] R1	0.0448
wR2 (reflections)	0. 0.0539
Npar	602

APPENDIX D

X-RAY CRYSTALLOGRAPHIC DATA FOR ***trans*-7e**

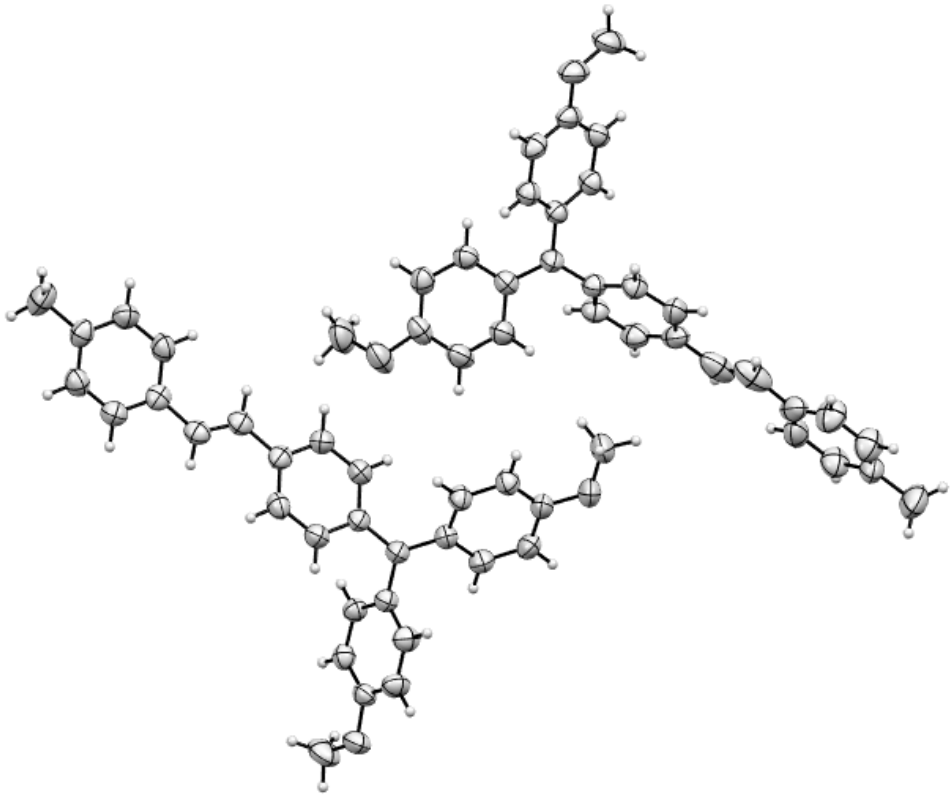

Empirical formula	$C_{29}H_{27}NO_2$
Formula weight	421.52
Temperature	293(2) K
Crystal dimensions (mm)	0.110 x 0.140 x 0.150
Wavelength	0.71073 Å
Crystal system, space group	Triclinic, P-1
Unit cell dimensions	a = 10.277(2) A alpha = 88.41(3) deg.

	b = 12.705(3) A beta = 81.69(3) deg. c = 18.381(4) A gamma = 77.29(3) deg.
Volume	2316.5(8) A^3
Z, Calculated density	4, 1.209 Mg/m^3
Absorption coefficient	0.075 mm^-1
F(000)	896
Theta range for data collection	1.64 to 27.11 deg.
Limiting indices	-13<=h<=13, -16<=k<=16, -23<=l<=23
Reflections collected / unique	70269 / 10185 [R(int) = 0.0390]
Completeness to theta = 27.11	99.5 %
Refinement method	Full-matrix least-squares on F^2
Data / restraints / parameters	10185 / 0 / 578
Goodness-of-fit on F^2	1.632
Final R indices [I>2sigma(I)]	R1 = 0.1123, wR2 = 0.3795
R indices (all data)	R1 = 0.1426, wR2 = 0.4159
Extinction coefficient	0.000(2)
Largest diff. peak and hole	1.462 and -0.408 e.A^-3

APPENDIX E

X-RAY CRYSTALLOGRAPHIC DATA FOR ***trans*-7g**

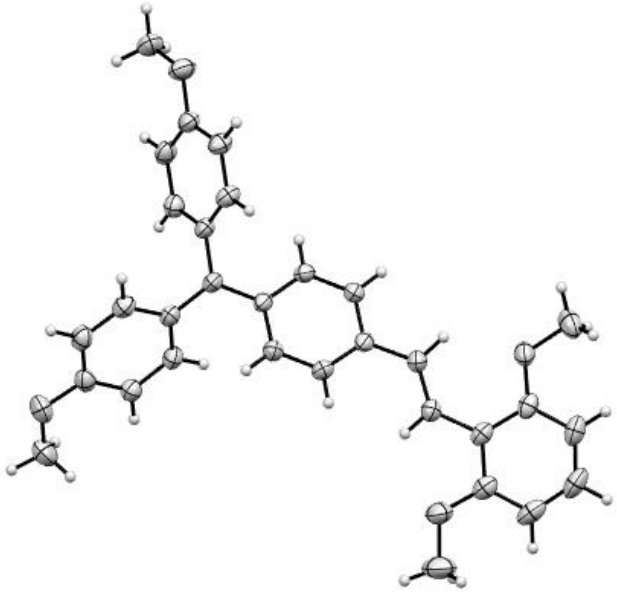

Identification code	***trans*-7g**
Empirical formula	$C_{30}H_{29}NO_4$
Formula weight	467.54
Temperature	293(2) K
Crystal dimensions (mm)	0.210 x 0.240 x 0.300
Wavelength	0.71073 Å
Crystal system, space group	Monoclinic, P2 (1)/C
Unit cell dimensions	a = 10.130(2) A alpha = 90 deg. b = 13.453(3) A beta = 100.10(3) deg. c = 18.394(4) A gamma = 90 deg.

Volume	2467.7(9) A^3
Z, Calculated density	4, 1.258 Mg/m^3
Absorption coefficient	0.083 mm^-1
F(000)	992
Theta range for data collection	1.89 to 27.22 deg.
Limiting indices	-12<=h<=13, -17<=k<=17, -23<=l<=23
Reflections collected / unique	56837 / 5486 [R(int) = 0.0292]
Completeness to theta =	27.22 99.7 %
Refinement method	Full-matrix least-squares on F^2
Data / restraints / parameters	5486 / 0 / 317
Goodness-of-fit on F^2	1.017
Final R indices [I>2sigma(I)]	R1 = 0.0401, wR2 = 0.1099
R indices (all data)	R1 = 0.0478, wR2 = 0.1175
Extinction coefficient	0.0060(9)
Largest diff. peak and hole	0.410 and -0.198 e.A^-3

APPENDIX F

EMISSION SPECTRUM OF 395-410 nm LED (7W)

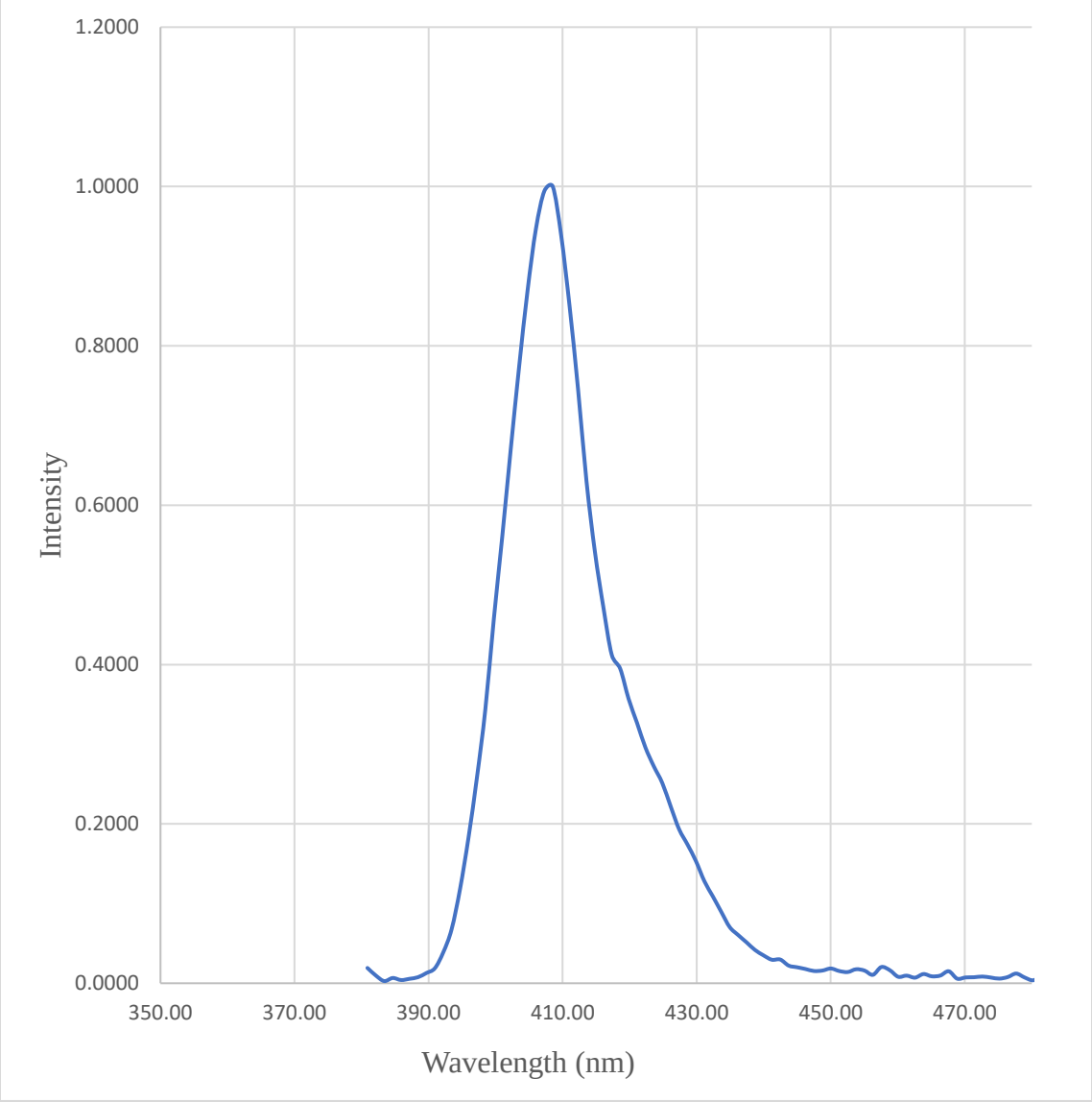

APPENDIX G

EMISSION SPECTRUM OF 430 nm LED (7W)

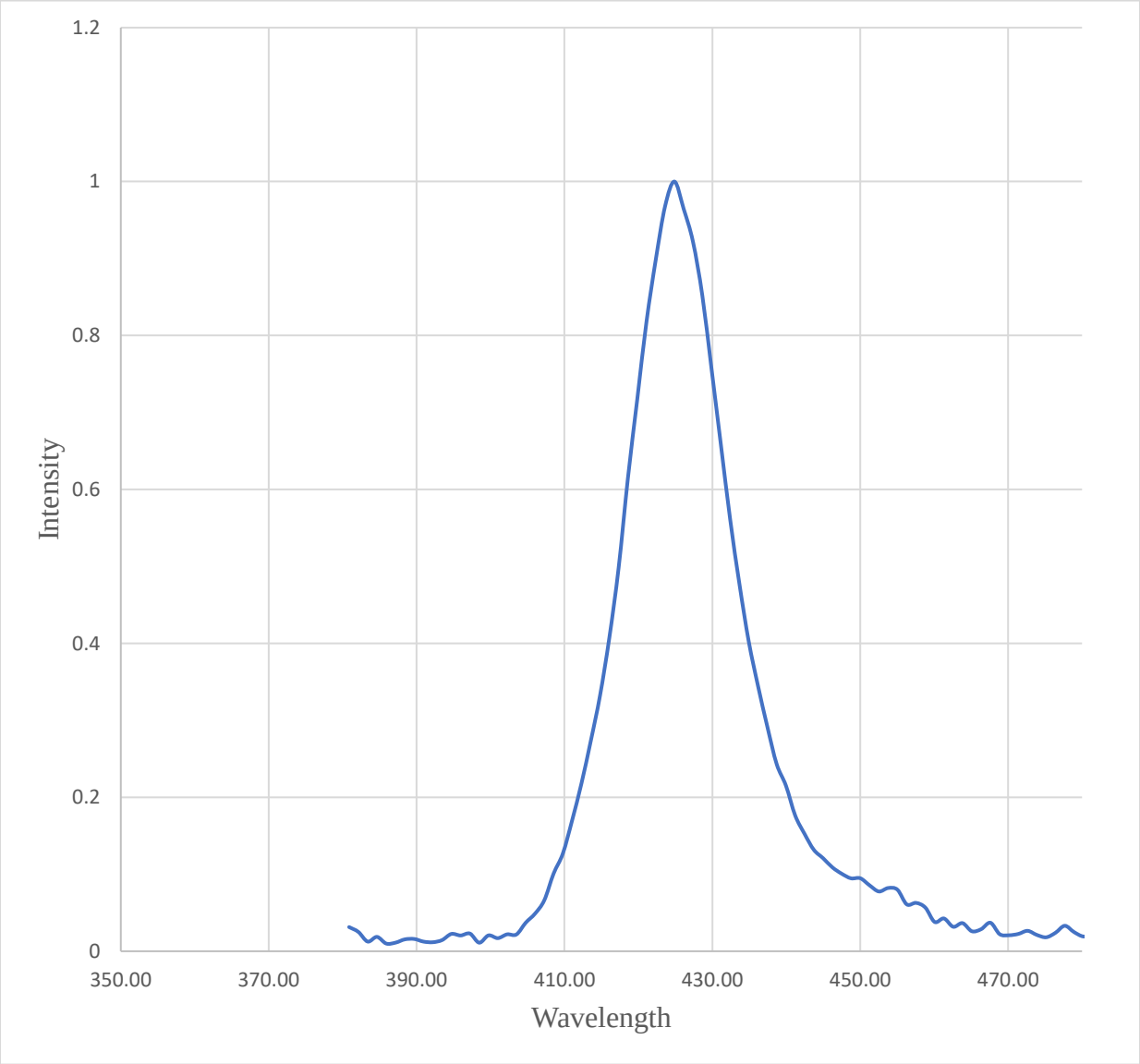

APPENDIX H

THERMAL ISOMERIZATION DATA FOR 0.0731 M ***cis*-7a-e**

H.1 Thermal isomerization of 0.0731 M ***cis*-7a** in DMSO at 150 °C.

H.2. Graph of ln[***cis*-7a**] vs time at 150 ºC.

H.3. Thermal isomerization of 0.0731 M ***cis*-7a** in DMSO at 130 °C.

H.4. Graph of ln[***cis*-7a**] vs time at 130 ºC.

H.5. Thermal isomerization of 0.0731 M ***cis*-7b** in DMSO at 150 °C.

H.6. Graph of ln[***cis*-7b**] vs time at 150 ºC.

H.7. Activation parameters of the thermal isomerization of ***cis*-7b** in DMSO

H.8. Thermal isomerization of 0.0731 M ***cis*-7c** in DMSO at 150 °C

H.9. Graph of ln[***cis*-7c**] vs time at 150 ºC.

H.10. Activation parameters of the thermal isomerization of ***cis*-7c** in DMSO.

H.11. Thermal isomerization of ***cis*-7d** in DMSO at 150 °C.

H.12. Graph of ln[***cis*-7d**] vs time at 150 ºC.

H.13. Thermal isomerization of ***cis*-7d** in DMSO at 135 °C

H.14. Graph of ln[***cis*-7d**] vs time at 135 ºC.

H.15. Activation parameters of the thermal isomerization of ***cis*-7d** in DMSO.

H.16. Thermal isomerization of ***cis*-7e** in DMSO at 150 °C

H.17. Graph of ln[***cis*-7e**] vs time at 150 ºC.

Time (minutes)	*cis* %	[*cis*]	ln[*cis*]
0	95.6	0.0699	-2.66
45	88.3	0.0645	-2.74
90	75.3	0.0550	-2.90
150	64.0	0.0468	-3.06
240	52.2	0.0382	-3.27
305	44.0	0.0321	-3.44
520	21.7	0.0159	-4.14
810	9.27	0.00678	-4.99

H.1 Thermal isomerization of 0.0731 M ***cis*-7a** in DMSO at 150 °C.

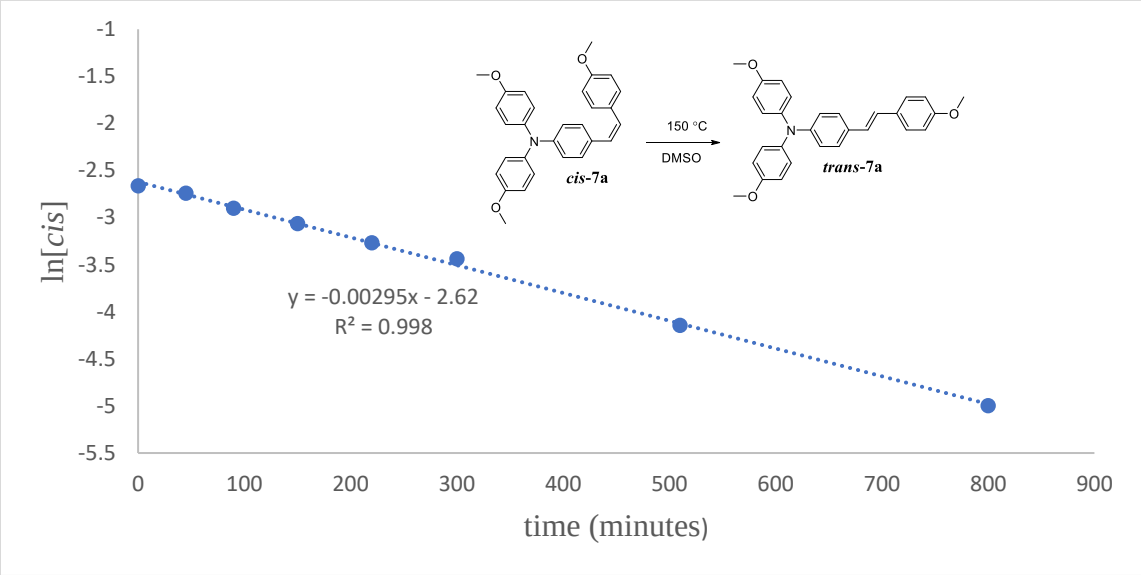

H.2. Graph of ln[***cis*-7a**] vs time at 150 ºC.

$k = 4.92 \pm 0.20 \times 10^{-5}\ s^{-1}$

$\Delta G^{\ddagger} = 33.4 \pm 0.8$ kcal/mol

Time (minutes)	% *cis*	[*cis*]	ln [*cis*]
0	95.6	0.0699	-4.20
210	90.4	0.0661	-4.25
310	84.4	0.0617	-4.32
547	75.2	0.0550	-4.43
1190	52.1	0.0381	-4.80
1890	38.4	0.0281	-5.10
2450	28.1	0.0205	-5.42
2780	24.6	0.0180	-5.55
3540	13.5	0.00987	-6.15

H.3. Thermal isomerization of 0.0731 M ***cis*-7a** in DMSO at 130 °C.

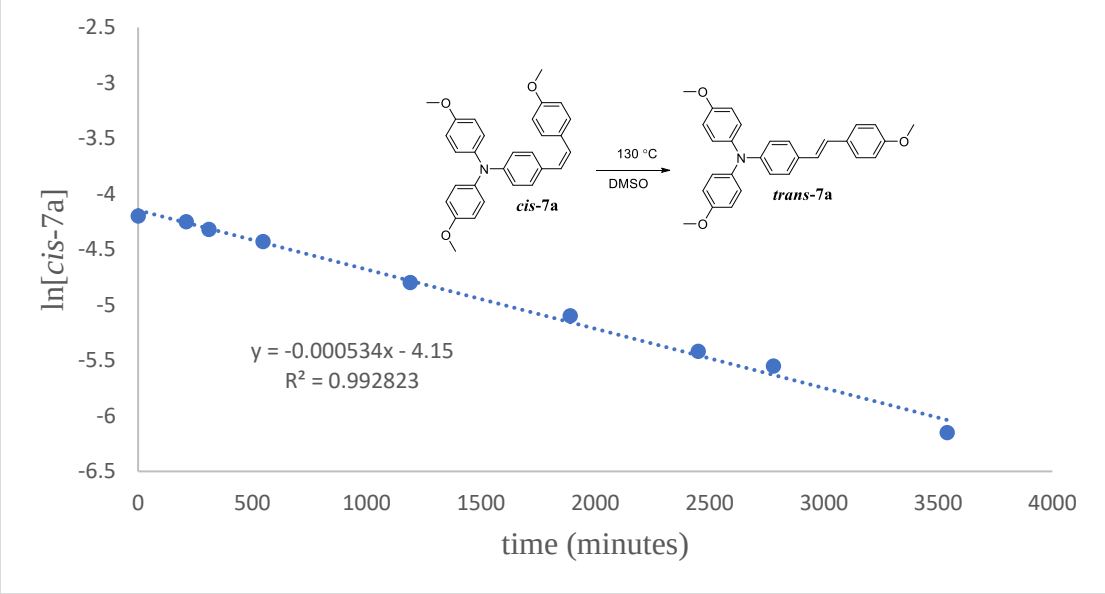

H.4. Graph of ln[***cis*-7a**] vs time at 130 ºC.

$k_{423K} = 8.90 \pm 0.04 \times 10^{-5}\ s^{-1}$

$\Delta G^{\ddagger}_{423K} = 33.6$ kcal/mol

Time (minutes)	% *cis*	[*cis*]	ln[*cis*]
0	97.2	0.0711	-2.64
60	84.2	0.0616	-2.79
200	75.6	0.0553	-2.90
320	67.3	0.0492	-3.01
550	49.2	0.0360	-3.32
805	27.6	0.0202	-3.90
1150	7.71	0.00564	-5.18

H.5. Thermal isomerization of 0.0731 M ***cis*-7b** in DMSO at 150 °C.

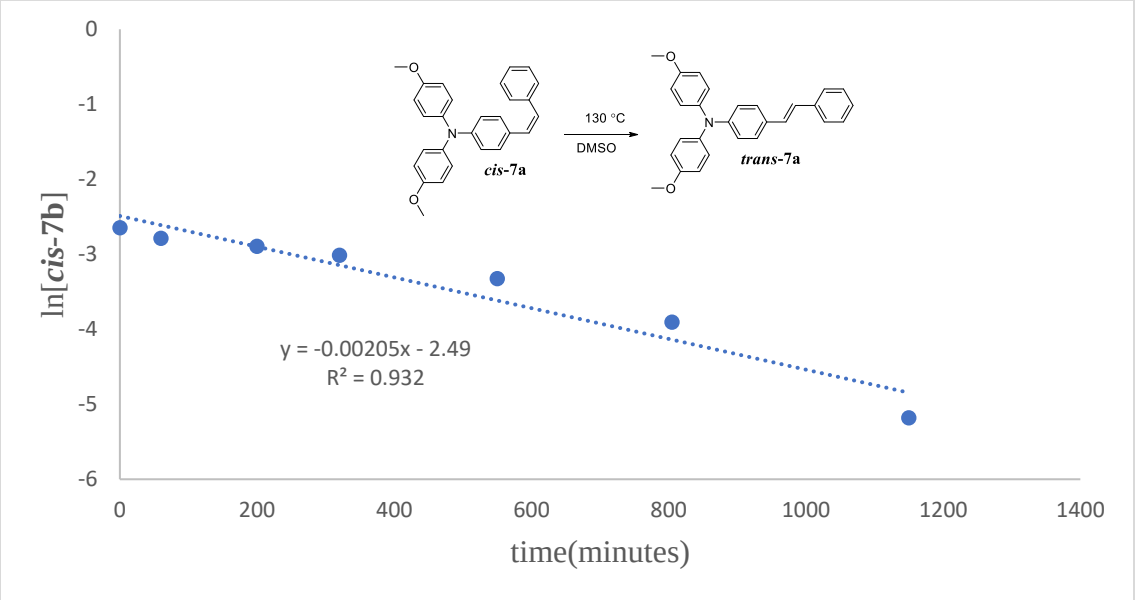

H.6. Graph of ln[***cis*-7b**] vs time at 150 ºC.

k_{423K} = 3.41 ± 0.10 x 10^{-5} s^{-1}

$\Delta G^{\ddagger}_{423K}$ = 33.7 ± 1.1 kcal/mol

Activation parameters	Experimental Values
$\Delta H^{\ddagger}$	21.1 ± 0.3 kcal/mol
$\Delta S^{\ddagger}$	-29.8 ± 1 cal mol^{-1} K^{-1}
$\Delta G^{\ddagger}_{413K}$	33.4 ± 1.1 kcal/mol

H.7. Activation parameters of the thermal isomerization of ***cis*-7b** in DMSO.

Time(minutes)	% *cis*	[*cis*]	ln [*cis*]
0	97.2	0.0711	-2.64
60	84.3	0.0616	-2.79
150	74.5	0.0545	-2.91
380	42.1	0.0308	-3.48
625	25.4	0.0186	-3.99
700	16.5	0.0121	-4.42
1092	2.49	0.00182	-6.31

H.8. Thermal isomerization of 0.0731 M ***cis*-7c** in DMSO at 150 °C

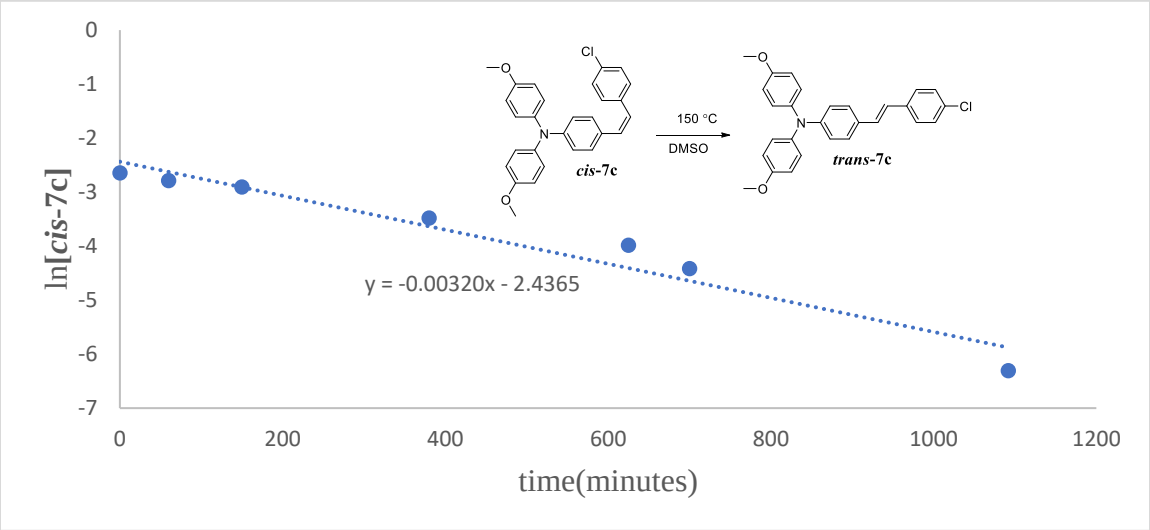

H.9. Graph of ln[***cis*-7c**] vs time at 150 ºC.

k_{423K} = 5.33 ± 0.10 x 10^{-5} s^{-1}

$\Delta G^{\ddagger}_{423K}$ = 33.3 ± 0.1 kcal/mol

Activation parameters	Experimental Values
$\Delta H^{\ddagger}$	18.8 ± 0.3 kcal/mol
$\Delta S^{\ddagger}$	-34.4 ± 1 cal mol^{-1} K^{-1}
$\Delta G^{\ddagger}_{413K}$	33.0 ± 1.1 kcal/mol

H.10. Activation parameters of the thermal isomerization of ***cis*-7c** in DMSO.

Time(minutes)	% *cis*	[*cis*]	ln[*cis*]
0	92.6	0.0677	-2.69
50	84.3	0.0616	-2.79
130	55.9	0.0409	-3.20
250	47.4	0.0346	-3.36
550	31.9	0.0233	-3.76
755	21.7	0.0159	-4.14
1220	4.01	0.00293	-5.83
1630	1.02	0.000746	-7.20

H.11. Thermal isomerization of ***cis*-7d** in DMSO at 150 °C.

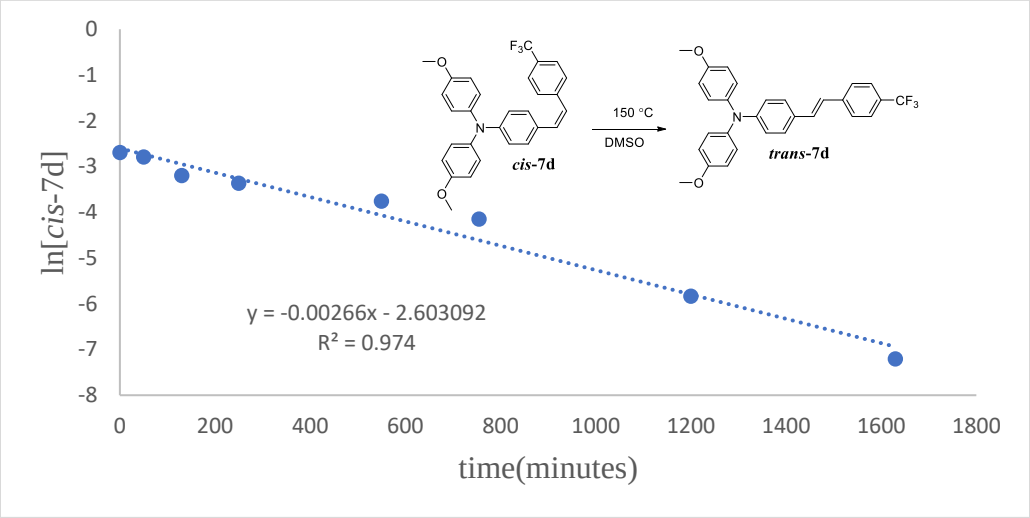

H.12. Graph of ln[***cis*-7d**] vs time at 150 ºC.

k_{423K} = 4.43 ± 0.20 x 10^{-5} s^{-1}

$\Delta G^{\ddagger}_{423K}$ = 33.5 ± 0.8 kcal/mol

Time (minutes)	% *cis*	[*cis*]	ln[*cis*]
0	92.6	0.0677	-2.69
50	75.4	0.0551	-2.90
80	72.9	0.0532	-2.93
130	69.9	0.0511	-2.97
250	63.3	0.0463	-3.07
550	45.5	0.0333	-3.40
1095	21.9	0.0160	-4.13
2170	5.33	0.00390	-5.55

H.13. Thermal isomerization of ***cis*-7d** in DMSO at 135 °C

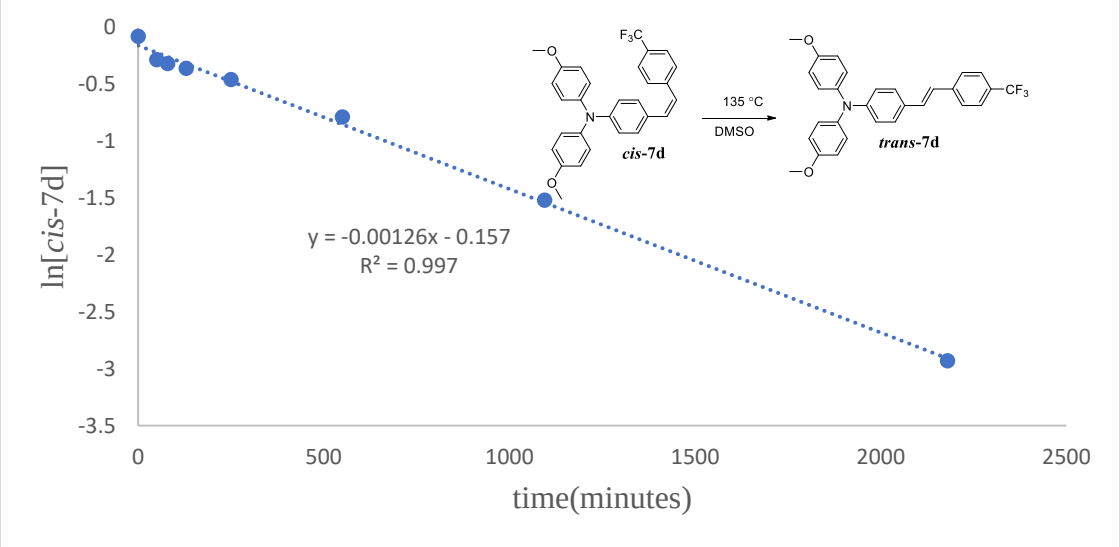

H.14. Graph of ln[***cis*-7d**] vs time at 135 ºC.

$k_{423K} = 2.10 \pm 0.20 \times 10^{-5}\ s^{-1}$

$\Delta G^{\ddagger}_{408K} = 32.9 \pm 0.8$ kcal/mol

Activation parameters	Experimental Values
$\Delta H^{\ddagger}$	17.1 ± 0.3 kcal/mol
$\Delta S^{\ddagger}$	-38.7 ± 1 cal mol^{-1} K^{-1}
$\Delta G^{\ddagger}_{413K}$	33.1 ± 1.1 kcal/mol

H.15. Activation parameters of the thermal isomerization of ***cis*-7d** in DMSO.

Time (minutes)	% cis	ln [cis]	ln(k)
0	95.6	0.0699	-2.66
30	90.1	0.0659	-2.72
60	83.4	0.0610	-2.80
120	74.3	0.0543	-2.91
220	53.1	0.0388	-3.25
360	38.5	0.0281	-3.57
420	30.7	0.0224	-3.80
510	22.3	0.0163	-4.12

H.16. Thermal isomerization of ***cis*-7e** in DMSO at 150 °C

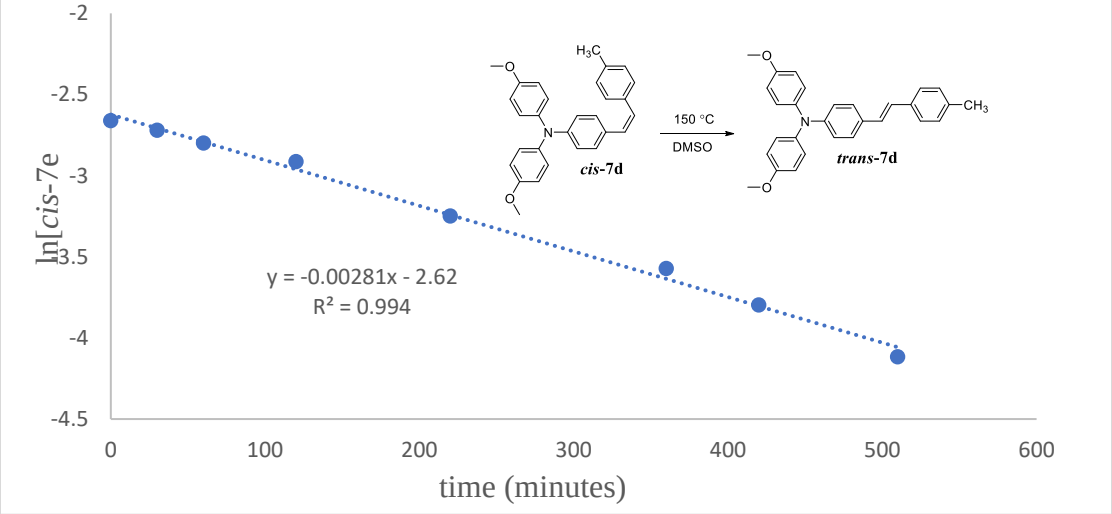

H.17. Graph of ln[***cis*-7e**] vs time at 150 ºC.

k_{423K} = 4.68 ± 0.20 x 10^{-5} s^{-1}

$\Delta G^{\ddagger}_{423K}$ = 33.4 ± 0.8 kcal/mol

APPENDIX I

RADICAL ISOMERIZATION DATA FOR ***cis*-7a**

I.1. RA promoted *cis-trans* isomerization of 3.05 x 10^{-5} M ***cis*-7a** in cyclohexane: benzene =98:2 using 6 mol % CRET in DCM at 30 ºC

I.4. First order plot of the ln[***cis*-7a**] vs time at 30 ºC for the redox auxiliary promoted *cis-trans* isomerization of ***cis*-7a** in cyclohexane: benzene =98:2 using 6 mol % CRET in DCM.

I.3. RA promoted *cis-trans* isomerization of 3.05 x 10^{-5} M ***cis*-7a** in cyclohexane: benzene =98:2 using 7 mol % CRET in DCM at 30 ºC

I.4. First order plot of the ln[***cis*-7a**] vs time at 30 ºC for the redox auxiliary promoted *cis-trans* isomerization of ***cis*-7a** in cyclohexane: benzene =98:2 using 7 mol % CRET in DCM.

I.5. RA promoted *cis-trans* isomerization of 3.05 x 10^{-5} M ***cis*-7a** in cyclohexane: benzene =98:2 using 8 mol % CRET in DCM at 30 ºC

I.6. First order plot of the ln**[*cis*-7a**] vs time at 30 ºC for the redox auxiliary promoted *cis-trans* isomerization of ***cis*-7a** in cyclohexane: benzene = 98:2 using 8 mol % CRET in DCM.

I.7. RA promoted *cis-trans* isomerization of 3.05 x 10^{-5} M ***cis*-7a** in cyclohexane: benzene =98:2 using 9 mol % CRET in DCM at 30 ºC

I.8. First order plot of the ln**[*cis*-7a**] vs time at 30 ºC for the redox auxiliary promoted *cis-trans* isomerization of ***cis*-7a** in cyclohexane: benzene = 98:2 using 9 mol % CRET in DCM.

I.9. RA promoted *cis-trans* isomerization of 3.05 x 10^{-5} M ***cis*-7a** in cyclohexane: benzene =98:2 using 10 mol % CRET in DCM at 30 ºC

I.10. First order plot of the ln[***cis*-7a**] vs time at 30 ºC for the redox auxiliary promoted *cis-trans* isomerization of ***cis*-7a** in cyclohexane: benzene =98:2 using 10 mol % CRET in DCM.

I.11. RA promoted *cis-trans* isomerization of 3.05 x 10^{-5} M ***cis*-7a** in cyclohexane: benzene =98:2 using 5 mol % CRET in DCM at 25 ºC

I.12. First order plot of the ln[***cis*-7a**] vs time at 25 ºC for the redox auxiliary promoted *cis-trans* isomerization of ***cis*-7a** in cyclohexane: benzene =98:2 using 5 mol % CRET in DCM.

I.13 RA promoted *cis-trans* isomerization of 3.05 x 10^{-5} M ***cis*-7a** in cyclohexane: benzene =98:2 using 5 mol % CRET in DCM at 35 ºC.

I.14 First order plot of the ln[***cis*-7a**] vs time at 35 ºC for the redox auxiliary promoted *cis-trans* isomerization of ***cis*-7a** in cyclohexane: benzene =98:2 using 5 mol % CRET in DCM.

I.15 RA promoted *cis-trans* isomerization of 3.05 x 10^{-5} M ***cis*-7a** in cyclohexane: benzene =98:2 using 5 mol % CRET in DCM at 40 ºC.

I.16 First order plot of the ln[***cis*-7a**] vs time at 40 ºC for the redox auxiliary promoted *cis-trans* isomerization of ***cis*-7a** in cyclohexane: benzene =98:2 using 5 mol % CRET in DCM.

I.17 RA promoted *cis-trans* isomerization of 3.05 x 10^{-5} M ***cis*-7a** in cyclohexane: benzene =98:2 using 5 mol % CRET in DCM at 45 ºC.

I.18 First order plot of the ln[***cis*-7a**] vs time at 45 ºC for the redox auxiliary promoted *cis-trans* isomerization of ***cis*-7a** in cyclohexane: benzene =98:2 using 5 mol % CRET in DCM.

Time(s)	% cis	[*cis*]	ln[*cis*]
0	91.6	2.77 E-05	-10.5
4	42.5	1.28 E-05	-11.3
12	23.0	6.95 E-06	-11.9
20	11.8	3.57 E-06	-12.5
28	3.81	1.15 E-06	-13.7
36	2.24	6.77 E-07	-14.2
44	0.567	1.71 E-07	-15.6

I.1 RA promoted *cis-trans* isomerization of 3.05 x 10^{-5} M ***cis*-7a** in cyclohexane: benzene =98:2 using 6 mol % CRET in DCM at 30 ºC

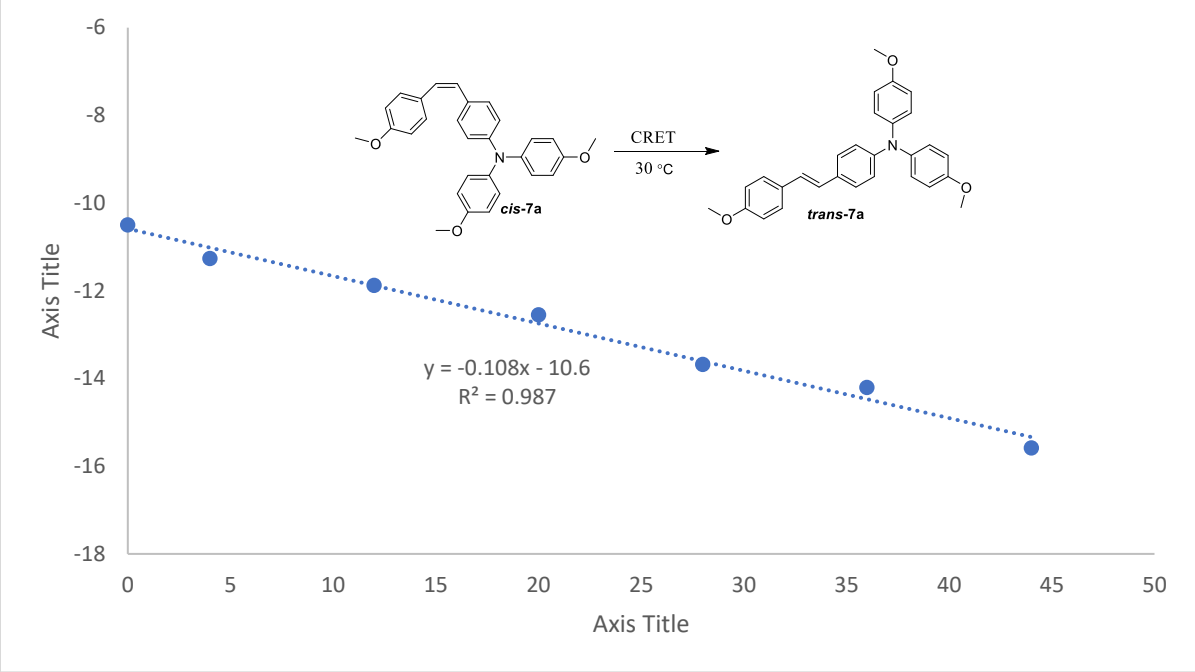

I.2. First order plot of the ln[***cis*-7a**] vs time at 30 ºC for the redox auxiliary promoted *cis-trans* isomerization of ***cis*-7a** in cyclohexane: benzene =98:2 using 6 mol % CRET in DCM.

Time (s)	% *cis*	[*cis*]	ln[*cis*]
0	91.2	2.75 E-05	-10.5
3	53.8	1.63 E-05	-11.0
6	33.7	1.02 E-05	-11.5
9	24.0	7.16 E-06	-11.8
12	17.8	5.36 E-06	-12.1
15	12.7	3.85 E-06	-12.5
18	9.31	2.81 E-06	-12.8
21	7.12	2.15 E-06	-13.0
24	5.38	1.62 E-06	-13.3
27	2.45	7.39 E-07	-14.1

I.3. RA promoted *cis-trans* isomerization of 3.05 x 10^{-5} M ***cis*-7a** in cyclohexane: benzene =98:2 using 7 mol % CRET in DCM at 30 ºC

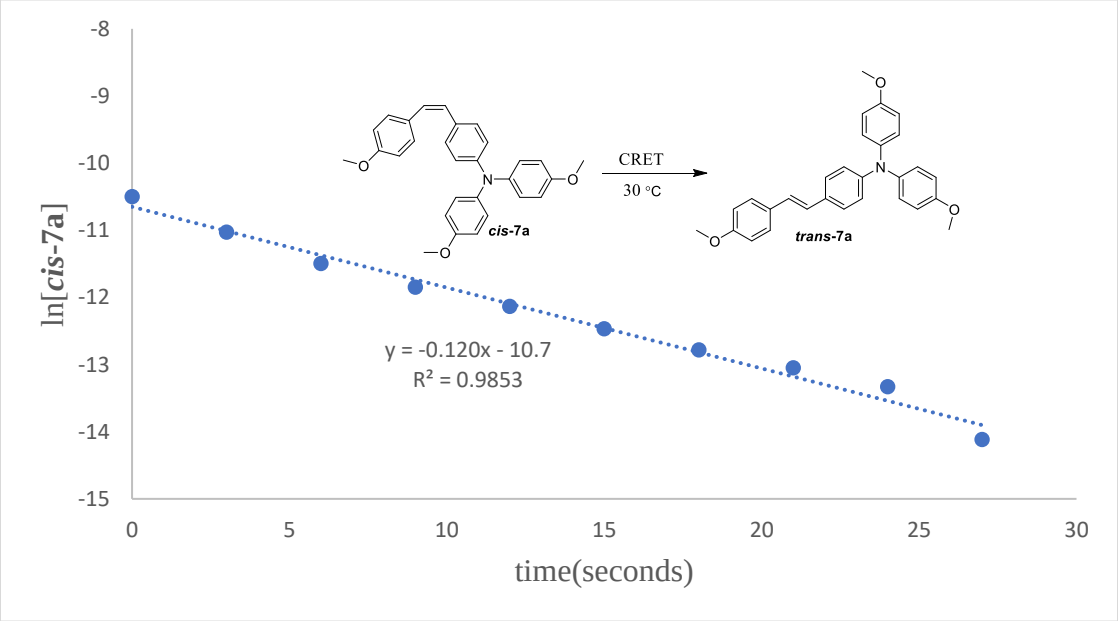

I.4. First order plot of the ln[***cis*-7a**] vs time at 30 ºC for the redox auxiliary promoted *cis-trans* isomerization of ***cis*-7a** in cyclohexane: benzene =98:2 using 7 mol % CRET in DCM.

Time (s)	% *cis*	[*cis*]	ln[*cis*]
0	95.9	2.90 E-05	-10.4
3	57.7	1.74 E-05	-11.0
6	37.3	1.13 E-05	-11.4
9	25.4	7.68 E-06	-11.8
12	18.1	5.45 E-06	-12.1
15	13.3	4.01 E-06	-12.4
18	9.33	2.82 E-06	-12.8
21	6.06	1.83 E-06	-13.2
24	3.97	1.20 E-06	-13.6
27	1.92	5.80 E-07	-14.4

I.5. RA promoted *cis-trans* isomerization of 3.05 x 10^{-5} M ***cis*-7a** in cyclohexane: benzene =98:2 using 8 mol % CRET in DCM at 30 ºC

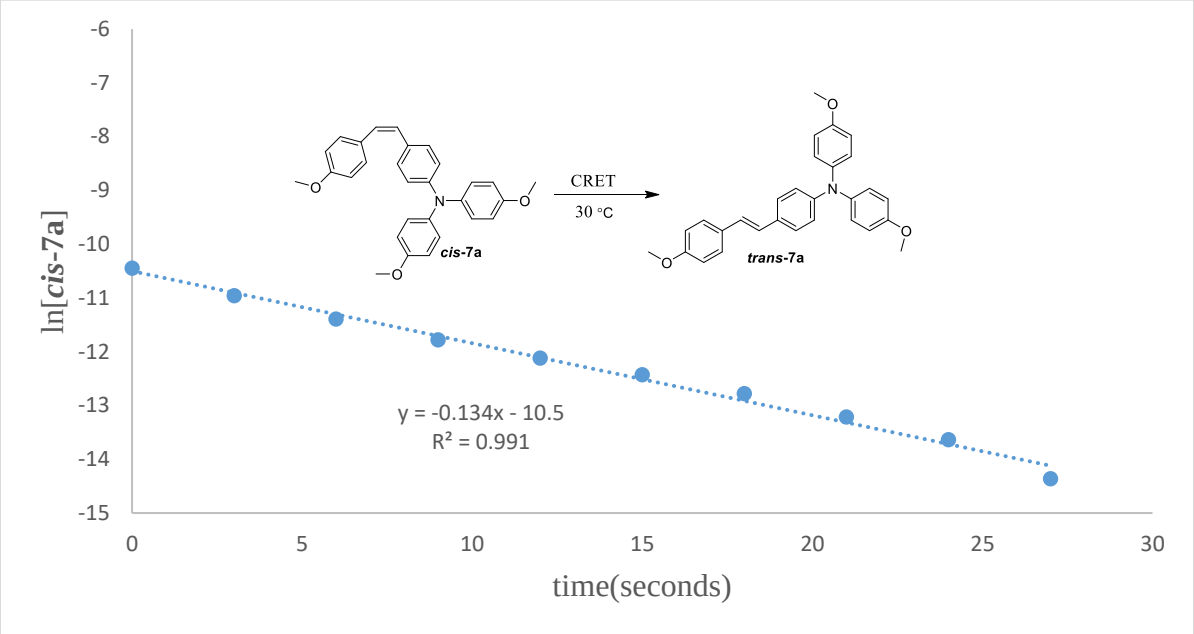

I.6. First order plot of the ln**[*cis*-7a]** vs time at 30 ºC for the redox auxiliary promoted *cis-trans* isomerization of ***cis*-7a** in cyclohexane: benzene = 98:2 using 8 mol % CRET in DCM.

Time (seconds)	% *cis*	[*cis*]	ln[*cis*]
0	94.2	2.84 E-05	-10.5
2	86.6	2.61 E-05	-10.6
5	52.8	1.56 E-05	-11.1
8	32.3	9.74 E-06	-11.5
11	20.8	6.28 E-06	-12.0
14	13.6	4.10 E-06	-12.4
17	8.16	2.46 E-06	-12.9
20	4.86	1.48 E-06	-13.4
23	2.47	7.45 E-07	-14.1

I.7. RA promoted *cis-trans* isomerization of 3.05 x 10^{-5} M ***cis*-7a** in cyclohexane: benzene =98:2 using 9 mol % CRET in DCM at 30 ºC

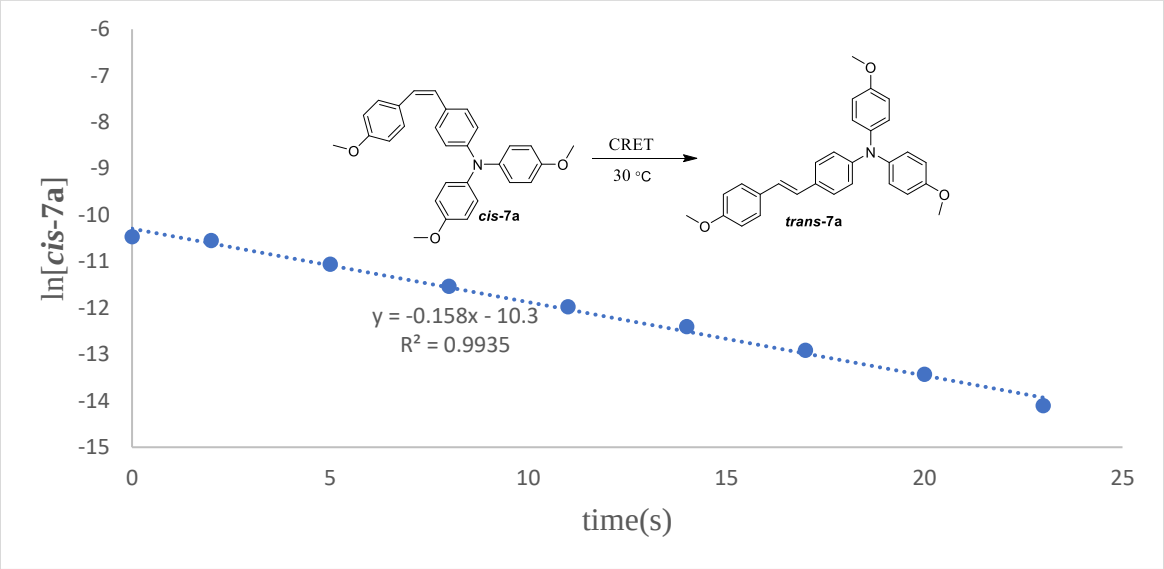

I.8. First order plot of the ln**[*cis*-7a]** vs time at 30 ºC for the redox auxiliary promoted *cis-trans* isomerization of ***cis*-7a** in cyclohexane: benzene = 98:2 using 9 mol % CRET in DCM.

Time (s)	% *cis*	*cis*	ln[*cis*]
0	95.6	2.89 E-05	-10.5
4	64.7	1.96 E-05	-10.8
6	40.2	1.21 E-05	-11.3
8	27.0	8.15 E-06	-11.7
10	18.8	5.69 E-06	-12.1
12	13.4	4.06 E-06	-12.4
14	9.90	2.99 E-06	-12.7
16	7.16	2.16 E-06	-13.0
18	5.00	1.51 E-06	-13.4
20	3.38	1.02 E-06	-13.8
22	2.32	6.99 E-07	-14.2
24	1.39	4.19 E-07	-14.7

I.9. RA promoted *cis-trans* isomerization of 3.05 x 10^{-5} M ***cis*-7a** in cyclohexane: benzene =98:2 using 10 mol % CRET in DCM at 30 ºC

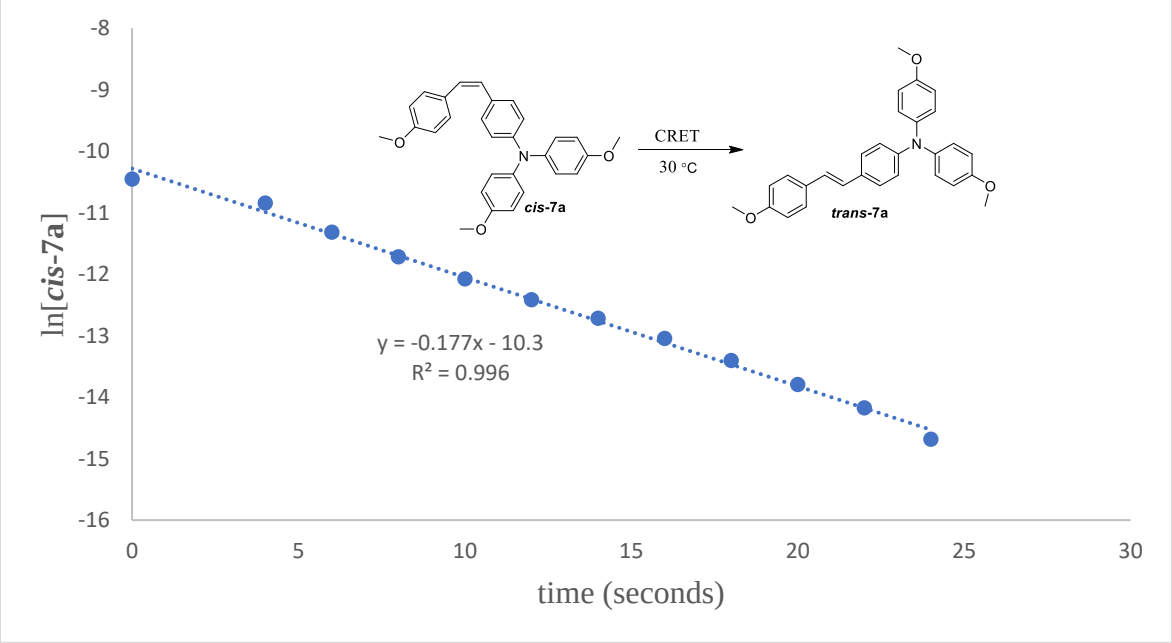

I.10. First order plot of the ln[***cis*-7a**] vs time at 30 ºC for the redox auxiliary promoted *cis-trans* isomerization of ***cis*-7a** in cyclohexane: benzene =98:2 using 10 mol % CRET in DCM.

Time (s)	% *cis*	[*cis*]	ln[*cis*]
0	97.5	2.97 E-05	-10.4
10	55.6	1.69 E-05	-11.0
20	31.6	9.64 E-06	-11.5
30	19.6	5.98 E-06	-12.0
40	12.2	3.73 E-06	-12.5
50	7.52	2.30 E-06	-13.0
60	4.29	1.31 E-06	-13.5
70	1.70	5.18 E-07	-14.5

I.11. RA promoted *cis-trans* isomerization of 3.05 x 10^{-5} M ***cis*-7a** in cyclohexane: benzene =98:2 using 5 mol % CRET in DCM at 25 ºC

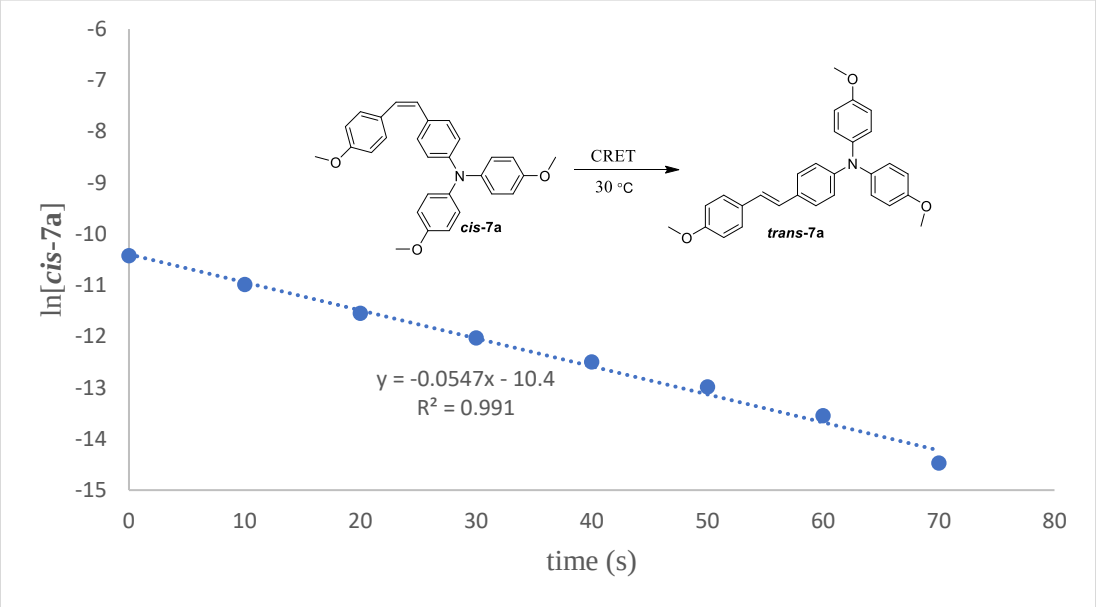

I.12. First order plot of the ln[***cis*-7a**] vs time at 25 ºC for the redox auxiliary promoted *cis-trans* isomerization of ***cis*-7a** in cyclohexane: benzene =98:2 using 5 mol % CRET in DCM.

Time (seconds)	% *cis*	[*cis*]	ln[*cis*]
0	98.2	3.00 E-05	-10.4
5	53.0	1.62 E-05	-11.0
10	29.3	8.93 E-06	-11.6
15	20.4	6.22 E-06	-12.0
20	14.8	4.52 E-06	-12.3
25	11.4	3.49 E-06	-12.6
30	7.36	2.24 E-06	-13.0
35	3.94	1.20 E-06	-13.6
40	1.02	3.10E-07	-15.0

I.13 RA promoted *cis-trans* isomerization of 3.05 x 10^{-5} M ***cis*-7a** in cyclohexane: benzene =98:2 using 5 mol % CRET in DCM at 35 ºC.

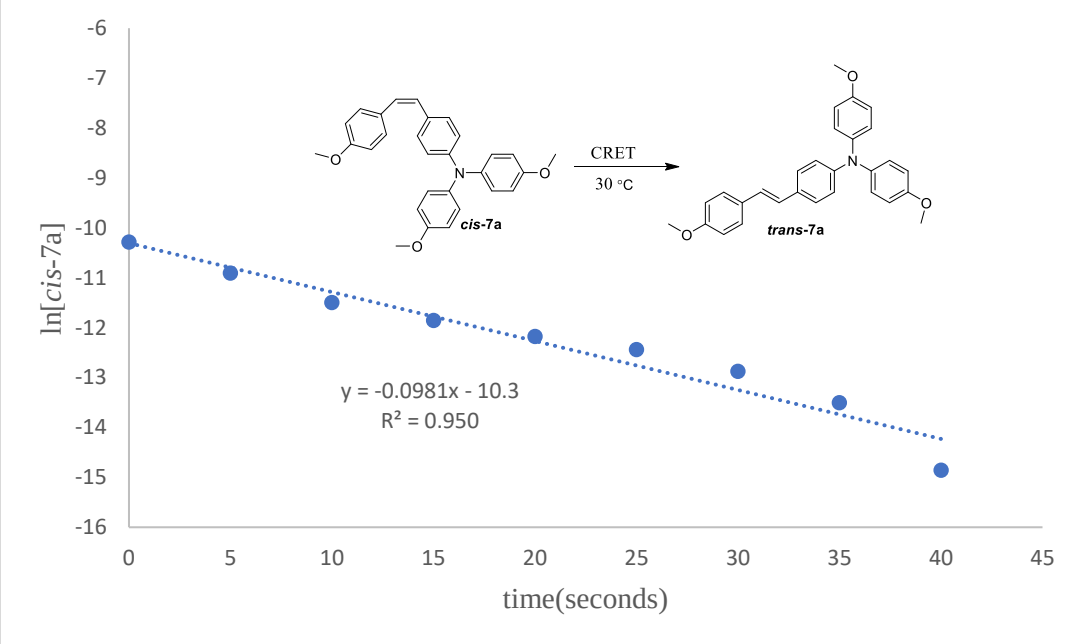

I.14 First order plot of the ln[***cis*-7a**] vs time at 35 ºC for the redox auxiliary promoted *cis-trans* isomerization of ***cis*-7a** in cyclohexane: benzene =98:2 using 5 mol % CRET in DCM.

Time (s)	% cis	[*cis*]	ln[*cis*]
0	97.9	2.99 E-05	-10.4
3	68.4	2.09 E-05	-10.8
6	33.9	1.03 E-05	-11.5
9	22.5	6.86 E-06	-11.9
12	15.8	4.83 E-06	-12.2
15	11.2	3.40 E-06	-12.6
18	7.92	2.42 E-06	-12.9
21	4.90	1.49 E-06	-13.4
24	3.01	9.19 E-07	-13.9

I.15 RA promoted *cis-trans* isomerization of 3.05 x 10^{-5} M ***cis*-7a** in cyclohexane: benzene =98:2 using 5 mol % CRET in DCM at 40 ºC.

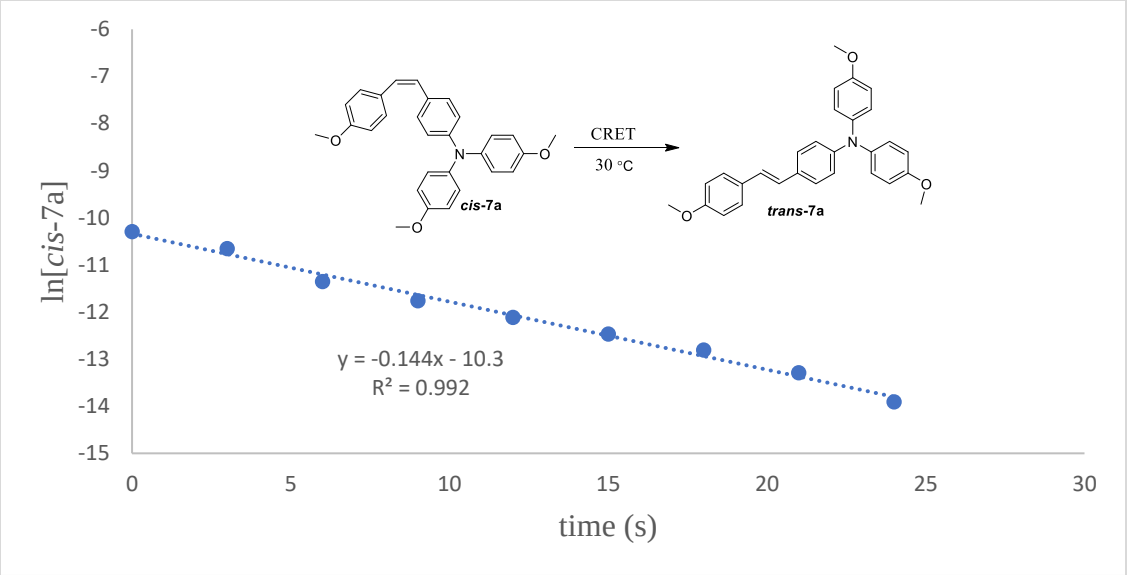

I.16 First order plot of the ln[***cis*-7a**] vs time at 40 ºC for the redox auxiliary promoted *cis-trans* isomerization of ***cis*-7a** in cyclohexane: benzene =98:2 using 5 mol % CRET in DCM.

Time (s)	% *cis*	[*cis*]	ln[*cis*]
0	97.9	2.99 E-05	-10.4
3	79.8	2.43 E-05	-10.6
6	42.2	1.29 E-05	-11.3
9	22.1	6.73 E-06	-11.9
12	13.3	4.06 E-06	-12.4
15	8.69	2.65 E-06	-12.8
18	4.93	1.50 E-06	-13.4
21	2.49	7.59 E-07	-14.1

I.17 RA promoted *cis-trans* isomerization of 3.05 x 10^{-5} M ***cis*-7a** in cyclohexane: benzene =98:2 using 5 mol % CRET in DCM at 45 ºC.

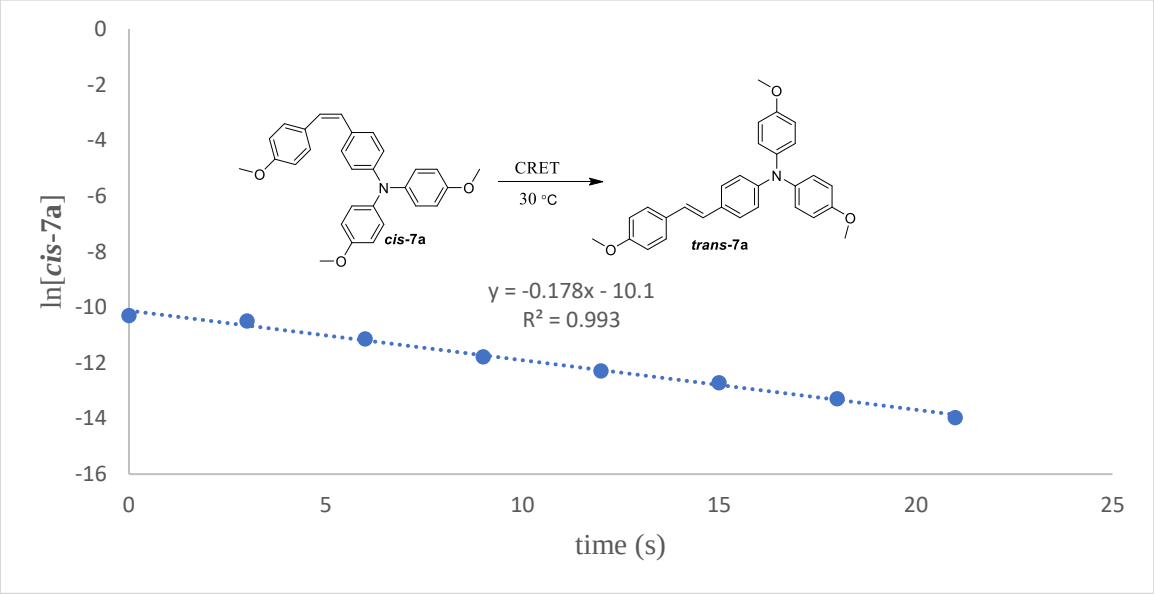

I.18 First order plot of the ln[***cis*-7a**] vs time at 45 ºC for the redox auxiliary promoted *cis-trans* isomerization of ***cis*-7a** in cyclohexane: benzene =98:2 using 5 mol % CRET in DCM.

APPENDIX J
The UV-Vis of CRET

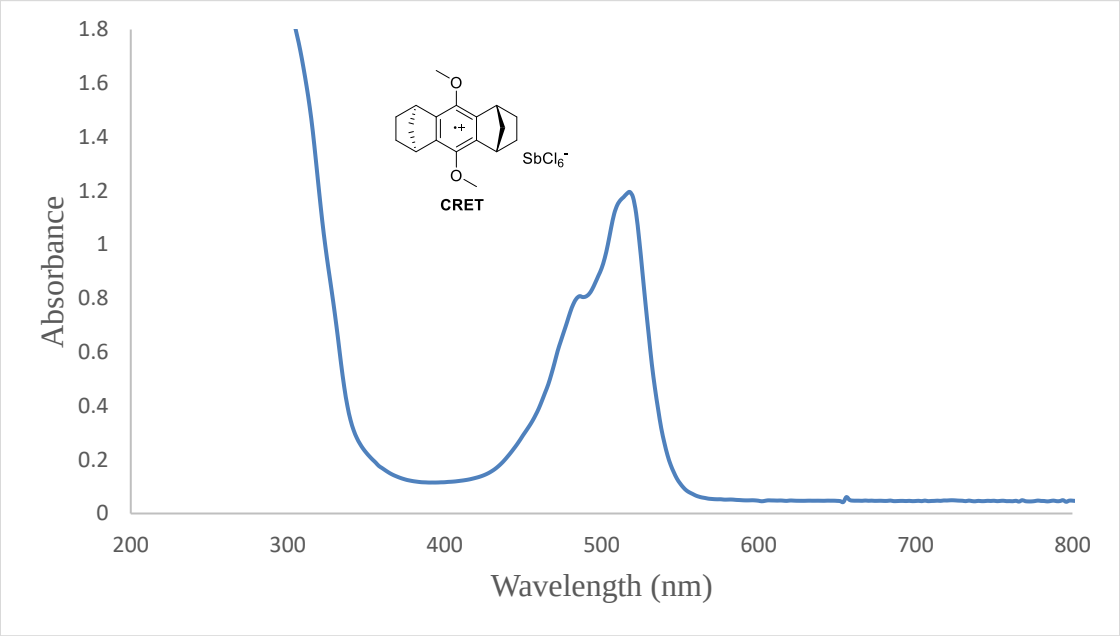

J.1 The UV-Vis spectrum of 1.65 x 10^{-4} M CRET in anhydrous DCM at room temperature

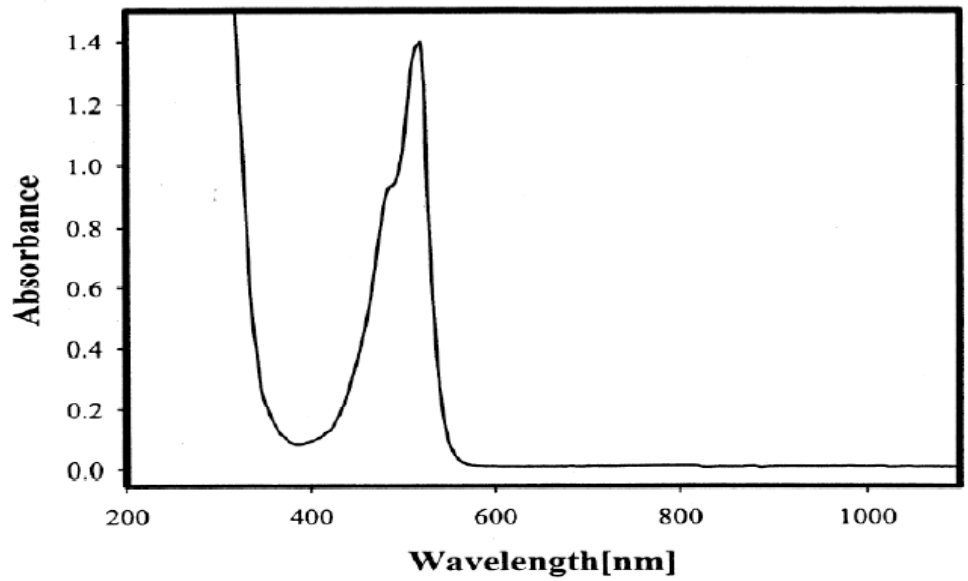

J.2 The UV-Vis spectrum of 1.92 x 10^{-4} M CRET in anhydrous DCM at room temperature[142]